Prokar Dasgupta
John Fitzpatrick
Roger Kirby
Inderbir S. Gill *Editors*

New Technologies in Urology

John Lumley *Series Editor*

Springer

New Technologies in Urology

Prokar Dasgupta • John Fitzpatrick
Roger Kirby • Inderbir S. Gill (Eds.)

New Technologies in Urology

Springer

Prof. Prokar Dasgupta
Medical Research Council (MRC) Centre
for Transplantation
King's College London
Department of Urology
Guy's Hospital, London SE1 9RT
United Kingdom
prokarurol@gmail.com

Prof. Dr. John Fitzpatrick
University College Dublin
Mater Misericordiae Hospital
Department of Surgery
47 Eccles Street
Dublin 7
Ireland
jfitzpatrick@mater.ie

Prof. Roger Kirby
Prostate Centre
32 Wimpole Street
London
United Kingdom W1G 8GT
Rogerkirby@theprostatecentre.com

Prof. Inderbir S. Gill
1441 Eastlake Ave, Suite
7416 Los Angeles CA 90089
Keck School of Medicine
USA
gillindy@gmail.com

ISBN: 978-1-84882-177-4 e-ISBN: 978-1-84882-178-1
DOI: 10.1007/978-1-84882-178-1
Springer Dordrecht Heidelberg London New York

Library of Congress Control Number: 2009938955

Dedicated to our families and friends

Preface

Technology seems to be an integral part of modern living. Urologists have over the years embraced new technological advances for patient benefit. On some occasions, however, the initial enthusiasm in something new has failed to endure rigorous scientific scrutiny. Thus, while being technological leaders, we urologists know better than most other surgical specialties that what is new is not necessarily good.

This textbook is aimed at urologists and surgeons at all levels and has contributions from international experts. The topics vary from robotics to lasers to single port laparoscopy. The comprehensive chapters should be of equal interest to uro-oncologists and those involved in treating benign urological diseases. While the contents are meant to bring the reader up to date with technological advances, the authors have attempted to balance their enthusiasm with basic science, translational research, and clinical outcomes. It will be obvious that some of the subjects mentioned here, such as nanotechnology, are still evolving, and it will be a while before they undergo clinical trials that establish their position in clinical medicine.

We hope you enjoy reading this book as much as we have enjoyed creating it.

London, UK — Prof. Prokar Dasgupta
Dublin, Ireland — Prof. John Fitzpatrick
London, UK — Prof. Roger Kirby
CA, USA — Prof. Inderbir S. Gill

Acknowledgements

The editors thank all authors for their time and valuable contributions.

We are also grateful to our developmental editors Joni Fraser and Barbara Lopez-Lucio.

Prokar Dasgupta acknowledges support from the UK Department of Health via the National Institute for Health Research (NIHR) comprehensive Biomedical Research Centre award to Guy's & St Thomas' NHS Foundation Trust in partnership with King's College London and King's College Hospital NHS Foundation Trust.

Contents

Contributors

Hashim U. Ahmed, MRCS (Ed), BM BCh (Oxon), BA (Hons) Division of Surgery and Interventional Sciences, University College London, London, UK

David M. Albala, MD Department of Urology, Duke University Medical Center, Durham, NC, USA

Kaspar Althoefer, PhD, Dip.-Ing. Department of Mechanical Engineering, King's College London, London, UK

Monish Aron, MD Department of Urology, Cleveland Clinic, Cleveland, OH, USA

Manit Arya, MBBS, BSc, MD, FRCS (Urol) Division of Surgery and Interventional Sciences, University College London, London, UK

Mohamed A. Attala, MD Smith Institute for Urology, New Hyde Park, NY, USA

Arie S. Belldegrun, MD Department of Urology, David Geffen School of Medicine, University of California Los Angeles, Los Angeles, CA, USA

James William Brewin, B Med Sci, BMBS, MRCS Department of Urology, Kings College Hospital, London, UK

Gareth J. Bydawell, MBChB, FRCR Department of Radiology, St. George's Hospital, London, UK

Jeffrey A. Cadeddu, MD Department of Urology, University of Texas Southwestern Medical Center, Dallas, TX, USA

Arthur Caire, MD Department of Urology, Duke University Medical Center, Durham, NC, USA

David Canes, MD Institute of Urology, Lahey Clinic, Burlington, MA, USA

Benjamin J. Challacombe, BSc, MS, FRCS (Urol) The Urology Centre, Guy's and St. Thomas' NHS Foundation Trust, London, UK

Department of Urology, Royal Melbourne Hospital, Melbourne, Australia

Shahin T. Chandrasoma, MD Department of Urology, University of Southern California, Los Angeles, CA, USA

Rafael Ferreira Coelho, MD Department of Urology, Florida Hospital Celebration Health, Celebration, FL, USA

Jose R. Colombo, MD Division of Urology, University of Sao Paulo, Sao Paulo, Brazil

Anthony J. Costello, MD, FRACS, MBBS Department of Urology, Royal Melbourne Hospital, Melbourne, Australia

Geoff Coughlin, MD, FRACS Department of Urology, Global Robotics Institute, Florida Hospital Celebration Health, Celebration, FL, USA

David W. Cranston, MBChB, DPhil, FRCS Nuffield Department of Surgery, University of Oxford, Oxford, UK

Ranan DasGupta, MBBChir, MA, MD, MRCS, FRCS (Urol) Department of Urology, Guy's Hospital, London, UK

Prokar Dasgupta, MSc (Urol), MD, DLS, FRCS, FRCS (Urol), FEBU The Urology Centre, Guy's Hospital, London, UK

King's Health Partners Academic Health Sciences Centre, London, UK

John Hugh Davis, BSc, MBBS, FRCS (Ed), FRCS (Urol) Department of Urology, Royal Surrey County Hospital, Guildford, UK

Roger E. De Filippo, MD Division of Urology, Childrens Hospital Los Angeles, Los Angeles, CA, USA

Jean J.M.C.H. de la Rosette, MD, PhD Department of Urology, Academic Medical Center, University of Amsterdam, Amsterdam, The Netherlands

Mihir M. Desai, MD Stevan Streem Center for Endourology, Cleveland Clinic Foundation, Cleveland, OH, USA

Oussama Elhage, MRCS Department of Urology, Guy's Hospital, London, UK

Mark Emberton, BSc, MBBS, MD, FRCS, FRCS (Urol) Interventional Oncology and Urological Surgery, University College London, London, UK

Michael Ferrandino, MD Department of Urology, Duke University Medical Center, Durham, NC, USA

John Fitzpatrick, MCh, FRCSI, FCS (Urol), SA FRCS (Glas), FRCS Mater Misericordiae University Hospital, Dublin, Ireland

Troy Gianduzzo, MBBS, FRCS (Urol) The Wesley Medical Centre, Auchenflower, Queensland, Australia

Inderbir S. Gill, MD, MCh Department of Urology, Keck School of Medicine, University of Southern California Los Angeles, Los Angeles, CA, USA

Peter J. Gilling, FRACS Department of Urology, Tauranga Hospital, Tauranga, New Zealand

Justin J. Gould, MD Institute of Urology, Lahey Clinic, Burlington, MA, USA

Stavros Gravas, MD, PhD Department of Urology, University Hospital of Larissa, Larissa, Greece

David M. Hartke, MD Department of Urology, Case Western Reserve University School of Medicine, Case Medical Center, Cleveland, OH, USA

Makoto Hashizume, MD, PhD Department of Advanced Medical Initiatives, Kyushu University, Fukuoka City, Japan

Nicholas Hegarty, MB, PhD, FRCS (Urol) Department of Urology, Guy's Hospital, London, UK

Alastair Henderson, MBBS, PhD, FRCS (Urol) Department of Urology, Royal Surrey County Hospital, Guildford, UK

Department of Urology, Guy's Hospital, London, UK

Brian H. Irwin, MD Division of Urology, University of Vermont College of Medicine, Burlington, VT, USA

Mohamed Ismail, MBChB, MRCS, PhD Department of Urology, Homerton University Hospital, London, UK

Jihad H. Kaouk, MD Section of Robotic Urologic Surgery, Glickman Urological and Kidney Institute, Cleveland Clinic, Cleveland, OH, USA

Louis R. Kavoussi, MD Smith Institute for Urology, New Hyde Park, NY, USA

Patrick A. Kenney, MD Institute of Urology, Lahey Clinic, Burlington, MA, USA

Roger S. Kirby, MA, MD, FRCS (Urol), FEBU The Prostate Centre, London, UK

Jeffrey C. La Rochelle, MD Department of Urology, University of California Los Angeles, Los Angeles, CA, USA

Tom A. Leslie, BSc, MBChB, Dphil, MRCSEd Nuffield Department of Surgery, University of Oxford, Oxford, UK

Charalampos Mamoulakis, MD, PhD, MSci, FEBU Department of Urology, Academic Medical Center, University of Amsterdam, Amsterdam, The Netherlands

Magnus J. Mansard, MS Department of Surgical Gastroenterology, Asian Institute of Gastroenterology, Hyderabad, India

Tsuneharu Miki, MD, PhD Department of Urology, Kyoto Prefectural University of Medicine, Kyoto, Japan

Caroline Moore, BSc, MBBS, MD, MRCS Division of Surgery and Interventional Sciences, University College London, London, UK

Declan G. Murphy, MB, FRCS (Urol) The Urology Center, Guy's and St. Thomas' NHS Foundation Trust, London, UK

Azad Najmaldin, MB, ChB, MS, FRCS (Ed), FRCS (Eng) St. James's University Hospital, Leeds, UK

Masahiko Nakamoto, PhD Department of Radiology, Graduate School of Medicine, Osaka University, Suita, Japan

Timothy G. Nedas, MBBS, MRCS, MSc (Urol) Department of Urology, Eastbourne District General Hospital, Eastbourne, UK

Shu Pan, BS Smith Institute for Urology, New Hyde Park, NY, USA

Sijo J. Parekattil, MD Department of Urology, University of Florida, Gainesville, FL, USA

Uday Patel, MB, ChB, FRCR, MRCP Department of Radiology, St. George's Hospital, London, UK

Vipul R. Patel, MD Global Robotics Institute and Urologic Oncology Program, Florida Hospital Celebration Health, Celebration, FL, USA

Thomas J. Polascik, MD Department of Surgery/Urology, Duke University, Durham, NC, USA

Lee E. Ponsky, MD Department of Urology, Center for Urologic Oncology & Minimally Invasive Therapies, Cleveland, OH, USA

University Hospitals Case Medical Center, Case Western Reserve University, Cleveland, OH, USA

Frédéric Pouliot, MD, PhD, FRCSC Department of Urology, David Geffen School of Medicine, University of California Los Angeles, Los Angeles, CA, USA

Guduru V. Rao, MS, MAMS Department of Surgical Gastroenterology, Asian Institute of Gastroenterology, Hyderabad, India

Pradeep P. Rao, MB, DNB (Surg), FRCSEd, DNB (Urol) Department of Urology, Mamata Hospital, Mumbai, India

Duvvuru N. Reddy, MD, DM, DSc, FAMS, FRCP Department of Gastroenterology, Asian Institute of Gastroenterology, Hyderabad, India

Peter Rimington, FCS (Urol) Department of Urology, East Sussex Hospitals, Eastbourne, East Sussex, UK

Jorge Rioja Zuazu, MD, PhD Department of Urology, AMC University Hospital, Amsterdam, The Netherlands

Yoshinobu Sato, PhD Department of Radiology, Graduate School of Medicine, Osaka University, Suita, Japan

Mohammad Shamim Khan, OBE, FRCS (Urol), FEBU Department of Urology, Guy's Hospital, London, UK

King's Health Partners Academic Health Sciences Centre, London, UK

Philippa L. Skippage, MBChB, MRCP, FRCR Department of Radiology, St. George's Hospital, London, UK

Naomi Smith, MA (Hons), MBBS, MRCS Department of Urology, Guy's and St. Thomas' NHS Foundation Trust, London, UK

Robert J. Stein, MD Department of Urology, Cleveland Clinic Foundation, Cleveland, OH, USA

Dan Stoianovici, PhD Department of Urology, Johns Hospital University, Baltimore, MD, USA

Li-Ming Su, MD Department of Urology, University of Florida, Gainesville, FL, USA

Kay Thomas, MBBS, MD, FRCS (Urol) Department of Urology, Guy's and St. Thomas' NHS Foundation Trust, London, UK

Chad R. Tracy, MD Department of Urology, University of Texas Southwestern Medical Center, Dallas, TX, USA

Sheaumei Tsai, MD Institute of Urology, Lahey Clinic, Burlington, MD, USA

Vassilios Tzortzis, MD Department of Urology, University Hospital of Larissa, Larissa, Greece

Osamu Ukimura, MD, PhD Department of Urology, Kyoto Prefectural University of Medicine, Kyoto, Japan

Wesley M. White, MD Section of Laparoscopic and Robotic Urologic Surgery, Glickman Urological and Kidney Institute, Cleveland Clinic, Cleveland, OH, USA

Hessel Wijkstra, MSc, PhD Department of Urology, Academic Medical Center, University of Amsterdam, Amsterdam, The Netherlands

Liam C. Wilson, FRACS Department of Urology, Tauranga Hospital, Tauranga, New Zealand

Lawrence L. Yeung, MD Department of Urology, University of Florida, Gainesville, FL, USA

Part I

Robots

Prokar Dasgupta and Roger Kirby

Robotic-Assisted Laparoscopic Radical Prostatectomy

1

Rafael Ferreira Coelho, Geoff Coughlin, and Vipul R. Patel

Introduction to Robotics

History of Robotics

The word "robot" was originally coined by Karel Capek in his play, Rossum's universal robots, in 1921.[1] It is derived from the Czechoslovakian term robota, meaning forced work. His original vision dealt with a world in which robots help humans with everyday tasks but eventually turn on their masters and attempt world domination. The first truly robotic flexible arm, known as the Programmable Universal Manipulation Arm (PUMA), was developed in 1978, by Victor Scheinman, and quickly became the industry standard. The first surgical application of this technology was in 1985 when the PUMA 560 was used to orientate a needle for a radiologically guided brain biopsy.[2] Soon after, robots were utilized in other surgeries including the PROBOT, to perform transurethral resection of the prostate, and the ROBODOC, for use in hip replacements.[3–6]

The contemporary generation of surgical robots consists of "master–slave" systems made by Intuitive Surgical Inc. (Sunnyvale, CA). These systems resulted from research initially conducted by the Stanford Research Institute, the National Aeronautics and Space Agency (NASA), and the Department of Defense. The concept of surgeons being able to perform surgery from a remote location with use of such a master–slave system would be optimal for use in space travel for astronauts and to remove specialist surgeons from the battlefield.[7]

The da Vinci® Robotic System

The da Vinci is an advanced master–slave robotic system. The basic principle involves control of three or four robotic arms by a surgeon sitting at a remote console. The system has three components: (a) a surgeon console, (b) a surgical robot with three or four arms, and (c) an endoscopic stack (Fig. 1.1). The console contains the master tool manipulators, the visual supply, and foot pedals for camera and tool manipulation. The surgeon's hands are inserted in the free-moving finger controls (masters). These controls convert

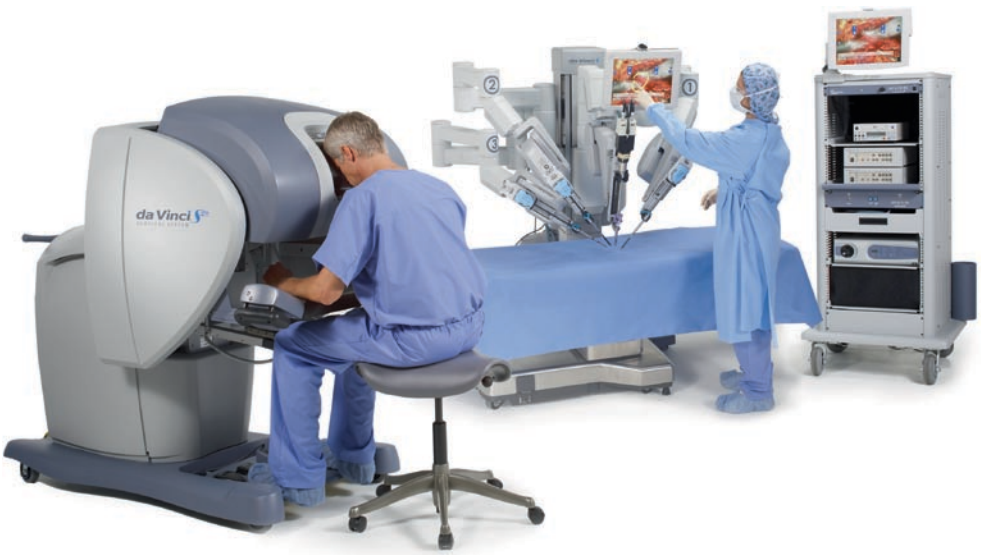

Fig. 1.1 The da Vinci S surgical system. The three components are shown: the surgeons console, the 4-armed surgical robot, and the endoscopic stack. Courtesy Intuitive Surgical, CA

P. Dasgupta et al. (eds.), *New Technologies in Urology,*
DOI: 10.1007/978-1-84882-178-1_1, © Springer-Verlag London Limited 2010

the movements of the surgeon's fingertips and wrist into electrical signals. These signals are translated to computer commands that direct the robot to replicate the movements with the robotic instruments in the operative field. The console is connected to the video and surgical component of the robot via cables. The patient-side surgical robot has an arm to control the camera and two or three arms to hold the operating instruments. These instruments are articulated at the wrist and have seven degrees of freedom and two degrees of axial rotation. This master–slave robotic system overcomes many of the limitations of conventional laparoscopy. It provides the surgeon with 3D 10× magnified vision, wristed instrumentation, tremor filtration, and motion scaling. The system produces an *immersive telerobotic environment* ideally suited for surgical precision and reconstructive applications.

Evolution of Minimally Invasive Laparoscopic Prostatectomy

Data from the Surveillance, Epidemiology, and End Results (SEER) registry indicate that the incidence of prostate cancer in men under 50 years of age has risen over the past 10 years, with an annual increase of 9.5%.[8] Prostate cancer accounts today for nearly 33% of all newly diagnosed cancers in men.[9] For patients with prostate confined disease, a number of treatment alternatives are now available. However, radical prostatectomy (RP) remains the gold standard for long-term cure.[10] Since its first description in 1905 by Young, RP procedure has been associated with significant perioperative morbidity, including excessive blood loss, urinary incontinence, and impotency.[11] In the late 1970s and early 1980s, several detailed anatomic studies provided important insights into the periprostatic anatomy, especially that of the dorsal venous complex,[12] neurovascular bundle,[13] and striated urethral sphincter.[14] These observations allowed the development of an anatomic approach to radical prostatectomy with significant reduction in operative morbidity.

With the increasing use of screening for prostate cancer detection, younger and healthier men are presently being diagnosed with the condition. These patients desire treatments that not only provide good oncological and functional outcomes but also treatments that can also be performed in a minimally invasive nature with short hospitalization times and minimal convalescence. In an effort to further decrease the morbidity of open radical prostatectomy, a minimally invasive surgical approach was first described by Schuessler and colleagues in 1997.[15] These authors performed the first successful laparoscopic radical prostatectomy (LRP). With their initial experience, the authors noted the challenging nature of the operation with long operative times and hospital stays. The operation was advanced in the late 1990s, as European surgeons tackled the difficult learning curve and reported feasibility with results comparable with the open surgical approach.[16–18] Despite this, the technical demands of the surgery and the protracted learning curve has prevented the widespread adoption of LRP by most urologic surgeons.

The recent introduction of advanced robotic devices such as the da Vinci Surgical System (Intuitive Surgical, Inc., Sunnyvale, CA) has simplified complex laparoscopic procedures and added new hopes of reducing operative times and the learning curve for a minimally invasive approach to radical prostatectomy.[19] Robotically assisted laparoscopic radical prostatectomy (RALP) offers the additional advantages of 10× magnified three-dimensional visualization, motion scaling with tremor filtration, improved surgical ergonomics and miniature wristed, articulating instruments with 7-degrees of freedom. The surgeon can dissect with improved operative precision and robotic technology greatly simplifies the reconstructive element of the procedure. The first robotic prostatectomy was performed in 2000 by Binder and Kramer in Germany.[20] Subsequently, the procedure has undergone significant innovation and improvement. Menon, Guillonneau, and Vallancien refined the technique at Henry Ford Hospital later in the same year and its growth has been exponential since then.[21]

Robotic-Assisted Laparoscopic Radical Prostatectomy (RALP)

Indications

The indications for RALP are identical to that for open surgery. Patients with clinical stage T2 or less prostate cancer with no evidence of metastasis, either clinically or radiographically, are candidates for RALP. Absolute contraindications include uncorrectable bleeding diatheses, increased intracranial pressure, or the inability to undergo general anesthesia due to severe cardiopulmonary compromise.

Some predictable situations provide a technical challenge to the entire robotic operative team. Though these scenarios certainly are not contraindications, they should be avoided by inexperienced teams during their initial experience with the procedure. These scenarios include patients with: prior major abdominal or pelvic surgery, morbid obesity, large prostate size, prior TURP, presence of a median lobe, prior pelvic irradiation, neoadjuvant hormonal therapy, or a history of prostatitis. As the experience of the robotic team increases, these challenging scenarios can be approached with more skill and confidence.

Table 1.1 Criteria for selection of ideal initial patients

Prostate size: 60 g
BMI < 30
No previous prostatic or abdominal surgery
Erectile dysfunction
Low-risk disease: PSA < 10 ng/mL, Gleason score <7, cT1 or T2a
No androgen ablation therapy or history of prostatitis

The ideal criteria for patient selection during the initial learning curve for RALP are shown in Table 1.1. From an oncological and functional viewpoint, patients with low-risk disease and erectile dysfunction are ideal. These characteristics reduce the risk of positive surgical margins and nerve sparing is a less important operative consideration. From a technical standpoint, patients with a BMI < 30, no prior abdominal surgery, prostate size < 60 g with no prior TURP, no median lobe, no prior androgen ablation, and no history of prostatitis is desirable. By eliminating these predictable challenges, the technical aspect of the operation is simplified. As experience is gained, these factors become less important considerations. This stepladder approach allows the surgeon to continually develop skills to deal with even the most challenging patients.

RALP and the "Learning Curve"

As robotic technology is introduced to surgery, there is a time period where surgeons develop the knowledge and skills required to utilize the technology with efficiency. This time is generally referred to as the learning curve and can be reduced by factors such as standardization of the surgical procedure, specialized resident or fellowship training, or case proctorship/mentorship. Initial reports on the learning curve for RALP suggested that approximately 20 cases were required for the surgeon to acquire basic proficiency at the procedure.[22–24] With increasing experience and standardization of the operation, it has become evident that far greater experience is required for the surgeon to be confident and provide good patient outcomes.[25]

Outcomes of RALP

Intraoperative Outcomes

Berryhill et al[26] reviewed the outcomes of radical prostatectomy via robotic, laparoscopic, and open approaches. Twenty-two robotic prostatectomy series were identified with pertinent reported outcomes. Many institutions were represented, including studies from Institute Mutualiste Montsouris (Paris, France), Goethe University of Frankfurt (Germany), Vattikuti Urology Institute (Detroit, Michigan), and University of California-Irvine. They found a mean operative time of 164 min (varying from 55 min to 13 h) for RALP. The mean EBL was 152 mL (range of means, 50–570 mL). The intraoperative and postoperative RALP transfusion rates were generally minimal, with a mean of 2.9% of cases requiring blood. This was compared favorably with LRP and open RP where mean EBL was 406 and 697 mL, respectively. The LRP studies reported a mean of 8.3% of cases requiring transfusion, while the open RP articles reported an even higher mean transfusion rate of 24%.

We reviewed our perioperative outcomes for fifteen hundred consecutive RALPs performed by a single surgeon (VRP).[27] Operative times fell with increasing experience of both the surgeon and team. While some of our initial cases were between 4 and 6 h, our operative times have averaged 105 min over the last 300 cases. Mean EBL was 111 mL (50–500) with no patient requiring intraoperative transfusion and 0.4% of patients receiving postoperative transfusion. Two rectal injuries occurred during the initial 25 cases that were recognized intraoperatively and repaired with no sequelae.

The comparative results for operative time and blood loss from some different robotic series are presented in Table 1.2.

Postoperative Complications

The same current review by Berryhill and colleagues reported a mean overall postoperative complication rate for RALP of 6.6%.[26] This is consistent with our findings where 63 of our first 1,500 patients (4.3%) suffered a perioperative complication.[27] As our experience progresses, we have observed a decreased trend in complications from 9.3% in the first 300 to 2.6% in the last 300 cases. In addition, more than half of the radiologically detected anastomotic leaks occurred during the first 300 patients. Though complications such as anastomotic leaks and rectal injury disappeared relatively early in our learning curve, occasional complications such as MI, DVT/PE, and postoperative bleed continue to occur sporadically at a low rate.

Oncological Outcomes

Given that the first RALP was performed in 2000, data regarding long-term cancer-specific survival will not be matured for some time. Likewise, evidence for biochemical recurrence free survival is also sparse. At present, positive surgical margin rates are being used as a surrogate marker to assess the oncological efficacy of RALP.

Table 1.2 RALP outcomes

Study (reference)	*N*	Age (year)	OR Time (minutes)	Mean EBL (mL)	Positive margin rate (%)			Continence outcomes		Potency outcomes			
					pT2	pT3	Overall	Time of assessment (months)	Continence rate (%)	Time of assessment (months)	BNS % intercourse	UNS % intercourse	Percentage of intercourse
Ahlering et al[28]	45	61.4 (46–71)	209 (150–600)	145 (25–350)	14.8	62.5	35.5	3	81	<12	33	0	33
Bentas et al[29]	40	61.3 (45–72)	500 (246–780)	570 (100–2,500)	8	67	30	3	84	12	–	–	21.1
Tewari et al[30]	200	59.9 (42–76)	160 (71–315)	153 (25–750)	–	–	6	6	96	<12	50	–	50
Wolfram et al[31]	81	62.9 (43–78)	250 (150–390)	300 (100–1,500)	12.7	42	22	–	–	–	–	–	–
Ahlering et al[32]	200	62.9 (43–78)	–	108 (25–400)	6.5	32	20.4	3	77	–	–	–	–
Ahlering et al[33]	109	56.1	–	92 (25–250)	–	–	13	–	–	<12	24.4	14.3	–
Chien et al[34]	56	58.9	356 (240–480)	356 (25–1,200)	–	–	10.7	–	–	12	35.7	40	40
Joseph et al[35]	50	59.6–1.6	202–38	206–63	–	–	12	3	90	<12	–	–	46
Menon et al[36]	1,142	60.2 (39–80)	154 (71–387)	142 (10–750)	–	–	13	12	95	12	97	74	–
Patel et al[37]	500	63.2	130 (51–330)	50 (10–300)	2.5	13.8	9.4	6	95	12	–	–	78
Tewari et al[38]	700	62.1			–	–	5,2	6	97	12	87	–	87
Badani et al[39]	2,766		154 (71–387)	142 (10–1,350)	13	35	12.3			12	79.2	–	79.2
Patel et al[27]	1,500	60.7	105	111	4	34	9.3	–	–	–	–	–	–

When stratified by pathological stage, positive margin rates following RALP range from 2.5 to 22% for pT2 and 13.5 to 67% for pT3 disease.[27–29,32,37,39] Only two prospective, nonrandomized comparative studies have compared robotic and open radical prostatectomy. They showed higher positive surgical margin rates in patients who had undergone open RP when compared with those treated with RALP.[30,39]

The overall positive margin rate for our first 1,500 cases was 9.3%.[27] When stratified for pathological stage, positive surgical margin rates were 4% for pT2, 34% for pT3, and 40% for pT4. The median Gleason score was 6 (range 5–10) and Gleason grade of 4, 5, 6, 7, 8, 9, and 10 was found in 0.69, 2.78, 62.36, 26.68, 5.18, 2.16, and 0.15% of prostate specimens. Pathologic stage was T2a, T2b, T2c, T3a, T3b, and T4 in 15, 3.07, 60.23, 13.76, 5.69, and 1.46%, respectively.

In Henry Ford's series of 2,766 patients, the positive margin rate for pT2 tumors declined from 7% in the first 200 cases to 4% in the last 200.[39] The pT3 positive margin rate for the overall cohort was 35%, and the overall positive margin rate was 13%.

The oncological results based on positive surgical margins for RALP are very encouraging. The centers experienced at this procedure are reporting results as good as the best published series for open RP (Table 1.2).

Functional Outcomes: Erectile Dysfunction

Mature data on erectile function after nerve-sparing RALP is presently limited. As more series mature in the near future, this information will be more abundant. Robotic-assisted surgery has the potential to improve nerve-sparing techniques during radical prostatectomy. Magnified stereoscopic vision, the relatively bloodless field provided by pneumoperitoneum, and the wristed instrumentation allow the surgeon to operate in a very precise manner during this intricate portion of the dissection. We find the benefits of robotic technology to be essential when performing our nerve preservation technique of "early retrograde release of the neurovascular bundles." Utilizing this approach for bilateral nerve sparing on 98 consecutive patients with a preoperative SHIM score ≥21, 87.7% were potent at 12 months follow-up with or without the use of oral PD5 inhibitors. Using the same technique on 48 men with mild erectile dysfunction preoperatively (SHIM 17–20), 73% of men were potent 12 months postoperatively.[40]

The available 12-months follow-up data suggest that between 20 and 97% of patients regain potency after nerve-sparing RALP.[26,29,36] Comparing postoperative potency rates between different centers and different techniques is quite difficult. Varying definitions of "potent" combined with several methods of data collection introduce the potential for significant variations in outcomes.

Menon and colleagues at the Vattikuti Institute in Detroit, recently reported potency results for their technique of lateral prostatic fascia-sparing (Veil of Aphrodite) RALP.[39] Erectile function was measured with the SHIM questionnaire. Complete follow-up erectile function data were available for 910 patients. Preoperative SHIM scores were >17 in 721 of 910 patients. Of these, 79.2% reported successful sexual intercourse postoperatively (defined as a SHIM score of at least 2 on the second question of the SHIM questionnaire: "When you had erections with sexual stimulation, how often were your erections hard enough for penetration?"). Phosphodiesterase-5 inhibitors (PDE5) were used in 44.2% of patients.

With regard to surgical technique, Ahlering et al demonstrated in a prospective, nonrandomized, comparative study that the adoption of a cautery-free technique for preservation of the neurovascular bundles produced a significantly higher potency rate 3 months postoperatively than the then standard bipolar cautery technique.[33] Erectile function was assessed through self-administered questionnaires and defined as erections sufficient for vaginal penetration with or without PDE-5 inhibitors. After 3 months of follow-up, 43% of men in the cautery-free group were potent when compared with 8.3% of the control group. At present, leading centers control the prostatic pedicle and perform nerve sparing without the use of any cautery.

According to the nonrandomized, comparative study of Tewari and colleagues,[30] RALP could allow better and earlier potency recovery when compared with open RP. These authors reported a prospective comparison between 100 open RPs and 200 RALPs. They demonstrated a more rapid return of erections with RALP (50% at a mean follow-up of 180 days vs. 50% at a mean of 440 days after open RP) as well as a quicker return to intercourse with RALP (50% at 340 days vs. 50% at 700 days for open RP).

The potency rates in various RALP series are shown in Table 1.2.

Functional Outcomes: Urinary Incontinence

As for erectile function, direct comparisons for urinary continence between different prostatectomy series are difficult due to variations in definitions, data collection methods, and length of follow-up. Despite these difficulties, current literature suggests both a quicker return to urinary continence as well as slightly improved overall continence rate with RALP when compared with both open RP and LRP.

In our earlier series of 500 patients, we reported continence rates of 89, 95, and 97% at 3, 6, and 12 months postoperatively.[37] Continence was defined as the use of no absorbent pads. Twenty-seven percent of these patients were continent immediately after catheter removal. The improved

visualization of robotics aids in preserving the urethral sphincter and functional urethral length during the apical dissection of RALP. We feel that these factors along with the addition of some key technical refinements (described subsequently) are of utmost importance to the early return of urinary continence for patients postoperatively.

Menon and colleagues evaluated the continence rates in 1,100 patients who had a minimum of 1 year of follow-up after RALP.[39] Continence was defined as "no pads or a single pad for security purposes only and failure to leak urine on provocative maneuvers." They reported a 93% continence rate at 12 months following lateral prostatic fascia-sparing RALP and 23.7% of these men reported having complete urinary control immediately at the time of catheter removal (0 pads). The median time to complete urinary control was 3 weeks (range, 0–120 weeks). When stratifying patients according to the year of surgery, they found that those patients operated on in 2001 and 2002 had a longer median time to continence (on average, 5 weeks), whereas no difference was demonstrated in those operated on in 2003–2005 (on average, <3 weeks). The authors concluded that the impact of experience and learning curve resulted in reproducibility of return to continence.

Tewari and coworkers recently reported continence rates for 182 patients treated with RALP and their technique of total reconstruction of the vesico-urethral junction.[38] Continence was defined as no pad usage or one small liner used for security purposes only. Postoperative continence rates of 38, 83, 91, and 97% were found at 1, 6, 12, and 24 weeks, respectively.

The continence rates in various RALP series are shown in Table 1.2.

Technical Refinements to Improve Early Postoperative Functional Outcomes

Our experience with RALP is now over 2,300 cases. Throughout this experience, we have continuously modified our technique in a quest to improve surgical outcomes. Here, we describe two of the refinements in our surgical technique, which we feel have had the greatest impact on the early functional outcomes following RALP.

Athermal Early Retrograde Release of the Neurovascular Bundle

Our approach to RALP is the traditional antegrade transperitoneal technique.[26] One significant refinement in our approach, however, has been to release the neurovascular bundles in a retrograde direction prior to control and division of the prostatic pedicles. This technique is a hybrid of both the traditional open and laparoscopic approaches to nerve sparing. After dividing the bladder neck and completing the

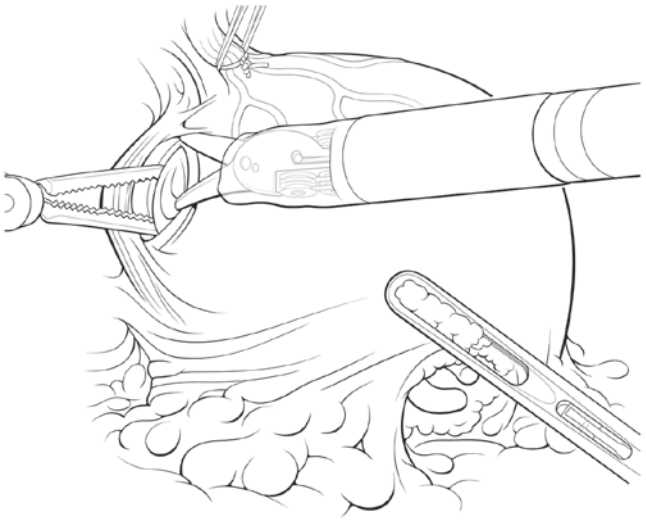

Fig. 1.2 Early retrograde release of the neurovascular bundle. The interfascial plane is developed between the neurovascular bundle laterally and the prostatic fascia medially. The bundle is stabilized with the PK dissector in the left hand, while the prostate is swept medially off the bundle with the monopolar scissors. Reprinted from Coughlin et al[41] with permission from Springer

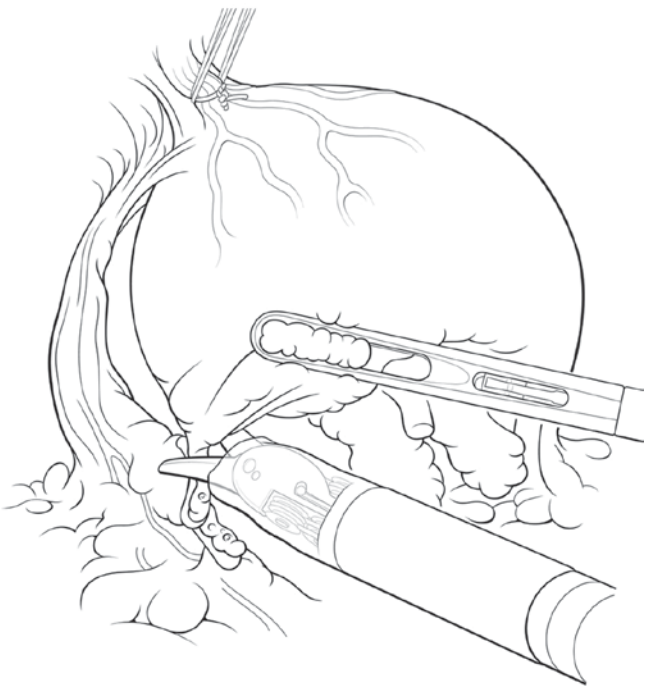

Fig. 1.3 Early retrograde release of the neurovascular bundle. The vascular pedicle is ligated with a hemolock clip. The clip is placed above the path of the neurovascular bundle. Releasing the bundle early and delineating its path avoids inadvertent damage to it at this point. Reprinted from Coughlin et al[41] with permission from Springer

posterior dissection, we incise the levator fascia along the length of the prostate. Using gentle blunt dissection, we develop the interfascial plane for nerve sparing and release the neurovascular bundle from the posterolateral surface of the prostate (Fig. 1.2). This approach allows us to clearly delineate the path of the neurovascular bundle prior to the placement of hemolock clips on the prostatic pedicles (Fig. 1.3). We are therefore able to avoid inadvertent injury to the cavernous nerves at this point of the dissection.

Modified Posterior Reconstruction of the Rhabdosphincter

Temporary urinary incontinence after radical prostatectomy for prostate cancer remains a disadvantage of surgical treatment. Though long-term continence rates after radical prostatectomy are excellent, the time it takes to regain continence has a significant impact on the patient's quality of life in the initial postoperative period. Several technical modifications have been proposed to promote an earlier return of continence, including bladder-neck sparing, preservation of the puboprostatic ligaments, intussusception of the reconstructed bladder neck, and posterior reconstruction of the rhabdosphincter.[38]

Posterior reconstruction of the rhabdosphincter was initially described in 2001, by Rocco and colleagues, and consisted of a two-layered reconstruction with apposition of the free edge of Denovilliers' fascia and the posterior bladder with the posterior aspect of the rhabdosphincter and posterior median raphe.[42] The technique provides posterior support for the sphincteric mechanism and also draws the bladder caudally into a supported position, taking all tension of the vesicourethral anastomosis. The same authors reported significantly quicker times to recovery of urinary continence following open radical prostatectomy using this technique.[43]

The benefits of robotic technology are ideally suited for such precise suturing in the confines of the male pelvis. We adopted and modified this technique for use in RALP. The principles are consistent with the two-layer reconstruction originally described by Rocco with some minor technical modifications. The reconstruction is performed utilizing a continuous suture of two 3–0 monocryl sutures (RB1 needles) of different colors that are tied together with each individual length being 12 cm. The free edge of the remaining Denovilliers' fascia is identified following prostatectomy. This edge is approximated to the posterior aspect of the rhabdosphincter with a running suture using one arm of the continuous monocryl suture. Typically, four bites of Denovilliers' fascia and the rhabdosphincter/posterior median raphe are taken and the edges are approximated. The second layer of the reconstruction is then commenced with the other arm of the monocryl suture. This layer approximates the posterior bladder (2 cm posterosuperior to the bladder neck) to the initial reconstructed layer of posterior rhabdosphincter and Denovilliers' fascia. A continuous modified Van Velthoven vesicourethral anastomosis[44] is then performed with a running suture.

Our initial pilot study using this technique revealed a complete "early continence" rate (no pads) of 58% at 1 week postoperatively. If the definition of continent is broadened to also include mild urinary incontinence (0 or 1 pad per day), the rate was 72%.[45] Other authors have also demonstrated improvements in early postoperative continence rates following LRP and RALP utilizing a similar reconstruction.[46,47]

Conclusion

Since the first RALP was performed in 2000, the operation has undergone significant standardization and modification. The use of this operation has increased exponentially in the United States and a similar pattern is likely to be seen in other continents. Today, RALP offers men a minimally invasive approach to radical prostatectomy with good oncological and functional outcomes. Owing to refinements in technique, the majority of patients will experience a quick return to normal daily activities with minimal impact on their health-related quality of life.

References

1. Capek K. *Rossum's universal srobots* [Playfair N, Selver P, trans. Landes WA, ed]. New York: Doubleday; 1923
2. Kwoh YS, Hou J, Jonckheere EA, Hayati S. A robot with improved absolute positioning accuracy for CT guided stereotactic brain surgery. *IEEE Trans Biomed Eng*. 1988;35:153–160
3. Davies B. A review of robotics in surgery. *Proc Inst Mech Eng*. 2000;214:129–140
4. Davies BL, Hibberd RD, Coptcoat MJ, Wickman JEA. A surgeon robot prostatectomy – a laboratory evaluation. *J Med Eng Technol*. 1989;13:273–277
5. Bann S, Khan M, Hernandez J, et al Robotics in surgery. *J Am Coll Surg*. 2003;196:784–795
6. Bauer A, Borner M, Lahmer A. Clinical experience with a medical robotic system for total hip replacement. In: Nolte LP, Ganz R, eds. *Computer Assisted Orthopedic Surgery*. Bern, Switzerland: Hogrefe & Huber; 1999:128–133
7. Satava RM. Robotic surgery: from past to future – a personal journey. *Surg Clin North Am*. 2003;83:1–6
8. Surveillance, Epidemiology, and End Results (SEER) Program (www.seer.cancer.gov). *SEER*Stat Database: incidence – SEER 9 Regs Public-Use, Nov 2004 Sub (1973–2002)*. National Cancer Institute, DCCPS, Surveillance Research Program, Cancer Statistics Branch, released April 2005, based on the November 2004 submission
9. Meng MV, Elkin EP, et al Predictors of treatment after initial surveillance in men with prostate cancer: results from CaPSURE. *J Urol*. 2003;170(6 Pt 1):2279–2283

10. Myers RP. Radical prostatectomy: making it a better operation in the new millennium. *Int J Urol*. 2001;8(7):S9–S14
11. Young HH. The early diagnosis and radical cure of carcinoma of the prostate. Being a study of 40 cases and presentation of a radical operation which was carried out in four cases. 1905 *J Urol*. 2002; 168(3):914–921
12. Reiner WB, Walsh PC. An anatomical approach to the surgical management of the dorsal vein and Santorini's plexus during radical retropubic surgery. *J Urol*. 1979;121:198–200
13. Walsh PC, Donker PJ. Impotence following radical prostatectomy: insight into etiology and prevention. *J Urol*. 1982;128:492–497
14. Oelrich TM. The urethral sphincter muscle in the male. *Am J Anat*. 1980;158:229–296
15. Schuessler WW, Schulam PG, Clayman RV, Kavoussi LR. Laparoscopic radical prostatectomy: Initial short-term experience. *Urology*. 1997;50:854–857
16. Guillonneau B, Vallancien G. Laparoscopic radical prostatectomy: the Montsouris experience. *J Urol*. 2000;163:418–422
17. Rassweiler J, Sentker L, Seemann O, et al Laparoscopic radical prostatectomy with the Heilbronn technique: an analysis of the first 180 cases. *J Urol*. 2001;166:2101–2108
18. Eden CG, Cahill D, Vass JA, et al Laparoscopic radical prostatectomy: the initial UK series. *BJU Int*. 2002;90:876–882
19. Menon M, Tewari A, Baize B, et al Prospective comparison of radical retropubic prostatectomy and robot-assisted anatomic prostatectomy: the Vattikuti Urology Institute experience. *Urology*. 2002; 60:864–868
20. Binder J, Kramer W. Robotically-assisted laparoscopic radical prostatectomy. *BJU Int*. 2001;87(4):408–410
21. Pasticier G, Rietbergen JBW, Guillonneau B, Fromont G, Menon M, Vallancien G. Robotically assisted laparoscopic radical prostatectomy: feasibility study in men. *Eur Urol*. 2001;40:70–74
22. Menon M, Shrivastava A, Tewari A, et al Laparoscopic and robot assisted radical prostatectomy: establishment of a structured program and preliminary analysis of outcomes. *J Urol*. 2002;168(3): 945–949
23. Ahlering TE, Skarecky D, Lee D, et al Successful transfer of open surgical skills to a laparoscopic environment using a robotic interface: Initial experience with laparoscopic radical prostatectomy. *J Urol*. 2003;170:1738–1741
24. Bhandari A, Peabody JO, et al Does surgical robot assist in safe learning of laparoscopic radical prostatectomy? AUA Abstract [presented 05/10/04]
25. Hugh JL, Thaly R, Shah K, Patel V. The advanced learning curve in robotic prostatectomy: a multi-institutional survey. AUA abstract [presented 05/20/07]
26. Berryhill R Jr, Jhaveri J, Yadav R, et al Robotic prostatectomy: a review of outcomes compared with laparoscopic and open approaches. *Urology*. 2008;72(1):15–23
27. Patel VR, Palmer KJ, Coughlin G, Samavedi S. Robotic-assisted laparoscopic radical prostatectomy: perioperative outcomes of 1500 cases. *J Endourol*. 2008;22(10):1–7
28. Ahlering TE, Skarecky D, Lee D, et al Successful transfer of open surgical skills to a laparoscopic environment using a robotic interface: initial experience with laparoscopic radical prostatectomy. *J Urol*. 2003;170:1738–1741
29. Bentas W, Wolfram M, Jones J, et al Robotic technology and the translation of open radical prostatectomy to laparoscopy: the early Frankfurt experience with robotic radical prostatectomy and one year follow-up. *Eur Urol*. 2003;44:175–181
30. Tewari A, Srivasatava A, Menon M, et al A prospective comparison of radical retropubic and robot-assisted prostatectomy: experience in one institution. *BJU Int*. 2003;92:205–210
31. Wolfram M, Brautigam R, Engl T, et al Robotic-assisted laparoscopic radical prostatectomy: the Frankfurt technique. *World J Urol*. 2003;21:128–132
32. Ahlering TE, Woo D, Eichel L, Lee DI, Edwards R, Skarecky DW. Robot-assisted versus open radical prostatectomy: a comparison of one surgeon's outcomes. *Urology*. 2004;63:819–822
33. Ahlering TE, Eichel L, Skarecky D. Rapid communication: early potency outcomes with cautery-free neurovascular bundle preservation with robotic laparoscopic radical prostatectomy. *J Endourol*. 2005;19:715–718
34. Chien GW, Mikhail AA, Orvieto MA, et al Modified clipless antegrade nerve preservation in robotic-assisted laparoscopic radical prostatectomy with validated sexual function evaluation. *Urology*. 2005;66:419–423
35. Joseph JV, Vicente I, Madeb R, et al Robot-assisted vs pure laparoscopic radical prostatectomy: are there any differences? *BJU Int*. 2005;96:39–42
36. Menon M, Kaul S, Bhandari A, et al Potency following robotic radical prostatectomy: a questionnaire based analysis of outcomes after conventional nerve sparing and prostatic fascia sparing techniques. *J Urol*. 2005;174:2291–2296
37. Patel VR, Thaly R, Shah K. Robotic radical prostatectomy: outcomes of 500 cases. *BJU Int*. 2007;9(9):1109–1112
38. Tewari A, Jhaveri J, Rao S, et al Total reconstruction of vesicourethral junction. *BJU Int*. 2008;101:871–877
39. Badani KK, Kaul S, Menon M. Evolution of robotic radical prostatectomy assessment after 2766 procedures. *Cancer*. 2007;110(9): 1951–1958
40. Shah K, Palmer KJ, Coughlin G, Patel VR. Early retrograde release of the neurovascular bundle during robotic-assisted laparoscopic radical prostatectomy. *J Endourol*. 2007;21(suppl 1):27
41. Coughlin G, Dangle P, Palmer K, et al Athermal early retrograde release of the neurovascular bundle during nerve sparing robotic assisted laparoscopic radical prostatectomy. *J Robotic Surg*. 2009 Mar;3(1)
42. Rocco F, Gadda F, Acquati P, et al Personal research: reconstruction of the urethral striated sphincter. *Arch Ital Urol Androl*. 2001;73: 127–37
43. Rocco F, Carmignani L, Acquati P, et al Early continence recovery after open radical prostatectomy with restoration of the posterior aspect of the rhabdosphincter. *Eur Urol*. 2007;52:376–83
44. Van Velthoven RF, Ahlering TE, Peltier A, Skarecky DW, Clayman RV. Technique for laparoscopic running urethrovesical anastomosis: the single knot method. *Urology*. 2003;61(4):699–702
45. Coughlin G, Dangle P, Patil N, et al Modified posterior reconstruction of the rhabdosphincter: application to robotic assisted laparoscopic prostatectomy. *BJU Int* 2008 Nov;102(10):1482–5
46. Rocco B, Gregori A, Stener S, et al Posterior reconstruction of the rhabdosphincter allows a rapid recovery of continence after transperitoneal videolaparoscopic radical prostatectomy. *Eur Urol*. 2007;51:996–1003
47. Nguyen MM, Kamoi K, Stein RJ, et al Early continence outcomes of posterior musculofascial plate reconstruction during robotic and laparoscopic prostatectomy. *BJU Int*. 2008;101:1135–1139

Robotic-Assisted Radical Cystectomy

2

Prokar Dasgupta, Oussama Elhage, Peter Rimington, and Mohammad Shamim Khan

Introduction

Radical cystectomy/anterior exenteration is currently regarded as the gold standard for managing invasive bladder cancer, extensive uncontrollable superficial cancer, and refractory carcinoma in situ (CIS). At specialized centers, the 5-year recurrence-free survival for muscle invasive disease is 56–73%.[1] Optimum standards for this procedure include 10% positive surgical margins overall and 15% in patients with T3 and T4 tumors. The median number of lymph nodes retrieved should be 10–14.[2] Although open radical cystectomy (ORC) has become safer in expert hands, it remains a formidable procedure with a complication rate of around 30–50%. Excessive bowel handling, fluid loss, and opiates can lead to prolonged ileus. In spite of improvements in surgical techniques, blood loss during ORC is often significant. The hospital stay is consequently quite prolonged with 18–21 days, quoted as the UK average.[3]

Urologists experienced in advanced laparoscopy have reported promising results of laparoscopic radical cystectomy (LRC) in the hope of reducing patient morbidity. Within our own group, LRC is performed by a team consisting of two experienced urologists to reduce surgical fatigue.[4] The procedure is sometimes difficult owing to reduced maneuverability of laparoscopic instruments, and the complication rate can be high even in expert hands. The overall complications during hospital stay and after discharge have been reported as 46 and 19%, respectively.[5] Another large LRC series of 84 patients showed that the complication rate can be reduced to 18%, which is better than reported in most series of ORC.[6] The da Vinci™ system (Intuitive Surgical, CA) has the potential to overcome some of the technical difficulties of LRC. We published the first experience of UK with this system[7] and now review the oncological and functional outcomes of robotic-assisted radical cystectomy (RARC).

Surgical Technique

Our technique is derived from ORC and LRC and has evolved over 5 years.[8] Patients are given clear fluids orally, an enema the day before their operation, and overnight intravenous normal saline to prevent dehydration. This is part of an enhanced recovery program derived from colorectal surgery, where formal bowel preparation is deliberately avoided. Intravenous cefuroxime and metronidazole and subcutaneous low molecular weight heparin are administered perioperatively. Patients above 60 years of age are digitalized as recommended by urologists experienced in open cystectomy, to prevent atrial fibrillation.[9] They are placed in the extended lithotomy position with a 45° Trendelenberg tilt (Fig. 2.1). A disposable sigmoidoscope is introduced per rectum in male and a methylene blue soaked swab per vaginum in female patients. After sterile catheterization, a six port transperitoneal approach is used as previously described

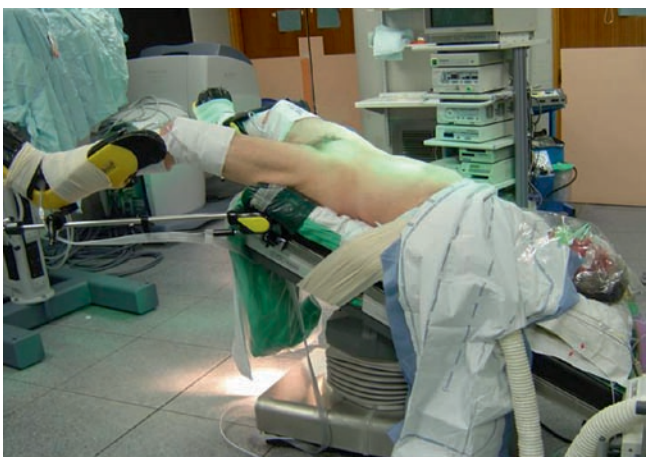

Fig. 2.1 Position of patient during robotic cystectomy. Reprinted from Murphy et al[19], Copyright 2008, with permission from Elsevier

P. Dasgupta et al. (eds.), *New Technologies in Urology,*
DOI: 10.1007/978-1-84882-178-1_2, © Springer-Verlag London Limited 2010

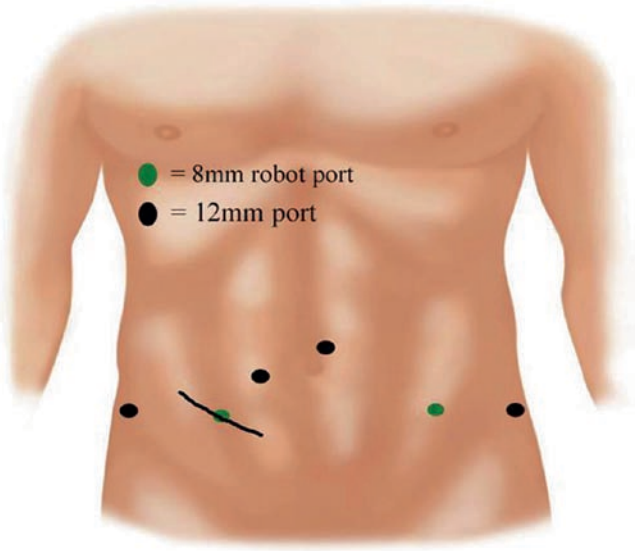

Fig. 2.2 Schematic diagram of port positioning. Reprinted from Murphy et al[19], Copyright 2008, with permission from Elsevier

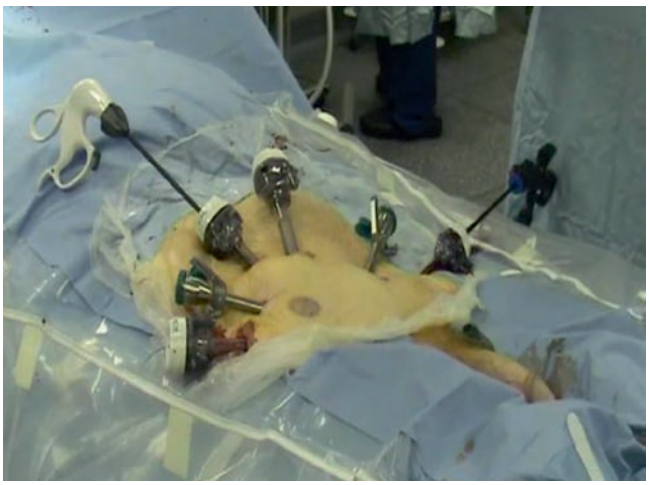

Fig. 2.3 Port positioning

(Fig. 2.2).[10] The ports are usually placed in a fan-shaped or W configuration (Fig. 2.3). The procedure involves three surgeons – one at the console and one on each side of the patient. With the da Vinci S HD, a fourth robotic arm is used in place of the left side assistant.

Posterior Dissection

The ureters are mobilized in the pelvis while keeping adequate tissue around them so as not to compromise their vascularity. The distal ends are clipped and cut and sent for frozen section analysis. An inverted U-shaped incision is made in the peritoneum of the cul-de-sac (Pouch of Douglas) (Fig. 2.4). The posterior layer of Denonvillier's fascia is then incised in the midline and the plane between the rectum and the prostate developed. In patients wishing to preserve potency, diathermy is avoided at the tips of the seminal vesicles to avoid injury to the pelvic plexus. In females, the ovarian vessels are controlled with Hem-o-lok clips (Weck Closure Systems, NC) and divided. The plane between the rectum and uterus is developed and the uterine arteries are controlled with Hem-o-loks.

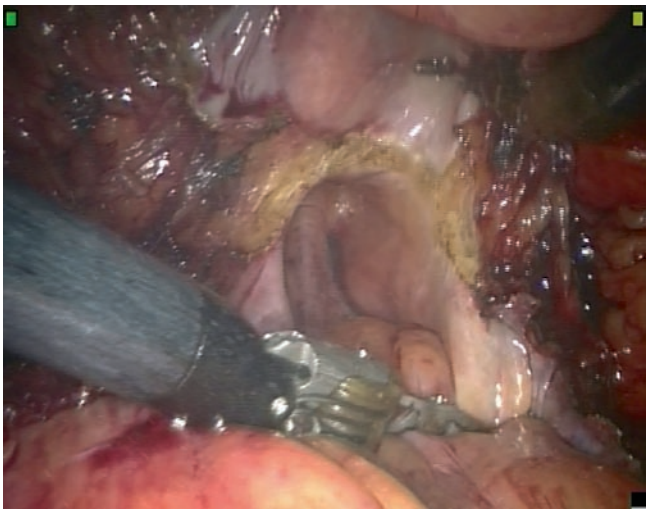

Fig. 2.4 Posterior dissection

Lateral Dissection

Dissection is continued medial to the external iliac veins to carefully preserve the obturator nerves and expose the lateral pelvic wall. This delineates the lateral pedicles to the bladder (and uterus in females). We initially used Hem-o-lok clips for control of the lateral pedicles but subsequently switched to an Endopath™ATW45 linear stapler (Ethicon Endosurgery, Livingston, UK). This was prompted by our perception that blood loss was somewhat higher with clips. Currently, an ACE Harmonic™ scalpel (Ethicon Endosurgery, Livingston, UK) seems to be the most efficient (Fig. 2.5a–c) for this purpose. It is also more cost effective, ~£300 for harmonic as opposed to £1,200 for staplers, since multiple firings of cartridges are required.

Anterior Dissection

The bladder is filled with 200 mL of formol–saline for easy identification and dropped by an inverted U incision to

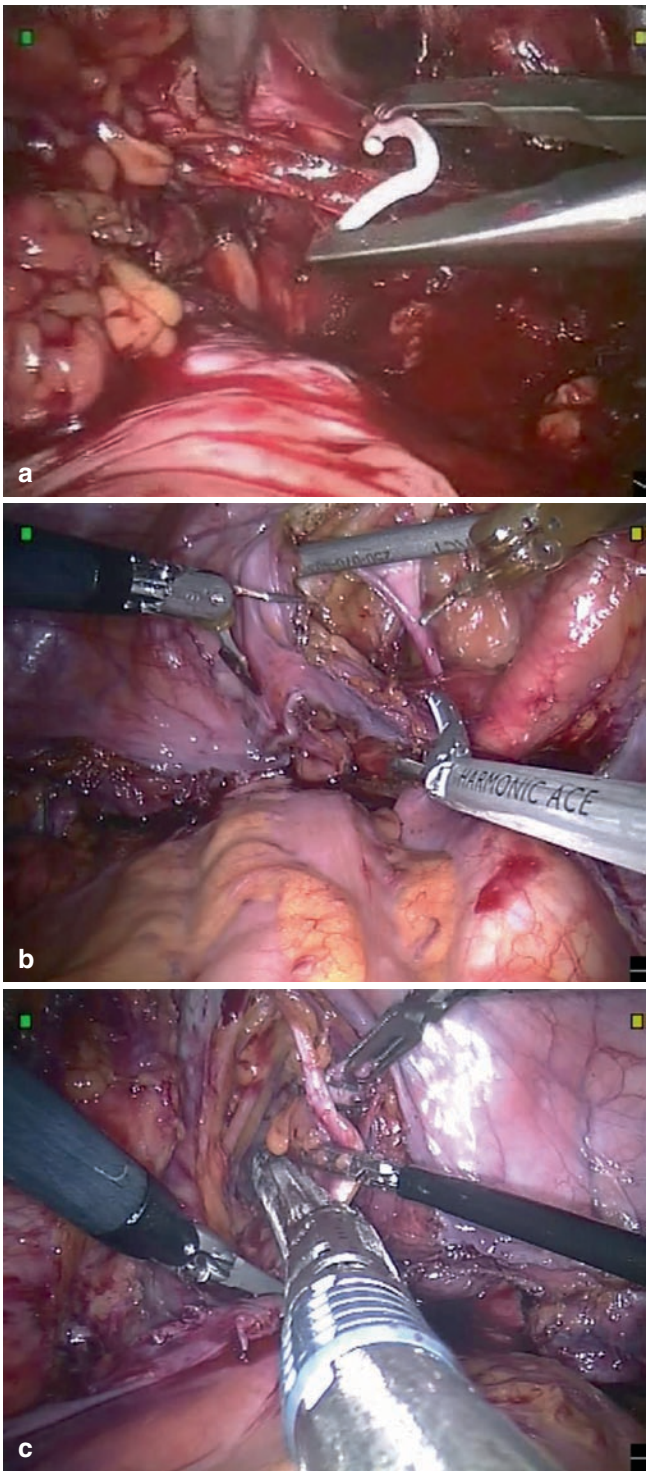

Fig. 2.5 (**a**) Control of lateral pedicles of the bladder with clips. (**b**) Control of lateral pedicles of the bladder with harmonic scalpel. Reprinted from Murphy et al[19], Copyright 2008, with permission from Elsevier. (**c**) Control of lateral pedicles of the bladder with staples

include the urachus. The endopelvic fascia is opened and the dorsal vein is controlled by a stitch. Nerve sparing is performed in potent patients. The dorsal vein complex and urethra are cut and a clip placed on the specimen side of the urethra to prevent any spillage. The distal urethral margin is sent for frozen section. In females, the urethra is dissected fully to the external meatus. The posterior vaginal fornix is opened. The previously placed methylene blue swab becomes visible indicating that the correct plane had been entered. The lateral vaginal walls are transected. The cystectomy specimens are placed in a 15 mm EndoCatch II™ bag (Tyco Healthcare, Hampshire, UK) for later retrieval. Leakage of carbon dioxide from the vagina is reduced by a water proof dressing applied externally. The vagina is then closed longitudinally by continuous intracorporeal suturing.

Lymphadenectomy, Transposition of Left Ureter

Using robotic bipolar forceps and scissors, careful bilateral lymphadenectomy is performed. The limits of the dissection are the genitofemoral nerve laterally, the bifurcation of the common iliac artery proximally and the node of Cloquet distally. Care is taken to preserve the obturator nerve. The da Vinci S-HD gives better quadrantic access and it is possible to extend the lymph node dissection to the aortic bifurcation with this new system. The lymph nodal packs are placed in separately marked laparoscopic sacks. An Endoloop™ (Ethicon Endo-surgery, Livingston, UK) is applied on the distal end of the left ureter, which is then transposed under the sigmoid mesocolon to the left by pulling the Endoloop through. The distal ends of the ureters are held together with a laparoscopic grasper introduced through the left-sided 5 mm assistant port.

Urinary Diversion

It is easier and quicker to perform urinary diversions extracorporeally although complete robotic-assisted intracorporeal diversion has been reported. For ileal conduits, a 15 cm segment of ileum about 15 cm proximal to the ileo-caecal junction is held in laparoscopic graspers introduced through the most lateral right-sided 10 mm port. The robot is undocked. The previously bagged bladder and lymph nodal specimens are extracted through a 5–7 cm incision (Fig. 2.6). In thin patients, an appendix muscle-splitting incision is made by extending a lateral port while in overweight patients (BMI > 30 kg/m^2) a subumbilical midline incision is preferred for easier left ureteric access. The graspers holding the ureters and ileal segment are brought to the surface through this incision. The ileal loop is isolated on its mesentery, bowel continuity is restored with staplers, and the mesenteric window is

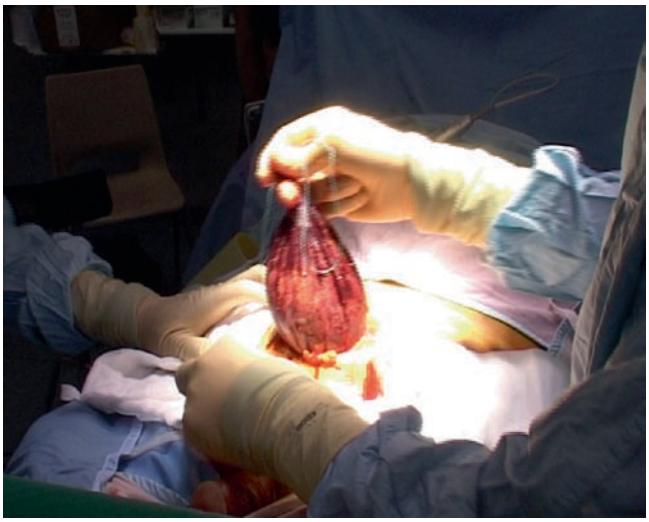

Fig. 2.6 Specimen extraction in laparoscopic sack

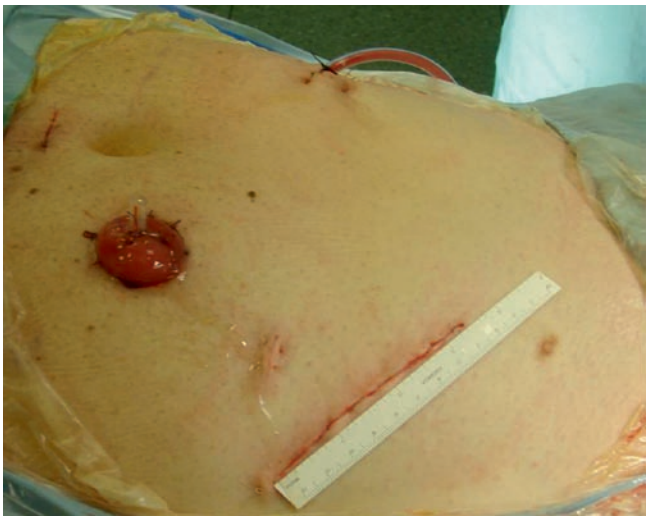

Fig. 2.8 Postoperative wounds. Reprinted from Murphy et al[19], Copyright 2008, with permission from Elsevier

closed. Uretero-ileal anastomosis is performed over 8F feeding tubes by a Wallace I technique. The distal end of the conduit is fashioned as a stoma at a previously marked site on the abdominal wall. A sump drain is introduced into the conduit to prevent any anastomotic pressure and leak from subsequent stomal edema. Studer pouches are created through lower midline incisions and anastomosed to the urethral stump by six robotically placed 3–0 monocryl sutures (Fig. 2.7). Alternatively, a continuous 3–0 monocryl anastomosis can be performed as in radical prostatectomy, after re-docking the robot. A 20 F drain is placed in the pelvis. The port sites and wounds are closed with absorbable sutures (Fig. 2.8). A liter of icodextrin (Adept, ML Pharmaceuticals, Warrington, UK) is instilled into the abdomen and drained after an hour to reduce the risk of bowel adhesions.

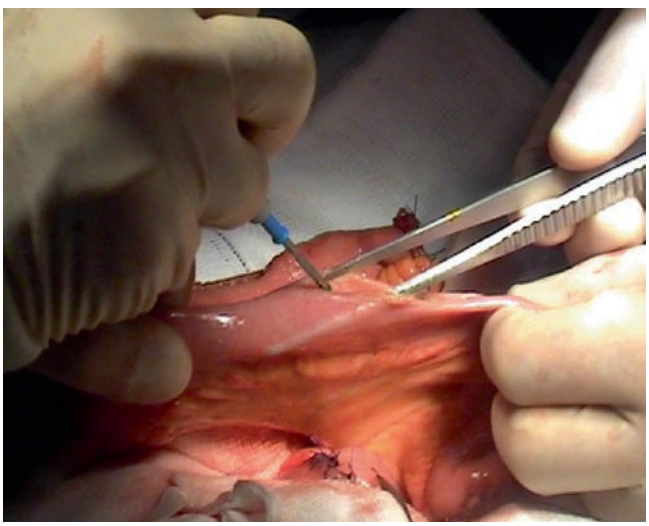

Fig. 2.7 Studer pouch formation through a small incision

Postoperative Care

All patients are electively managed in an overnight recovery or high dependency unit immediately after the operation. The naso-gastric tube is removed and oral liquids are administered based on the tolerence of the patient. Early mobilization and chest physiotherapy are encouraged. Most patients are discharged with their pelvic drains and ureteric catheters in situ, which are removed at 3 weeks. Patients are seen again at 6 weeks, have an abdominal ultrasound at 3 months, and CT scans at 6 months and then at 6 monthly intervals. At these visits, they also undergo clinical examination and assessment of serum hemoglobin, electrolytes, creatinine, chloride, and bicarbonate.

Outcomes of RARC

RARC and urinary diversion was initially reported in 2003.[11] Similar to LRC, it involved a six-port trans-peritoneal approach. The procedure was performed in three stages: initially pelvic lymphadenectomy and cystoprostatectomy, second extracorporeal formation of a neobladder, and third intra-corporeal urethro-neovesical anastomosis following re-docking of the robot. The operative times ranged from 260 to 308 min depending on whether an ileal conduit or orthotopic neobladder was formed. Blood loss was <150 mL and surgical margins were clear in all cases. One patient had N1 disease. Long-term oncological or functional results were not reported, although a port site metastasis was subsequently mentioned.[12] Around the same time, Beeken et al described robotic cystectomy and intra-corporeal Hautmann orthotopic

neobladder with an operating time of 8.5 h and a blood loss of 200 mL,[13] while Balaji et al successfully performed robotic-assisted totally intracorporeal laparoscopic ileal conduit urinary diversion in three patients with operative time of 630–830 min and hospital stay of 5–10 days.[14] The longest operative time was in one patient who underwent concomitant RARC. Menon's group has subsequently refined the robotic technique for women with preservation of the uterus and vagina.[15] Other authors have excluded patients with prior extensive abdominal surgery, pelvic irradiation, who have undergone neoadjuvant chemotherapy, and extravesical mass on CT from RARC,[16] making a selection bias quite likely. Guru et al reported their early results on 20 RARC with an average age of 70 and a BMI of 26 kg/m^2. The mean operative duration was 442 min, blood loss 555 mL, and hospital stay of 10 days. The procedure was unsuccessful in a patient with fixed pelvic mass and another needed conversion to open surgery as the patient could not tolerate the Trendelenburg position. There were three bowel obstructions, one of whom died of sepsis and one readmission with pyelonephritis. Thus, the overall complication rate was 20%. One patient had positive vaginal margins and 9 of 26 lymph nodes were positive.[17] The same group found that overweight and obese patients had similar operative times, estimated blood loss, and complications compared with patients with normal BMI. Overweight and obese patients with bulky disease (pT3–4) had significantly higher rates of positive surgical margins.[18]

In over 50 patients at Guy's, the operative time was between 5.5 and 8 h depending on whether an ileal conduit or Studer pouch was created. One patient needed blood transfusion owing to bleeding from an inferior epigastric artery and one patient with a large urethral adenocarcinoma needed a colostomy for rectal injury. Delayed functional complications occurred in three patients. One patient with a Studer pouch developed a neovesico-urethral stricture, which needed urethral dilatation. Another developed a left upper ureteric stricture at 6 months. This was assumed to be malignant and hence treated with nephroureterectomy. The final pathology was that of a benign inflammatory stricture. A third patient needed repair of an incisional hernia at 12 months. Serum creatinine levels were maintained in all patients. Three of four previously potent male patients who underwent nerve sparing were potent with Tadalafil. Our experience was published by Murphy et al in a recent Surgery in Motion DVD to aid urologists trying to learn this procedure. We described our technique in 23 patients, 19 of whom had ileal loop urinary diversion while 4 had Studer pouch reconstruction. Mean total operative time was 397 (295–600) min. Mean blood loss was 278 (100–1,150) mL. Surgical margins were clear in all patients with a median of 16 lymph nodes retrieved. The complication rate was 23%. At a mean follow-up of 17 (4–40) months, 1 patient has died of metastatic disease with 1 other alive with metastases.[19]

The operation has also been performed in patients without cancer. Two men, 41 and 38 years old, with complete posttraumatic C7–C8 quadriplegia underwent total intracorporeal cystoprostatectomy and ileal-conduit urinary diversion with robotic assistance. The procedures were completed without open conversion. The total surgical time was 9.25 and 6.75 h, respectively. There were no intraoperative complications. In the postoperative period, both patients had complications (pulmonary and urinary infections) that were treated medically. The postoperative hospital stay was 13 days.[20]

The International Robotic-Assisted Cystectomy Consortium (IRCC) reported on data on 369 patients from 11 centers at the American Urological Association, 2008. The mean operative time was 397 min, estimated blood loss 390 mL, transfusion rate 10.5%, hospital stay 9 days, and positive margins 8%.

Comparison of ORC and RARC

Rhee et al compared 23 ORC to seven RARC and found that although blood loss was lower for RARC, four of seven patients (57%) needed transfusion. The operative duration was 638 min for RARC vs. 507 min for ORC and hospital stay 11 and 13 days, respectively.[21] In another study of 37 patients, 24 (64.9%) had ORC and 13 (29.7%) were treated with RARC. RARC resulted in significantly lower blood loss, hospital stay, and longer operating time compared with ORC. Four (16.7%) perioperative complications occurred in the open group compared with 2 (15.4%) in the robotic group.[22] Pruthi and Wallen compared 20 men undergoing RARC and extracorporeal urinary diversion to 24 matched men who underwent ORC. Mean operative time for RARC was 6.1 h as opposed to 3.8 h for ORC. Mean blood loss was significantly less for RARC. On surgical pathology, 14 RARC cases were pT2 or less, four were pT3, and two were N +. There were no positive surgical margins. A mean of 19 lymph nodes was removed. Mean time to flatus and bowel movement was significantly shorter than in men undergoing ORC. There were six postoperative complications (30%) in five patients.[23] Likewise, Wang et al compared 20 ORC and 33 RARC patients and found similar complication rates (24% open, 21% robotic). The open cohort had more patients with extravesical disease (57 vs. 28%) and nodal metastasis (34 vs. 19%), although this may be a reflection of small sample size. There were three patients in the open group and two in the robotic with positive margins. The median number of lymph nodes removed was similar between the groups.[24]

Table 2.1 Comparison of ORC, LRC, RARC

Op	Op time (min)	Blood loss (mL)	Complication (%)	Hospital stay (days)	Recovery (weeks)	Oncologic follow-up
ORC	325	1,300	60	16	8	60% RFS@5year
LRC	345	350	50	16	3	60% RFS@4year
RARC	365	150	20	10.5	4	90% RFS@3year

RFS recurrence-free survival

Comparison of ORC, LRC, and RARC

Thirty age-matched patients (10 in each group) had ORC, LRC, or RARC and ileal conduit diversion by three surgeons. RARC and LRC took longer than ORC but were associated with less blood loss and quicker recovery (Table 2.1). Hospital stay was shortest for RARC, which also had the lowest complication rate.[25,26]

Oncological Outcomes

For RARC to stand the test of time, the oncological outcomes have to be equivalent to ORC and LRC. In their series of 1,054 patients undergoing ORC, Stein et al reported recurrence-free survival at 5 and 10 years of 68 and 66%, respectively.[27] The recurrence-free survival appears to be worse for patients with stage >pT2N0.[1] Based on their results in 10 LRC patients, five of whom died, Simonato et al reported poorer oncologic outcomes with LRC when compared with ORC.[28] In a recent study of 37 patients undergoing LRC, followed up for up to 5 years, Haber and Gill reported actuarial overall and recurrence-free survival of 63 and 92%, respectively. However, only eight patients had completed 5 years of follow-up, and oncological data were not available in seven patients. Assuming that all these seven patients had died from metastatic disease, the recalculated 5-year overall and cancer-specific survival were 58 and 68%, respectively. The outcomes were poorer in those with concomitant CIS, extra-organ disease, and nodal metastasis. Patients having extended laparoscopic lymph node dissection had slightly better cancer-specific survival when compared with those having a limited template lymphadenectomy, although not reaching statistical significance.[5] With the da Vinci S HD system, excellent lymph node yield can be achieved during RARC. In a cohort study, the mean number of lymph nodes retrieved was 18 (6–43) with an operative time of 44 min. Neither BMI nor previous major abdominal surgery affected the nodal yield. There was one vascular injury.[29] With strict adherence to oncological principles during RARC to prevent spillage of cancer cells, we reported 100% overall and recurrence-free survival at 2 years.[30] At a maximum follow-up of 3.5 years, the actuarial overall and recurrence-free survival were 95 and 90%, respectively. A median of 16 (6–28) lymph nodes were removed. In our patient group, 10% had lymph nodal disease, 10% incidental prostate cancer, and 10% prostatic urethral CIS. There were no positive margins, no local pelvic recurrences, and no port site metastasis. Lymph node metastastis, higher grade, and concomitant CIS were predictors of poor medium-term outcome.[26]

Bulky tumors removed with RARC may be associated with an increased rate of intraoperative transfusion, higher stage disease, and higher rate of margin positivity. In patients with large-volume tumors on preoperative assessment, wider dissection may decrease the margin-positive rates.[31]

Quality of Life and Patient Satisfaction

Using quality of life questionnaires, Guru et al found that time to normal activity was 4 weeks, time to driving 6 weeks, and time to strenuous activity 10 weeks.[17] Using the SF-8 validated questionnaire, we found no change in physical quality of life scores at 6 weeks after RARC but significantly better mental scores (Fig. 2.9). Patient satisfaction was high (median 30 out of a maximum of 32 on a validated client satisfaction-8 survey; range 27–32). We found that 93% of patients read and understood the patient information leaflet provided and 60% elected to watch a robotic patient information video. This had been screened by the British Broadcasting Corporation (BBC) after appropriate patient consent.

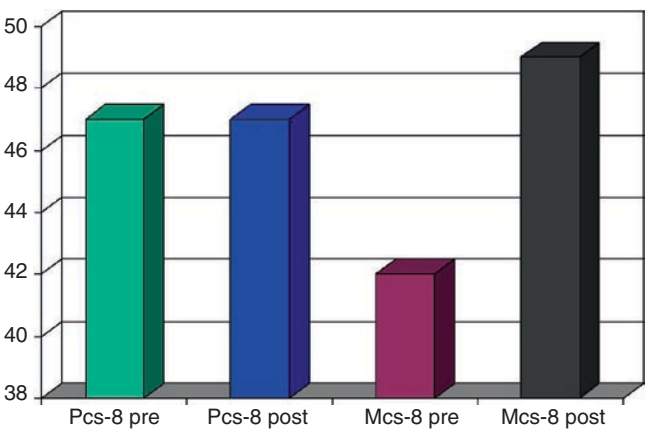

Fig. 2.9 Assessment of physical and mental quality of life after robotic cystectomy

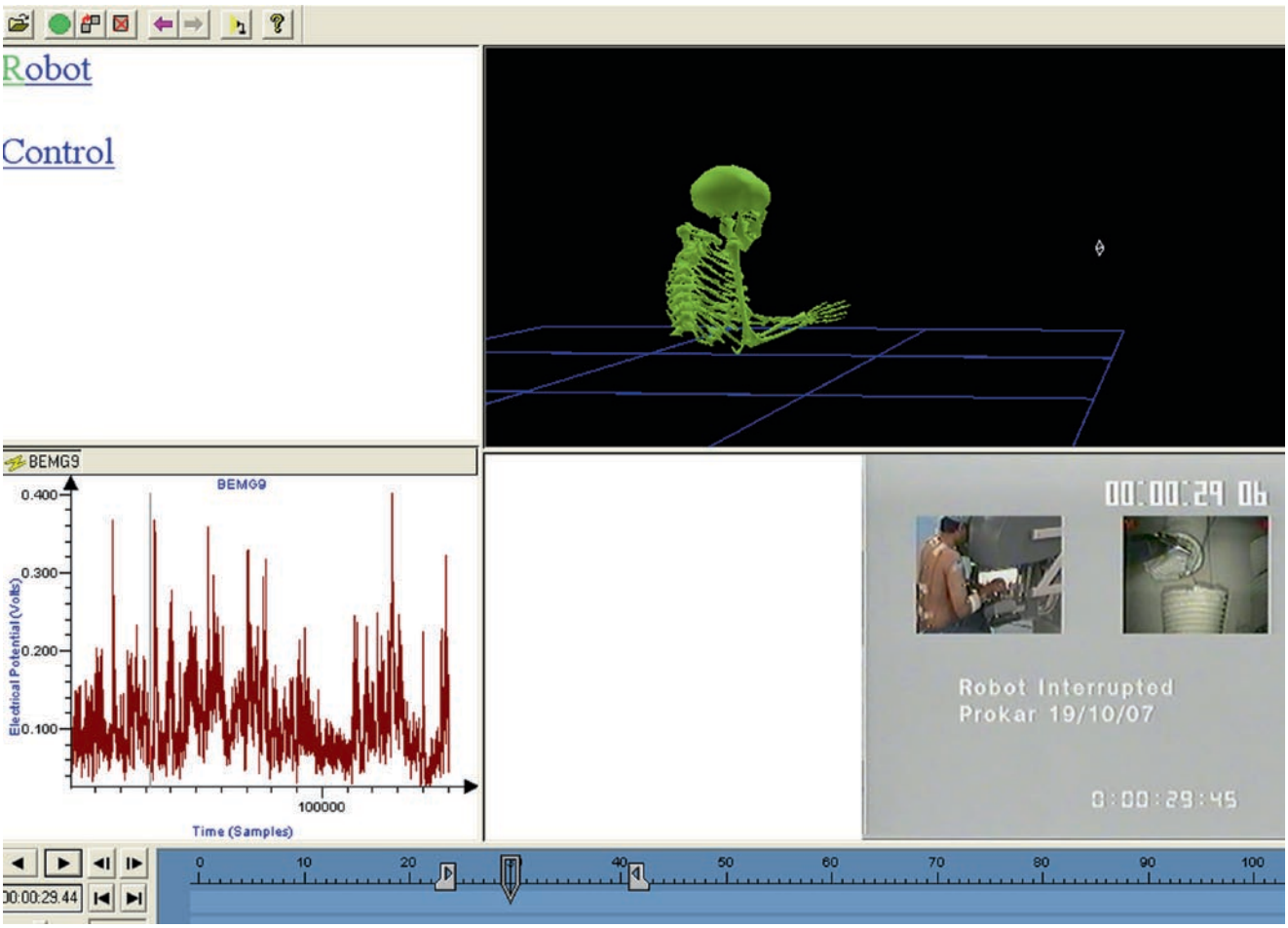

Fig. 2.10 Assessment of surgical fatigue by motion analysis in a gait laboratory (courtesy of Adam Shortland)

Ergonomics

One of the advantages of RARC over ORC and LRC may be reduced surgical fatigue during a long procedure.[32] This has been studied using motion analysis and EMG recordings in a gait lab (Fig. 2.10). These elegant experiments showed that while laparoscopy was associated with the most fatigue and progressive errors over time, robotics combined the best of laparoscopy and open surgery. With robotics, the patients enjoyed the generic benefits of minimal access, while the surgeon had the least fatigue and errors as in open surgery.

Conclusions

The medium term surgical, oncologic, and functional outcomes of RARC are encouraging. A randomized controlled trial of ORC, LRC, and RARC is planned and will include detailed health economic modeling.

Acknowledgments Guy's and St. Thomas' Charity, British Urological Foundation.

References

1. Madersbacher S, Hochreiter W, Burkhard F, et al Radical cystectomy for bladder cancer today–a homogeneous series without neoadjuvant therapy. *J Clin Oncol*. 2003;21:690–696
2. Herr H, Lee C, Chang S, Lerner S; for the bladder cancer collaborative group. Standardization of radical cystectomy and pelvic lymph node dissection for bladder cancer. A collaborative group report. *J Urol*. 2004;171:1823–1828
3. Nuttall MC, van der Meulen J, McIntosh G, Gillatt D, Emberton M. Changes in patient characteristics and outcomes for radical cystectomy in England. *BJU Int*. 2005;95:513–516
4. Rimington P, Dasgupta P. Laparoscopic and robotic radical cystectomy. *BJU Int*. 2004;93:460–461
5. Haber G-P, Gill IS. Laparoscopic radical cystectomy for cancer: oncological outcomes at up to 5 years. *BJU Int*. 2007;100:137–142
6. Cathelineau X, Arroyo C, Rozet F, Barret E, Vallancien G. Laparoscopic assisted radical cystectomy: the Montsouris experience after 84 cases. *Eur Urol*. 2005;47:780–784

7. Dasgupta P, Hemal A, Rose K; Guy's and St. Thomas' Robotics Group. Robotic urology in the UK: establishing a programme and emerging role. *BJU Int*. 2005;95:723–724
8. Raychaudhuri B, Khan MS, Challacombe B, Rimington P, Dasgupta P. Minimally invasive radical cystectomy. *BJU Int*. 2006;98:1064–1067
9. Stein JP, Skinner DG. Surgical atlas radical cystectomy. *BJU Int*. 2004;94:197–221
10. Hemal AK, Eun D, Tewari A, Menon M. Nuances in the optimum placement of ports in pelvic and upper urinary tract surgery using the da Vinci robot. *Urol Clin North Am*. 2004;31:683–92; viii
11. Menon M, Hemal A, Tewari A, et al Nerve-sparing robot-assisted radical cystoprostatectomy and urinary diversion. *BJU Int*. 2003;92: 232–236
12. El-Tabey NA, Shoma AM. Port site metastases after robot-assisted laparoscopic radical cystectomy. *Urology*. 2005;66:1110
13. Beecken WD, Wolfram M, Engl T, et al Robotic-assisted laparoscopic radical cystectomy and intra-abdominal formation of an orthotopic ileal neobladder. *Eur Urol*. 2003;44:337–339
14. Balaji KC, Yohannes P, McBride CL, Oleynikov D, Hemstreet GP III. Feasibility of robot-assisted totally intracorporeal laparoscopic ileal conduit urinary diversion: initial results of a single institutional pilot study. *Urology*. 2004;63:51–55
15. Menon M, Hemal AK, Tewari A, et al Robot-assisted radical cystectomy and urinary diversion in female patients: technique with preservation of the uterus and vagina. *J Am Coll Surg*. 2004; 198: 386–393
16. Miller NL, Theodorescu D. Status of robotic cystectomy in 2005 *World J Urol*. 2006;24:180–187
17. Guru KA, Kim HL, Piacente PM, Mohler JL. Robot-assisted radical cystectomy and pelvic lymph node dissection: initial experience at Roswell Park Cancer Institute. *Urology*. 2007;69:469–74
18. Butt ZM, Perlmutter AE, Piacente PM, et al Impact of body mass index on robot-assisted radical cystectomy. *JSLS*. 2008;12:241–5
19. Murphy DG, Challacombe BJ, Elhage O, et al Robotic-assisted laparoscopic radical cystectomy with extracorporeal urinary diversion: initial experience. *Eur Urol*. 2008;54:570–80
20. Hubert J, Chammas M, Larre S, et al Initial experience with successful totally robotic laparoscopic cystoprostatectomy and ileal conduit construction in tetraplegic patients: report of two cases. *J Endourol*. 2006;20:139–143
21. Rhee JJ, Lebeau S, Smolkin M, Theodorescu D. Radical cystectomy with ileal conduit diversion: early prospective evaluation of the impact of robotic assistance. *BJU Int*. 2006;96:1059–1063
22. Galich A, Sterrett S, Nazemi T, et al Comparative analysis of early perioperative outcomes following radical cystectomy by either the robotic or open method. *JSLS*. 2006;10:145–150
23. Pruthi RS, Wallen EM. Robotic assisted laparoscopic radical cystoprostatectomy: operative and pathological outcomes. *J Urol*. 2007; 178(3 Pt 1):814–818
24. Wang GJ, Barocas DA, Raman JD, et al Robotic vs open radical cystectomy: prospective comparison of perioperative outcomes and pathological measures of early oncological efficacy. *BJU Int*. 2008; 101:89–93
25. Elhage O, Keegan J, Varma P, et al A comparative analysis of open, laparoscopic and robotic radical cystectomy for bladder cancer. *J Endourol*. 2007;21(S1):142A
26. Dasgupta P, Rimington P, Murphy D, Elhage O, Challacombe B, Khan MS. Robotically assisted radical cystectomy. *BJU Int*. 2008; 101:1489–90
27. Stein JP, Lieskovsky G, Cote R, et al Radical cystectomy in the treatment of invasive bladder cancer: long-term results in 1054 patients. *J Clin Oncol*. 2001;19:666–675
28. Simonato A, Gregori A, Lissiani A, et al Laparoscopic radical cystoprostatectomy: our experience in a consecutive series of 10 patients with a 3 years follow-up. *Eur Urol*. 2005;47:785–790
29. Guru KA, Sternberg K, Wilding GE, et al The lymph node yield during robot-assisted radical cystectomy. *BJU Int*. 2008;102:231–234
30. Dasgupta P, Rimington P, Murphy D, et al Robot-assisted radical cystectomy for bladder cancer and 2 year follow-up. *BJUInt*. 2007; 99(S1):P62
31. Yuh B, Padalino J, Butt ZM, et al Impact of tumour volume on surgical and pathological outcomes after robot-assisted radical cystectomy. *BJU Int*. 2008;102:840–843
32. Elhage O, Murphy D, Challacombe B, Shortland A, Dasgupta P. Ergonomics in minimally invasive surgery. *Int J Clin Pract*. 2007; 61:186–188

Robotic Pyeloplasty

3

Michael Ferrandino, Arthur Caire, and David M. Albala

Introduction

Laparoscopic pyeloplasty was first reported in the literature by Schuessler and colleagues in 1993.[1] This procedure was developed in an attempt to duplicate the high success rates achieved with open pyeloplasty while offering the advantages of minimally invasive techniques. Their series consisted of 5 patients with symptomatic ureteropelvic junction (UPJ) obstruction. Symptoms were completely resolved in all patients and the advantages of minimally invasive surgery could be seen as their patients returned to normal activity within 1 week.

The advantages of minimal invasive surgery are shorter hospital stays, decreased perioperative pain, and faster recovery times. The morbidity associated with open pyeloplasty is due to the large incision necessary to expose the ureteropelvic junction. This results in pain and prolonged convalescence. In recent years, many groups have transitioned to laparoscopic pyeloplasty to eliminate this unnecessary morbidity. Unfortunately, the technical difficulty associated with laparoscopic suturing has limited this procedure to highly skilled laparoscopic surgeons.

Robotic pyeloplasty was developed in part to manage the anatomical challenges of operating in the tight confines of the retroperitoneum and allows for tremor filtering, movement scaling, improved ergonomics, better vision of the operative field, and increased range of motion.[2] Robotic pyeloplasty maintains the clinical advantages seen with laparoscopy including a shorter hospital stay, decreased perioperative pain, and decrease blood loss, and its surgeon friendly interface allows for more widespread usage.[3]

Patient Presentation, Diagnosis, Indications, and Treatment Options

The classic symptom of obstruction of the upper urinary tract is flank discomfort, which is exacerbated by the intake of fluids. In many patients, it is not uncommon for them to be asymptomatic. In the pediatric population, the typical presentation ranges from a palpable flank mass to an incidental finding. Adults classically present with intermittent vague flank pain that may be associated with nausea or vomiting. Other manifestations of UPJ obstruction include hematuria, hypertension, recurrent urinary tract infection (UTI), and occasionally, azotemia. UPJ obstruction is twice as common in males as in females, and the sex differential is most striking in infants, in whom this condition is five times more common in the male than in the female. The left kidney is involved twice as often as the right.

A variety of studies can be done to better identify the obstruction and the function of the kidney. Computerized tomography (CT) is initially used to evaluate flank pain and, in the setting of UPJ obstruction, will demonstrate hydronephrosis initiated at the level of the obstruction.

Once the diagnosis of UPJ obstruction is established, patients generally undergo intravenous urography (IVU), which demonstrates a dilated pelvicalyceal system and a stenosis at the UPJ. An anatomic narrowing does not always correlate with symptoms or a functional obstruction. Unless distal ureteral filling occurs, the length of the obstructive segment is difficult to determine. Although often obtained in the evaluation of symptoms and follow-up, IVU has given way to accurate functional studies such as the Lasix renal scan. A CT angiogram with three-dimensional reconstructions is occasionally performed prior to operative intervention to assess the presence of crossing vessels. Retrograde urography is generally performed intraoperatively to avoid infecting the operative field prior to intervention.

Surgical correction of the UPJ should be performed only after adequate imaging studies have documented UPJ obstruction and have eliminated the possibility of other ureteral abnormalities. Urine cultures must be sterile. Accepted indications for operative intervention include deteriorating renal function, obstructive symptoms, stone formation, and infection. After all the appropriate studies have been completed demonstrating obstruction, a variety of techniques may be used to repair the UPJ. Operative interventions include open, laparoscopic, and robotic pyeloplasty as well as endopyelotomy. The goal of surgical intervention is to reconstitute a

P. Dasgupta et al. (eds.), *New Technologies in Urology,*
DOI: 10.1007/978-1-84882-178-1_3, © Springer-Verlag London Limited 2010

nonobstructed pathway to restore renal function and alleviate symptoms. Open pyeloplasty has classically been the operation of choice, but the morbidity associated with this procedure has shifted the focus toward less invasive procedures.

Endopyelotomy is a contemporary procedure of pyeloplasty. This technique was brought to the United States in 1915; however, it was not until the 1940s when Davis popularized this approach and renamed it "intubated ureterotomy," the method gained popularity. Wickham named this procedure "pyelolysis." With this procedure, an indwelling stent was left for 4 weeks. It was not until 1986 when Arthur Smith popularized this procedure in the United States. He renamed it "endopyelotomy" as both the renal pelvis and ureter were incised under endoscopic control. Although endopyelotomy has many minimally invasive benefits in comparison with an open pyeloplasty, success rates vary from 76 to 90%.[4–6] The potential for a second procedure is considered, as open repair becomes more difficult in patients who have undergone endopyelotomy. In addition to having lower success rates than open pyeloplasty, endopyelotomy also has an increased risk of hemorrhage in patients with a crossing vessel.

The goal of the laparoscopic pyeloplasty was to combine the success rate of an open pyeloplasty, but in a less morbid fashion. Laparoscopic pyeloplasty has had similar success rates (97–98%) as open pyeloplasty; however, the popularity of this procedure never materialized due to multiple technical challenges.[7–10] The major challenge was that of laparoscopic suturing; this created longer operating room times and despite repeated efforts, an effective alternative to laparoscopic suturing was never developed.

Robotic pyeloplasty was first described by Sung and colleagues in 1995.[11] The minimally invasive advantages and success rates of laparoscopy are maintained while creating a surgeon friendly interface that allows for more widespread use of the procedure.[3] The aforementioned advantages of robotic pyeloplasty make it the procedure of choice in the future.

Preoperative Evaluation and Management

Preoperative evaluation for patients with supposed UPJ obstruction includes a standard history and physical exam, laboratory examination, and imaging studies – both functional and anatomic. Important preoperative findings include any history of previous abdominal surgery, bleeding disorders, recurrent urinary tract infections, adequate description of the flank pain, and physical identification of abdominal/flank scars and a palpable abdominal mass. It is beneficial to thoroughly document the patient's description of pain, including analog pain scores, particularly if this is the patient's chief or sole complaint.

Laboratory evaluation should be undertaken to assess overall renal function and the presence of urinary tract infection. Urinalysis and urine culture should be performed to identify any underlying infection due to stagnation of urine. If infection is documented, it should be treated prior to and at the time of surgical repair. Serum chemistry should be sent for creatinine to assess the patient's overall renal function.

A combination of diagnostic imaging studies are often employed to assess renal and ureteral anatomy, as well as, delineation of function and degree of obstruction. Standard techniques include ultrasonography, intravenous urography (IVU), retrograde/antegrade pyelogram, diuretic renography, and computed tomographic imaging (CT). The differing modalities have inherent benefits and limitations; therefore a combination of studies is employed prior to undergoing operative intervention.

Ultrasonography (US) is a rapid examination often available in clinicians' offices. It does not subject the patient to ionizing radiation; however, it is quite user dependent and its yield is limited to anatomic information regarding renal parenchyma, degree of hydronephrosis, presence of vasculature, etc… It should be noted that enhancements in ultrasound technology and techniques have improved its ability of identify vasculature. Crossing vessels have been reliably imaged with the use of contrast-enhanced color Doppler imaging and endoluminal ultrasonography.[12,13] Imaging of associated renal calculi is also limited with the use of ultrasound. Owing to its limitations, ultrasound is often an initial diagnostic test but not one on which surgical decisions are based.

Intravenous urography is informative regarding both the anatomic and functional aspects of the kidneys. A properly performed IVU will indicate the presence of calculi (if radiopaque), renal parenchymal thickness, hydronephrosis, delay/lack of excretion, and level of obstruction. One concern with this imaging modality is the lack of information with respect to renal vasculature, particularly the presence or absence of crossing vessels. One study has suggested that particular findings on IVU can reliably detect crossing vessels with a sensitivity of 82% and specificity of 100%.[14] The authors identified an acute posteriorly angulated ureteral deformity just below a patent UPJ. Despite its value in evaluation of UPJ obstruction, IVU is decreasingly utilized likely due to the ubiquity of CT scanners and the more objective data obtained from diuretic nuclear scintigraphy. Intravenous urography remains an important diagnostic modality and continues to play a role in the postoperative evaluation of UPJ obstruction.

Nuclear scintigraphy (diuretic renography) documents important information regarding differential function (right vs. left), and clearance time but lacks anatomic detail.[15] A Lasix renal scan is the most common functional study used in patients with UPJ obstruction. The most commonly applied agent is 99m Tc-MAG3 owing to its more favorable dosing and imaging characteristics.[16] Radionuclide that is to

be excreted into the collecting system is administered intravenously and allowed to collect in the area of interest (collecting system). Imaging determining the level of radioactivity (counts) is obtained at 5 min intervals until the collecting system is filled. If the curve demonstrates obstruction (increasing counts), intravenous Lasix (1 mg/kg) is administered. Imaging is repeated at 5 min intervals and computerized curves of the counts remaining in the collecting system are determined. This process of uptake and excretion by the kidneys occurs in a fairly reproducible manner. After perfusion and uptake/clearance of the agent from the renal parenchyma, excretion of the radiopharmaceutical should occur. The normal time it takes for half the radiotracer to leave the collecting system (T½) is less than 10 min. A normal renogram excludes significant renal obstruction. Studies with T½ between 10 and 20 min are considered equivocal and those with T½ greater than 20 min are indicative of obstruction.[16] Diuretic renography therefore provides objective data with which to diagnose and follow patients after surgical repair. The lack of anatomic detail, however, leads most surgeons to combine this test with further imaging.

Currently, the most common diagnostic study is CT because of its rapidity, ubiquity, and ability to diagnose a multitude of ailments in the patient presenting with flank pain. CT provides excellent anatomic detail with respect to renal parenchyma, degree of hydronephrosis, renal calculi, and level of obstruction, and is capable of identifying crossing vessels. Functional assessment is limited but subjective evaluation owing to delay in contrast enhancement of renal parenchyma and excretion of contrast dye is useful. Interestingly, a recent analysis of CT-measured renal parenchyma area accurately predicted and correlated with renal function assessment of nuclear scintigraphy.[17] These findings notwithstanding, CT is still not the standard method of functional assessment.

Because of the limited functional assessment, CT imaging does not play a routine role in the postoperative follow-up of patients after robotic pyeloplasty.

Retrograde pyelography is a beneficial study for assessing degree of hydronephrosis, level of ureteral obstruction, and presence of additional ureteral anatomic abnormalities. Retrograde studies generally require an additional visit to the operating room if used as part of preoperative diagnostic evaluation and therefore is often performed only at the time of planned surgical repair. If patients require preoperative stenting due to pain or infection, a retrograde pyelogram should be performed. Antegrade pyelography is also uncommon as a preoperative diagnostic study because it requires placement of a percutaneous nephrostomy tube; however, if placed, anatomic details similar to retrograde pyelography can be obtained. Additionally, if concern remains regarding the significance of hydronephrosis and the actual presence of obstruction, a Whitaker test can be performed via the percutaneous nephrostomy tube.[18] This is a renal collecting system/ureteral perfusion test at a set flow rate to determine if functional obstruction is present. Owing to its invasive nature, it is rarely used except in equivocal cases.

A thorough review of the available clinical data is paramount prior to surgical intervention. Once the proper diagnosis is made, it is the role of the urologist to educate the patient on the surgical risks, benefits, and alternatives.

Surgical Approach

The most common approach to robotic pyeloplasty is transperitoneal. This technique is most familiar to minimally invasive surgeons and provides the greatest working space for the surgeon. The familiarity with anatomy and increased range of motion make this approach easier to learn and therefore more rapidly disseminated. Alternatively, a retroperitoneal approach has been described and successful outcomes have been demonstrated.[19] Though limited by a smaller working space and less familiar anatomic landmarks, the potential advantages of containment of potential urinoma and application to patients with prior abdominal surgery make the retroperitoneal approach a fertile area of investigation. Currently, however, the standard technique for robotic pyeloplasty remains as transperitoneal access to the renal hilum.

Variations exist regarding ureteral stent placement. Ureteral stents are placed prior to arrival in the operating room (OR), retrograde in the OR just prior to positioning for pyeloplasty, or antegrade during reconstruction of the UPJ. Some authors advocate retrograde placement at the time of the procedure combined with a retrograde pyelogram, which permits assessment of length and level of anatomic obstruction.[20] Additionally, the retrograde pyelogram will occasionally demonstrate a distal ureteral obstruction, thereby altering surgical management. Others prefer antegrade stent placement during the time of reconstruction.[21] Arguments for antegrade stent placement include improved visualization of the renal pelvis and site of obstruction, because the pelvis is not decompressed, and the ability to start in the lateral decubitus position as opposed to lithotomy for cystoscopy followed by repositioning. The decision when to place a ureteral stent remains a matter of surgical preference.

Operating Room Setup

On arrival to the operating room, the patient has sequential compressive devices placed on the lower extremities and general anesthesia is induced. If the patient is to have a cystoscopy, retrograde pyelogram, and stent placement prior to robotic pyeloplasty, the patient is placed in standard

lithotomy position. Routine cystoscopy and stent placement is performed followed by Foley catheterization of the urinary bladder. The anesthesia team places an orogastric tube for decompression of the stomach.

Once the stent has been placed, or if it is to be placed antegrade during reconstruction, the patient is placed on the operating table in the lateral decubitus position with the surgical side up. The decubitus positioning for robotic pyeloplasty has been described as ranging from 45 to 70° flank position. Patients are secured to the table and supported with a variety of equipment ranging from egg-crates to gel pads to a bean bag depending upon institutional and physician preference. Typically, the umbilicus is placed at the level of the bed's break point. The bed is then gently flexed to increase the working space between the iliac crest and the ribs.

The equipment is placed as appropriate for the OR being utilized. Generally, the anesthesia cart is located cephalad to the patient's bed, the sterile surgical table is placed cephalad and posterior to the bedside assistant, and the robotic console is located where appropriate with respect to room space. Importantly, the robot is located cephalad and lateral to the surgical side. The robot can then be brought in at a 60° angle over the posterior aspect of the patient, permitting an optimal approach to the upper urinary tract. The assistant is stationed anterior to the abdominal wall at the level of the lowest assistant port. The surgical tech/scrub nurse is located along side but posterior to the surgical assistant.

Surgical Site and Trocar Placement

After the patient is properly positioned, adequately padded, and secured, the patient is prepped and draped in a standard sterile manner. The surgical field extends from the level of the xyphoid to the anterior superior iliac spine. Laterally, the field extends to the mid-axillary line for the transperitoneal approach.

The initial incision is a semicircular peri-umbilical incision on the ipsilateral side of the surgical site. This is then carried down to the level of the rectus fascia. A Veress needle is inserted and the peritoneal cavity is insufflated. Securing the rectus fascia with a suture or clamp for counter traction can be beneficial at the time of Veress insertion. Once the pneumoperitoneum is properly established, a 12-mm trocar is placed through the abdominal wall. The camera can now be inserted and the peritoneal cavity inspected. Prior to the placement of additional ports, the abdomen should be evaluated for injuries, adhesions, as well as the presence of additional intra-abdominal pathology.

The two robotic arms can now be inserted. Generally, the goal is to triangulate the renal pelvis while maintaining adequate separation to avoid the arms from hindering each other. The camera is utilized for visualization of the reusable 8 mm robotic trocars during their insertion. The cephalad arm is located 8 cm superior to the umbilicus in the midline. The caudal arm is placed 8 cm away from the umbilical port in line toward the ipsilateral anterior superior iliac spine. Various locations and port sizes have been described for the assistant port. Assistant ports have been described in the midline both inferior and superior to the umbilical camera port, subcostally in the ipsilateral anterior axillary line, and in the contralateral lower abdominal area.[21–24] The important point is to avoid obstruction of the assistant's movement by the robotic arms. The assistant port used has been reported as 5, 10, and 12 mm depending on the surgeon's preference. The advantage of the larger trocars is that they provide access for different sized instruments and passage of suture material. This may lead to decreased cosmesis and potentially require surgical closure. For obese patients, the trocar sites are transposed laterally in the direction of the surgical site.

Exposure of the Ureteropelvic Junction

Once the trocars have been safely placed and any intraabdominal adhesions that would limit progress of the procedure have been mobilized, the dissection may begin. Some authors prefer to perform the initial dissection of the colon and renal pelvis with standard laparoscopic instruments and utilize the robot for the reconstructive portion of the procedure, while others prefer to perform the entire procedure with robotic assistance.[21–25] Both techniques are capable of accomplishing the same task, thereby, making the decision one of surgeon's preferences.

If the operative site is the right renal pelvis, the line of Toldt is incised and the colon reflected medially from the level of the hepatic flexure to the pelvis. The posterior peritoneal reflection is mobilized off the anterior surface of Gerota's fascia, thereby exposing the renal hilum. It may be necessary to perform a Kocher maneuver on the duodenum if it is found to be overlying the operative site. Once the kidney with the overlying Gerota's fascia is properly exposed, the renal hilum and proximal ureter can be dissected out of the peri-renal fat. Care is taken to not dissect the proximal ureter to far distally or disturb an excessive amount of its adventitia so as to not strip it of its blood supply.

For patients with left-sided UPJ obstruction, mobilization of the line of Toldt from the level of the splenic flexure to the sigmoid attachment is often necessary. Additionally, if the site of obstruction is medially displaced, it may be necessary to mobilize the spleen, including the splenophrenic and splenorenal ligaments. Alternatively, if the patient is thin and the UPJ is laterally located, a trans-mesenteric approach has

been used. The course of the gonadal vein on the left can be used as a guide to identification of the ureter and subsequently the renal pelvis.

As the dissection of the UPJ proceeds, either from the renal pelvis toward the ureter or vice versa, care should be taken to identify potential crossing vessels. The use of preoperative imaging should have indicated the presence of such structures but will occasionally miss smaller vessels. Extensive dissection and manipulation of the ureter should be avoided. Grasping of the ureter should be kept to a minimum or completely avoided to prevent crush injuries due to the lack of tactile feedback when using the robot.

After exposure of the UPJ and the obstruction, some authors advocate the use of a "hitch" stitch. This is either passed through the abdominal wall or inserted through the assistant's trocar. This suture is passed through the renal pelvis and the abdominal wall in an attempt to elevate the collecting system off the retroperitoneum and out of any pooled urine or blood.

Pyeloplasty

Multiple techniques exist for performing the pyeloplasty portion of the procedure, both dismembered and non-dismembered – Anderson–Hynes dismembered pyeloplasty, Fengerplasty, Y-V plasty, Heine-Mikulicz, etc… The authors prefer the Anderson-Hynes technique of dismembered pyeloplasty owing to its versatility. It is applicable for the removal of functionally or anatomically abnormal segments, as well as transposition of the UPJ in the presence of crossing vessels. It is the procedure of choice for a patient with a large renal pelvis or a high insertion due to the need for "tailoring" of the UPJ.

The ureter is transected caudal to the obstruction. Care is taken to avoid damaging any previously placed ureteral stent. The ureter is mobilized distally as necessary to allow for spatulation and a tension-free anastamosis. If the ureteral stent was placed earlier, it is brought out of the renal pelvis. Close attention to anatomic landmarks or placement of a marking stitch are important to prevent malrotation of the ureter. The ureter is spatulated laterally, for a distance of 1 cm, using standard robotic scissors. The ureter must be mobilized anteriorly if a crossing vessel is identified.

Once the ureter has been prepared, the renal pelvis is incised on the medial aspect, cephalad to the blockage. This incision is carried obliquely in a caudal, lateral direction until the UPJ is free from the pelvis. The specimen is retrieved through the assistant's trocar and sent to pathology. If a crossing vessel is present, the renal pelvis can be transposed anteriorly. The pelvis must be carefully freed of all its attachments to the crossing vessel and retroperitoneum to minimize tension and permit proper anterior translocation. If the renal pelvis is redundant, additional tissue can be resected to allow for optimal drainage through the new anastamosis.

The posterior aspect of the anastamosis is performed first. Either an interrupted or continuous closure can be performed. An absorbable 4–0 monofilament suture is employed for the anastamosis. The most caudal portion of the renal pelvis is sutured to the most caudal aspect of the ureteral spatulation with the knot located outside the anastamosis. Closure proceeds medially and cephalad until the posterior wall is closed. If the ureteral stent was not placed prior to dissection, it can be placed at this point. A guide wire is inserted through the assistant's trocar or alternatively through a small stab incision in the abdominal wall. The wire is passed into the ureter and down into the urinary bladder under direct vision. The stent is advanced over the guide wire until the proximal coil is located at the level of the renal pelvis and the wire is then removed. The proximal coil is placed into the renal pelvis. The anterior portion of the anastomosis can now be completed. If the renal pelvis requires further closure, further suturing can be performed to completely close the superior aspect of the incision.

Upon completion of the anastomosis, the intraabdominal pressure is decreased and the operative field is inspected for adequate hemostasis. To ensure a water-tight anastamosis, a drain is placed through the inferior robotic trocar prior to de-docking of the robot.

Closure

Some authors advocate reattachment of the colon to the lateral side-wall to retroperitonealize the kidney and ureter.[23] Most surgeons, however, do not bother with this step as no data exists regarding outcomes from this technique. All trocars are removed under direct vision to ensure adequate hemostasis at the trocar sites. The 12 mm trocar sites are closed with an absorbable suture at the fascial level. Skin is then closed with subcuticular suture and/or skin adhesive. Sterile dressings are placed and the patient can now be repositioned into the supine position and awaken from anesthesia.

Immediate Postoperative Course

The patient is left with a Foley catheter and an indwelling double J ureteral stent. The Foley catheter remains in place for 24–48 h; however, if high output from the drain is encountered, it is advisable to continue urethral catheterization until the drainage diminishes. If high drain output is identified, it

is beneficial to send the fluid for a creatinine level to assess whether it is due to urinary leakage, peritoneal fluid, bowel injury, or retained irrigation fluid (if used). Once the drain output is less than 50 mL/8 h, it is generally safe to remove the Foley catheter. The drain output should remain low at this point. If the output increases significantly, it is advisable to replace the Foley catheter and continue until the drainage becomes scant. Patients can be discharged with a Foley catheter and the drain in place and return to the office for removal, once low output occurs.

Postoperative pain is managed with standard narcotics and/or Ketorolac (renal function permitting). Patients should be ambulating on the first postoperative day. A clear diet can be started on postoperative day 1 and advanced as tolerated. The average hospitalization is expected to range from 1 to 5 days.[22,24,26–29] The ureteral stent is removed at 3–6 weeks postoperatively in the office setting. It is reasonable to follow pain scales at the time of stent removal in an attempt to generate objective assessment of outcomes. The initial follow-up imaging should be a diuretic renal scan or IVP at 3 months postoperatively.

Complications

Gettman et al reported no intraoperative complications or open conversions in their initial series of 9 patients.[24] One patient required an open re-exploration to repair a leaking renal pelvis; however, all of the procedures were successful on a subjective as well as radiographic analysis, although follow-up was limited to 3 months.

In a series of 35 patients published in 2005, no open conversions or intraoperative complications were noted.[21] Postoperative complications included a nephrectomy secondary to nonrecovery of renal function, and persistent pain on the affected side. Another patient had an asymptomatic stricture at the site of the anastomosis; this was successfully treated with a laser incision of the stricture. Again follow up was limited with a mean of 7.9 months.

Yee et al, retrospectively compared eight open and eight robotic pyeloplasties in children and did not find any intraoperative complications in either group.[30] Immediate postoperative complications were limited to a prolonged ileus in one patient who underwent robotic pyeloplasty; however, no long-term complications were seen in the robotic arm with a mean follow-up of 14.7 months. The open cohort had one failure due to ureteropelvic stricture, which was diagnosed approximately 6 months postoperatively.

A cohort of 31 patients who underwent robotic pyeloplasty with an average follow-up of 6 months was reported by Weise et al.[31] The authors documented one febrile UTI and one urine leak causing a postoperative ileus. Both patients were managed nonoperatively and recovered without incident. Of their robotic pyeloplasty series, five patients continued to have partial obstruction as documented by early postoperative renography, although none were symptomatic. One patient had high-grade obstruction, and once imaging confirmed no anatomical obstruction, a laparoscopic nephrectomy was performed.

A series of 92 patients who underwent transperitoneal robotic pyeloplasty were evaluated by Schwentner et al with a mean follow-up of 39.1 months.[22] They reported no intraoperative complications and all cases were completed without open conversion. Three early complications were reported including insufficient closure of the collecting system, postoperative hemorrhage, and improper stent placement. There were no long-term complications reported in just over 3 years of follow-up.

In the largest cohort to date, Mufarrij et al evaluated 140 patients from three medical centers.[27] Their postoperative complications at mean follow up of 29 months included: a renal pelvis clot, stent migration, febrile UTI, delayed anastomotic closure, and a ureteral stricture. Stent migration was the most common major complication seen in their cohort. Stent migration was suggested to be in part due to the improper placement. They suggested using blue-dyed saline and allowing it to reflux to confirm proper stent placement. Ureteral strictures generally lead to a second procedure: pyeloplasty or endopyelotomy. The strictures were attributed to technical errors or ureteral ischemia. Minor complications encountered were a febrile UTI and a delayed anastomotic closure.

Unfortunately as seen earlier, outcomes data is limited in caseload and follow-up time. A prospective analysis with longer follow-up times is needed to properly assess the complications associated with robotic pyeloplasty. However, initial data suggests this procedure offers the benefits of minimally invasive surgery with complications similar in nature and number to other laparoscopic procedures.

Outcomes

As previously stated, the goal of robotic pyeloplasty is to emulate the high success rate of open pyeloplasty while reproducing the benefits of minimally invasive surgery. The complications, outlined previously, demonstrate that robotic pyeloplasty is a safe procedure with a low number of complications. Once safety is documented, it is important for any procedure to establish successful outcomes to gain acceptance and use. For robotic pyeloplasty, success can be reported as peri-operative (i.e., length of hospitalization, complications, etc…) and cure (i.e., asymptomatic and relief of obstruction). Both sets of measures illustrate the high

Table 3.1 Perioperative and surgical outcomes

Author	Year	Number of patients	Operative time (min)	Estimated blood loss (mL)	Length of hospitalization (days)	Mean follow-up (months)	Symptomatic success (%)	Radiographic success (%)
Bentas et al[28]	2003	11	197	Negligible	5.5	21	100	100
Patel[3]	2005	50	122	40	1.1	11.7	100	100
Mendez-Torres et al[26]	2005	32	300	50	1.1	10.3	94	94
Siddiq et al[29]	2005	26	245	69	2	6	95	100
Schwentener et al[22]	2007	92	108	N/A	4.6	39	96.7	100
Kaouk et al[19]	2008	70	175	50	2	30	100	100
Mufarrij et al[27]	2008	140	217	59.4	2.1	29	92.4	95.7

success rate of this surgical approach to UPJ obstruction. As illustrated in Table 3.1, operative time ranges from 108 to 300 min, with a low estimated blood loss. The length of hospitalization is relatively short (1.1–5.5 days), averaging 2.5 days. The long-term outcomes of radiographic and symptomatic success are comparable with the reported success rates of both open and laparoscopic repair.[32,33] Symptomatic success is slightly lower (92.4–100%) than radiographic success (94–100%), both of which are the acceptable rates for any surgical intervention.

Follow-Up

The patient initially returns in 3–6 weeks time after robotic pyeloplasty for cystoscopy and stent removal. Assessment of abdominal wounds, postoperative pain, and a thorough review of systems (i.e., return of bowel function, activity level, etc…) should be included at this visit, as it is expected that the patient has returned to his/her preoperative baseline. All subsequent visits should evaluate the patient's analog pain scores, serum assessment of renal function, and imaging.

Various authors advocate the use of renal ultrasound, intravenous urography, and diuretic renography, alone or in combination. The goal of follow-up imaging is to determine return of function and normal anatomy. Functional assessment with diuretic renography or intravenous urography is performed 3 months postoperatively and then repeated at 6 and 12 months. The authors find it helpful to alternate between renal scan and IVP at each subsequent visit in an attempt to overcome the inherent limitations of each study. Others have recommended diuretic renogram at 3, 6, and 12 months followed by ultrasound or renogram annually thereafter.[34] Adequate guidelines on the length of follow-up do not exist; however, evidence continues to mount indicating that long-term follow-up is imperative in these patients.[34]

Special Considerations

Concomitant Nephrolithiasis

Nephrolithiasis is not uncommonly associated with UPJ obstruction; this may be due to a combination of urinary stasis and underlying metabolic or dietary predilection for stone formation. The potential presence of stones should be considered preoperatively and investigated during routine work-up with diagnostic imaging. If identified, stones can be addressed at the time of pyeloplasty. Removal of renal calculi at the time of robotic pyeloplasty has been documented in a number of series.[27,35] Insertion of a flexible cystonephroscope through one of the robotic trocars sites and into the renal pelvis is performed. Once in the collecting system, all calyces can be readily inspected and graspers or baskets are utilized to grasp and remove the calculi. Atug et al reported irrigating smaller fragments into the peritoneal cavity and using the assistant's suction to remove these stones.[35]

Horseshoe Kidney

Limited data exists regarding the application and outcome of robotic pyeloplasty in horseshoe kidneys. To date seven patients have been described as successfully having undergone robotic pyeloplasty.[22,27,36,37] Notably, Pe et al reported successful repair following failed endopyelotomy.[37] All authors report successful outcomes with up to 1 year follow-up.

Conclusion

Robotic pyeloplasty is a safe and effective treatment option for patients who present with signs and symptoms of UPJ obstruction. Proper documentation of patients' preoperative

status – symptomatically, anatomically, functionally – is imperative to optimize outcomes. As techniques and equipment continue to advance, it is likely to become the "gold standard" treatment of UPJ obstruction.

References

1. Schuessler WW, Grune MT, Tecuanhuey LV, et al Laparoscopic dismembered pyeloplasty. *J Urol*. 1993;150:1795
2. Patel RP, Casale P. Robotic pediatric urology. *Minerva Urol Nefrol*. 2007;59:425
3. Patel V. Robotic-assisted laparoscopic dismembered pyeloplasty. *Urology*. 2005;66:45
4. Matin SF, Yost A, Streem SB. Ureteroscopic laser endopyelotomy: a single-center experience. *J Endourol*. 2003;17:401
5. Motola JA, Badlani GH, Smith AD. Results of 212 consecutive endopyelotomies: an 8-year followup. *J Urol*. 1993;149:453
6. Kletscher BA, Segura JW, LeRoy AJ, et al Percutaneous antegrade endopyelotomy: review of 50 consecutive cases. *J Urol*. 1995; 153:701
7. Moon DA, El-Shazly MA, Chang CM, et al Laparoscopic pyeloplasty: evolution of a new gold standard. *Urology*. 2006;67:932
8. Janetschek G, Peschel R, Frauscher F. Laparoscopic pyeloplasty. *Urol Clin North Am*. 2000;27:695
9. Zhang DH, Yu DM, Ding GQ, et al Experience with transperitoneal laparoscopic dismembered pyeloplasty. *Chin Med J (Engl)*. 2005; 118:246
10. Inagaki T, Rha KH, Ong AM, et al Laparoscopic pyeloplasty: current status. *BJU Int*. 2005;95(suppl 2):102
11. Sung GT, Gill IS, Hsu TH. Robotic-assisted laparoscopic pyeloplasty: a pilot study. *Urology*. 1999;53:1099
12. Mitterberger M, Pinggera GM, Neururer R, et al Comparison of contrast-enhanced color Doppler imaging (CDI), computed tomography (CT), and magnetic resonance imaging (MRI) for the detection of crossing vessels in patients with ureteropelvic junction obstruction (UPJO). *Eur Urol*. 2008;53:1254
13. Lin L, Bagley DH, Liu JB. Role of endoluminal sonography in evaluation of obstruction of the ureteropelvic junction. *AJR Am J Roentgenol*. 2008;191:1250
14. Wang W, LeRoy AJ, McKusick MA, et al Detection of crossing vessels as the cause of ureteropelvic junction obstruction: the role of antegrade pyelography prior to endopyelotomy. *J Vasc Interv Radiol*. 2004;15:1435
15. Goldfarb CR, Srivastava NC, Grotas AB, et al Radionuclide imaging in urology. *Urol Clin North Am*. 2006;33:319
16. Roarke MC, Sandler CM. Provocative imaging. Diuretic renography. *Urol Clin North Am*. 1998;25:227
17. Feder MT, Blitstein J, Mason B, et al Predicting differential renal function using computerized tomography measurements of renal parenchymal area. *J Urol*. 2008;180:2110
18. Whitaker RH. Methods of assessing obstruction in dilated ureters. *Br J Urol*. 1973;45:15
19. Kaouk JH, Hafron J, Parekattil S, et al Is retroperitoneal approach feasible for robotic dismembered pyeloplasty: initial experience and long-term results. *J Endourol*. 2008;22:2153
20. Canes D, Berger A, Gettman MT, et al Minimally invasive approaches to ureteropelvic junction obstruction. *Urol Clin North Am*. 2008;35:425
21. Palese MA, Stifelman MD, Munver R, et al Robot-assisted laparoscopic dismembered pyeloplasty: a combined experience. *J Endourol*. 2005;19:382
22. Schwentner C, Pelzer A, Neururer R, et al Robotic Anderson-Hynes pyeloplasty: 5-year experience of one centre. *BJU Int*. 2007; 100:880
23. Peschel R, Neururer R, Bartsch G, et al Robotic pyeloplasty: technique and results. *Urol Clin North Am*. 2004;31:737
24. Gettman MT, Neururer R, Bartsch G, et al Anderson-Hynes dismembered pyeloplasty performed using the da Vinci robotic system. *Urology*. 2002;60:509
25. Gettman MT, Peschel R, Neururer R, et al A comparison of laparoscopic pyeloplasty performed with the daVinci robotic system versus standard laparoscopic techniques: initial clinical results. *Eur Urol*. 2002;42:453
26. Mendez-Torres F, Woods M, Thomas R. Technical modifications for robot-assisted laparoscopic pyeloplasty. *J Endourol*. 2005;19: 393
27. Mufarrij PW, Woods M, Shah OD, et al Robotic dismembered pyeloplasty: a 6-year, multi-institutional experience. *J Urol*. 2008; 180:1391
28. Bentas W, Wolfram M, Brautigam R, et al Da Vinci robot assisted Anderson-Hynes dismembered pyeloplasty: technique and 1 year follow-up. *World J Urol*. 2003;21:133
29. Siddiq FM, Leveillee RJ, Villicana P, et al Computer-assisted laparoscopic pyeloplasty: University of Miami experience with the daVinci Surgical System. *J Endourol*. 2005;19:387
30. Yee DS, Shanberg AM, Duel BP, et al Initial comparison of robotic-assisted laparoscopic versus open pyeloplasty in children. *Urology*. 2006;67:599
31. Weise ES, Winfield HN. Robotic computer-assisted pyeloplasty versus conventional laparoscopic pyeloplasty. *J Endourol*. 2006;20:813
32. Bauer JJ, Bishoff JT, Moore RG, et al Laparoscopic versus open pyeloplasty: assessment of objective and subjective outcome. *J Urol*. 1999;162:692
33. Jarrett TW, Chan DY, Charambura TC, et al Laparoscopic pyeloplasty: the first 100 cases. *J Urol*. 2002;167:1253
34. Yanke BV, Lallas CD, Pagnani C, et al The minimally invasive treatment of ureteropelvic junction obstruction: a review of our experience during the last decade. *J Urol*. 2008;180:1397
35. Atug F, Castle EP, Burgess SV, et al Concomitant management of renal calculi and pelvi-ureteric junction obstruction with robotic laparoscopic surgery. *BJU Int*. 2005;96:1365
36. Chammas M Jr, Feuillu B, Coissard A, et al Laparoscopic robotic-assisted management of pelvi-ureteric junction obstruction in patients with horseshoe kidneys: technique and 1-year follow-up. *BJU Int*. 2006;97:579
37. Pe ML, Sterious SN, Liu JB, et al Robotic dismembered pyeloplasty in a horseshoe kidney after failed endopyelotomy. *JSLS*. 2008; 12:210

Robotic-Assisted Laparoscopic Partial Nephrectomy

4

Brian H. Irwin, Monish Aron, and Inderbir Gill

Introduction

Laparoscopy came into existence in Urology the first time when Kelling introduced a cystoscope into the abdomen of a living dog via a trocar placed through the abdominal wall in 1901.[1] Since that time, laparoscopic surgical techniques have been honed to allow urologic surgeons to perform the entire gamut of urologic procedures in a minimally invasive manner. With new advances in robotic technologies, the surgical repertoire has grown to include an ever-expanding array of complex extirpative and reconstructive procedures. While partial nephrectomy and, to a lesser extent, laparoscopic partial nephrectomy have been accepted as the gold standard for the treatment of small incidentally found solid renal tumors, there is only limited literature available about the role of robotic-assisted laparoscopic partial nephrectomy (RALPN).[2–9] This is an emerging procedure, which has yet to find its role in the mainstream of urologic practice; however, it does offer several clear and intriguing advantages over current technology when placed in the correct hands.

Between the years 1975 and 1995, the incidence of renal cancers rose between 2 and 4% each year owing in large part to a significant increase in the use of cross-sectional imaging.[10–13] The most striking increase was seen in incidentally found, localized tumors potentially amenable to surgical cure.[12] Currently, this group represents between 48 and 66% of all renal masses in contemporary series.[14] Despite the relatively new development of renal ablative techniques for the treatment of such tumors, the mainstay of treatment remains surgical excision.

Open partial nephrectomy became the standard of care for the treatment of T1 renal tumors, as the cancer control was shown to be equivalent to radical nephrectomy.[15–20] As it became clear that up to 20–30% of solid enhancing renal masses in contemporary series represent benign pathology,[21–23] a major push to minimize morbidity through minimally invasive nephron sparing surgery has advanced to the forefront. To date, the world's literature on laparoscopic partial nephrectomy includes well over 2,000 patients. Minimally invasive nephron sparing surgery mimics the oncologic principles of open nephron sparing surgery.[22,23] These include careful identification and excision of the tumor under direct vision with attempts at minimizing the required warm ischemia time (WIT) and intraoperative confirmation of negative surgical margins.

Surgical robotics offers several distinct benefits over the abilities available with conventional laparoscopy in performing complex urologic procedures. The prototype for reproducing an open procedure using minimally invasive techniques is the robotic-assisted laparoscopic radical prostatectomy.[24] Though more robotic systems exist, and are currently being developed, the vast majority of the experience in the published literature has been performed with the DaVinci system (Intuitive Surgical, Sunnyvale, CA). This surgical system includes a surgical console, in which the surgeon sits to control the slave surgical robotic cart through a set of hand and foot controls. A slave robotic cart stands immediately at the side of the patient and holds a 3-dimensional camera and articulating working instruments, which are passed through the abdominal wall via specially designed trocars. For purposes of this chapter, the remainder of the discussion will focus specifically on this surgical system except where otherwise stated.

The DaVinci system provides a magnified 3-dimensional view of the entire surgical field under the direct control of the surgeon. This provides a very stable and clear view without the need for constant communication with the assistant regarding camera distance and position. The articulating instruments provide 6 degrees of freedom via the use of an endowrist located near the end of the instrument. The motion of these instruments can be both scaled down as well as set to provide tremor reduction allowing for very precise dissection and suturing capabilities. The current system does not, however, provide for any tactile feedback to the surgeon. With experience, most surgeons are quickly able to compensate for this by the use of subtle visual cues allowed by the high-level optics.

Indications for Procedure

Indications for robotic-assisted minimally invasive nephron sparing surgery are essentially identical to those seen in the conventional laparoscopic experience. With experience, the

P. Dasgupta et al. (eds.), *New Technologies in Urology,*
DOI: 10.1007/978-1-84882-178-1_4, © Springer-Verlag London Limited 2010

added benefits of improved visualization, tissue handling, and suturing abilities, the robotic platform may allow a surgeon with less conventional laparoscopic training and experience to perform more complex resections in a minimally invasive fashion. Special consideration to tumor location, size, depth of invasion into the renal parenchyma, and proximity to the renal hilum must be taken into account. These must also be balanced with the surgeon's skill set to come up with an optimal approach to maintain oncologic principles, while minimizing morbidity from access to the site. Minimally invasive nephron sparing approaches are particularly applicable to patients with solitary kidneys, preexisting chronic kidney disease, multiple or bilateral tumors, or those with a genetic predisposition for the development of multiple renal tumors such as von Hippel–Lindau disease, tuberous sclerosis syndrome, or hereditary papillary renal cell carcinoma (RCC).

Procedure

Room Setup

Space is at a premium in most surgical suites. This space constraint is exaggerated when a relatively large amount of space is required for storage, movement, and function of the robotic surgical cart. The room is set up to allow for maneuvering of the robotic surgical cart and ease of passage of instruments from the scrub nurse/tech to the surgical assistant, while allowing the anesthesia team room to manipulate the airway and access sites as needed as shown in Fig. 4.1. Monitors should be placed at an ergonomically comfortable height and position to allow all members of the surgical team (assistant, scrub tech, anesthesia team) to closely monitor the progression of the procedure to insure prompt availability of all required instruments and interventions during critical portions of the case.

Patient Preparation

A metastatic work-up, creatinine clearance determination, and differential function testing should be completed prior to considering nephron sparing surgery. Informed consent regarding the risks, benefits, expectations, and alternatives during the preoperative, intraoperative, and postoperative periods is obtained prior to initiating any surgical procedure. A bowel preparation is administered to patients the day before surgery, and NPO status is maintained during the day of surgery. Necessary medications are allowed according to the guidelines set forth by the department of Anesthesia at our institution.

Anesthetic Considerations

The patient will be positioned in such a way that access to the endotracheal tube and vascular access sites may be limited to during surgery. For this reason, it is imperative that all access be secured prior to positioning the patient. Dissection during the case will be in proximity to the great vessels and, as such, there exists the potential for significant blood loss should there be an injury to these or nearby structures. For this reason, it is recommended that a current specimen for type and cross and two units of packed red blood should be available and at least two large bore intravenous accesses are obtained prior to positioning. Additional vascular access in the form of arterial lines and central venous access/monitors should be placed at the discretion of the anesthesiologist.

Prophylaxis

Pneumatic anti-embolism stockings are placed immediately upon entering the operative suite and should be functioning well before and during the induction of anesthesia. A first-generation cephalosporin is typically given as prophylaxis against surgical site infection within 60 min of the time of incision. Repeat doses are administered at 4 h intervals during the duration of the case.

Cystoscopic Ureteral Catheter Insertion

Routine cystoscopic open-ended ureteral catheter placement is performed prior to positioning in the flank position in all cases of laparoscopic nephrectomy. The patient is placed in modified lithotomy position and is padded appropriately. A glide wire is used to obtain access to the ureteral orifice to prevent ureteral trauma during passage of the ureteral stent. This stent allows for retrograde injection of dilute methylene blue/saline mixture following excision and initial parenchymal closure to look for sites of entry into the renal collecting system. Though small, peripheral, exophytic tumors may be excised without this step, it is felt that the minimal extra effort required for ureteral catheter placement allows for the most conservative management when tumors require more extensive resections than initially suspected. As such, this has become the standard at our institution.

The patient is then repositioned into the 45-degree flank position as shown in Fig. 4.2. The bed is flexed to allow for optimal working space during the transperitoneal approach. An axillary roll is placed and all pressure points are padded, taking care to protect the legs, knees, ankles, and hip well before securing the patient to the bed. The head and arms should be

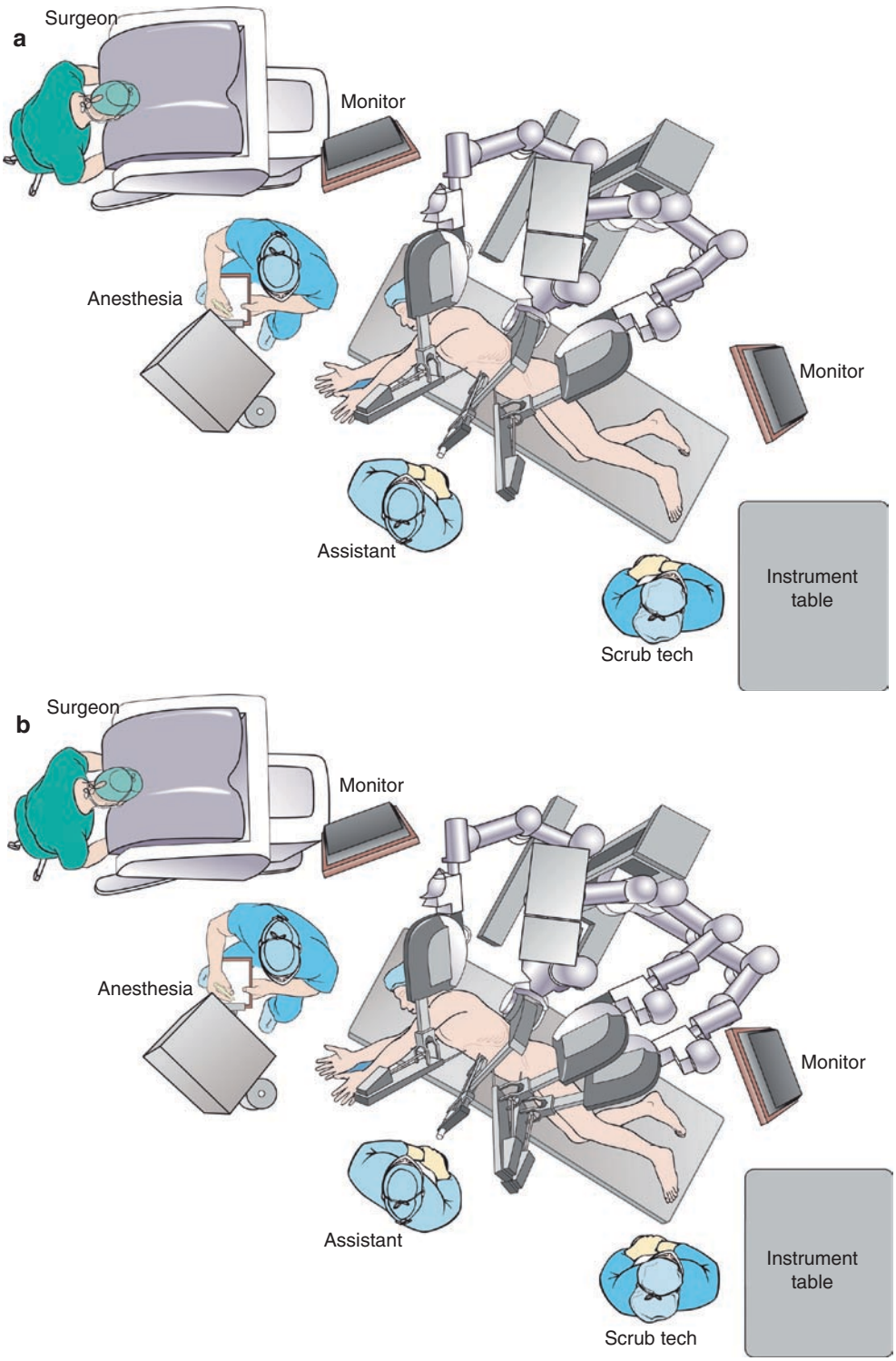

Fig. 4.1 Room equipment configuration during robotic-assisted laparoscopic partial nephrectomy with the (**a**) 3-arm and (**b**) 4-arm DaVinci (Intuitive Surgical, Sunnyvale, CA) robotic surgical systems

placed in a neutral position and secured in place after the anesthesia team has confirmed good function of all vascular access sites and secured the airway following repositioning.

Access is then gained into the peritoneal cavity to create a pneumoperitoneum. If the Varress needle technique is used to obtain access, confirmatory tests (i.e., the "drop test") to insure intraperitoneal placement must be performed prior to insufflation with carbon dioxide gas.[25–27] The initial port is placed carefully after creation of the pneumoperitoneum to a level of 20 cm of water to avoid inadvertent visceral injury. This level is then decreased to 15 cm of water after all ports have been placed and is maintained for the remainder of the

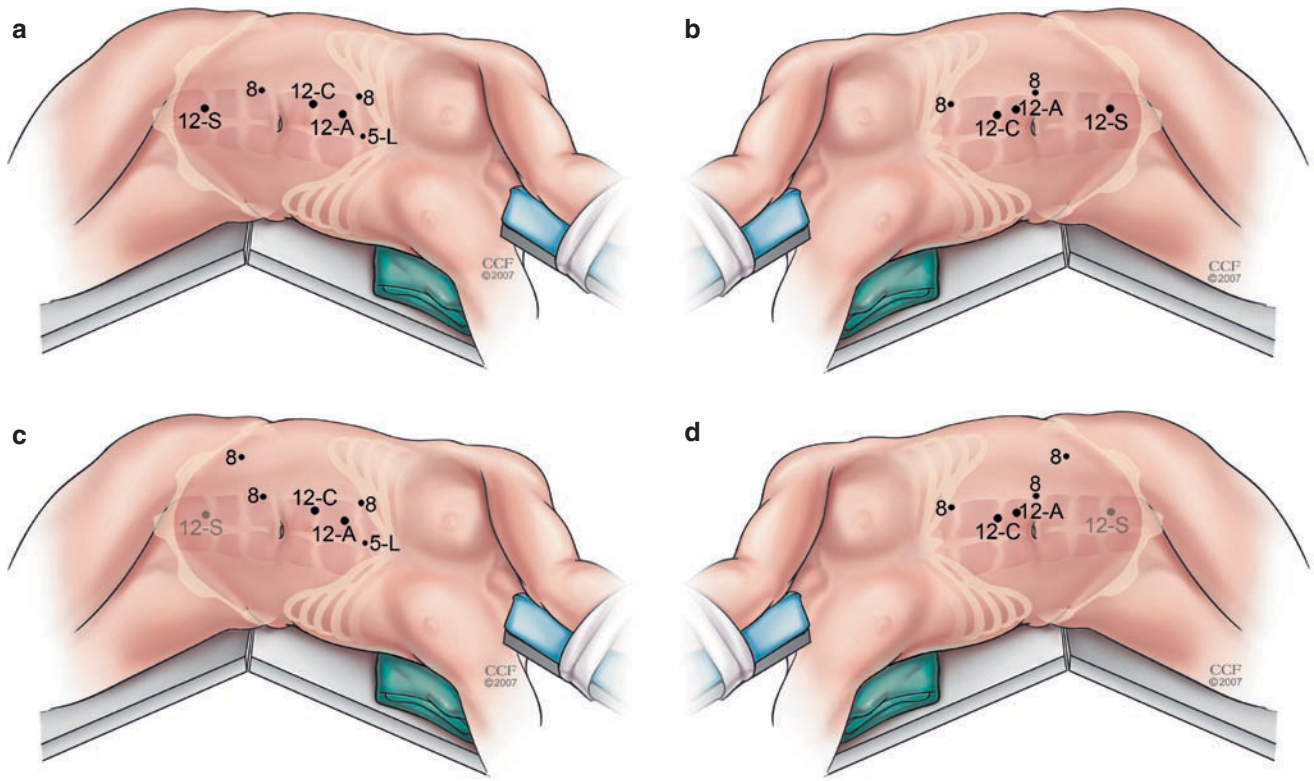

Fig. 4.2 Patient position and port placement for performing robotic-assisted laparoscopic partial nephrectomy on both the right (**a**, **c**) and left (**b**, **d**) sides using the 3-arm (**a**, **b**) and 4-arm (**c**, **d**) DaVinci (Intuitive Surgical) robotic surgical systems. *C* camera port; *S* satinsky port; *A* assistant port; *L* liver retractor port

case. Additional ports are placed under direct vision. It is important to maintain adequate distance between ports to allow for triangulation of the instruments. This will allow maximum range of motion for the robotic arms during dissection and reconstructive portions of the case. In general, the three primary robotic ports are placed into a diamond configuration with the pathology, in this case, the renal hilum and/or tumor, opposite the camera and the working arms located at the apices of the diamond on either side as shown in Fig. 4.2.

Alternatively, some authors have supported the use of a more lateral placement of the camera port and use of a 30-degree down lens with more medial placement of the working arms stating that it gave better visualization of the hilum while obviating the need for colonic retraction.[3] This modification may be particularly helpful for excising more posteriorly located tumors. A "port-in-port" technique has been described in which the 8 mm robotic working ports are placed through conventional laparoscopic 12 mm ports enabling seamless transition from the laparoscopic to the robotic portions of the case and back again as necessary.[6,7]

When using a fourth assistant arm, the remaining robotic port is placed laterally and inferiorly to allow for retraction and stabilization of the kidney/tumor during excision and reconstruction. An additional 12 mm port is placed between the camera port and the more inferior primary robotic working port to allow for passage of needles, suction, and the use of vascular bulldog clamps if desired. En bloc clamping of the artery and vein within the vascular pedicle can be performed with a Satinsky clamp placed through a lower midline 12 mm port. In thin patients, we have found that this clamp can be placed directly through the abdominal wall through a small skin incision without the need for an additional port that requires fascial closure. It must be placed in a location that it will not allow external interaction with the lower-most robotic arm while clamped in place on the renal hilum. On the right side, a 5 mm port is placed in the subxiphoid region for retraction of the liver with a locking clamp secured to the inner aspect diaphragm laterally.

Colonic Mobilization

The colon and mesocolon are mobilized completely from the anteromedial aspect of the kidney as seen in Fig. 4.3a. It is important to find the plane between this leaflet of mesentery and the anterior surface of Gerota's fascia, as it will allow for an easy identification of the hilar structures. Avoidance of the use of diathermy in this area can help to avoid inadvertent

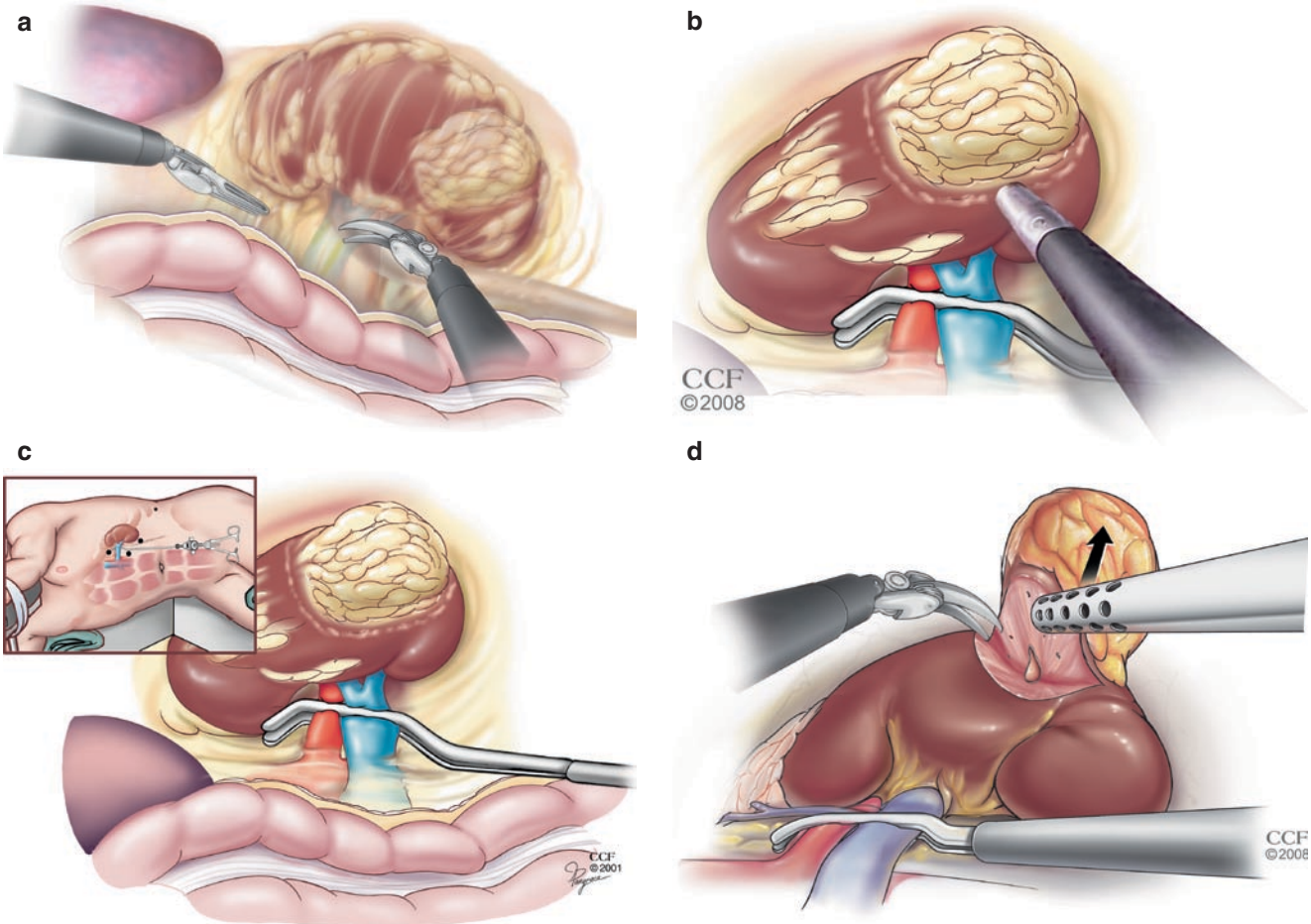

Fig. 4.3 Surgical steps of robotic-assisted laparoscopic partial nephrectomy including mobilization of the colon (**a**), intraoperative ultrasonographic examination to identify and score the boundaries of the tumor (**b**), prior to hilar clamping (**c**), and excision of the tumor (**d**)

bowel injury. Rotating the operative table away from the robotic cart helps to allow the colon to fall medially away from the hilum maximizing exposure.[28] On the left side, care must be taken not to injure the spleen or the tail of the pancreas during mobilization. On the right side, the duodenum must be carefully Kockerized off of the anterior aspect of the hilum. Again, the use of sharp dissection without electrocautery should be emphasized in this region as duodenal injuries can be caused easily and may have devastating results.

Mobilization of the Kidney

The kidney is typically completely mobilized to facilitate achieving the correct orientation for safe and precise excision of the tumor and renorrhaphy after excision. Mobilization of the medial, inferior, and superior aspects of the kidney should be performed first to allow access to the hilar structures. The lateral attachments are best left intact at this point in the dissection to allow for hilar exposure to be maintained without the need for further retractors. Mobilization of the kidney can be performed in two distinct planes; outside of Gerota's fascia or directly on the capsule of the kidney beneath Gerota's fat. Mobilization within the Gerota's fat may facilitate nephropexy at the end of the case by allowing simple reapproximation of the perinephric fat, thus securing the kidney back in its original anatomic location.

Preparation of the Hilum for En Bloc Clamping

The ureter is identified near the lower pole of the kidney on the anterior aspect of the psoas muscle. It is then retracted gently anterolaterally and followed toward the level of the hilum. At this juncture, any lower pole accessory renal arteries will be encountered and should be noted and carefully spared. The gonadal vein is likely to be seen at this time and can be allowed, in most cases, to simply fall medially. On the left side, the gonadal vein enters the renal vein and may need to be taken to allow safe en bloc clamping of the renal vein

and artery. This should be done in such a manner that if, in an emergent situation, the hilum is needed to be stapled to prevent massive blood loss; it could be performed safely while avoiding any surgical clips interfering with the stapling device. If en bloc clamping is not feasible, or if additional renal arteries are encountered, the renal vascular pedicle can be controlled with laparoscopic bulldogs as well. It is important to have the entire hilum prepared for clamping prior to planning the tumor excision. Doses of mannitol and furosemide are given approximately 30 min prior to clamping and immediately prior to unclamping the hilum.

Defatting of the Kidney

Strategic defatting of the kidney should be performed to maintain fat directly over the tumor for the purpose of cancer control as well as to allow manipulation of the tumor without compromising the integrity of the tumor. Maintaining fat over uninvolved portions can be helpful as well, as this can be used as a handle for manipulating and securing the kidney in a stable position during tumor excision and renorrhaphy. During the defatting of the kidney, the kidney would likely be rotated into several different orientations. During this process, it is important to be cognizant of the relationships of the hilar structures to the surface of the kidney. The ureter can be easily inadvertently injured near the lower pole during these maneuvers if care is not taken to identify it and spare it from the area of dissection. Likewise, the renal artery will be encountered posteriorly with aggressive mobilization after the kidney is flipped anteriorly.

Intraoperative Ultrasonography

Intraoperative ultrasonographic examination is performed routinely through the 12 mm assistant port. This allows for accurate identification of the size, location, and depth of invasion of the tumor. It also allows for an assessment of the remainder of the kidney to insure that multifocal disease does not exist. Under ultrasound guidance, the borders of the resection are scored into the renal capsule with the electrocautery as shown in Fig. 4.3b.

Docking of the Robotic Cart

The robotic cart is docked after the above steps have been performed using conventional laparoscopic techniques. This allows the surgeon to take advantage of the flexibility of conventional laparoscopy for mobilization and orientation of the kidney and tumor, while still taking advantage of the precision and dexterity of the robotic assistance. The robotic cart is docked over the ipsilateral shoulder/flank as depicted in Fig. 4.1. It is important to insure that there is ample room between the arms of the robot. On the first generation DaVinci system, the elbows of the working arms should be allowed to be spread as far to the sides as possible to provide the largest range of motion. Positioning with the newer 4-arm DaVinci-S robotic system, it is imperative that the numbers on the robotic working arms face directly toward the surgical field and that the camera arm is positioned within the “sweet spot” as indicated on the elbow joint. When using the fourth arm for retraction, it is also helpful to position the camera arms elbow to the side opposite the fourth arm to allow for maximum freedom of motion of all arms.

Application of the Satinsky Clamp

With the primary surgeon seated at the console, the assistant carefully applies the Satinsky clamp to the renal pedicle as shown in Fig. 4.3c. Prior to this crucial step, it is imperative that the surgical team have a clear plan and vision for excision and renorrhaphy specific to the tumor involved. Care must be taken not to avulse any posterior lumber veins or other small branches from the main renal vein during this maneuver. For this reason, the renal hilum should be skeletonized enough to allow safe passage of the clamp under direct vision. It cannot be overemphasized that the Satinsky clamp should not interact with the caudal-most robotic arm while clamped to the renal hilum. Because this area will likely be out of the surgeon’s view during excision of the tumor, the assistant must remain cognizant of this potential interaction and monitor the proximity of the two pieces of equipment as significant injury could potentially result. During this time of warm ischemia, the entire surgical team must remain focused on the task at hand. In an attempt to minimize ischemic injury, a renal cooling protocol was described during RALPN by Gettman et al, similar to that used at their institution during conventional laparoscopic partial nephrectomy.[4]

Tumor Excision

The tumor is excised sharply from the underlying parenchyma using the previously scored lines in the renal capsule as a guide as can be seen in Fig. 4.3d. During this excision process, the assistant should remain vigilant and provide

expert but judicious and unobtrusive suctioning to maintain a bloodless field. Though during conventional laparoscopy it has become our practice to apply Hem-o-lok clips (Weck Closure Systems, Research Triangle Park, NC) to distinct vessels during tumor excision within the bed of resection, this is often more difficult and time-consuming with the robotic techniques and this step is eliminated. As an alternative, the robotic Maryland bipolar electrocautery device can be used to control these vessels during excision.[3,7] After complete excision, the specimen is placed to the side of the surgical field and renorrhaphy is performed immediately. The specimen will be trapped in a laparoscopic specimen bag and removed via an extended port site incision for frozen section margin analysis immediately following renorrhaphy.

Parenchymal Suture Placement

The initial closure of the renal defect is performed in a running fashion with polyglycolic acid absorbable braided suture as in Fig. 4.4b. The choice of needle size depends on the size of the defect to be closed, but most typically a CT-1 or CT-X is chosen. The aim of the initial closure is to control transected vessels in the sinus fat with direct ligation and to close the collecting system. The collecting system is identified and the edges of any calyceal/pelvis violation are carefully approximated. Since the robotic surgical system lacks tactile feedback, suture breakage can be expected early in the surgeon's robotic experience and care must be taken to avoid suture cut-through within the parenchyma. It should also be pointed out that unlike both open and conventional laparoscopic needle drivers, the needle drivers for the DaVinci system do not have locking mechanisms when activated. With very little experience, most surgeons make the transition without a significant learning curve. Retrograde injection of blue-dyed saline is then performed through the previously placed open-ended ureteral catheter to confirm a water-tight closure and to identify any areas that need further suturing as seen in Fig. 4.4a.

At this point, the hilar clamp is carefully removed by the surgical assistant as part of an "early unclamping" protocol[29] during which the defect is not closed in its entirety prior to clamp removal in an attempt to decrease WIT and to allow for the identification of vessels, which might otherwise bleed without further ligation prior to completely closing the defect. This technique was developed in response to criticism that the WITs in laparoscopic partial nephrectomy series is ~10 longer than in comparable open series.[30] If arterial bleeding is identified after clamp removal, further sutures are placed, thus providing definitive surgical hemostasis.[31] The remainder of the defect is then closed with or without the use of an oxidized cellulose bolster at the discretion of the surgeon. If a bolster is chosen, it is sized to fit well within the edges of the defect. It should not be allowed to lie directly against the ureteral wall within the defect, as it may cause ureteral obstruction in this position (Fig. 4.4c). Once surgical hemostasis is assured, hemostatic agents are applied to the defect in combination with an oxidized cellulose covering.

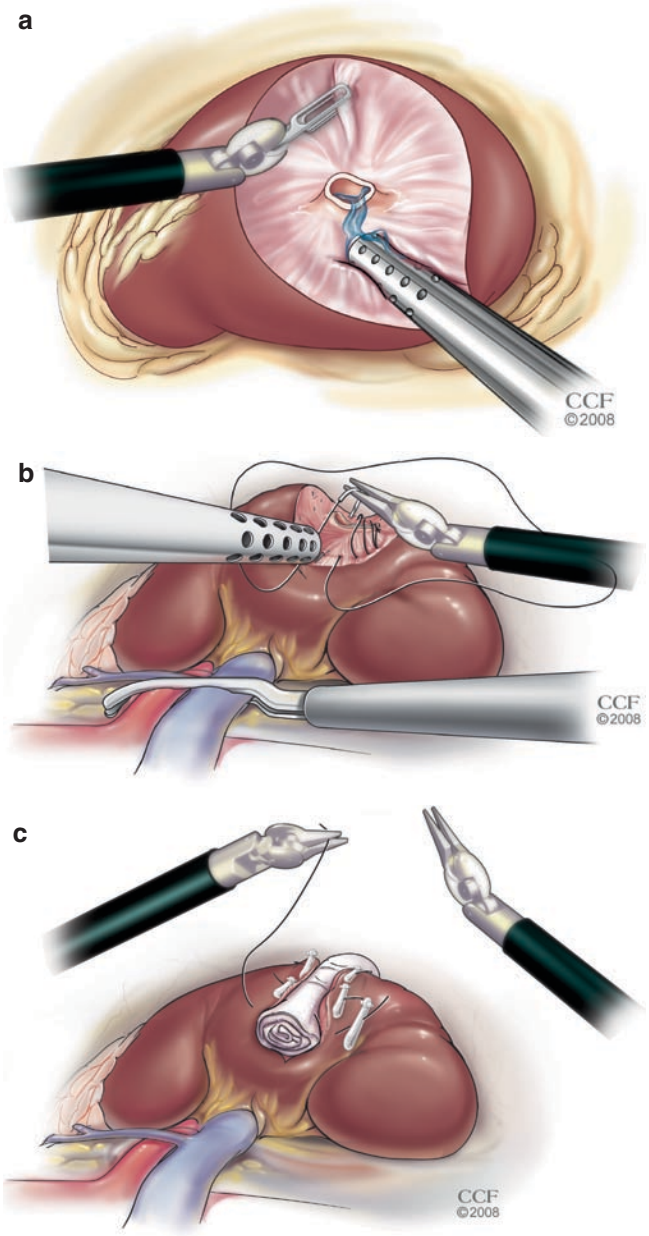

Fig. 4.4 Renorrhaphy technique including identification of collecting system violation via retrograde injection of blue-dyed saline through a previously placed open-ended ureteral catheter (**a**), running parenchymal suture to control transected vessels in the defect bed (**b**), and placement of an oxidized cellulose bolster (**c**)

Because the kidney has been completely mobilized for tumor identification, excision, and reconstruction, the kidney can theoretically torse about its hilar axis. For this reason, a

nephropexy is performed with at least two-point fixation reapproximating the perinephric fat over the anterior surface of the kidney to the lateral body wall. A closed suction drain is then placed in the paracolic gutter and is secured to the skin. All 12 mm port sites are then closed at the fascial level and all ports are removed under direct vision.

Complications

To date, there have been eight series reported in the literature detailing the experience with RALPN representing over 100 patients.[2–9] The details of these are shown in Table 4.1. Complications following RALPN mimic those seen in the

Table 4.1 Published series of RALPN

Variable	Study							
	Gettman et al[4]	Phillips et al[5]	Caruso et al[6a]	Kaul et al[2]	Rogers et al[3]	Deane et al[7,8]	Aron et al[9]	Bhayani et al[6b]
Type of study	Case series	Case series (technique report)	Case–control	Case series	Case series	Case–control	Matched-pair	Case Series
No. RALPN	13	12	10	10	8 (14 tumors)	11	12	35
Mean(range) tumor size (cm)	3.5 (2–6)	1.8	2	2.3 (1–3.5)	2.4 (0.8–6.4)	3.1 (2.5–4)	2.4 (1.4–3.8)	2.5(1–5)
Side (R/L)	7/6	NR	NR	6/4	3/5	4/7	7/5	NR
Tumor location	U 3; M 5; L 5	NR	U 3; M 3; L 4	U 3; L 3; NR 4	Hilar 5; U + M 1; U + L 1; U 1	U 8; L 3	U 2; M 4; L 6	NR
Technique	Pure robotic 11 trans, 2 retro	Robotic assisted all trans	Robotic assisted all trans	Pure robotic all trans	Pure robotic all trans	Robotic assisted all trans	Robotic assisted all trans	Pure robotic all trans
Hilar clamping method	Bulldogs	Bulldogs	Bulldogs	Bulldogs	Bulldogs	Bulldogs	Satinsky	Bulldogs or fourth arm with atraumatic grasper
Mean (range) operative time (min)	215 (130–262)	265 (NR)	279 (NR)	155 (120–185)	192 (165–214)	228.7 (98–375)	242 (130–360)	142 (69–219)
EBL (ml)	170 (50–300)	240 (NR)	240 (NR)	92 (NR)	230 (100–450)	115.0 (75–500)	329 (50–1,000)	133 (25–500)
WIT (range) (min)	(n = 5) 22 (15–29)	26 (NR)	26.4 (NR)	21 (18–27)	31 (24–45)[c]	32.1 (30–45)	23 (13–36)	20 (0–40)
Cold IT (range) (min)	(n = 8) 33 (18–43)							
Positive margin on final pathology	1	NR	0	0	0	0	0	0
Mean LOS (range) (days)	4.3 (2–7)	2.7	2.6	3.5 (1–21)	2.6 (2–3)	2.0	4.7 (2–10)	2.5 (1–7)
No. RCC (% of tumors RCC)	10 (77)	NR	8 (80)	8 (80)	7 (87)	9 (82)	9 (75)	24 (66)
Follow-up (months)	2–11, all NED	NR	NR	15 (16–28) all NED	3 NR, all NED	4.5 (1–8), all NED	7.4, all NED	NR
Complications	Ileus, 1	Conversion to: HAL 1, SL 1, Open 1	Conversion to: HAL 1, Open 1; Retention, 1	Urine leak, 1; Re-exploration for bleed, 1		HAL re-exploration for bleed 1	Conversion to: SL 2; PE and angio-embolization 1	Conversion to: Open 1, SL cryoablation, DVT 1, MI 1, HTN'ive crisis 1, transfusion 2

RALPN robotic-assisted laparoscopic partial nephrectomy; *NR* not reported; *U* upper pole; *M* middle pole; *L* lower pole; *trans* transperitoneal; *retro* retroperitoneal; *EBL* estimated blood loss; *WIT* warm ischemia time; *Cold IT* cold ischemia time; *LOS* length of stay; *RCC* renal cell carcinoma; *HAL* hand-assisted laparoscopy; *SL* straight laparoscopy; *PE* pulmonary embolism; *DVT* deep venous thrombosis; *MI* myocardial infarction; *HTN'ive* hypertensive

[a]Pertain to the same data set from the same institution

[b]Does not include 20 min robot setup time

[c]Some smaller lesions were excised without hilar clamping after the index tumor was excised with the hilum clamped

conventional laparoscopic series. In the early series that have been reported, the most commonly reported complication is conversion to a conventional or hand-assisted laparoscopic approach and in one case an open approach. Most of these conversions have been required to control significant bleeding,[7,8] although conversion due to focal positive margin on frozen section examination and robotic camera malfunction necessitating conversion to a conventional laparoscopic technique have also been described.[6] Re-exploration for bleeding was reported in two separate series,[3,5] one of which required a nephrectomy to be performed.[3] The remainder of reported complications included urine leak[3] and postoperative hemorrhage requiring transfusion[9] and angioembolization[6] as well as ileus,[4,6] myocardial infarction (MI), DVT[9]/pulmonary embolism, postoperative atrial fibrillation, congestive heart failure,[6] and asymptomatic perinephric hematoma.[6,9]

Future Directions

Surgical robotics will inevitably undergo many modifications and advancements in the near future. The next generations of these systems will undoubtedly incorporate tactile feedback in more streamlined housings with less obtrusive maneuvering mechanisms. These may have advanced instruments designed for specific procedures and working with more freedom of movement. New systems are being developed that can integrate multiple imaging modalities in real time to allow for more accurate location of the tumor within the renal parenchyma. Advanced optics may be developed, which allow for more accurate visual discrimination between tumor and normal tissue as well as to clearly identify individual vessels through the use of various filters with or without the use of photo-pharmaceuticals. Whatever the future brings, this remains an invigorating time rife with an opportunity for innovation.

Conclusion

Overall, RALPN represents an exciting and new procedure which, while in its infancy, has demonstrated both feasibility and safety comparable with that of contemporary series of both open and laparoscopic partial nephrectomy series. With continued improvements in the available and future robotic surgical platforms, the technical difficulties of such complex urologic procedures may continue to be diminished leading to improved oncologic and functional outcomes for our patients.

References

1. Kelling G. Die Tamponade der Bauchhohle mit Luft zur Stillung lebensgefahrlicher Intestinalblutungen. *Munch Med Wochenschr*. 1901;48:1535–1538
2. Rogers CG, Singh A, Blatt AM, et al Robotic partial nephrectomy for complex renal tumors: surgical technique. *Eur Urol*. 2008;53:514
3. Kaul S, Laungani R, Sarle R, et al da Vinci-assisted robotic partial nephrectomy: technique and results at a mean of 15 months of follow-up. *Eur Urol*. 2007;51:186
4. Gettman MT, Blute ML, Chow GK, et al Robotic-assisted laparoscopic partial nephrectomy: technique and initial clinical experience with DaVinci robotic system. *Urology*. 2004;64:914
5. Deane LA, Lee HJ, Box GN, et al Robotic versus standard laparoscopic partial/wedge nephrectomy: a comparison of intraoperative and perioperative results from a single institution. *J Endourol*. 2008;22:947
6. Aron M, Koenig P, Kaouk JH, et al Robotic and laparoscopic partial nephrectomy: a matched-pair comparison from a high-volume centre. *BJU Int*. 2008;102:86
7. Phillips CK, Taneja SS, Stifelman MD. Robot-assisted laparoscopic partial nephrectomy: the NYU technique. *J Endourol*. 2005;19:441
8. Caruso RP, Phillips CK, Kau E, et al Robot assisted laparoscopic partial nephrectomy: initial experience. *J Urol*. 2006;176:36
9. Bhayani SB, Das N. Robotic assisted laparoscopic partial nephrectomy for suspected renal cell carcinoma: retrospective review of surgical outcomes of 35 cases. *BMC Surg*. 2008;8:16
10. La Vecchia C, Negri E, Levi F. Increasing incidence of renal cell cancer. *JAMA*. 1999;282:2120
11. Katner HP, Baynham SA. Increasing incidence of renal cell cancer. *JAMA*. 1999;282:2119
12. Chow WH, Devesa SS, Warren JL, et al Rising incidence of renal cell cancer in the United States. *JAMA*. 1999;281:1628
13. Mathew A, Devesa SS, Fraumeni JF Jr, et al Global increases in kidney cancer incidence, 1973–1992 *Eur J Cancer Prev*. 2002;11:171
14. Abaza R, Picard J. A novel technique for laparoscopic or robotic partial nephrectomy: feasibility study. *J Endourol*. 2008;22:1715
15. Herr HW. Partial nephrectomy for unilateral renal carcinoma and a normal contralateral kidney: 10-year followup. *J Urol*. 1999;161:33
16. Fergany AF, Hafez KS, Novick AC. Long-term results of nephron sparing surgery for localized renal cell carcinoma: 10-year followup. *J Urol*. 2000;163:442
17. Leibovich BC, Blute ML, Cheville JC, et al Nephron sparing surgery for appropriately selected renal cell carcinoma between 4 and 7 cm results in outcome similar to radical nephrectomy. *J Urol*. 2004;171:1066
18. Patard JJ, Shvarts O, Lam JS, et al Safety and efficacy of partial nephrectomy for all T1 tumors based on an international multicenter experience. *J Urol*. 2004;171:2181
19. Lau WK, Blute ML, VWeaver AL, et al Matched comparison of radical nephrectomy vs nephron-sparing surgery in patients with unilateral renal cell carcinoma and a normal contralateral kidney. *Mayo Clin Proc*. 2000;75:1236
20. Lee CT, Katz J, Shi W, et al Surgical management of renal tumors 4 cm. or less in a contemporary cohort. *J Urol*. 2000;163:730
21. Frank I, Blute ML, Cheville JC, et al Solid renal tumors: an analysis of pathological features related to tumor size. *J Urol*. 2003;170:2217
22. Fujii Y, Komai Y, Saito K, et al Incidence of benign pathologic lesions at partial nephrectomy for presumed RCC renal masses: Japanese dual-center experience with 176 consecutive patients. *Urology*. 2008;72:598
23. Kutikov A, Fossett LK, Ramchandani P, et al Incidence of benign pathologic findings at partial nephrectomy for solitary renal mass presumed to be renal cell carcinoma on preoperative imaging. *Urology*. 2006;68:737

24. Badani KK, Kaul S, Menon M. Evolution of robotic radical prostatectomy: assessment after 2766 procedures. *Cancer*. 2007;110: 1951
25. Azevedo OC, Azevedo JL, Sorbello AA, et al Evaluation of tests performed to confirm the position of the Veress needle for creation of pneumoperitoneum in selected patients: a prospective clinical trial. *Acta Cir Bras*. 2006;21:385
26. Azevedo JL, Guindalini RS, Sorbello AA, et al Evaluation of the positioning of the tip of the Veress needle during creation of closed pneumoperitoneum in pigs. *Acta Cir Bras*. 2006;21:26
27. Bemelman WA, Dunker MS, Busch OR, et al Efficacy of establishment of pneumoperitoneum with the Veress needle, Hasson trocar, and modified blunt trocar (TrocDoc): a randomized study. *J Laparoendosc Adv Surg Tech A*. 2000;10:325
28. Phelan MW, Perry KT, Gore J, et al Laparoscopic partial nephrectomy and minimally invasive nephron-sparing surgery. *Curr Urol Rep*. 2003;4:13
29. Berger A, Crouzet S, Canes D, et al Minimally invasive nephron-sparing surgery. *Curr Opin Urol*. 2008;18:462
30. Gill IS, Kavoussi LR, Lane BR, et al Comparison of 1,800 laparoscopic and open partial nephrectomies for single renal tumors. *J Urol*. 2007;178:41
31. Nguyen MM, Gill IS. Halving ischemia time during laparoscopic partial nephrectomy. *J Urol*. 2008;179:627

Robotic Sacral Colpopexy

5

Wesley M. White and Jihad H. Kaouk

Introduction

The demand for the repair of female pelvic organ prolapse has increased significantly as the general population has aged, yet remained active and focused on the quality of life.[1] The majority of evidence-based studies cite the importance of apical support in obtaining optimal and durable prolapse repair.[2,3] Although transvaginal repairs, with or without the use of synthetic mesh, have demonstrated adequate and reproducible outcomes; support of the vaginal apex is generally not emphasized during these procedures. As a consequence, remote objective failures and symptomatic recurrences are not uncommon.[3]

Contemporary clinical trials have demonstrated the superiority of abdominal-based prolapse repairs, including abdominal sacral colpopexy (ASC), in providing durable anatomical restoration and lower rates of dyspareunia.[3,4] However, open ASC is associated with increased morbidity and postoperative discomfort when compared with the transvaginal route. Indeed, the morbidity of open abdominal prolapse surgery has been a major impediment to its widespread application with many patients accepting lower success rates with vaginal surgery in exchange for improved aesthetics and faster recovery. In response to these shortcomings, laparoscopic ASC was introduced and refined during the last decade.[5] Laparoscopic ASC essentially mimics the open approach while decreasing the latter's attendant morbidity. Cumulative outcomes with laparoscopic ASC have been compared favorably with the open approach with decreased blood loss and pain and faster recovery.[5–9] Despite these advantages, laparoscopic ASC is associated with longer operative times and a steep learning curve that has largely limited its use.[10] Robotic ASC was introduced in 2004 in an attempt to overcome these limitations.[11] Thus far, outcomes have been equivalent or superior to laparoscopic ASC with a significantly shorter learning curve. In this chapter, we will review the preoperative evaluation for robotic ASC, describe our operative technique, and provide a balanced and concise review of the published literature on the subject.

Patient Evaluation

The indications for robotic ASC parallel those for laparoscopic and open ASC and include post-hysterectomy vaginal vault prolapse, prolapse recurrence following primary vaginal repair, primary prolapse when concomitant abdominal surgery is required, and, in appropriate circumstances, the repair of primary pelvic organ prolapse in females who have not undergone prior hysterectomy (sacral uteropexy).[12] Optimal candidates demonstrate symptomatic Stage II or greater anterior, apical, or posterior prolapse and, though not a specific contraindication, no or minimal prior abdominal surgeries are preferred. The goals of surgery should be the durable restoration of anatomy and the relief of urinary, sexual, bowel, and local symptoms. Certainly, treatment must be individualized and should consider the patient's risk factors, goals for treatment, and should optimally address all pathologies simultaneously.[13,14]

All patients should undergo a thorough history and physical examination. Specific attention should be paid to the patient's presenting symptoms and an attempt should be made to reconcile the symptom complex with physical exam findings.[15] In general, urinary, bowel, sexual, and other local symptoms (vaginal pressure, heaviness, or pain) predominate, and their impact on the quality of life should be elicited. It is often helpful to administer quality of life questionnaires (urogenital distress inventory (UDI-6) or Incontinence Impact Questionnaire (IIQ-7)) to establish a baseline for later reference.[16]

Urinary symptoms are frequently encountered in women with pelvic organ prolapse, and it is essential to elucidate the nature and severity of these symptoms.[17] Patients often report urgency and frequency of urination with or without concomitant urge incontinence, nocturia, hesitancy of urination, especially in the setting of severe prolapse, and stress urinary incontinence.[12,18] A voiding log and postvoid residual measurement are administered to all patients and are invaluable in objectively translating patient complaints. Pad weight testing is appropriate in patients with significant incontinence. The ancillary and judicious use of urodynamic testing is frequently helpful in objectively demonstrating and quantifying symptoms, especially in the circumstance of suspected stress

P. Dasgupta et al. (eds.), *New Technologies in Urology,*
DOI: 10.1007/978-1-84882-178-1_5, © Springer-Verlag London Limited 2010

urinary incontinence, in which leakage can be masked by severe prolapse more than 80% of the time.[18–20]

The physical examination should be thorough, focused, and systematic. The abdomen should be inspected for any scars or evidence of prior surgery. A bimanual examination should be performed to determine the size and location of the uterus if present and to rule out the presence of any adnexal pathology. With the use of a bivalved speculum or its equivalent, the vagina is evaluated for hypoestrogenism, urethral hypermobility (Q-tip test), prolapse, and the integrity of the perineal body and rectal sphincter.[12,21,22] Optimally, the anterior, apical, and posterior walls of the vagina should be individually inspected for the evidence of prolapse and quantified utilizing the pelvic organ prolapse quantification (POPQ) system.[23] Cystoscopic evaluation is generally not indicated in patients with an uncomplicated clinical picture.[24,25]

Preoperative medical clearance, especially among women of advanced age, is appropriate and should be individualized. Similarly, preoperative formal imaging is rarely indicated. Although magnetic resonance imaging is an accurate and reproducible means of diagnosing and staging pelvic organ prolapse, its utility is as yet unproven.[26–28]

Operative Technique

Patients are brought to the operating room and placed in the supine position for induction. After general anesthesia is administered, the patient's arms are tucked and hands are padded with the thumb in the upright position. After removing and/or lowering the foot of the bed, the patient's perineum is centered at the distal end of the bed. Both legs are placed in Allen stirrups with each knee facing the contralateral shoulder (low lithotomy position). Padding is placed laterally to protect the peroneal nerves. An additional pad is placed across the patient's chest, and the patient is secured to the table with 2 in. silk tape. The abdomen and perineum are prepped widely with betadine or chlorhexadine solution. Particular attention should be paid to the preparation of the vagina, as vaginal sizer will be used to reduce the apex to an appropriate location during graft positioning. A Foley catheter is placed and left to gravity drainage. A sterile drape specifically designed for laparoscopy (pre-fabricated service pockets and Velcro straps) is employed. When appropriately used, these drapes can provide order during the operative procedure and efficiency of instrument exchange.

Following the identification of relevant landmarks, an approximate 12 mm peri-umbilical incision is made. Ideally, this incision should be no less than 14 cm from the pubic bone to ensure adequate intraoperative visualization. The rectus fascia is palpated, a Veress needle is introduced through the fascia into the peritoneal cavity, and intra-peritoneal access confirmed with a saline drop test. The Veress needle should always be aspirated to rule out vascular or visceral transgression. Alternatively, an open Hasson technique can be used. The abdomen is insufflated with CO_2 gas to a maximum pressure of 15 mmHg. Once adequate pneumoperitoneum has been achieved, the Veress needle is removed and exchanged for a 12 mm operative trocar (port 1). A standard operative laparoscope or the robotic camera is introduced through this initial port and the peritoneal cavity is inspected. The patient is placed in steep Trendelenburg and the operating table is lowered maximally. Under direct vision, two additional 8 mm robotic trocars (ports 2 and 3) are placed approximately 9 cm lateral and just caudad to the peri-umbilical trocar. If employing a 4-armed da Vinci® robot (Intuitive Surgical, Sunnyvale, CA), an additional 8 mm robotic trocar (port 6) is placed 2 cm cephalad and medial to the left anterior superior iliac spine. If a 3-armed robot is to be used, a 5 mm standard trocar is placed in this location for bedside assistance. A 12 mm standard trocar (port 4) is placed on the patient's right side for suction/irrigation and the passage of mesh/sutures. An additional 5 mm trocar (port 5) can be placed as needed for additional assistance (Fig. 5.1).

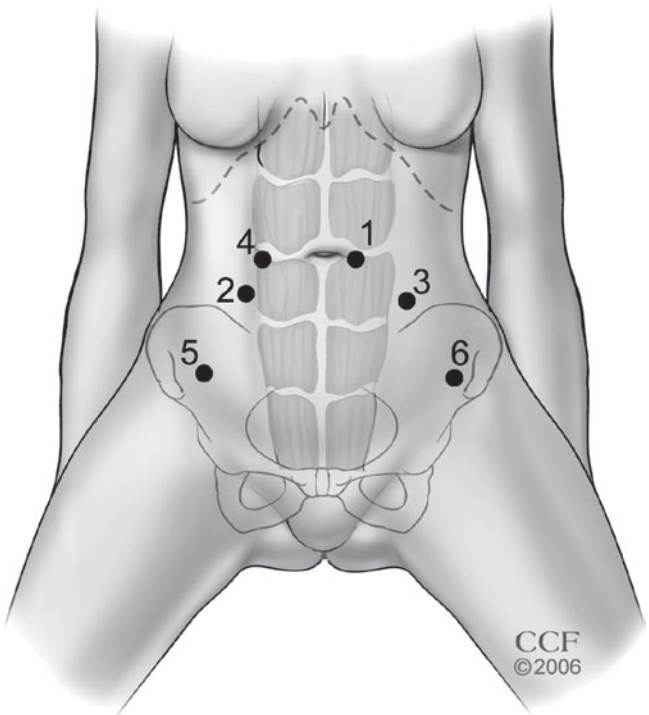

Fig. 5.1 Schematic representation of port configuration during robotic-assisted laparoscopic abdominal sacral colpopexy. The patient is placed in the lithotomy position with arms tucked at the side. The robotic camera is placed in port 1 and robotic instruments are placed in ports 2 and 3. Port 4 is used by the bedside assistant for suction/irrigation and the passage of mesh/sutures. Ports 5 and 6 may be placed as needed for additional assistance. Reprinted with the permission of The Cleveland Clinic Center for Medical Art & Photography © 2008. All Rights Reserved

The da Vinci® robot is positioned with its base equidistance between the patient's legs. The base of the robot should be far enough away from the end of the table to allow an assistant to place a vaginal sizer during dissection of the vaginal cuff. The camera arm is connected to port 1 and instrument arms are connected to ports 2, 3, and 6 (if a 4-armed robot is used). A 0° scope is used. Monopolar shears or hook cautery are applied to the right hand and atraumatic grasping forceps are applied to arms 2 and 3. An assistant is positioned on the patient's right side to exchange instruments (suction/irrigator or atraumatic small bowel grasper) and introduce suture and mesh through ports 4 and 5.

The sigmoid colon is identified and retracted laterally to the left with arm 3 to facilitate exposure of the sacral promontory. If a first generation robot is used, an assistant may use a locking grasper to retract the colon. In either situation, atraumatic grasping forceps should be used and the colon should be grasped by its taenia coli and held under appropriate but not excessive static tension (Fig. 5.2). Alternatively, a silk stitch may be introduced percutaneously from the left side and a figure-of-eight suture placed through the taenia coli to retract the sigmoid colon.

The sacral promontory and presacral space are visualized and its borders confirmed by the bedside assistant through tactile feedback. The posterior peritoneum overlaying the sacrum is incised superficially. Deep dissection is discouraged as sacral veins are encountered at this level. It is important to incise the peritoneum evenly to avoid difficulty with its eventual closure. A vaginal sizer is placed to facilitate subsequent dissection and to reduce the vagina to a normal anatomical position in preparation for mesh placement. The bladder is dissected from the anterior vagina and the posterior vagina is dissected from the colon. A pre-fashioned Y-shaped polypropylene mesh is introduced by the assistant through port 4 or 5. With the vagina appropriately reduced, the mesh is sutured to the apex of the vagina anteriorly and posteriorly with 0 nonabsorbable (Ethibond, Ethicon, New Brunswick, NJ) suture (Fig. 5.3). The tail of the mesh is affixed to the sacral promontory at the level of S1–S2 with a laparoscopic tacking device, suture through the superficial periosteum, or a commercially available drill designed specifically for sacral colpopexy (American Medical Systems, Minnetonka, MN). The mesh should adequately reduce the vagina to a normal anatomic position but should not be under

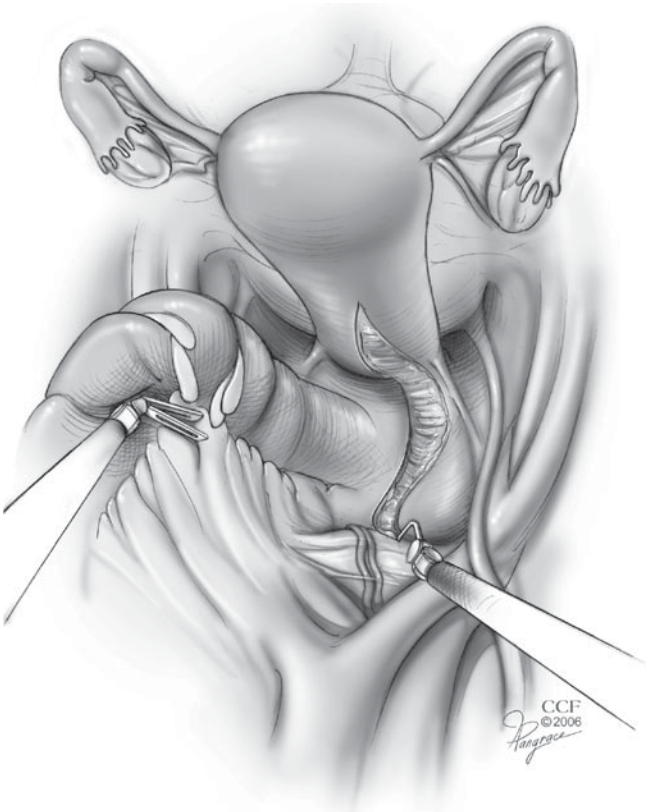

Fig. 5.2 The sigmoid colon is reflected laterally using a ProGrasp instrument in the left hand and the posterior peritoneum of the cul-de-sac is incised superficially with a J-hook to expose the underlying sacral promontory. Reprinted with the permission of The Cleveland Clinic Center for Medical Art & Photography © 2008. All Rights Reserved

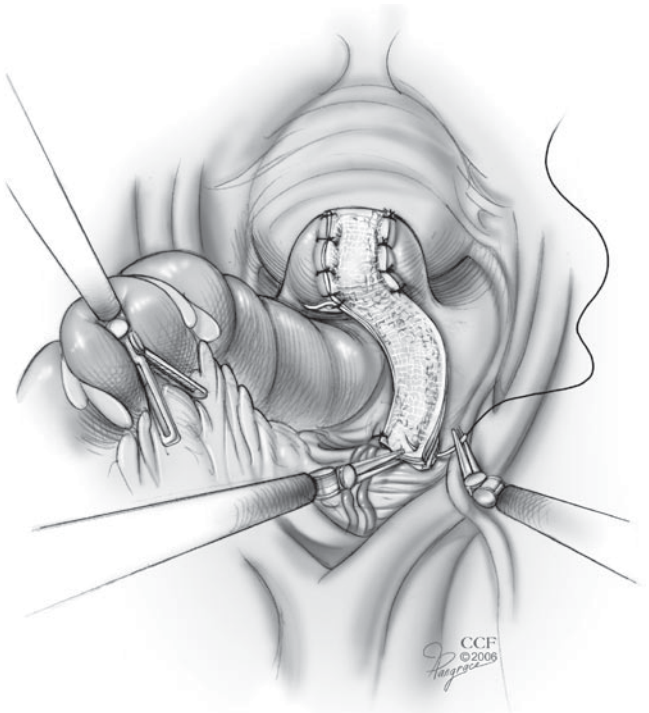

Fig. 5.3 A pre-fashioned Y-shaped portion of mesh is sutured to the vaginal cuff and affixed under appropriate tension to the sacral promontory to effect vaginal reduction. Reprinted with the permission of The Cleveland Clinic Center for Medical Art & Photography © 2008. All Rights Reserved

any undue tension. Cystoscopy is performed to rule out transvesical placement of any suture material. The excess mesh is excised and the peritoneal flaps are closed over the graft with 2–0 absorbable suture. When necessary or at the discretion of the operating surgeon, a culdoplasty may be performed.

The abdomen is inspected thoroughly and the sigmoid colon is returned to its normal anatomic position. The robot arms are disengaged and the robot undocked. The 12 mm ports are sequentially removed and the fascia closed with 1–0 Vicryl suture with the aid of a Carter-Thompson needle. All skin incisions are closed with a running, subcuticular 5–0 Monocryl suture. Following skin closure, the vagina should be reinspected and a decision is rendered regarding the need for additional procedures including anterior plication. Additionally, transvaginal or transobturator sling placement for stress urinary incontinence should be performed at this time if needed. A vaginal pack is placed and may be soaked in betadine or estrogen cream.

Patients are admitted for 23 h following surgery. A clear liquid diet is allowed during the night following surgery and bed rest is prescribed. Postoperative laboratory testing is generally unnecessary. Oral narcotics and intravenous breakthrough ketorolac are used for pain control. The vaginal pack and Foley catheter are removed in the morning of postoperative day 1. The patient is ambulated and the diet is advanced as tolerated. Once the patient has adequate pain control with oral narcotics, is tolerating a regular diet, and is voiding freely, she is discharged home. Patients are instructed to avoid heavy lifting (>15 pounds) and sexual intercourse for a minimum of 4 weeks. A stool softener should be prescribed to avoid postoperative constipation and resultant straining. Patients are re-evaluated at the first and third month following surgery with repeated POPQ evaluation.

Comparative Outcomes with Robotic Abdominal Sacral Colpopexy

First proposed in 1962, open ASC has changed little since its inception and original description.[29,30] Cumulative outcomes with open ASC have been excellent with reported success rates (absence of apical prolapse) of between 80 and 100% at a mean follow-up of 6 months to 3 years.[2,31] Complications have been relatively uncommon and include hemorrhage and hematoma (3%), injury to adjacent organs (1.6%), and the need for re-exploration for bowel obstruction or other abdominal pathology (3%).[31] The rate of reoperation for prolapse following ASC approaches 4%.[2] When compared directly with vaginal apical restorative surgery in prospective and retrospective trials, open ASC has consistently demonstrated a lower objective rate of recurrent vault prolapse and dyspareunia.[32] However, the anatomical superiority of open ASC comes at the expense of increased costs, longer operative times, and higher morbidity.[3] Patients must therefore choose between an objectively superior abdominal procedure with more discomfort and risk or a less successful vaginal procedure with lower attendant morbidity. Although the morbidity of open ASC has never been specifically identified as an impediment to its broad application, it is generally reserved for younger patients with better overall vitality, those patients who have failed prior vaginal reconstruction, and/or those with concomitant abdominal pathology.[12]

Recognizing the limitations of open ASC, urologists and urogynecologists described and refined laparoscopic ASC in the mid 1990s.[5–9] Laparoscopic ASC essentially recreates the open procedure with some minor modifications, and ostensibly offers superior visibility, less postoperative pain, and improved cosmesis. Indeed, objective and subjective success rates with laparoscopic ASC have rivaled or surpassed outcomes with open ASC. Nearly 1,000 laparoscopic ASC cases have been reported thus far with favorable outcomes in greater than 90% (Table 5.1). Of note, one dedicated, retrospective comparative cohort study was performed by Paraiso and colleagues in 2005, in which open ASC was compared with laparoscopic ASC.[9] The laparoscopic cohort demonstrated longer operative times, decreased blood loss, and a shorter duration of hospitalization. The objective success and complication rates were similar between the two groups.

Table 5.1 Comparative outcomes of laparoscopic and robotic ASC

Author	Method of repair	Number of patients	Duration of follow-up	Success rate (%)
Nezhat et al[7]	Laparoscopic	15	3–40 months	100
Ross[38]	Laparoscopic	89	1 year	94
Cosson et al[39]	Laparoscopic	83	<1 year	94
Wattiez et al[6]	Laparoscopic	125	32 months	93.4
Antiphon et al[8]	Laparoscopic	104	17 months	75
Rozet[40]	Laparoscopic	363	14.6 months	96
Paraiso et al[9]	Laparoscopic	55	13.5 months	87.5
DiMarco et al[11]	Robotic	5	4 months	100
Elliott et al[35]	Robotic	19	5.1 months	100
Elliott et al[36]	Robotic	30	24 months	96.6
Daneshgari et al[37]	Robotic	12	3.1 months	100

Despite the tangible and reproducible benefits offered by laparoscopic ASC, this procedure has similarly experienced limited widespread applicability owing to its generous learning curve.[12] Much like laparoscopic radical prostatectomy and laparoscopic partial nephrectomy, laparoscopic ASC demands expertise in intracorporeal suturing and a resolute commitment by the operating surgeon to develop and maintain this skill set.

The introduction and FDA approval of robotics in 2000 revolutionized urologic surgery by offering the advantages of laparoscopy with a considerably shorter learning curve. Although initially used exclusively for radical prostatectomy by most urologists, its application and advantages in the field of extirpative and reconstructive renal and pelvic surgery is now being realized. The robotic platform is ideally suited for reconstructive procedures given its superior optics, its capacity to filter tremor, and its ability to operate freely and precisely in a confined field. Moreover, myriad studies have successfully demonstrated that robotic reconstructive procedures can be performed with confidence and safety even among surgeons with little to no formal laparoscopic experience.[33,34]

Robotic ASC combines the gold standard anatomical repair of open ASC with the decreased morbidity of laparoscopy, and makes it accessible, feasible, and reproducible across the entire field of urology and urogynecology. The first published reports of robotic ASC came from Elliott and colleagues at the Mayo Clinic in 2004.[11,35] Their initial experience in the treatment of 20 patients with symptomatic vaginal vault prolapse was very favorable. Nineteen of 20 patients underwent successful robotic ASC without complications. The mean length of stay was approximately 1 day. At a mean follow-up of 5.1 months, one patient developed recurrent prolapse (rectocele only) and nearly all patients (90%) were subjectively satisfied with the results of their operation. The authors concluded that robotic ASC "facilitated precise intracorporeal suture placement so that the procedure could be done in a fashion similar to the open method." Additional studies published in 2004 and 2006 corroborated their findings and documented durability of the repair.[35,36]

In 2007, a second report of robotic ASC was published by Daneshgari and colleagues from the Cleveland Clinic.[37] Twelve patients with symptomatic pelvic organ prolapse underwent successful robotic ASC with preoperative and postoperative POPQ examination. Mean POPQ stage preoperatively was 3.1. Mean estimated blood loss was 81 mL and mean operative time was 317 min. The mean length of hospitalization was 2.4 days. At a mean follow-up of 3.1 months, the mean POPQ stage was 0. The authors concluded that robotic ASC was safe and feasible but not without technical limitations. They cited a longer initial learning curve than the traditional laparoscopy owing to the increased technological burden that is inherent to robotics (i.e., positioning of trocars, set-up of the robotic arms and joints, etc). However, they found that simple modifications to their initial operation and setup yielded significantly shorter operative times and fully exploited the ergonomic advantages of the robot, namely complex dissection in a swift, precise manner.[37]

In our experience, robotic ASC is safe, expedient, and can be easily performed by urologists who are familiar with the robotic platform and are adept at robotic suturing. By employing our aforementioned set-up and operative technique, many of the limitations inherent to robotic ASC should be obviated and, as a result, the learning curve should be curtailed. Certainly, any discussion of robotics must address not only the technical limitations and benefits of robotics, but also issues related to capital overhead and the cost of disposables. One must bear in mind that although robotic ASC is, in our opinion, a significant advance, its utility and clinical superiority have yet to be proven in prospective, multi-center trials.

Conclusion

The essential tenet of surgery for pelvic organ prolapse is the durable restoration and repositioning of the pelvic structures in a fashion that relieves symptoms, treats concomitant pelvic disease, and improves urinary, bowel, and sexual function. The preponderance of evidence-based studies and systematic reviews cite apical support as the cornerstone of effective and durable treatment. Though abdominal procedures offer anatomically superior apical support, patients are often reluctant to undergo a potentially morbid and cosmetically unpleasing procedure. Robotic ASC offers equivalent objective outcomes with lower attendant morbidity, and makes the procedure accessible and reproducible among junior or inexperienced laparoscopists. Despite these advantages, future long-term studies are needed to answer two questions: does robotic ASC offer improved and discernable patient outcomes, and is robotic ASC cost-effective? As the field of laparoscopy trends further toward robotics as a whole and improved robotic instrumentation and platforms are introduced, we believe the answer to these two questions is yes.

References

1. Olsen AL, Smith VJ, Bergstrom JO, et al Epidemiology of surgically managed pelvic organ prolapse and urinary incontinence. *Obstet Gynecol*. 1997;89:501–506
2. Nygaard IE, McCreery R, Brubaker L, et al Abdominal sacrocolpopexy: a comprehensive review. *Obstet Gynecol*. 2004;104:805–823
3. Maher C, Baessler K, Glazener CM, et al Surgical management of pelvic organ prolapse in women. *Cochrane Database Syst Rev*. 2007;(3):CD004014

4. Maher CF, Qatawneh AM, Dwyer PL, et al Abdominal sacral colpopexy or vaginal sacrospinous colpopexy for vaginal vault prolapse: a prospective randomized study. *Am J Obstet Gynecol*. 2004;190:20–26
5. Rozet F, Mandron E, Arroyo C, et al Laparoscopic sacral colpopexy approach for genito-urinary prolapse: experience with 363 cases. *Eur Urol*. 2005;47:230–236
6. Wattiez A, Canis M, Mage G, et al Promontofixation for the treatment of prolapse. *Urol Clin North Am*. 2001;28:151–157
7. Nezhat CH, Nezhat F, Nezhat C. Laparoscopic sacral colpopexy for vaginal vault prolapse. *Obstet Gynecol*. 1994;84:885–888
8. Antiphon P, Elard S, Benyoussef A, et al Laparoscopic promontory sacral colpopexy: is the posterior, recto-vaginal, mesh mandatory? *Eur Urol*. 2004;45:655–661
9. Paraiso MF, Walters MD, Rackley RR, et al Laparoscopic and abdominal sacral colpopexies: a comparative cohort study. *Am J Obstet Gynecol*. 2005;192:1752–1758
10. Miklos JR, Moore RD, Kohli N. Laparoscopic surgery for pelvic support defects. *Curr Opin Obstet Gynecol*. 2002;14:387–395
11. DiMarco DS, Chow GK, Gettman MT, et al Robotic-assisted laparoscopic sacrocolpopexy for treatment of vaginal vault prolapse. *Urology*. 2004;63:373–376
12. Herschorn SH. Vaginal reconstructive surgery for sphincteric incontinence and prolapse. In: Kavoussi LR, Novick AC, Partin AW, Peters CA, and Wein AJ, eds. *Campbell-Walsh Urology*. 9th ed. Philadelphia, PA: Saunders; 2007:2187–2233
13. Wall LL, Versi E, Norton P, et al Evaluating the outcome of surgery for pelvic organ prolapse. *Am J Obstet Gynecol*. 1998;178:877–879
14. Kobashi KC, Leach GE. Pelvic prolapse. *J Urol*. 2000;164:1879–1890
15. Bump RC, Mattiasson A, Bo K, et al The standardization of terminology of female pelvic organ prolapse and pelvic floor dysfunction. *Am J Obstet Gynecol*. 1996;175:10–17
16. Donovan J, Bosch R, Gotoh M, et al Symptom and quality of life assessment. In: Abrams P, Cardozo L, Khoury S, Wein A, eds. *Incontinence: 3rd International Consultation*. Plymouth, UK: Health Publications; 2005:519–584
17. McGuire EJ. Bladder instability and stress incontinence. *Neurourol Urodyn*. 1988;7:563–567
18. Romanzi LJ, Chaikin DC, Blaivas JG. The effect of genital prolapse on voiding. *J Urol*. 1999;161:581–586
19. Fianu S, Kjaeldgaard A, Larson B. Preoperative screening for latent stress incontinence in women with cystocele. *Neurourol Urodyn*. 1985;4:3–7
20. Rosenzweig B, Pushkin S, Blumenfeld D, et al Prevalence of abnormal urodynamic test results in continent women with severe genitourinary prolapse. *Obstet Gynecol*. 1992;79:539–542
21. Fantl JA, Cardozo L, McClish DK. Estrogen therapy in the management of urinary incontinence in postmenopausal women: a meta-analysis. First report of the Hormones and Urogenital Therapy Committee. *Obstet Gynecol*. 1994;83:12–18
22. Crystle CD, Charme LS, Copeland WE. Q-tip test in stress urinary incontinence. *Obstet Gynecol*. 1971;38:313–315
23. Bump RC, Hurt WG, Theofrastous JP, et al Randomized prospective comparison of needle colposuspension versus endopelvic fascia plication for potential stress incontinence prophylaxis in women undergoing vaginal reconstruction for stage III or IV pelvic organ prolapse. The Continence Program for Women Research Group. *Am J Obstet Gynecol*. 1996;175:326–333
24. Fantl JA, Newman DK, Colling J, et al *Urinary Incontinence in Adults: Acute and Chronic Management*. Clinical Practice Guideline No. 2 Update. Rockville, MD: U.S. Department of Health and Human Services, Public Health Service, Agency for Health Care Policy and Research; 1996
25. Vasavada SP, Comiter CV, Raz S. Cytoscopic light test to aid in the differentiation of high-grade pelvic organ prolapse. *Urology*. 1999; 54:1085–1087
26. Yang A, Mostwin JL, Rosenshein NB, et al Pelvic floor descent in women: dynamic evaluation with fast MR imaging and cinematic display. *Radiology*. 1991;179:25–33
27. Singh K, Reid WM, Berger LA. Assessment and grading of pelvic organ prolapse by use of dynamic magnetic resonance imaging. *Am J Obstet Gynecol*. 2001;185:71–77
28. Tubaro A, Artibani W, Bartram CI, et al Imaging and other investigations. In: Abrams P, Cardozo L, Khoury S, Wein A, eds. *Incontinence: 3rd International Consultation*. Plymouth, UK: Health Publications; 2005:707–797
29. Birnbaum SJ. Rational therapy for the prolapsed vagina. *Am J Obstet Gynecol*. 1973;115:411–419
30. Sutton GP, Addison WA, Livengood CH III, et al Life-threatening hemorrhage complicating sacral colpopexy. *Am J Obstet Gynecol*. 1981;140:836–837
31. Beer M, Kuhn A. Surgical techniques for vault prolapse: a review of the literature. *Eur J Obstet Gynecol Reprod Biol*. 2005;119:144–155
32. Maher CF, Qatawneh AM, Dwyer PL, et al Abdominal sacral colpopexy or vaginal sacrospinous colpopexy for vaginal vault prolapse: a prospective randomized study. *Am J Obstet Gynecol*. 2004; 190:20–26
33. Yohannes P, Rotariu P, Pinto P, et al Comparison of robotic versus laparoscopic skills: is there a difference in the learning curve? *Urology*. 2002;60:39–45
34. Bentas W, Wolfram M, Brautigam R, et al daVinci robot assisted Anderson-Hynes dismembered pyeloplasty: technique and 1 year follow-up. *World J Urol*. 2003;21:133–138
35. Elliott DS, Frank I, DiMarco DS, et al Gynecologic use of robotically assisted laparoscopy: sacrocolpopexy for the treatment of high-grade vaginal vault prolapse. *Am J Surg*. 2004;188:52–56
36. Elliott DS, Krambeck AE, Chow GK. Long-term results of robotic assisted laparoscopic sacrocolpopexy for the treatment of high grade vaginal vault prolapse. *J Urol*. 2006;176:655–659
37. Daneshgari F, Kefer JC, Moore C, et al Robotic abdominal sacrocolpopexy/sacrouteropexy repair of advanced female pelvic organ prolapse (POP): utilizing POP-quantification-based staging and outcomes. *BJU Int*. 2007;100:875–879
38. Ross JW. Laparoscopic approach for severe pelvic vault prolapse. *J Am Assoc Gynecol Laparosc*. 1996;3:S43
39. Cosson M, Bogaert E, Narducci F, et al Laparoscopic sacral colpopexy: short-term results and complications in 83 patients. *J Gynecol Obstet Biol Reprod*. 2000;29:746–750
40. Rozet F, Mandron E, Arroyo C, et al Laparoscopic sacral colpopexy approach for genito-urinary prolapse: experience with 363 cases. Eur Urol. 2005;47:230–236

Principles of Robotic-Assisted Surgery in Children

6

Azad Najmaldin

Introduction

The application of intra-luminal endoscopy and laparoscopy in children was virtually unknown until 1971, when Gans and Berci reported the procedures as safe diagnostic measures.[1] Since then, the feasibility, safety, and benefits of therapeutic endoscopy (minimal access surgery-thoracoscopy and laparoscopy) in infants and children have been widely reported, and the number and types of procedures performed endoscopically have grown at a rate consistent with improvements in the advances of technology, training of surgeons and patients, and media awareness of the advantages of the techniques. Children may be expected to have laparoscopic nephrectomy as a day case and Nissen's fundoplication and pyeloplasty with an overnight hospital stay and minimal, if any, narcotic analgesia, and infants undergo colonic procedures, lung resection, and esophageal atresia repair with minimal morbidity and short hospital stay.[2]

Telerobotic surgery represents an advance for minimal access surgery. Although its advantages in radical prostatectomy are well documented,[3] the application of the new technique in both adult and pediatric surgical practice remains in its early infancy.

This chapter highlights the aspects of the current status of robotic-assisted surgery in children.

Pediatric Surgeons and Telerobotics

In 1998, clinical robotics was introduced to the world of adult surgery.[4] In the year 2000, pediatric surgeons from Europe and USA investigated the feasibility and potentials of robotic-assisted surgery for fundoplication and pyeloplasty.[5–7] Since then, increasing numbers of surgeons have reported the success of the new technique in a growing range of pediatric surgical subspecialties, namely cervical and transoral, thoracic, cardiovascular, gastrointestinal, and urological (Table 6.1).

In a prospective study, Lehnert et al[8] compared ten robotic Thall anti-reflux procedures with ten manual laparoscopic similar problems. The patients' mean age was 11.4 ± 1.4 years. There were no operative or postoperative complications and the overall operating time was similar. However, the authors concluded that the Da Vinci robotic system was superior and faster for dissection and suturing, but the setup time was longer. Anderberg et al[9] compared postoperative data from six Da Vinci robotic Nissen's fundoplications with historic data from six manual laparoscopic and six open procedures in children matched for age (2–11 years old) and severity of the preexisting condition. They had no complications and concluded that the operative time for the robot was comparable with that of the laparoscopy but longer than open procedures and analgesia requirements and hospital stay were similar in the robotic and laparoscopic groups, but shorter than open.

Meehan and Sandler[10] reported a large series of children who underwent robotic surgery using the Da Vinci system. This report included 100 cases, 89% abdominal and 11% thoracic. Although the majority of procedures had never been performed using minimally invasive techniques by the authors, 31 different types of procedures were attempted in patients whose age ranged from 1 day to 23 years with the average being 8.4 years and 22% being less than 10 kg of body weight (range 2.2–103 kg). They had a 13% conversion rate for nonrobot-related complications. However, five of these patients suffered significant bleeding as a result of accessory conventional laparoscopic instrumentation. The authors concluded that robotic surgery in infants and children is safe and ideal for complex hepatobiliary and thoracic conditions. Luebbe and associates[11] reported the first series of 20 abdominal procedures with a total complication rate of 15%. In this report, the mean age of the patients was 8.4 years, the youngest being 4 months old. One patient developed a pneumothorax during the Morgagni diaphragmatic hernia repair and another two suffered significant bleeding during splenectomies, but none of the patients encountered hemodynamic instability or required blood transfusions. The authors concluded that even in the learning phase, complications following telerobotic surgery appear low.

In 2002, Le Bret and associates[12] described the success of robotic-assisted ligation of patent ductus arteriosis in a large series of children with an average age of 20 months using the Zeus robotic system. Suematsu et al[13] reported the use of the

P. Dasgupta et al. (eds.), *New Technologies in Urology,*
DOI: 10.1007/978-1-84882-178-1_6, © Springer-Verlag London Limited 2010

Table 6.1 Robotic pediatric operations (urological procedures are highlighted)

Transaxillary thyroid	Cases
Transoral larynx	Short series
Patent ductus and vascular ring	Series
Pulmonary	Cases
Esophageal atresia	Cases
Anterior and posterior mediastinal masses and cysts	Cases
Congenital diaphragmatic hernia	Cases
Tumor – benign and malignant – chest, abdomen, and retroperitoneal	Short series
Heller myotomy	Cases
Hiatal repair and fundoplication	Large series
Gastrostomy	Short series
Cholecystectomy	Large series
Biliary atresia and choledochal cyst	Cases
Splenectomy	Short series
Duodenal and pylorus	Cases
Pancreas	Cases
Small intestine – variety	Cases
Large intestine	Cases
Rectal pull-through and prolapse	Cases
Adrenal	Cases
Nephrectomy/partial nephrectomy	Large series
Pyeloplasty	Large series
Ureter	Short series
Bladder	Cases
Urinary stone	Cases
Mullerian remnants	Cases
Ovarian	Cases
Urachus	Cases
Testis	Cases
Experimental	Short reports
Fetal – experimental	Cases

Da Vinci system in 15 children between the ages 3 and 18 who underwent closure of patent ductus arteriosis and division of vascular ring. The authors concluded that the system was safe and that future technologic improvement, including miniaturization of instruments and the incorporation of tactile feedback, might allow the technique to be applied in young infants and intracardiac procedures. Robotic retroperitoneal[6] and transperitoneal[7] pyeloplasty in children were reported in the early 2000s. In a retrospective case-controlled study, Lee et al[7] compared 33 robotic with 33 open pyeloplasties in children whose age ranged from 0.2 to 19 years. There were no conversions or operative complications. However, one patient in the robotic group required redo surgery for recurrent obstruction. The mean operating time was significantly longer in the robotic group (219 and 181 min, $p = 0.031$), but the postoperative narcotic requirements ($p = 0.001$) and hospital stay (2.3 and 3.5 days, $P < 0.001$) were significantly less. The authors have also quoted that with experience the robotic operating time decreased and approached the open technique experience.

In an interesting report by Rahbar et al[14] using the Da Vinci system, the application and safety of transoral intraluminal robotic surgery in the pediatric airway was tested. The authors tried four pediatric cadaver larynxes at first followed by five children with laryngeal cleft defects (age 1–14 years). They had two successes and three failures with the size of the equipment and instruments being the limiting factor.

Other authors have published successful case reports of robotic procedures covering the pediatric age groups and a wide variety of conditions including thyroid surgery,[15] thoracic,[10,11] upper and lower gastrointestinal procedures,[10] biliary including choledochal cyst, biliary atresia,[10,16] and renal bladder and pelvic surgery.[17]

The feasibility and safety of intrauterine (fetal) robotic surgery has also been investigated in animal models with specific reference to congenital defects such as myelomeningocele and diaphragmatic hernia.[18,19]

Personal Experience

From March 2006 to March 2009 (including the learning phase), using the Da Vinci system, the author has personally carried out 144 procedures in 115 patients involving 23 different types of transperitoneal procedures with 44% being gastrointestinal and 56% urological. The mean age at the time of surgery was 6.8 ± 3.7 (7 months–16 years) including three patients weighing <7 kg. At the start of the new program, our setup and operating times were long.[20] Nowadays and with an experienced theater team, the nursing setup time can be as short as 25 min, robot docking time 4 min (robot moved into position, arms and instruments fixed and ready to use), and console time for pyeloplasty 120 min and fundoplication 58 min. We have had five (4.3%) conversions: robotic related one (mechanical failure) and non-robotic related four. On a few occasions, procedures were delayed for 13–32 min owing to the faulty signals within the system. So far, we have had no robot-related complications, and outcomes of surgery have been comparable with that of conventional laparoscopic and open techniques. In our hands, the requirements for preoperative and postoperative analgesia and duration of hospital stay were no different from that of laparoscopic surgery.

Table 6.2 Results of robotic-assisted pyeloplasty (one surgeon – including the learning curve)

Patients	34 (9 months–15 years)
Conversion	2 – Mechanical robot failure = 1 Difficulty with stent insertion = 1
Operating time	
Nursing preparation	20–45 min
Docking	10.9 min (4–20)
Console	167 min (120–200)
Total	217 min (180–280)
Postoperative analgesia	13 h (0–23) narcotics
Complications	
Robotic	None
Nonrobotic	1 – Stent displacement and extravasation
Hospital stay	2 days (1–6)
Follow-up	5 weeks–36 months
	U/S ± MAG3

Table 6.2 illustrates the results of the most common robotic procedure carried out by the author.

Advantages and Limitations of Pediatric Robotics

The complexity and reconstructive nature of many pediatric surgical procedures, and patients' spectrum that spans from unborn fetuses and infants to older children and adolescents demands high grades of operating view, dexterity, and precision. The three-dimensional panoramic high-resolution views with depth, perception, ability to directly control a stable visual operating field with increased magnification, intuitive increased freedom of movements, motion scaling, near normal restoration of eye and hand coordination, and superior ergonomics, make the robot a near ideal tool for pediatric and neonatal surgery.

Other, but potential, advantages of the system include: the reduced learning curve for new and established minimal access surgical procedures,[21] and delivering safe, advanced, and emergency procedures in smaller locations where specialist skills are absent.[22]

The robotic system has overcome many difficulties in the development of minimal access surgery and enhanced the surgeon's ability to execute complex surgical procedures that were previously thought to be technically demanding.[10,12,14] However, the system is not without limitations. A complete lack of haptics necessitates surgeons to take extra care while handling pediatric delicate tissues and microsuture materials. Other disadvantages emanate from the size of the mobile slave unit and instruments. The size discrepancy may restrict anesthetist's access to the patient (upper abdomen and thoracic procedures, and small children) and allow arm and instrument collision outside and inside the patient, respectively (infants and small children). The recently developed 8 mm telescope represents an improvement over the 12 mm telescope. The 5 mm telescope is capable of delivering two-dimensional images. Both 5 and 8 mm instruments are effective; however, smaller instruments would undoubtedly enhance the surgeon's ability to work in a smaller working space and further reduce surgical trauma.

The capital and maintenance costs of the Da Vinci system are significantly higher than conventional open and minimal access surgery equipment. However, the cost of consumables is comparable with that of disposable minimal access surgery instruments.

Operative Considerations

The ability to perform safe and successful robotic procedures relies greatly on the understanding of general and specific principles of surgery/minimally invasive surgery, and appropriate application of the equipment and instruments as well as safe access and the creation of an operative space. Failure to do this produces unnecessary complications and puts patients at risk.

The procedure is performed under general anesthesia with intubation, full muscle relaxation and controlled ventilation. There is no place for local, regional, or spinal/epidural anesthesia in pediatric robotic surgery. During induction, gaseous distension of the gastrointestinal tract should be avoided as even a slight dilatation can jeopardize safe access and increases the risks of conversion to open method surgery. This is particularly so in infants and small children. Nasogastric aspiration via a tube improves access in the upper abdomen and minimizes the risks of pulmonary aspiration. In children, preoperative colon preparation is rarely required for lower abdominal/pelvic surgery. A palpable bladder can be adequately emptied by expression, and catheterization is required only in prolonged lower abdominal procedures.[23]

In thoracic procedures, endotracheal intubation with or without lung retraction and/or low pressure CO_2 (4–6 mmHg) insufflation provides adequate exposure to all hemithoracic compartments including the mediastinum. Double lumen intubation, which is an ideal technique, is not suitable in children weighing <25 kg. Selective bronchial intubation, with or without contralateral bronchial occlusion with a balloon catheter is technically demanding and may prove helpful in certain circumstances.

In both thoracoscopic and laparoscopic procedures, postoperative analgesia is provided effectively with local anesthetic

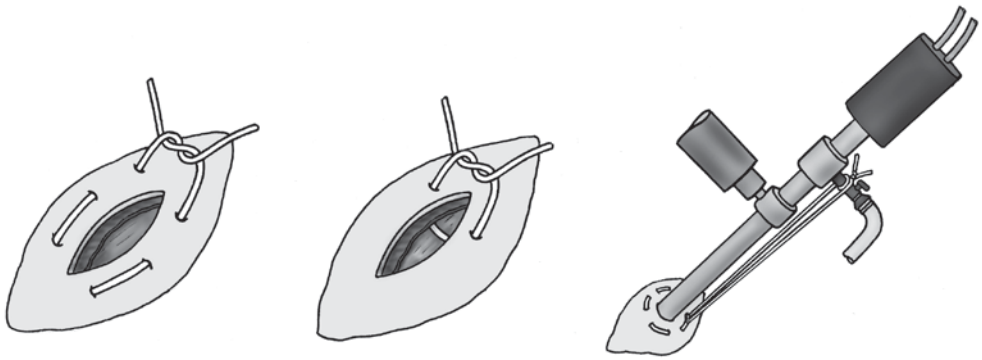

Fig. 6.1 Open technique insertion of primary port

infiltration of the port sites at the start or end of the procedure. This may be supplemented with 12–24 h of Oromorph, intravenous Opiate or Paracetamol, or epidural analgesia depending on the age and general health of the child and the exact nature of the procedure to be executed, e.g., patients who undergo extensive intraperitoneal/pleural dissection or those who are expected to ooze blood, bile, or urine during the immediate postoperative period, or require wound extension to retrieve solid organs are more likely than not requiring stronger and longer duration of postoperative analgesia.[2]

It is important to recognize that in children, particularly infants, the surface area for access is small, the body wall is thin and highly compliant, intercostal spaces are narrow, the liver margin is below the rib cage, the bladder is largely an intraabdominal structure, the viscera and major blood vessels are close to the body surface and the working spaces are small. In infants, only 200–500 mL of CO_2 may be required to establish a pneumoperitoneum/pneumothorax. These anatomical characteristics make access and manipulation in children more difficult and complicated when compared to adults. However, most children have well-defined anatomical landmarks owing to lack of excess fat, making recognition and dissection of structures a relatively easy exercise.

Although our system, Da Vinci, has four arms, the author prefers the use of three robotic arms with or without an accessory conventional laparoscopic port in most pediatric cases. This is because:

- Many pediatric procedures can easily be performed using two instruments within two working arms.
- The fourth arm takes wider space at and around the operating table.
- The fourth arm (third working port) does not allow for easy suction irrigation, insertion and retrieval of suturing materials, and stapling guns, needles, and specimen bag and has limited choice of retractors and sealing devices.
- An accessory laparoscopic/thoracoscopic port may prove more versatile and be used for:
  - Multiple purposes and different types of instruments and suturing materials or stapling gun.
  - Cost-cutting measure.
  - Avoiding extra (unnecessary) port site wounds whenever possible.

In pediatric abdominal procedures, open technique (modified Hasson) is the preferred method for insertion of the primary "telescope" port and creation of a pneumoperitoneum.[24,25] An incision to fit the size of the primary port is made. A purse-string or single suture through the fascia and peritoneum with a double throw prevents gas leak around the port. Hitching the suture around the gas inlet port prevents outward displacement of the port (Fig. 6.1). The exact location of primary port depends on the site and nature of the procedure to be executed. In general, a periumbilical (transperitoneal) or mid-axillary line in fifth to seventh intercostal space (transpleural) position serves most purposes. An insufflation pressure of 6–8 mmHg at a CO_2 flow of 0.1–0.5 L/min in neonates and infants, and 8–10 mmHg at a flow 0.5–1.5 L/min in older children are adequate parameters for all abdominal procedures. In the chest, if insufflation is required, a pressure of 4–6 mmHg at a CO_2 flow of 0.1–1 L/min is adequate. In children (who are normal otherwise), physiological changes that may follow CO_2 insufflation are of no clinical significance provided the pressure is kept below 15–18 mmHg for laparoscopy and 8–12 mmHg for thoracoscopy.[26,27]

The placement of two or three 5–8 mm robotic working ports and one or more (if necessary) accessory conventional laparoscopic ports under direct telescopic vision are also modified according to the type of surgical procedure to be completed. In general, the positions of the ports are similar to those of equivalent conventional laparoscopic/thoracoscopic procedures.[23,25] However, care must be taken not to allow for collision between:

- Robotic arms.
- Robotic arms and patient's head, prominent bony landmarks, operating table and anesthetic apparatus (Fig. 6.2).
- Robotic arms and assistant's arm and accessory laparoscopic instruments.
- All instruments inside the patient.

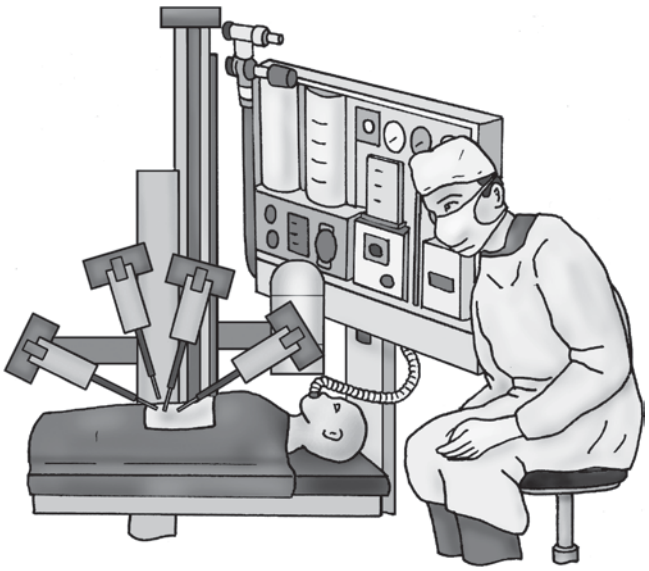

Fig. 6.2 Position of the robotic arms in relation to the patient, operating table, and the anesthetic machine for renal and adrenal surgery

The working spaces for both instrument function and dissection may be reduced critically if too much of the ports are placed inside the peritoneal/pleural space. In infants and small children and in certain anatomical locations (e.g., retroperitoneal space), only 5–10 mm of the ports may be allowed inside the working space (Fig. 6.3). The position of the Da Vinci slave usually depends on the type of procedure to be executed and size of the patient. The slave is placed at the head of the table for cervical and thoracic inlet procedures, left or right shoulders for left and right upper abdominal procedures, respectively, behind (semiprone patients) posterior mediastinum, in front (semisupine/lateral patient) of anterior mediastinum and left and right retroperitoneal renal surgery, behind with a slight turn toward the foot (semi-supine patient) for transperitoneal renal surgery, left or right (supine patient) for small and large bowels, left or right foot of the table (supine patient) for left and right lower abdominal procedures, respectively, and direct foot of the table (supine in infants and small children, Lloyd–Davis in older children) for lower abdominal midline structures.

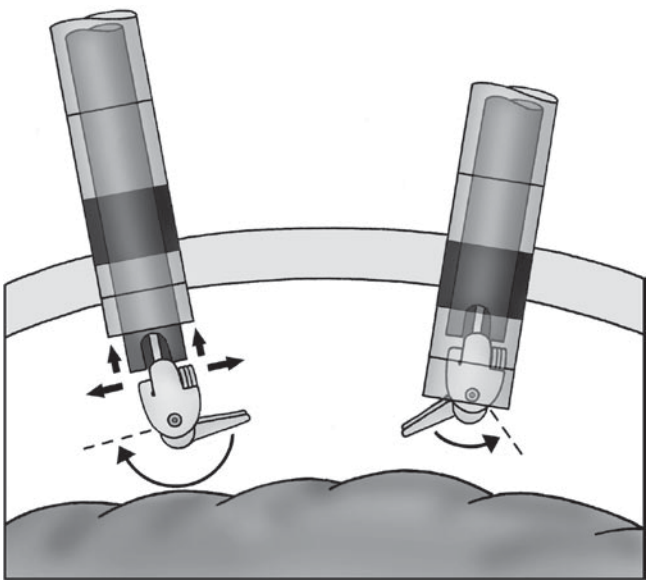

Fig. 6.3 The restricted working space in pediatric robotic surgery – note the position of the port and its effect on the functioning instrument

Dissection and suturing, and the use of energy sources are carried out in a manner similar to that of a conventionally performed open/endoscopic operation. However, pediatric surgeons are to be particularly careful while handling tissues and microsutures because of a complete lack of haptics.

The importance of teaching and training a dedicated pediatric theater team cannot be overemphasized and probably is more critical than they are for adults. This is because the spectrum of patients who would benefit from robotic surgery varies widely in terms of age, size, complexity, and pathology (multidisciplinary) and due to the lack of specialized equipment and instruments as a whole, including minimal access/robotic surgery.

Conclusions

In children, telerobotic surgery is safe and applicable to a wide range of pediatric surgical conditions. The technique holds more promise for pediatric surgeons than adult surgeons. This is because pediatric surgery covers a wider range of patients, age groups, and procedures, many of which are complex and reconstructive by nature. In its current format, it has already improved aspects of conventional minimal access surgery. However, the system has limitations and a smaller system and miniaturization of instruments and lower costs are worthy investments.

References

1. Gans SL, Berci G. Advances in endoscopy of infants and children. *J Pediatr Surg*. 1971;6:199–223
2. Najmaldin A, Rothenberg S, Crabbe D, Beasley S, eds. *Operative Endoscopy and Endoscopic Surgery in Infants and Children*. London: Hodder Arnold; 2005
3. Tewari A, Srivasatava A, Menon M. A prospective comparison of radical retropubic and robot-assisted prostatectomy: experience in one institution. *BJU Int*. 2003;92:205–210
4. Cadierre GB, Himpens J. Feasibility of robotic laparoscopic surgery: 146 cases. *World J Surg*. 2001;25:1467–1477
5. Heller K, Gutt CN, Schaeff B, et al Use of the robot system da Vinci for laparoscopic repair of gastro-oesophageal reflux in children. *Eur J Pediatr Surg*. 2002;12:239–242

6. Olsen LH, Jorgeusen TM. Robotic vs standard retroperitonescopic pyeloplasty in children. *BJU Int*. 2003;91:73
7. Lee RS, Retik AB, Borer JG, Peters CA. Paediatric robot assisted laparoscopic dismembered pyeloplasty: comparison with a cohort of open surgery. *J Urol*. 2006;175:683–687
8. Lehnert M, Richter B, Beyer PA, Heller K. A prospective study comparing operative time in conventional laparoscopic and robotically assisted fundoplication in children. *J Pediatr Surg*. 2006;41: 1393–1396
9. Anderberg M, Kockum CC, Arnbjornsson E. Robotic fundoplication in children. *Pediatr Surg Int*. 2007;23:123–127
10. Meehan JJ, Sandler A. Paediatric robotic surgery: a single-institutional review of the first 100 consecutive cases. *Surg Endosc*. 2008; 22:177–182
11. Luebbe B, Woo R, Wolf S, Irish M. Robotically assisted minimally invasive surgery in technical considerations and description of the da Vinci surgical system. *Paediatr Endosurg Innov Tech*. 2003;7: 385–402
12. Le Bret E, Papadatos S, Folliguet T, et al Interruption of patent ductus arteriosus in children; robotically assisted versus videothoracoscopic surgery. *J Thorac Cardiovasc Surg*. 2002;123:973–976
13. Suematsu Y, Mora BN, Mihaljevic T, del Nido PJ. Totally endoscopic robotic-assisted repair of patent ductus arteriosus and vascular ring in children. *Ann Thorac Surg*. 2005;80:2309–2313
14. Rahbar R, Ferrari LR, Borer JG, Peters CA. Robotic surgery in the paediatric airway: application and safety. *Arch Otolaryngol Head Neck Surg*. 2007;133:45–50
15. Lobe TE, Wright SK, Irish MS. Novel uses of surgical robotics in head and neck surgery. *J Laparoendosc Adv Surg Tech A*. 2005;15: 647–652
16. Woo R, Le D, Albanese CT, Kim SS. Robot-assisted laparoscopic resection of a type 1 choledochal cyst in a child. *J Laparoendosc Adv Surg Tech A*. 2006;16:179–183
17. Passerotti C, Peters CA. Robot-assisted laparoscopy applied to reconstructive surgeries in children. *World J Urol*. 2006;24:193–197
18. Aaronson OS, Tulipan NB, Cywes R, et al Robot-assisted endoscopic intrauterine myelomeningocele repair: a feasibility study. *Pediatr Neurosurg*. 2002;36:85–89
19. Knight C. Applying the Zeus robotic surgery system to fetal sheep surgery. In: *22nd Annual Meeting of the International Fetal Medicine and Surgery Society*, Zermatt, Switzerland; 2003:27–30
20. Najmaldin A, Antao B. Early experience of telerobotic surgery in children. *Int J Med Robotics Comput Assist Surg*. 2007;3:199–202
21. Youhannes P, Rotariu P, Pinto P, et al Comparison of robotic versus laparoscopic skills: is there a difference in the learning curve? *Urology*. 2002;60:39–45
22. Anwari M. Remote telepresence surgery: the Canadian experience. *Surg Endosc*. 2007;21:537–541
23. Najmaldin A. Laparoscopy: basic technique. In: Najmaldin et al, eds. *Operative Endoscopy and Endoscopic Surgery in Infants and Children*. London: Arnold; 2005
24. Humphrey GM, Najmaldin A. Modification of the Hasson technique in paediatric laparoscopy. *Br J Surg*. 1994;81:1320–1323
25. Najmaldin A, Guillou P. *A Guide to Laparoscopic Surgery*. Oxford: Blackwell Science; 1998
26. Lister DR, Rudston-Brown B, Warriner CB, et al Carbon dioxide absorption is not linearly related to intraperitoneal carbon dioxide insufflation pressure in pigs. *Anaesthesiology*. 1994;80:129–136
27. Sfez M, Guerard A, Desruelle P. Cardiorespiratory changes during laparoscopic fundoplication in children. *Paediatr Anaesth*. 1995;5:89–95

Emerging Robotics

7

Ben Challacombe, Kaspar Althoefer, and Dan Stoianovici

> This is perhaps the most beautiful time in human history; it is really pregnant with all kinds of creative possibilities made possible by science and technology which now constitute the slave of man – if man is not enslaved by it.
>
> Jonas Salk

Introduction

We live in exciting times and the pace of change in medical and surgical technology has never been more rapid. Gordon Moore's 1965 law stated that the power (memory) of computers would double every 18 months.[1] Almost every measure of the capabilities of digital electronic devices remains linked to Moore's law: processing speed, memory capacity, and even the number and size of pixels in digital cameras. This law continues to be true today in the field of surgical robotics. What have changed while technology continues to expand are the demands and expectations of our increasingly well-informed, demanding, and internet-literate patients. Patients want the best for themselves and their families and market forces themselves are driving expansion and development in many instances.

At present, robotic urological surgery is dominated by the da Vinci™ robotic system and the procedure of robotic-assisted laparoscopic radical prostatectomy (RALRP), although there is significant expansion in renal and bladder surgical applications; however, technology does not stand still and there are a huge and diverse number of robotic systems in development throughout the globe. There are many systems with enormous clinical potential in the pipeline that are likely to be further refined and developed in the coming years before being released into the clinical arena. Urologists have been quick to embrace robotic surgery and other new technologies and RALRP is easily the most common robotic procedure performed worldwide. From 766 cases performed in 2002, over 48,000 are projected for 2008.[2] This accounts for over 40% of the radical prostatectomy market in the USA.

We will look at the robotic systems being developed in some of the premier robotic engineering institutions in the world and assess their clinical applications.

Robotic Developmental Directions

Robotic laboratories throughout the world are attempting to produce robotic systems that are superior to those already in clinical use and remedy some of the problems experienced by the current machines. The da Vinci S™ is far lighter than the standard da Vinci system, but it remains a bulky piece of equipment that is difficult to maneuver and store in many standard operating theaters. Groups are looking at reducing these issues by installing ceiling-mounted robotic devices that swing down onto the patient when required and are easily housed above the patient when no longer required. Other options include simply debulking the robot cart still further by the use of lightweight polymers and downsizing the robotic arms and instruments. Another issue presented by the da Vinci system is the lack of force feedback and there are now miniature robots capable of entering via a laparoscopic port to provide the surgeon with enhanced and detailed haptic feedback.

Other than trying to improve on the robotic systems already in clinical use, various engineering teams are also looking at percutaneous and transrectal needle placing robots that can be used within CT/MRI scanners, robots used in natural orifice and single port surgery, and developing nano-robotic technology. This chapter will look more closely at these exciting areas.

Force Sensing and Tissue Identification: Current and Future Developments

With the advent of specialized surgical robots such as the da Vinci S™ surgical system, urological surgeons have been provided with specialist end-effectors that assist during complex laparoscopic operations and help to improve the outcomes including blood loss, analgesia requirements, and length of hospital stay while reducing the overall morbidity of surgical procedures. These highly sophisticated robotic devices incorporate advanced technologies such as precision mechanics, enhanced and magnified stereo vision, and advanced motion

P. Dasgupta et al. (eds.), *New Technologies in Urology,*
DOI: 10.1007/978-1-84882-178-1_7, © Springer-Verlag London Limited 2010

control algorithms enabling tremor-free handling of the operating instruments. However, there are limitations to even the updated da Vinci S system. Most notably, the surgeon loses all tactile sensation when operating with the aid of a robot. This sense of touch, which is readily available during open surgery and also present to a lesser degree in traditional laparoscopic procedures, provides the surgeon with valuable information about the nature of the tissues and potential extent of disease and margins of safety. The inability to palpate organs and soft tissues during an operation can lead to a misjudgment and result in inadvertent injury to neighboring organs or an incomplete surgical resection. Recent studies have revealed that the lack of tactile sensation during robot-aided surgery can lead to an increase in tissue trauma and accidental tissue damage, and surgeons provided with force feedback significantly improved their performance.[3,4] This risks leaving cancer behind and getting a positive surgical margin. Open surgeons often avoid this by feeling the tumor and going wide at the suspicious areas to obtain a negative margin and excise the cancer completely. In urological surgery using the da Vinci robot, the lack of tactile feedback is particularly difficult during surgery for locally advanced T3 prostate cancer and large bulky muscle invasive bladder cancer. In these situations, tactile feedback via an indentation probe with an applied sense of "feel" would thus be clinically very useful.

Current research at a number of research institutes aims at equipping surgical robots with sensors and feedback mechanisms to reestablish the surgeon with tactile perception and feedback. Owing to advances in microtechnologies, there is now a clear trend toward developing miniaturized sensors that can measure the manipulation forces at the point where the tool comes into contact with soft tissue through a laparoscopic port. Recently, a surgical gripper at the end of a laparoscopic instrument has been integrated with a strain gauge sensor.[5] The sensor's hexapod structure made from an aluminum alloy provides a light-weight and rigid solution to acquire force and torque signals along all six axes with a high resolution of 0.05 and 0.25 N in the radial and axial direction, respectively, with a range of up to 20 N. A MEMS microgripper driven by a piezoelectric actuator integrated with semiconductor strain gauges mounted on a microfabricated elastic surface (flexure) has been developed allowing soft tissue property characterization and realistic palpation using a haptic interface.[6]

Advances have also been made in employing piezoelectric materials to measure the contact forces at the tip of surgical tools. Micromachined force array sensors have been developed that can be mounted on surgical tools.[7,8] The developed sensors claim to have a high sensitivity and linear behavior over a wide range of up to 15 N, allowing realistic palpation feedback. Very promising results have also been achieved based on fiber-optic measuring principles. Miniature force sensors can be created using fiber-optic cables that carry light signals – which are modulated in response to the applied forces – from a sensing region to an optoelectronic converter. Recently, a 5-mm diameter force sensor integrating three fiber-optic sensor elements into the tip of a surgical tool was developed. This sensor can measure forces along three axes with a sensitivity of 0.04 N and a range of up to 2.5 N.[9] The main advantages of these sensors are that they are not affected by electromagnetic interference and are compatible with magnetic resonant imaging systems potentially enabling procedures to be performed during MR imaging. Exploiting this, a three degree-of-freedom optical fiber force sensor was used in an MR-compatible neurosurgery robot to measure tool–tissue interaction forces.[10]

Accurate sensors and appropriate actuators that reconstruct the measured forces in the user's hand are both necessary components of haptic interfaces that provide genuine remote touch sensing. The major problem in providing haptic feedback to the surgeon is the difficulty in sensing the forces during movement in multiple directions/degrees of freedom as well as the need for sophisticated control systems to drive the actuation mechanisms necessary to create the sensation of touch in the hands of the surgeons. These problems are further compounded by the miniaturization and sterilization requirements of minimally invasive surgical instruments.[11] Attempting to avoid the complicated control systems needed for the surgeon to "feel" the tissue interaction, smart instruments are being created to measure mechanical soft tissue properties (i.e., areas of increased stiffness or softness in tissue) and transmit this information to aid the surgeon in tissue diagnosis. A uniaxial stretching device has been used by Brouwer et al to measure porcine tissue response both in vivo and ex vivo.[12] Another device was developed to investigate the in vivo viscoelastic properties of tissue under uni axial small deformations.[13] A motorized endoscopic grasper, which was used to test abdominal porcine tissues in vivo and in situ with cyclic and static compressive loadings, is also described.[14] An ultrasound indentation device, which integrates an ultrasound transducer and a load cell, is integrated to simultaneously monitor the tissue strain, and the response tissue stress under compressive load has been used for measuring breast tissue in vivo.[15] The use of a transrectal probe equipped with tactile sensors to identify prostate tumors has been described.[16] Tactile feedback systems have also been proposed for the identification and characterization of pulmonary tumors,[17] lesions in the breast,[18] and for identifying arteries during robotic surgery.[19]

The previous research aims to estimate tissue properties by applying an external stimulus while measuring the corresponding tissue response. The difficulty is that, in many cases, small and deep lesions are not easily detected using this technique. To overcome this, a technique known as elastography that can provide a relative stiffness image of a

target area deep inside tissue has been proposed and utilized in soft tissue diagnosis. Sonoelastography is an imaging technique where low-amplitude, low-frequency ultrasound shear waves are propagated through an organ to measure tissue elasticity. This has been used to measure the elasticity of in vitro muscle[20] and reconstruct three-dimensional tumor volumes of in vitro prostate samples based on the measurement of tissue elasticity.[21] Others have used the concept of harmonic motion imaging (HMI), which can be used to differentiate soft tissue stiffness.[22] This technique applies a radiation force produced by focused ultrasound to induce a harmonic motion deep inside a tissue. In a further study, HMI[23] has been used to measure the elastic modulus of in vitro bovine liver using a mechanical model and computational scheme. Magnetic resonance elastography (MRE) imaging has also been described[24] and this technique can directly visualize and quantitatively measure propagating acoustic strain waves allowing the calculation of local quantitative values of shear modulus and the generation of images that depict tissue elasticity or stiffness.

Recently conducted research at King's College, London, is aiming to develop devices that look at a series of distributions measured as either a wheeled probe (Figs. 7.1 and 7.2) or an air-cushion spherical probe (Fig. 7.3) that slide across a tissue surface. This approach differs from those previously mentioned, which includes static indentations, as the wheeled probe and spherical probe allow the assessment of larger regions of organ tissue in a relatively short time.[25,26] Both probes can fuse the kinaesthetic information from the wheel–tissue rolling interaction into a pseudo-color map that can indicate the spatial variation of tissue stiffness caused by the differences of the internal tissue structure.[27] These devices have been trialed with success in excised porcine liver and kidneys[28,29] allowing the stiffness distribution of the subject area (embedded rubber "tumor" nodules) to be visualized in a form of force/tactile map with good face validation to the original tissue.[30–33]

Fig. 7.2 Photograph of the force-sensitive probe during initial trials

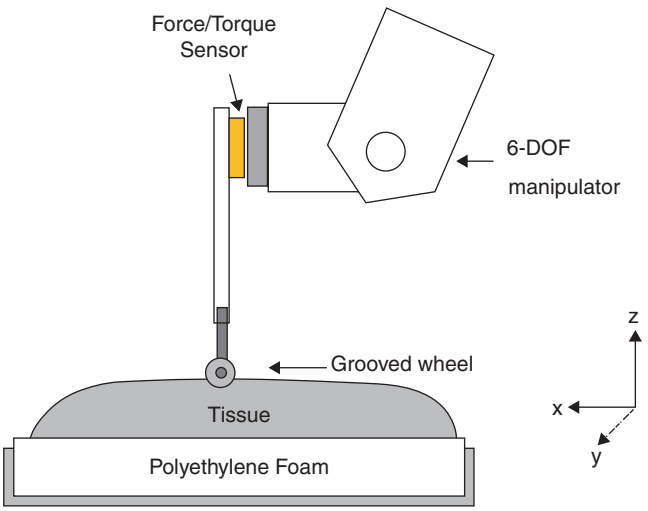

Fig. 7.1 Diagram of the force-sensitive probe with a grooved wheel end-effector

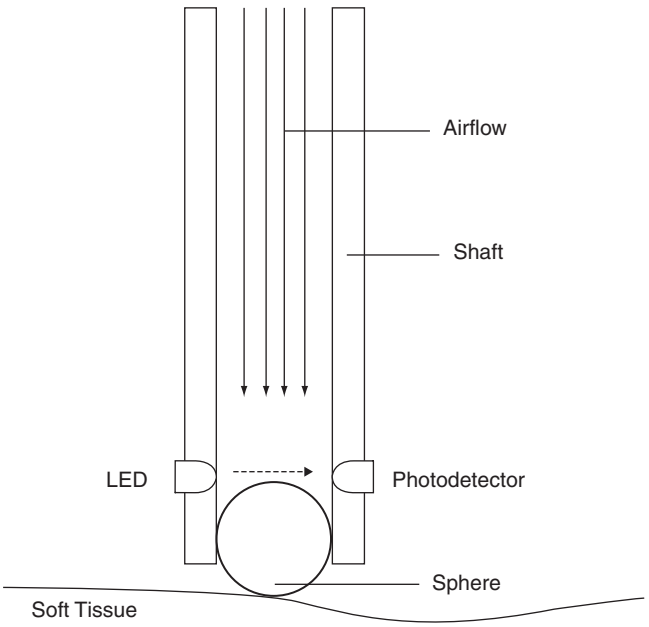

Fig. 7.3 Air cushion spherical tactile sensor

Robotic Needle Placement

The ability to accurately place a needle into a patient is a feature of numerous medical procedures. In urological surgery, this is particularly useful during the first stage of percutaneous nephrolithotomy, for radioactive seed placement in prostate brachytherapy, in ablative renal procedures such as cryotherapy and radiofrequency ablation, and also to accurately target a biopsy for a variety of organs. Inaccuracies in needle or electrode placement for these procedures and lack of navigation devices to aid placement may result in increased procedure time, morbidity, inaccurate diagnosis, or tumor recurrence. In recent years, robot-assisted needle insertion has attracted significant attention because of its capabilities to provide assistance throughout a range of minimally invasive procedures. These systems may provide a safer working environment for the physician by reducing radiation exposure. In addition, there is the potential to enhance outcomes by improving repeatability and accuracy, which could allow standardization of surgical ability.

One of the leaders in the field of percutaneous robotic biopsy and needle placement is the Urology Robotics Laboratory at Johns Hopkins University. This laboratory initially developed the percutaneous access to the kidney robot (PAKY) which was used in the first randomized trial of telerobotic surgery[34] and also successfully for PCNL in patients where robotic insertions compared favorably with manual insertions when time to access, number of attempts, and estimated blood loss were looked at.[35] This robot consisted of a seven DOF lockable manipulator, or passive arm, connected to a three DOF active arm. The arm houses a radiolucent needle driver and was mounted using a side rail onto the operating table. Following on from this, they have developed the Acubot device, which like its predecessor is based on the remote center of motion (RCM) device. Clinical feasibility studies in 2 patients with hepatic metastases have been described by Solomon et al[36] to develop a tumor ablation treatment system that utilizes the AcuBot robot system for accurate applicator placement.

The RCM is a key concept in surgical robotics (Fig. 7.4). It consists of a fulcrum point that is located distal to the mechanism itself, typically at the skin entry point/laparoscopic port site in percutaneous devices. This allows the RCM to precisely orientate a surgical instrument/needle in space while maintaining the needle tip at the skin entry point (or another specified location) without placing unwanted traction or pressure on this point. Current examples of RCM robots include the da Vinci™ itself along with the Zeus™, AESOP™, and AcuBot® devices.

When equipped with a force feedback device, the AcuBot robot can detect changes in resistance upon successful entry to the renal collecting system or other tissues and thus can confirm percutaneous access.

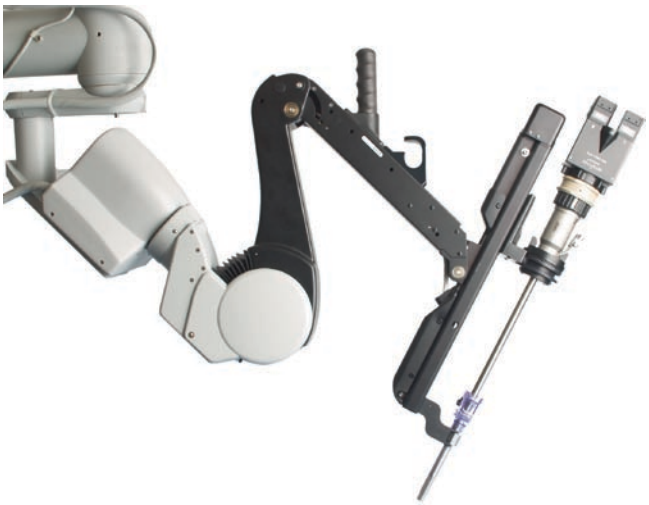

Fig. 7.4 The da Vinci™ surgical arm

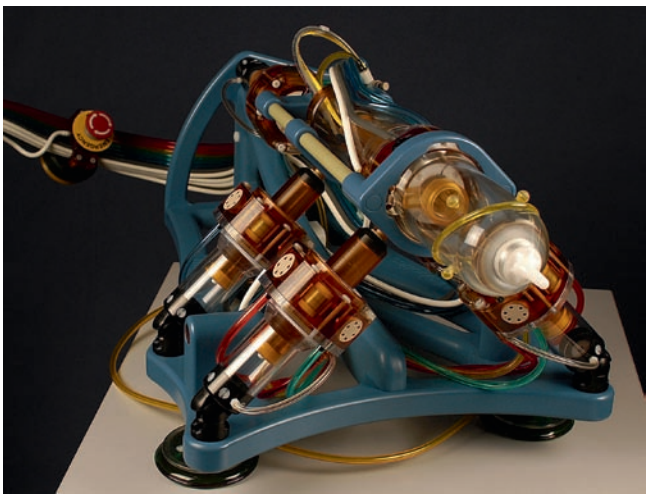

Fig. 7.5 MrBot prostate robot

A derivative of the AcuBot is the MrBot robot (Fig. 7.5), a fully actuated robot for image-guided access of the prostate gland. For MRI compatibility, this robot is exclusively constructed from nonmagnetic and dielectric materials such as plastics, ceramics, and rubbers and is electricity free. The system utilizes a new type of motor specifically designed for this application, the pneumatic stepper motor (PneuStep).[37] These uniquely provide easily controllable precise and safe pneumatic actuation. Fiber-optical encoding is used for feedback, so that all electric components are distally located outside the imager's room.[38]

Imager compatibility tests performed in scanners up to 7 T showed outstanding MRI compatibility, independent of the field strength. MRI-guided needle targeting experiments showed that the tip of the needle may be placed within 1 mm of a desired target selected in the image. This robot has

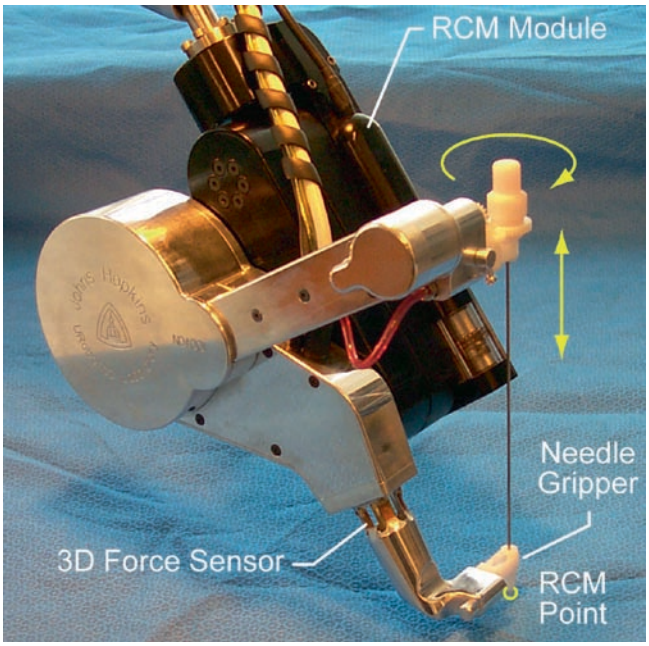

Fig. 7.6 Revolving needle driver (RND) connected to the AcuBot CT-guided robot for needle positioning and orientation

recently been shown in to be capable of accurate MR imaging-guided prostatic needle intervention within a standard MR imager in vivo in a canine model.[39]

The latest device from the Urobotics lab is the revolving needle driver (RND). This is a fully actuated driver for needle insertion, spinning, release, and force measurement and is perhaps the most complex, feature-rich needle driver reported to date (Fig. 7.6). It can be connected to the AcuBot CT-guided robot for needle positioning and orientation. Using a novel kinematic design for inserting the needle, the RND creates the translation motion with a mechanism of rotary joints. This has resulted in a compact design, so that the driver is less tall than the needle. Beside its actuated needle insertion mechanism, the RND is also capable of spinning the needle, so that the needle is advanced in a drill-like motion. To engage the needle, standard biopsy needles are placed in a custom adapter fitted with a gear. The RND supports the needle from its head, and provides an additional needle support guide in close proximity of the skin entry point. This is similar to holding the needle with two finger-like grippers, one from its head and one from its barrel next to the skin.

The top one pushes the needle in and out, while the lower holds the guide to support the direction of the needle as close as possible to the skin. The guide or needle nozzle also encases the sharp needle point before insertion to protect the patient and medical personnel. Both grippers can simultaneously release the needle automatically. Finally, the new driver is also equipped with a set of force sensors to measure the interaction of the nozzle with the patient and the force of needle insertion. These can be used either with a haptic interface to reproduce the interaction of the physician in handling the needle, or to provide additional information that is not typically used in the manual case, such as respiratory motion tracking. This device has been assessed using a porcine model and been found to be effective for lung and liver biopsy.[40] Reduced force was required for insertions using needle rotation.

Nanotechnology

Nanotechnology or nanotech is an emerging technology seeking to exploit distinct technological advances by controlling the structure of materials at a reduced dimensional scale approaching that of individual molecules and their aggregates or supramolecular structures. In the same way as the development of microtechnology in the 1980s led to new tools for urological and other surgery, emerging nanotechnologies will similarly permit further advances toward better diagnosis and new devices for medicine. Nanorobots are expected to permit significant new capabilities for the diagnosis and treatment of the disease, for patient monitoring, and for minimally invasive surgery.[41,42] The ability to manufacture nanorobots results from new methodologies in fabrication, computation, transducers, and manipulation, e.g., electrospinning techniques for the preparation of nanofibers and macroporous scaffolds intended for drug delivery and tissue engineering.

The hardware architecture for a medical nanorobot must include the necessary devices for monitoring the most important aspects of its operational workspace: the human body. Teams of nanorobots may cooperate to perform predefined complex tasks in medical procedures.[43] With this goal in mind, data processing, energy supply, and data transmission capabilities can be addressed through embedded integrated circuits, using advances in technologies derived from nanotechnology and very large system integration (VLSI design).[44]

Complementary metal semi-conductor (CMOS) VLSI design using deep ultraviolet lithography provides a high precision and commercial way for manufacturing early nanodevices and nanoelectronics systems. The CMOS industry may successfully drive the pathway for the assembly processes needed to manufacture nanorobots, where the joint use of nanophotonic, carbon nanotubes, and nanocrystals may even accelerate further the actual levels of resolution ranging from 248 to 157 nm devices.[45] The appropriate interdisciplinary effort will impact on assembly nanodevices and nanoeletronics to build nanorobots.[46] To validate designs to achieve a successful implementation, the use of Verification Hardware Description Language (VHDL) is the most common methodology utilized in the integrated circuit manufacturing industry. Nanorobots can be useful in a large range of biomedical applications for future drug delivery

applications, such as dosage regimens based on predicted pharmacokinetic parameters for chemotherapy in anti-cancer treatments.[47] A range of different signals are directly correlated to specific medical problems. Chemical signals can serve for medical target identification and actuation. A single tumor cell can be characterized as a typical endothelial cell mutation with profound consequences for patients suffering from cancer. Endothelial cells have a large number of functions and may play an important role in human health. They also serve as part of the structure forming the inside blood vessels, which are spread throughout every single organ or system comprising our body.

Factors like low energy consumption and high sensitivity are among some of the advantages of nanosensors. Nanobioelectronics using nanowires as material for circuit assembly can achieve maximal efficiency for applications involving chemical changes, enabling new medical applications.[46] Using chemical sensors, nanorobots can be programmed to detect different levels of E-cadherin and beta-catenin as medical targets in primary and metastatic phases. Integrated nanosensors can be utilized for such a task to find different concentrations of E-cadherin signals.[48] Beyond sensors, nanorobots may be designed with appropriated space to carry chemotherapeutic agents for future cancer drug delivery. This approach enables the drug carrier to be maintained for as long a time as necessary in the bloodstream, and therefore avoiding the extravasation toward non-reticuloendothelial-located cancers and the side-effects of premature degeneration.[49]

The Future of Surgical Robotic Science

The da Vinci robot is highly unlikely to represent the ultimate robotic surgical system and it should be seen as the current most highly sophisticated master–slave system on a stepwise progression of robotic development. The devices themselves will become smaller, lighter, and integrated into telesurgical systems, which may have fully robotic surgical theater nurses and equipment nurses. This will allow the seamless integration of patient data and imaging into the robotic console permitting real-time intraoperative visualization of pathology and other tissues. This augmented reality surgery combining laparoscopic images with virtual 3D images will help identify and avoid injury to key structures. Instruments will continue to decrease in size to true needlescopic (2 mm) end-effectors and a haptic feedback system is likely to arrive within a few years.

Other areas of development include the snake-like or serpentine robots, which are now being targeted toward the field of natural orifice surgery. Known as NOTES™ (natural orifice trans-luminal endoscopic surgery), these robots have multiple degrees of freedom, do not fail if one joint locks/blocks, and can be used transgastrically.[50] One such device is the CardioARM (Articulated Robotic MedProbe), a snake-like surgical robot developed at Carnegie Mellon University, which hopes to allow cardiac surgeons to perform procedures through a single subxiphoid incision (Fig. 7.7). The robot has a series of joints that automatically adjust to follow the course plotted by the robot's head, providing greater precision than a flexible endoscope can offer.

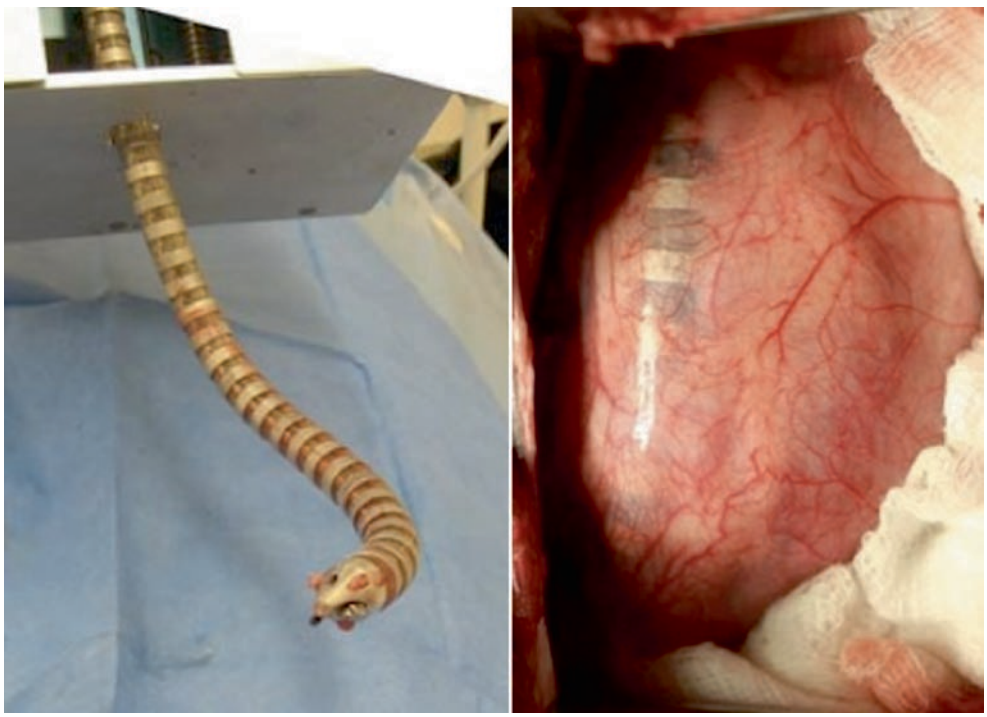

Fig. 7.7 The CardioARM in the laboratory and in animal trials™

It is 12 mm in diameter, has 102 degrees of freedom, three of which can be activated at once and "memory" as device remembers its configuration as it moves, so each segment follows the previous segment's path.[51] The same company is also developing a laparoARM™, gastroARM™, and arthroARM™, which will provide platforms for various endoscopic and laparoscopic procedures. These and other similar devices open the door for single incision or external woundless/scarless surgery and procedures including cholecystectomies, appendicectomies, and tubal ligations that have already occurred. Once the ability to exchange and manipulate a variety of end-effectors has been developed, this type of robot may become the future of robotic surgery. The field of surgical robotics continues to move at a rapid pace and many of these concepts that we find difficult to grasp at present will rapidly become standard surgical practice throughout the globe.

> Any sufficiently advanced technology is indistinguishable from magic.
>
> Arthur C. Clarke

Acknowledgment The authors would like to acknowledge contributions from Mr. Hongbin Liu, Mr. Dinusha Zzbyszewski, Mr. David Noonan, Professor Lakmal Seneviratne, and Dr. Adriano Cavalcanti.

References

1. GE. Cramming more components onto integrated circuits. *Electron Mag*. 1965;38:8
2. Peplinski R. Past, present and future of the Da Vinci robot. *2nd UK Robotic Urology Course*; 2006
3. Wagner C, Stylopoulos N, Howe R. The role of force feedback in surgery: analysis of blunt dissection. In: *Proceedings of the IEEE 10th Symposium on Haptic Interfaces for Virtual Environmental &Teleoperator systems*; 2002
4. Deml B, Ortmaier T, Seibold U. The touch, and feel in minimally invasive surgery. In: *IEEE International Workshop on Haptic Audio Visual Environment, and Their Applications*, Ottawa, ON; 2005: 33–38
5. Seibold U, Kuebler B, Hirzinger G. Prototype of instrument for minimally invasive surgery with 6-axis force sensing capability. In: *Proceeding of the IEEE International Conference on Robotics, and Automation*, Barcelona, Spain; 2005:496–501
6. Menciassi A, Eisinberg A, Carrozza M et al Force sensing microinstrument for measuring tissue properties, and pulse in microsurgery. *IEEE/ASME Trans Mechatron*. 2003;8:10
7. Ottermo M, Stavdahl O, Johansen T. Palpation instrument for augmented minimally invasive surgery. In: *Proceedings of the IEEE/RSJ International Conference on Intelligent Robots, and Systems*, Sendai, Japan; 2004:3960–3964
8. Dargahi J, Parameswaran M, Payandeh S. A micromachined piezoelectric tactile sensor for an endoscopic grasper-theory, fabrication, and experiments. *J Microelectromech Syst*. 2000;9:329
9. Peirs J, Clijnen J, Reynaerts D, et al A micro optical force sensor for force feedback during minimally invasive robotic surgery. *Sensors Actuators A*. 2004;115:447
10. Sutherland G, McBeth P, Louw D. *NeuroArm: An MR Compatible Robot for Microsurgery*. Amsterdam: Elsevier Science; 2003 International congress series, 1256: 504
11. Okamura AM. Methods for haptic feedback in teleoperated robot-assisted surgery. *Ind Rob Int J*. 2004;31(6):499–508
12. Brouwer I, Ustin J, Bentley L, et al Measuring in-vivo animal soft tissue properties for haptic modelling in surgical simulation. *Stud Health Technol Inform*. 2001;81:69–74
13. Ottensmeyer M. In-vivo measurement of solid organ visco-elastic properties. *Stud Heatlh Technol Inform*. 2002;85:328
14. Brown J, Rosen J, Kim Y, et al In-vivo and in-situ compressive properties of porcine abdominal soft tissues. *Stud Health Technol Inform*. 2003;94:26–32
15. Wellman P, Howe R. Modelling probe and tissue interaction for tumour feature extraction. In: *ASME summer Bioengineering conference*, Sun River, OR; 1997
16. Egorov V, Ayrapetyan S, Sarvazyan AP. Prostate mechanical imaging: 3-D image composition and feature calculations. *IEEE Trans Med Imag*. 2006;25(10):1329–1340
17. Miller AP, Peine WJ, Son JS, et al Tactile imaging system for localizing lung nodules during video-assisted thoracoscopic surgery. In: *Proceedings of the IEEE International Conference on Robotics and Automation*, Rome, Italy; 2007:2996–3001
18. Wellman SP. Tactile imaging of breast masses: first clinical report. *Arch Surg*. 2001;136:204–208
19. Beasley RA, Howe RD. Tactile tracking of arteries in robotic surgery. *Proc IEEE Int Conf Rob Autom*. 2002;4:3801–3806
20. Levinson SF, Shinagawa M, Sato T. Sonoelastic determination of human skeletal muscle elasticity. *J Biomech*. 1995;28(10): 1145–1154
21. Taylor LS, Porter BC, Rubens DJ, Parker KJ. Three-dimensional sonoelastography: principles and practices. *Physics Med Biol*. 2000; 45(6):1477–1494
22. Konofagou EE, Hynynen K. Localized harmonic motion imaging theory, simulations and experiments. *Ultrasound Med Biol*. 2003;29: 1405–1413
23. Shan B, Pelegri A, Maleke C, Konofagou E. A mechanical model to compute elastic modulus of tissues for harmonic motion imaging. *J Biomech*. 2008;41(10):2150–2158
24. Manducam A. : non-invasive mapping of tissue elasticity. *Med Image Anal*. 2000;5(4):237–254
25. Noonan D, Liu H, Zweiri Y et al A dual-function wheeled probe for tissue viscoelastic property identification during minimally invasive surgery. In: *International Conference on Robotics And Automation*, Rome, Italy; 2007
26. Murphy D, Challacombe B, Nedas T, et al Equipment and technology in robotics. *Arch Esp Urol*. 2007;60(4):349–355
27. Liu H, Noonan DP, Zweiri YH, Althoefer K, Seneviratne LD. The development of nonlinear viscoelastic model for the application of soft tissue identification. In: *IEEE/RSJ International Conference on Intelligent Robots and Systems*; 2007:208–213
28. Puangmali P, Althoefer K, Seneviratene LD, Murphy D, Dasgupta P. State-of-the-art in force and tactile sensing for minimally invasive surgery. *IEEE Sens J*. 2008;8(4):371–381
29. Al-jaafreh TM, Seneviratne LD, Zweiri YH, Althoefer K. Modelling soft tissue-mechatronic tool interactions during indentation. *Int J Model, Identif Control (IJMIC)*. 2008;4(4):337–347
30. Al-ja'afreh TM, Zweiri YH, Seneviratne LD, Althoefer K. A new soft tissue indentation model for estimating "force-displacement" characteristics using circular indenters. Proceedings of the Institution of Mechanical Engineers (IMechE), Part H. *J Eng Med*. 2008;222(5):805–815
31. Althoefer K, Zbyszewski D, Liu H, et al Air-cushion force sensitive probe for soft tissue investigation during minimally invasive surgery. In: *7th IEEE Conference on Sensors*, Lecce, Italy; 2008 [unconditionally accepted for inclusion in 7th IEEE Conference on Sensors]

32. Zbyszewski D, Liu H, Puangmali P, et al Wheel/tissue force interaction: a new concept for soft tissue diagnosis during MIS. In: *Proceedings of 2008 International IEEE Engineering in Medical and Biological Society Conference*, Vancouver, BC, Canada;2008
33. Puangmali P, Liu H, Althoefer K, Seneviratne LD. Optical fiber sensor for soft tissue investigation during minimally invasive surgery. In: *IEEE International Conference on Robotics and Automation (ICRA'08)*, Pasadena, CA; 2008:2934–2939
34. Challacombe B, Patriciu A, Glass J, et al A randomized controlled trial of human versus robotic and telerobotic access to the kidney as the first step in percutaneous nephrolithotomy. *Comput Aided Surg*. 2005;10(3):165–171
35. Su L-M, Stoianovici D, Jarrett TW, et al Robotic percutaneous access to the kidney; comparison with standard manual access. *J Endourol*. 2002;16:471–475
36. Solomon SB, Patriciu A, Stoianovici DS. Tumor ablation treatment planning coupled to robotic implementation: a feasibility study. *J Vasc Interv Radiol*. 2006;17(5):903–907
37. Stoianovici D, Patriciu A, Mazilu D, Petrisor D, Kavoussi L. A new type of motor: pneumatic step motor. *IEEE/ASME Trans Mechatron*. 2007;12(1):98–106 http://urology.jhu.edu/urobotics/pub/2007-stoianovici-tmech.pdf
38. Stoianovici D, Song D, Petrisor D, et al "MRI stealth" robot for prostate interventions. *Minim Invasive Ther Allied Technol*. 2007;16:241–248
39. Muntener M, Patriciu A, Petrisor D, et al Transperineal prostate intervention: robot for fully automated MR imaging–system description and proof of principle in a canine model. *Radiology*. 2008;247(2):543–549
40. Shah S, Kapoor A, Ding J, et al Robotically assisted needle driver: evaluation of safety release, force profiles, and needle spin in a swine abdominal model. *Int J CARS*. 2008;3(2):173–179
41. Cavalcanti A. Assembly automation with evolutionary nanorobots and sensor-based control applied to nanomedicine. *IEEE Trans Nanotechnol*. 2003;2:82.
42. Freitas RA Jr. Nanomedicine – basic capabilities. www.nanomedicine.com; 1999
43. Cavalcanti A, Freitas RA Jr. Nanorobotics control design: a collective behaviour approach for medicine. *IEEE Trans Nanobiosci*. 2005;4:133
44. Srivastava N, Banerjee K. Performance analysis of carbon nanotube interconnects for VLSI applications. In: *IEEE/ACM ICCAD International Conference on Computer-Aided Design*; 2005:383–390
45. Bogaerts W, Baets R, Dumon P, et al Nanophotonic waveguides in silicon-on-insulator fabricated with CMOS technology. *J Lightwave Technol*. 2005;23:401
46. Cavalcanti A, Shrinzadeh B, Freitas RA, et al Medical Nanorobot Architecture Based on Nanobioelectronics. Recent Patents on Nanotechnology. 1st ed. Pennington: Bentham Science; 2007
47. Kawasaki ES, Player A. Nanotechnology, nanomedicine, and the development of new, effective therapies for cancer. *Nanomed Nanotechnol Biol Med*. 2005;1:101–109
48. Janda E, Nevolo M, Lehmann K, et al Raf plus TGFbeta-dependent EMT is initiated by endocytosis and lysosomal degradation of E-cadherin. *Oncogene*. 2006;25:7117
49. Couvreur P, Gref R, Andrieux K, et al Nanotechnologies for drug delivery: application to cancer and autoimmune diseases. Progress in solid state. *Chemistry*. 2006;34:231
50. Hochberger J, Lamade W. Transgastric surgery in the abdomen: the dawn of a new era? *Gastrointest Endosc*. 2005;62(2):293–296
51. Ota T, Patronik NA, Schwartzman D, Riviere CN, Zenati MA. Minimally invasive epicardial injections using a novel semiautonomous robotic device. *Circulation*. 2008;118(14 suppl):S115–S120

Part II

Lasers

Roger Kirby and John Fitzpatrick

The Holmium Laser in the Treatment of Benign Prostatic Enlargement

8

Wilson L. C. and Gilling P. J.

Introduction

The holmium laser has the ideal characteristics for an endourological tool. It is a precise, safe, versatile instrument that can be utilized anywhere in the urinary tract. Most importantly, it has diverse applications being able to be used in treating the prostate, urinary calculi, strictures, and other soft tissue disorders in the urinary tract. This makes it a unique technology for urological practice. This chapter will focus on the use of the holmium laser for the treatment of benign prostatic enlargement (BPE).

Physics of the Holmium Laser

The holmium laser is a pulsed solid-state laser with a wavelength of 2,140 nm. As the prostate is 60–70% water, the light absorption length in the prostate is very short at 0.4 mm – the resulting energy density being high enough to create a temperature greater than 100°C, which results in tissue vaporization without coagulation. This enables precise cutting and incision, while the dissipating heat coagulates the small- and medium-sized vessels to a depth of 2–3 mm.[1] The fact that saline can be used as the operative irrigant means that the consequences of using hypo-osmolar solutions can be avoided. Our unit has not had a case of TUR Syndrome in over 5,000 cases and this means that the operating time need not be restricted as it is for transurethral resection of prostate (TURP).

Holmium Laser and Benign Prostatic Enlargement

BPE is a common cause of lower urinary tract symptoms (LUTS). The mainstay of surgical intervention in the past has been TURP and while this has proven efficacy, alternative techniques have been sought to avoid TURP's perioperative morbidity, which occurs in up to 15% of patients.

Lasers have been at the forefront of alternative treatments for the treatment of BPE. Early generation Neodymium:YAG lasers were beset by several problems; only prostate coagulation was able to be performed, and this created prolonged sloughing of prostate tissue with consequent postoperative urinary symptoms. The lack of tissue removal also contributed to the procedure's lack of durability and unpredictable results.

With the advent of the high-powered holmium laser, surgical techniques evolved beyond ablation. The characteristics of the holmium wavelength allowed precise incision and resection, and so for the first time there was a technique that could mimic TURP while avoiding the perioperative morbidity and shortening inpatient hospital stay. This procedure was holmium laser resection of the prostate (HoLRP). With the development of the tissue morcellator, however, holmium enucleation of the prostate (HoLEP) evolved and became an endourological equivalent of the Open Prostatectomy, with no restriction on the size of the prostate that could be treated. Well-designed randomized controlled trials from several centers have proven that HoLEP has superior perioperative outcomes when compared with TURP or Open Prostatectomy, as well as equivalent clinical outcomes.

HoLEP Procedure

The indications for HoLEP include, but are not limited to, those for TURP. In general, anticoagulants are stopped 7 days prior to surgery, but the hemostatic properties of the holmium laser allow patients who are unable to cease taking these medications to undergo HoLEP.[2] In addition, the use of normal saline rather than glycine as irrigant means that there is no risk of TUR Syndrome, and therefore there is no limitation to the size of prostate treated. The largest adenoma retrieved at our institution is 1,100 g.

A 100 W laser is usually used (Lumenis, Yokneam, Israel). A 550 μm laser fiber is passed through an interlink injection port (Baxter, Deerfield, IL) via a 6 F open-ended ureteric catheter. The end of the ureteric catheter should be just visible, with the end of the laser fiber a few millimeters beyond

P. Dasgupta et al. (eds.), *New Technologies in Urology,*
DOI: 10.1007/978-1-84882-178-1_8, © Springer-Verlag London Limited 2010

the ureteric catheter. The laser may require advancing at times during the procedure to prevent damage to the ureteric catheter, or more importantly, the scope.

The laser resectoscope is a 26 F, continuous-flow, with an inner sheath (27040 XAL), with an incorporated stabilizing guide (Storz, Tuttlingen, Germany). A 30° telescope (27005 BA) with a long bridge (27068CD) is also required.

An alternative setup involves a combined laser-bridge and inner sheath (A21500A) passed through a 27 F outer sheath (Olympus, Hamburg, Germany).[3]

The principles of HoLEP are sequential retrograde enucleation of the three prostatic lobes in their entirety. Hemostasis is achieved by utilizing the defocused laser on bleeding vessels.

After identifying the ureteric orifices, bladder neck incisions are made at the 5 and 7 o'clock positions to define the median lobe (Fig. 8.1). The depth of incision is made down to the prostatic capsule, easily identifiable by the transversely running connective tissue fibers. These incisions are vital to ensure the effectiveness of the remainder of the operation, particularly the enucleation of the lateral lobes. The two incisions are joined just proximal to the verumontanum, and the median lobe is enucleated in a retrograde direction. In many cases, a single incision can be employed with the median lobe tissue included with one of the lateral lobes and a bi-lobed dissection taking place.

Dissection then continues from the previously made bladder neck incision laterally and anteriorly at the level of the veru (Fig. 8.2). Once the limit of this dissection is achieved (ideally at the 2 o'clock position), a further bladder neck incision is made at the 12 o'clock position. This is continued laterally and inferiorly (Fig. 8.3). The two incisions are then joined at the level of the veru, and the lateral lobe is then enucleated retrogradely off the capsule. The same process is repeated on the contralateral side (Fig. 8.4).

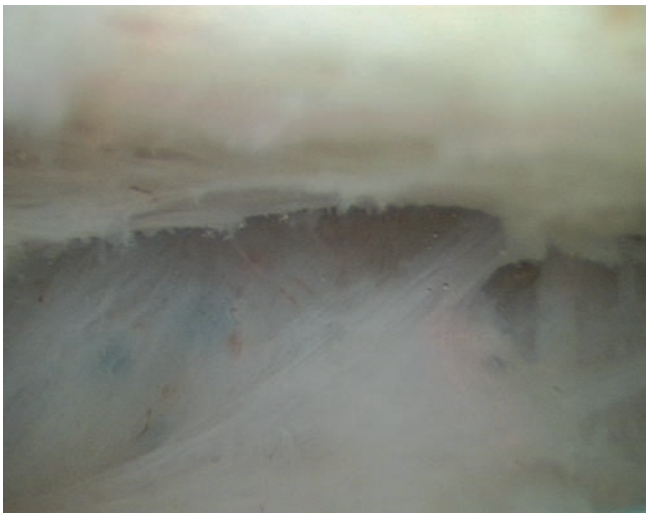

Fig. 8.2 Initial incision enucleating the lower border of right lateral lobe

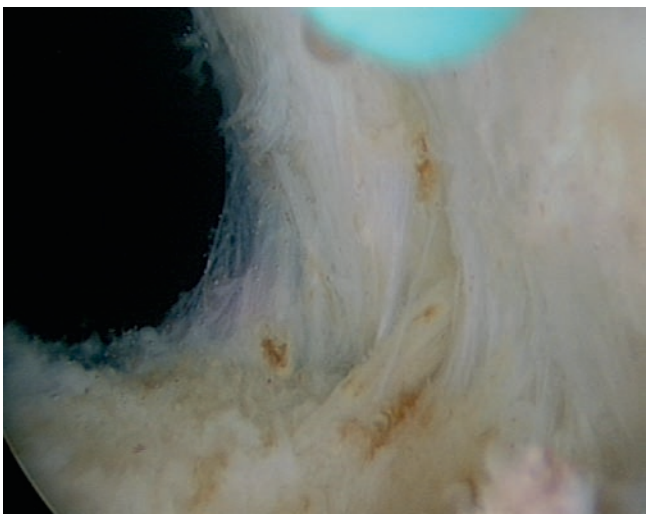

Fig. 8.3 Junction between capsule and lateral lobe

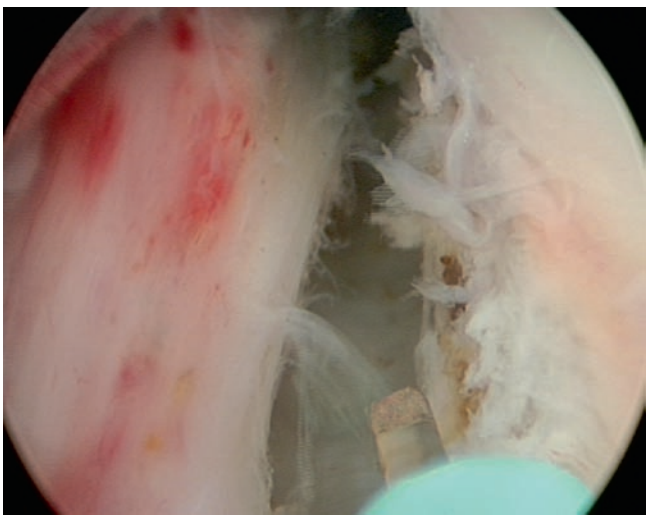

Fig. 8.1 5 o'clock bladder neck incision

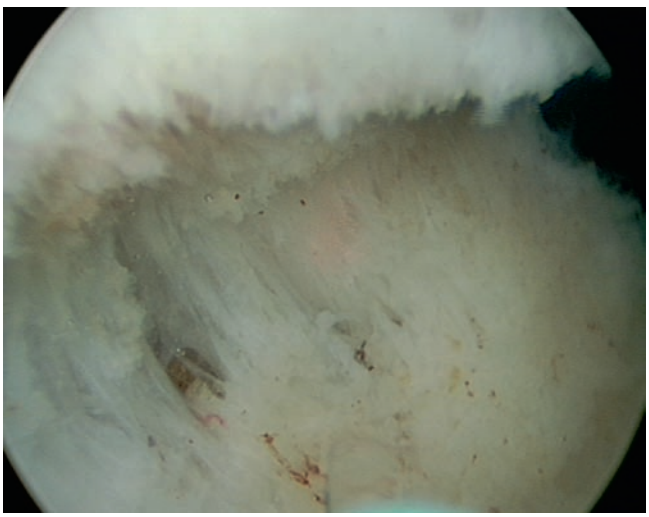

Fig. 8.4 Enucleating left lateral lobe from above

Following enucleation, morcellation is performed. This is achieved by passing the morcellator (comprising hand piece, reciprocating blades, and graduated foot pedal and controller box – Versacut, Lumenis) via a long nephroscope.

The morcellator is often cited as a drawback preventing widespread HoLEP uptake, but if simple principles are maintained, complications are rare. These principles are ensuring meticulous hemostasis (which is efficiently achieved, with blood transfusion rates much less than 1%) to allow vision to be maintained, constant distention of the bladder, and precise placement of the morcellator in the bladder cavity just inside the bladder neck. Small fragments can be removed with a retrieval loop (Storz), or Toomey syringe.[3]

Postoperatively, 95% of patients require a standard 20 F indwelling catheter, the remaining 5% requiring continuous irrigation. The vast majority of men have their catheter removed the next morning.

Comparative Trials vs. TURP

The holmium laser treatment of BPE has been extensively and thoroughly studied; several large, well-designed, randomized controlled trials have been published, and these are in contrast to the majority of literature concerning alternative treatments for BPE. This is particularly true for the green light laser literature, the majority of which is single institution case series of short duration.

Three well-designed randomized controlled trials comparing HoLEP and TURP have demonstrated the following: reduced perioperative complications, reduced catheter time, and reduced hospital stay.

Tan et al[4] published the first prospective randomized trial comparing TURP and HoLEP in 2003. All patients had extensive preoperative workup, including video urodynamics. HoLEP was superior with respect to catheter time (17.7 vs. 44 h) and hospitalization (27.6 vs. 49 h). Efficiency was equivalent but the urodynamic findings were superior with HoLEP in terms of relief of obstruction. There were no differences between the two modalities with respect to maximum urinary flow (*Q*max) or IPSS scores at 12 months of follow-up.

Kuntz et al[5] published results of a larger prospective randomized trial in 2004. There were 100 patients in each treatment arm, and again the results were consistent, with reduced catheter time (27.6 vs. 43.4 h) and hospitalization (53.3 vs. 85.8 h) in the HoLEP group. Up to 12 months of follow-up, there were similar improvements in urinary flow rates, but HoLEP was significantly superior with regard to the reduction in both symptom scores and post void residual volumes (PVR).

Montorsi et al published the first multi-center randomized trial comparing HoLEP with TURP.[6] All patients had extensive preoperative workup including urodynamics and IPSS, QOL, and IIEF questionnaires. Though operating time was longer in the HoLEP group (74 vs. 57 min), significantly more tissue was removed in the HoLEP group (36.08 vs. 25.4g). Catheterization time (31 vs. 57.78 h), and Hospital Stay (59 vs. 85.8 h) were superior in the HoLEP group. These differences were statistically significant.

A meta-analysis of HoLEP vs. TURP trials demonstrated that those undergoing HoLEP had reduced postoperative blood loss, a shorter catheterization time, and a shorter hospital stay. There were no differences in clinical outcomes between the two groups at 6 and 12 months.[7]

Perioperative Morbidity

HoLEP's perioperative morbidity is low. Blood loss is mild, with an average postoperative decrease in Hemoglobin just over 1 g/dL.[5] There were no transfusions required in the HoLEP groups of the three randomized trials.[4–6] TUR Syndrome also did not occur. The reintervention rate was 0% in Tan's paper[4] and 1% in both Montorsi's and Kuntz's studies.[5,6] Postoperative urinary retention rates are 0–8%. Specific to HoLEP, minor bladder mucosal injury caused by the morcellator occurred in up to18%, but this did not prevent timely catheter removal. Transient dysuria and urge incontinence also occurs, but was not a feature at 6 month postoperative follow-up and has been shown to be similar to TURP.[6]

Operating Time

Though HoLEP is often slower than TURP in treating moderate-sized glands, significantly more prostate tissue is removed with HoLEP and therefore the efficiency of the operation is equivalent to TURP. As prostate volume increases, HoLEP becomes significantly more efficient than TURP, and in very large glands, HoLEP needs to be compared with open prostatectomy, and in this comparison it compares very favorably.

Delayed Morbidity

Further enhancing the benefits of HoLEP, delayed morbidity for this procedure is low and not significantly different from TURP morbidity. In Montorsi's paper, 1 patient in the HoLEP group developed a urethral stricture vs. 4 in the TURP group.[6] This is consistent with Tan's findings. A pooled analysis of over 1,800 patients demonstrated that incontinence occurred in 1.1% of patients, urethral stricture in 1.9% of patients, and bladder neck contracture in 1.5%.[1]

Sexual Function

Earlier comparative studies of Holmium and TURP commenced prior to the establishment of standardized sexual function questionnaires. More recently, Briganti et al specifically compared the impact of HoLEP and TURP on sexual function. Apart from the expected impact on orgasmic function (owing to postoperative retrograde ejaculation, which was equal in both groups), there was no difference in sexual function compared with the preoperative state. There was no difference in outcome between the two surgical groups.[8]

Urodynamic Evaluation

In Tan's paper, at 6 months of postoperative follow-up, the HoLEP group had superior urodynamic parameters when compared with the TURP group, with lower PdetQmax and lower Schafer grades.[4] This is the first study showing a procedure to be urodynamically superior to TURP and is to be expected given that the prostate volume has been shown to reduce by 62–77% after HoLEP.

PSA Reduction

Several studies have shown that the reduction in PSA after treatment correlates well with the amount of adenoma resected. This is important indirect evidence to consider when comparing established techniques such as TURP and HoLEP with ablative techniques such as the KTP laser, where no tissue is removed. After HoLEP, PSA commonly drops by 81–86%.[9] In larger prostates, it has been proven that PSA can reduce by 90%.[10] A recent study demonstrated that PSA reduces by 71% after TURP,[11] but only reduces by 30–42% after treatment with KTP laser.[12,13]

Histology

One concern with HoLEP was that the effect of the holmium laser as well as mechanical morcellation would affect the ability of the histopathologist to accurately assess the adenoma specimen. This was studied by Naspro et al, who concluded that this was not the case and that the diagnosis of incidental prostate cancer is not affected.[14]

Hospital Stay

The reduced perioperative morbidity means that HoLEP can be performed as day case surgery. A randomized study of men with prostates less than 40 g demonstrated that day stay HoLEP surgery was achievable, with a mean hospital stay of 12.3 h. In our experience and that of others, over 90% of men can be treated on an outpatient basis.[15]

HoLEP vs. Open Prostatectomy

A large, well-designed randomized trial by Kuntz et al demonstrated significant advantages for HoLEP when treating large prostates. Blood loss and transfusion rates were significantly lower in the HoLEP group, as was the median hospital stay (2 vs. 10 days).[16] Significantly, there was no difference in the amount of prostate tissue removed, vindicating statements that HoLEP mimics the index finger of open prostatectomy, without the perioperative morbidity.

Naspro et al performed a well-designed, prospective randomized trial with 24 months of follow-up, comparing HoLEP with open prostatectomy for men with prostate volumes greater than 70 g. Though operating time was longer in the HoLEP group (72 vs. 58 min), catheter time and hospital stay were significantly shorter. Blood loss and transfusion rates (4 vs. 13%) were also superior in the HoLEP group. Symptomatically, there was no difference in the two groups out to 24 months of follow-up. There was no difference in the rates of late complications.[17]

HoLEP Durability

A common issue with alternative treatments for BPE is the lack of treatment durability, with deterioration in objective and subjective parameters and higher reoperation rates due to lack of adequate prostate tissue removal. Quality data are emerging supporting the sustained benefits of HoLEP.

Wilson et al published 24-month data from the randomized trial comparing HoLEP and TURP in urodynamically obstructed patients with prostate volumes between 40 and 200 g. There was no difference in symptom scores, *Q*max scores, or quality of life scores between the two surgical groups at 2 years. Two of the patients in the TURP group required reintervention vs. none in the HoLEP group.[18]

Vavassori et al have published 3-year follow-up data on 330 consecutive patients. This demonstrated that the clinical improvement was sustained at 3 years of follow-up. The reoperation rate for recurrent/residual adenoma was 2.7%.[19] Ahyai et al published the 3-year data comparing HoLEP and

TURP in 200 patients. At 2 years, symptom scores were significantly lower in the HoLEP group. At 3 years, there was no difference in outcome measures or reoperation rates between the two groups.[20] Elzayat et al have also published long-term data, which at a mean follow-up of 48 months demonstrate similar prolonged efficacy and low late complication rates. Interestingly, when analyzing their reoperation rates, 4 of the 5 patients who required reintervention occurred early in the HoLEP learning curve.[21] Gilling et al have recently published 6-year data. This demonstrated persistent reductions in IPSS scores (8.5 vs. 25.7), QOL score (1.8 vs. 4.9), and *Q*max (19 vs. 8.1). The reoperation rate was 1.4%. Ninety-two percent of patients were satisfied or extremely satisfied with the results of surgery.[22] We have also recently presented our 7-year data from the trial comparing HoLEP with TURP. At mean follow-up of 7.6 years, there was no difference in outcomes between the two groups. At this duration of follow-up, no patient in the HoLEP groups required reintervention vs. 3 patients in the TURP arm.[23]

These results obviously compare more favorably with TURP but also highlight the lack of long-term data for other alternative treatments for BPE. It is rare to find any quality data for other alternative treatments beyond 12 months of follow-up. In Kuntz's pooled analysis, 1.8% of 1,800 patients required reoperation after HoLEP.[1]

Large Prostates

Kuntz et al described their 5-year data comparing open prostatectomy to HoLEP for prostates >100 g. At 5 years, both groups had similar outcomes, with mean IPSS scores of 3.0, and mean *Q*max of 24.4 mL/s. There does not appear to be any increase in complications when treating large prostates. Reoperation rates were low, 5% in the HoLEP groups and 6.7% in the open prostatectomy group. There was no difference in the incidence of delayed urethral stricture formation or bladder neck contracture.[24]

Learning Curve

One of the commonly cited reasons that HoLEP has not become more popular is the "learning curve." This is commonly mentioned in editorials, usually by urologists who have minimal experience or understanding of the technique. There is no doubt that training and mentoring are required, but there are some advantages over learning over TURP. As there is no risk of TUR syndrome and hemostasis is much easier to achieve, there is no restriction of vision and no operative time constraints as there is for TURP. The procedure is technically satisfying and uses anatomical planes for the dissection and in our experience, is easier to teach and learn, than TURP, for novices.

Like most facets of HoLEP, the learning curve associated with it has been well studied. El Hakim concluded that 20 cases were required to achieve competence. Although good outcomes are achieved early in the operative series, enucleation efficiency improves with time.[25] Other studies demonstrate that results equivalent to published experts can be achieved after 50 cases when self-taught.[26] When learning HoLEP, a short intense period of instruction and mentoring is important, as well as careful case selection of prostates less than 60 g (ultrasound measurement).

This learning-curve data further support the broad applicability of HoLEP; it has wide clinical applications, but also need not be restricted to a talented few. When compared with many other "standard" urological procedures, such as open retropubic prostatectomy, laparoscopic nephrectomy, or robotic-assisted prostatectomy, HoLEP is easier to master.

Economics/Cost Effectiveness

A study by Salonia et al, analyzing the inpatient costs of HoLEP when compared with open prostatectomy, concluded that there was a cost advantage for HoLEP of about 10%.[27] At our institution, comparing the cost of Holmium laser resection with that of TURP also demonstrated a cost advantage for HoLRP of nearly 25%.[28] We would expect this cost advantage to be maintained for HoLEP when compared with TURP as more adenoma is removed and the addition of morcellation has made the operation more efficient.

Other Holmium Laser Techniques

Holmium Laser Bladder Neck Incision (HoBNI)

Aho et al performed a randomized study comparing HoBNI to HoLEP as an outpatient procedure in men with prostate volumes <40 g. HoBNI was significantly faster to perform, but 10% of patients in the HoBNI group required recatheterization. There was no significant difference in catheter time, or more importantly hospital time (12.3 h in HoBNI group vs. 13.7 h in HoLEP group). However, fewer patients remained obstructed at 6 months following HoLEP, but this appeared to be true only for prostates between 30 and 40 g.[29] This study supports the fact that like other alternative treatments for BPE, day-stay surgery is achievable in the vast majority of patients with both HoBNI and HoLEP.

HoBNI as a catheterless day-stay procedure was described by Cornford et al in 1998. Ninty-seven of 100 patients voided successfully postoperatively. There were significant improvements in symptom scores and urinary flow rates, which were sustained at 2 years of follow-up.[30]

Holmium Laser Ablation of the Prostate (HoLAP)

The use of the high-powered holmium laser has evolved to the current technique of enucleation but the older techniques of ablation and resection may still play a role for some urologists. Ablation was the first technique used with the holmium laser (HoLAP), and has the advantage of being simple to perform. A side-firing fiber is used to create a TURP-like cavity.

HoLAP has been compared with TURP; this demonstrated improved perioperative outcomes for ablation, with reduced bleeding, catheter time, and hospital stay in the ablation group.

In one of the very few studies to analyze the long-term outcome of HoLAP, a paper by Tan et al reported 7-year data. Although, like in most BPE studies, there were a significant percentage of patients lost to follow-up, the study showed that *Q*max improved by a mean of 83% and IPSS score reduced by 47%. The reoperation rate was 15%.[31] This highlights one of the several problems with the ablation technique. In addition, the technique is inefficient, and very slow when used for treating large prostates. In common with all ablation procedures, it is also aesthetically inferior when compared with more refined anatomical techniques.

With the promotion of the high-powered KTP laser, ablation has been repopularized.[32] In response, HoLAP has been remarketed and may have a role to play in treating the smaller prostate although data have recently been presented concerning its use in large glands.

Holmium Laser Resection of the Prostate

Prior to the development of a morcellator, the holmium laser was used to resect tissue rather than enucleate whole lobes. The prostate was resected in pieces small enough to be removed whole (less than 1–2 g), or be resected once they were in the bladder. Though this is a more effective use of the holmium laser's unique properties, it is inefficient when compared with whole lobe enucleation and morcellation.

Nevertheless, HoLRP has been well studied. A prospective randomized trial comparing HoLRP with TURP showed perioperative advantages for HoLRP; nursing requirements, catheter time, and duration of hospital stay were superior. There were no differences in outcome between the two groups at 12 months.[33] Westenberg published 48-month data for this comparative study. There was no difference in outcomes between the two groups, with similar improvements in symptom scores and urinary flow rates.[34]

While HoLEP is the mainstay of treatment, HoLRP has an advantage of avoiding morcellation, which may appeal to some urologists. It is also commonly employed in malignant "channel" prostatectomy and for reoperations. However, this is really only a viable primary option for smaller prostates, as operating time is long.

Conclusion

HoLEP has been proven to be a safe and effective means of treating BPE and can be used to treat prostates of any size. It has reduced the burden of postoperative care with less postoperative bleeding and reduced irrigation requirements. It has obvious patient and economic advantages with shorter hospitalization times when compared with the incumbent procedure, TURP. The postoperative outcomes between the two procedures are at least equivalent, and HoLEP has proven durability out to 7 years of follow-up. This is in stark contrast to other alternative treatments for BPE.

References

1. Kuntz RM. Current role of lasers in the treatment of BPH. *Eur Urol*. 2006;49(6):961–969
2. Elzayat E, Habib E, Elhilali M. Holmium laser enucleation of the prostate in patients on anticoagulant therapy or with bleeding disorders. *J Urol*. 2006;175(4):1428–1432
3. Gilling PJ. Holmium laser enucleation of the prostate (HoLEP). Surgery illustrated. *BJUI Int*. 2008;101(1):131–142
4. Tan AHH, Gilling PJ, Kennett KM, et al Randomized trial comparing holmium laser enucleation of prostate with transurethral resection of prostate for treatment of bladder outlet obstruction secondary to benign prostatic hyperplasia in large glands (40 to 200 grams). *J Urol*. 2003;170:1270
5. Kuntz R, Ahyai S, Lehrich K, Fayad A. Transurethral holmium laser enucleation of the prostate versus transurethral electrocautery resection of the prostate: a randomized prospective trial in 200 patients. *J Urol*. 2004;172(3):1012–1016
6. Montorsi F, Naspro R, Salonia A, et al Holmium laser enucleation versus transurethral resection of the prostate: results from a 2-center prospective randomized trial in patients with obstructive benign prostatic hyperplasia. *J Urol*. 2008;179(5 suppl):S87–S90
7. Tan A, Liao C, Mo Z, et al Meta-analysis of holmium laser enucleation versus transurethral resection of the prostate for symptomatic prostatic obstruction. *Br J Surg*. 2007;94(10):1201–1208
8. Briganti A, Naspro R, Gallina A, et al Impact on sexual function of holmium laser enucleation versus transurethral resection of the prostate: results of a prospective, 2-center, randomized trial. *J Urol*. 2006;175(5):1817–1821

9. Tinmouth WW, Habib E, Kim SC, et al Change in serum prostate specific antigen concentration after holmium laser enucleation of the prostate: a marker for completeness of adenoma resection? *J Endourol*. 2005;19(5):550–554
10. Matlaga BR, Kim SC, Kuo RL, et al Holmium laser enucleation of the prostate for prostates of >125 mL. *BJU Int*. 2006;97(1):81–84
11. Fonseca RC, Gomes CM, Meireles EB, et al Prostate specific antigen levels following transurethral resection of the prostate. *Int Braz J Urol*. 2008;34(1):41–48
12. Sulser T, Reich O, Wyler S, et al Photoselective KTP laser vaporization of the prostate: first experiences with 65 procedures. *J Endourol*. 2004;18:976–981
13. Volkan T, Ihsan T.A, Yilmaz O, et al Short term outcomes of high power (80 W) potassium-titanyl-phosphate laser vaporization of the prostate. *Eur Urol*. 2005;48:608–613
14. Naspro R, Freschi M, Salonia A, et al Holmium laser enucleation versus transurethral resection of the prostate. Are histological findings comparable? *J Urol*. 2004;171(3):1203–1206
15. Larner TR, Agarwal D, Costello AJ. Day-case holmium laser enucleation of the prostate for gland volumes of <60 mL: early experience. *BJU Int*. 2003;91(1):61–64
16. Kuntz R, Ahyai S, Lehrich K. Transurethral holmium laser enucleation of the prostate compared with transvesical open prostatectomy: 18-month follow-up of a randomized trial. *J Endourol*. 2004; 18(2):189–191
17. Naspro R, Suardi N, Salonia A, et al Holmium laser enucleation of the prostate versus open prostatectomy for prostates >70 g: 24-month follow-up. *Eur Urol*. 2006 ;50(3):563–568
18. Wilson LC, Gilling PJ, Williams A, et al A randomised trial comparing holmium laser enucleation versus transurethral resection in the treatment of prostates larger than 40grams: results at 2 Years. *Eur Urol*. 2006;50(3):569–573
19. Vavassori I, Valenti S, Naspro R, et al Three-year outcome following holmium laser enucleation of the prostate combined with mechanical morcellation in 330 consecutive patients. *Eur Urol*. 2008;53(3):599–604
20. Ahyai S, Kuntz R, Lehrich K. Holmium laser enucleation versus transurethral resection of the prostate: 3-year follow-up results of a randomized clinical trial. *Eur Urol*. 2007;52(5):1456–1463
21. Elzayat E, Elhilali M. Holmium laser enucleation of the prostate (HoLEP): long-term results, reoperation rate, and possible impact of the learning curve. *Eur Urol*. 2007;52(5):1465–1471
22. Gilling PJ, Aho TF, Frampton CM, King CJ, Fraundorfer MR. Holmium Laser Enucleation of the prostate: results at 6 Years. *Eur Urol*. 2008;53(4):744–749
23. Gilling PJ, Wilson LC, Westenberg AM, Fraundorfer MR. A randomized trial comparing the long-term results of HOLEP and TURP in urodynamically obstructed patients: results at 7 years. *J Urol*. 2008;179:671; Abstract.
24. Kuntz R, Lehrich K, Ahyai S. Holmium laser enucleation of the prostate versus open prostatectomy for prostates greater than 100 grams: 5-year follow-up results of a randomised clinical trial. *Eur Urol*. 2008;53(1):160–166
25. El-Hakim A, Elhilali MM. Holmium laser enucleation of the prostate can be taught: the first learning experience. *BJU Int*. 2002;90(9):863–869
26. Elzayat EA, Elhilali MM, Holmium laser enucleation of the prostate (HoLEP): long-term results, reoperation rate, and possible impact of the learning curve. *Eur Urol*. 2007;52(5):1465–1471
27. Salonia A, Suardi N, Nasproi R, et al Holmium laser enucleation versus open prostatectomy for benign prostatic hyperplasia: an inpatient cost analysis. *Urology*. 2006;68(2):302–306
28. Fraundorfer MR, Dunton N, Das A, Gilling PJ. Holmium laser resection of the prostate is more cost-effective than transurethral resection of the prostate: actual values based on a randomised prospective trial. *ANZ J Surg*. 1999;696:A115
29. Aho T, Gilling P, Kennett K, Westenburg AM, Fraundorfer MR, Frampton CM. Holmium laser bladder neck incision versus holmium laser enucleation of the prostate as outpatient procedures for prostates less than 40 grams: a randomized trial. *J Urol*. 2005;174: 210–214
30. Cornford PA, Biyani CS, Powell CS. Transurethral incision of the prostate using the holmium:YAG laser: a catheterless procedure. *J Urol*. 1998;159(4):1229–1231
31. Tan A, Gilling PJG, Kennett K, Fletcher H, Fraundorfer M. Long term results of holmium laser ablation of the prostate. *BJUI*. 2003; 92:707–709
32. Kumar SM. Photoselective vaporization of the prostate: a volume reduction analysis in patients with lower urinary tract symptoms secondary to benign prostatic hyperplasia and carcinoma of the prostate. *J Urol*. 2005;173(2):511–513
33. Gilling PJ, Kennett KM, Fraundorfer MR. Holmium laser resection of the prostate (HoLRP) versus transurethral resection of the prostate (TURP): results of a randomised trial with 2 years follow-up. *J Endourol*. 2000;14:757–760
34. Westenberg A, Gilling P, Kennett K, Frampton C, Fraundorfer M. Holmium laser resection of the prostate (HoLRP) versus transurethral resection of the prostate (TURP): results of a randomised trial with long-term follow-up (4 year minimum). *J Urol*. 2004;172: 16–619

Lasers and Urinary Calculi

9

Ranan DasGupta and Nicholas Hegarty

The application of novel technology and innovative surgical techniques has contributed greatly to the advance of endourology over the past two decades. Key developments include endoscopic access to the urinary tract and advances in intra- and extra-corporeal stone fragmentation techniques. Of these techniques, laser technology has also been applied to other branches of urology including prostate surgery, ablation of urothelial tumors, and treating urinary strictures. The safe introduction of this potentially hazardous technology has required defining stringent safety guidelines, which encompass protection of both the patient and the user. In this chapter, physics of laser is discussed, along with the review of its application in treating stones.

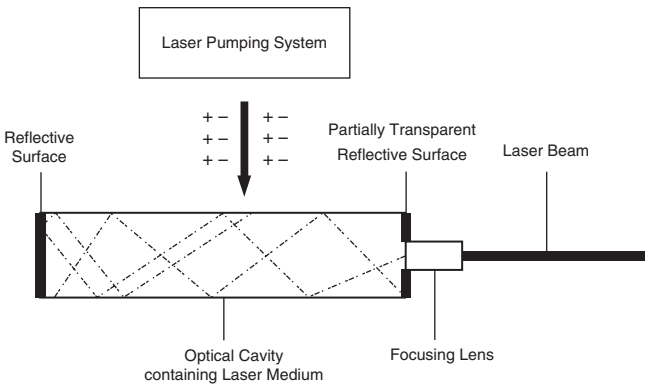

Fig. 9.1 Basic summary of generation of laser beam

Background

The foundations for the development of this technology can be traced to theories developed by Albert Einstein and Satyendranath Bose whose work on photons were the basis of the stimulated emission of radiation. In the early 1950s, Charles Townes and colleagues developed a "maser," based on microwave amplification, which was applied to atomic clocks, receivers in radio telescopes, and other uses. In fact, Townes did publish a paper in 1958 describing the theoretical possibility of a laser, with light rather than microwaves being amplified; he subsequently went on to share the Nobel Prize for Physics in 1964.

The acronym LASER (light amplification by stimulated emission of radiation) dates from the late 1950s when Gordon Gould used the term in his doctoral thesis.[1]

How Lasers Work

The laser beam is generated by passing light through a "lasing medium," which is a material with properties that allow it to amplify light by stimulated emission of photons (Fig. 9.1). The medium may be solid, liquid, gas, or plasma. As the medium absorbs energy, electrons are raised into a higher-energy state; upon dropping down to a lower-energy level, photons are emitted. When the photons collide, further photons are emitted. Photons are reflected along the optical chamber with opposing mirrors at either end generating the laser beam.

The characteristics of a laser beam are that it is *coherent*, *collimated*, and *monochromatic.* This means that the energy waves are in phase, do not diverge (i.e., are focused), and are of a single wavelength (unlike white light). The wavelength is determined by the lasing medium used, and this in turn helps to determine the depth of penetration of the beam.

As the laser beam encounters tissue, it will be absorbed, scattered, and reflected depending on the characteristics of the tissue and laser, respectively. The most important of these is absorption, with the intensity of the laser beam decreasing exponentially as the beam enters the absorbing medium (Lambert-Beer law). The laser energy is converted to heat, which thereby causes tissue coagulation or vaporization.

Classification of Lasers

Lasers are generally classified as to the type of laser medium or by their effect on human tissue (principally their propensity to damage skin and retina). Differences between medical lasers and other applications are summarized in Table 9.1.

P. Dasgupta et al. (eds.), *New Technologies in Urology,*
DOI: 10.1007/978-1-84882-178-1_9, © Springer-Verlag London Limited 2010

Table 9.1 Classification of lasers

Class	Power	Examples	Precautions
I	Very low	CD and DVD players, laser printers	None required
II	Low (<1 mW)	Laser pointers	Avoid pointing toward eye
IIIa	Intermediate (1–5 mW)	Laser scanners	Do not view directly
IIIb	Intermediate (5–500 mW)	Light shows, spectrometry	Protective eye wear. Operate in "laser controlled area"
IV	High >500 mW	Surgical lasers, industrial cutting lasers	Protective eye wear. Limit reflective surfaces. Operate in "laser controlled area." Do not place body parts in laser firing line

Solid State

Common solid-state lasers include Nd:YAG (neodymium yttrium aluminum garnet) which has a wavelength of 1,064 nm and Ho:YAG (holmium) with a wavelength of 2,100 nm. Of these, the Holmium has generated the greater interest in the past few years, possibly related to its application in a range of surgeries including calculi as well as prostates and strictures. The wavelength approaches that of water (1,910 nm), and both prostate and renal stones contain significant amounts of water and therefore absorb holmium laser energy. Mucosal effects are limited, even with direct contact, to a depth of penetration of 0.4 mm, thereby limiting collateral damage.

Another laser finding widespread application more recently in urology is the KTP (potassium titanyl phosphate). This is in fact a modification of Nd:YAG, the product of which is passed through a KTP crystal, thus halving its wavelength to 532 nm. As this wavelength is well absorbed by hemoglobin, this laser is particularly suited to photoselective vaporization of prostate (PVP) tissue. The depth of penetration is 1–2 mm. Another variation is the FREDDY laser (or frequency doubled double pulse Nd:YAG laser), which switches between the 1,064 and 532 nm wavelengths, allowing the same laser to be used for both lithotripsy and prostate ablation.

Like Holmium, Thulium is also a rare earth metal, and has been developed as a laser in recent years. Factors including cost have prevented its widespread use so far, but there are now several studies supporting its use in the treatment of bladder outflow obstruction.

Gas

Gas lasers include those using CO_2 (9.6, 10.6 μm) and Argon (350–500 nm). The CO_2 laser is an infrared laser, with a long wavelength (10,640 nm) that produces a very short depth of penetration (less than 0.2 mm), lending itself to treating superficial lesions (e.g., penile lesions).

Dye

Pulsed dye lasers were used during the early development of laser technology in urology, but advances in laser technology have generally replaced these lasers, which were based on organic dyes as the medium.

Applications of Lasers in Urology

Laser for Stone Management

The four main modalities for endoscopic stone fragmentation are pneumatic (electrokinetic), ultrasonic, electrohydraulic, and laser. Laser lithotripsy is now generally synonymous with holmium laser treatment. The basis for stone fragmentation with the holmium laser depends on a combination of photothermal, photomechanical, and cavitation-bubble effects. Unlike the mechanical modalities of ultrasound or pneumatic lithotripsy, the laser involves absorption of its particular wavelength by the water molecules of the stone. Vaporization of these molecules then leads to bubble formation within the stone, and their collapse leads to fragmentation. A second effect is that of a thermochemical reaction at the stone surface, such that the laser causes crater formation by "stone meltdown" at the stone surface. Third, the laser generates a spherical cavitation bubble, which then produces a shock wave upon its collapse; this shock wave produces the photoacoustic effect of stone fragmentation upon hitting the stone. The longer the pulse width of the laser (duration of each pulse of laser energy), the greater the energy involved in generating the cavitation bubble – this mechanism is similar to pneumatic lithotripsy, for example, but is only one of the several mechanisms of action of the laser as mentioned. Comparisons of laser with other modalities are shown in Table 9.2.

A key advantage of the laser is that there is less retropulsion of the stone. There is some migration of the stone (due to generation of internal shock waves and creation of vapor bubbles, which push away the stone) but less so than the pneumatic lithotrite, for example. Other modalities create a

Table 9.2 Comparison of stone fragmentation rates

Study	Comparison	Results	
Bapat et al[6]	Laser vs. pneumatic	Fragmentation (97% laser vs. 81% pneumatic)	Secondary procedures (2% laser vs. 14% pneumatic)
Manohar et al[7]	Laser vs. pneumatic	Stone-free rates (84% laser vs. 88% pneumatic)	Secondary procedures (12% laser vs. 16% pneumatic)
Ziaee et al[8]	URS vs. ESWL	Stone-free rates (72% URS vs. 79% ESWL)	
Hautmann et al[9]	URS vs. ESWL	Stone-free rate (97% URS vs. 78% ESWL)	

very strong shock wave with "scatter" of energy and potential injury to the adjacent urothelium. As this is less apparent with laser fragmentation, its use is favored for ureteric stones. Furthermore, the laser's ability to break stones to dust particles gives the benefit of not needing to remove fragments endoscopically (e.g., with graspers or baskets) and even possibly avoiding the need for a stent. The smaller diameter fibers (200 or 365 μm) used with a holmium laser enable fragmentation of upper tract stones that are accessed using a flexible ureterorenoscope; this is not achievable with mechanical lithotrites as they do not permit deflection of their probes.

Power settings vary, but typically holmium laser stone fragmentation is performed with incremental increases in power from 0.5 to 1.0 J at 6–10 Hz, with higher settings being usually reserved for the kidney or ablative procedures.

Choice of laser machine depends on the likely uses – more expensive high-energy machines offer the versatility of application to ablative, e.g., prostate surgery, though the energy for this is far higher (at 80–100 W); if solely used for stone treatment, a lower energy holmium machine (20–30 W) can be used, with considerable cost savings albeit less versatile.

Lasers for Prostate Surgery

Discussion of lasers in prostate surgery is beyond the scope of this chapter, except for a broad outline. Since the introduction of pulsed coumarin dye lasers in the 1980s,[2] urology has witnessed a reemergence of the popularity of this therapy with the arrival of the ablation and enucleation techniques. The KTP (or "Greenlight") laser uses a wavelength of 504 nm, and produces a vaporization of the prostate by its side-firing ablative delivery – the PVP. The holmium laser (wavelength 2,100 nm) has also been applied in an ablative role, though its end-firing fiber can also be used to *enucleate* the prostate, a similar principle to transurethral resection of prostate (TURP) – the so-called holmium enucleation of prostate (HoLEP). One of the advantages of the enucleative technique is that it provides tissue for histological analysis, though there have been comments about the longer learning curve when compared with the relatively easier method of vaporization, and also removal of the enucleated prostate lobes requires a dedicated morcellation device. Nevertheless, HoLEP provides the advantages of reduced bleeding, avoidance of TUR syndrome (by using saline instead of glycine), and option of treating larger glands than the traditional TURP as there are no safety time constraints (akin to Millin's prostatectomy).

Lasers for Transitional Cell Carcinoma

There is increasing familiarity with the use of the laser with a flexible cystoscope in the treatment of small bladder tumor recurrences, which have traditionally been diathermized. The practical limitations of laser availability for these cases are more restrictive than the actual technical aspects of this treatment.

In the upper tract, there appears to be increasing acceptance of laser treatment of small, focal, low-grade low volume disease, which traditionally would have been dealt with by radical nephroureterectomy. Although the latter is still arguably the "gold standard" for the treatment of upper tract transitional cell tumors, there is increasing long-term evidence for the safe use of laser ablation of tumors.[3]

Lasers for Stricture and PUJ Obstruction

Although there may be a role for lasers in the management of strictures in the ureter and pelvi-ureteric junction, this field is more controversial. The primary management of an idiopathic PUJ obstruction remains a pyeloplasty, though some advocate the use of endopyelotomy following failed pyeloplasty. The use of lasers to perform this incision has been proposed in some centers,[4] just as incision of ureteric strictures has been performed using the holmium laser by some.[5] The long-term success or failure of these procedures may be a reflection of the actual operation itself rather than the energy modality (e.g., laser) used to carry it out.

Comparison of Holmium Lithotripsy with Other Stone Treatments

The management of stones in different clinical settings will often be determined by the availability of an energy source to break the stone and the range of endoscopic equipment on hand. While a distal ureteric stone can be successfully cleared with electrokinetic force as well as laser, a higher ureteric stone or a stone in the kidney may need greater versatility as seen with a laser probe through a flexible ureterorenoscope. Several studies have compared laser with other treatments for ureteric stones, in particular for those in the proximal ureter. These include recent comparisons with pneumatic lithotripsy[6,7] and also ESWL.[8,9]

Lasers and Specific Stones

One of the concerns of holmium usage has been with uric acid calculi owing to the release of cyanide as a by-product. Incremental increases in cyanide production are seen with higher energy settings with a recommendation to keep power settings below 1.0 J,[10,11] though systemic absorption of this leading to death has not been reported. Other stones that may be refractory to laser treatment include calcium oxalate monohydrate.

Lasers and Pregnancy

The recently updated EAU guidelines on the management of ureteric stones include recommendation for safe use of ureteroscopy. This mentions studies describing safe use of holmium laser during ureteroscopy in pregnancy, and proposed that this is a reasonable option in specialist centers after failure of conservative treatment. Watterson et al described eight pregnant patients at two tertiary centers who were treated for symptomatic urolithiasis or encrusted stents, and reported no obstetric complications of ureteroscopy with holmium laser treatment.[12]

Safety Procedures

Safety training is mandatory for all staff involved in laser treatments. These measures include those relating to the treatment area (e.g., operating room), staff, and patient. The operating room must have clear warning signs prohibiting entry during laser use, be locked while the laser is in use, have darkened or shielded windows to prevent errant laser light; the laser machine should be stored in a safe location, and the starting key/switch be the responsibility of a named individual. Energy use should be documented in a book each occasion the laser is used.

The patient should be given protective eyewear even if the eyes are closed during a general anesthetic. Similarly, all staff in the operating room require protective eyewear. Clear instructions should be given for when the laser is to be activated and switched off.

Future Developments

Future improvements in laser technology are discussed in a review paper by Pierre and Albala.[13] Changes in the laser machines (based on the lasing medium) as well as the optical laser fibers for delivery of the laser energy are described. Other factors such as patient demands and market costs will also influence choice of lasers in the future.

References

1. Gould G, Gordon R. The LASER, light amplification by stimulated emission of radiation. In Franken PA, Sands RH, eds. *The Ann Arbor Conference on Optical Pumping*. University of Michigan;1959
2. Watson GM, Wickham JE. Initial experience with a pulsed dye laser for ureteric calculi. *Lancet*. 1986;1:1357–1358
3. Lucas SM, Svatek RS, Olgin G, et al Conservative management in selected patients with upper tract urothelial carcinoma compares favourably with early radical surgery. *BJUI*. 2008;102(2):172–176
4. Biyani CS, Cornford PA, Powell CS. Retrograde endoureteropyelotomy with the holmium:YAG laser. Initial experience. *Eur Urol*. 1997;32(4):471–474
5. Bagley D, Erhard M. Use of the holmium laser in the upper urinary tract. *Tech Urol*. 1995;1(1):25–30
6. Bapat SS, Pai KV, Purnapatre SS, et al Comparison of holmium laser and pneumatic lithotripsy in managing upper-ureteral stones. *J Endourol*. 2007;21(12):1425–1427
7. Manohar T, Ganpule A, Desai M. Comparative evaluation of Swiss LithoClast 2 and holmium:YAG laser lithotripsy for impacted upper-ureteral stones. *J Endourol*. 2008;22(3):443–446
8. Ziaee SA, Halimiasl P, Aminsharifi A, et al Management of 10–15-mm proximal ureteral stones: ureteroscopy or extracorporeal shockwave lithotripsy? *Urology*. 2008;71(1):28–31
9. Hautmann S, Friedrich MG, Fernandez S, et al Extracorporeal shockwave lithotripsy compared with ureteroscopy for the removal of small distal ureteral stones. *Urol Int*. 2004;73(3):238–243
10. Teichman JM, Vassar GJ, Glickman RD, et al Holmium:YAG lithotripsy: photothermal mechanism converts uric acid calculi to cyanide. *J Urol*. 1998;160(2):320–324
11. Corbin NS, Teichman JM, Nguyen T, et al Laser lithotripsy and cyanide. *J Endourol*. 2000;14(2):169–173
12. Watterson JD, Girvan AR, Beiko DT, et al Ureteroscopy and holmium:YAG laser lithotripsy: an emerging definitive management strategy for symptomatic ureteral calculi in pregnancy. *Urology*. 2002;60(3):383–387
13. Pierre SA, Albala DM. The future of lasers in urology. *WJU*. 2007;25:275–283

Lasers for Bladder Tumors

10

Naomi Smith and Kay Thomas

Introduction

Bladder cancer is the fourth most common cancer in men with 8,373 new diagnoses of bladder cancer made in the United Kingdom in 2006[1] (Incidence of 29.3 per 100,000 in men; 9.3 in women). Initial diagnosis is usually made endoscopically using both macroscopic appearances and microscopic features of the tumor. Tissue is commonly obtained via transurethral resection of bladder tumor (TURBT) using diathermy, but if the tumors are small and/or the bladder is thin, cold cup biopsy forceps with diathermy coagulation may be used.[2] The mainstay of surveillance currently is outpatient local anesthetic flexible cystoscopy. Any recurrences identified are then initially treated with TURBT or biopsy and cystodiathermy with further treatments given depending on the clinical indications.

With the advent of laser technology and its use in other areas of urology, much interest has been generated in the use of lasers to treat bladder tumors. Laser therapy for bladder cancer was first reported in Germany in the 1970s and approved for use in the USA in 1984 but is still not the standard of care. In particular, the perceived benefit of improved hemostasis (allowing catheter-free treatment and facilitating treatment of patients on anticoagulants) and the possibility of performing procedures under local anesthetic make this an attractive option. This chapter reviews the potential role of different types of lasers in bladder cancer management, looking at the evidence for both ablation and, more recently, resection using this technology.

Laser Technology in Treatment of Bladder Tumors

General Features of Lasers

Lasers deliver energy as photons of light generated by excited atoms returning to their resting energy state.[3] The wavelength is determined by the properties of the lasing medium. Tissues contain chromophores that selectively absorb light of different wavelengths; effects are generated via thermal energy – coagulating or vaporizing tissues depending on the amount of heat involved. If coagulative necrosis is achieved, the tissue maintains its structure and heals via deposition of collagen.

Surgical lasers have differing properties depending on the substance used to produce the laser (the lasing material, which determines the wavelength) and chromophore that absorbs the laser energy in tissues, e.g., blood or water. The laser's penetration is measured by the extinction length, the depth at which 90% of the incident laser energy is absorbed and converted into heat. Lasers with different extinction length are suitable for different therapies.

Lasers are already widely used in urological surgery to ablate and resect prostates, fragment stones, incise strictures, treat genital warts, and ablate upper tract transition cell carcinoma. They are particularly suited to endourological surgery because the fibers are small enough to fit down the working channel of scopes, relatively flexible, and can be targeted to produce a relatively small area of heating effect – to treat the pathology and spare healthy tissue. Of crucial importance, lasers have good hemostasis on soft tissues and can maintain the endoscopic field of view.

Advantages of lasers in the Treatment of Bladder Tumors

Lasers can be used for bladder tumor ablation and/or tumor resection depending on the type of laser used and its power settings.[4–8] An advantage of using laser in bladder tumor ablation is that it seems to be less painful than standard electrocautery, which some authors have suggested is due tothe rapid heating *destroying* neural tissue in contrast to electrocautery, which causes current to propagate backward along nerve fibers (Table 10.1). This potentially allows ablative treatment under local anesthetic in an out-patient setting.

It has also been reported that laser treatment does not excite the obturator nerve, negating the need for paralysis of

P. Dasgupta et al. (eds.), *New Technologies in Urology,*
DOI: 10.1007/978-1-84882-178-1_10, © Springer-Verlag London Limited 2010

Table 10.1 Advantages and disadvantages of lasers in the treatment of bladder tumors

Advantage	Disadvantage
Improved hemostasis	Inadequate histology specimen
Minimal pain	Perforation of bladder ± bowel
Reduced need for catheter	Inadequate depth of penetration to treat tumor
No stimulation of obturator nerve	Staff training and expertise
Resection using saline not glycine	Equipped theater
Reduced cost of out-patient procedure	Expensive machine

patients with tumor on the lateral wall of the bladder. In theory, this should allow a more complete resection of tumor in this notoriously difficult location. It is also useful for the treatment of tumors in other difficult locations – bladder diverticulum and near the ureteric orifice.

The bleeding is less when using a laser compared with diathermy and therefore a decreased requirement for irrigation.[9] This allows the treatment of patients with coagulopathies or on anticoagulants with less morbidity. Also, the decreased requirement for irrigation facilitates catheter-free surgery and, therefore, day case treatment.[10,11] Intraoperatively, saline is used for irrigation rather than glycine, thus avoiding the rare complication of TUR syndrome.

Disadvantages of Lasers in the Treatment of Bladder Tumors

The main disadvantage of using a laser for the treatment of bladder tumors is the loss of tissue for histological analysis, which has often limited its use to low-grade, superficial, recurrent tumors.[5–8] There are specific changes that are induced in the urothelium in response to the laser – coagulation necrosis, ulceration, granulation, and healing by fibrosis – which make histological interpretation difficult particularly with respect to accurate staging.[12]

The potential for perforation of the bladder or nearby pelvic organs (especially bowel) is a complication of the Nd:YAG laser but with the newer lasers the depth of penetration is so much lower that this is largely a historical complication.[13,14] However, the lack of depth of penetration can lead to inadequate treatment of tumor.

Regardless of the type of laser used, the theater staff and surgeon must be formally trained in its use and be available when required. There are strict legal requirements for laser safety: staff and patient wearing goggles, room to have limited access, all windows are covered, signs outside the theater, etc.

The expense of the treatment (laser machine and fibers) can be either a disadvantage or an advantage depending on whether it is being bought specifically for this purpose or if procedures previously requiring admission and general anesthesia are now day cases.

Specific Types of Lasers

The neodymium:YAG laser was the most commonly used at the outset of laser treatment of bladder cancer and many of the published studies are, therefore, based on this laser.[15–22] Recently, however, it has been superseded by the holmium:YAG laser, perhaps not only due to its use in other areas of urology – causing it to be more readily available in departments – but also due to its safer tissue penetration.[23–30] In the last year, reports of thulium:YAG laser offer a new and potentially exciting development in the use of lasers for bladder cancer treatment.[31–33]

Neodymium:YAG

The Nd:YAG laser was the first laser to achieve widespread use in urology. This laser uses a Neodymium:YAG crystal (Yttrium Aluminum Garnet) and produces an invisible light of continuous 1,064 nm wavelength. The long extinction length and penetration of 5–10 mm are due to its poor absorption by both water and tissue. The Nd:YAG laser causes damage by coagulative necrosis. Macroscopically, the tissue appears ulcerated and covered with eschar in the acute phase. Microscopically, areas of necrotic tissue are seen, which are sharply delineated from adjacent tissue. At about 8 weeks, these lesions show healing and marked granulation tissues and chronically dense fibrosis occurs.[12]

The deep penetration gives effective coagulation and can achieve transmural coagulation of the bladder wall without perforation; however, the long extinction length can also result in tissue damage to pelvic organs beyond the bladder, e.g., bowel in the *absence* of bladder perforation.[13,14] This is particularly pertinent in thinned areas, e.g., the dome of the bladder and, in these cases, it is important to keep the bladder relatively empty to reduce this risk. In a series of over 2,000 cases, the rate of intestinal perforation was 0.01%. The authors advised a lower power of 30 W with the Nd:YAG laser in patients who have had previous laser therapy to the bladder or tumors on the posterior bladder wall.[15]

The standard noncontact Nd:YAG technique uses 30–40 W of energy, with the fiber held 3–4 mm from the lesion surface; energy is then applied in a continuous fashion to coat the surface. The tumor undergoes whitish discoloration

as it is coagulated, and these areas may then be displaced to treat deeper layers. Hemostasis is such that continuous irrigation and routine postoperative catheterization are rarely needed. The dangers of bladder injury and occult bowel perforation have led to the Nd:YAG largely losing favor for treatment of bladder tumors.

KTP:YAG

When an Nd:YAG laser is used in combination with potassium titanyl phosphate crystal, a visible green light laser is produced with a wavelength of 532 nm. This laser therefore has short extinction length with tissue penetrance of 1–2 mm. In well vascularized tissues, penetrance can be as little as 1–2μm creating high temperatures, which vaporize tissue. The absorption in water is low leading to concerns about the effect of scattered photons or the misfired laser beam. This laser could be used for treating superficial lesions and potentially has a greater margin for safety, but would be very slow. There are no reports of its use in the literature for the treatment of bladder cancer probably due to the better efficacy of holmium:YAG.

Holmium:YAG

A greater understanding of the behavior of light and tissue interactions led to the development of the 2,100 nm Holmium:YAG laser.[3] There are also thulium ions present, which provide cross-relaxation preventing the laser from generating an excessive amount of heat and allowing it to fire at a repetitive pulsed rate at room temperature. The holmium laser experiences a short extinction length both in tissue and in irrigation fluid, as it is absorbed by water. The laser can produce both coagulation and tissue vaporization depending on power properties and because it is absorbed well by water, penetrance is limited to 0.5–1 mm. This makes it safer in the bladder than Nd YAG, but it can be more time-consuming and care must be taken to ensure adequate penetration of the tumor base.

Thullium:YAG

The most recent development is the Thullium:YAG laser, a continuous laser on a similar wavelength to the holmium:YAG laser (2,000 nm), but the thulmium ions are excited directly by high-power laser diodes.[3] This increased power efficiency avoids excessive heat generation and so negates the requirement for elaborate cooling and insulation mechanisms. The pulsed holmium laser creates a tearing action on tissues, whereas the continuous output from the thullium laser gives smoother incisions and better vaporization and coagulation. Early results using this laser for prostate vaporization and more recently for ablation of bladder tumors are emerging in the literature.[31–33]

Methods of Using Lasers for Treatment of Bladder Tumors

Ablation

Transurethral resection although still the standard treatment for bladder cancer has a number of limitations, one of which is that cutting into the tumor and shedding viable tumor cells into the bladder may be one of the factors responsible for tumor recurrence.[34–36] Laser ablation allows noncontact tumor necrosis, which may explain the decrease in local recurrence reported with laser ablation.[17–19]

Several techniques for ablating bladder tumors have been described over the years. Initially, the Nd:YAG laser was used with energy applied circumferentially to the tumor including a margin of 0.5–1 cm to ensure treatment of surrounding precancerous areas, coagulation of vessels, and in particular, lymphatics around the tumor.[8] However, subsequent studies have not confirmed the "sealing" of lymphatics and no dynamic scintography trials have confirmed this hypothesis. Depending on the clinical factors, the tumor was then sampled using biopsy forceps and the remaining tissue was ablated with the laser. More recently, Holmium and then Thulium lasers have been used to ablate tumors and this has usually been achieved by noncontact "painting" of the laser onto the tumor until white discoloration is seen indicating coagulation. If this could not be achieved, then the contact technique was used to vaporize the tissue.[23–26]

Laser Ablation Under General/Regional Anesthetic

Beer et al report their experience of using an Nd:YAG laser to treat 400 patients with superficial bladder cancer over an 8-year period.[17] A 0.6 mm quartz fiber with a continuous wave output and power of 40–50 W was applied to each area for 3–4 s to coagulate bladder tumors under spinal or local anesthetic. In tumors >0.5 cm diameter and in patients with evidence of infiltration, a preoperative staging transurethral resection was also performed. In smaller tumors, tissue for

histological examination was first removed using biopsy forceps. They found that the general recurrence rate (33–54%) was not significantly different to the recurrence rate amongst similar patients undergoing electrocautery but the local recurrence rate was significantly reduced in those treated with laser (7 vs. 25%).

A similar finding was seen in an earlier prospective randomized trial of standard TURBT with laser ablation for T1 and T2 tumor recurrences of bladder cancer.[18] Local recurrence was reduced in the laser treatment group but overall tumor recurrence rate was similar. This has been confirmed in other studies.[19]

To assess the effect of laser ablation on invasive bladder tumors, Tarantino and colleagues used an Nd:YAG laser to ablate tumors in 18 patients with clinical T1 to T3 disease prior to radical cystectomy but after an initial transurethral resection of tumor.[20] Eleven of the 18 patients had pathology at cystectomy, which was unchanged or had progressed since the patients' original transurethral resection. Seven of the patients had a lower pathological stage (three had no residual tumor). Results were more favorable in the group of patients who had a shorter time between laser ablation and cystectomy, suggesting that progression may have been due to recurrence rather than incomplete original resection.

There are more limited studies published using laser to treat invasive bladder cancer. The depth of penetration of the Nd:YAG laser is an advantage here allowing treatment through to the tumor base to be applied endoscopically. A management strategy combining transurethral resection by electrocautery and laser ablation was used in 15 patients with T2 disease. Ten patients were followed for a mean of 57 months without evidence or recurrence, one patient died of an unrelated disease and was found to have no evidence of disease at autopsy, and the remaining four patients failed treatment and went on to either cystectomy or external beam radiotherapy.[21]

The depth of penetration of Nd:YAG although useful in treating invasive cancer increases the potential for bowel injury. Combination of laser ablation and transperitoneal laparoscopy with mobilization of bowel away from the bladder wall and continuous visual monitoring has been described. This allows treatment of more invasive tumors and treatment of tumor on the serosal surface of the bladder. The laparoscopic technique also permits bladder biopsy and assessment of pelvic lymph nodes but does not seem to offer an advantage over standard TURBT. This technique is reported in a small series of 5 patients with T2–T3a bladder cancer who were unfit for cystectomy.[22] The treatment was trialed as palliation in these patients, who had frequent recurrences of problematic bleeding. A power of 50 W was used endoscopically and 20 W laparoscopically in two patients. Four of the 5 patients developed local recurrences within 1–4 months postoperatively and 3 required transurethral resection for symptom control. The advanced stage of disease is demonstrated in the fact that 3 patients had distant metastases within 9 months.

Laser Ablation Under Local Anesthetic

The properties of laser ablation with respect to improved coagulation and lower anesthetic requirements have led to an interest in its use in those with superficial bladder tumors and/or significant comorbidities.[23–26]

The relatively low intensity of pain when compared with electrocautery techniques combined with the fact that laser fibers can be used in combination with flexible cystoscopes enable this treatment to be delivered in the out-patient setting and under local anesthetic (Fig. 10.1). Clearly, this is particularly advantageous in patients with multiple comorbidities in

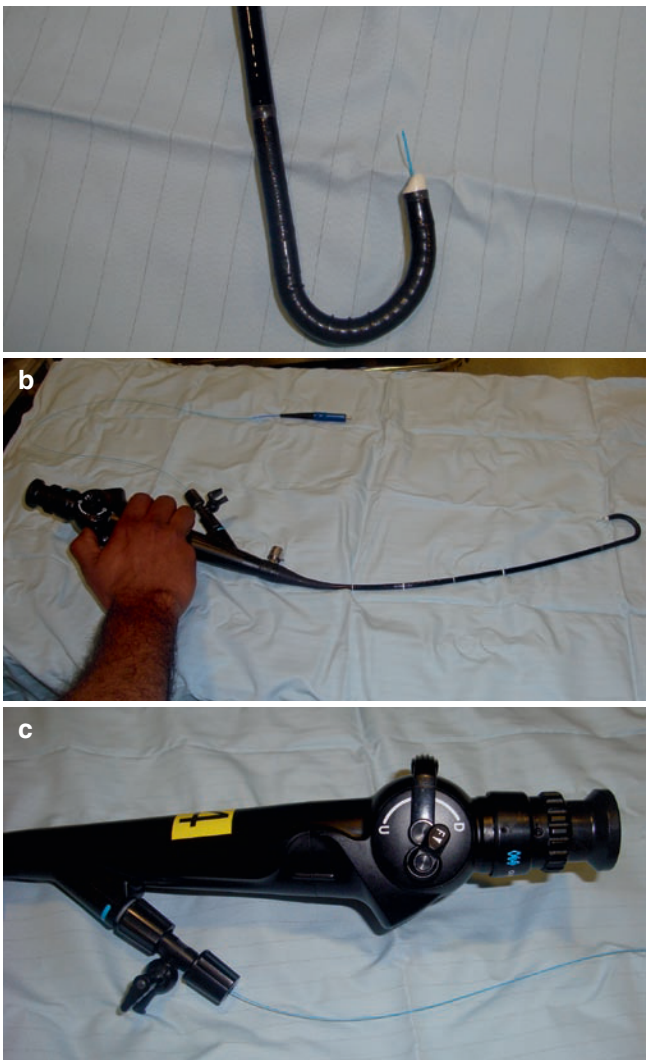

Fig. 10.1 Flexible cystoscope with laser fiber in situ

whom resection under general anesthetic carries a significant risk. Laser ablation is reported to achieve better hemostasis than standard electocautery and diathermy, and many series describe treatment of anticoagulated patients without incident. However, this has not always been the experience of the authors. Decreased blood loss is important in those with comorbidities and the patient can be catheter-free immediately post procedure, which also allows the procedure to be performed without requiring an overnight stay.

The largest series reported as yet is that of Jonler et al from Denmark.[23] This series of 88 procedures in 52 patients describes the treatment of superficial (TaG1) bladder tumor recurrences with holmium:YAG laser under lignocaine gel anesthesia. They used a 40 W holmium:YAG laser delivered through a 0.2–0.4 mm fiber held a few millimeters from the tumor. The tumor was then coagulated or vaporized depending on the energy delivered. An average of two tumors was treated in each patient ranging in size from 2 to 30 mm (mean 5 mm). The procedure took approximately 15 min. Eighty-six percent of procedures were completed with no complaint of pain from the patient and no procedures were terminated owing to pain. On questioning, all of the patients would chose this method of treatment over a standard general anesthetic TURBT should they develop further suitable tumors. In 88 procedures, three complications arose: one patient required urethral catheterization post procedure, one required intervention for bleeding, and a third developed epididimo-orchitis.

Of note, the authors reported the technique to have a short learning curve. The five surgeons performing the local anesthetic procedures were questioned as the difficulty of each procedure. Seventy-eight percent were described as easy. The surgeons halved their operating time between the first and last cases of their own series, and reported confidence in tackling larger or more numerous tumors.

The local anesthetic laser ablation was 350€ cheaper than a comparable day case TURBT and 1,350€ cheaper than a TURBT requiring overnight stay. Since the procedure could be carried out in clinic, the further advantages were freeing up of the department's operating theater for other procedures and the requirement of a substantially smaller team to operate (two compared with five for a TURBT).

Soler-Martinez and colleagues used a 10 W holmium laser (less expensive than the higher-power lasers) through a flexible cystosope to ablate early recurrences of superficial bladder tumors (pTaG1).[24] Thirty-six patients were treated under local anesthetic and intravenous sedation. All patients had a cold cup biopsy taken at the beginning of the procedure and at the end of the procedure 40 mg of mitomycin was instilled intravesically. Patients tolerated this well and were discharged the same day catheter-free. This technique had an overall recurrence rate of 25% at 12 months.

A study carried out by German et al has shown that 5–10% of patients with superficial bladder cancer will develop recurrences that are small in size and number.[37] If laser ablation under local anesthetic proves to be comparable with cystodiathermy in the longer term as current research suggests, these patients could be treated in the out-patient setting without the risks and resources associated with a general anesthetic procedure.

In summary, from the literature and our own experience, holmium laser ablation of superficial bladder tumors under local anesthetic seems safe, effective, and well tolerated by patients. The technique appears easy to learn and presents several resource advantages in that it can save money and theater operating time. It is a particularly attractive technique for use in the elderly and those with multiple comorbidities.

Resection

Though evidence is mounting to suggest laser ablation of tumors may be comparable with TURBT in terms of tumor recurrence rate and favorable with respect to complications, there remains a significant limitation to the technique. The coagulation and vaporization of bladder tumors affects the volume and quality of tissue available for histological analysis. Tumor histology is clearly important for prognosis and also for differentiating superficial from muscle invasive cancers (Fig. 10.2). Radiological imaging has proven unreliable at demonstrating muscle invasion, leaving biopsy as the only method. These problems have largely prevented the use of lasers to treat primary tumors. Research on lasers and bladder tumors has mainly been in cancer recurrences where the initial tumor was superficial on histology and where the recurrences were also judged by the surgeon to be superficial. Exciting new developments have been reported in the literature using holmium and thullium lasers for en bloc resection of bladder tumors.[28,29] (Fig. 10.3). The anticipated oncological benefits of such a technique are: ability to resect tumors en bloc for histological analysis, coagulation of the tumor margins at resection by the laser potentially decreasing tumor cell scatter, and use of the laser to treat the tumor base.

Das et al published their work in 1998 reporting the use of holmium laser to resect bladder tumors (HoLRBT).[27] Using a modified resectoscope and an end firing fiber, they performed resections on 23 patients with newly diagnosed bladder transitional cell carcinoma (TCC). Cold cup biopsies were then taken of the tumor base and compared with the resection specimens. These biopsy specimens did not alter the stage of the bladder tumor in any case implying that the laser resection gave an accurate way of staging the tumor.

In 2008, Zhu and colleagues working in Beijing published work with holmium laser resection of bladder tumor (HoLRBT) as a primary treatment for clinically nonmuscle invasive bladder tumors.[28] One-hundred and one patients

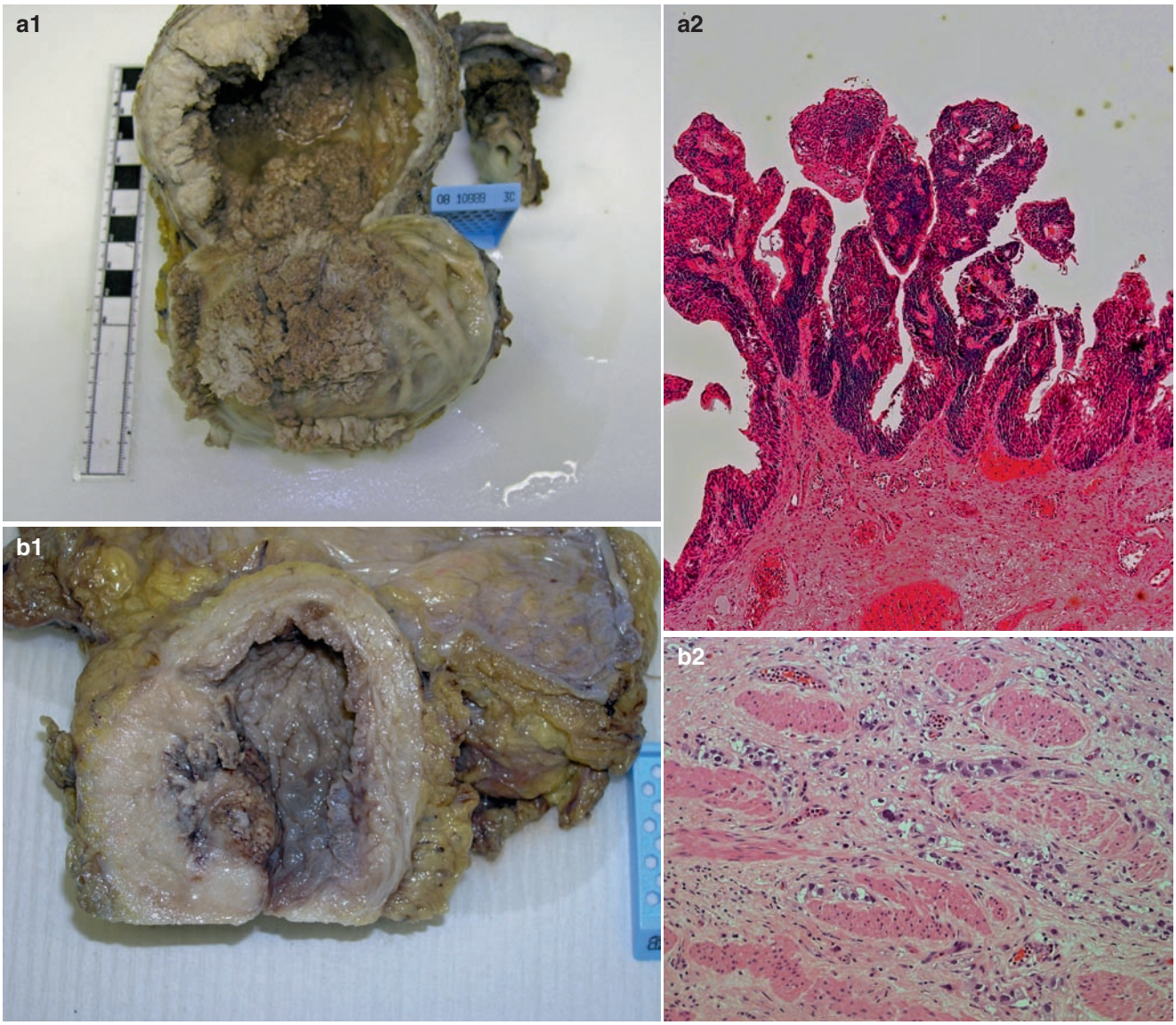

Fig. 10.2 Examples of bladder tumor specimens: (**a**) superficial (**b**) invasive

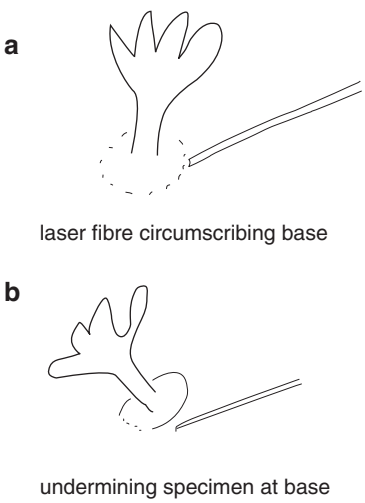

Fig. 10.3 "En bloc" resection using 550 μm laser fiber. (**a**) Laser fiber circumscribing base. (**b**) Undermining specimen at base

were treated with an en bloc resection (allowing histological analysis) and coagulation of the base of the tumor followed by a postoperative intravesical mitomycin C regimen. For the HoLRBT group, a 100 W Holmium:YAG laser was used with a 550 μm fiber through a 5F open-ended ureteric catheter. These patients were compared with 111 similar patients who underwent conventional transurethral electroresection of bladder tumor (TURBT). Both groups had a similar disease-free survival. The patients undergoing HoLRBT had a significantly longer operative time but significantly shorter length of catheterization. There were no obturator kicks in the HoLRBT group but 7/111 in the TURBT group with three perforations. Histology was adequate with minimal effect from thermal artefact. The authors conclude that HoLRBT may represent a promising alternative to TURBT.

It is not yet clear how treatment with the newly developed thulium laser can be compared with holmium laser for the resection of bladder tumors.[32,33] A recently published case series reports its use in the treatment of recurrent superficial bladder cancer (ThuRBT).[31] Thirty-two patients were treated via flexible cystoscopy under general anesthetic. A 200 μm fiber was used at power levels of 5–15 W in a continuous and pulsed mode. After coagulating the tumor, it was removed with biopsy forceps and random biopsies were taken off the tumor base, margin, and bladder. Mean tumor size was 1.5 cm and mean operation time was 25 min. Two patients required irrigation postoperatively and all had a urinary catheter, which was removed the following day. Recurrence rates were 28% at 12 months. In the discussion, the authors commented that while vaporization with the holmium laser results in little or no tissue left for histological examination, in contrast, tissue was obtained in all cases with ThuRBT. Unfortunately, however, the architectural detail was distorted, so that while tumor grade was available for every case, the pathologist was not always able to stage the tumor.

Combined Gene and Laser Therapy: A Novel Strategy

A novel approach to the treatment of bladder tumors is to use gene therapy to influence the disease at genetic level. Although some advances have been made in this area, the major difficulty has been delivering the gene and transporting it into the cell. Transfection rates of naked DNA into a cell are poor. Work published in 2002 by Knoll and colleagues from Mannheim, Germany, looked at the effect of laser energy on DNA transfection rate in vitro.[38] A suspension of transitional carcinoma cells was mixed with DNA plasmids and subjected to laser energy from neodymium:YAG or holmium:YAG lasers. FACS analysis looking for the reporter gene in cancer cells showed that Nd:YAG was not effective but holmium:YAG laser was found to increase the transfection rates to satisfactory levels. Transfection rate further increased with increasing frequency and energy levels (optimum 10 Hz, 2,000 mJ) (rates rose from 18.3 to 58.3%). With further analysis, gene therapy could offer an alternative intravesical therapy to decrease implantation of tumor cells at the time of transurethral resection.

Conclusion

Laser technology has been used to resect and ablate bladder tumors over the past 30 years. A variety of lasers have been tried but neodyium:YAG, holmium:YAG, and more recently thulium:YAG are the only ones with clinical application for the bladder. Initial studies used a neodyium:YAG laser with a penetration depth of 4–6 mm but holmium:YAG laser is now in common use for prostate and stone surgery and therefore available in many departments. It has a wavelength of 2,140 nm and depth of penetration of only 0.3–0.4 mm making it an attractive option for resection in the bladder. Several studies have shown laser TURBT using a 550 μm fiber to be feasible, but there are still questions regarding the adequacy of the specimen for histology. The main advantages of laser *resection* are improved hemostasis potentially facilitating catheter-free day case treatment, resection in saline, and en bloc resection. An exciting potential for laser treatment in bladder tumor is the *ablation* of recurrent papillary tumors under local anesthetic using a holmium or thulium laser fiber through a flexible cystoscope. The advantage offered over electrocautery is less discomfort and bleeding allowing outpatient treatment of higher volume tumors and patients on anticoagulation. Given the high incidence of TCC of the bladder, the co-morbidity of the patients, cost of inpatient admission, risks of general anesthesia, frequent recurrence and the indolent nature of many tumors, and treatment under local anesthetic in the "office" setting are attractive for both the patient and the surgeon.

References

1. Office for National Statistics. *Cancer Statistics Registrations: Registrations of Cancer Diagnosed in 2006*, England. Series MB1 no.37. London: National Statistics; 2008
2. Thomas K, O'Brien TS. Improving transurethral resection of bladder tumour: the gold standard for diagnosis and treatment of bladder tumours. *Eur Urol.* 2008;(suppl 7):524–528
3. Teichmann HO, Herrmann TR, Bach T. Technical aspects of lasers in urology. *World J Urol*. 2007;25(3):221–225
4. Pietrow PK, Smith JA Jr. Laser treatment for invasive and noninvasive carcinoma of the bladder. *J Endourol*. 2001;15:415–418
5. Eschenbach A. The neodymium-yittrium aluminium garnet (Nd:YAG) laser in urology. *Urol Clin North Am.* 1986;13(3):381–392
6. Smith JA. Endoscopic applications of laser energy. *Urol Clin North Am.* 1986;13(3):405–420
7. Holzbierelein JM, Smith JA. Surgical management of noninvasive bladder cancer (stages Ta/T1/CIS). *Urol Clin North Am.* 2000;27(1):15–24
8. Smith JA. Laser surgery for transitional cell carcinoma. *Urol Clin North Am.* 1992;19(3):473–483
9. Hossain MZ, Khan SA, Salam MA, Hossain S, Islam R. Holmium laser treatment of superficial bladder carcinoma. *Mymensingh Med J.* 2005;14(1):13–15
10. Muraro GB, Grifoni R, Spazzafumo L. Endoscopic therapy of superficial bladder cancer in high-risk patients: holmium laser versus transurethral resection. *Surg Technol Int.* 2005;14:222–226
11. Johnson DE. Use of the holmium:YAG laser for treatment of superficial bladder carcinoma. *Lasers Surg Med.* 1994;14(3):213–218
12. Lopez-Beltran A, Luque RJ, Mazzucchelli R, et al. Changes produced in the urothelium by traditional and newer therapeutic procedures for bladder cancer. *J Clin Pathol*. 2002;55:641–647

13. Ruiz-Tovar J, González R, Conde S, Morales V, Martinez-Molina E. Jejunal and bladder perforation: complication of intravesical Nd-YAG laser irradiation of bladder tumour. *Acta Chir Belg.* 2008; 108(5):595–596
14. Greskovich FJ III, von Eschenbach AC. Bladder perforation resulting from the use of the neodymium:YAG laser. *Lasers Surg Med*. 1991;11(1):5–7
15. Hofstetter AG. Application of lasers in bladder cancer. *Semin Surg Oncol*. 1992;8(4):214–216
16. Gross AJ, Herrmann TR. History of lasers. *World J Urol*. 2007;25(3): 217–220
17. Beer M, Jocham D, Beer A, et al. Adjuvant laser treatment of bladder cancer: 8 years' experience with the Nd:YAG laser 1064 nm. *Br J Urol.* 1989;63:479–478
18. Beisland HO, Seland O. A prospective randomized study on neodymium:YAG laser irradiation versus TUR in the treatment of urinary bladder cancer. *Scand J Urol Nephrol.* 1986;20:209–212
19. Kardos R, Magasi P, Karsza A. Nd-Yag laser treatment of bladder tumours. *Int Urol Nephrol*. 1994;26(3):317–322
20. Tarantino AE, Aretz HT, Libertino JA, et al. Is the neodymium: YAG laser effective therapy for invasive bladder cancer? *Urology.* 1991;38:514
21. Beisland HO, Sander S. Neodymium:YAG laser irradiation of stage T2 muscle-invasive bladder cancer: Long-term results. *Br J Urol.* 1990;65:24
22. Gerber GS, Chodak GW, Rukstalis DB. Combined laparoscopic and transurethral neodymium: yttrium-aluminum-garnet laser treatment of invasive bladder cancer *Urology.* 1995;45:230–233
23. Jønler M, Lund L, Bisballe S. Holmium:YAG laser vaporization of recurrent papillary tumours of the bladder under local anaesthesia. *BJU Int.* 2004;94:322
24. Soler-Martínez J, Vozmediano-Chicharro R, Morales-Jiménez P, et al. Holmium laser treatment for low grade, low stage, noninvasive bladder cancer with local anesthesia and early instillation of mitomycin C. *J Urol.* 2007;178(6):2337–2339
25. Syed H, Biyani C, Bryan N, Brough S, Powell C. Holmium:YAG laser treatment of recurrent superficial bladder carcinoma: initial clinical experience. *J Endourol.* 2001;15:625–627
26. Morten J, Lund L, Bisballe S. Holmium:YAG laser vaporisation of recurrent papillary tumours if the bladder under local anaesthesia. *BJU Int.* 2004;94:322–325
27. Das A, Gilling P, Fraundorfer M. Holmium laser resection of bladder tumors (HoLRBT). *Tech Urol.* 1998;4:12
28. Zhu Y, Jiang X, Zhang J, Chen W, Shi B, Xu Z. Safety and efficacy of holmium laser resection for primary nonmuscle-invasive bladder cancer versus transurethral electroresection: single-center experience. *Urology*. 2008;72(3):608–612
29. Saito S. Transurethral en bloc resection of bladder tumours. *J Urol.* 2001;166:2148–2150
30. Fraundoerfer M, Cresswell M, Gilling P, Kabalin J. Bladder tumour resection with the holmium laser. *BJU Int.* 1997;80(suppl 2):39
31. Gao X, Ren S, Xu C, Sun Y. Thulium laser resection via a flexible cystoscope for recurrent non-muscle-invasive bladder cancer: initial clinical experience. *BJU Int*. 2008;102(9): 1115–1118
32. Fried NM, Murray KE. High-power thulium fiber laser ablation of urinary tissues at 1.94 mm. *J Endourol.* 2005;19:25–31
33. Bach T, Herrmann TR, Cellarius C, Gross AJ. Bladder neck incision using a 70 W 2 micron continuous wave laser (RevoLix). *World J Urol.* 2007;25:263–267
34. Boyd P, Burnand K. Site of bladder tumour recurrence. *Lancet.* 1974;2:1290–1292
35. Hafner C, Knuechel R, Zanardo L, et al. Evidence for oligoclonality and tumour spread by intraluminal seeding in multifocal urothelial carcinomas of the upper and lower urinary tract. *Oncogene.* 2001; 20:4910–4915
36. Ray E, O'Brien TS. Should urologists be spending more time on the golf course? *BJU Int.* 2007;100:728–729
37. German K, Hasan ST, Derry C. Cystodiathermy under local anaesthesia using the flexible cystoscope. *Br J Urol.* 1992;69: 518–520
38. Knoll T, Trojan L, Langbein S, Sagi S, Alken P, Michel MS. Impact of holmium:YAG and neodymium:YAG lasers on the efficacy of DNA delivery in transitional cell carcinoma. *Lasers Med Sci*. 2004; 19(1):33–36

Lasers in Laparoscopic Surgery

11

Troy Gianduzzo

Introduction

Laser energy has been increasingly used in recent times in urology, most notably in the treatment of stone disease and benign prostatic hyperplasia. In the laparoscopic realm, laser energy has remained experimental. This chapter will review the current status of laser applications in laparoscopic urology.

Laser Physics

The principles of laser physics and laser-tissue interactions are well described in a number of excellent reviews.[1–4] In essence, the well-known laser acronym stands for ***l***ight ***a***mplification through the ***s***timulated ***e***mission of ***r***adiation. Laser light is (1) coherent, whereby the light wave trains travel in phase in both time and space, (2) collimated, whereby the radiation beams travel in parallel, (3) monochromatic, whereby the photon waves are of the same wavelength, and (4) of high energy.

The production of laser light requires a laser generator, an excitation source, a lasing medium, and a resonator to produce amplification via optical feedback (see Fig. 11.1a).[3] Atoms within the lasing medium are energized by the excitation source so that the electrons in the resting ground state, E^0, are stimulated to higher and progressively higher energy levels (E^1–E^n). Typically, only a small proportion of the atoms exist in these higher energy states. When most of the atoms of the lasing medium are energized, population inversion occurs, which is critical to the laser process. Spontaneous emission then occurs whereby energized atoms spontaneously decay after a given time E^0 and thereby emit photons at a given wavelength as monochromatic light (see Fig. 11.1b). This spontaneous emission then precipitates stimulated emission, in which the emitted photons interact with other high-energy-state electrons and stimulate their subsequent decay and associated photon emission. Hence, amplification occurs whereby one photon is able to stimulate the emission of additional photons and so on (see Fig. 11.1c). As long as population inversion continues, the laser light continues to be amplified. The photons are reflected back and forth by mirrors within the resonator, and continued photonic interaction with high-energy-state electrons results in further amplification (see Fig. 11.1a). Additionally, this reflection process aligns the photon wave trains in space and time producing coherence and collimation of the laser light. Typically, one of the mirrors of the resonator, the optical coupler, is semi-transparent and allows the collimated, coherent monochromatic photon waves to be released from the lasing medium as a laser beam, which is subsequently directed toward the target tissue.

The interaction of laser light with tissues is governed by photomechanical, photochemical, and photothermal mechanisms.[2] Photomechanical effects occur when short pulses of high wattage laser energy are applied and disrupt the cellular architecture via photoacoustic shocks, whereas photochemical interactions occur when low-energy laser light induces a chemical reaction within the cell. Photothermal interactions are the most characteristic in laser surgery and are governed by the tissue-specific absorption characteristics. At temperatures of 45–50°C, enzymatic changes occur, at 60°C, protein denaturation occurs and results in coagulation, and cellular vaporization occurs at 90–100°C. Continued heating to several hundred degrees results in tissue carbonization and burning.[2] These photothermal effects are governed by the applied power density, also known as the irradiance, which is expressed as a function of energy per unit area or watts/cm^2.

$$\text{Irradiance} = \text{intensity/area} = \text{watts/cm}^2.$$

The energy density expressed as a function of time is known as the fluence and is the product of irradiance, and the exposed time is expressed as Joules (J)/cm^2.

$$\text{Fluence} = (\text{intensity} \times \text{time})/\text{area} = \text{watts.s/cm}^2 = \text{J/cm}^2.$$

Increasing irradiance increases the tissue temperature and favors vaporization and tissue cutting. This effect is favored by small diameter fibers, which produce a small spot size, higher laser output power, maintenance of the fiber tip close

P. Dasgupta et al. (eds.), *New Technologies in Urology,*
DOI: 10.1007/978-1-84882-178-1_11, © Springer-Verlag London Limited 2010

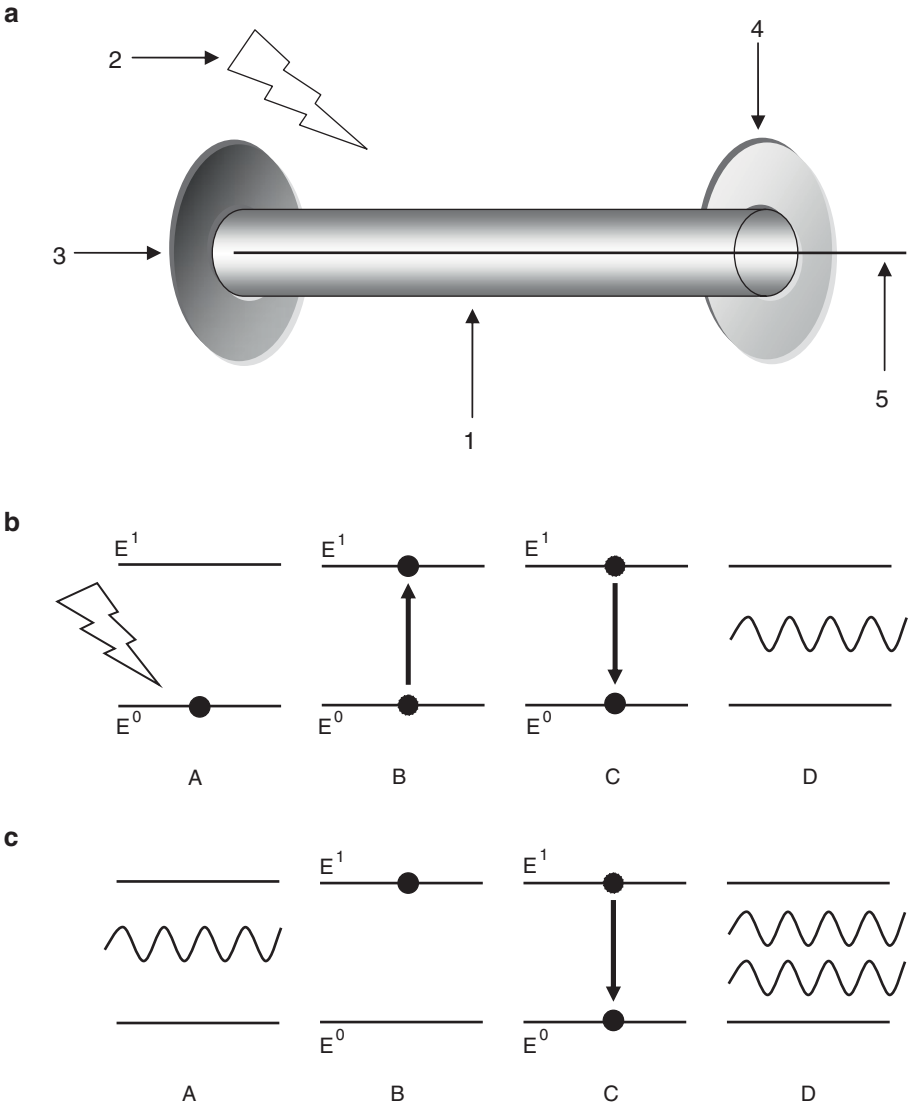

Fig. 11.1 (**a**) Laser generator. (**b**) Spontaneous emission. Resting state electrons are energized via the excitation source (*A*) to a higher energy level (*B*). The electrons then decay back to the resting state (*C*) and in the process emit a given wavelength of ionizing radiation (*D*). (**c**) Stimulated emission. Emitted ionizing radiation (*A*) interacts with high-energy state electrons of energized atoms (*B*) to precipitate their decay to the resting state (*C*) thus producing further ionizing radiation of the same wavelength (*D*)

to the tissue to minimize beam divergence, and the application of the beam at right angles to the tissue to focus the laser spot. Conversely, the reciprocal of these factors decreases the irradiance and favors coagulation and hemostasis.

When laser light is applied to a tissue, it can be transmitted, absorbed, scattered, or reflected.[3] The absorption of laser light by the tissue produces the resultant effects of the laser beam. The presence of chromophores such as melanin and hemoglobin and the water content of the tissues govern the laser absorption profile. In the ultraviolet and visible range of the spectrum from approximately 100 nm to 800 nm, there is very little water absorption. Water absorption begins at approximately 1,000 nm and has a large peak at 3,000 nm. In the visible light spectrum, hemoglobin and melanin dominate absorption. The Hemoglobin curve has three main absorption peaks at 418, 542, and 577 nm and decreases by approximately 600 nm. Melanin has a broad overlapping absorption band ranging across the ultraviolet, visible, and near infrared spectrum.

Laser Types

The principal laser types, which may be suitable for laparoscopic use, are the carbon dioxide (CO_2), neodymium-doped yttrium-aluminum-garnate (Nd:YAG), the holmium-doped yttrium-aluminum-garnate (Ho:YAG), the potassium-titanyl-phosphate (KTP), or lithium triborite (LBO) crystals, which generate the 532 nm wavelength, and most recently the thulium laser.

The CO_2 laser has a wavelength in the far infrared spectrum with a wavelength of 10,600 nm and thus has shallow penetration because of the high water content of body tissues.

It is not as hemostatic as other laser types and typically seals vessels up to 0.5 mm in diameter.[5] In addition, this laser type has traditionally required rigid delivery systems that limit its laparoscopic use. Its main mechanism is via a photothermal effect. Omniguide® flexible photonic band-gap fibers have recently been developed (Omniguide Inc., Cambridge, MA) to allow flexible delivery of CO_2 laser light. Nonetheless it is unlikely that this laser would be suitable to achieve hemostasis in laparoscopic urological procedures because of the larger sizes of the vessels involved such as in laparoscopic partial nephrectomy (LPN).

The 1,064 nm Nd:YAG laser is not preferentially absorbed by water or by tissue chromophores, but it penetrates deeply into the tissue. It is hemostatic and coagulates vessels up to 3–5 mm in diameter and has predominantly photothermal effects.[6,7] In contrast, the 2100 nm Ho:YAG laser is a high-energy pulsed laser, which produces its effect by predominant photomechanical mechanisms. The depth of penetration is typically 0.5 mm.[8] The photomechanical effects on tissues tend to produce irregular cut margins and also theoretically may disseminate malignant cells during oncological procedures through tissue splattering.[9] Additionally, these photomechanical properties have been noted to splatter tissue fragments onto the laparoscope lens and interfere with the laparoscopic view.[10]

The 532 nm KTP laser is produced by passing an Nd:YAG laser beam through a frequency doubling KTP crystal. This wavelength is in the green light spectrum and is absorbed predominantly by hemoglobin.[4] It vaporizes tissues through photothermal effects and has excellent hemostatic properties. These properties have led to its widespread use and development in the treatment of benign prostatic hyperplasia with the development of the high-powered 80 W Greenlight® PV and 120 W Greenlight® HPS systems developed by Laserscope (San Jose, CA), now recently acquired by American Medical Systems (Minnetonka, MN). The HPS system now utilizes the more stable LBO crystal to generate the 532 nm wavelength. These laser generators produce very rapid pulses of high-powered 532 nm laser energy in a quasicontinuous mode.

The most recent laser type to be examined is the 2,013 nm thulium laser. This laser penetrates to a depth of approximately 0.5 mm and has properties similar to that of the holmium laser, but is delivered in a continuous wave form, and therefore avoids the photomechanical splattering effects associated with the holmium laser.[11]

Laparoscopic Pyeloplasty

Most work in laser laparoscopic applications has centered on the upper tract, principally with laser LPN. Initially, however, the work focused on laser welding of the pyeloureteral anastomosis in laparoscopic pyeloplasty. This was based on the initial difficulties associated with intracorporeal suturing when laparoscopic urology was in its infancy. Laser welding utilizes the photothermal properties of laser light whereby laser energy is applied to a solder, typically 50% human albumin, in conjunction with laser wavelength specific chromophores such as indocyanine green or flourescein to facilitate laser light absorption. The dyed solder thus absorbs most of the light energy and increases the temperature at the repair site, which denatures the solder and results in a coagulum, which initially increases the initial strength at the repair site.

Eden and Copcoat in 1996 described the use of laser welding as a means of facilitating the pyeloureteral anastomosis in laparoscopic pyeloplasty.[12] In this study using the acute and survival porcine model, KTP human albumin laser welding was compared with gelatine resorcin formaldehyde (GRF) glue and fibrin glue. GRF glue produced anastomotic adhesion, which was insufficiently flexible to withstand rotation of the anastomosis and was thus abandoned. Both laser welding and fibrin glue produced supraphysiological leak pressures, but the fibrin glue was significantly faster to perform and easier to apply in comparison with laser welding. Laser welding was found to be demanding and required dry tissue edges that needed to be precisely aligned without any shear force. Also the end point of laser welding was felt to be subjective and easily exceeded, resulting in significant tissue thermal injury. The authors thus opted to proceed with fibrin glue as their anastomotic method of choice in an initial clinical series.[13]

In a similar study, Wolf and coworkers in 1997 laparoscopically repaired 22 proximal ureterotomies in 14 pigs using either fibrin glue, laser welding, Endo-Stitch® suturing, or free suturing.[14] Urine leak was assessed immediately via the retrograde instillation of methylene blue, while long-term survival analysis was performed at 12 weeks using retrograde pyelography, pressure-flow assessment, bursting pressures, and histological analysis. Fibrin glue produced more favorable radiographic findings and flow characteristics when compared with KTP human albumin laser welding and suturing. Though laser welding was faster then free suturing, it was not superior to free suturing in other aspects. The authors concluded that given the expense of laser systems, laser welding would need to be significantly superior to free suturing to justify its routine clinical use. Barrieras et al in 2000 assessed 53 pyelpplasties in 50 pigs and found that neither laser welding using an 804 nm diode laser nor fibrin glue was superior to standard suturing in the long term and was associated with a higher incidence of urinoma formation.[15] Recently, Shumalinsky et al in 2004 demonstrated successful laser welding of the pyeloureteral anastomosis in ten farm pigs using a fiber-optic CO_2 laser soldering system.[16] In this assessment, the authors developed a unique, flexible, fiber-optic CO_2 laser delivery system, which included a real-time infrared thermal sensor that regulated the laser output within

a 2–3°C temperature range. Successful tissue welding of the pyeloureteral anastomosis was demonstrated at up to 1 month following the procedure as assessed with postoperative intravenous urography, ultrasound, and histology.

Ultimately, however, laser welding of the pyeloureteral anastomosis has not demonstrated an advantage over standard suturing techniques. As laparoscopy has evolved, intracorporeal suturing is readily learned by residents in training and forms an integral part of the laparoscopic urologist's armamentarium and is not considered the technically demanding highly advanced skill that it once was. Accordingly, laser welding of the pyeloureteral anastomosis is not performed in routine clinical practice.

Laser Laparoscopic Partial Nephrectomy

Most investigation of laser applications in laparoscopic urology has centered on LPN. Approximately, 35,000 renal tumors are diagnosed annually in the US.[17] The incidence of renal cell carcinoma (RCC) has been increasing in recent years largely due to an increasing use of imaging modalities detecting incidental, small, asymptomatic renal masses.[18,19] Many of these tumors are small, <4 cm, and as such may be candidates for partial nephrectomy (PN).

Recently, LPN has been developed and offers equivalent oncological and renal function outcomes but with improved convalescence when compared with open partial nephrectomy (OPN).[20] However, LPN is a technically demanding procedure that is practiced only in selected centers of expertise and is difficult to master. The most accepted technique replicates the open procedure and involves hilar clamping, cold scissor excision, collecting system closure, and sutured hemostasis with the application of a Surgicel Nu-Knit® (Ethicon Inc., NJ) bolster and Floseal® (Baxter, IL) for additional hemostasis.[21] Hilar clamping is limited to 30 min to minimize the impact of warm ischemia. Such time constraints add to the technical demands of the operation. Renal parenchymal reconstruction is complex and requires rapid, free-hand suturing that is technically challenging, which in conjunction with the time constraints of hilar clamping, has limited the widespread dissemination of the technique.

The ideal LPN scenario would be to excise the renal mass with minimal blood loss, without hilar clamping, and in a technically straightforward manner while maximizing oncological control and minimizing any impact on renal function in a safe manner. A number of modalities and energy sources have been explored in an attempt to meet these aims such as microwave tissue coagulation,[22] radiofrequency dissection,[23,24] bipolar energy,[25] argon beam coagulation,[26] ultrasonic shears,[26] and water-jet dissection;[27] however, none has been proved universally successful.

Lasers of various types have been investigated as potential hemostatic energy sources in PN for many years; however, none gained widespread acceptance as laser OPN offered no advantage when compared with the standard open surgical technique. However, the complexity of LPN has led to resurgence in the investigation of laser PN to simplify LPN and to eliminate warm ischemia.

The CO_2 laser was the first laser type to be investigated in OPN by Hughes and Scott in 1972, who initially described CO_2 laser PN in dogs.[5] Further animal and clinical investigations were performed;[28–31] however, the CO_2 laser alone was not sufficient for hemostasis in these reports and additional ligatures were required to control the larger vessels. As the CO_2 laser coagulates small vessels of up to 0.5 mm, it is unlikely that this laser will play a significant role in PN.

The Nd:YAG laser was the next to be investigated.[6,32–44] Techniques included cold scalpel excision with spot lasing of transected vessels and straight laser transection with and without hilar clamping in cooled and uncooled kidneys. The Nd:YAG laser was also combined with the CO_2[44] and KTP[40] lasers in an attempt to limit the degree of thermal injury. Overall collecting system closure was inadequate and hemostasis was variable; however, Malloy et al in 1986 successfully used the Nd:YAG laser without hilar clamping in a clinical series of 6 patients with solitary kidneys,[38] while Korhonen et al 1993 used the Nd:YAG laser under cold ischemia in 6 patients with VHL.[35]

Johnson et al in 1992 then examined the Ho:YAG laser in clamped PN in the canine model and demonstrated a twofold reduction in the depth of necrosis using the Ho:YAG laser when compared with the Nd:YAG.[45] They also noted that collecting system closure was inadequate.[45]

Thus ended the open era in which the CO_2, Nd:YAG, KTP, and Ho:YAG lasers were assessed. The overall conclusions were that laser dissection, though achievable, offered no advantage to standard open surgical techniques. In contrast to the open era where open laser PN offered no advantage to open surgery, laser PN offers the potential of allowing the wide spread dissemination of an otherwise difficult technique that is performed only in selected centers of expertise.

The Nd:YAG laser was the first to be examined in the laparoscopic context by Janetscheck et al in 1998, who in a series of seven LPNs for small renal masses described its use in combination with the argon beam coagulator in the unclamped kidney in 1 patient.[46]

The Ho:YAG laser has been investigated more extensively. Though it appears effective, tissue splattering limits its usefulness. Lotan et al 2001 initially presented a video of Ho:YAG laser LPN in an unclamped porcine model at the 19th World Congress of Endourology and SWL.[47] Estimated blood loss was <50 mL. Blood splattering onto the laparoscope and smoke generation were particular problems. In 2002, the authors described the clinical use of the Ho:YAG

laser in three cases of a complex cyst, a nonfunctioning lower-pole moiety in a duplex system in an 8-year boy, and a case of RCC.[10] The hilum was not clamped in 2 of 3 cases. In case 1, fibrin glue was applied to the cut surface to prevent secondary hemorrhage. Estimated blood loss was <50 mL. The second case involved the excision of a nonfunctioning lower pole moiety in a duplex system. The lower pole vessels were clipped and divided. Blood loss was < 100 mL and oxidized cellulose was applied to the cut renal surface. The third case, a 2.5 cm exophytic RCC, was resected without hilar clamping. The estimated blood loss was 500 mL. The argon beam coagulator and fibrin glue were also applied. In these cases, splattering was particularly troublesome when larger vessels were transected. Then in 2004 this same group performed five acute and five survival lower pole laser transperitoneal LPNs in five pigs using the Ho:YAG laser.[10] Fibrin glue was applied to the cut surface to seal the collecting system. Blood loss was <50 mL for each procedure. Extravasation was noted in two of the survival kidneys. Again blood splattering and smoke generation were problematic.

Diode lasers have also been trailed. Ogan et al in 2002 performed ten laparoscopic transperitoneal partial nephrectomies in five 45–50 kg female farm pigs without hilar clamping using a 980 nm diode laser.[48] After transection fibrin glue was applied to seal the collecting system. The laser was insufficient for hemostasis in three of the ten partial nephrectomies and adjunctive hemostatic clips were necessary to stop bleeding from larger vessels toward the center of the parenchyma. The mean laser time was 84 min and the mean blood loss was 150 mL. There was minimal extravasation in three kidneys on ex vivo retrograde pyelography. The depth of necrosis was up to 2 mm. In 2003, this group examined the 810 nm pulsed diode laser combined with 50% liquid-albumin-indocyanine green solder to weld the parenchyma to achieve hemostasis and seal the collecting system.[49] Five survival and five acute heminephrectomies were assessed in five farm pigs. The renal pedicle was clamped and the heminephrectomy was performed with scissors. The solder and the laser were then applied to the cut renal surface. The mean blood loss was 43.5 mL and the warm ischemia time 11.7 min. Two of the acute kidneys demonstrated minimal urine extravasation on ex vivo retrograde pyelography, although none of the survival kidneys demonstrated any clinically relevant urine leak.

Recently, high-power 532 nm wavelength laser systems have been developed. The 80 and 120 W Greenlight® PV and HPS systems (Laserscope®) have become established as effective treatment options in the management of bladder outflow obstruction from benign prostatic hyperplasia. Moinzadeh et al in 2005 examined KTP laser LPN in the unclamped calf model using the Greenlight® PV system.[50] This study is unique in that it was the first to use the robust calf model, which the authors theorize as more closely representing the human scenario, because of its large kidney size. In this study, six Jersey calves weighing 76–94 kg underwent 12 staged bilateral transperitoneal LPNs in the unclamped kidney including left kidney chronic LPN with 1 month follow-up in 6 and right kidney acute LPN with immediate sacrifice in 6. Two techniques were investigated, which included ablative vaporization of renal tissue in five subjects and wedge resection in seven. Eleven of the 12 procedures were performed without hilar clamping. The mean total operating time was 2.9 h and the mean blood loss was 119 mL. The mean lasing time was 56 min. At 1 month follow-up there was no evidence of urine-leak on pyelography or AV fistula on arteriography. The procedures were performed using the 80 W quasi-continuous KTP Greenlight® PV system with a 600 μm bare-tip end-firing fiber delivered through a 5 mm suction irrigation hand-piece. Smoke generation was noted and necessitated the use of a smoke evacuator system and two insufflators to counteract the loss of the pneumoperitoneum. Collecting system entries were repaired with running suture. Acute necrosis was minimal at 0.8 mm.

Hindley et al in 2006 performed transperitoneal KTP laser LPN in four pigs. In this study, the Greenlight® PV system delivering high power 80 W KTP laser energy via a 600 μm fiber without renal cooling or hilar clamping.[51] The mean blood loss was <30 mL. In one procedure, a 7 mm vein was transected that required a single laparoscopic clip to secure hemostasis. The mean operating time was 42 min. The zone of necrosis was 1 mm. The authors report that the hemostatic properties of the KTP laser were excellent, but also noted that smoke production was a particular problem.

In an attempt to overcome the problem of smoke production, Liu et al in 2006 examined saline irrigation during KTP laser LPN in the porcine model.[52] The authors initially theorized that different insufflation gasses may affect smoke formation. An initial ex vivo study was performed where resected kidneys were placed in a sealed container filled with either argon, helium, or CO_2, and the kidney was cauterized by electrocautery passed through laparoscopic ports. There was no difference in smoke production with the various gasses and the authors concluded that the smoke was generated from the laser-tissue interaction. Similar findings were noted in vivo. Fourteen LPNs were performed without hilar occlusion in four pigs with continuous saline irrigation to suppress smoke production. Thirteen of the fourteen partial nephrectomies were performed without hilar clamping and with successful suppression of smoke. The laser fiber fractured in the suction cannula through which the fiber was passed in one procedure, which could then not be completed. The mean PN time was 13.14 min and the mean blood loss was 28.57 mL.

Anderson et al in 2007 examined the KTP laser LPN in six pigs.[53] The technique was developed in the first two pigs after which the remaining four pigs underwent a right-sided laser LPN followed by a left-sided laser LPN 2 weeks later,

in which a mean of 30 g of renal tissue approximating a sizeable 25% of the kidney mass was resected. The hilum was clamped in all cases. The 80 W KTP laser was used at a setting of 80 W for tissue cutting and 30 W for coagulation delivered via a 365 μm fiber. Hemostasis was successful in all cases and no perioperative complications occurred. Mean blood loss was 80 mL, mean laser time was 35 min and the mean warm ischemia time was 34 min. Urinary extravasation was noted in 7 out of 8 kidneys on retrograde pyelography. Saline irrigation eliminated smoke formation but slowed the time of resection. Hilar clamping decreased smoke formation and charring and greatly facilitated dissection. Smoke production although less was still a factor and a smoke evacuator was required at a suction rate of 5 L/min. Fibrin glue was used to seal the collecting system. The zone of necrosis was up to 5 mm in the acute specimens, which the authors hypothesize to be due to hilar clamping; however, this is at odds with the results found by Benderev et al in 1987, who found that hilar clamping decreased the necrotic zone with the Nd:YAG laser.[54] It may be that the larger amount of excised tissue in this study may have accounted for this difference as more energy would have been likely to be required, although the energy use was not reported.

We recently examined the clinical applicability of laser Robotic-assisted LPN at the Cleveland Clinic in a pilot series of 5 patients (manuscript in preparation). In this series, the Greenlight® HPS 120 W system was used in conjunction with the da Vinci® robotic unit to facilitate laser delivery (see Fig. 11.2). Specific purpose-built, prototype robotic instrumentation was engineered for this study. As the green laser light saturates the robotic camera system, KTP filters were incorporated into the camera adapter to prevent laser flare from obscuring the operative view. A prototype laser delivery device was also developed whereby a 5 mm da Vinci® instrument (Intuitive Surgical, Sunnyvale, CA) was assembled to allow the passage of the laser fiber through the center of the instrument. This instrument allowed precise multidirectional delivery of the laser beam. The laser beam was delivered via a purpose-built, end-firing 600 μm fiber using the Greenlight® HPS (AMS/Laserscope) laser system to a maximum setting of 80 W.

Following transperitoneal laparoscopic renal mobilization, the tumor mass was defined using intraoperative laparoscopic ultrasound and the proposed line of parenchymal incision was circumferentially scored with an electrocautery robotic J-hook. The laser fiber was passed via the custom-built laser instrument and activated using the Greenlight® HPS laser system to a maximum setting of 80 W and was used to incise the renal parenchyma and excise the mass without hilar clamping. A CT-1 needle with 3-zero polyglactin suture was used to perform meticulous running repair of any collecting system defects.

The results of this pilot series are given in Table 11.1. Hemostasis was problematic throughout the series. We found that the Greenlight® laser did not coagulate vessels larger than 4–5 mm such as the more centrally placed interlobar arteries. All cases required additional hemostatic maneuvers such as clips, suture, Floseal®, or surgical bolster. The mean blood loss for the series was 400 mL. In the last three cases,

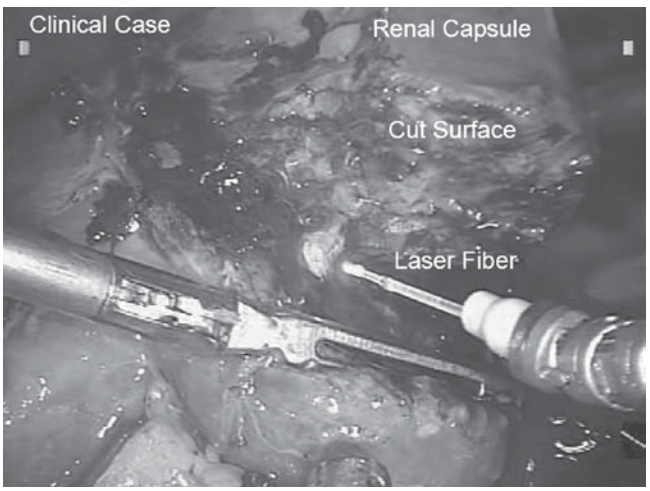

Fig. 11.2 Greenlight® laser robotic partial nephrectomy without hilar clamping. An upper pole Greenlight® laser robotic partial nephrectomy is performed in the perfused kidney using a custom-made da Vinci® 5 mm delivery instrument through which a 600 μm laser fiber was delivered

Table 11.1 Greenlight® laser robotic-assisted partial nephrectomy without Hilar clamping

	Median	Range
Age (years)	51	46–65
BMI (kg/m^2)	29	28–48
Preoperative creatinine (g/dL)	1.0	0.7–1.3
Tumor size (cm)	1.8	1.6–4.0
Hb pre (g/dL)	14.2	13.9–15.4
Hb post (g/dL)	10.8	10.2–12.8
Hct pre (%)	43	41.7–47.2
Hct post (%)	32.3	31.5–38.4
OT time (min)	310	180–360
Mass excision time (min)	54	36–96
Warm ischemia time (min)	0	0–14
Total energy (J)	20,931	9,949–29,158
Lasing time (min)	8.5	3.2–17.1
Specimen weight (g)	9.1	4.5–61.5
Blood loss (mL)	400	200–1,300
Length of stay (days)	3	3–7

continuous suturing of the renal parenchyma was done, as dissection proceeded to assist with hemostasis. Despite this, hemostasis was difficult to achieve and the dissection proceeded slowly and mass excision times were in the order of 36–96 min. The high affinity of the 532 nm wavelength laser light for hemoglobin resulted in absorption of the laser light by free blood, which in turn decreased the cutting efficiency of the laser beam. Therefore, continuous suction and irrigation of the operative field was essential. One case required hilar clamping with 14 min of warm ischemia time. This case was complicated by postoperative hemorrhage requiring embolization and a subsequent four unit blood transfusion. The intraoperative blood loss in the final patient was 1,300 mL and a two unit intraoperative blood transfusion was required. Final histology revealed two oncocytomas, two clear cell RCCs and one papillary tumor. One margin was focally positive. We found that laser transection resulted in significant charring of the renal parenchyma which obscured the intrarenal dissection planes and it is likely that this was a major contributing factor to the focally positive margin.

Smoke generation during the procedures was problematic and high flow insufflation at 40 L/min in conjunction with active smoke evacuation by smoke suction units was required. In addition, continuous irrigation by saline helped to decrease smoke plume. In summary, Greenlight® laser robotic LPN did not achieve adequate hemostasis, was slow with significant smoke generation, and resulted in significant charring of the renal parenchyma, which made intraoperative margin assessment difficult.

Since this initial clinical robotic experience, Honeck et al 2008 compared the hemostatic potential of the Habib® 4× bipolar resection device, the Greenlight® KTP laser, the Ligasure® and Sonosurg® devices in an ex vivo porcine model both with and without clamping, in which scalpel resection was used as a control.[55] While KTP laser excision was rapid and simple to handle, the blood loss without hilar occlusion as assessed by measured sponge weights, was significant and was similar to scalpel excision. The authors concluded that none of the evaluated devices were sufficiently hemostatic for LPN. Certainly, the comment by these authors and others that facilitation and acceleration of the standard laparoscopic technique to reduce warm ischemia while operating in a nearly bloodless field as the more promising approach is well worth noting.[55,56]

Finally, the 2,013 nm Thulium laser has been evaluated in both animal and clinical series. Bui et al 2007 assessed the 30 W thulium laser delivered via a 365 μm fiber passed through a flexible cystoscope in conjunction with continuous saline irrigation in a survival porcine model without hilar clamping.[57] Laser LPN was completed successfully in all cases with an estimated blood loss of <50mL with minimal smoke and minimal tissue charring. Fibrin glue was also however applied to the exposed parenchyma. A limitation of this study is that only the renal cortex was treated, and in the authors' initial nonsurvival pilot assessment, they state that the laser was unable to control the more centrally placed larger medullary vessels near the hilum.

In an open series, Gruschwitz et al in 2008 reported success with the thulium laser in 5 patients with tumor sizes ranging from 1.2 to 3.8 cm at 30 W without hilar clamping via an open loin approach.[11] Operative time was reported in one patient and was stated to be less than 20 min. The authors state that the thulium laser can coagulate vessels up to 1.5 mm and that because of the short operative time, minimal blood loss, and absence of clamping, the thulium laser may be useful in high-risk patients. Whether these results will be reproducible, particularly in a laparoscopic environment, remains to be determined.

The collective data to date is insufficient to support the routine use of laser energy during LPN. It is unlikely that laser LPN will have the capacity to treat all renal masses. Laser energy does not appear capable of sealing the larger, more centrally placed vessels, and additionally is not likely to effect the collecting system closure of its own accord. Therefore larger, centrally placed tumors are unlikely to be suitable for laser resection. Additionally, smoke production is problematic and dissection times are slow. Tissue charring also appears to interfere with intraoperative margin assessment. At this juncture, laser LPN is unlikely to replace standard LPN with sutured parenchymal reconstruction.

Laser Laparoscopic Radical Prostatectomy

Much less work has been done with regard to lower tract laser laparoscopic applications. However, laser laparoscopic radical prostatectomy (LRP) has recently been investigated. The ultimate aim of radical prostatectomy is to maximize outcomes in the triad of cancer control, continence, and potency. The description of the cavernous nerves and their relationship to the prostate as initially described by Walsh and Donker represents one of the most significant advances in urological practice in recent times.[58] Classically, the neurovascular bundles (NVBs) containing the cavernous nerves are described to pass distally within the leaves of the lateral endopelvic fascia on the postero-lateral aspect of the prostate.[58,59] However, more recent data indicates that the pelvic autonomic neural pathways are more extensive than had been initially appreciated and are prone to injury at multiple sites. Significant numbers of nerve fibers exist on the ventral and lateral aspects of the prostate, although their functional significance is undetermined.[60,61] Takenaka et al[62] demonstrated that the pelvic splanchnic nerves continue to join the NVB distal to the vesico-prostatic junction. Tewari et al[63] described the trizonal neural architecture around the prostate gland that

comprises the proximal neurovascular plate (PNP), the predominant neurovascular bundles (PNB), and the presence of accessory neural pathways (ANP). The PNP ranged from 3 to 10 mm lateral to the seminal vesicles, 0–7 mm from the proximal prostate and lateral pedicles, 4–15 mm from the bladder neck and 2–7 mm from the endopelvic fascia.[63] The PNB coursed along the posterolateral aspect of the prostate in the groove between the prostate and the rectum but also extended medially behind the prostate, while ANPs were noted in the layers of levator fascia and the lateral pelvic fascia on the antero-lateral and posterior aspects of the prostate.

It is thus apparent, that the pelvic autonomic neural anatomy is more complex and more extensive than has been previously appreciated. Therefore, collateral tissue injury must be minimized to effectively preserve these structures. Methods currently used to achieve hemostasis during laparoscopic and robotic radical prostatectomy include ultrasonic shears,[64] bipolar diathermy,[65] laparoscopic clips,[66] and lateral vascular pedicle control with laparoscopic bulldog clamps.[67] Ultrasonic shears, bipolar diathermy, and monopolar diathermy have all been shown to adversely affect cavernous nerve function[68] and injure tissues across distances of 0.9, 1.3 and 2.1 cm, respectively, depending on the tissue type and duration of activation.[69] Monopolar diathermy may also injure tissues several centimeters from the site of instrument activation.[69] Given the close proximity of the proximal neural plate to the bladder neck, lateral pedicle, and prostate base, diathermy used at sites distant to the actual cavernous nerves such as at the bladder neck may theoretically damage these proximal neural structures.

Athermal techniques (ATs) have been developed to minimize thermal injury to the cavernous nerves. However, theoretical concerns have been raised regarding the application of bulldog clamps, mass suturing, bulk clipping, or stapling of the pedicle, which may physically traumatize the adjacent cavernous nerves and pelvic plexus.[63,70,71] As a result, clipless techniques have been advocated; however, these rely on the use of bipolar energy.[71] In addition, despite recommendations for the avoidance of thermal energy near the NVBs, thermal energy is still used by many for bladder neck division[62] and also for lateral pedicle control,[72] while many practitioners continue to use ultrasonic shears extensively for the dissection of NVBs and posterolateral prostatic dissection simply because of the speed of dissection and general ease of use.

As a result of these challenges, laser energy has been trialled. Laser energy potentially allows for precise dissection with good hemostasis and minimal adjacent tissue injury. Current laser fibers typically have diameters of 100–1,000 μm and are much finer than the working surfaces of either bipolar forceps or of ultrasonic shears. They are also finer than bulldog clamps and the 5–10 mm clips used laparoscopically. Laser energy is a direct photonic beam which, in contrast to diathermy does not have an associated electrical field, the diffusion of which may result in widespread thermal injury. These theoretical benefits in concert with the advantages of robotic-assisted radical prostatectomy (RARP) by way of the highly magnified 3D view, wristed instrumentation, complete absence of tremor, and fine movement scaling could theoretically allow for extremely fine and accurate dissection with a minimum of collateral neural damage and improved operative outcomes, particularly with respect to potency.

An initial pilot series of Nd:YAG laser nerve-sparing LRP in 5 patients observed an acute mean depth of injury of 615 μm to the NVBs, a reduction in total operative blood loss of 213 mL with laser dissection when compared with 292 mL with standard dissection and no laser-related complications.[73] Following this, a series of studies has investigated the potential application of laser energy facilitating LRP in the canine model.[74–76] Initially, the canine model was assessed for its suitability as a nerve-sparing radical prostatectomy model.[74] Then, the effects of the KTP laser on NVB function was assessed and compared with cold scissor dissection.[75] In this assessment, laparoscopic KTP laser dissection of the NVBs was shown to be equivalent to cold scissor dissection and superior to ultrasonic shears in preservation of cavernous nerve function.[75] In this study, 36 adult male dogs underwent laparoscopic mobilization of a unilateral NVB using KTP laser (n = 12), ultrasonic shears (US) (n = 12), or AT using cold scissors and titanium clips (n = 12). Half the dogs in each group were sacrificed acutely while the remaining half survived for 1 month. Peak penile intracavernosal pressure normalized against simultaneously recorded mean arterial pressure measurements (ICP%MAP) in response to cavernous nerve stimulation were recorded from each bundle initially prior to mobilization and again immediately following NVB mobilization. Peak ICP%MAP was again recorded at 1 month in the survival dogs immediately prior to sacrifice. KTP laser mobilization was performed using a 15 W Aura XP™ laser unit (Laserscope), in which a 200 μm Endostat™ end-firing fiber was passed through a custom-made 5 mm laser-delivery instrument.

The ICP%MAP following KTP laser dissection was comparable with that of cold scissor dissection both immediately postoperatively and at 1 month. US dissection resulted in a significant decrease in the mean ICP%MAP response when compared with both the KTP and AT groups (*acute* ICP%MAP: KTP 92%, AT 96%, US 49%. KTP vs. AT p = 0.54, US vs. KTP $p < 0.001$, US vs. AT $p < 0.001$; *chronic* ICP%MAP: KTP 95%, AT 98%, US 58%. KTP vs. AT p = 0.71, US vs. KTP $p = 0.02$, US vs. AT $p = 0.02$). Histological assessment of the prostate specimens from the laser group demonstrated a zone of laser-induced necrosis of 600 μm (range: 500–2,000) when compared with a median of 1,200 μm (range: 500–1,300) in the US group and 450 μm (range: 300–1,200) of crush injury in the AT group. Thermographic

mapping of the ex vivo prostate specimens demonstrated significant spread of heat onto the region of the NVBs with the US, while there was less heat diffusion with the KTP laser. Serial sectioning of the strips of harvested peritoneum demonstrated a significantly greater area of thermal spread with US shears than with KTP laser (median thermal spread >60°C KTP 1.07 mm vs. US 6.42 mm, $p < 0.01$). The temperatures at the tip of the US shears exceeded 150°C and required 40 s to return to below 60°C. In comparison, heat was not retained at the tip of the laser fiber.

On the basis of these findings, laser RARP was then assessed.[76] Laser RARP was performed in ten male dogs. The study was divided into two phases. The first five dogs constituted the acute, nonsurvival phase of the study, in which the utility of laser prostatectomy using the robotic approach was assessed and the technique was standardized. An additional five dogs constituted the survival phase in which the dogs were sacrificed 72 h postoperatively. Pre and post dissection ICP%MAP were again recorded. Laser RARP was performed completely using the KTP and Nd:YAG lasers delivered from an 800 Series KTP/YAG™ Surgical Laser System (Laserscope). The majority of the dissection was performed using the KTP laser while the Nd:YAG laser was used selectively for hemostasis of larger vessels as required. In the acute study, the optimal power settings for each laser type were determined and these settings were used for the final five survival dogs.

All ten procedures were entirely completed with the use of laser energy. Laser dissection was easy to perform and proceeded efficiently. The median laser prostatectomy excision time (not including the urethrovesical anastomosis) was 65 min (range: 57–100). No additional hemostatic maneuvers such as clips, ultrasonic shears, or electrocautery were required in any case. The median operative blood loss was 50 mL (range: 20–200), which included 200 mL blood loss from a trocar-related splenic injury in one case. The median postoperative hemoglobin and hematocrit were not significantly decreased when compared with the preoperative values in the five survival animals (preoperative Hb 14.4 mg/dL and postoperative Hb 12.6 mg/dL, $p = 0.06$; preoperative Hct 45.1% and postoperative Hct 40.2%, $p = 0.06$).

The median postdissection ICP%MAP was slightly reduced; however, this was not statistically significant (preoperative ICP%MAP 99.3%, postoperative 77.0%, $p = 0.12$). Histological assessment of the excised acute specimens demonstrated a zone of necrosis typically extending 0.5–1.0 mm from the cut edge of the prostatic fascia, extending focally to a maximum of 1.5 mm in some sections with areas of injured but non-necrotic tissue of up to 2 mm beyond the cut edge. There were no laser-related complications.

Finally, KTP laser robotic-assisted LRP was performed in 10 patients as a phase 1 clinical assessment (see Fig. 11.3).[77] In this initial series, complete laser robotic radical prostatectomy was performed successfully using a low power 15 W AuraXP™ KTP (Laserscope/AMS) laser unit. Additional hemostatic maneuvers using clips, sutures, or diathermy were required on an average of eight occasions per case. The mean perioperative values were operative time 217 min, blood loss 290 mL, hospital stay 39.9 h, mean laser time 65.9 min, and laser energy 20,862 J. Eight patients had pT2 disease and two had pT3. All surgical margins were negative. There were no laser-related complications. There was one urine leak and one drain site infection.[77] The mean preoperative SHIM score was 20.4 (range: 9–25) and at 6 months was 7.3 (range: 5–16) (unpublished data).

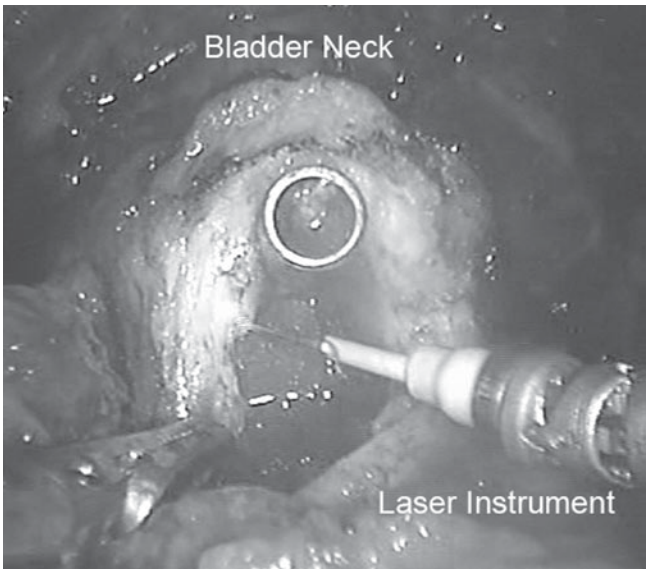

Fig. 11.3 Laser robotic-assisted laparoscopic radical prostatectomy (LRP). Laser robotic-assisted LRP is performed using the 15 W Aura XP™ laser unit delivered via a custom-made 5 mm da Vinci® robotic instrument

From this series of studies, it appears that laser RARP is feasible; however, it is unclear as to whether this offers any benefit over standard laparoscopic and robotic techniques. Certainly, thermal energy should be avoided wherever possible in the region of the NVBs in accordance with standard athermal dissection techniques. Whether laser energy offers any benefit during laparoscopic or robotic radical prostatectomy over current athermal practices remains to be seen and the application of this technology to LRP and RARP is unproven at this time.

Conclusion

In summary, lasers have been investigated in laparoscopic urological applications ranging from laser tissue welding in laparoscopic pyeloplasty through to laser laparoscopic and

laser robotic radical prostatectomy, while most development has centered on LPN. Despite extensive investigation, laser usage during laparoscopic urological procedures has not gained widespread acceptance and remains experimental at this time.

References

1. Carroll L, Humphreys TR. LASER-tissue interactions. *Clin Dermatol*. 2006;24(1):2–7
2. Knappe V, Frank F, Rohde E. Principles of lasers and biophotonic effects. *Photomed Laser Surg*. 2004;22(5):411–417
3. Reinisch L. Laser physics and tissue interactions. *Otolaryngol Clin North Am*. 1996;29(6):893–914
4. Stein BS. Laser physics and tissue interaction. *Urol Clin North Am*. 1986;13(3):365–380
5. Hughes BF, Scott WW. Preliminary report on the use of a CO_2 laser surgical unit in animals. *Invest Urol*. 1972;9(4):353–357
6. Taari K, Salo JO, Pitkaranta P, Kivisaari L, Schroder T, Rannikko S. Efficacy and complications of the Nd:YAG laser in partial nephrectomy: experimental study in piglets. *Scand J Urol Nephrol*. 1991; 25(4):303–306
7. Benson RC Jr. Laser use in open surgery and external lesions. *Urol Clin North Am*. 1986;13(3):421–434
8. Lotan Y, Gettman MT, Lindberg G, et al Laparoscopic partial nephrectomy using holmium laser in a porcine model. *JSLS*. 2004;8(1): 51–55
9. Zenk J, Geisthoff UW, Hamadi I, Iro H. In vitro tissue effects of a combined Ho:YAG/Nd:YAG laser: sprinkling of tissue fragments by Ho:YAG laser light may be problematic for oncological interventions. *Lasers Surg Med*. 1999;25(5):396–400
10. Lotan Y, Gettman MT, Ogan K, Baker LA, Cadeddu JA. Clinical use of the holmium: YAG laser in laparoscopic partial nephrectomy. *J Endourol*. 2002;16(5):289–292
11. Gruschwitz T, Stein R, Schubert J, Wunderlich H. Laser-supported partial nephrectomy for renal cell carcinoma. *Urology*. 2008;71(2): 334–336
12. Eden CG, Coptcoat MJ. Assessment of alternative tissue approximation techniques for laparoscopy. *Br J Urol*. 1996;78(2):234–242
13. Eden CG, Sultana SR, Murray KH, Carruthers RK. Extraperitoneal laparoscopic dismembered fibrin-glued pyeloplasty: medium-term results. *Br J Urol*. 1997;80(3):382–389
14. Wolf JS Jr, Soble JJ, Nakada SY, et al Comparison of fibrin glue, laser weld, and mechanical suturing device for the laparoscopic closure of ureterotomy in a porcine model. *J Urol*. 1997;157(4):1487–1492
15. Barrieras D, Reddy PP, McLorie GA, et al Lessons learned from laser tissue soldering and fibrin glue pyeloplasty in an in vivo porcine model. *J Urol*. 2000;164(3 Pt 2):1106–1110
16. Shumalinsky D, Lobik L, Cytron S, et al Laparoscopic laser soldering for repair of ureteropelvic junction obstruction in the porcine model. *J Endourol*. 2004;18(2):177–181
17. Jemal A, Tiwari RC, Murray T, et al Cancer statistics, 2004 *CA Cancer J Clin*. 2004;54(1):8–29
18. Hock LM, Lynch J, Balaji KC. Increasing incidence of all stages of kidney cancer in the last 2 decades in the United States: an analysis of surveillance, epidemiology and end results program data. *J Urol*. 2002;167(1):57–60
19. Novick AC, Derweesh I. Open partial nephrectomy for renal tumours: current status. *BJU Int*. 2005;95(suppl 2):35–40
20. Novick AC. Laparoscopic and partial nephrectomy. *Clin Cancer Res*. 2004;10(18 Pt 2):6322S–6327S
21. Haber GP, Gill IS. Laparoscopic partial nephrectomy: contemporary technique and outcomes. *Eur Urol*. 2006;49(4):660–665
22. Terai A, Ito N, Yoshimura K, et al Laparoscopic partial nephrectomy using microwave tissue coagulator for small renal tumors: usefulness and complications. *Eur Urol*. 2004;45(6):744–748
23. Sprunger J, Herrell SD. Partial laparoscopic nephrectomy using monopolar saline-coupled radiofrequency device: animal model and tissue effect characterization. *J Endourol*. 2005;19(4):513–519
24. Herrell SD, Levin BM. Laparoscopic partial nephrectomy: use of the TissueLink hemostatic dissection device. *J Endourol*. 2005;19(4): 446–449; discussion 449–450
25. Ong AM, Bhayani SB, Hsu TH, et al Bipolar needle electrocautery for laparoscopic partial nephrectomy without renal vascular occlusion in a porcine model. *Urology*. 2003;62(6):1144–1148
26. Simon SD, Ferrigni RG, Novicki DE, Lamm DL, Swanson SS, Andrews PE. Mayo Clinic Scottsdale experience with laparoscopic nephron sparing surgery for renal tumors. *J Urol*. 2003;169(6): 2059–2062
27. Moinzadeh A, Hasan W, Spaliviero M, et al Water jet assisted laparoscopic partial nephrectomy without hilar clamping in the calf model. *J Urol*. 2005;174(1):317–321
28. Barzilay B, Lijovetzky G, Perlberg S, Caine M. Comparative experimental study on the use of the carbon dioxide laser beam in partial nephrectomy. *Lasers Surg Med*. 1982;2(1):73–80
29. Barzilay B, Lijovetzky G, Shapiro A, Caine M. The clinical use of CO_2 laser beam in the surgery of kidney parenchyma. *Lasers Surg Med*. 1982;2(1):81–87
30. Meiraz D, Peled I, Gassner S, Ben-Bassat M, Kaplan I. The use of the CO_2 laser for partial nephrectomy: an experimental study. *Invest Urol*. 1977;15(3):262–264
31. Rosemberg SK. Clinical experience with carbon dioxide laser in renal surgery. *Urology*. 1985;25(2):115–118
32. Benderev TV, Schaeffer AJ. Efficacy and safety of the Nd:YAG laser in canine partial nephrectomy. *J Urol*. 1985;133(6):1108–1111
33. Benderev TV, Schaeffer AJ. Preliminary study of the Nd:YAG laser in canine partial nephrectomy. *Lasers Surg Med*. 1985;5(4):415–421
34. Johnson DE, Wishnow KI, von Eschenbach AC, Grignon D, Ayala AG. Partial nephrectomy using the Nd:YAG laser: a comparison of the 1.06 mu and 1.32 mu lasers employing different delivery systems. *Lasers Surg Med*. 1988;8(3):241–247
35. Korhonen AK, Talja M, Karlsson H, Tuhkanen K. Contact Nd:YAG laser and regional renal hypothermia in partial nephrectomy. *Ann Chir Gynaecol Suppl*. 1993;206:59–62
36. Landau ST, Wood TW, Melzer RB, Lee RG, Smith JA Jr. Renal evaluation after CUSA plus Nd:YAG laser for partial nephrectomy. *Lasers Surg Med*. 1986;6(2):146–149
37. Landau ST, Wood TW, Smith JA Jr. Evaluation of sapphire tip Nd:YAG laser fibers in partial nephrectomy. *Lasers Surg Med*. 1987;7(5):426–428
38. Malloy TR, Schultz RE, Wein AJ, Carpiniello VL. Renal preservation utilizing neodymium:YAG laser. *Urology*. 1986;27(2):99–103
39. Melzer RB, Wood TW, Landau ST, Smith JA Jr. Combination of CUSA and neodymium:YAG laser for canine partial nephrectomy. *J Urol*. 1985;134(3):620–622
40. Merguerian PA, Seremetis G. Laser-assisted partial nephrectomy in children. *J Pediatr Surg*. 1994;29(7):934–936
41. Salo JO, Savolainen H, Schroder T, Nordling S, Verkkala K, Rannikko S. Nd: YAG contact laser in partial nephrectomy. An experimental study in piglets. *Scand J Urol Nephrol*. 1991;25(2):151–155
42. Taari K, Salo JO, Kairemo KJ, et al Renal function after partial nephrectomy with the Nd-YAG laser. Experimental study in piglets. *Br J Urol*. 1991;68(5):459–462
43. Taari K, Salo JO, Kivisaari L, Rannikko S, Nordling S, Lindell O. Contact fibre Nd:YAG laser for partial nephrectomy: experimental study in pigs. *Urol Res*. 1993;21(4):301–304
44. Taari K, Salo JO, Rannikko S, Nordling S. Partial nephrectomy with a combined CO_2 and Nd:YAG laser: experimental study in pigs. *Lasers Surg Med*. 1994;14(1):23–26
45. Johnson DE, Cromeens DM, Price RE. Use of the holmium:YAG laser in urology. *Lasers Surg Med*. 1992;12(4):353–363

46. Janetschek G, Daffner P, Peschel R, Bartsch G. Laparoscopic nephron sparing surgery for small renal cell carcinoma. *J Urol*. 1998;159(4):1152–1155
47. Lotan Y, Gettman MT, Lindberg G, et al Laparoscopic partial nephrectomy using holmium laser (video). *J Endourol*. 2001;15(suppl 1):134
48. Ogan K, Wilhelm D, Lindberg G, et al Laparoscopic partial nephrectomy with a diode laser: porcine results. *J Endourol*. 2002;16(10): 749–753
49. Ogan K, Jacomides L, Saboorian H, et al Sutureless laparoscopic heminephrectomy using laser tissue soldering. *J Endourol*. 2003; 17(5):295–300
50. Moinzadeh A, Gill IS, Rubenstein M, et al Potassium-titanyl-phosphate laser laparoscopic partial nephrectomy without hilar clamping in the survival calf model. *J Urol*. 2005;174(3):1110–1114
51. Hindley RG, Barber NJ, Walsh K, Petersen A, Poulsen J, Muir GH. Laparoscopic partial nephrectomy using the potassium titanyl phosphate laser in a porcine model. *Urology*. 2006;67(5):1079–1083
52. Liu M, Rajbabu K, Zhu G, Petersen A, Muir GH, Poulson J. Laparoscopic partial nephrectomy with saline-irrigated KTP laser in a porcine model. *J Endourol*. 2006;20(12):1096–1100
53. Anderson JK, Baker MR, Lindberg G, Cadeddu JA. Large-volume laparoscopic partial nephrectomy using the potassium-titanyl-phosphate (KTP) laser in a survival porcine model. *Eur Urol*. 2007; 51(3):749–754
54. Benderev TV, Chmiel JS, Carone FA, Schaeffer AJ. Dosimetry study of Nd:YAG laser damage to canine renal cortex. *Lasers Surg Med*. 1987;7(4):363–369
55. Honeck P, Wendt-Nordahl G, Bolenz C, et al Hemostatic properties of four devices for partial nephrectomy: a comparative ex vivo study. *J Endourol*. 2008;22(5):1071–1076
56. Hacker A, Albadour A, Jauker W, et al Nephron-sparing surgery for renal tumours: acceleration and facilitation of the laparoscopic technique. *Eur Urol*. 2007;51(2):358–365
57. Bui MH, Breda A, Gui D, Said J, Schulam P. Less smoke and minimal tissue carbonization using a thulium laser for laparoscopic partial nephrectomy without hilar clamping in a porcine model. *J Endourol*. 2007;21(9):1107–1111
58. Walsh PC, Donker PJ. Impotence following radical prostatectomy: insight into etiology and prevention. *J Urol*. 1982;128(3):492–497
59. Lepor H, Gregerman M, Crosby R, Mostofi FK, Walsh PC. Precise localization of the autonomic nerves from the pelvic plexus to the corpora cavernosa: a detailed anatomical study of the adult male pelvis. *J Urol*. 1985;133(2):207–212
60. Eichelberg C, Erbersdobler A, Michl U, et al Nerve distribution along the prostatic capsule. *Eur Urol*. 2007;51(1):105–110; discussion 110–101
61. Tewari A, Peabody JO, Fischer M, et al An operative and anatomic study to help in nerve sparing during laparoscopic and robotic radical prostatectomy. *Eur Urol*. 2003;43(5):444–454
62. Takenaka A, Leung RA, Fujisawa M, Tewari AK. Anatomy of autonomic nerve component in the male pelvis: the new concept from a perspective for robotic nerve sparing radical prostatectomy. *World J Urol*. 2006;24(2):136–143
63. Tewari A, Takenaka A, Mtui E, et al The proximal neurovascular plate and the tri-zonal neural architecture around the prostate gland: importance in the athermal robotic technique of nerve-sparing prostatectomy. *BJU Int*. 2006;98(2):314–323
64. Dahl DM, L'Esperance J O, Trainer AF, et al Laparoscopic radical prostatectomy: initial 70 cases at a U.S. university medical center. *Urology*. 2002;60(5):859–863
65. Guillonneau B, Vallancien G. Laparoscopic radical prostatectomy: the Montsouris technique. *J Urol*. 2000;163(6):1643–1649
66. Eden CG, King D, Kooiman GG, Adams TH, Sullivan ME, Vass JA. Transperitoneal or extraperitoneal laparoscopic radical prostatectomy: does the approach matter? *J Urol*. 2004;172(6 Pt 1): 2218–2223
67. Gill IS, Ukimura O, Rubinstein M, et al Lateral pedicle control during laparoscopic radical prostatectomy: refined technique. *Urology*. 2005;65(1):23–27
68. Ong AM, Su LM, Varkarakis I, et al Nerve sparing radical prostatectomy: effects of hemostatic energy sources on the recovery of cavernous nerve function in a canine model. *J Urol*. 2004;172(4 Pt 1): 1318–1322
69. Tulikangas PK, Smith T, Falcone T, Boparai N, Walters MD. Gross and histologic characteristics of laparoscopic injuries with four different energy sources. *Fertil Steril*. 2001;75(4):806–810
70. Walz J, Graefen M, Huland H. Basic principles of anatomy for optimal surgical treatment of prostate cancer. *World J Urol*. 2007; 25(1):31–38
71. Chien GW, Mikhail AA, Orvieto MA, et al Modified clipless antegrade nerve preservation in robotic-assisted laparoscopic radical prostatectomy with validated sexual function evaluation. *Urology*. 2005;66(2):419–423
72. Stolzenburg JU, Rabenalt R, Do M, Tannapfel A, Truss MC, Liatsikos EN. Nerve-sparing endoscopic extraperitoneal radical prostatectomy: University of Leipzig technique. *J Endourol*. 2006; 20(11):925–929
73. Gianduzzo TR, Chang CM, El-Shazly M, Mustajab A, Moon DA, Eden CG. Laser nerve-sparing laparoscopic radical prostatectomy: a feasibility study. *BJU Int*. 2007;99(4):875–879
74. Gianduzzo TR, Colombo JR, El-Gabry E, Haber GP, Gill IS. Anatomical and electrophysiological assessment of the canine periprostatic neurovascular anatomy: perspectives as a nerve sparing radical prostatectomy model. *J Urol*. 2008;179(5):2025–2029
75. Gianduzzo T, Colombo JR Jr, Haber G-P, et al Laser nerve-sparing laparoscopic radical prostatectomy: effects of potassium-titanyl-phosphate laser on cavernous nerve function in a survival canine model. *J Urol*. 2007;177(4):804
76. Gianduzzo T, Colombo JR Jr, Haber GP, et al Laser robotically assisted nerve-sparing radical prostatectomy: a pilot study of technical feasibility in the canine model. *BJU Int*. 2008;102(5): 598–602
77. Gianduzzo T, Kaouk J, Colombo JR, et al KTP laser robotic nerve-sparing radical prostatectomy: development and initial clinical experience. In: *Engineering and Urology Society 22nd Annual Meeting;* 2007:Abstract 212

Part III

Other New Technologies

John Fitzpatrick

Cryosurgical Ablation for Prostate Cancer

12

Alastair Henderson, Mohamed Ismail, and John Davies

Introduction

Prostate cancer is the most commonly diagnosed malignancy in the UK representing 24% of male cancers; the death rate from prostate cancer is significant at 3% of all male deaths.[1] In many cases, the disease has a long period of asymptomatic growth before developing into locally advanced or metastatic disease with symptoms.

There are several existing options for the control of early prostate cancer including radical prostatectomy (RP), utilizing open surgical, laparoscopic, or robotic techniques, external beam radiotherapy (EBRT), and brachytherapy (BXT) using either low dose or high dose rate techniques. More recently, prostate cryotherapy has become available and new technologies including high intensity focused ultrasound (HIFU), interstitial treatment with photosensitizers and laser radiation are evolving into clinically relevant entities.

Despite the range of technologies employed to target early prostate cancer, none has become the definitive treatment for the most common of male malignancies. This is due to the fact that all have significant drawbacks, as well as advantages, over each other and compared with conservative therapy for early prostate cancer. The literature on radical treatment for early prostate cancer has few randomized trials. In this difficult intellectual terrain, we describe the current and future place of prostate cryotherapy.

Aims of Treatment for Early Prostate Cancer

The aims of treatment for organ confined prostate cancer are to prevent progression from early disease to metastatic, locally advanced disease or symptomatic disease within the patient's lifetime or as a cause of a shortened lifespan via the mechanisms described in Fig. 12.1. Its additional aim should be to achieve this without causing new symptoms or disease in the patient.

The late Dr Whitmore as director of urology at the Memorial Sloane Kettering Cancer Centre noted, of existing treatments for prostate cancer, "When cure is possible is it necessary and when it is necessary, is it possible?" This question is equally valid today and the value of cryotherapy may lie mainly in the group of men with significant primary or recurrent disease in whom the possibility of cure remains a challenge.

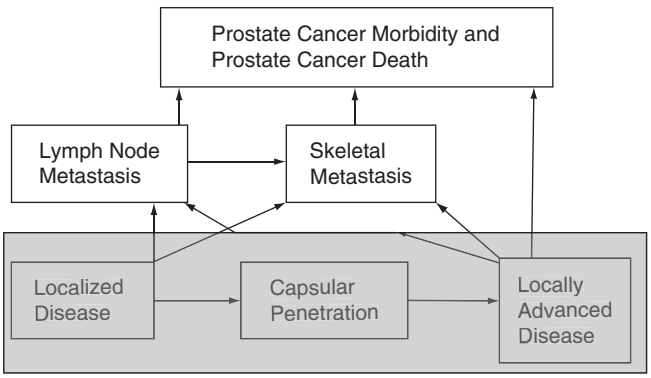

Fig. 12.1 Possible patterns of prostate cancer progression

Cryotherapy has been applied to all the stages of nonmetastatic prostate cancer described in the gray-shaded area of Fig. 12.1. This chapter will describe current results of cryotherapy treatment as well as the theory underpinning the technique and possible areas for future development.

The History and Development of Cryosurgery for Prostate Cancer

The history of prostate cryotherapy was recently reviewed by Ahmed et al[2]. Though modern cryotherapy is a relatively recent and constantly evolving technique, the recognition that cold could be used to treat tumors is not novel. Therapeutic cryotherapy started with the work of Dr James Arnott from Brighton, UK. In the 1840s, he described the use of ice slush for topical anesthesia and to treat tumors including cervical cancer using a wide speculum to achieve freezing. He made an important conclusion following his observation on the use of cryotherapy in the treatment of cancer "Congelation

P. Dasgupta et al. (eds.), *New Technologies in Urology,*
DOI: 10.1007/978-1-84882-178-1_12, © Springer-Verlag London Limited 2010

arresting the accompanying inflammation, and destroying the vitality of the cancer cell, is not only calculated to prolong life for a great period, but may not improbably, in the early stage of the disease, exert a curative action." He published his work in the Lancet in 1850 and his cryotherapy apparatus was shown in the Great Exhibition in London in 1851.[3]

Topical applications of ice slush were not suitable for reliably achieving adequately reduced temperatures in the −20 to −40°C range, and although gas liquefaction by adiabatic expansion systems for cooling were invented in the 1870s, delivery systems were not developed until the late 1890s. The early 1900s saw an increase in the availability of liquid nitrogen, which led to the possibility of topical treatment of superficial lesions either by direct application of liquid nitrogen or application of a cooled metal probe.

It was not until 1961 that the neurosurgeon, Irving Cooper and engineer, Arnold Lee developed a vacuum-insulated needle delivery system for liquid nitrogen. This allowed an iceball to be formed at the needle tip and variants of this system were used to treat benign and malignant conditions at a variety of sites including malignant brain tumors.[4] Gonder[5] used a transurethral probe with digital rectal monitoring to freeze the prostate using liquid nitrogen. This process was complicated by a high incidence of urethral sloughing and recto-urethral fistulae.[5]

The modern renaissance of prostate cryosurgery was heralded by several developments. The description by Onik et al of transrectal ultrasound guided cryotherapy in 1993[6] using dual liquid nitrogen cryoprobes heralded the era of modern cryotherapy. The availability of more accurate thermocouples[7] and the urethral warming catheter[8] led to reductions in the significant complications of urethral sloughing and rectal fistulae, which had been encountered in early cryotherapy.

Lastly, the progression from single- or dual-probe, liquid nitrogen–based systems to the current multi-probe argon–helium systems has led to better control of the cooling phase, ability to actively warm the probe, and reduced trauma as an effect of reduced probe size.

Currently available systems utilize the Joule-Thompson effect. This is characterized by a change in temperature, produced in this scenario at the probe tip, when high pressure gas is released to a lower pressure, and exits via the outer lumen of the probe. The temperature at the probe tip may be reduced or increased depending on the physical properties of the gas chosen. Rapid cooling to temperatures as low as −186°C may be achieved using argon; helium produces warming to temperatures of up to 40°C. Figure 12.2 illustrates the iceball generated during probe testing on a modern device.

Two systems are currently in widespread use. Galil Medical introduced their third-generation cryotherapy system (Seednet™) in the late 1990s. They developed ultra thin 17-gauge needle probes, which allowed more uniform coverage of the prostate. In 2003, Endocare introduced their fourth-generation cryotherapy system (Cryocare™) CS), which superseded their previous argon-helium system, introduced in the mid-1990s.

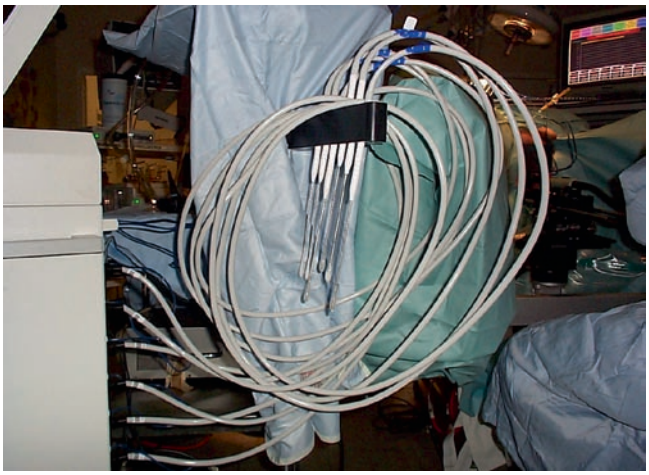

Fig. 12.2 Iceball generated during cryoprobes testing prior to procedure

The latest developments of the technique resulted from the constant improvement in the quality of transrectal ultrasound images due to the evolution of high-definition multiplanar ultrasound arrays over the last 20 years. This has led to an ability to more accurately monitor the iceball (which can be seen as a hyperechoic rim with acoustic shadowing[6]) and more accurately place the thermocouples used for temperature monitoring.

This evolution in the technique, with evidence of a significant reduction in complications as advances in technology occured[8] does mean that care is necessary in interpreting the published results of prostate cryotherapy.

Mechanism of Tissue Injury in Prostate Cryotherapy

The aim of prostate cryotherapy is to destroy neoplastic tissue and preserve vital structures around the prostate including the bladder, rectum, and ideally the neurovascular bundles. This requires precise freezing process to achieve the maximum tissue ablation within the prostate without damage to the critical structures.

In modern prostate cryotherapy, several cryoprobes are used and cells are exposed to variable thermal parameters depending on their location from the freezing probe. Larson et al[9] reported two areas of tissue damage surrounding the cryotherapy probe. Areas near the probe undergo coagulative necrosis; while at a greater distance from the probe, tissues undergo squamous metaplasia and hemorrhage, which is replaced by polymorphonuclear leukocytes infiltrate.[10] It is

well known that two mechanisms are responsible for cell death: direct injury caused by ice formation and indirect ischemic effect caused by microvascular changes. During freezing, extracellular ice forms at a temperature range between −7 and −20°C. A hyperosmolar extracellular environment draws water from the cells and lead to cell dehydration and shrinkage (the solute effect injury). At even lower temperatures (<−15°C), ice will extend to the intracellular space.[11] Homogenous intracellular ice crystals are noticed at temperature lower than −40°C, which is almost always lethal to the cells.[11]

During thawing, the extracellular space is hypotonic and water enters the cells to augment the solute effect and results in cell rupture. Microvascular effects start with vasoconstriction and tissue anoxia during the freezing phase, which results in tissue necrosis. This is followed by vasodilatation, increased vascular permeability, and tissue edema during the thawing phase which contributes to the solute effect cell injury. Following freezing, blood vessels show endothelial cell damage and microthrombus formation and complete cessation of circulation follows in few hours.[12] Apoptotic cell death can be identified in the peripheral zone of the cryolesion, where cells are exposed to sublethal freezing temperature.[13]

Physical Parameters in Prostate Cryotherapy

Several physical parameters appear to influence the biological tissue changes described earlier. These include the freezing rate, temperature nadir, thawing rate, duration of freeze, and number of freeze cycles.

Freezing Rate

Rapid freezing is essential for intracellular ice formation and is associated with higher rate of cell death.[14] However, there was no agreed definition of rapid freezing. In vitro studies demonstrated that intracellular ice formation can be achieved with freezing rate between 3 and 50°C/min,[15,16] while Tatsutani et al[17] demonstrated that a freezing rate of 25°C/min is essential for intracellular ice formation and complete cell death. Factors affecting the freezing rate include the distance of the tissue from the center of the ice ball, vascularity, and water content of the treated organ.[17]

Target Temperature

The critical temperature that results in complete ablation of the prostate tissue is not well defined. Early reports demonstrated a temperature of −20°C or less is essential to kill the cells.[18,19] More recently, studies have shown that −40°C is required for complete destruction of prostate tissue.[20] Larson et al[9] reported on six prostate cancer patients who underwent prostate cryotherapy using single cryotherapy probe followed by RP, as a definitive treatment. They identified that the critical temperature required to achieve uniform coagulative necrosis was −41.4°C in the double freeze cycle compared with −61.7°C in the single freeze cycle, though clearly, further tissue changes might have occurred if a greater time had been allowed to elapse between cryotherapy and prostatectomy.

Thawing Rate

Thawing phase is an important mechanism that results in cell destruction during the freeze–thaw cycle. During thawing phase, cells are exposed to different damaging mechanisms including solute effect, ice crystal recrystallization, and reperfusion injury.[21] It was demonstrated that slow thawing rates are associated with a significant increase in cell death when compared with active thawing.[20] Slow thawing exposes tissues to prolonged time of osmotic imbalance, oxidative stress, and growth of ice crystals and hence is associated with increased cell death.[22]

Duration of Freezing

Although the optimum duration of freezing is not yet well defined, it is known that the length of exposure to freezing temperatures affects cell viability post cryotherapy.[15] Early reports suggested that duration of freezing is less important when the tissue is treated to a temperature less than −40°C as a smaller amount of water remain unfrozen.[21] Klossner et al[20] demonstrated that prostate cancer cells held at the critical temperature of −40°C for 2 min showed the maximum ablative level (~93%) when compared with cells, which just reached the critical temperature (24%).

Repetition of the Freeze–Thaw Cycle

The importance of double freeze-thaw cycle for complete ablation of prostate tissue has been identified in an in vivo study.[9] The volume of necrotic tissue significantly increased from 4 to 13% following double freeze–thaw cycle. A recent report demonstrated enhanced lethal effect of cryotherapy following the second freeze–thaw cycle.[20] The mechanism

behind increased cell death following the second freeze–thaw cycle is not well understood. Cellular disruption and loss of cell membrane integrity following the first freeze causes an increase in thermal conductivity during the second freeze, which results in faster and more extensive tissue freezing during the second freeze–thaw cycle.[23] In addition, extended exposure to cold injury may sensitize cancer cells following the first freeze.[20]

Indications for Cryotherapy

Primary Therapy for Organ Confined Disease

Organ confined prostate cancer remains amenable to cryotherapy today, although increasing competition from other treatment options means that this is infrequently used for primary treatment in the UK when compared with radiotherapy and RP. Guidance was issued from the UK National Institute of Clinical Excellence (NICE), based on their literature review which was prepared in 2004.[24] This stated that in view of the current scarcity of evidence on the efficacy and safety of primary cryotherapy, it was not recommended for men with localized prostate cancer other than in the context of controlled clinical trials comparing their outcomes with those of more established interventions.

The Cochrane review group considered cryotherapy for localized prostate cancer in 2007[25] and their findings supported these conclusions. The American Urological Association (AUA) has stated that there are insufficient published data to perform a meta-analysis of the results of cryosurgery for early prostate cancer and include this modality in the 2007 guidelines on the management of clinically localized prostate cancer.[26]

Best practice guidelines from the AUA on prostate cryotherapy suggest that although there is a scarcity of evidence, short-term outcomes for intermediate and high risk organ confined disease may be similar to those from radiotherapy at follow-up durations <8 years.[27] The latest publications detailed in the results section include patients with 10-year follow-up.

Primary Therapy for Locally Advanced Disease

Cryotherapy has also been used to treat locally advanced prostate cancer. However, a recent randomized controlled trial in T2c-T3b (bilateral organ confined, capsular penetration, or seminal vesical invasion) by Chin et al[28] has suggested that biochemical disease-free survival was poorer in men who underwent cryotherapy as their primary treatment modality than in those who underwent primary EBRT. Clearly, the subgroup of patients with capsular penetration and a contraindication to EBRT may wish to consider cryotherapy as primary therapy.

Salvage Therapy After External Beam Radiotherapy or Brachytherapy

The failure rates for contemporary EBRT in biochemical control of organ-confined prostate cancer range from 24 to 85% depending on the risk profile of the assessed group and the planning and delivery of radiotherapy.[29–31] Owing to the widespread use of EBRT often at lower radiation doses than are used currently, this is potentially the largest group of patients who are suitable for prostate cryotherapy. The workload of such patients who may require cryotherapy is also higher, in part due to the relative lack of other established modalities, which are recognized as effective in the treatment of locally recurrent disease after radiotherapy.

Patient Selection for Primary Cryotherapy

Guidelines by the AUA and the NICE, UK, detail appropriate investigations to confirm staging prior to local ablative therapy in patients with pathologically confirmed prostate cancer.[32,33] Use of established staging nomograms (Roach[32] or Partin[34]) should be encouraged and the possibility of lymph node (LN) sampling considered if the chance of LN involvement is >15%.[32] As in patients undergoing primary treatment, a prostate volume of more than 40 cm^3 requires 3 months cytoreductive hormone therapy to facilitate the procedure and reduce the risk to the surrounding structures.[35]

Patient Selection for Salvage Cryotherapy

Rising serum prostate specific antigen (PSA) level is usually the first sign of treatment failure in prostate cancer. The PSA may fluctuate in the first 18 months following radiotherapy.[36] If there is a persistent rise in PSA, which fulfils the Phoenix definition of biochemical failure (nadir PSA + 2.0 mmol/dL) then staging investigations for salvage therapy may be instigated.[37]

The possibility of lower urinary tract infection should be excluded. Restaging pelvic MRI scan and bone scan is mandatory to exclude patients with metastatic disease prior to prostate biopsy. Prostate biopsy is mandatory to confirm local recurrence. Saturation prostate biopsy (20–40 cores) is more

sensitive than transrectal biopsy (10 cores) in detection of recurrent cancer in irradiated patients.[38] Cytoreductive androgen deprivation should be employed when prostate volume is >40 cm^3. The role of pelvic LN dissection should be considered in men at higher risk of having locally advanced disease based on the characteristics of their initial presentation (using the Roach or Partin nomograms identified earlier).

The Technique of Cryosurgical Ablation of the Prostate

Our protocol requires a phosphate enema on the morning of surgery, after which the patient is anesthetized, usually with general or regional anesthetic. In the lithotomy position, the patient is draped and the perineum prepared with aqueous iodine solution. A flexible cystoscopy is performed to check for possible urethral problems, which might prevent the placement of the warming system, and the patient then has a catheter placed. A volume measurement is then performed and the number of probes necessary is calculated. A stepping unit mounted either on the floor or attached directly to the operating table may be used. Commercial software is available to optimize placement of the cooling probes based on the gland volume and the location of the critical structures (rectum and urethra); however, this is not widely used and most operators place the cryoprobes freehand via a perineal template. For typical salvage cases, this would result in the placement of 6–12 of the Galil Seednet probes in 2–3 rows, at approximately 10 mm intervals. Thermocouples are then placed in four locations; anterior to Denonviliers fascia, in the anterior prostate, at the prostatic apex, and in the sphincter, all under ultrasound control. The catheter is then removed and a flexible cystoscopy performed to allow placement of a guidewire in the bladder and the urethral warmer is placed over the guidewire. A typical setup for cryotherapy is reproduced in Fig. 12.3. The two freeze cycles are then commenced with careful monitoring of the freeze using the temperature probes and the ultrasound images. This technique was used to produce the results in the series of patients treated at our institution.[39]

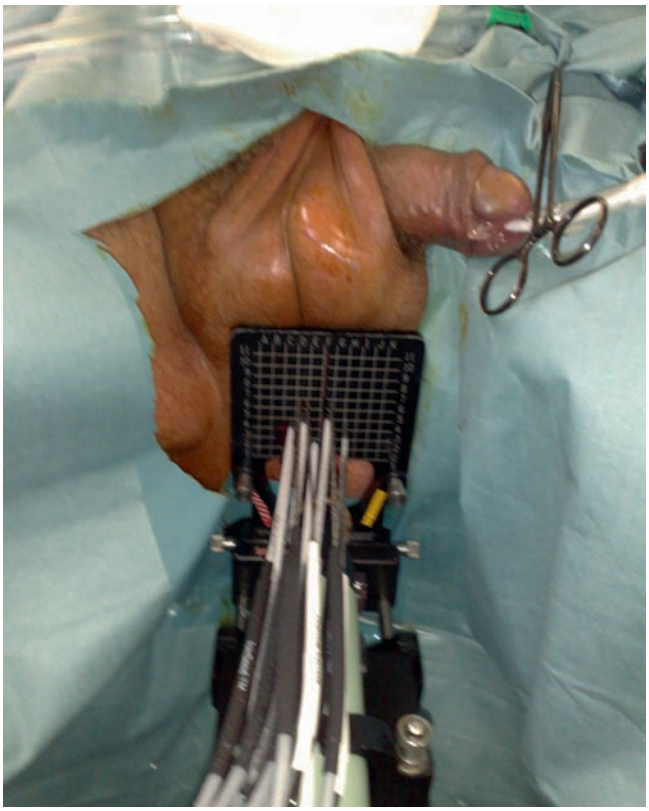

Fig. 12.3 Setup for prostate cryotherapy with urethral warmer in situ, black cryoprobes and white thermocouples inserted via a perineal template

Primary Cryotherapy of the Prostate

Biochemical recurrence free survival (BRFS) rates after primary cryotherapy are variable ranging from 60 to 90% at the last follow-up. This depends on the criteria used in defining the cutoff PSA recurrence rate. The outcome also varies depending on the risk groups with better outcome in the low-risk patients (those with a PSA level ≤10 ng/mL, a Gleason score ≤6 and a clinical stage ≤T2b) when compared with the high-risk patients (those with two or more unfavorable risk factors from a PSA level >10 ng/mL, a Gleason score ≥7, and clinical stage >2b).[40] The use of preoperative hormone ablation therapy impacts on the long-term results of the procedure. Tables 12.1 and 12.2 summarize the results and complications of the recent studies of primary prostate cryosurgery. Cohen et al[41] assessed 370 patients who had undergone prostate cryotherapy as primary treatment for locally advanced prostate cancer. The 10-year actuarial biochemical recurrence-free survival (BRFS) for low risk, medium risk, and high risk was 80.56, 74.16, and 45.54%, respectively. The 10-year positive biopsy rate was 23%. Hubosky et al[42] retrospectively reviewed 89 patients for 11 months who had undergone primary cryotherapy of the prostate. Their results were comparable with those of Cohen et al[41] series with regard to the local cancer control. Long et al[43] presented a multi-institutional report following primary prostate cryotherapy. A total of 975 patients were treated over 5 years. Two PSA thresholds were used (0.5 and 1 ng/mL) to define biochemical disease recurrence. Seventy-five percent of the patients were in the intermediate and high-risk group. The 5-year actuarial BRFS rates were 60% in the low-risk patients

Table 12.1 Results of the primary cryotherapy series

Series	Year	Number of patients	Follow-up (mean) months	Negative biopsy %	PSA failure	Percentage of BRFS (risk group)		
						Low	Intermediate	High
Cohen et al[41]	2008	370	150	76.9	Nadir + 2	80.5	74.16	45.5
Hubosky et al[42]	2007	89	11	N/A	≤0.4	74	70	60
Polascik et al[45]	2007	50	18	96	<0.5	90 all patients		
El Hayek et al[47]	2007	21	41	42	<1	42.8 at 60 months		
Prepelica et al[48]	2005	65	35	87.5	ASTRO	83 all patients		
Han et al[49a]	2003	106	12	N/A	<0.4	75 at 12 months		
Bahn et al[44]	2002	590	(65)	87	ASTRO	92	89	89
Donnelly et al[46]	2002	87	(50)	98.6	<0.3	60	77	48
Long et al[43]	2001	975	24	82	<1	76	71	61
Koppie et al[50]	1999	176	(30.8)	62	<0.5	70		45
Wong et al[51]	1997	83	30	17[b] 90	–	–	–	–
Shinohara et al[52]	1996	102	–	77	Undetectable	41	54	3
Miller et al[53]	1994	62	(24)	79	<0.4	51 at 20 months		
Onik et al[6]	1993	55	(23)	93	Biopsy results	–	–	–

[a]Mixed primary and salvage cases

[b]Without temperature monitoring

Table 12.2. Complication rates following primary cryotherapy of the prostate

Series	Impotence (%)	Incontinence (%)	Recto-urethral fistula (%)	Urethral slough (%)	Pain (%)	Stricture/ retention (%)
Cohen et al[41]	N/A	N/A	N/A	N/A	N/A	N/A
Hubosky et al[42]	N/A	N/A	N/A	N/A	N/A	N/A
Polascik et al[45]	50	4	0	0	0	0
El Hayek et al[47]	96	8	0	N/A	N/A	N/A
Prepelica et al[48]	N/A	3.1	0	N/A	3.1	3.1
Han et al[49a]	87	8	0	5	2.6	3.3
Bahn et al[44]	89.8	15.9	0.004	N/A	N/A	5.5
Donnelly et al[46]	53	1.3	N/A	3.9	N/A	N/A
Long et al[43]	93	7.5	0.5	N/A	2.3	13
Koppie et al[50]	N/A	N/A	N/A	N/A	N/A	N/A
Wong et al[51]	94	4	0	37	N/A	4
Shinohara et al[52]	84	4	1	N/A	3	23
Miller et al[53]	N/A	2.7	0	1.3	N/A	1.3
Onik et al[6]	64	0	2.9	4.4	N/A	N/A

[a]Mixed primary and salvage cases

when compared with 36% in the high-risk group (PSA cut-off 0.5 ng/mL). The positive biopsy rates ranged from 18 to 24%. Bhan et al[44] reported on 590 patients who underwent cryoablation of the prostate and followed for 7 years; BRFS rate was defined as PSA level <0.5 ng/mL. The 7-year actuarial BRFS rate were 61, 68, and 61% for the low-risk, intermediated-risk, and high-risk groups, respectively, with a positive biopsy rate of 13%.

Complications of Primary Cryotherapy of the Prostate

Complication rates are low following primary prostate cryotherapy apart from erectile dysfunction, which remains a serious problem.[42] Table 12.2 summarizes the complication rate following primary cryotherapy of the prostate. Rectourethral fistulae are very uncommon in modern primary cryotherapy series (<0.5% in reports from the last decade).[45] The impotence rate in the primary cryotherapy ranges from 53 to 96%. Donnelly et al[46] reported that the nerves have the potential to recover 12 months following cryotherapy and half of their patients had recovered potency by 36 months. Incontinence rates varied considerably but were <10% in most series.

Oncological Results of Salvage Cryotherapy

There has been controversy in evaluating the clinical response following cryotherapy of the prostate. PSA level cutoffs of 0.1, 0.2 (above nadir), 0.3, 0.4, and 0.5 ng/mL have been used to define biochemical failure.[35–49,54–57] Connolley et al[57] demonstrated that PSA cutoff value of ≥0.5 ng/mL is a strong predictor of positive biopsy at 12 months post cryotherapy. Table 12.3 summarizes the outcome of the recent salvage cryotherapy case series.

In our center the first 100 salvage cryotherapy patients were followed with 3 monthly serum PSA level over mean follow-up period of 33 months. We used the American Society for Therapeutic Radiology and Oncology (ASTRO) definition and cutoff value ≥0.5 ng/mL to define the biochemical failure. Using the ASTRO definition, 60% of men remained disease free at 3 years follow-up. Unsurprisingly, high-risk patients showed the least favorable outcome. This may reflect undetected subclinical systemic disease, persistent local cancer progression, or involvement of the seminal vesicle[58]. Seventy-three percent of low-risk patients with no risk factor remained free from biochemical recurrence at 5 years follow-up.

A recent retrospective case series reported on 279 patients who had undergone salvage cryotherapy for recurrent prostate cancer.[59] At 5 years, 59% were free from biochemical failure and 67.4% had a negative biopsy following the procedure. Bahn et al[56] presented the longest follow-up series of salvage cryotherapy. At 7 years follow-up, the combined BRFS using PSA cutoff of 0.5 ng/mL was 59%. At the London Health Sciences Centre in Ontario, 187 patients with locally recurrent prostate cancer have been treated with salvage cryotherapy.[60] They reported BRFS of 56% with a mean follow-up of 39 months. Preoperative PSA level was an independent predictor for BRFS and patients with preoperative PSA less than 4 ng/mL had better outcome.

Complications of Salvage Cryotherapy Series

Almost all patients following salvage cryotherapy will have some degree of lower urinary tract symptoms (LUTS) secondary to urethral slough, most of which will resolve in the first 6 months (Table 12.4). Urethral slough rates have been reduced from 40[61] to 5%[54,55] in many series since the introduction of urethral warming catheter, which protects urethral mucosa during cryotherapy. In contemporary salvage cryotherapy series, the urinary incontinence rate has dropped

Table 12.3. Results of the salvage cryotherapy series

Series	Year	Number of patients	Follow-up (mean) months	Negative biopsy (%)	PSA failure (%)	Percentage of BDF survival (risk group)		
						Low	Intermediate	High
Pisters et al[59]	2008	279	21.6	67.4	ASTRO	58.9 all groups		
Ng et al[60]	2007	187	(39)	83.4	Nadir + 2	56 all groups		
Ismail et al[64]	2007	100	(33.5)	N/A	≥0.5	73	45	11
Robinson et al[67]	2006	46	24	N/A	≥0.3	48 at 2 years		
Lam et al[66]	2005	72	6	N/A	N/A	90 at 6 months		
Bahn et al[56]	2003	59	(72.5)	100	≥0.5	61	62	50
Ghafar et al[35]	2001	38	20.7	N/A	>0.3 above nadir	74 at 2 years		
Chin et al[54]	2001	118	(18.6)	94	>0.5	34 all groups		
de la Taille et al[55]	2000	43	(21.9)	63(5/8)	<0.1	66 at 1 year		
Pisters et al[58]	1997	150	(13.5)	77 (85/110)	≥0.2 above nadir	58		
Bales et al[61]	1995	23	12–23	59 (13/22)	<0.3	14 at 1 year		

Table 12.4 Complication associated with salvage cryotherapy

Series	Impotence (%)	Incontinence (%)	Recto-urethral fistula (%)	Urethral slough (%)	Pain (%)	Stricture/retention (%)
Pisters et al[59]	69.2	4.4	1.2	3.2	N/A	6.8
Ng et al[60]	N/A	3 (severe)	2		14	21
Ismail et al[64]	86	6 (severe)	1	16	4	2
Robinson et al[67]	56	29 (moderate to severe)	2 (early series)	24 (early series)	16	6 (early series)
Lam et al[66]	83.3	17.5	0	N/A	5	9
Bahn et al[56]	N/A	8	3.4	N/A	N/A	N/A
Ghafar et al[35]	N/A	7.9	0	0	39.5	0
Chin et al[54]		6.7	3.3	5.1		8.5
de la Taille et al[55]	N/A	9	0	N/A	26	5
Pisters et al[58]	72	73	1	22	8	67
Bales et al[61]	100	95.5	N/A	N/A	N/A	40.9

dramatically with recent studies reporting incontinence rates of 3–6%.[45–62] Although urethral warming has been successful in reducing urinary morbidity, it may compromise cancer control by protecting a rim of prostatic tissue around the urethra from freezing.[63]

Erectile dysfunction is the most frequently occurring complication following prostate cryotherapy,[47,64] primarily due to the ice ball extending into the neurovascular bundles when attempting to completely eradicate the tumor. The impotence rate in salvage cases range from 56 to 100%. In salvage cryotherapy most patients suffer from a degree of erectile dysfunction owing to previous hormone therapy and pelvic irradiation.[65]

The most serious complication of salvage cryotherapy is the development of recto-urethral fistula. New treatment advances and better control of the procedure have significantly reduced this complication to <4% in salvage cases.[54,66]

Areas for Potential Advances in the Management of Organ Confined Prostate Cancer Using Cryotherapy

Focal Nerve Sparing Cryotherapy

In prostate cryotherapy, the whole prostate gland is frozen including the periprostatic tissue with neurovascular bundles to eradicate all tumor cells. As a result, the incidence of erectile dysfunction is high. In an attempt to preserve potency, Onik et al[68] described focal nerve sparing prostate cryotherapy where they treated part of the prostate which contained the tumor. After a mean follow-up of 50 months, 95% of the treated patients had stable PSA and 80% maintained their potency. In a different approach, the neurovascular bundle was successfully preserved by active warming, but this resulted in an incomplete ablation of prostate tissue.[69] Lambert et al[70] presented 28 months (range 9–72 months) follow-up of 25 patients treated with primary focal cryotherapy. Eighty-four percent of patients had not experienced biochemical failure and only 14% showed positive biopsy on the treated site. Potency was maintained in 71% and no patient reported any worsening LUTS or incontinence. Focal nerve sparing cryotherapy has not been applied in salvage treatment.

Laser-Assisted Cryotherapy (LAC)

LAC is a new technique that attempts to protect healthy tissue around the prostate without limiting the cryoablation of unwanted tissue. Laser radiation administered from the urethra into the prostate during freezing process maintains the temperature in the urethral wall and surrounding region above the damaging level, and at the same time lethal temperature is achieved in the surrounding prostate tissue. The margin of laser protected area increases with injecting light absorbing dye into the periurethral tissue.[71]

Rectal Wall Protection

The rate of recto-urethral fistula following prostate cryotherapy is low; however, this remains a potentially catastrophic complication. Avoiding excessive freezing at the posterior margin of the prostate protects the rectum from freezing

injury. Therefore, whole gland ablation which is necessary for complete eradication of prostate cancer will always be associated with the risk of fistula. Modifying the cryotherapy technique to achieve lethal temperature (<–40°C) posteriorly while avoiding potential rectal injury was attempted using different techniques. Cytron et al[72] inserted two cryotherapy needles into the Denonvellier's fascia for active warming using the thawing phase when the temperature drops below 0°C in the posterior prostate. This approach successfully maintained a PSA level of <0.5 ng/mL in 80.6% of the patients treated and no rectal injury was reported. Other studies have addressed this issue by manipulating the transrectal ultrasound probe to increase the distance between the rectal wall and the prostate. The mean distance was increased by 7.1 mm without impairing the ultrasound quality image.[73]

Adjuvant Treatment with Cryotherapy

There are limitations to the maximum improvement technical innovations in the delivery of cold to the prostate can achieve, given the close relationship between the critical structures that surround the prostate. Other options for improving outcomes include the application of treatments adjuvant to the application of cold.

Cryochemotherapy

Freezing results in necrotic cell death; 3mechanisms are responsible for this:[15]

(a) Extracellular ice crystal formation, which leads to cell hyperosmolarity and post hypertonic lysis
(b) Direct cell damage caused by intracellular ice crystal formation
(c) Vascular stasis and tissue ischemia

The use of anticancer drugs as sensitizing agents to enhance apoptotic cell death at the peripheral zone of the cryogenic lesion may improve the efficacy of cryotherapy. Clarke et al[74] demonstrated that the combination of cryotherapy and Tumor necrosis factor-Related Apoptosis-Inducing Ligand (TRAIL) resulted in enhanced prostate cancer cell death owing to apoptosis at −10°C. The same group demonstrated enhanced efficacy of cryotherapy when combined with sublethal concentration of 5-fluorouracil in vitro.[75]

Goel et al[76] investigated the ability of tumor necrosis factor alpha (TNF-α) to enhance cryoinjury in vivo. Temperature threshold for necrosis was increased with the addition of TNF-α prior to cryotherapy and the combined treatment resulted in growth delay of the tumor in the experimental animals which require further investigation.

Cryo-Immunotherapy

Systemic antitumor immune response has been postulated following prostate cryotherapy. Clinical case reports observed regression of metastatic disease and symptoms relief following prostate cryotherapy, which implies that a protective immune response may be induced.[77,78] The mechanism of such clinical observation was not clear. Local tumor destruction by cryotherapy results in the release of a large amount of cryonecrotic tissue and tumor antigens. This may enhance the uptake of these antigens by local dendritic cells and priming of naïve T cells in regional LNs resulting in tumor-specific immune response and tumor eradication.[79] The cryoimmune response has been studied in several animal models. Both immunostimulatory and immunoinhibitory effects have been reported.[80–83]

The precise mechanism of the immunostimulatory effect is not clear. Early cytokine-mediated response,[80,81] the involvement of T-cell immunity and enhanced natural killer (NK) cells cytotoxicity,[81,84] and the development of antitumor antibodies[85] have all been suggested as possible immune stimulations. Suppressed immunity and enhanced tumor growth and metastases have also been reported following cryotherapy.[82,83]

Conclusions

Prostate cryotherapy may be used to treat a variety of presentations including localized primary prostate cancer, locally advanced disease, and for salvage after failed radiotherapy. The most established of the three roles is currently in salvage treatment. The relative merits of primary treatment with cryotherapy for localized and locally advanced disease compared with other existing modalities have yet to be fully explored with comparative studies. Contemporary randomized trials would be useful in each of the disease subgroups. The possible cryoimmune effects of treatment require further investigation.

References

1. UK CR. *Prostate Cancer Incidence Statistics UK*. London: Cancer Research; 2007
2. Ahmed S. A history of cryosurgery. In: Mattelaer JJ, ed. *de Historia Urologiae Europaeae. Vol 13*. Belgium: Historical Committee EAU; 2006:145–155
3. Arnott J. Practical illustrations of the remidial efficacy of very low or anaesthetic temperature. I. In Cancer. *Lancet*. 1850;2:257–259
4. Cooper IS, Lee AS. Cryostatic congelation: a system for producing a limited, controlled region of cooling or freezing of biologic tissues. *J Nerv Ment Dis*. 1961;133:259–263
5. Gonder MJ, Soanes WA, Shulman S. Cryosurgical treatment of the prostate. *Invest Urol*. 1966;3(4):372–378

6. Onik GM, Cohen JK, Reyes GD, Rubinsky B, Chang Z, Baust J. Transrectal ultrasound-guided percutaneous radical cryosurgical ablation of the prostate. *Cancer*. 1993;72(4):1291–1299
7. Lee F, Bahn DK, McHugh TA, Onik GM, Lee FT Jr. US-guided percutaneous cryoablation of prostate cancer. *Radiology*. 1994;192(3): 769–776
8. Cohen JK, Miller RJ, Shuman BA. Urethral warming catheter for use during cryoablation of the prostate. *Urology*. 1995;45(5):861–864
9. Larson TR, Rrobertson DW, Corica A, Bostwick DG. In vivo interstitial temperature mapping of the human prostate during cryosurgery with correlation to histopathologic outcomes. *Urology*. 2000; 55(4):547–552
10. Seifert JK, Gerharz CD, Mattes F, et al A pig model of hepatic cryotherapy. In vivo temperature distribution during freezing and histopathological changes. *Cryobiology*. 2003;47(3):214–226
11. Gage AA. History of cryosurgery. *Semin Surg Oncol*. 1998;14(2): 99–109
12. Whittaker DK. Mechanisms of tissue destruction following cryosurgery. *Ann R Coll Surg Engl*. 1984;66(5):313–318
13. Baust JG, Gage AA. Progress toward optimization of cryosurgery. *Technol.Cancer Res Treat*. 2004;3(2):95–101
14. Mazur P. Freezing of living cells: mechanisms and implications. *Am J Physiol*. 1984;247(3 pt 1):125–142
15. Bischof JC, Smith D, Pazhayannur PV, Manivel C, Hulbert J, Roberts KP. Cryosurgery of dunning AT-1 rat prostate tumor: thermal, biophysical, and viability response at the cellular and tissue level. *Cryobiology*. 1997;34(1):42–69
16. Hong JS, Rubinsky B. Patterns of ice formation in normal and malignant breast tissue. *Cryobiology*. 1994;42(1):59–68
17. Tatsutani K, Rubinsky B, Onik G, Dahiya R. Effect of thermal variables on frozen human primary prostatic adenocarcinoma cells. *Urology*. 1996;48(3):441–447
18. Cooper IS. Cryobiology as viewed by the surgeon. *Cryobiology*. 1964;51:44–51
19. Dow JA, Waterhouse K. An experimental study in lethal freezing temperatures of the prostate gland. *J Urol*. 1970;103(4):454–457
20. Klossner DP, Robilotto AT, Clarke DM, et al Cryosurgical technique: assessment of the fundamental variables using human prostate cancer model systems. *Cryobiology*. 2007;55(3):189–199
21. Gage AA, Baust J. Mechanisms of tissue injury in cryosurgery. *Cryobiology*. 1998;37(3):171–186
22. Baust JG, Gage AA. The molecular basis of cryosurgery. *BJU Int*. 2005;95(9):1187–1191
23. Poppendiek HF, Randall R, Breeden JA, Chambers JE, Murphy JR. Thermal conductivity measurements and predictions for biological fluids and tissues. *Cryobiology*. 1967;3(4):318–327
24. NICE. Interventional procedures overview of cryotherapy as a primary treatment for prostate cancer. London: National Institute of Clinical Excellence; 2005:1–15
25. Shelley M, Wilt TJ, Coles B, Mason MD. Cryotherapy for localised prostate cancer. *Cochrane Database Syst Rev*. 2007;(3):CD005010
26. Thompson I, Thrasher JB, Aus G, Burnett AL, Canby-Hagino ED, Cookson MS. Guideline for the management of clincially localised prostate cancer: 2007 update. *J Urol*. 2007;177:2106
27. Babaian RJ, Donnelly B, Bahn D, et al Best practice statement on cryosurgery for the treatment of localized prostate cancer. *J Urol*. 2008;180(5):1993–2004
28. Chin JL, Ng CK, Touma NJ, et al Randomized trial comparing cryoablation and external beam radiotherapy for T2C-T3B prostate cancer. *Prostate Cancer Prostatic Dis*. 2008;11(1):40–45
29. Vicini FA, Kestin LL, Martinez AA. Prostatectomy, external beam radiation therapy, or brachytherapy for localized prostate cancer. *JAMA*. 1999;281(17):1583–1584; discussion 1585–1586
30. Potters L, Klein EA, Kattan MW, et al Monotherapy for stage T1–T2 prostate cancer: radical prostatectomy, external beam radiotherapy, or permanent seed implantation. *Radiother Oncol*. 2004;71(1): 29–33
31. D'Amico AV, Crook J, Beard CJ, DeWeese TL, Hurwitz M, Kaplan I. In: Kavoussi LR, Novick AC, Partin AW, Peters CA, eds. *Campbell's Urology*. Philadelphia: Saunders; 2007:3014–3031
32. NICE. *Prostate Cancer: Diagnosis and Treatment*. Cardiff: Velindre NHS Trust, Cardiff, Wales; 2008
33. Thompson I, Thrasher JB, Aus G, et al Guideline for the management of clinically localized prostate cancer: 2007 update. *J Urol*. 2007;177(6):2106–2131
34. Partin AW, Kattan MW, Subong EN, et al Combination of prostate-specific antigen, clinical stage, and Gleason score to predict pathological stage of localized prostate cancer. A multi-institutional update. *JAMA*. 1997;277(18):1445–1451
35. Ghafar MA, Johnson CW, De La Taille A, et al Salvage cryotherapy using an argon based system for locally recurrent prostate cancer after radiation therapy: the Columbia experience. *J Urol*. 2001; 166(4):1333–1337; discussion 1337–1338
36. Katz AE, Ghafar MA. Selection of salvage cryotherapy patients. *Rev Urol*. 2002;4(suppl 2):S18–S23
37. Dudderidge T, Payne H, Emberton M. An algorithm for managing the failure of external beam radiotherapy in prostate cancer. *BJU Int*. 2007;100(3):518–527
38. Chan TY, Chan DY, Stutzman KL, Epstein JI. Does increased needle biopsy sampling of the prostate detect a higher number of potentially insignificant tumors? *J Urol*. 2001;166(6):2181–2184
39. Ahmed S, Lindsey B, Davies J. Salvage cryosurgery for locally recurrent prostate cancer following radiotherapy. *Prostate Cancer Prostatic Dis*. 2005;8(1):31–35.
40. Blasko JC, Grimm PD, Sylsvester JE, Cavanagh W. The role of external beam radiotherapy with I-125/Pd-103 brachytherapy for prostate carcinoma. *Radiother Oncol*. 2000;57(3):273–278
41. Cohen JK, Miller RJ Jr, Ahmed S, Lotz MJ, Baust J. Ten-year biochemical disease control for patients with prostate cancer treated with cryosurgery as primary therapy. *Urology*. 2008;71(3):515–518
42. Hubosky SG, Fabrizio MD, Schellhammer PF, Barone BB, Tepera CM, Given RW. Single center experience with third-generation cryosurgery for management of organ-confined prostate cancer: critical evaluation of short-term outcomes, complications, and patient quality of life. *J Endourol*. 2007;21(12):1521–1531
43. Long JP, Bahn D, Lee F, Shinohara K, Chinn DO, Macaluso JN Jr. Five-year retrospective, multi-institutional pooled analysis of cancer-related outcomes after cryosurgical ablation of the prostate. *Urology*. 2001;57(3):518–523
44. Bahn DK, Lee F, Badalament R, Kumar A, Greski J, Chernick M. Targeted cryoablation of the prostate: 7-year outcomes in the primary treatment of prostate cancer. *Urology*. 2002;60(2 suppl 1):3–11
45. Polascik TJ, Nosnik I, Mayes JM, Mouraviev V. Short-term cancer control after primary cryosurgical ablation for clinically localized prostate cancer using third-generation cryotechnology. *Urology*. 2007;70(1):117–121
46. Donnelly BJ, Saliken JC, Ernst DS, et al Prospective trial of cryosurgical ablation of the prostate: five-year results. *Urology*. 2002;60(4):645–649
47. El Hayek OR, Alfer W Jr, Reggio E, Pompeo AC, Arap S, Srougi M. Percutaneous prostate cryoablation as treatment for high-risk prostate cancer. *Clinics*. 2007;62(2):109–112
48. Prepelica KL, Okeke Z, Murphy A, Katz AE. Cryosurgical ablation of the prostate: high risk patient outcomes. *Cancer*. 2005;103(8): 1625–1630
49. Han KR, Cohen JK, Miller RJ, et al Treatment of organ confined prostate cancer with third generation cryosurgery: preliminary multicenter experience. *J Urol*. 2003;170(4 pt 1):1126–1130
50. Koppie TM, Shinohara K, Grossfeld GD, Presti JC Jr, Carroll PR. The efficacy of cryosurgical ablation of prostate cancer: the

University of California, San Francisco experience. *J Urol*. 1999; 162(2):427–432
51. Wong WS, Chinn DO, Chinn M, Chinn J, Tom WL. Cryosurgery as a treatment for prostate carcinoma: results and complications. *Cancer*. 1997;79(5):963–974
52. Shinohara K, Connolly JA, Presti JC Jr, Carroll PR. Cryosurgical treatment of localized prostate cancer (stages T1 to T4): preliminary results. *J Urol*. 1996;156(1):115–120; discussion 120–121
53. Miller RJ Jr, Cohen JK, Merlotti LA. Percutaneous transperineal cryosurgical ablation of the prostate for the primary treatment of clinical stage C adenocarcinoma of the prostate. *Urology*. 1994; 44(2):170–174
54. Chin JL, Pautler SE, Mouraviev V, Touma N, Moore K, Downey DB. Results of salvage cryoablation of the prostate after radiation: identifying predictors of treatment failure and complications. *J Urol*. 2001;165(6 pt 1):1937–1941; discussion 1941–1942
55. de la Taille A, Hayek O, Benson MC, et al Salvage cryotherapy for recurrent prostate cancer after radiation therapy: the Columbia experience. *Urology*. 2000;55(1):79–84
56. Bahn DK, Lee F, Silverman P, et al Salvage cryosurgery for recurrent prostate cancer after radiation therapy: a seven-year follow-up. *Clin Prostate Cancer*. 2003;2(2):111–114
57. Connolly JA, Shinohara K, Carroll PR. Cryosurgery for locally advanced (T3) prostate cancer. *Semin Urol Oncol*. 1997;15(4): 244–249
58. Pisters LL, von Eschenbach AC, Scott SM, et al The efficacy and complications of salvage cryotherapy of the prostate. *J Urol*. 1997;157(3):921–925
59. Pisters LL, Rewcastle JC, Donnelly BJ, Lugnani FM, Katz AE, Jones JS. Salvage prostate cryoablation: initial results from the cryo on-line data registry. *J Urol*. 2008;180(2):559–563; discussion 563–564
60. Ng CK, Moussa M, Downey DB, Chin JL. Salvage cryoablation of the prostate: followup and analysis of predictive factors for outcome. *J Urol*. 2007;178(4 pt 1):1253–1257; discussion 1257
61. Bales GT, Williams MJ, Sinner M, Thisted RA, Chodak GW. Short-term outcomes after cryosurgical ablation of the prostate in men with recurrent prostate carcinoma following radiation therapy. *Urology*. 1995;46(5):676–680
62. Pisters LL. Treatment failure after primary and salvage therapy for prostate cancer. *Cancer*. 2008;112(2):225–227
63. Gould RS. Total cryosurgery of the prostate versus standard cryosurgery versus radical prostatectomy: comparison of early results and the role of transurethral resection in cryosurgery. *J Urol*. 1999;162(5):1653–1657
64. Ismail M, Ahmed S, Kastner C, Davies J. Salvage cryotherapy for recurrent prostate cancer after radiation failure: a prospective case series of the first 100 patients. *BJU Int*. 2007;100(4): 760–764
65. Perrotte P, Litwin MS, McGuire EJ, Scott SM, von Eschenbach AC, Pisters LL. Quality of life after salvage cryotherapy: the impact of treatment parameters. *J Urol*. 1999;162(2):398–402
66. Lam JS. Salvage cryosurgical ablation for radiorecurrent prostate cancer using third generation cryoneedles: the University of California-Los Angeles experience. *J Urol*. 2005;173:181
67. Robinson JW, Donnelly BJ, Coupland K, et al Quality of life 2 years after salvage cryosurgery for the treatment of local recurrence of prostate cancer after radiotherapy. *Urol Oncol*. 2006;24(6): 472–486
68. Onik G. Rationale for a "male lumpectomy," a prostate cancer targeted approach using cryoablation: results in 21 patients with at least 2 years of follow-up. *Cardiovasc Intervent Radiol*. 2008;31(1): 98–106
69. Janzen NK, Han KR, Perry KT, Said JW, Schulam PG, Belldegrun AS. Feasibility of nerve-sparing prostate cryosurgery: applications and limitations in a canine model. *J Endourol*. 2005;19(4):520–525
70. Lambert EH, Bolte K, Masson P, Katz AE. Focal cryosurgery: encouraging health outcomes for unifocal prostate cancer. *Urology*. 2007;69(6):1117–1120
71. Romero-Mendez R, Franco W, Aguilar G. Laser-assisted cryosurgery of prostate: numerical study. *Phys Med Biol*. 2007;52(2):463–478
72. Cytron S, Paz A, Kravchick S, Shumalinski D, Moore J. Active rectal wall protection using direct transperineal cryo-needles for histologically proven prostate adenocarcinomas. *Eur Urol*. 2003; 44(3):315–320; discussion 320–321
73. Jones JS. Ultrasound probe positioning to minimize the risk of recto-urethral fistula during cryosurgical ablation of prostate cancer. *BJU Int*. 2007;100(1):58–62; discussion 62
74. Clarke DM, Robilotto AT, VanBuskirk RG, Baust JG, Gage AA, Baust JM. Targeted induction of apoptosis via TRAIL and cryoablation: a novel strategy for the treatment of prostate cancer. *Prostate Cancer Prostatic Dis*. 2007;10(2):175–184
75. Clarke DM, Baust JM, Van Buskirk RG, Baust JG. Addition of anticancer agents enhances freezing-induced prostate cancer cell death: implications of mitochondrial involvement. *Cryobiology*. 2004; 49(1):45–61
76. Goel R, Swanlund D, Coad J, Paciotti GF, Bischof JC. TNF-alpha-based accentuation in cryoinjury-dose, delivery, and response. *Mol Cancer Ther*. 2007;6(7):2039–2047
77. Gursel E, Roberts M, Veenema RJ. Regression of prostatic cancer following sequential cryotherapy to the prostate. *J Urol*. 1972;108(6): 928–932
78. Soanes WA, Ablin RJ, Gonder MJ. Remission of metastatic lesions following cryosurgery in prostatic cancer: immunologic considerations. *J Urol*. 1970;104(1):154–159
79. den Brok MH, Sutmuller RP, van der Voort R, et al In situ tumor ablation creates an antigen source for the generation of antitumor immunity. *Cancer Res*. 2004;64(11):4024–4029
80. Joosten JJ, Muijen GN, Wobbes T, Ruers TJ. In vivo destruction of tumor tissue by cryoablation can induce inhibition of secondary tumor growth: an experimental study. *Cryobiology*. 2001;42(1):49–58
81. Sabel MS, Nehs MA, Su G, Lowler KP, Ferrara JL, Chang AE. Immunologic response to cryoablation of breast cancer. *Breast Cancer Res Treat*. 2005;90(1):97–104
82. Friedman EJ, Orth CR, Brewton KA, Ponniah S, Alexander RB. Cryosurgical ablation of the normal ventral prostate plus adjuvant does not protect Copenhagen rats from Dunning prostatic adenocarcinoma challenge. *J Urol*. 1997;158(4):1585–1588
83. Hoffmann NE, Coad JE, Huot CS, Swanlund DJ, Bischof JC. Investigation of the mechanism and the effect of cryoimmunology in the Copenhagen rat. *Cryobiology*. 2001;42(1):59–68
84. Hayakawa K, Yamashita T, Suzuki K, et al Comparative immunological studies in rats following cryosurgery and surgical excision of 3-methylcholanthrene-induced primary autochthonous tumors. *Gann*. 1982;73(3):462–469
85. Moore FT, Blackwood J, Sazenbacher L, Pace WG. Cryotherapy for malignant tumors. Immunologic response. *Arch Surg*. 1968;96(4): 527–529

Prostate Focal Therapy

13

Frédéric Pouliot, Jeffrey C. LaRochelle, Thomas J. Polascik, and Arie S. Belldegrun

Introduction

Rationale of Focal Therapies

Treatment decisions regarding prostate cancer (PCa) are difficult because of the protracted course of the disease and the morbidity associated with treatment.[1] With the increased incidence of localized prostate cancers at diagnosis, new treatment modalities have been developed to decrease morbidity without affecting oncologic results. Though cancers are multifocal in the majority of cases, approximately 20% are unifocal. This affords the opportunity for the application of treatment targeted to a solitary focus of cancer, which would potentially decrease morbidity associated with whole gland treatment.

Natural Evolution of Localized Prostate Cancer on Watchful Waiting

The importance of treating localized prostate cancer has been demonstrated by the prospective, randomized Scandinavian study that compared active surveillance to radical prostatectomy (RP). This study has shown that RP increases both prostate cancer-specific and overall survival after a median follow-up of 10.8 years.[1] Evolution of the disease was slow for the first 10 years of follow-up, after which they observed a difference in overall survival between the two groups.[1] Interestingly, a difference in overall survival was seen only in patients less than 65 years old, a category of patients for which erectile function is often of prime importance. In another study, Johansson et al showed that 16% (35/233) of patients diagnosed with cT0-T2 prostate cancers and followed by watchful waiting died of prostate cancer after a mean follow-up of 21 years.[2] Of the patients who died, 45 and 40% had localized and low-grade lesions, respectively. Finally, results from the Connecticut Tumor Registry,[3] which included 1,618 patients 75 years or younger who underwent surgery, external beam radiation therapy or initial observation for clinically localized prostate cancer demonstrated that at an average follow-up of 13.3 years, 13% of patients had died of PCa. Patients who elected observation had significantly worse cancer-specific survival than those who underwent elected surgery. Taken together, these three studies show that treatment can increase cancer-specific and overall survival and that localized disease can lead to death after more than 15 years. It also suggests that patients undergoing active surveillance may need effective definitive treatment if life expectancy is more than 15 years.

Definitions for Focal Therapy of the Prostate

The reports from the Consensus Conference on Focal Treatment of Prostatic Carcinoma defined focal therapy as an individualized treatment that selectively ablates known disease and preserves existing functions, with the overall objective of minimizing lifetime morbidity without compromising life expectancy.[4] Focal therapy can involve the local application of treatment to a specific focus, and the term "image-guided focal therapy" is used when it is done under real-time imaging.[5–7] Focal therapy have been further subdivided into hemiablation when treatment involves a complete lobe and subtotal ablation when both lobes are targeted with the exception of a rim of parenchyma close to the neurovascular bundle(s).[8–13] Others have used the term "conformal cryoablation" to define bilateral ablation with preservation ablation of one neurovascular bundle on the unaffected side.[6]

Indications for Focal Therapies

There are currently no widely accepted indications for focal therapy for prostate cancer. Selection of patients should be based on their preoperative risk for extraprostatic and bilateral disease. Recently, a group termed the International Task Force on Prostate Cancer and the Focal Lesion Paradigm has published its recommendations for clinical use of focal ablation therapies. These are summarized in Table 13.1.[8]

P. Dasgupta et al. (eds.), *New Technologies in Urology,*
DOI: 10.1007/978-1-84882-178-1_13, © Springer-Verlag London Limited 2010

Table 13.1 Proposed clinical, biopsy, and imaging criteria for focal therapy patient selection[a]

Clinical
Clinical stage T1 or T2a
PSA less than 10 ng/mL
PSA density less than 0.15 ng/ml/g of prostate
PSA velocity less than 2 ng/mL yearly in the year prior to diagnosis
Biopsy
Minimum of 12 cores
No Gleason grade 4 or 5
Maximum percentage of cancer in each core (e.g., 20%)
Maximum length of cancer in each core (e.g., 7 mm)
Maximum percentage of total cores with cancer (e.g., 33%).
Imaging
Single lesion with a maximum size (e.g., 12 mm)
Maximum length of capsular contact (e.g., 10 mm)
No evidence of extraprostatic extension or seminal vesicle invasion

[a]This article was published in Eggener et al[8], Copyright Elsevier 2007

Table 13.2 Important questions to answer when considering focal ablation therapy

Questions	Answers (%)
What is the prevalence of unilateral prostate cancer in low-risk disease?	20[11,14,15a]
What is the prevalence of prostate cancers with adverse features[b] on the controlateral side when TRUS-biopsy show unilateral prostate cancer?	20[16a]
What is the PPV of TRUS biopsies to detect unilateral prostate cancer?	6-core biopsy: 27[17a] 10–12 core biopsy: 46–67[6,18 a, c] 3D-template biopsy: 80[d]
What is the PPV of repeated TRUS biopsies to detect unilateral prostate cancer after a first set of unilateral TRUS biopsies?	53[6c]

[a]Relative to pathology on radical prostatectomy specimens
[b]Adverse features are defined as tumor volume >0.5 cm^3, positive margins, extraprostatic extension, and Gleason score >6
[c]Relative to pathology on 3D template biopsies
[d]Seventy-six percent sensitivity for unilateral cancer, based on ex vivo simulation.[19] PPV is a personal communication from Werahera based on the data from his paper

These recommendations are guidelines, but data are currently lacking to encourage widespread use of these therapies. Assuming that the targeted focus of prostate cancer is completely ablated by focal therapy, the main challenge in the establishment of indications for focal therapies is to accurately select patients with localized, unifocal prostate cancer and for which the treatment would improve the overall survival. Therefore, the success of focal therapy does not rely solely on the ability of the therapy to eradicate cancerous prostate tissue but also on the accuracy of the clinical predictive models, biopsy, and imaging techniques to identify a unilateral and localized prostate cancer.

Clinical Staging of Prostate Cancer

When considering focal ablative therapy for prostate cancer, some questions exist regarding prostate cancer biology and the ability to characterize it accurately. These questions are summarized in Table 13.2, with the applicable studies described in the subsequent text.

Prevalence of Unilateral Prostate Cancer

Many studies have looked at the prevalence of unifocal prostate cancer on RP specimens. Mouraviev et al analyzed paraffin-embedded RP specimens from patients with clinically localized PCa with low-risk features.[14] Pathologic assessment of 1,184 specimen paid particular attention to laterality. Completely unilateral cancers were identified in 227 (19.2%) patients. Similar results were obtained by Iczkowski et al when they analyzed a series of 393 perineal RP specimens and observed that prostate cancers were unifocal in 23%, unilateral in 23%, and organ-confined in 89%.[15] Ohori et al analyzed 1,000 RP specimens from early stage PCa patients finding a similar frequency of unilateral lesions in 18%.[20] The index lesion represented an average of 80% of the total cancer volume. In those with extracapsular extension (ECE), the largest focus of cancer was responsible in 90%. This raises the question as to whether therapy should be extended beyond the prostatic capsule to eradicate potentially extraprostatic disease.

Rukstalis et al presented a retrospective analysis of 112 nonselected consecutive RP specimens.[11] They observed that 21% of patients had unifocal prostate cancer, with a median number of two foci for multifocal prostate cancers. They hypothesized the effect of focal targeted therapy assuming that the largest tumor would be the one targeted. By limiting treatment to 3, 6, or 9 out of 12 prostate zones (thereby sparing the contralateral neurovascular bundle), cancer control could be accomplished with a 37, 34, and 21% risk of significant (i.e., >0.5 mL) residual disease, respectively. Importantly, they did not consider other parameters such as PSA, clinical staging, and extent of biopsy to select their patients. Since some cancers had a Gleason score of 8 or a PSA above 100, the postulated efficacy of focal therapy might have been increased if more stringent preoperative criteria had been chosen. However, despite these limitations, this concept

serves as a basis for the clinical implementation of subtotal glandular therapy.

Adverse Contralateral Pathological Features in Low-Risk Patients with Unilateral Disease at Biopsy

In a study from John Hopkins, Yoon et al reviewed the prostatectomy specimens for which the preoperative biopsy predicted limited disease (Gleason score 6 or less, less than three positive core, less than 50% of cancer in any core).[16] Sixty-five percent had cancers present on the contralateral side with an average volume of 0.2 cm^3 per nodule. Thirteen percent had a significant tumor (>0.5 cm^3) contralateral to the index tumor, half of them located in the transition zone. At RP, 20% of the patients had an adverse pathological feature on the contralateral side of the biopsy, described as tumor volume >0.5 cm^3, positive margins, extraprostatic extension, or Gleason score >6. However, one limitation of that study is that there was no detail about the number of biopsy cores obtained preoperatively.

Determination of Unilateral Disease by Image-Guided Biopsy of Early Stage PCa

Owing to the present inability to reliably image PCa, clinicians rely mainly on information obtained by extended prostate biopsy. Iczkowski et al reviewed a series of 393 RPs and compared the results to preoperative biopsies.[15] Patients had a mean of 11 core biopsies preoperatively. Unilateral prostate cancer at biopsy and at RP were 62 and 23%, respectively, for a correlation of 0.7. Unilateral prostate cancers at prostatectomy were predicted preoperatively by unilaterality and unifocality at biopsy with odd ratios of 2.6 and 4.3, respectively. Unilaterality at biopsy could better predict unilaterality at prostatectomy when 9-core or more biopsies were obtained. This is in agreement with the results of Mayes et al who reported that 73% of unilateral prostate cancers after six core transrectal ultrasonography (TRUS) biopsies were bilateral at prostatectomy, demonstrating the importance of adequate prostate sampling before treatment decision.[17] In another study, Bulbul et al showed that when 12-core biopsies showed unilateral PCa, pathology after RP showed unilateral disease in 67% of cases.[18]

Ability of Repeat TRUS-Guided Biopsy to Detect Unilateral Disease

Barzell et al used template-guided transperineal, 3D mapping to identify clinically significant PCa prior to recommending treatment.[6] These authors performed an average of 1.88 biopsies per cm^3 of prostate in patients who had unilateral PCa on TRUS-guided biopsy. The average and median numbers of cores obtained on initial biopsy were 11 and 12, respectively. After template-guided transperineal biopsies, 46% redemonstrated unilateral disease.[6]

Ability of 3D-Template Biopsy to Detect Unilateral Disease

Crawford et al simulated a template saturation biopsy (TSB) protocol on 86 prostates with carcinoma after autopsy.[19] They applied a protocol where biopsies were taken at each 5 or 10 mm. The 5 mm protocol was more precise that the 10 mm protocol, but necessitated a mean of 54 biopsies per prostate. Using the 5 mm protocol, they could detect unilateral cancers with a sensitivity of 76%. The positive predictive value of TSB for unilateral prostate cancer was 80% (Werahera, personal communication). Moreover, the sensitivity of TSB for clinically significant cancers was 95% (defined as ≥0.5 cm^3, or Gleason >6) and Gleason patterns 4 or 5 were detected in all ten tumors where they were present. These results suggest that TSB might have a role in the evaluation of patients before focal therapy of the prostate.

Taken together, these data show that before considering focal ablation therapy:

1. At least 12 or more cores should be obtained at TRUS biopsy and should include some additional biopsies in the transition zone.
2. The positive predictive value of standard repeat TRUS biopsy for unilateral disease may be, at the best, 46%.
3. Twenty percent of prostate cancers on TRUS have adverse pathologic features on the contralateral side at prostatectomy.
4. Better sampling using template-guided transperineal, 3D pathologic mapping to identify clinically significant PCa might be useful after initial biopsy to recommend treatment.

Imaging

MRI

At this time, there is no imaging modality that can determine the exact localization of small volume PCa.[21] Some investigators have conducted correlation studies between radiographic images and whole-mount RP pathology slides.[21–23] Villers et al evaluated suspicious areas within the prostate by pelvic phased array dynamic contrast-enhanced magnetic resonance imaging (MRI) for predicting the intraprostatic location and volume of clinically localized PCa in 24

patients.[22] Sensitivity, specificity, and positive and negative predictive values for small PCa lesions in the transition or peripheral zones were 90, 88, 77, and 95%, respectively, for foci greater than 0.5 cc. However, in another study by Nakashima et al, endorectal MRI correlated with histological examination for tumors only larger than 1.0 cm in diameter in 95 patients.[23] The ability of endorectal MRI for detecting tumors less than 1.0 cm regarding accuracy, sensitivity, and positive predictive value were 24, 26, and 76%, respectively.

Contrast-Enhanced Doppler Ultrasound

Prostate cancer is more vascularized than normal prostate tissue.[24] This characteristic served as a basis to study contrast-enhanced Doppler ultrasound (CEDUS) to detect prostate cancer. Ultrasound contrast agents consist of small encapsulated gas bubbles that are administered intravenously and remain intravascular. These microbubbles are detected in the bloodstream and increasethe sensitivity of color (CD) and power Doppler (PD) imaging. The role of CEDUS has been recently reviewed by Wink et al[25]. Using, CEDUS, Goossen et al were able to lateralize the tumor in 78% of cases.[26] A large patient group was evaluated with CEDUS before RP and 68–79% of all tumor foci larger than 5 mm were detected. Unal et al showed that sensitivity and specificity of the CEDUS were 87% (26/30) and 79% (23/29), respectively, for the expert observer.[27] When combined with PSA, the sensitivity was still 87% but the specificity increased to 100%. Mitterberger et al showed that CEDUS-targeted biopsy detected more cancers than random biopsies with a reduced number of biopsy cores, and it detected cancers with higher Gleason scores and more cancers than random biopsy.[28,29] Therefore, CEDUS could be a useful tool to use in the context of focal therapy to localize the tumor side, increase sensitivity of TRUS biopsies, and image the tumor during treatment.

Focal Therapies for PCa

As stated previously, focal therapy for prostate cancer implies any treatment that can target a focus of cancer within the prostate gland. Treatment may freeze (cryotherapy), heat (thermoablation), or irradiate (radiosurgery) the focus of cancer. Focal therapy for prostate cancer can be divided into clinically tested and experimental technologies. The first category implies that the efficacy of the technology has been tested by posttherapy biopsies and evaluated clinically for side effects on continence and erectile functions. The experimental technologies are those for which the physical principles have shown efficacy in ablating tumors in patients, but for which follow-up with posttreatment biopsies and assessment of side effects are missing. Only cryotherapy falls in the first category of technologies while experimental technologies include high intensity focal ultrasound (HIFU), vascular targeted photodynamic therapy (VTP), radiosurgery, focal brachytherapy, and Interstitial Laser Thermoablation.

Cryotherapy

Cryobiology

The main mechanism of cytotoxicity of cryotherapy is coagulative necrosis. Cryotherapy induces cell injury by four main mechanisms: osmotic shock, mechanical injury, cell hypoxia, and induction of immune response. Molecular mechanisms of action include protein denaturation, cell membrane rupture, accumulation of a toxic concentration of cellular elements, vascular thrombosis, and apoptosis,[30] which can be divided into direct and indirect mechanisms. Direct mechanisms occur in successive steps that occur when tissue is cooling or thawing.[31] First, when interstitial fluid reach 0°C, crystallization begins and osmotic pressure in the nonfrozen interstitial fluid increases. This causes a shift of fluid from intracellular to extracellular compartments and subsequently cell constituent changes. When temperature reaches −15°C, all extracellular fluid is frozen, which leads to mechanical shearing forces on the cellular membranes. At these steps, many cells are threatened but most cell death occurs when intracellular ice is formed. Intracellular crystal formation is most likely to occur when rapid cooling temperature is used since it does not allow water to exit cells before freezing. A temperature of less than −40°C is required for homogenous intracellular ice crystal formation.[31] During thawing, when tissue is around −20 to 25°C, a process called recrystallization occurs, which further damages the cells by creating large crystals. This process results from the fusion of crystals during warming of ice. Other direct injuries to cells are caused by the movement of hypotonic extracellular fluid created by thawing that reenters the cells, causing cell swelling, membrane disruption, and death.

Indirect injuries to tissue by cryotherapy mainly involve vascular changes. Vascular changes are thought to be the main mechanism of cell death in cryotherapy. It occurs around −20°C and involves vasoconstriction, platelet occlusion, and microthrombi formation, which lead to cellular hypoxia and death. Technical aspects, such as the number of freeze–thaw cycles, temperatures reached, velocity of freezing and thawing, duration of freezing, and the presence of heat sinks affect the cytoxicity of cryotherapy.

Techniques for Cryotherapy

Cryosurgical ablation of prostatic tissue is performed using a system of cryoprobes that are inserted into the prostate under TRUS guidance. Measurements of the prostate, particularly length, are taken to ensure that the entire length of the prostate is treated. Wider prostates can be treated with the use of additional probes. Longer prostates, at least until recently, were treated by moving the probes apically after treating the base and mid-gland. However, newer probes are able to produce longer zones of freezing that eliminate the need for a "pull-back."

Probes are placed into the prostate with or without the use of a template grid. Position is checked in both the transverse and longitudinal planes. The tips of the cryoprobes should extend to the capsule at the base of the bladder. Temperature probes are placed at the prostatic apex, external sphincter, Denonvillier's fascia, rectal wall, and adjacent to the neurovascular bundles. A recent breakthrough in cryotherapy has come with the development of third-generation cryotechnology, such as the IceRod™ (Oncura, Amersham) 17-gauge cryoneedle with an advanced heat exchanger and the Multitemp™ 1601 temperature monitoring system (TMS, InvivoSense, Trondheim, Norway). It facilitates a potentially more safe and targeted treatment technique.[9] Probes can be selected based on the size of the iceball desired, and the temperature probes have an ability to give multiple temperature readings at various positions along their length.

Once an adequate number of probes have been placed, the bladder and urethra are inspected by performing a flexible cystoscopy to ensure no probes traverse them, which is a function of the width of the iceball that is produced by the probes being used. A urethral warming catheter is placed, and the freezing cycle is started. Progression of the iceball is monitored visually by TRUS and by the temperature readings. Frozen tissue does not transmit US, so it appears entirely anechoic. For this reason, freezing is initiated anteriorly. Starting posteriorly would prevent visual monitoring of anterior ice formation. Once −40°C is reached in the desired tissue and it is entirely encompassed by ice for a brief period, thawing is initiated. A second freezing cycle is performed once the tissue has thawed. It is important to make sure that the ice extends slightly beyond the tissue being ablated, as the lethal zone lies just inside the edge of the iceball. Great care is also taken to not freeze the wall of the rectum or external sphincter. Visualizing the progression of the ice and watching the temperatures make avoiding any injury to these structures straightforward.

Unilateral and Focal Cryotherapy: Oncological Results

Hemiablation

Table 13.3 summarizes the first pilot clinical trials of focal hemiablation for unilateral lesions and targeted cryoablation of a presumed unifocal lesion. Lambert et al reported data on patients treated with hemiablation.[32] The authors defined their biochemical failure as a PSA nadir greater than 50% of the pretreatment PSA level. Of the 25 patients, 21

Table 13.3 Cancer control and complication rates after focal and unilateral cryoablation

Reference	Number of patients	Number of Bx cores	Median follow-up (months)	CryoUnit	DFS[a] (%)	PSA cutoff	Bx-proven recurrence	Potency preserved
Unilateral cryoablation of unilateral lesions								
Lambert et al (3.5-year data)[32]	25	12	28	SeedNet[a]	84	<50% nadir, nadir +2	12% 8%untreated lobe, 4% treated lobe	71%
Bahn et al (5-years data)[b] [33]	31	6–12	70	Cryocare[c]	93	ASTRO[d]	4% untreated lobe	88.9% total, 48.1% fully recovered; 40.8% medically assisted
Focal cryoablation of unifocal lesion								
Onik et al (6-year data)[34]	21	7–8	50 (mean)	Cryocare	95	ASTRO	0 (in 1 case caner was found on MRIS in untreated lobe)	80%
Ellis e al[35]	60	ND[e]	12	Cryocare	80.5	ASTRO	23%[f]	70.6%

Bx biopsy; *bDFS* biochemical disease-free survival; *PSA* prostate specific survival; *MRIS* MRI spectroscopy

[a]SeedNet, Galil Medical, Plymouth, PA

[b]Results from a two center trial

[c]Cryocare Endocare, Irvine, CA

[d] Three consecutive rise in PSA

[e]Not determined

[f]Twenty-three percent for the whole series of 60 patients but only 35 patients were biopsied. Forty percent (14/35) of those biopsied had positive biopsy, 13/14th on the contralateral side of cryotherapy

(84%) demonstrated PSA failure-free survival over a median follow-up of 28 months. Repeat prostate biopsy revealed PCa in the contralateral lobe in 8% of patients and in the treated lobe in 4% (2 and 1 patients, respectively). Seventeen (71%) of 24 patients who were potent preoperatively remained so postoperatively. All patients preserved complete urinary continence.

Bahn et al reported the results of 31 patients from two institutions with clinically organ-confined, unilateral PCa confirmed by targeted and systematic biopsy using color Doppler TRUS-guidance.[33] Tumor control data at a mean follow-up of 70 months were excellent. Using the ASTRO definition of PSA recurrence (three consecutive rises in PSA), they reported biochemical disease-free survival (bDFS) in 92.8% of patients with a 96% negative-biopsy rate. The one patient with a positive biopsy in the apex of the contralateral untreated lobe was disease-free after retreatment with full-gland cryotherapy. The total potency-preservation rate was 88.9%. There were no cases of incontinence or other complications.

Focal Targeted Cryoablation

Onik recently published an updated series of 21 patients treated with targeted focal cryoablation of a unifocal tumor. Preoperatively, all patients had two series of prostate biopsies using color Doppler TRUS examination to identify and target any suspicious areas of abnormally increased flow or altered echogenicity.[7] All patients were potent preoperatively. Five patients had intermediate risk and five had high risk based on D'Amico criteria. At an average follow-up of 50 months, biochemical disease-free survival was obtained in 95% of patients by ASTRO definition. Nineteen patients had a prostate biopsy after 1 year, and no cancer was found in the treated or contralateral side. Potency was maintained in 80% with no complications reported. This series suggests the effectiveness of focal therapy when patients are accurately staged preoperatively using repeating TRUS biopsies and color doppler ultrasound.

High-Intensity Focal Ultrasound (HIFU)

HIFU Biology

Ultrasound is a high-frequency vibration produced by a transducer at a range higher than the ear can detect.[36] If the frequency of ultrasound is increased and focused on a precise point, it can lead to tissue destruction. HIFU destroys tissue by two mechanisms that lead to coagulation necrosis: thermal injury and cavitation. Thermal injuries occurs after the tissue absorbs the ultrasounds and converts it to heat. Temperature in the tissue on which HIFU is targeted can reach up to 100°C in a few seconds. The energy generated during HIFU therapy results in destruction of lipid-based membranes and protein degradation, which constitutes the main disruptive action on the tumor. The cavitation mechanism involves the formation of microbubbles in the targeted tissue. Collapse of these bubbles further destroys the tissue. This latter effect, which could be considered undesirable depending on whether one wants to achieve collateral damage to surrounding structures, may need to be minimized depending on the clinical situation.

HIFU Technique and Devices

Two types of devices are currently on the market: Ablatherm (EDAP TMS S.A., Vaulx-en-Velin, France) and the Sonablate (Focus Surgery, Inc, Indianapolis, IN). The Ablatherm device uses two different therapeutic (3 MHz) and imaging (7.5 MHz) transducers, while the Sonablate uses a single transducer (4 MHz) for both imaging and treatment.[36] Treatment is performed under gray-scale ultrasonography under a rectal cooling device, which prevents thermal rectal injuries.

HIFU as Focal Therapy

Given its ability to focally direct energy, HIFU can be potentially applied as focal therapy. Muto et al recently published a series of 29 patients with prostate cancer treated by focal HIFU using the Sonoblate 500 device.[37] Patient selection was based on TRUS biopsy showing unilateral disease. Posttreatment biopsies were positive in 23.5% (4/17) of patients in 1 year. Urethral stricture was reported in one case, and no change on IPSS was observed after therapy. No data were reported relative to erectile function. Further studies with better-defined preoperative criteria must be done to ascertain the efficacy of HIFU as a focal therapy.

Technologies in Development

Vascular Targeted Photodynamic Therapy

Biology of Vascular Targeted Photodynamic Therapy

VTP is based on the activation of a photosensitive drug that is toxic to cells when excited at a specific wavelength.[38] Neither light nor the photosensitive drug are toxic alone but, when combined, produce oxygen metabolites that cause apoptosis by targeting the mitochondria, lysosomes, and cell membranes. Vascular damage and immunologic stimulation are also secondary mechanisms.

Focal VTP

VTP may be suitable for minimally invasive outpatient procedure with reproducible cancer control and minimal side effects.[39] This novel therapy uses a new generation of an intravenously administered bacteriochlorophyl-derived photo sensitizer Tookad (WST09) that absorbs light in the visible-near-infra-red (VIS-NIR) wavelength with maximum light energy absorption at 763 nm.

A phase I/II non-randomized study at University College Hospital of London is enrolling men with previously untreated PCa in a focal therapy clinical trial. To date, a total of 27 men have been treated, 14 with a two-fiber VTP and 13 with a multifiber VTP. The interim results from this trial demonstrate a dose response that appears to correspond to an increase in the volume of hypoperfusion observed on post-treatment MRI with increasing total light energy delivered to the prostate.[39] Further development of this type of therapy also includes a search for other photosensitizing agents.

Radiotherapy

Traditionally, radiotherapy has been administrated as a whole gland therapy, and it is associated with side effects on surrounding organs. Its biology is well known and beyond the scope of this chapter. Development of new techniques such as conformal- and intensity modulated-radiotherapy allows radio-oncologists to target specific regions in the prostate. These techniques decrease irradiation of surrounding organs. Furthermore, development of real-time localization of the prostate during therapy has allowed better accuracy in prostate irradiation. The advances in conformal radiotherapy and imaging have led to the development of focal radiosurgery.

Radiosurgery

Radiosurgery is the application of high dose of radiation therapy directly to a tumor under precise imaging.[40] It has been studied mainly in the treatment of lung and brain tumors with successes over 80% for lung cancer. A study has recently started for localized prostate cancer using the Cyberknife (Accuray, Inc. Sunyvale, CA). The Cyberknife technology uses a robotic arm that is automatically repositioned to track the targeted tissue with a high level of accuracy. This technology could potentially be used to treat focal lesions.[41]

Brachytherapy

Brachytherapy has been used as a whole gland therapy for more than 15 years. It is recognized as an effective therapy for low to low-intermediate risk prostate cancer. With accurate localization of a focal lesion, radioactive seeds could be placed in and around the area of interest. A pilot study has been performed by D'Amico et al on nine patients with localized prostate cancer. No data have yet been reported regarding the oncological outcomes of this treatment.[42]

Interstitial Laser Thermotherapy

Biologic Effects of Interstitial Laser Thermotherapy

Interstitial laser thermotherapy use photothermal energy created by one or two sources placed in the vicinity of the tumor. This causes coagulation of the tissue in an ellipsoid form of 1.5 cm in length and 1cm in diameter.[43] This procedure takes 20–30 min and heats the tissue to 90ºC.

Focal Interstitial Laser Thermotherapy

A pilot study by Trachenberg has been done in five patients using focal interstitial laser thermotherapy. Follow-up biopsy was done at 6 months in two patients, and it showed absence of residual tumor in the treated area. However, one tumor was found on the contralateral side in one patient. After laparoscopic prostatectomy in this patient, no residual tumor was found in the treated region, demonstrating efficacy of the technique to eradicate tumor.[43]

Follow-Up After Prostate Focal Therapy

There is no established manner to follow a patient after focal therapy. Biopsy is probably the most accurate method to evaluate the efficacy of focal therapy in eliminating the cancer in the treated zone. Some studies have used systematized posttreatment biopsies to determine the success of therapy.[7,37] A problem with follow-up biopsy is the possible detection of nonsignificant cancers on the contralateral side, which might create anxiety for the patient. After such a diagnosis, should patients be placed on active surveillance? Should patients receive whole gland treatment? Obviously, there is no answer to this question, but when considering focal therapy we believe that this possibility should be discussed before intervention. On the basis of data from Yoon et al, the patient can be counseled that the risk of significant contralateral prostate cancer is about 20%.[16] The accuracy of the preoperative evaluation is important to decrease the chance of postoperative detection of contralateral lesions.

Some urologists have used PSA and the ASTRO criteria to evaluate recurrence.[7,32,33] Lambert also used a nadir of less

than 50% as a criterion of failure.[32] Others have used MRI to follow their patients and evaluate treatment efficacy.[34] The significance of these techniques regarding oncologic success is unknown.

Outcomes expected from focal ablative therapy for prostate cancer

Oncological outcomes with RP and radiotherapy for low-risk prostate cancer are excellent, but these oncologic outcomes might be due in part to the prolonged natural history of screening-detected prostate cancer.[44] Since currently the main indication for focal therapy is in localized low-risk prostate cancer, quality of life outcomes after RP, radiotherapy, and brachytherapy are very important aspects to be considered. For a focal therapy to be justified, it would have to demonstrate at least equivalent quality of life outcomes when compared with standard therapies, without compromising oncologic outcomes. Erectile dysfunction in previously potent men has been estimated to be around 36–83% after brachytherapy,[45,46] 39–53% after external beam radiotherapy,[47,48] and approximately 35% after bilateral nerve-sparing RP.[49,50] Incontinence after RP is approximately 5% at 1 year.[49] While 37% of patients have voiding symptoms during the first 60 days after brachytherapy, persistent urinary symptoms occur in 1–5% of patients.[51] Moderate to severe urinary symptoms are observed in 3–23% of patients after radiotherapy. Rectal complications are rare after RP but occur in 3–32% of patients after external radiotherapy. Rectal bleeding occurs in 1–4% after brachytherapy.[47] The term "trifecta" has been proposed as the perfect combination of three main outcomes: absence of PSA-recurrence, preservation of erectile function, and continence.[49] The "trifecta" is obtained in 62% of patients after RP. Before widespread adoption, focal therapy in prostate cancer should demonstrate the same or better "trifecta" rates than classic therapy for prostate cancer.

Conclusions

Focal ablation of the prostate is a new minimally invasive approach that is still experimental. Our conclusions based on the available published data are:

1. Low-risk patients should be those to whom this therapy should be offered.
2. Since success of this approach is based on adequate preoperative staging, diagnosis of unilateral prostate cancer should be based on 12-core biopsies with additional 6–12 core biopsies on the negative side. Since repeat negative biopsy does not guarantee absence of cancer on the contralateral side on follow-up biopsy, patients should be informed of the possibility of subsequent active surveillance or whole-gland treatment. The role of 3D-template saturation biopsies may significantly improve staging of patients prior to therapy.
3. Short-term outcomes should be assessed by posttreatment biopsy since the significance of outcomes based on PSA-values (Nadir, ASTRO criteria) or imaging are unknown.
4. Outcomes on erectile and urinary functions should be included in studies since preservation of these functions is the main goal of focal ablation of the prostate.

References

1. Bill-Axelson A, Holmberg L, Filen F, et al Radical prostatectomy versus watchful waiting in localized prostate cancer: the Scandinavian prostate cancer group-4 randomized trial. *J Natl Cancer Inst*. 2008;100(16):1144–1154
2. Johansson JE, Andren O, Andersson SO, et al Natural history of early, localized prostate cancer. *JAMA*. 2004;291(22):2713–2719
3. Albertsen PC, Hanley JA, Penson DF, Barrows G, Fine J. 13-year outcomes following treatment for clinically localized prostate cancer in a population based cohort. *J Urol*. 2007;177(3):932–936
4. Bostwick DG, Waters DJ, Farley ER, et al Group consensus reports from the consensus conference on focal treatment of prostatic carcinoma, celebration, Florida, February 24, 2006 *Urology*. 2007;70(6 suppl):42–44
5. Barqawi AB, Crawford ED. The current use and future trends of focal surgical therapy in the management of localized prostate cancer. *Cancer J*. 2007;13(5):313–317
6. Barzell WE, Melamed MR. Appropriate patient selection in the focal treatment of prostate cancer: the role of transperineal 3-dimensional pathologic mapping of the prostate – a 4-year experience. *Urology*. 2007;70(6 suppl):27–35
7. Onik G. The male lumpectomy: rationale for a cancer targeted approach for prostate cryoablation. A review. *Technol Cancer Res Treat*. 2004;3(4):365–370
8. Eggener SE, Scardino PT, Carroll PR, et al Focal therapy for localized prostate cancer: a critical appraisal of rationale and modalities. *J Urol*. 2007;178(6):2260–2267
9. Polascik TJ, Mouraviev V. Focal therapy for prostate cancer. *Curr Opin Urol*. 2008;18(3):269–274
10. Ahmed HU, Emberton M. Active surveillance and radical therapy in prostate cancer: can focal therapy offer the middle way? *World J Urol*. 2008;26:157–467
11. Rukstalis DB, Goldknopf JL, Crowley EM, Garcia FU. Prostate cryoablation: a scientific rationale for future modifications. *Urology*. 2002;60(2 suppl 1):19–25
12. Jones JS. Focal or subtotal therapy for early stage prostate cancer. *Curr Treat Options Oncol*. 2007;8(3):165–172
13. Mouraviev V, Polascik TJ. Update on cryotherapy for prostate cancer in 2006 *Curr Opin Urol*. 2006;16(3):152–156
14. Mouraviev V, Mayes JM, Madden JF, Sun L, Polascik TJ. Analysis of laterality and percentage of tumor involvement in 1386 prostatectomized specimens for selection of unilateral focal cryotherapy. *Technol Cancer Res Treat*. 2007;6(2):91–95
15. Iczkowski KA, Hossain D, Torkko KC, et al Preoperative prediction of unifocal, unilateral, margin-negative, and small volume prostate cancer. *Urology*. 2008;71(6):1166–1171

16. Yoon GS, Wang W, Osunkoya AO, Lane Z, Partin AW, Epstein JI. Residual tumor potentially left behind after local ablation therapy in prostate adenocarcinoma. *J Urol*. 2008;179(6):2203–2206; discussion 6
17. Mayes JM, Mouraviev V, Sun L, Madden JF, Polascik TJ. WITHDRAWN: can the conventional sextant prostate biopsy reliably diagnose unilateral prostate cancer in low-risk, localized, prostate cancer? *Prostate Cancer Prostatic Dis*. 2008
18. Bulbul MA, El-Hout Y, Haddad M, et al Pathological correlation between needle biopsy and radical prostatectomy specimen in patients with localized prostate cancer. *Can Urol Assoc J*. 2007; 1(3):264–266
19. Crawford ED, Wilson SS, Torkko KC, et al Clinical staging of prostate cancer: a computer-simulated study of transperineal prostate biopsy. *BJU Int*. 2005;96(7):999–1004
20. Ohori M, Eastham J, Koh H, et al Is focal therapy reasonable in patients with early stage prostate cancer (PCa): an analysis of radical prostatectomy (RP) specimens. *J Urol*. 2006;175(supplement):507
21. Ahmed HU, Calleary J, Arya M, Emberton M, Illing RO, Allen C. Re: dynamic contrast enhanced, pelvic phased array magnetic resonance imaging of localized prostate cancer for predicting tumor volume: correlation with radical prostatectomy findings. A. Villers, P. Puech, D. Mouton, X. Leroy, C. Ballereau and L. Lemaitre, J Urol. 2006; 176: 2432–2437 *J Urol*. 2007;177(6):2395; author reply 2395–2396
22. Villers A, Puech P, Mouton D, Leroy X, Ballereau C, Lemaitre L. Dynamic contrast enhanced, pelvic phased array magnetic resonance imaging of localized prostate cancer for predicting tumor volume: correlation with radical prostatectomy findings. *J Urol*. 2006;176(6 Pt 1):2432–2437
23. Nakashima J, Tanimoto A, Kikuchi E, et al Clinical implications of tumor size and local extent of primary prostatic lesions in prostate cancer patients with metastases: value of endorectal magnetic resonance imaging in patients with metastases. *Urology*. 2007;70(1): 86–90
24. Weidner N, Carroll PR, Flax J, Blumenfeld W, Folkman J. Tumor angiogenesis correlates with metastasis in invasive prostate carcinoma. *Am J Pathol*. 1993;143(2):401–409
25. Wink M, Frauscher F, Cosgrove D, et alContrast-enhanced ultrasound and prostate cancer; a multicentre european research coordination project. *Eur Urol*. 2008;54:982–992
26. Goossen TE, de la Rosette JJ, Hulsbergen-van de Kaa CA, van Leenders GJ, Wijkstra H. The value of dynamic contrast enhanced power Doppler ultrasound imaging in the localization of prostate cancer. *Eur Urol*. 2003;43(2):124–131
27. Unal D, Sedelaar JP, Aarnink RG, et al Three-dimensional contrast-enhanced power Doppler ultrasonography and conventional examination methods: the value of diagnostic predictors of prostate cancer. *BJU Int*. 2000;86(1):58–64
28. Mitterberger M, Pinggera GM, Horninger W, et al Comparison of contrast enhanced color Doppler targeted biopsy to conventional systematic biopsy: impact on Gleason score. *J Urol*. 2007;178(2): 464–468; discussion 468
29. Mitterberger M, Horninger W, Pelzer A, et al A prospective randomized trial comparing contrast-enhanced targeted versus systematic ultrasound guided biopsies: impact on prostate cancer detection. *Prostate*. 2007;67(14):1537–1542
30. Cooper IS, Hirose T. Application of cryogenic surgery to resection of parenchymal organs. *N Engl J Med*. 1966;274(1):15–18
31. Gage AA, Baust J. Mechanisms of tissue injury in cryosurgery. *Cryobiology*. 1998;37(3):171–186
32. Lambert EH, Bolte K, Masson P, Katz AE. Focal cryosurgery: encouraging health outcomes for unifocal prostate cancer. *Urology*. 2007;69(6):1117–1120
33. Bahn DK, Silverman P, Lee F Sr, Badalament R, Bahn ED, Rewcastle JC. Focal prostate cryoablation: initial results show cancer control and potency preservation. *J Endourol*. 2006;20(9): 688–692
34. Onik G, Vaughan D, Lotenfoe R, Dineen M, Brady J. The "male lumpectomy": focal therapy for prostate cancer using cryoablation results in 48 patients with at least 2-year follow-up. *Urol Oncol*. 2008;26(5):500–505
35. Ellis DS, Manny TB Jr, Rewcastle JC. Cryoablation as primary treatment for localized prostate cancer followed by penile rehabilitation. *Urology*. 2007;69(2):306–310
36. Murat FJ, Poissonnier L, Pasticier G, Gelet A. High-intensity focused ultrasound (HIFU) for prostate cancer. *Cancer Control*. 2007;14(3):244–249
37. Muto S, Yoshii T, Saito K, Kamiyama Y, Ide H, Horie S. Focal therapy with high-intensity-focused ultrasound in the treatment of localized prostate cancer. *Jpn J Clin Oncol*. 2008;38(3):192–199
38. Pinthus JH, Bogaards A, Weersink R, Wilson BC, Trachtenberg J. Photodynamic therapy for urological malignancies: past to current approaches. *J Urol*. 2006;175(4):1201–1207
39. Moore CM, Nathan TR, Lees WR, et al Photodynamic therapy using meso tetra hydroxy phenyl chlorin (mTHPC) in early prostate cancer. *Lasers Surg Med*. 2006;38(5):356–363
40. Timmerman RD, Kavanagh BD, Cho LC, Papiez L, Xing L. Stereotactic body radiation therapy in multiple organ sites. *J Clin Oncol*. 2007;25(8):947–952
41. Pawlicki T, Cotrutz C, King C. Prostate cancer therapy with stereotactic body radiation therapy. *Front Radiat Ther Oncol*. 2007;40:395–406
42. D'Amico AV, Cormack R, Tempany CM, et al Real-time magnetic resonance image-guided interstitial brachytherapy in the treatment of select patients with clinically localized prostate cancer. *Int J Radiat Oncol Biol Phys*. 1998;42(3):507–515
43. Trachtenberg J HM, Weersink R, et al Image guided laser thermotherapy for focal ablation of prostate cancer. In: *Abstracts of the Eighth Annual Meeting of the Society of Urologic Oncology*; 29 November–1 December 2007; Bethesda, Maryland: USA Urology Oncology: Extraordinary Opportunities for Discovery; 2007:96–97
44. D'Amico AV, Moul J, Carroll PR, Sun L, Lubeck D, Chen MH. Cancer-specific mortality after surgery or radiation for patients with clinically localized prostate cancer managed during the prostate-specific antigen era. *J Clin Oncol*. 2003;21(11):2163–2172
45. Cesaretti JA, Kao J, Stone NN, Stock RG. Effect of low dose-rate prostate brachytherapy on the sexual health of men with optimal sexual function before treatment: analysis at > or = 7 years of follow-up. *BJU Int*. 2007;100(2):362–367
46. Merrick GS, Butler WM, Wallner KE, et al Erectile function after prostate brachytherapy. *Int J Radiat Oncol Biol Phys*. 2005;62(2): 437–447
47. Zelefsky MJ, Wallner KE, Ling CC, et al Comparison of the 5-year outcome and morbidity of three-dimensional conformal radiotherapy versus transperineal permanent iodine-125 implantation for early-stage prostatic cancer. *J Clin Oncol*. 1999;17(2):517–522
48. Mantz CA, Nautiyal J, Awan A, et al Potency preservation following conformal radiotherapy for localized prostate cancer: impact of neoadjuvant androgen blockade, treatment technique, and patient-related factors. *Cancer J Sci Am*. 1999;5(4):230–236
49. Eastham JA, Scardino PT, Kattan MW. Predicting an optimal outcome after radical prostatectomy: the trifecta nomogram. *J Urol*. 2008;179(6):2207–2210; discussion 2210–2211
50. Carini M, Masieri L, Minervini A, Lapini A, Serni S. Oncological and functional results of antegrade radical retropubic prostatectomy for the treatment of clinically localised prostate cancer. *Eur Urol*. 2008;53(3):554–561
51. Gelblum DY, Potters L, Ashley R, Waldbaum R, Wang XH, Leibel S. Urinary morbidity following ultrasound-guided transperineal prostate seed implantation. *Int J Radiat Oncol Biol Phys*. 1999;45(1): 59–67

Radiofrequency Ablation

14

Chad R. Tracy and Jeffrey A. Cadeddu

Introduction

Increasing use of sonography, computed tomography (CT), and magnetic resonance imaging (MRI) has led to a rapid rise in the discovery of small renal tumors and an increase in the detection of renal cell cancer (RCC). Although these incidentally discovered masses tend to be smaller and of lower grade than symptomatic lesions,[1,2] the majority (65–80%) of these tumors are renal cell carcinomas (RCC) when pathologically analyzed.[3] In addition, nearly 60% of these lesions will exhibit growth during active surveillance (mean 0.26 cm/year), such that given a long life expectancy, lesions in younger patients may grow sufficiently to become symptomatic or to metastasize.[4]

Radical nephrectomy has traditionally been considered the "gold standard" for the treatment of renal masses. Nephron-sparing surgery, such as partial nephrectomy, was developed to preserve renal function in patients with bilateral renal masses, hereditary cancer syndromes, or renal insufficiency. With intermediate term and long-term cancer control rates similar to radical nephrectomy,[5,6] indications for partial nephrectomy have expanded to patients without imperative indications, and successful surgery is now only limited by technical factors such as proximity to the renal hilum or collecting system.[7,8]

Morbidity and prolonged convalescence of open surgery led to the development of laparoscopic partial nephrectomy. Though laparoscopic partial nephrectomy improves postoperative pain and is a viable option in some patients with small renal masses, the surgery is technically demanding and associated with complication rates similar to open partial nephrectomy.[9,10] Owing to these limitations and the increased detection of tumors in younger patients, there has been a recent push toward the development of minimally invasive therapies for renal tumors, including tissue ablative techniques.

In situ ablation methods such as radiofrequency ablation (RFA) and cryotherapy offer potential benefits when compared with the extirpative approach, including a decreased complication rate, shorter convalescence, absence of an ischemic period, and the possibility of using intravenous sedation over general anesthesia.[2,11] All of these potential benefits are clearly desirable in the increasingly older, sicker patients who represent an increasing proportion of patients with incidental renal masses. While these potential benefits make renal tumor ablation attractive for both patient and surgeon, successful cancer control and long-term outcomes of the therapy are required prior to broad adoption of these technologies.

In this chapter, we review the current status of RFA for treatment of the small renal mass including the mechanism of tissue destruction, technical considerations, anatomic considerations, surgical technique, postoperative follow-up, cancer control outcomes, and complications. Other ablative techniques are covered comprehensively by other authors within this text.

Mechanism of Radiofrequency Ablation

RFA uses monopolar alternating electric current that is delivered directly into the target tissue at a frequency of 450–1,200 kHz. This high-frequency current leads to vibration of ions within tissue as the current alternates polarity, resulting in molecular friction and heat production. Increasing temperature within the target tissue leads to cellular protein denaturation and cell membrane disintegration. Heat, therefore, is not directly supplied by the probe itself, but rather by the agitation of ions within the tissue.[12] As RFA is a temperature-based technology, heat distribution in the tissue surrounding the probe is affected by tissue impedance, native tissue temperature, thermal conductivity, and heat loss through blood circulation, with the temperature decreasing as the distance increases from the probe (temperature≈1/radius).[13,14]

The ability of RFA to ablate the target tissue relies on the power delivered to the probe as well as the maximum temperature obtained and the duration of the ablation. In in vitro studies using human prostate tissue, Bhowmick et al achieved irreversible cell injury when benign and malignant cell lines were heated to 45°C for 60 min, 55°C for 5 min, and 70°C for 1 min.[15,16] Histological analysis in these studies demonstrated coagulative necrosis, characterized by membrane disruption, protein denaturation, and vascular thrombosis.[17]

P. Dasgupta et al. (eds.), *New Technologies in Urology,*
DOI: 10.1007/978-1-84882-178-1_14, © Springer-Verlag London Limited 2010

Subsequent work in both human and animal models demonstrated that treated tissue is initially characterized by a well-circumscribed necrotic area with extensive cellular edema and localized tissue inflammation. After 3–7 days, the tissue begins to demonstrate the effects of coagulative necrosis with extensive nuclear degeneration and chronic inflammation. By day 30, there is a total loss of the cytoplasmic borders with no remaining normal renal architecture, and by day 90 there is a near total resorption of the necrotic focus with ultimate autoamputation.[18,19] Repeating these studies in renal cancer cell lines in the mouse model confirmed the effectiveness of ablation in both benign and malignant tissues.[20]

Technical Considerations

RFA can be performed with either a temperature-based or impedance-based system. Temperature-based systems work by measuring tissue temperatures at the tip of the electrode and are based on achieving a specific temperature for a given period of time. Though these systems accurately measure the temperature of the tissue at the electrode tip, they do not measure the temperature of the surrounding parenchyma. Alternatively, impedance-based systems measure the tissue impedance (resistance to alternating current) at the electrode tip and are based on achieving a predetermined impedance level that indicates complete tissue ablation. While these systems are able to measure the actual tissue desiccation at the electrode tip, they have been associated with incomplete ablation in animal models.[21]

Another major classification in RFA technology is the differentiation between dry and wet RFA. As tissue desiccation increases in the target lesion, the charring effect on tissue leads to increased impedance and resistance to the alternating current of the electrode, limiting the size of the ablation zone. Wet RFA probes deliver a constant saline infusion to mitigate the charring effect and premature rise in impedance. Although lesions tend to be larger using the wet electrode, there is less control of the exact size of ablation, which may lead to overtreatment of the target zone and disruption of adjacent normal parenchyma.[22]

There are several products currently approved for performing RFA.[23] Two of the RFA systems use Christmas tree or umbrella-shaped multitine electrodes. The RITA device (Aniodynamics, Queensbury, NY) uses thermistors embedded in five of the nine electrodes to modulate energy based on the temperature of each electrode as well as the average temperature of the electrodes in aggregate. The LeVeen system (Boston Scientific, Natick, MA) is an umbrella-shaped device that is based on tissue impedance rather than temperature. The Valleylab system (Mansfield, MA) uses an impedance-based system composed of a single 17-gauge (“cool tip”) electrode that is cooled internally with chilled saline to prevent charring of tissue adjacent to the probe. Although randomized human trials of various systems do not exist, a direct comparison of these systems in the porcine liver demonstrated larger zones of ablation with the wet-RFA and “cool tip” systems, more spherical ablation volumes with the 12-tinned electrodes, and better reproducibility with the 9-tine electrodes.[24]

Anatomic and Tumor Considerations

High blood flow volumes in the region of tissue ablation act as a “heat sink” for radiofrequency energy, such that target temperatures may not be obtained on a consistent basis when lesions are close to large vessels. This is a particularly relevant factor in renal malignancy as the kidney receives 20% of cardiac output and RCC is notoriously vascular. On the basis of this phenomenon, tumors that are closer to the renal hilum and segmental renal arteries can be difficult to treat as target temperatures may not be reached owing to countercurrent heat exchange. Temporary clamping of the renal hilum during RFA increases the size of the initial treatment lesion and shortens the time to reach the target temperature.[25] However, over time the size of the lesions appear to equilibrate, such that after 4 weeks there is no difference in the size of the treated area in patients who undergo clamping vs. those who do not. As such, hilar clamping is not currently recommended owing to the risk of arterial thrombosis and ischemia-reperfusion injury to normal parenchyma.

To prevent complications of hilar clamping, some authors have advocated selective arterial embolization when performing RFA. Hall et al reported an innovative combination of embolization with polyvinyl alcohol and percutaneous RFA in a 67-year-old patient with a 2.5 × 3.0 cm tumor in a solitary kidney.[26] A CT scan performed at 8 weeks post ablation showed a complete lack of contrast enhancement in the treated area. At 3 months post ablation, a biopsy revealed fibrous tissue and necrotic cellular debris with no evidence of malignancy. We have successfully employed this same technique in a few central or large (≥4 cm) tumors to reduce the circulatory heat sink.

Tumor location is the most important determinant for the choice of surgical approach. Injury to adjacent organs, including bowel, liver, spleen, and the renal collecting system, from high frequency energy, may lead to significant morbidity. To avoid these injuries, anterior tumors within 1 cm of colon or small bowel and those in close proximity to the liver, spleen, ureter, or renal pelvis should be managed with a laparoscopic approach (lap-RFA). Posterior or laterally-based tumors that are far removed from adjacent structures may be ablated percutaneously (perc RFA) under CT or MR guidance.[27]

Indications

Prospective clinical trials validating exact clinical indications for RFA of renal masses are lacking in the literature. Early studies of RFA included mostly patients who were determined to be poor surgical candidates owing to significant co-morbidities, had multiple bilateral tumors, or those with compromised renal function. As experience with RFA has increased and results have continued to appear promising, more treatments are being carried out on healthier patients with solitary small renal masses.

At our institution, candidates for RFA include patients with small solid renal masses (<4 cm) with contrast enhancement (≥10–12 Houndsfield Units) on CT or MRI. In addition, tumors must be located >0.5 cm from the ureteropelvic junction or renal pelvis and >1 cm from segmental renal vessels. RFA is offered as an alternative to open partial nephrectomy, laparoscopic partial nephrectomy, or laparoscopic radical nephrectomy in these patients.

Patients participate in a thorough discussion of the risks, benefits, and alternatives to RFA before consenting to this procedure. Specifically, patients are informed that while cancer control data are extremely encouraging for renal RFA, long-term follow-up to 5 years and beyond is just now becoming available.[28] Patients are also counseled about the risks of various complications and the expected convalescence period after ablation vs. laparoscopic or open partial nephrectomy.[29] Patients must agree to a strict protocol of radiographic follow-up, and understand that recurrence may require repeat RFA or even radical nephrectomy.

Percutaneous RFA

After induction of anesthesia, the patient is positioned on the CT table to perform the ablative procedure. Though most patients will be placed in the prone position for treatment of posteriorly located tumors, some patients may require variable positioning to best expose their tumor for placement of the percutaneous probe. For instance, a patient who has difficult access to the tumor due to the spleen lying within close proximity may be placed in the right lateral decubitus position over a small kidney cushion to role the spleen anteriorly and allow for direct percutaneous access. Once the positioning is felt to be appropriate, an initial CT scan is performed to observe whether there is a clear path to the kidney. If positioning appears appropriate and the patient's creatinine clearance permits, intravenous contrast is administered and the scan is repeated to further delineate the lesion.

Once the lesion location and a clear access path have been confirmed, a 20-Guage Chiba needle is directed such that the tip of the needle is located adjacent to the rim of the central portion of the tumor. Placement of this "finder needle" is important as it less traumatic than the ablative probe and limits bleeding as well as the risk of damage to the surrounding structures such as the bowel or pleura. The CT scan is repeated at that time and if positioning is correct, the ablative probe is advanced to the rim of the tumor and the tines are deployed to create an ablation zone approximately 5–10 mm beyond the tumor margin. After the tines have been deployed, an 18-Guage true-cut biopsy needle is used to obtain 2–3 biopsy specimens. Biopsy should not be performed prior to probe placement, as bleeding from the tumor may obscure the radiographic appearance of the mass.

After CT scan confirms appropriate deployment of the tines, ablation is carried out using temperature-based RFA with the RITA Medical Systems model 1500 RF generator coupled to a 14-Gauge Starburst XL probe. The generator modulates power up to 150 W, to achieve an average temperature of 105°C, as measured by five of the nine tines in the Starburst XL probe. Once the target temperature is reached, tumors requiring tine deployment less than 2 cm are ablated for 5 min, tine deployment between 2 and 3 cm ablated for 7 min, and tine deployment over 3 cm for 8 min. A 30 s cool-down period is followed by a second ablation cycle of identical duration. If the was not adequately covered by the tines during the first ablative procedure, the probe can be repositioned and the ablation repeated until the tumor has been adequately treated. To prevent bleeding of the electrode site and minimize the risk of tract seeding, the tract is ablated by withdrawing the tines into the probe and then gradually removing the probe from the renal fossa, keeping probe temperature above 70°C. Once the probe has been removed, a contrast CT scan can be performed to confirm complete tumor ablation.

Laparoscopic RFA

General contraindications to laparoscopic surgery apply to laparoscopic RFA, including multiple intra-abdominal adhesions, history of peritonitis, bowel distention, and severe chronic obstructive pulmonary disease (COPD). As previously mentioned, laparoscopy should be considered the primary approach for all patients with anterior lesions and for those with lesions located within close proximity to other intra-abdominal organs. After induction of general anesthesia, the patient is positioned in the modified flank position at 30–45° and strapped to the table using 2-in. cloth tape. Three trocars are placed with a 12-mm trocar in the umbilicus, a 5-mm trocar one-third of the way down between the xyphoid and umbilicus, and a 12-mm trocar in the mid-clavicular line 2–4 cm below the umbilicus.

After reflecting the bowel and exposing Gerota's fascia, the perinephric fat is dissected away from the kidney to

fully expose the lesion. A laparoscopic ultrasound probe is brought through the inferior laparoscopic port to confirm the lesion characteristics including the size and depth of penetration. Once the lesion has been exposed, the RFA probe is introduced through a separate stab incision along a perpendicular orientation to the tumor surface. The electrode is brought to the surface of the lesion and the tines are deployed to the base of the tumor using ultrasound guidance. Tines are positioned to create a zone of ablation 0.5–1 cm beyond the tumor margin and tine deployment is reconfirmed with ultrasound prior to beginning the ablation in an identical manner to that used with the percutaneous approach.

There are two key differences to account for while performing laparoscopic ablation when compared with the percutaneous route. First, whereas biopsy during percutaneous RFA can only be performed with needle core biopsies, laparoscopic RFA allows for large tumor biopsies using a 5-mm toothed biopsy forceps. To decrease bleeding from the relatively large biopsy site, we routinely perform biopsy *after* the ablation is complete, in contrast to percutaneous RFA where biopsies are performed before the ablation procedure. We have previously shown that postablation biopsies are fully interpretable by pathologists and equivalent to pretreatment biopsy specimens.[30]

The second major difference between laparoscopic and percutaneous ablation is that real-time monitoring of the ablation during laparoscopic ablation is not possible with the use of ultrasound owing to radiofrequency interference and formation of microbubbles at the periphery of the lesion that limit ultrasound visualization. However, because the temperatures at the margin of ablation are constantly monitored by the Starburst probe, tissue ablation is predictable and real-time monitoring is unnecessary. To date, there have been no studies indicating that real-time monitoring of the lesion increases cancer-free survival in RFA. In fact, there are some indications that patients undergoing laparoscopic RFA, where real-time monitoring is not possible, have better ablation success than those undergoing percutaneous procedures.[31]

Postoperative Follow-Up and Imaging

Owing to the fact that RFA is still a relatively new technology, close follow-up of patient outcomes is required. At our institution, each patient undergoes biannual physical examination, chest radiography, liver function tests, alkaline phosphatase measurement, and contrast-enhanced CT at 6 weeks, 6 months, and annually thereafter. A radiologist and urologist review all CT or MRI images to evaluate for any remaining tumor or recurrence of the lesion (Fig. 14.1). With further experience at our institution and internationally, the follow-up imaging protocols continue to be refined.

RFA leads to desiccation of tissue, localized inflammation, coagulative necrosis, and eventual replacement of the lesion with fibrosis. Immediate imaging following RFA demonstrates circumferential high attenuation corresponding to the hyperemic inflammatory response demonstrated in surrounding normal parenchyma on histological examination. It is important to recognize this as a normal postRFA response, as areas of hyperemia may be mistaken for persistent contrast enhancement of viable tumor.[32,33] The true extent of ablation is not fully realized until 7 days after the procedure, corresponding to the histological completion of coagulative necrosis.[34] As such, initial postoperative imaging should be completed at 6 weeks, at which time the zone of treatment can be adequately assessed.

Incomplete ablation is defined as any enhancement within the tumor ablation zone on CT or MR seen at the initial 6 week study. As RFA is delivered in a spherical distribution, any untreated tissue is typically found at the periphery of the lesion in a crescent-shaped distribution (Fig. 14.2). Recurrence is defined as any enhancement within the tumor ablation zone after an initially normal 6-week CT or MRI. Unlike incomplete ablation, recurrence may be seen anywhere in the ablation zone. Over time, tumors will involute to a degree and may significantly decrease in volume.[35] However, as previously described, shrinkage of the ablated lesion, in contrast to cryotherapy, is not a requirement for ablation success, as long as growth and contrast enhancement are absent.[36]

Some investigators have questioned the validity of a radiographic definition of ablative success.[37,38] The majority of these investigators, however, utilize traditional hematoxylin and eosin (H & E) staining in evaluating posttreatment biopsies, which is inadequate for assessing cell viability since cellular architecture is preserved after RFA and therefore not indicative of viability.[30,39] Problems with H & E staining as a measurement of tissue viability are overcome by utilizing nicotinamide adenine dinucleotide (NADH) diaphorase staining, which indicates viability by the reduction of tetrazolium salts to a water-based blue dye called formazan.[40] Though the majority of studies using NADH diaphorase staining have identified only nonviable cells within biopsies of RF-treated lesions, some studies have revealed persistent positive staining of tumor cells immediately after tissue ablation, raising the concern of viable cells within the ablation zone. To clarify the extent of tissue viability in RF-treated lesions, Anderson et al performed NADH diaphorase staining on RFA ablated renal tissue in the porcine model.[40] Overall, 14% biopsies showed viable tissue when analyzed less than 150 min after ablation, while no lesion showed persistent NADH diaphorase activity 3 h after ablation. Therefore, it is essential to take timing into

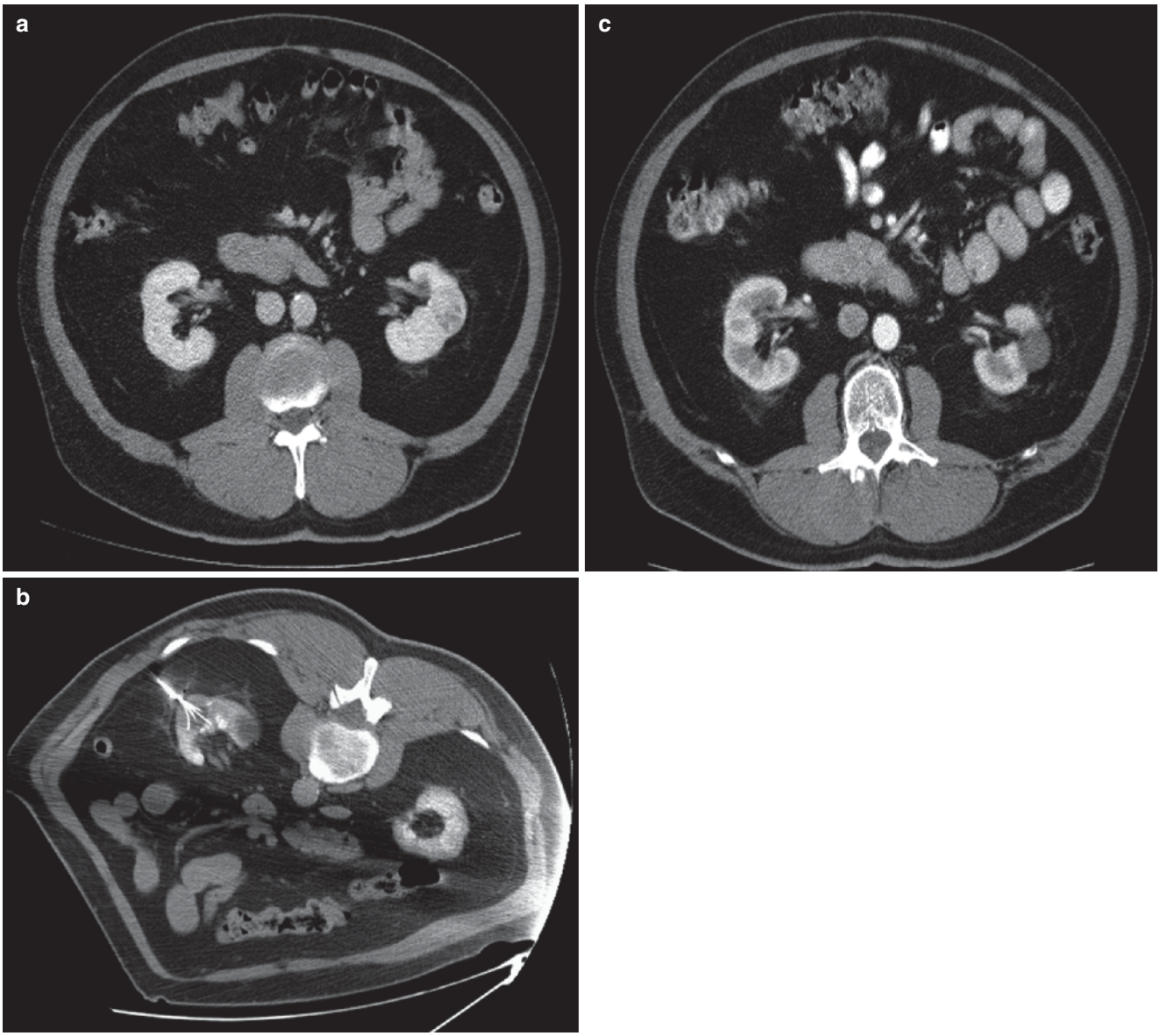

Fig. 14.1 (**a**) Pretreatment contrast enhanced CT scan demonstrates a 2.7 cm enhancing renal mass in the mid pole of the left kidney. (**b**) Intraprocedural CT scan with patient placed in the prone position. The multitined RITA electrode is deployed to achieve an ablation zone 0.5–1 cm beyond the margin of the tumor. (**c**) Postoperative contrast CT scan demonstrating the ablated renal mass with absence of contrast enhancement

account when evaluating for persistent cellular viability following RFA and any study evaluating persistence of viability immediately after ablation should be read with close scrutiny.

Owing to the fact that routine postoperative biopsies are often difficult to obtain in patients who have clear evidence of response based on imaging, and the fact that comprehensive studies assessing tissue viability and persistence of malignancy have confirmed complete cell death, we do not currently recommend postoperative biopsy to patients with normal imaging.

Safety and Complications

A recent meta-analysis of RFA found an overall major complication rate of 3.1% for percutaneous procedures and 7.4% for laparoscopic procedures.[31] Major complications in laparoscopic cases included significant blood loss in 3%, conversion to open surgery in 2%, and one case each of liver laceration, congestive heart failure, hemorrhage leading to nephrectomy, pulmonary embolism, myocardial infarction, pancreatic injury, ureteropelvic junction obstruction, and urine leak. Minor complications occurred in approximately

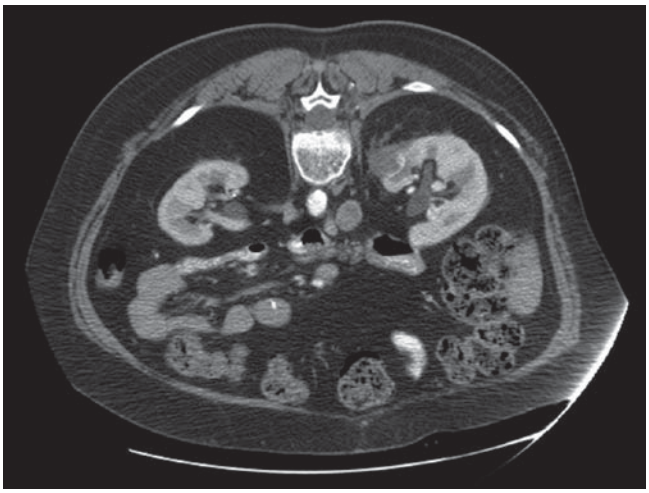

Fig. 14.2 Six week posttreatment contrast CT (prone) showing residual crescent-shaped peripheral enhancement of posterior mid pole renal tumor consistent with incomplete ablation. This patient underwent a successful repeat RFA with complete ablation of remaining tumor

10% of cases, with perirenal hematoma, transient hematuria, increased serum creatinine, and probe site pain or parasthesias being the most common. As with all invasive procedures, the complication rate has diminished with more RFA experience, owing to an appreciation of the potential pitfalls.

Results

Though short-term studies have been overwhelmingly positive in favor of RFA, the true utility must be measured with long-term follow-up studies. The initial human studies demonstrated the safety and feasibility of RFA by performing the procedure in patients immediately prior to performing radical or partial nephrectomy.[32,34] In 1999, McGovern et al reported the first use of RFA with the intent to treat renal carcinoma[41] in an elderly individual who refused surgery for a 3.5 cm enhancing renal mass. Contrast enhanced CT scan performed 2 h following the ablation showed a nonenhancing region at the site of the previous tumor, which was confirmed by 1 and 3 month follow-up CTs. These authors later reported their experience treating nine tumors in 8 patients (including the initial patient above) with tumor sizes ranging from 1.2 to 5 cm.[42] Two of the larger tumors (4.4 and 5.0 cm) demonstrated persistent enhancement and were treated with additional RFA. With a mean follow-up of 10.3 months (range 3–21) no patient demonstrated recurrence of metastatic renal cell carcinoma.

Since the initial results with RFA of renal masses, several authors have confirmed its effectiveness in regard to short-term and intermediate-term cancer-specific survival.[43] In their review of published data on RFA of renal cancer in 337 patients, Park et al found an excellent disease-specific survival (94.8%) after RF ablation of small tumors (mean size 2.4 cm), with a mean follow-up of 19 months. It is important to remember that in the majority of the ablation literature, cancer-specific survival rates often include patients who have undergone a second or third ablation for an incompletely treated lesion. In this review, Park found that 8.8% of patients required reablation for incompletely treated lesions following RFA.

Though initial success is encouraging, intermediate-term and long-term results are only now being reported. When evaluating intermediate-term results of a new treatment modality, it is important to report results with minimum follow-up rather than the average follow-up of the group. Accordingly, there are only three currently available long-term studies on patients undergoing RFA for renal masses (Table 14.1). In patients with biopsy-proven RCC and a minimum follow-up of 3 years, the recurrence-free survival appears to be comparable with that of early studies, approaching 95%. These results confirm that the majority of renal cell recurrences occur within the first 3 years and are likely owing to incomplete ablation rather than recurrent cancer.

Table 14.1 Reported results for radiofrequency ablation of renal tumors with at least 36 months of follow-up

Author	Approach (number)	Number of tumors	Number with RCC	Mean tumor size (range, cm)	Mean follow-up (range, months)	Number of recurrences after 3 years	Time from treatment to recurrence (range, months)	Recurrence-free survival[a] (%)	Overall survival (%)
McDougal et al[44]	Percutaneous	20	16 (80)	3.2 (1.1–7.1)	60(48–72)	1	Not specified	94	69
Levinson et al[45]	Percutaneous (33) Laparoscopic (1)	34	18 (53)	2 (1–4)	61(41–80)	3	7–30	80	71
Tracy et al[46]	Percutaneous (68) Laparoscopic (34)	102	66 (72%)	2.3 (0.9–5.4)	51 (36–84)	1	3–36[b]	94	90

[a]Recurrence-free survival of all patients in cohort with biopsy-confirmed RCC, including those who recurred prior to the minimum follow-up of 3 years

[b]Number of recurrences occurring after minimum follow-up of 3 years, which does not include early recurrences

Conclusion

As the incidence of small renal masses increases, so does the desire to pursue minimally invasive therapies for their treatment. RFA represents one of the unique therapies for this purpose. When approached laparoscopically, ablation is associated with minimal morbidity that appears favorable in comparison with open or laparoscopic partial nephrectomy. Percutaneous treatment allows for the outpatient management of small renal masses with considerable improvement in convalescence when compared with extirpative surgery. With medium to long-term follow-up, cancer recurrence rates remain low with nearly 95% of patients having no evidence of recurrence after 3 years and up to 7 years. Further long-term results are required to determine if cancer outcomes are equivalent to traditional surgery.

References

1. Pantuck AJ, Zisman A, Rauch MK, Belldegrun A. Incidental renal tumors. *Urology*. 2000;56(2):190–196
2. Luciani LG, Cestari R, Tallarigo C. Incidental renal cell carcinoma-age and stage characterization and clinical implications: study of 1092 patients (1982–1997). *Urology*. 2000;56(1):58–62
3. Remzi M, Memarsadeghi M. [Small incidental renal tumors. Evaluation and biological parameters]. *Urologe A*. 2007;46(5):478; 480–474
4. Abouassaly R, Lane BR, Novick AC. Active surveillance of renal masses in elderly patients. *J Urol*. 2008;180(2):505–508; discussion 508–509
5. Lane BR, Novick AC, Babineau D, Fergany AF, Kaouk JH, Gill IS. Comparison of laparoscopic and open partial nephrectomy for tumor in a solitary kidney. *J Urol*. 2008;179(3):847–851; discussion 852
6. Gill IS, Kavoussi LR, Lane BR, et al Comparison of 1,800 laparoscopic and open partial nephrectomies for single renal tumors. *J Urol*. 2007;178(1):41–46
7. Fergany AF, Hafez KS, Novick AC. Long-term results of nephron sparing surgery for localized renal cell carcinoma: 10-year followup. *J Urol*. 2000;163(2):442–445
8. Thompson RH. Radical nephrectomy: too radical for small renal masses? *Lancet*. 2006;368(9538):823–824
9. Matin SF, Gill IS, Worley S, Novick AC. Outcome of laparoscopic radical and open partial nephrectomy for the sporadic 4 cm. or less renal tumor with a normal contralateral kidney. *J Urol*. 2002;168(4 pt 1):1356–1359; discussion 1359–1360
10. Ramani AP, Desai MM, Steinberg AP, et al Complications of laparoscopic partial nephrectomy in 200 cases. *J Urol*. 2005;173(1):42–47
11. Allaf ME, Varkarakis IM, Bhayani SB, Inagaki T, Kavoussi LR, Solomon SB. Pain control requirements for percutaneous ablation of renal tumors: cryoablation versus radiofrequency ablation–initial observations. *Radiology*. 2005;237(1):366–370
12. Cosman ER, Nashold BS, Ovelman-Levitt J. Theoretical aspects of radiofrequency lesions in the dorsal root entry zone. *Neurosurgery*. 1984;15(6):945–950
13. Patel VR, Leveillee RJ, Hoey MF, Herron AJ, Zaias J, Hulbert JC. Radiofrequency ablation of rabbit kidney using liquid electrode: acute and chronic observations. *J Endourol*. 2000;14(2):155–159
14. Organ LW. Electrophysiologic principles of radiofrequency lesion making. *Appl Neurophysiol*. 1997;39(2):69–76
15. Bhowmick P, Coad JE, Bhowmick S, et al In vitro assessment of the efficacy of thermal therapy in human benign prostatic hyperplasia. *Int J Hyperthermia*. 2004;20(4):421–439
16. Bhowmick S, Coad JE, Swanlund DJ, Bischof JC. In vitro thermal therapy of AT-1 Dunning prostate tumours. *Int J Hyperthermia*. 2004;20(1):73–92
17. Rehman J, Landman J, Lee D, et al Needle-based ablation of renal parenchyma using microwave, cryoablation, impedance- and temperature-based monopolar and bipolar radiofrequency, and liquid and gel chemoablation: laboratory studies and review of the literature. *J Endourol*. 2004;18(1):83–104
18. Hsu TH, Fidler ME, Gill IS. Radiofrequency ablation of the kidney: acute and chronic histology in porcine model. *Urology*. 2000;56(5): 872–875
19. Crowley JD, Shelton J, Iverson AJ, Burton MP, Dalrymple NC, Bishoff JT. Laparoscopic and computed tomography-guided percutaneous radiofrequency ablation of renal tissue: acute and chronic effects in an animal model. *Urology*. 2001;57(5):976–980
20. Walsh LP, Anderson JK, Baker MR, et al In vitro assessment of the efficacy of thermal therapy in human renal cell carcinoma. *Urology*. 2007;70:380–384
21. Gettman MT, Lotan Y, Corwin TS, et al Radiofrequency coagulation of renal parenchyma: comparison of effects of energy generators on treatment efficacy. *J Endourol*. 2002;16(2):83–88
22. Frich L EB, Brabrand K, et al Percutaneous saline-enhanced radiofrequency ablation of colorectal liver metastases in a patient with adhesionsin the peritoneal cavity. *Am J Roenterol*. 2005;16: 83–88
23. Winter TC, Laeseke PF, Lee FT Jr. Focal tumor ablation: a new era in cancer therapy. *Ultrasound Q*. 2006;22(3):195–217
24. Pereira PL, Trubenbach J, Schenk M, et al Radiofrequency ablation: in vivo comparison of four commercially available devices in pig livers. *Radiology*. 2004;232(2):482–490
25. Corwin TS, Lindberg G, Traxer O, et al Laparoscopic radiofrequency thermal ablation of renal tissue with and without hilar occlusion. *J Urol*. 2001;166(1):281–284
26. Hall WH, McGahan JP, Link DP, deVere White RW. Combined embolization and percutaneous radiofrequency ablation of a solid renal tumor. *AJR Am J Roentgenol*. 2000;174(6):1592–1594
27. Ogan K, Jacomides L, Dolmatch BL, et al Percutaneous radiofrequency ablation of renal tumors: technique, limitations, and morbidity. *Urology*. 2002;60(6):954–958
28. Matsumoto ED, Johnson DB, Ogan K, et al Short-term efficacy of temperature-based radiofrequency ablation of small renal tumors. *Urology*. 2005;65(5):877–881
29. Johnson DB, Saboorian MH, Duchene DA, Ogan K, Cadeddu JA. Nephrectomy after radiofrequency ablation-induced ureteropelvic junction obstruction: potential complication and long-term assessment of ablation adequacy. *Urology*. 2003;62(2):351–352
30. Margulis V, Matsumoto ED, Lindberg G, et al Acute histologic effects of temperature-based radiofrequency ablation on renal tumor pathologic interpretation. *Urology*. 2004;64(4):660–663
31. Hui GC, Tuncali K, Tatli S, Morrison PR, Silverman SG. Comparison of percutaneous and surgical approaches to renal tumor ablation: metaanalysis of effectiveness and complication rates. *J Vasc Interv Radiol*. 2008;19(9):1311–1320
32. Zlotta AR, Wildschutz T, Raviv G, et al Radiofrequency interstitial tumor ablation (RITA) is a possible new modality for treatment of renal cancer: ex vivo and in vivo experience. *J Endourol*. 1997;11(4): 251–258
33. Goldberg SN, Gazelle GS, Compton CC, Mueller PR, Tanabe KK. Treatment of intrahepatic malignancy with radiofrequency ablation: radiologic-pathologic correlation. *Cancer*. 2000;88(11):2452–2463
34. Walther MC, Shawker TH, Libutti SK, et al A phase 2 study of radio frequency interstitial tissue ablation of localized renal tumors. *J Urol*. 2000;163(5):1424–1427

35. Rutherford EE, Cast JE, Breen DJ. Immediate and long-term CT appearances following radiofrequency ablation of renal tumours. *Clin Radiol*. 2008;63(2):220–230
36. Matsumoto ED, Watumull L, Johnson DB, et al The radiographic evolution of radio frequency ablated renal tumors. *J Urol*. 2004; 172(1):45–48
37. Hegarty N KJ, Remer E, O'Malley C, Novick A, Gill I. Lack of enhancement on 6-month MRI does not guarantee complete cancer cell kill following radiofrequency ablation of small renal tumors. In: *Abstract presentation. AUA Annual meeting*; 2006
38. Michaels MJ, Rhee HK, Mourtzinos AP, Summerhayes IC, Silverman ML, Libertino JA. Incomplete renal tumor destruction using radio frequency interstitial ablation. *J Urol*. 2002;168(6): 2406–2409; discussion 2409–2410
39. Marcovich R, Aldana JP, Morgenstern N, Jacobson AI, Smith AD, Lee BR. Optimal lesion assessment following acute radio frequency ablation of porcine kidney: cellular viability or histopathology? *J Urol*. 2003;170(4 pt 1):1370–1374
40. Anderson JK, Baker M, Jaffers O, Pearle MS, Lindberg GL, Cadeddu JA. Time course of nicotinamide adenine dinucleotide diaphorase staining after renal radiofrequency ablation influences viability assessment. *J Endourol*. 2007;21(2):223–227
41. McGovern FJ, Wood BJ, Goldberg SN, Mueller PR. Radio frequency ablation of renal cell carcinoma via image guided needle electrodes. *J Urol*. 1999;161(2):599–600
42. Matlaga BR, Zagoria RJ, Woodruff RD, Torti FM, Hall MC. Phase II trial of radio frequency ablation of renal cancer: evaluation of the kill zone. *J Urol*. 2002;168(6):2401–2405
43. Park S, Cadeddu JA. Outcomes of radiofrequency ablation for kidney cancer. *Cancer Control*. 2007;14(3):205–210
44. McDougal WS, Gervais DA, McGovern FJ, Mueller PR. Long-term followup of patients with renal cell carcinoma treated with radio frequency ablation with curative intent. *J Urol*. 2005;174(1):61–63
45. Levinson AW, Su LM, Agarwal D, et al Long-term oncological and overall outcomes of percutaneous radio frequency ablation in high risk surgical patients with a solitary small renal mass. *J Urol*. 2008;180(2):499–504; discussion 504
46. Tracy CR RJ, Bagrodia A, Cadeddu JA. Outcomes of radiofrequency ablation (RFA) for small renal tumors: experience in 102 tumors with more than 3 years of follow-up. In: *Abstract presentation. 26th World Congress of Endourology, Shanghai, China*; 2008

High-Intensity Focused Ultrasound in the Management of the Small Renal Mass

15

Tom A. Leslie and David W. Cranston

Introduction

High-intensity focused ultrasound (HIFU) is an attractive new option in the management of the small renal mass, especially in view of its noninvasive or minimally invasive applications. Using well-established principles, this ablative therapy can be used to treat a variety of solid tumors with few side effects. As a result, there is a great deal of research being carried out in this field, and a number of commercially available devices already exist.

The History of HIFU

HIFU has been investigated as an ablative technique for many years. Wood et al were the first to describe bio-effects from a plane ultrasound transducer in 1920s.[1] Further, basic scientific research resulted in the first clinical application of the technology in the 1950s when Fry et al used HIFU for the treatment of focal neurological conditions such as Parkinson's disease.[2, 3] However, as the ability to create a predictable lesion improved, it became clear that the rate-limiting step was targeting. Without reliable imaging to accurately assess, target, and monitor the ablated area or "lesion," the early investigators strived to create reversible damage to allow them to site the definitive treatment lesions[4] and thus attempt controlled and accurate ablation. This method was not good enough, and it was only with the advent of vastly improved imaging techniques, such as ultrasound, computerized tomography (CT), and magnetic resonance imaging (MRI), that HIFU research began to move forward again. With these advances, clinicians and scientists once again became interested in applying HIFU as a noninvasive method of treating tumors, especially urological malignancy.

Over the last 20 years, a great deal of experimental work has been carried out, both laboratory based and in the form of clinical trials, aimed at developing devices that can deliver treatments with safe and effective outcomes. This has led to the development of commercial devices that can now deliver HIFU accurately and in a reproducible fashion, and the goal of a noninvasive cancer treatment draws ever nearer.

Principles

Unlike diagnostic ultrasound, which usually employs frequencies in the range of 1–20 MHz, frequencies of 0.8–4 MHz are generally used during the clinical applications of HIFU, and the energy levels carried in the HIFU beam are several orders of magnitude greater than those of a standard diagnostic ultrasound beam.[5] The intensity of the energy in the ultrasound beam is increased by up to 10,000 times greater than those of a standard diagnostic ultrasound beam, and focused tightly, causing the temperature at the focus to rise rapidly above 80°C.[6] Even for very short exposures, this level of heating should lead to effective cell killing.[7] This area of coagulative necrosis or "lesion" occurs with little damage to overlying or surrounding tissue and can be targeted from outside the body, thus providing noninvasive tissue damage. A typical lesion is cigar shaped and approximately 12 × 3 mm; the size does vary with the transducer design (Fig. 15.1).

Heating and Cavitation

Ultrasound causes tissue damage through two predominant mechanisms. The first is by the conversion of mechanical energy into heat and the second is through cavitation. As an ultrasound beam propagates through a tissue, some of its energy is converted to heat. The rate of ultrasound-mediated heating dQ/dt within a unit volume of tissue depends on its absorptive properties and can be predicted by the following equation:

$$dQ/dt = 2\alpha I$$

where α is the absorption coefficient. Under normal circumstances, this heat will dissipate rapidly through both direct

P. Dasgupta et al. (eds.), *New Technologies in Urology,*
DOI: 10.1007/978-1-84882-178-1_15, © Springer-Verlag London Limited 2010

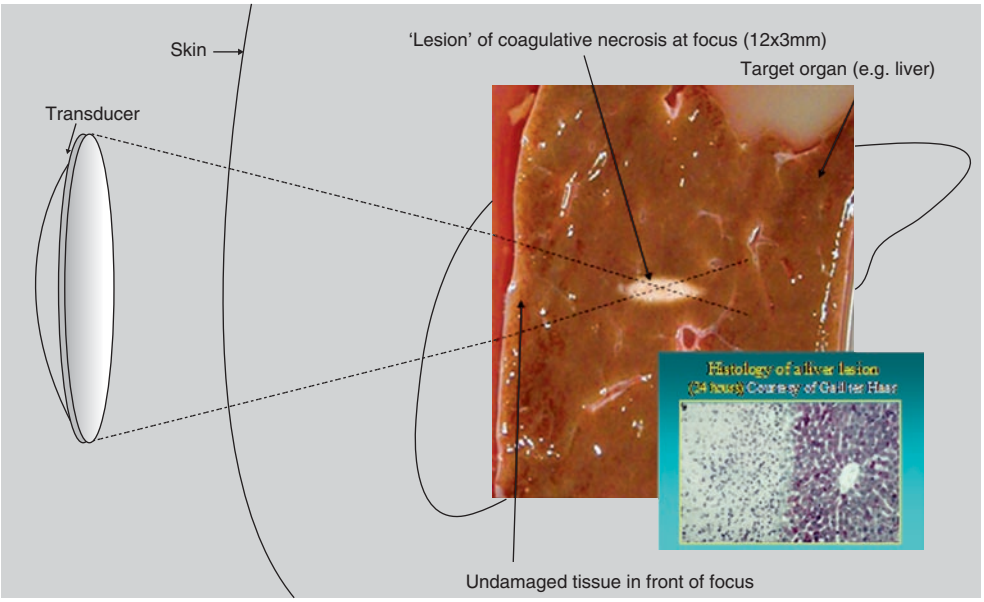

Fig. 15.1 Diagram of high-intensity focused ultrasound (HIFU) lesion

thermal conduction and convection from the flowing blood (convection). If the rate of heating exceeds the rate of cooling, the result will be a local temperature rise. Arrest of cellular reproduction will occur if the temperature is maintained above 43°C for 60 min or longer. This is of particular relevance for existing "hyperthermia" or "thermotherapy" treatments, where the aim is to raise the temperature of the target tissues to a precise temperature (usually just above 42.8°C) for a defined period of time. In contrast, HIFU relies on the fact that, above a threshold of 56°C for 1 s, rapid thermal toxicity occurs, causing irreversible cell death through coagulative necrosis. During HIFU treatments, the temperature at the focus can rise rapidly above 80°C,[6] which, even for very short exposures, should lead to effective cell killing,[7] and thus, precise monitoring of temperature is unnecessary. There is a steep temperature gradient between the focus and the neighboring tissue, which is demonstrated by the sharp demarcation between the volume of necrotic tissue (lesion) and normal surrounding cells seen on histology (Fig 15.1).[8] The cooling effect of perfusion may limit the reliability of other forms of hyperthermia treatment, for which there is sufficient time during exposures for local thermal diffusion and heat dissipation from the target region. This factor can be practically eliminated during HIFU treatment by keeping individual exposure times below 3 s.[9] The size of an individual lesion will vary with drive frequency, and beam geometry, and is also dependent on exposure parameters such as intensity, time, target tissue, and the focal depth in the tissues.

Acoustic cavitation is complex, and unpredictable, but the end result is also cell necrosis induced through a combination of mechanical stresses and thermal injury. Ultrasound causes the tissues to vibrate, and the molecular structure is subjected to alternating compression and rarefaction. During rarefaction, gas can be drawn out of solution to form bubbles, which oscillate in size (stable or noninertial cavitation) or collapse rapidly (unstable or inertial cavitation), causing mechanical stresses and generating temperatures of 2,000–5,000 K in the microenvironment.[10] The maximum displacement amplitude of tissue particles during a wave cycle is in the order of micrometers and is proportional to the pressure amplitude within the tissue. This is determined by the energy carried in the wave at that site and is proportional to the square root of the incident intensity at any given frequency. The maximum displacement amplitude is also inversely proportional to the drive frequency at any given intensity.[11] Cavitation is therefore dependent on frequency, negative pressure amplitude, and intensity, and the cavitation threshold also lowers as temperature increases.[12] Diagnostic ultrasound exposures generally operate at frequencies >2 MHz and have lower pressure amplitudes than do therapeutic exposures, but during HIFU exposures, it is not possible to eliminate the possibility of the occurrence of cavitation entirely.

The effect of heating is both more repeatable and more predictable than cavitation,[13] which made it the preferred mode of cell killing in early clinical applications of HIFU. More recently, bubble appearance has been used as an indicator of successful ablation,[14] and in fact, work is now underway to investigate whether ultrasound contrast agents can be used safely to increase the volume of tissue ablation in a given time.[15] The mechanisms behind any such potential effect remain unclear, but it may be that the contrast agents act as seeds to promote cavitation.

Histological Assessment of Renal Ablation

The observed tissue changes following HIFU begin characteristically with appearances of homogeneous coagulative necrosis.[16] As a result, following treatment a volume of necrotic tissue is left, which should correspond to the targeted tissue. However, histological evidence of coagulation necrosis following thermal ablation requires at least 24–48 h[17] to develop; thus, lesions that are examined immediately after ablation do not show changes characteristic of necrosis. Subtle changes including erythrocyte homogenization, variation of shape, size, and lysis of red cells within blood vessels, endothelial damage and granular protein deposits on vessel walls, homogenization of vascular smooth muscle, shrinkage and loss of cell membrane detail of tumor cells, and pyknosis of nuclei can be seen on H&E staining. However, none of these features is entirely specific, especially given the morphological heterogeneity seen in renal cell carcinoma (RCC). Indeed, RCCs commonly have areas of necrosis, hemorrhage, and hyalinization of stroma in untreated tumors, and these vary within each tumor.

A handful of published investigational studies of nephrectomies following radiofrequency (RF) ablation have yielded mixed results from pathological assessment of ablation. Michaels et al[18] reported that the vast majority of their 15 patient series revealed residual tumor viability immediately after ablation, whereas Matlaga[19] reported complete treatment in eight out of ten patients after just a single 12-min RF ablation treatment. In addition to the different methodologies used to perform RF ablation, other factors, such as the possible uncertainties about the true area ablated, may play a role in these discrepant results. For example, it has been shown in the liver that specialized stains are required to identify ablated tumor, particularly in the acute post-ablation period.[20] Hence, the precise role of pathological assessment after RF ablation patients has been questioned.[21]

A method that may avoid the problems of routine histological examination of acutely ablated tissue is nicotinamide adenine dinucleotide (NADH) diaphorase staining. NADH is a coenzyme present in cytoplasm and mitochondria. It is integral to oxidation and reduction reactions in glycolysis, the Krebs cycle, and cellular respiration. NADH diaphorase is a ubiquitous cellular enzyme that catalyzes substrate reduction by the transfer of electrons from NADH, yielding reduced substrate and NAD^+. One such substrate is p-nitroblue tetrazolium (Sigma-Aldrich). Diaphorase has been shown to be active only in viable cells, and its activity ceases immediately after cellular death.[22]

In a porcine model, negative NADH staining has correlated well with effective ablation.[21, 23, 24] NADH staining has been used as an adjunct to routine H&E staining to study the effects of renal RF ablation.[25, 26] However, there continues to be some debate as to the best timing of specimen staining. Stern et al[27] commented that although negative NADH staining is consistent with nonviability, their results suggested that false-positive staining can occur immediately following radiofrequency ablation (RFA), making the predictive value of positive NADH diaphorase staining unclear. This was supported by Anderson et al[23] who observed that tissue that is apparently viable on NADH staining within 2.5 h of RFA may in fact have been ablated. From the literature, there is no clear resolution to this problem, but H&E alone may not be sufficient, and at this time, a combination of H&E and NADH is probably optimal when assessing ablation in a specimen that has been resected immediately after ablation (Fig. 15.2).

When the ablated tissue is left in situ, the subsequent inflammatory response includes granulation tissue formation at the periphery of the necrotic region after approximately 7 days, showing the presence of immature fibroblasts and new capillary formation[8] and the migration of polymorphonuclear leucocytes deep into the treated volume. Two weeks following HIFU, the periphery of the treated region is replaced by proliferative repair tissue. The repair process has not been investigated in detail at the cellular level beyond this time frame, but sequential anatomical imaging records a gradual shrinkage of treated volumes over time, which indicates replacement of the necrotic region with fibrous scar tissue.[28]

Methods of Targeting HIFU Treatments

There are several ways to monitor an HIFU treatment, and this has led to the development of a variety of devices, a few of which are now commercially available. These devices, although applying the same basic principles for ablation using HIFU, use different imaging modalities to target organs and monitor the effect of the treatment given. Accurate treatment monitoring is essential. Today, HIFU is monitored and guided by either ultrasound or MRI.

Diagnostic ultrasound is the most common imaging modality used to direct therapeutic ultrasound. It is widely available, relatively inexpensive, mobile, and easily applied. Using the same modality for imaging and ablation is logical, as the limitations of the imaging will correspond to the limitations of the HIFU beam and as such enable the operator to assess the suitability of a given approach. The diagnostic imaging transducer is usually built into the treatment transducer and is directed in the same plane as the treatment head. This means that real-time assessment is possible, and thus adjustment to treatment parameters during treatment can be made to optimize efficacy and safety. Real-time gray-scale changes seen immediately following ablation are used to judge the extent of treatment.[29] These gray-scale changes or "bright-ups" are thought to represent boiling tissue and therefore guarantee sufficient temperatures for cell death.

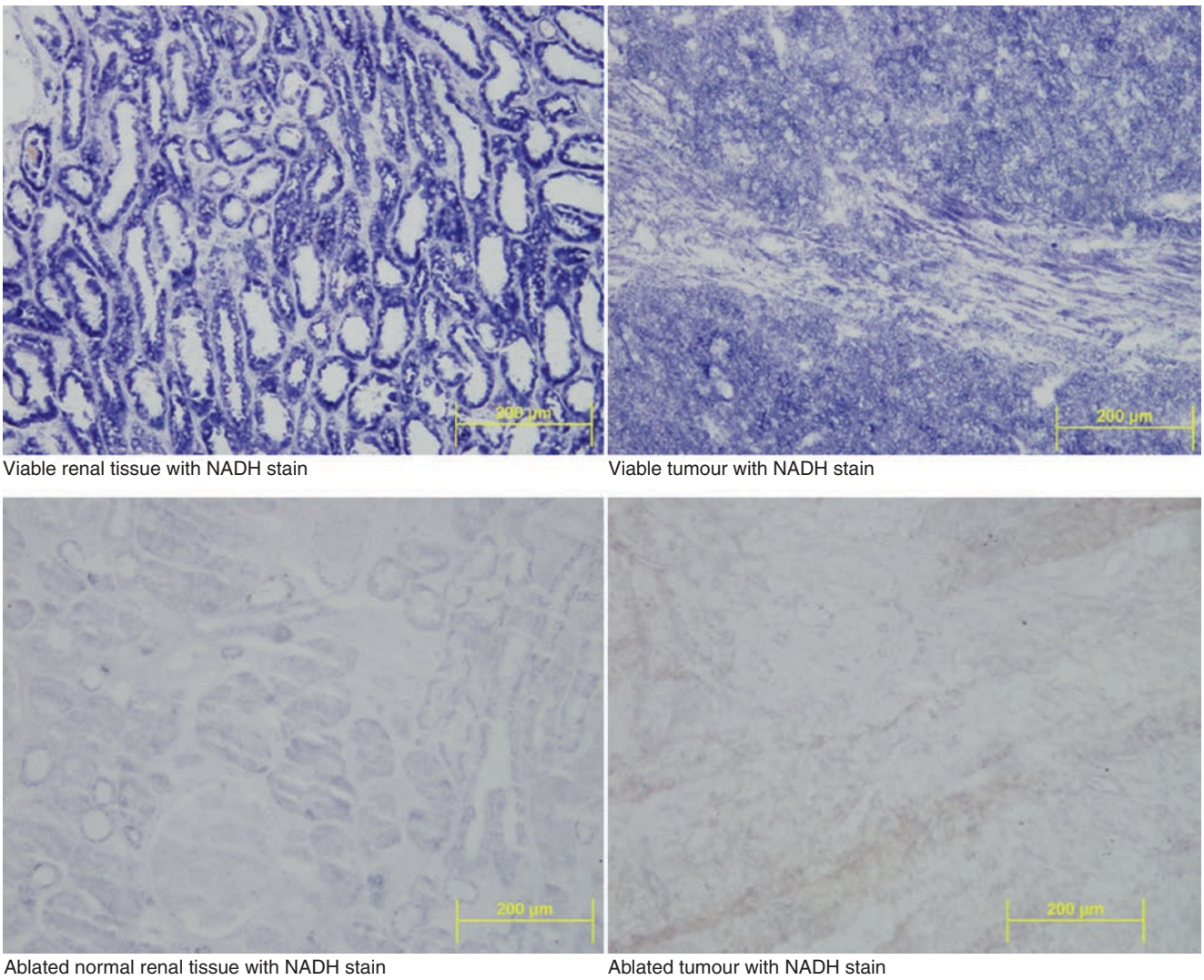

Fig. 15.2 Viability staining of ablated kidney tissue

The clear disadvantage of ultrasound is the relatively poor image quality, which can be difficult to interpret. The image quality can degrade rapidly as a consequence of changes in the acoustic properties of tissues[14]; this may occur when heating or when edema has occurred in the targeted tissue or within the tissue in front of the target, e.g., perinephric fat.

MRI is increasingly being used to guide HIFU treatments. MR is highly sensitive in localizing tumors and provides precise anatomical resolution for tumor targeting. MR has many parameters that are temperature sensitive, and small temperature elevations (±1°C) can be detected.[30] As a result, the HIFU focus can be located at relatively low powers, and the accuracy of targeting can be verified. In addition, by using temperature-sensitive MR imaging sequences, focal temperature elevations and effective thermal doses may be estimated.[31] The disadvantages of MR include its cost and size. Practically, MR has lower spatial resolution than ultrasound and real-time assessment of treatment relies on relatively slow, computer-generated assumptions of temperature change; as a result, treatment time is also prolonged.

Side-Effects and Limitations

The HIFU technique has been investigated extensively in small and large animals and been shown to be successful for the treatment of liver tumors in the former[32] and in the selective destruction of normal liver, bladder, muscle, and kidney in the latter.[33, 34] Small animal studies have also shown that HIFU does not increase the risk of tumor metastasis.[35]

The evidence from both animal-based research and human clinical trials is that local pain, transient fever, and skin toxicity are the most frequently occurring adverse events.[36, 37]

Pain is usually transient, mild, and short-lived, while fever is thought to be caused by a combination of the release of intracellular ions, nucleic acids, proteins, and their metabolites into the extracellular space.[28] Skin toxicity is usually limited to small superficial burns, but significant burns can occur as Leon-Villapalos et al[38] describe in their case report on a patient with full thickness burns following MR-guided HIFU treatment of uterine fibroids. Skin burns occur because outside the focal region, energy deposition is maximal at interfaces between tissues of differing acoustic impedances, and the most significant of these interfaces is the skin surface. There are other potential complications of HIFU treatment such as inadvertent injury to hollow viscera adjacent to the target tumor, and abscess formation following bacterial colonization of the necrotic volume following successful ablation.[37] These are very rare and have been reported in less than 0.1% of cases.

HIFU Devices

With these factors in mind, there are three generic types of HIFU device: extracorporeal, transrectal, and laparoscopic.

Extracorporeal devices are large devices and can be used to treat a variety of conditions including liver, kidney, pancreatic, pelvic, and bone tumors. These extracorporeal devices use transducers with a longer focal length (10–15 cm) and use either ultrasound or MRI to target the organ. The first commercially available extracorporeal device was designed and developed in Chongqing, China. The Model JC HIFU device (HAIFU™ Technology Company, China)[39] was the first commercially available extracorporeal HIFU device, and the majority of the published clinical data come from work with this device. This is the only ultrasound-guided extracorporeal device that has a CE Mark (Conformité Européene), the European kite mark that is awarded to a device once it has been proven to be safe in humans. The second extracorporeal device is the MR-guided focused ultrasound (MRgFUS) system (ExAblate 2000, InSightec, Haifa, Israel)[30]; this device is only licensed for use with uterine fibroids.

Transrectal probes were designed for the treatment of prostatic disease. Transrectal devices are smaller, with short focal lengths (4–5 cm), operating at higher frequencies than extracorporeal devices, and they use ultrasound guidance. There are two devices in use around the world: The Ablatherm (Ablatherm, Technomed International; Lyon, France)[40] and the Sonablate®-500 (Focus Surgery, Indianapolis, IN, USA).[41] These devices rely on similar principles, and as such, their results are comparable. This device cannot be used in the management of renal tumors.

Laparoscopic HIFU is delivered using a transducer mounted in a probe, which can be passed through an 18-mm port. Thus, the transducer is small, with an even shorter focal length (2.5–3.5 cm) and once again operates under ultrasound guidance. The Sonablate®-Laparoscopic HIFU system (Focus Surgery, Indianapolis, IN, USA and Misonix Inc., Farmingdale, NJ, USA) is the first device of this kind to have reached clinical trials.

HIFU in the Kidney

Renal tumors comprise 3% of all solid neoplasms, and the incidence of RCC has risen by 2.3–4.3% annually over the last three decades, with 51,190 new cases and 12,890 deaths expected in the USA in 2007.[42] With the advent of high-quality and easily accessible imaging, the rate of detection of small renal masses has greatly increased. Luciani et al[43] studied a series of more than 1,000 patients and found that the incidental discovery of renal tumors increased from 13 to 59% in the period between 1982 and 1997. Almost half of those with incidentally found masses were more than 65 years old. In the UK, there are around 6,000 new cases each year, most commonly occurring in the seventh and eighth decades.[44]

With this ever-growing group of newly diagnosed patients, the management of the small renal mass has become an important area of debate. Nephron-sparing surgery by partial nephrectomy (where indicated) is still seen as the gold standard,[45] and active surveillance remains a popular option for these small renal masses; however, there is a growing place for low morbidity, ablative techniques in the management of this patient group, many of whom are elderly. Cryotherapy,[46] RFA,[47] and extracorporeal HIFU[48] have all been proposed as treatment options for small RCC (<4 cm).

The kidney has been used as an animal model for HIFU ablation. Linke et al (1973)[49] were the first to report successful kidney tissue ablation using HIFU on rabbits. The test animals were kept for more than 1 year following HIFU exposure. Long-term assessment showed the treated area of healthy kidney was replaced with a thin fibrous scar on gross histological analysis of the specimens.

Adams et al (1996)[50] treated implanted VX-2 tumors in rabbit kidneys as part of a two-phase trial. The first phase involved the ablation of implanted tumors during an open procedure, whereas in the second phase the implanted tumors were ablated in an extracorporeal fashion. The kidneys were excised shortly after exposure and assessed histologically for ablation. The authors found areas of discrete renal damage in all nine tumors treated in the first phase. In the second phase, seven out of nine tumors showed evidence of ablation; however,ablation was seen throughout the implanted tumors in only two cases. Accurate targeting of the tumors remained difficult at that time.

Watkin et al (1997) used a large animal model to assess the feasibility of noninvasive renal tumor ablation.[51] An extracorporeal HIFU transducer was used to evaluate the time/exposure thresholds for kidney damage in ex vivo pig kidney. Eighteen porcine kidneys were treated in vivo at a depth of 40 mm from the skin surface, with acute damage detected in 13 kidneys (67%). The lesions appeared well circumscribed with a pale central area surrounded by a hemorrhagic rim.

Extracorporeal HIFU in the Management of Small Kidney Tumors

Clinical trials looking at the use of HIFU in the management of small kidney tumors remain few. Vallancien et al (1993)[52] reported the first clinical feasibility study. Eight patients received extracorporeal HIFU exposures followed by nephrectomy. They reported evidence of ablation in the treated areas following excision of the kidney, but encountered a high rate of skin burns with 10% of patients suffering from this complication.

Marberger et al (1993)[53] reported a series of 16 patients who had renal tumors treated with HIFU. In 14 patients, a 10-mm^3 volume of renal tumor was treated with HIFU, and this was followed by immediate surgical resection of the kidney. In nine patients, areas of acute tissue necrosis were seen, although the lesions only measured between 15 and 35% of the original targeted volume. Two patients were treated with curative intent; however, both had incomplete ablation with residual disease visible on follow-up MRI.

Wu et al (2003)[54] have described a series of 13 patients with renal tumors who have received HIFU treatment. They only comment on the ten patients who were treated with palliative intent, the three receiving HIFU with curative intent were not analyzed. They showed that nine out of ten patients described a reduction in tumor-related pain, while hematuria resolved in seven out of eight cases.

Hacker et al (2006)[55] used an experimental hand-held extracorporeal technology to ablate 43 porcine and human kidneys. However, technical success was mixed, and the authors concluded that further work was required in the dosage and application of this system.

The first prospective, nonrandomized clinical trial to evaluate the safety and effectiveness of HIFU in the treatment of small kidney tumors has been carried out by our group at the University of Oxford; the results are as yet unpublished, although interim results were published by Illing et al (2005).[56] Twenty-one patients with kidney tumors were treated, six receiving HIFU prior to nephrectomy, allowing histological assessment, and 15 undergoing HIFU followed by radiological follow-up. MRI changes suggestive of tumor response to HIFU treatment have been seen in 12/21 cases (57%). Fourteen patients within the radiology group were eligible for assessment: complete ablation was seen in four cases (29%) and complete or partial ablation in eight patients (57%). Mild, transient discomfort was reported by 12/21 patients, and moderate discomfort in 4/21, but severe pain needing prolonged opiate analgesia was not encountered. Minor skin toxicity was seen in 5/21 patients. Recovery time was short with none of the patients remaining in hospital for more than 24 h, and the treatment has proven to be repeatable in those patients with a partial response. We have shown that it is feasible to ablate small renal tumors, and importantly, neither renal function nor overall health were adversely affected (Fig. 15.3).

Laparoscopic HIFU for the Small Renal Mass

Published preliminary results have shown some evidence of ablation in all trials looking at HIFU for kidney tumors. However, we have shown that less than a third of patients with small renal tumors achieve complete ablation. Specific reasons for these low-complete ablation rates have yet to be fully elucidated, but are likely to include rib interaction and body habitus. A laparoscopic probe may overcome the practical constraints of extracorporeal HIFU posed by the ribcage, allowing direct ablation of the tumor under direct ultrasound visualization. This approach may provide a nephron-sparing procedure without the associated risks of bleeding or urinary leakage.

The Sonablate®-Laparoscopic HIFU system (Focus Surgery, Indianapolis, IN, USA and Misonix Inc., Farmingdale, NJ, USA) has been tested in both ex vivo and in vivo in large animal models. A team at the University of Chicago department of surgery, led by Professor Shalhav,[57, 58] used eight female farm pigs weighing between 27 and 36 kg to assess the equipment. A total of 16 kidneys were treated, with the animals divided into two groups for the evaluation of the tissue effects of the laparoscopic HIFU equipment: an acute group (n = 4, killed at 4 days post-HIFU treatment) and a subacute group (n = 4, killed at 14 days post-HIFU treatment). Following HIFU treatment and sacrifice according to group, the kidneys were analyzed by a single, blinded pathologist.

The results from this in vivo study confirmed that kidney ablation was feasible with a mean volume of necrosis of 4.5 ± 2.94 cm^3 (range 0.8–10.5). Only two intra-operative complications were described. The first occurred in the first lesion performed in the study. Only limited dissection had been performed, and postmortem assessment revealed thermal injury to the adjacent back muscle wall. The second complication occurred on animal no. 4 where the ipsilateral ureter was included in the treatment zone, and thermal

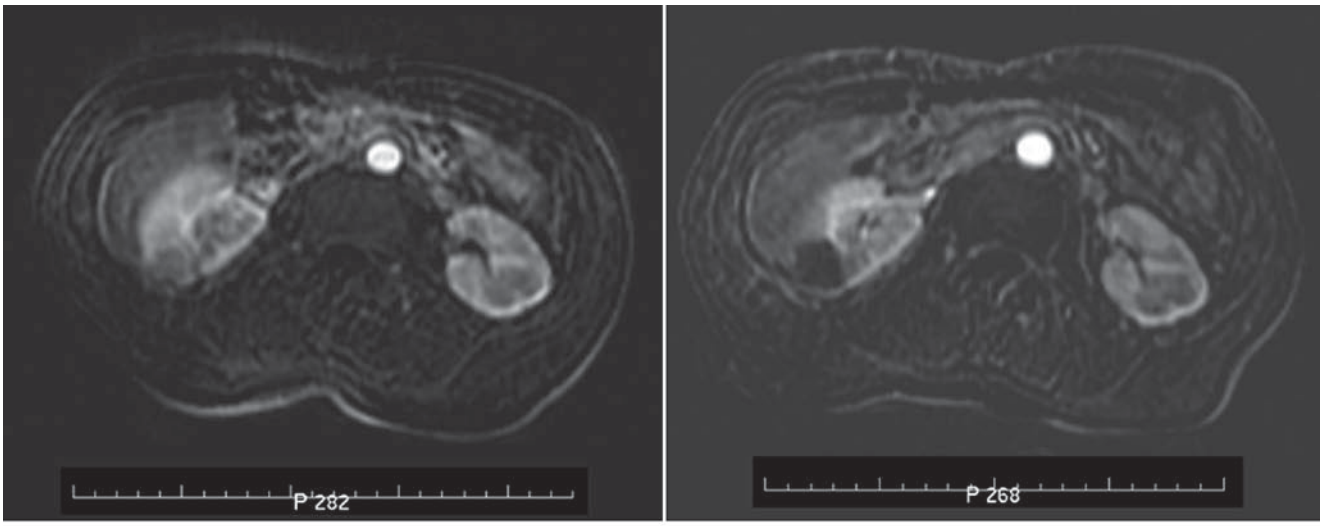

Before HIFU

12 days after HIFU

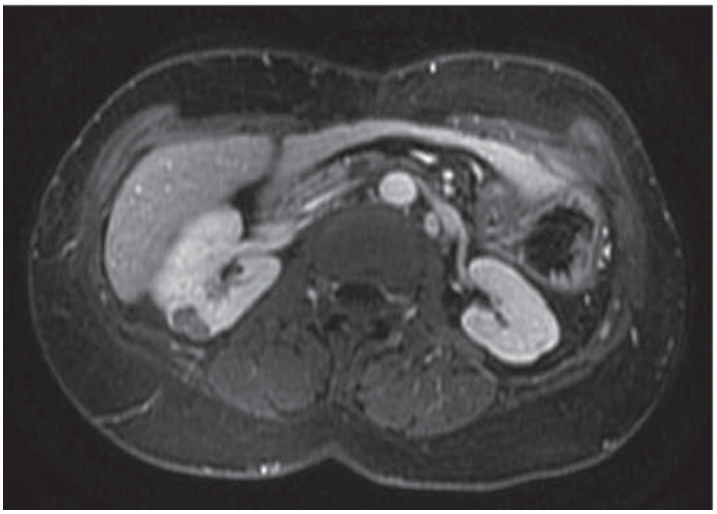

1.5 years after HIFU

Fig. 15.3 Primary *right* renal tumor treated with extracorporeal HIFU

damage was noted to this structure as a result. They concluded that the 18-mm probe could be inserted through a standard port so that effective HIFU could be delivered to a healthy porcine kidney, and that complications were minimal.

Klingler et al[59] have used the laparoscopic HIFU device to treat ten kidneys with solitary renal tumors. In the first two patients with 9-cm tumors, a defined marker lesion was placed prior to laparoscopic radical nephrectomy. In eight patients with a mean tumor size of 22 mm (range, 11–40), the tumor was completely ablated as in curative intent, followed by laparoscopic partial nephrectomy in seven tumors. One patient had post-HIFU biopsies and was followed radiologically. Specimens were studied by detailed and whole-mount histology, including NADH stains. At histological evaluation, both marker lesions showed irreversible and homogeneous thermal damage within the targeted site. Of the seven tumors treated and removed after HIFU, four showed complete ablation of the entire tumor. Two tumors had a 1–3-mm rim of viable tissue immediately adjacent to where the HIFU probe was approximated, and one tumor showed a central area with about 20% vital tissue. There were no intra- or postoperative complications related to HIFU.

In Oxford, the laparoscopic device has been used to treat seven patients with small renal tumors prior to laparoscopic radical nephrectomy. Our experience is similar to that of the Vienna group. The treatment has proven to be safe and by the end of the series effective. Phase II trials are now planned to assess the use of this device in patients with small renal tumors (<3 cm) (Fig. 15.4).

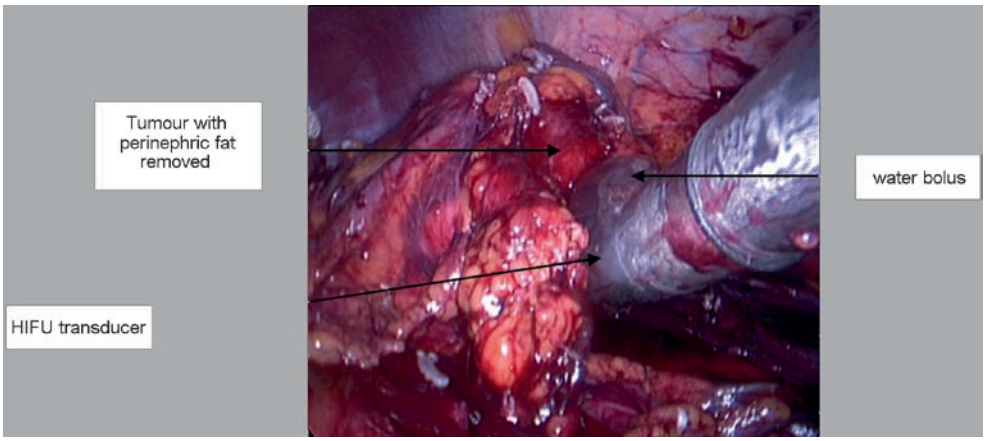

Fig. 15.4 Laparoscopic image showing the probe placement and tumor

Conclusion

HIFU is an exciting prospect for the noninvasive treatment of kidney tumors. The position and size of small renal tumors makes them an ideal target for this treatment. The data to date have shown that it is not straightforward. Targeting and successfully treating an entire tumor consistently has proven to be difficult with rib interaction, perinephric fat, and body habitus suggested as possible reasons for a 30% success rate in the only prospective, curative trial to date. A laparoscopic approach may overcome these problems, and early works suggest that complete ablation is possible; however, this approach is more invasive and will need to be proven to be safer than and as effective as other minimally invasive procedures such as cryoablation and RF.

However, despite mixed results to date, further work is underway, and more clinical trials are proposed with new technology to try and overcome some of the limiting factors. Extracorporeal HIFU remains the only noninvasive option for this growing group of patients and can be performed as a day case. If the success rate can be improved, HIFU would seem to be a reasonable option for many patients in the first instance, with repeat treatments possible or salvage surgery as an option if the treatment proves unsuccessful. If this were the case, a large group of patients would have their kidney cancer cured without ever having to see a knife or a hospital ward, a prospect that continues to drive the research teams forward in an effort to perfect the treatments.

References

1. Wood RW, Loomis AL. The physical and biological effects of high-frequency sound waves of great intensity. *London Edinburgh Dublin Phil Mag J Sci.* 1927;4:417–436
2. Fry WJ, Mosberg WH, Barnard JW, Fry FJ. Production of focal destructive lesions in the central nervous system with ultrasound. *J Neurosurg.* 1954;11:471–478
3. Fry WJ, Barnard JW, Fry FJ, Krumins RF, BJ F. Ultrasonic lesions in the mammalian central nervous system. *Science.* 1955;122:517–518
4. Lele PP. Production of deep focal lesions by focused ultrasound – current status. *Ultrasonics*. 1967;5:105
5. Kennedy JE, Ter Haar GR, Cranston D. High intensity focused ultrasound: surgery of the future? *Br J Radiol.* 2003;76(909):590–599
6. ter Haar G, Clarke RL, Vaughan MG, Hill CR. Trackless surgery using focused ultrasound: technique and case report. *Minimally Invasive Therapy.* 1991;1:13–19
7. Hill CR, ter Haar GR. Review article: high intensity focused ultrasound: potential for cancer treatment. *Br J Radiol.* 1995;68(816):1296–1303
8. Chen L, Rivens I, ter Haar G, Riddler S, Hill CR, Bensted JP. Histological changes in rat liver tumours treated with high-intensity focused ultrasound. *Ultrasound Med Biol.* 1993;19(1):67–74
9. Chen L, ter Haar G, Hill CR, et al Effect of blood perfusion on the ablation of liver parenchyma with high-intensity focused ultrasound. *Phys Med Biol.* 1993;38(11):1661–1673
10. Mason TJ. A sound investment. *Chem Ind*. 1998;878–882
11. Williams AR. *Ultrasound: biological effects and potential hazards*. London: Academic; 1983
12. Hynynen K. The threshold for thermally significant cavitation in dog's thigh muscle in vivo. *Ultrasound Med Biol.* 1991;17(2):157–169
13. Hill CR, Rivens IH, Vaughan MG, ter Haar G. Lesion development in focused ultrasound surgery: a general model. *Ultrasound Med Biol.* 1994;20(3):259–269
14. Wu F, Wang Z, Wang Z, et al Changes in ultrasonic image of tissue damaged by high intensity ultrasound in vivo. *J Acoust Soc Am.* 1998;103:2869
15. Tran BC, Seo J, Hall TL, Fowlkes JB, Cain CA. Microbubble-enhanced cavitation for noninvasive ultrasound surgery. *IEEE Trans Ultrason Ferroelectr Freq Control.* 2003;50(10):1296–1304
16. Wu F, Chen WZ, Bai J, et al Pathological changes in human malignant carcinoma treated with high-intensity focused ultrasound. *Ultrasound Med Biol.* 2001;27(8):1099–1106
17. Rendon RA, Gertner MR, Sherar MD, et al Development of a radiofrequency based thermal therapy technique in an in vivo porcine model for the treatment of small renal masses. *J Urol.* 2001;166(1):292–298
18. Michaels MJ, Rhee HK, Mourtzinos AP, Summerhayes IC, Silverman ML, Libertino JA. Incomplete renal tumor destruction using radio frequency interstitial ablation. *J Urol.* 2002;168(6):2406–2409; discussion 2409–2410
19. Matlaga BR, Zagoria RJ, Woodruff RD, Torti FM, Hall MC. Phase II trial of radio frequency ablation of renal cancer: evaluation of the kill zone. *J Urol.* 2002;168(6):2401–2405
20. Goldberg SN, Gazelle GS, Compton CC, Mueller PR, Tanabe KK. Treatment of intrahepatic malignancy with radiofrequency ablation: radiologic-pathologic correlation. *Cancer.* 2000;88(11):2452–2463

21. Marcovich R, Aldana JP, Morgenstern N, Jacobson AI, Smith AD, Lee BR. Optimal lesion assessment following acute radio frequency ablation of porcine kidney: cellular viability or histopathology? *J Urol.* 2003;170(4 Pt 1):1370–1374
22. Neumann RA, Knobler RM, Pieczkowski F, Gebhart W. Enzyme histochemical analysis of cell viability after argon laser-induced coagulation necrosis of the skin. *J Am Acad Dermatol.* 1991;25(6 Pt 1):991–998
23. Anderson JK, Baker M, Jaffers O, Pearle MS, Lindberg GL, Cadeddu JA. Time course of nicotinamide adenine dinucleotide diaphorase staining after renal radiofrequency ablation influences viability assessment. *J Endourol.* 2007;21(2):223–227
24. Corwin TS, Lindberg G, Traxer O, et al Laparoscopic radiofrequency thermal ablation of renal tissue with and without hilar occlusion. *J Urol.* 2001;166(1):281–284
25. Gettman MT, Lotan Y, Corwin TS, et al Radiofrequency coagulation of renal parenchyma: comparison of effects of energy generators on treatment efficacy. *J Endourol.* 2002;16(2):83–88
26. Crowley JD, Shelton J, Iverson AJ, Burton MP, Dalrymple NC, Bishoff JT. Laparoscopic and computed tomography-guided percutaneous radiofrequency ablation of renal tissue: acute and chronic effects in an animal model. *Urology.* 2001;57(5):976–980
27. Stern JM, Anderson JK, Lotan Y, Park S, Cadeddu JA. Nicotinamide adenine dinucleotide staining immediately following radio frequency ablation of renal tumors-is a positive stain synonymous with ablative failure? *J Urol.* 2006;176(5):1969–1972; discussion 1972
28. Kennedy JE. High-intensity focused ultrasound in the treatment of solid tumours. *Nat Rev Cancer.* 2005;5(4):321–327
29. Illing RO, Leslie TA, Kennedy JE, Calleary JG, Ogden CW, Emberton M. Visually directed high-intensity focused ultrasound for organ-confined prostate cancer: A proposed standard for the conduct of therapy. *BJU Int.* 2006;98(6):1187–1192
30. Hynynen K, Pomeroy O, Smith DN, et al MR imaging-guided focused ultrasound surgery of fibroadenomas in the breast: a feasibility study. *Radiology.* 2001;219:176–185
31. Hynynen K, Darkazanli A, Unger E, Schenck JF. MRI-guided noninvasive ultrasound. *Med Phys.* 1993;20(1):107–115
32. ter Harr G, Rivens I, Chen L, Riddler S. High intensity focused ultrasound for the treatment of rat tumours. *Phys Med Biol.* 1991;36(11):1495–1501
33. Vaughan MG, ter Haar GR, Hill CR, Clarke RL, Hopewell JW. Minimally invasive cancer surgery using focused ultrasound: a preclinical, normal tissue study. *Br J Radiol.* 1994;67:267–274
34. Chapelon JY, Margonari J, Theillere Y, et al Effects of high-energy focused ultrasound on kidney tissue in the rat and the dog. *Eur Urol.* 1992;22(2):147–152
35. Oosterhof GON, Cornel EB, Smits GAHJ, Debruyne FMJ, Schalken JA. Influence of high-intensity focused ultrasound on the development of metastases. *Eur Urol.* 1997;32:91–95
36. Kennedy JE, Wu F, Ter Haar GR, et al High-intensity focused ultrasound for the treatment of liver tumours. *Ultrasonics.* 2004; 42(1–9):931–935
37. Wu F, Wang ZB, Chen WZ, et al Extracorporeal focused ultrasound surgery for treatment of human solid carcinomas: early Chinese clinical experience. *Ultrasound Med Biol.* 2004;30(2):245–260
38. Leon-Villapalos J, Kaniorou-Larai M, Dziewulski P. Full thickness abdominal burn following magnetic resonance guided focused ultrasound therapy. *Burns.* 2005;31(8):1054–1055
39. Wu F, Chen W, Bai J. Effect of high-intensity focused ultrasound on patients with hepatocellular cancer – preliminary report. *Chin J Ultrasonog.* 1999;8(4):213–216
40. Chaussy C, Thuroff S. High-intensity focused ultrasound in prostate cancer: results after 3 years. *Mol Urol.* Fall 2000;4(3):179–182
41. Madersbacher S, Kratzik C, Szabo N, Susani M, Vingers L, Marberger M. Tissue ablation in benign prostatic hyperplasia with high-intensity focused ultrasound. *Eur Urol.* 1993;23(suppl 1):39–43
42. Jemal A, Siegel R, Ward E, Murray T, Xu J, Thun MJ. Cancer statistics, 2007 *CA Cancer J Clin.* 2007;57(1):43–66
43. Luciani LG, Cestari R, Tallarigo C. Incidental renal cell carcinoma-age and stage characterization and clinical implications: study of 1092 patients (1982–1997). *Urology.* 2000;56(1):58–62
44. *Cancer Research UK*. UK Kidney Cancer Statistics 2001; 2006
45. Fergany AF, Hafez KS, Novick AC. Long-term results of nephron sparing surgery for localized renal cell carcinoma: 10-year followup. *J Urol.* 2000;163(2):442–445
46. Stein RJ, Kaouk JH. Renal cryotherapy: a detailed review including a 5-year follow-up. *BJU Int.* 2007;99(6):1265–1270
47. McDougal WS. Radiofrequency ablation of renal cell carcinoma. *BJU Int.* 2007;99(6):1271–1272
48. Marberger M. Ablation of renal tumours with extracorporeal high-intensity focused ultrasound. *BJU Int.* 2007;99(6):1273–1276
49. Linke CA, Carstensen EL, Frizzell LA, Elbadawi A, Fridd CW. Localized tissue destruction by high-intensity focused ultrasound. *Arch Surg.* 1973;107(6):887–891
50. Adams JB, Moore RG, Anderson JH, Strandberg JD, Marshall FF, Davoussi LR. High-intensity focused ultrasound ablation of rabbit kidney tumors. *J Endourol.* 1996;10(1):71–75
51. Watkin NA, Morris SB, Rivens IH, ter Haar GR. High-intensity focused ultrasound ablation of the kidney in a large animal model. *J Endourol.* 1997;11(3):191–196
52. Vallancien G, Chartier-Kastler E, Harouni M, Chopin D, Bougaran J. Focused extracorporeal pyrotherapy: experimental study and feasibility in man. *Semin Urol.* 1993;11(1):7–9
53. Marberger M, Schatzl G, Cranston D, Kennedy JE. Extracorporeal ablation of renal tumours with high-intensity focused ultrasound. *BJU Int.* 2005;95(suppl 2):52–55
54. Wu F, Wang ZB, Chen WZ, Bai J, Zhu H, Qiao TY. Preliminary experience using high intensity focused ultrasound for the treatment of patients with advanced stage renal malignancy. *J Urol.* 2003; 170(6 Pt 1):2237–2240
55. Hacker A, Michel MS, Marlinghaus E, Kohrmann KU, Alken P. Extracorporeally induced ablation of renal tissue by high-intensity focused ultrasound. *BJU Int.* 2006;97(4):779–785
56. Illing RO, Kennedy JE, Wu F, et al The safety and feasibility of extracorporeal high-intensity focused ultrasound (HIFU) for the treatment of liver and kidney tumours in a Western population. *Br J Cancer. Oct 17*. 2005;93(8):890–895
57. Shalhav A. *High intensity focused ultrasound renal tissue ablation: a laparoscopic porcine model*. Chicago: Department of Surgery, University of Chicago; 2005
58. Paterson R, Barret E, Siqueira T, et al Laparoscopic partial kidney ablation with high intensity focused ultrasound. *J Urol.* 2003;169(1): 347–351
59. Klingler HC, Susani M, Seip R, Mauermann J, Sanghvi N, Marberger MJ. A novel approach to energy ablative therapy of small renal tumours: laparoscopic high-intensity focused ultrasound. *Eur Urol.* 2008;53(4):810–816; discussion 817–818

Prostate High-Intensity Focused Ultrasound

16

Hashim Uddin Ahmed, Caroline Moore, Manit Arya, and Mark Emberton

Introduction

The management of localized prostate cancer has centered on surveillance or radical therapy such as prostatectomy or radiotherapy. Furthermore, because of the reduction in disease severity as a result of early detection, it is quite likely that the small absolute risk reduction – of approximately 5% over 10 years that has been demonstrated in a randomized controlled trial comparing surgery with watchful waiting – in men with low-to-moderate risk disease is likely to be reduced even further.[1] The advent of active surveillance with selective delayed intervention is also very likely to make this difference in mortality between surveillance and radical therapy less significant. As radical treatments carry significant morbidity with operative complications (wound infection, hemorrhage, and hospital stay) and can cause significant long-term toxicity (incontinence, impotence, and rectal problems), there has been a demand to develop ablative therapies that attempt to reduce treatment burden while retaining cancer control and avoiding the psychological morbidity associated with surveillance. Although a number of minimally invasive therapies have been described, e.g., cryosurgery, high-intensity-focused ultrasound (HIFU), radiofrequency ablation, and photodynamic therapy, each one is at a different stage in its evaluation and diffusion into clinical practice.

Basic Science

Ultrasound refers to mechanical vibrations above the threshold of human hearing (16 kHz) and has the ability to interact with tissue to produce biological changes. Ultrasound is generated by applying an alternating voltage across a piezoelectric material such as lead zirconate titanate. These materials oscillate at the same frequency as the alternating current causing ultrasound wave that can propagate through tissues. This in turn causes alternating cycles of increased and reduced pressure (compression and rarefaction, respectively). Diagnostic ultrasound usually uses frequencies in the range of 1–20 MHz, but therapeutic HIFU uses frequencies of 0.8–3.5 MHz with delivery of energy within the ultrasound beams that are several times greater than the energy levels within diagnostic ultrasound (Fig. 16.1). Therapeutic ultrasound can be conveniently divided into two broad categories:

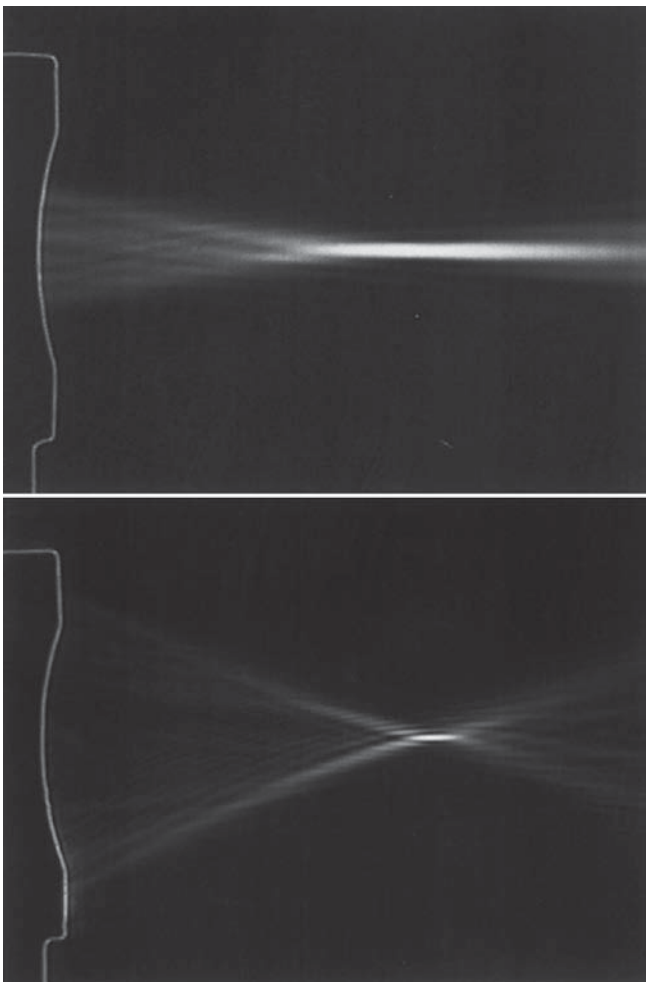

Fig. 16.1 Schelieren images of the ultrasound transducer during imaging and HIFU therapy modes. During the HIFU mode, the entire transducer crystal surface is excited with RF high voltage to generate a sharp and narrow beam for treatment of the tissue. During imaging, ultrasound transducer uses only the center segment of the crystal to generate a long and uniform beam. From Sanghvi et al.[2] Copyright 2009, with permission from Elsevier

P. Dasgupta et al. (eds.), *New Technologies in Urology,*
DOI: 10.1007/978-1-84882-178-1_16, © Springer-Verlag London Limited 2010

"low" intensity (0.125–3 W/cm^2) and "high" intensity (>5 W/cm^2). The former can stimulate normal physiological responses to injury and accelerate other processes such as the transport of drugs across the skin. The high-intensity ultrasound can selectively destroy tissue if delivered in a focused manner.[3]

HIFU relies on the physical properties of ultrasound, which allows it to be brought into a tight focus, using an acoustic lens, a bowl-shaped transducer, or an electronic-phased array. As ultrasound propagates through a tissue, zones of high and low pressure are created. When the energy density at the focus is sufficiently high (during the high-pressure phase), tissue damage occurs. The volume of ablation (or lesion) following a single HIFU pulse or exposure is small and varies according to transducer characteristics. It is typically cigar shaped with dimensions in the order of 1–3 mm (transverse) × 8–15 mm (along beam axis). To ablate larger volumes of tissue for the treatment of solid cancers, these lesions are placed adjacent to each other. The two predominant mechanisms of tissue damage are by the conversion of mechanical energy into heat and "inertial cavitation." If tissue temperatures are raised above 56°C, then immediate thermal toxicity can occur, provided the temperature is maintained for at least 1 s. This will lead to irreversible cell death from coagulative necrosis. In fact, during HIFU, the temperatures achieved are much greater than this, typically above 80°C, so even short exposures can lead to effective cell death. Inertial cavitation occurs at the same time, but is neither as controllable nor predictable. It occurs because of the alternating cycles of compression and rarefaction. At the time of rarefaction, gas can be drawn out of solution to form bubbles, which then collapse rapidly. The mechanical stress and a degree of thermal injury induce cell necrosis[4] (Fig. 16.2). Histologically, the tissue changes that occur are homogeneous coagulative necrosis, with an inflammatory response that follows, leading to the formation of granulation tissue – indicated by the presence of immature fibroblasts and new capillary formation – at the periphery of the necrotic area at about a week after treatment. Polymorphonuclear leukocytes migrate deep into the treated tissue, and then at 2 weeks, the boundary of the treated region is replaced by proliferative repair tissue. The repair process has not been investigated in detail at the cellular level beyond this time, but imaging techniques using contrast-enhanced ultrasound or magnetic resonance imaging show an eventual shrinkage of treated volumes, indicating that the necrotic area has been replaced by fibrous scar tissue.

The placement of the small HIFU lesions requires precise planning for an entire tumor to be ablated reliably. Furthermore, patient movement can lead to areas of viable malignant tissue remaining after treatment, and even in ideal situations, other factors can prevent a successful treatment. The most important of these include the heat-sink effect and calcification. The heat-sink effect relates to one area that overheats in the HIFU pulses pathway and thus prevents adequate ultrasound propagation to the targeted area; such a phenomenon occurs if the time between HIFU pulses is inadequate for tissue cooling or if an area is high in water content, such as a cyst. In addition, highly vascularized tissues might be more resistant to thermal ablation owing to the heat-sink effect of their blood supply. Calcification simply leads to reverberation and shielding of the targeted area from parts of the HIFU pulse, leading to inadequate heating of the tissue.

Transrectal Devices for Treating the Prostate

Currently, there are two commercially available transrectal devices that can treat the prostate gland – the Ablatherm®

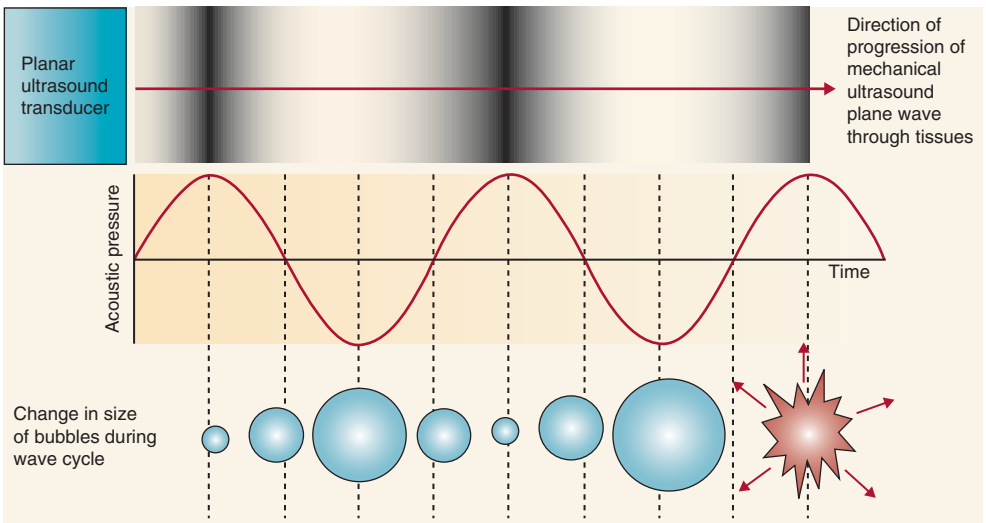

Fig. 16.2 Inertial cavitation. An ultrasound wave progresses through tissue causing alternating cycles of increase and decreased pressure. Gas is drawn out during rarefaction to create bubbles that can collapse and release energy to raise local temperature at the microscopic level. From Kennedy.[4] With permission from Nature Publishing Group

device (Edap-Technomed, Lyon, France) and the Sonablate® 500 (Focus Surgery, Indianapolis, IN).

Ablatherm

The Ablatherm® device until very recently had separate imaging (7 MHz) and therapy transducers (3 MHz), which had a fixed focal length of 4 cm. Prostate imaging during treatment was not possible but performed between treatment zones by inserting the imaging transducer through the therapeutic transducer. The latest modification to the Ablatherm® combines treatment and planning probes so that visual feedback is possible during treatment. However, because the Ablatherm® uses algorithm-driven treatment protocols with preset energy levels, individual pulse-energy levels cannot be modified by the operator. Other features include the incorporation of the probe into a table that holds the pump and cooling mechanism and on which the patient is placed in the right lateral position. Treatment is done to each lobe in turn and performed anterior to posterior within a complete block that incorporates the full anterior–posterior height of the prostate. A number of safety features that monitor the rectal-wall energy deposition are in place to prevent damage to this area. Many centers that use the Ablatherm® combine transurethral resection of the prostate (TURP) or bladder neck incision to reduce gland size and stricture formation.

Sonablate 500

The Sonablate® system consists of a rectal probe (containing the transducer) with an operating frequency of 4 MHz that attempts to optimize the combined imaging and therapy roles of the transducer (Figs. 16.3 and 16.4). This has the advantage of allowing visualization of treatment effect, following each pulse of the treatment cycle. Degassed water is pumped through the system and is chilled to temperatures of 17–20 °C to prevent rectal-wall injury by heat buildup. Rectal-wall monitoring features are also in place with this probe. Treatment planning, execution, and monitoring are controlled using a user interface that allows the surgeon to precisely target the area of treatment, adjust the focal length of the transducer (currently 3, 4, or 4.5 cm), and alter the power intensity delivered to each focal zone individually (Fig. 16.5). Rather than a protocol-driven treatment, the power intensity of each pulse is guided by gray-scale changes within the targeted area that represent steam, so that greater certainty about cell kill is obtained.[5] In other words, the power is raised to obtain what we have deemed "Uchida" changes (or gray-scale "popcorning"), named after the Japanese urologist who pioneered work using the Sonablate 500. The Sonablate 500 delivers

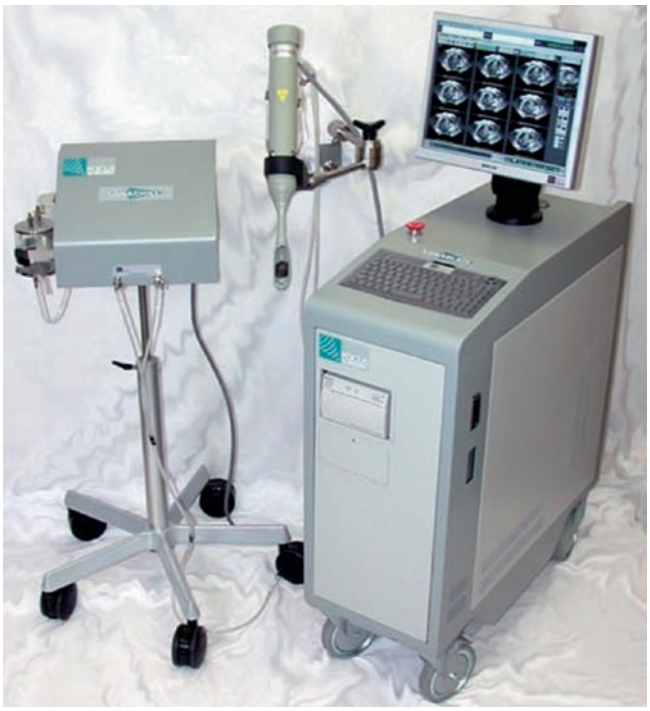

Fig. 16.3 The Sonablate 500 transrectal HIFU device

Fig. 16.4 The Sonablate 500 transrectal HIFUprobe and transducer

treatment to the prostate in three separate blocks. The anterior portion of the prostate is treated initially, followed by midzone, and then posterior gland (Fig. 16.6). The probe requires adjustment between each of these blocks. The posterior block is always treated using the 3-cm focal length and with lower energy levels. Within each zone, multiple overlapping lesions are created to enhance ablation (Fig. 16.7).

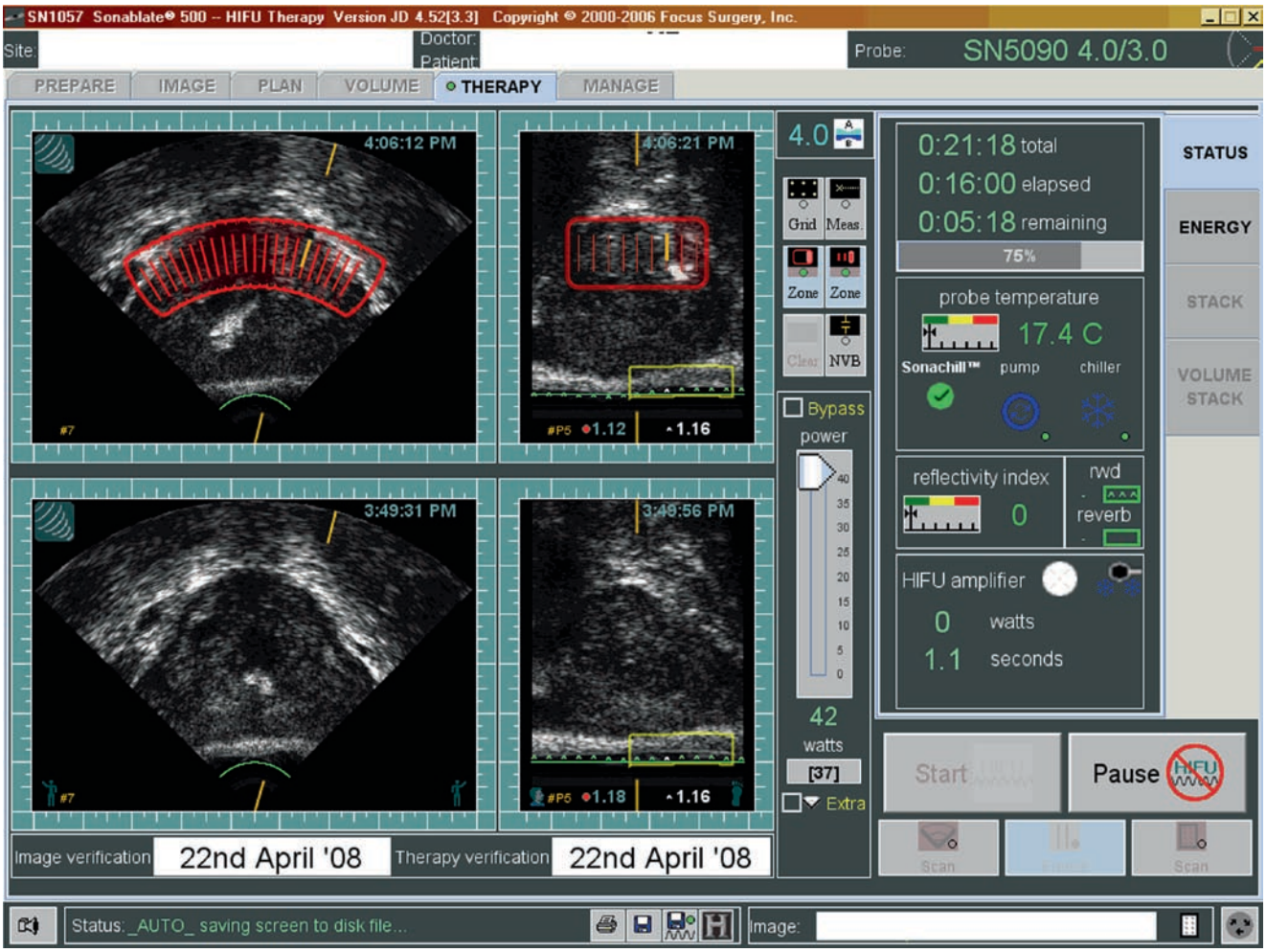

Fig. 16.5 Screen capture demonstrating what the operator sees during a Sonablate 500 treatment. The *lower* two images demonstrate pretreatment axial and sagittal images whereas the *upper* two images show the treatment with continual updates in images. This live comparison to the prostate prior to energy delivery allows adjustments to be made to energy on a pulse by pulse basis

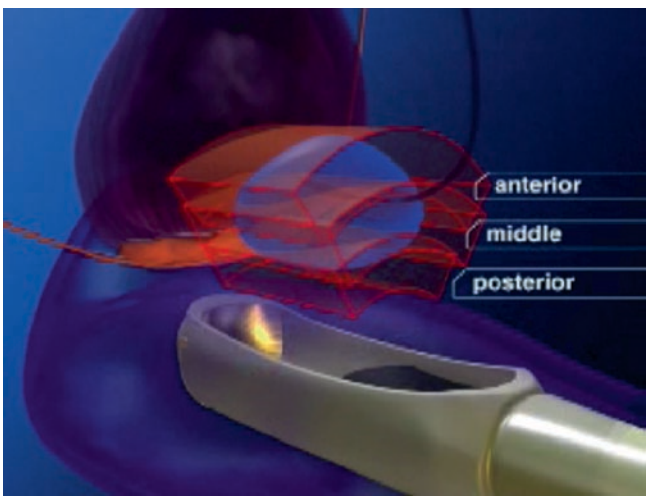

Fig. 16.6 Diagrammatic representation of the Sonablate 500 within the rectum and the treatment blocks, anterior, posterior, and middle as depicted

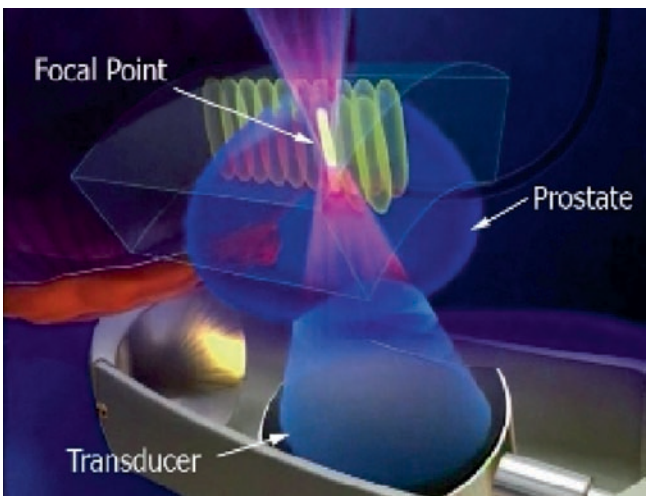

Fig. 16.7 Diagrammatic representation each HIFU pulse delivered to the anterior block. Rows of pulses adjacent to each other are used to ablate larger areas of prostate

HIFU Treatment of Benign Prostatic Hyperplasia

Historically, when extremes of care (surgery vs. no treatment) have been the only therapeutic options available in treating a condition, a predictable result can be observed. Within urology, there are several examples of this, but perhaps the best relates to the trend in relation to the management of benign prostatic hyperplasia (BPH). Until recently, there were only two options for a man with lower urinary tract symptoms, surgery or watchful waiting. Today, a man with lower urinary tract symptoms is very likely to reject both of these options and instead opt for either medical therapy or one of the minimally invasive approaches to the disease.[6] The trade-off that men make is acceptance of a slight reduction in efficacy in exchange for greater convenience and a better toxicity profile.[7]

BPH is a common condition in which the choice of treatment has been between watchful waiting and surgery. Surveillance carries the risk of progression of symptoms. Over the last 50 years, TURP has become the "gold-standard" for the surgical management of BPH. It can result in a significant clinical improvement in just over 90% of those who have severe symptoms.[8] However, there is need for general or regional anesthesia, postoperative catheterization, and a hospital stay of 2–3 days. Alongside a morbidity of one in five that includes transfusion (2–5%), erectile dysfunction (5%), urethral/bladder neck stricture, urinary incontinence (0.4–1.3%), and retrograde ejaculation (60–70%), TURP is not an easy alternative to surveillance or medication. Furthermore, the results in terms of symptomatic improvement following TURP for those men who have mild-to-moderate symptoms are less significant, with just below 80% showing improvement. At present, medical management with five alpha reductase inhibitors and alpha blockers have evolved to achieve a central role in the management of BPH, so much so that surgery is reserved in those that fail medical management or those that present with acute urinary retention. For this group of men, alternatives to the traditional TURP have been sought. HIFU has been investigated for use in BPH. The most recent studies that have used HIFU in treating BPH are summarized in Table 16.1.[2,9–13] Although HIFU did show improvements in urodynamic and symptomatic parameters, they were slow to materialize and of short duration with other significant complications. Importantly, a significant proportion of men, 5–44%, required a secondary TURP because of treatment failure within 1 or 2 years. Outcomes on impotence and incontinence, and other morbidity outcome data were poorly reported in these series. Consequently, using HIFU for BPH has not been popular, especially since new improved energy modalities, including the traditional TURP, have been shown to be far better. Other heat-based modalities, such as microwave therapy, and new laser energies to vaporize or resect prostate tissue have also come to the fore.

Table 16.1 Series demonstrating outcomes from use of HIFU in treating BPH

Study	*N*	Mean follow-up (months)	Prostate volume change	IPSS/AUA scores (%)	*Q* max (%)	Catheterization (days)	Secondary TURP (%)	Impotence	Incontinence	Other side effects
Lu et al (2007)	23	12	65.0–38.1 mL, $p < 0.05$	Improved ($p < 0.01$)	+286	3–19		–	–	Recurrent urinary retention ($n = 2$) and urethrorectal fistula ($n = 1$)
Madersbacher et al[9]	80	41.3	–	−53	+30% at 1 year +12% at 4 years	–	44	–	–	–
Schatzl et al[10]	20	24	–	−48	+22	–	15	–	–	–
Sullivan et al[11] (multicenter)	46	12	–	−35 to 59.	+30		24			Recatheterization (16%); hematospermia (13%); hematuria (9%); acute retention (4%); perineal pain (11%); epididymitis (9%)
Nakamura et al[12]	22	6	–	−56	+54	–	–	–	–	Transient urinary retention (18%); hematuria (23%); hematospermia (36%)
Sanghvi et al[2] (multicenter)	62	6	–	−55	+67	5	5	–	–	Retention (39%); hematospermia (7%); epididymitis (3%); hematuria (8%); dysuria (2%); UTI (1.5%)

HIFU in the Treatment of Primary Localized Prostate Cancer

The use of HIFU for the treatment of localized prostate cancer has until recently been nested within a small number of enthusiasts. They have refined the indications, developed the technology, and disseminated their early experience. Fourteen series have so far reported outcome data, with four using the Sonablate 500 and the remainder using the Ablatherm device.[14–28] There was double reporting of a number of series, but this was not always made explicit in the papers (Table 16.2). The number of patients treated ranged from 30 to 402, and mean follow-up ranged from 11 to 76.8 months. Morbidity data were inconsistently reported (Table 16.3). Incontinence rates were 0.5–15.4%, and impotence rates ranged from 13 to 53%. These did not always grade the incontinence, and where grading was used, these differed and were therefore not comparable across series. Definitions of impotence and potency had similar problems. Fistulae rates ranged from 0 to 2%, although most of the fistulae were in the early experience with prototype machines. Other symptoms were inconsistently and selectively reported in most series. Neoadjuvant hormonal therapy was primarily used for cytoreduction of gland size but represented a possible confounding factor for cancer-control rates. D'amico risk stratification was reported in six series, while one series categorized all patients as high risk using another definition (stage ≥T3a, Gleason score 8–10, PSA > 20 ng/mL). Biochemical outcome was reported using either mean PSA values at longest follow-up, PSA nadir values (<1, <0.5, <0.2, <0.3, and 0.1 ng/mL), old American Society for Therapeutic Radiology and Oncology (ASTRO) criteria, and ASTRO Phoenix criteria (validated for radiotherapy only). Biopsies were not carried out in all men in all series, but only one did not report on biopsy data. Most series included HIFU retreatments within the overall outcome data with the mean HIFU sessions ranging from 1.17 to 1.4 (Table 16.2). Second HIFU therapies were regarded as part of the treatment protocol rather than treatment failures per se, since one of the advantages of HIFU has been purported to be its repeatability, sometimes up to three times for men who have residual prostate cancer.

The exact follow-up protocol to be used and criteria for success or failure are yet to be ascertained in HIFU therapy of prostate cancer. A number of groups have demonstrated that gadolinium contrast-enhanced MRI may be of use in the early determination of cancer control. Areas of necrosis are obvious through lack of enhancement, and areas of residual undertreated tissue can be shown as early as 2 weeks after treatment with good correlation to biochemical outcome (Figs. 16.8 and 16.9). The exact role for contrast-enhanced MRI in follow-up of patients after HIFU is yet to be determined.[31,32]

The natural history of prostate cancer prevents the use of mortality as an outcome measure in most short- to medium-term reports. As a result, surrogates in the form of biochemical failure have emerged. However, the optimal definition of biochemical failure is far from clear. Indeed, because of this lack of certainty, the reporting of minimally invasive modalities has shown little consistency. The variability in biochemical outcome is demonstrated by the differing PSA nadirs used to define successful outcome with groups using any one of PSA <1, <0.5, 0.4, <0.3, <0.2, and <0.1 ng/mL. A PSA of <0.2 ng/mL has evidence within radical prostatectomy series demonstrating its effectiveness to predict long-term outcomes, but such evidence is insufficient for HIFU.[33] A number of series use three successive PSA rises to define treatment failure according to the old ASTRO criteria to define biochemical failure after radiotherapy.[34] This has its own drawbacks since the old ASTRO criteria are not appropriate for evaluating PSA elevations sooner than 3–5 years after treatment and were only developed for use in radiotherapy. Indeed, with the emergence of the ASTRO Phoenix criteria (nadir + 2 ng/dL),[35] the old definition is in itself questionable, although some HIFU series have attempted to use this new definition. The Phoenix definition of failure is being used by the Federal Drug Administration (FDA) as the key determinant of success against which HIFU will be assessed in FDA Phase II/III trials in the United States, so this may need to be adopted as a reasonable standard for the foreseeable future.

Equally, morbidity data are reported poorly. Most series do not define incontinence or impotence, while the majority show inconsistent reporting of other perceived minor complications. As the premise of minimally invasive ablative therapies is to reduce the morbidity of therapy for men with localized prostate cancer while retaining cancer control and thus overcome the therapeutic dilemma that such men presently face, such lack of open reporting regarding morbidity data is disappointing. Although such data are difficult within the constraints of retrospective case series, it is important that a minimum data set is agreed on for reporting complications.

Assessing health technology outcomes is difficult because of the hardware and software developments that occur, as well as improved treatment delivery from overcoming the initial learning curve. For this reason, comparison with other series using transrectal HIFU and other modalities is problematic, since not all publications make such changes explicit. The impact of these changes, as well as the introduction of rectal cooling, is evident by a reduction in the rectoprostatic fistula rate. It was not always clear, especially from the HIFU series, whether software modifications occurred and to what proportion of patients it was applied to. Using the Sonablate® 500, our own group has demonstrated that changing power levels in a real-time fashion so as to visualize gray-scale changes (so-called "Visually directed

Table 16.2 Biochemical and biopsy outcome in series reporting treatment of localized prostate cancer using HIFU

Study	Device	*N*	D'amico risk groups (unless otherwise specified)	Neoadjuvant hormonal therapy (%)	Follow-up (months) (mean/median)	Biochemical Control (PSA, ng/mL)	Positive biopsy
Challacombe et al[28]	Ablatherm	28 (pre-HIFU TURP)	Low 21.4%; intermediate 57.2%; high 21.4%	35.7	25	75% (PSA >0.5); 46.4% (Phoenix ASTRO)	Not done
Ahmed et al[29]	Sonablate 500	172 (1.0 sessions)	Low 28%; intermediate 38%; high 34%	29	12	92.4% No evidence of residual disease 61% (PSA <0.2) 83% (PSA <0.5)	7.6%
Mearini et al[15]	Sonablate 500	163 (1.17 sessions)	Low 49%; intermediate 29%; high 9%	0	23.8	78.2% (Phoenix) Median PSA nadir 0.15 70.3% (PSA <0.4)	33.9%
Uchida et al[16]	Sonablate 200/500	63 (1.2 HIFU sessions)	Low 35%; intermediate 41%; high 24%	0	22	75% (old ASTRO criteria)	13%
Uchida et al[17]	Sonablate 200/500	181 (1.2 HIFU sessions)	Low 29%; intermediate 45%; high 26%	52	18	84, 80 and 78% (at 1, 3, and 5 years, respectively [old ASTRO]	Not reported
Blana et al[18]	Ablatherm	163 (first 47 HIFU only; 116 pre-HIFU TURP) (1.2 sessions)	Low 51.5%; intermediate 48.5%	36.8	57.6	75% (Phoenix) 86% (PSA <1.0) 64% (PSA <0.2)	7.3% ("vital prostate cancer"
Misrai et al (2008)	Ablatherm	119 71% pre-HIFU TURP) (1.4 sessions)	Low 55%; intermediate 42%; high 3%	0	46.8	56.3% (Phoenix) Estimated 30% 5 years	65%
Blana et al[25]	Ablatherm	140 (1.3 HIFU sessions)	Low 51.4%; intermediate 48.6%	16	76.8	68.4% (PSA <0.5); 66 and 59% at 5 and 7 years (Phoenix ASTRO)	13.6%
Poissonnier et al[26]	Ablatherm	227 (pre-HIFU TURP) (1.4 HIFU sessions)	Not reported	33.5	27	84% (PSA <0.5); 66% Disease free survival at 5 years[b]	14%
Ficarra et al[27]	Ablatherm	30 (pre-HIFU TURP)	High risk 100%[a]	100 (3 years)	12	90% (PSA <0.3); 100% (PSA <1)	23%
Vallencien et al (2004)	Ablatherm	30 (pre-HIFU TURP)	Not specified	Not specified	20	Mean PSA 0.9	14%
Blana et al[21]	Ablatherm	146 (1.17 HIFU sessions)	Not specified	0	22	92% (PSA <1); 83% (PSA <0.5); 56% (PSA <0.1)	7%
Thuroff et al[22]	Ablatherm	402 (1.5 HIFU sessions)	Low 28%; intermediate 48%; high 23.6%	0	11	Median PSA 0.6; mean PSA 1.8	13%
Chaussy and Thuroff[24]	Ablatherm	271 (96 HIFU only; 175 pre-HIFU TURP)	Not available	Not available	19	80–84% (old ASTRO)	29–34%
Gelet et al[30]	Ablatherm	102	Not specified	Not available	19	66% (three consecutive increases in PSA + velocity >0.75/year or positive biopsy); 80–84% (old ASTRO)	25%

[a]Clinical stage of ≥T3a or Gleason score 8–10, or total PSA >20 ng/mL
[b]Any positive biopsy or a PSA > 1 ng/mL with three consecutive rises

Table 16.3 Morbidity outcome in series reporting treatment of localized prostate cancer using HIFU

Study	Complications			
	Incontinence	Erectile dysfunction	Fistulae (%)	Other
Challacombe et al[28]	0% (pad-free)	50%	0	Retention 3.5%; stricture 7.1%
Ahmed et al[29]	7.0% (Grade 1, no pads) 0.6% (grade 3)	70% (sufficient for penetrative sex) IIEF-15 scores at 0, 3, 6, 9, and 12 months: 33.8, 18.1, 39.1, 23.9 and 28.1	0	Stricture (14.6% suprapubic catheter; 44% urethral catheter); UTI/dysuria (23.5%); epididymitis 7.6%; mild-moderate debris/dysuria in all for 4–6 weeks
Mearini et al[15]	16% Mild, mixed; 0.6% Grade 3	IIEF decreased from 16 to 12	0.6	Urethral stricture (15%)
Uchida et al[16]	2% Grade 1	17% (of 34 "sexually active" prior to treatment)	2	All had transitory (2 months) frequency, urgency, difficulty urination; Stricture 24%
Uchida et al[17]	0.5% (Grade 1)	13% ("erectile dysfunction")	1	TURP 0.5%; stricture 22%; epididymitis 6%
Blana et al[18]	6.1% (Grade 1); 1.8% (grade 2); 0 (grade 3)	55.3% (erectile function sufficient for intercourse)	0	Bladder neck stricture/necrotic tissue (requiring surgery) 24.5%; UTI (7.8%); pelvic pain (3.7%)
Misrai et al (2008)	Not reported	Not reported	Not reported	Not reported
Blana et al[25]	5.8% Grade 1. No grade 2/3 incontinence.	53%	0.6	Most had transient urgency and frequency; UTI 4%; TURP/bladder neck incision 11.7%; perineal discomfort 1.4%
Poissonnier et al[26]	12% Grade 1–2; 1% Grade 3	39%	0	Stricture 12%; UTI 2%; hematuria 0.5%; perineal pain 3%; urgency 5%
Ficarra et al[27]	7%	Not reported	0	UTI 16%; stricture 10%
Vallencien et al (2004)	3%	32%	0	Acute urinary retention 6%; urinary infection 10%; Transient hematuria 66%; transient urgency 50%
Blana et al[21]	6% (5% Grade I, 0.7% grade II)	43%	0	UTI 7%; urinary obstruction 14%; pelvic pain 6%
Thuroff et al[22]	10.6% Grade 1; 2.5% grade 2; 1.5% grade 3	Not evaluable	1	UTI 13.5%; retention 8.6%; urethral stricture 3.6%
Chaussy and Thuroff[24]	15.4% pre-HIFU TURP; 6.9% HIFU only	Not reported	Not reported	UTI (47.9% pre-HIFU TURP vs. 11.4% HIFU only)
Gelet et al[23]	Not available	Not available	Not available	Not available

HIFU") within each focal-treatment zone leads to significantly lower PSA levels postoperatively in the primary setting.[36] This was the first attempt at standardizing HIFU treatment.

Another difficulty in comparing HIFU with other treatments for localized prostate cancer is best illustrated by examining the demographic features of published trials. Most HIFU reports include patients in their late seventies and mid-eighties, as the technology was initially used on men who were not suitable for other radical therapies. Such heterogeneity makes the interpretation of disease-free survival and overall survival between studies difficult. This group may benefit least from treatment and suffer a greater amount of morbidity from ablative techniques.

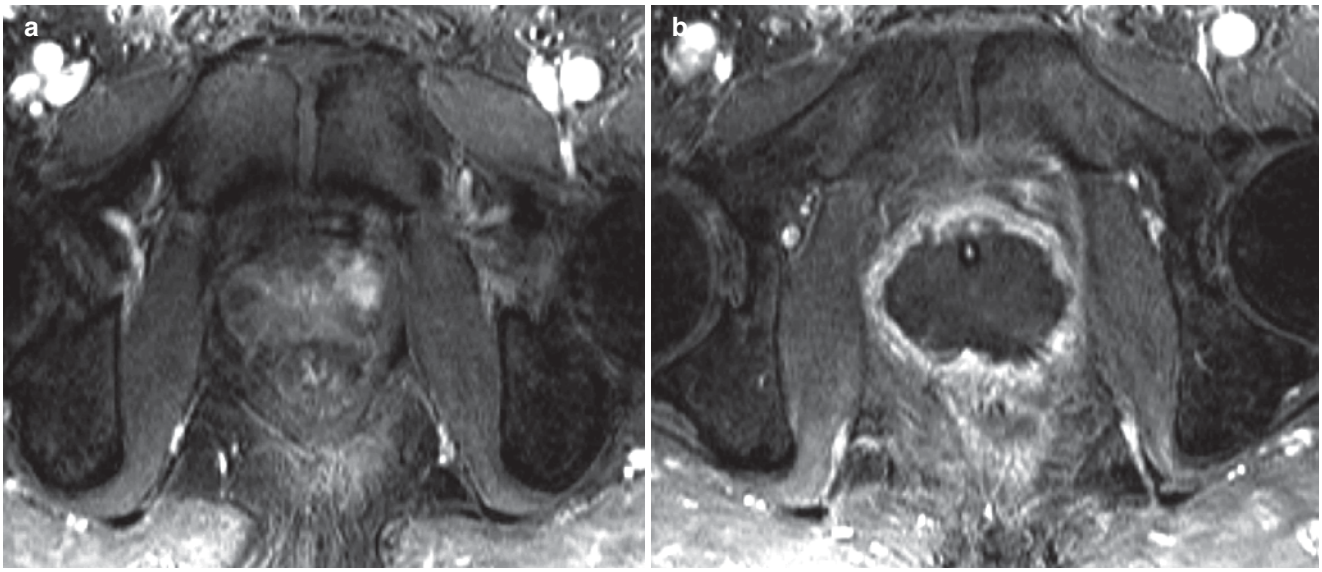

Fig. 16.8 (**a**) Pretreatment dynamic gadolinium contrast enhanced axial MRI demonstrating a malignant lesion in left upper quadrant of prostate at the midgland. (**b**) Post-HIFU (Sonablate 500) dynamic contrast enhanced axial MRI at the same level demonstrating entire prostate lacking blood supply (*dark area*). The catheter is seen. No residual cancer or prostate tissue was seen at 6 month biopsies, with an unrecordable PSA demonstrated at follow-up

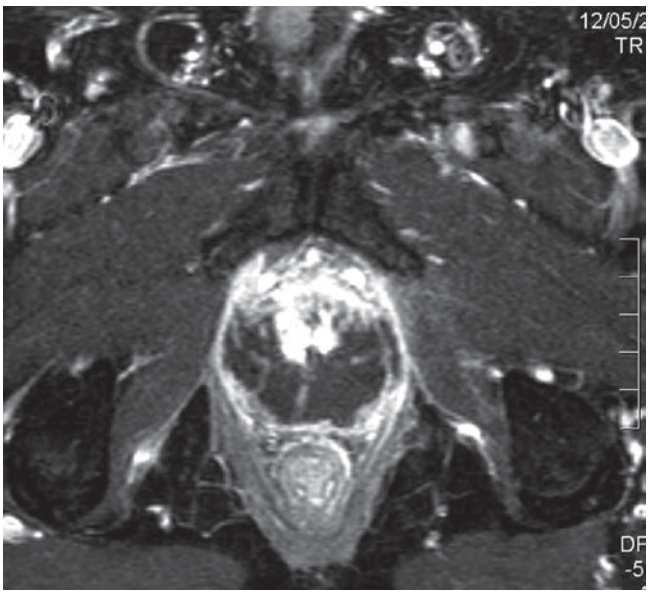

Fig. 16.9 Post-HIFU (Sonablate 500) dynamic contrast enhanced MRI in a different patient demonstrating viable tissue in the anterior region of the prostate as demonstrated by enhancement. Residual prostate cancer and a PSA >0.5 ng/mL was demonstrated at 6 months

HIFU as Salvage Treatment of Radiorecurrent Prostate Cancer

Men who have external beam radiation therapy (EBRT) or interstitial brachytherapy for clinically localized PCa have a 20–30% chance of experiencing biochemical failure defined by ASTRO criteria.[37–39] Salvage therapy using prostatectomy, cryosurgery, brachytherapy, and HIFU have been applied in the salvage setting for this group of men, provided that staging investigations demonstrate localized disease.[40] The success rates following salvage procedures are considerably lower than those that have been reported following primary treatments.[41] Patients experiencing biochemical recurrence following radical EBRT may have either a local recurrence or a metastatic disease, or both. Patients thought to have a localized recurrence after EBRT have historically been offered radical prostatectomy, androgen ablation therapy, or observation. These therapies are not without significant side effects, so other modalities such as cryotherapy and bracyhtherapy have recently been investigated in this setting. Surgery, brachytherapy, and cryotherapy have a cancer-control (estimated 5-years biochemical disease-free status rate) of 31–83%, 20–89%, and 18–74% (one series at 5-years and other series at 1–2 years), respectively. However, the average fistula rates were 4.7, 3.4, and 2.5%, respectively. Incontinence rates varied with modality and were 17–67%, 0–31%, and 4.3–96%, respectively.[42]

The use of salvage HIFU has been reported in a number of series using both the Ablatherm® and Sonablate 500 devices. Gelet et al demonstrated good early results in 71 men, with negative biopsy rates as high as 80 and 61%, achieving a PSA nadir of <0.5 ng/mL. Forty-four percent were reported as free of biochemical relapse at last review (mean, 14.8 months follow-up [range 6–86]).[30] In this same series, the rate of rectourethral fistula was 6%, with 7% suffering urinary incontinence requiring pads and 17%

developing a bladder neck stenosis. In the latest update to their series, this group has now reported on 167 patients treated with 194 HIFU sessions with a mean of 18.1 months follow-up (range 3–121). Bladder outlet obstruction occurred in 20% with 7.8% overall going into urinary retention within 3 months due to stricture or necrotic tissue. Overall, 49.5% developed urinary incontinence with grade 1, 2, and 3 in 18, 22, and 9.5%, respectively. Worryingly, 11% required artificial urinary-sphincter implantation. Such an outcome may be explained using a bladder neck incision in all men prior to HIFU, although this is uncertain. Fecal incontinence occurred in 1.2%, while 3% developed a fistula. The mean PSA nadir was 2.38 (±6.22 ng/mL) (median PSA nadir 0.19 ng/mL). Local cancer control was achieved in 73% as demonstrated by negative biopsies. Thirty-one percent had biochemical relapse but had negative biopsies. Seventeen patients developed metastatic disease; 11 of these patients died of prostate cancer.[43] Challacombe et al report on a small series of 12 patients who underwent salvage HIFU using the Ablatherm device.[28] Incontinence requiring pad usage was reported by two patients (16.7%) with one requiring an artificial urinary sphincter. One patient (8.3%) developed a urethral stricture, and worryingly, two men (16.7%) developed a rectourethral fistula. Forty-two percent of patients failed treatment after a mean of 22 (±SD 5.9) months using the ASTRO-Phoenix criteria, but 67% achieved a PSA of <0.5 ng/mL. In our own series, we have treated 31 men using the Sonablate 500 with a mean follow-up of 7.4 months (range 3–24). Side effects included stricture or intervention for necrotic tissue in 11 men (36%), urinary tract infection or dysuria syndrome in 8 (26%), and urinary incontinence in 2 (7%). The high stricture rate is probably explained by the avoidance of a bladder neck incision or TURP prior to HIFU. Rectourethral fistula occurred in two men, although one was due to patient movement as a result of inadequate anesthesia, so the true rate is probably closer to 3%. One half the patients had PSA levels of <0.2 ng/mL at last follow-up. Three had metastatic disease, while another two had local, histologically confirmed failure. A further four had evidence of biochemical failure only. Overall, 71% had no evidence of disease following salvage HIFU.[44] These series demonstrate the problem with accurate staging as current staging modalities cannot detect micrometastatic disease at the time of recurrence.

In the setting of salvage therapy for failed high-dose rate radiotherapy and where low-dose brachytherapy has been used in addition to external beam radiotherapy, we have shown that the risk of fistula formation is significant, affecting three of five men treated with salvage HIFU.[45] It may be that using transperineal biopsies to ascertain local histology rather than transrectal biopsies may aid in reducing the rectal damage that can occur. In addition, a focal salvage approach in which just the areas of cancer are treated to reduce the energy deposition within the compromised rectal mucosa may also help to reduce the morbidity with any salvage procedure.

Although salvage HIFU is able to significantly lower the PSA in men who have previously undergone radiotherapy for organ-confined prostate cancer, it carries significant side effects. Clearly, longer-term follow-up and prospective multicenter randomized controlled trials are required to assess whether these encouraging results are truly equivalent to other salvage treatments such as surgery, brachytherapy, and cryosurgery. The difficulty in accurately staging recurrent disease to exclude metastatic disease is still problematic, and such large trials will require strict inclusion criteria to minimize this difficulty.

Focal Therapy

Efforts to reduce such morbidity from treatment of localized prostate cancer have mainly centered on the refinement of surgery (laparoscopic and robotic prostatectomy) or radiotherapy (intensity modulation and conformal) so as to restrict damage to surrounding structures. However, as the premise of radical therapy has not changed, the success of such modifications in reducing genitourinary toxicity has been limited.[46,47]

Focal therapy involves treatment directed only at the cancer focus and a margin of tissue surrounding the cancer.[48,49] Most treatment-related side effects are due to injury to the immediate surroundings of the prostate and not due to treatment of the prostate per se. The surrounding structures can be described as capsule, pelvic nerves/ganglia, bladder neck, bladder, seminal vesicles, rhabdo-sphincter, Denonvilliers fascia, and rectum. Although the profile of treatment-related toxicities depends on the type of treatment given, they share a remarkable similarity and can be summarized as follows: erectile dysfunction, ejaculatory dysfunction, stress-related urinary incontinence, urge-related urinary incontinence, reduced functional bladder capacity, urethral or bladder neck strictures, and bowel dysfunction. In summary, radical radiotherapy on average causes moderate-to-severe rectoanal toxicity and urinary problems in almost one half of patients, with nearly all suffering minor symptoms. Surgery causes less damage rectally, but a third suffers chronic urinary symptoms. On average, both modalities give rise to impotence in about one half of men.[50,51]

Since unifocal or unilateral disease is present in up to 30–40% of men who are diagnosed in the PSA-screened era, it is feasible to attempt focal ablation of just the cancer areas or hemiablation or one side of the prostate in which unilateral disease is present. The modalities of cryosurgery, HIFU, photodynamic therapy, and radiofrequency ablation, as well as brachytherapy, are capable of creating localized focal

necrosis within the prostate of a predetermined size in a relatively controlled manner.[52]

To date, only case series carried out in single institutions have reported on their early results with focal therapy. Onik et al[53] first reported their results on hemiablation using cryotherapy. These results have recently been updated in 55 men completing at least 1-year follow-up.[54] Ninety-five percent (52/55) had stable PSA (as defined by ASTRO criteria) and of the 51 who were potent prior to the procedure, 44 (86%) remained potent afterwards. One had a previous TURP and was incontinent. However, four patients (7%) had to be retreated due to cancer left in the untreated area. This equates to the error rate quoted for transperineal template biopsies, which were used to verify unilateral cancer in this group of men. Transrectal biopsies by virtue of sampling error are inherently flawed in detecting all cancer foci. To reinforce this, data using transperineal template biopsies with sampling of the prostate at 5 mm intervals shows that just under half of patients deemed to have unilateral disease by TRUS biopsy were actually shown to have cancer in both sides.[55,56] This cryosurgery series has obvious limitations with the lack of clear recruitment data, lack of true trial conditions with institutional review board approval, and poor reporting. Bahn et al[57] have recently reported another series in which hemiablation was carried out using cryosurgery. At a mean follow-up of 70 months, biochemical disease-free status, according to the ASTRO definition, was maintained by 92.8% of patients (26/28) and a 96.0% negative-biopsy rate (24/25) was observed. The one biopsy-positive patient was subsequently treated with full-gland cryosurgery and remains disease free. Potency was maintained by 48.1% of patients (13/27), and another 40.7% (11/27) were potent with oral pharmaceutical assistance, yielding a total potency-preservation rate of 88.9%. These results are also encouraging, although in addition to the limitations described for the study by Onik et al, there is an additional problem. The investigators used color Doppler-guided TRUS biopsies to verify unilateral disease as well as posttreatment success. Since this technique does not carry the necessary accuracy for cancer detection, significant under-treatment and lack of verification by using the same diagnostic tool for follow-up biopsies was a major problem.[58,59] Another group demonstrated in 60 men, who underwent focal cryosurgery followed by penile rehabilitation with a vacuum device, that 73% of those potent prior to treatment maintained potency alongside a low incontinence rate of 3.6%.[60] After therapy, 35 patients underwent biopsy, with 14 showing positive findings (40.0%) at a mean of 12.0 months posttreatment. Thirteen out of fourteen patients were actually from the untreated side. This was not surprising since this group did not report on using any further evaluation beyond TRUS biopsy to establish the location of cancer. Lambert et al reported on a small series of 25 who underwent hemiablation cryosurgery for presumed unilateral disease, although again this was based on TRUS biopsy at diagnosis only.[61] Of the 24 patients potent prior to hemiablation cryosurgery, 17 (71%) were potent postoperatively. There was no rectal toxicity or incontinence. Recognizing that biochemical failure was difficult to define, this group used a PSA nadir greater than 50% of pretreatment levels as indicative of biochemical disease-free survival, giving rise to a value of 84%. Only seven patients were eligible for repeat biopsy using either a PSA nadir of more than 50% or a PSA nadir plus 2 ng/mL as determined by the investigators. Recurrent cancer was detected in three patients, with two recurrences on the contralateral side and one recurrence on the ipsilateral side of the cryosurgery. All were retreated successfully. Finally, Muto et al report on hemiablation using the Sonablate® 500 HIFU device.[62] Twenty-nine patients who were found to have unilateral disease on the basis of TRUS biopsy were treated to ablation of both peripheral zones and one half of the transition zone. Ten percent (3/28) had positive biopsies at 6 months, whereas 23.5% (4/17) had further positive biopsies at 12 months. There was no significant change in the IPSS, but there was one urethral stricture and one urinary tract infection. Although demonstrating feasibility of focal therapy using a transrectal HIFU device, the toxicity reporting in this series was very poor and the group tried to make comparison to a nonrandomized group that were treated with whole-gland HIFU.

This very limited data from uncontrolled case series suggests that treatment-related toxicity could be reduced by treating malignant areas while preserving a significant amount of prostate tissue. Equally, the data suggest that it might be possible to obtain clinically important periods of remissions from disease progression. Nonetheless, what is now required is a standardized assessment of a focal therapy intervention in a well-characterized group of men with a follow-up regimen under prospective trial conditions. Two prospective National Cancer Research Network (UK) HIFU trials using the Sonablate® 500 device, evaluating the role of hemiablation of unilateral disease and focal ablation of bilateral, low-volume disease verified by template transperineal prostate biopsies, are being undertaken at our center. At the time of writing this chapter, interim results have demonstrated the preservation of genitourinary function in 95% of men with residual cancer in the treated areas of approximately 10%.[29] A prospective ethically approved trial evaluating hemiablation cryosurgery using template biopsies to verify location of disease is also underway in Colorado, USA, and Duke Cancer Centre, USA.[58]

Focal therapy in treating organ-confined prostate cancer proposes a radical paradigm shift in our current thinking. Questions about whether such a treatment is ethical have now given way to questions about how best to localize disease, which modality is most efficacious in ablating discrete areas of tissue, and how best to define failure and monitor

untreated areas. More exciting is the proposition that if small, low-grade foci of cancer exist in association with large, high-grade "index" lesions, do we need to ablate all foci or can we ablate just the index lesion and obtain cancer control rates near equivalent to whole-gland treatment in the first 5–10 years of follow-up. If so, it may be possible to "postpone" the morbidity of whole-gland therapy until later in life to such a time as when there is progression of disease warranting further treatment. If there were no recurrence or disease progression, then this postponement could be indefinite.

Conclusion

Until controlled comparative trials are carried out, it will be difficult to determine whether HIFU or any of the competing devices delivering these energies is the optimal treatment. It is therefore an opportune time to begin a debate on standardizing the reporting of such series to allow comparison, and think about long-term prospective data collection, since randomized controlled trials are difficult to recruit in such settings.[59] HIFU for the treatment of prostate cancer has the desired short- to medium-term biochemical and histological outcomes combined with a reduction in healthcare and toxicity burden that would justify its further evaluation as a treatment for localized prostate cancer. The recent National Institute for Clinical Excellence (NICE) prostate cancer guidelines in the UK[63] have recommended that HIFU as well as cryotherapy be limited to clinical trials, although their latest recommendation for implementing the guidelines has accepted that registry data should be viewed as having equivalence to long-term prospective trials. This clearly must have the added proviso that all patients treated at a center are entered into the registry and data recorded in a prospective fashion at each follow-up to prevent selection bias.[64]The role of focal therapy as a future management strategy for men with early prostate cancer could represent a tremendous change that will ultimately benefit patients by delivering cancer treatment with a very low risk of sideeffects.

Conflicts of Interest

Hashim Uddin Ahmed and Mark Emberton receive funding from the Medical Research Council, Pelican Cancer Foundation, The Prostate Research Campaign, UK, and Prostate Cancer Research Centre, UK, for work in focal therapy of prostate cancer. In addition, Mark Emberton receives funding and is a consultant for Negma Lerads, France (manufacturers of TOOKAD, a photodynamic agent used in prostate cancer therapy), and Misonix/Focus Surgery/UKHIFU (manufacturers and distributors of the Sonablate® 500 HIFU device). Mark Emberton and Hashim Ahmed are approved proctors for training other surgeons in the use of the Sonablate 500 machine and have received fees for this activity.

Manit Arya has no conflict of interest.

References

1. Bill-Axelsen A, Holmberg L, Mirrja Ruuth, et al. Watchful waiting and prostate cancer. *NEJM*. 2005;352:1977–1984
2. Sanghvi NT, Foster RS, Bihrle R, et al Noninvasive surgery of prostate tissue by high intensity focused ultrasound: an updated report. *Eur J Ultrasound*. 1999;9(1):19–29
3. Hill CR, ter Haar GR. Review article: high intensity focused ultrasound–potential for cancer treatment. *Br J Radiol*. 1995;68(816): 1296–1303
4. Kennedy JE. High-intensity focused ultrasound in the treatment of solid tumours. *Nat Rev Cancer*. 2005;5(4):321–327
5. Haar GT, Coussios C. High intensity focused ultrasound: physical principles and devices. *Int J Hyperthermia*. 2007;23(2):89–104
6. O'Leary MP. Lower urinary tract symptoms/benign prostatic hyperplasia: maintaining symptom control and reducing complications *Urology*. 2003;62(3 suppl 1):15–23
7. Watson V, Ryan M, Brown CT, Barnett G, Ellis BW, Emberton M. Eliciting preferences for drug treatment of lower urinary tract symptoms associated with benign prostatic hyperplasia. *J Urol*. 2004;172(6 pt 1):2321–2325
8. Fowler FJ, Wennberg JE, Timothy RP, Barry MJ, Mulley AJ, Hanley D. Symptom status and quality of life following prostatectomy. *J Am Med Assoc*. 1988;259:3018–3022
9. Madersbacher S, Schatzl G, Djavan B, Stulnig T, Marberger M. Long-term outcome of transrectal high-intensity focused ultrasound therapy for benign prostatic hyperplasia. *Eur Urol*. 2000;37(6): 687–694
10. Schatzl G, Madersbacher S, Djavan B, Lang T, Marberger M. Two-year results of transurethral resection of the prostate versus four "less invasive" treatment options. *Eur Urol*. 2000;37(6):695–701
11. Sullivan L, Casey RW, Pommerville PJ, Marich KW. Canadian experience with high intensity focused ultrasound for the treatment of BPH. *Can J Urol*. 1999;6(3):799–805
12. Nakamura K, Baba S, Saito S, Tachibana M, Murai M. High-intensity focused ultrasound energy for benign prostatic hyperplasia: clinical response at 6 months to treatment using Sonablate 200. *J Endourol*. 1997;11(3):197–201
13. Lü J, Hu W, Wang W. Sonablate-500 transrectal high-intensity focused ultrasound (HIFU) for benign prostatic hyperplasia patients. *J Huazhong Univ Sci Technolog Med Sci*. 2007;27(6):671–674
14. Zacharakis E, Ahmed HU, Dudderidge T, et al Transrectal high intensity focused ultrasound in the treatment of localised prostate cancer – the first UK series. *J Urol*. 2008;179(4 suppl 1):493
15. Mearini L, D'Urso L, Collura D, et al Visually directed transrectal high intensity focused ultrasound for the treatment of prostate cancer: a preliminary report on the italian experience. *J Urol*. 2009; 181(1):105–111
16. Uchida T, Ohkusa H, Nagata Y, Hyodo T, Satoh T, Irie A. Treatment of localized prostate cancer using high-intensity focused ultrasound. *BJU Int*. 2006;97:56–61
17. Uchida T, Ohkusa H, Yamashita H, et al Five years experience of transrectal high-intensity focused ultrasound using the Sonablate

device in the treatment of localized prostate cancer. *Int J Urol*. 2006;13(3):228–233
18. Blana A, Rogenhofer S, Ganzer R, et al Eight years' experience with high-intensity focused ultrasonography for treatment of localized prostate cancer. *Urology*. 2008;72(6):1329–1333
19. Misraï V, Rouprêt M, Chartier-Kastler E, et al Oncologic control provided by HIFU therapy as single treatment in men with clinically localized prostate cancer. *World J Urol*. 2008;26(5):481–485
20. Vallancien G, Prapotnich D, Cathelineau X, Baumert H, Rozet F. Transrectal focused ultrasound combined with transurethral resection of the prostate for the treatment of localized prostate cancer: feasibility study. *J Urol*. 2004;171:2265–2267
21. Blana A, Walter B, Rogenhofer S, Wieland WF. High-intensity focused ultrasound for the treatment of localized prostate cancer: 5-year experience. *Urology*. 2004;63:297–300
22. Thuroff S, Chaussy C, Vallancien G, et al High intensity focused ultrasound and localized prostate cancer: efficacy results from the European multicentric study. *J Endourol*. 2003;17:673–677
23. Gelet A, Chapelon JY, Bouvier R, Rouvie`re O, Lyonnet D, Dubernard JM. Transrectal high intensity focused ultrasound for the treatment of localised prostate cancer: factors influencing the outcome. *Eur Urol*. 2001;40:124–129
24. Chaussy C, Thuroff S. The status of high-intensity focused ultrasound in the treatment of localized prostate cancer and the impact of a combined resection. *Curr Urol Rep*. 2003;4:248–252
25. Blana A, Murat FJ, Walter B, et al First analysis of the long-term results with transrectal HIFU in patients with localised prostate cancer. *Eur Urol*. 2008;53(6):1194–201
26. Poissonnier L, Chapelon JY, Rouvière O, et al Control of prostate cancer by transrectal HIFU in 227 patients. *Eur Urol*. 2007;51(2):381–387
27. Ficarra V, Antoniolli SZ, Novara G, et al Short-term outcome after high-intensity focused ultrasound in the treatment of patients with high-risk prostate cancer. *BJU Int*. 2006;98(6):1193–1198
28. Challacombe BJ, Murphy DG, Zakri R, Cahill DJ. High-intensity focused ultrasound for localized prostate cancer: initial experience with a 2-year follow-up. *BJU Int*. 2009;104:200–204
29. Ahmed HU, Sahu M, Govindaraju SK, et al High intensity focused ultrasound (HIFU) hemiablation trial in localised unilateral prostate cancer: interim results. In: *European Association of Urology, Annual Meeting*; 2009:Abstract 863
30. Gelet A, Chapelon JY, Poissonnier L, et al Local recurrence of prostate cancer after external beam radiotherapy: early experience of salvage therapy using high-intensity focused ultrasonography. *Urology*. 2004;63(4):625–629
31. Kirkham AP, Emberton M, Hoh IM, Illing RO, Freeman AA, Allen C. MR imaging of prostate after treatment with high-intensity focused ultrasound. *Radiology*. 2008;246(3):833–844
32. Rouvière O, Lyonnet D, Raudrant A, et al MRI appearance of prostate following transrectal HIFU ablation of localized cancer. *Eur Urol*. 2001;40(3):265–274
33. Ganzer R, Rogenhofer S, Walter B, et al PSA nadir is a significant predictor of treatment failure after high-intensity focussed ultrasound (HIFU) treatment of localised prostate cancer. *Eur Urol*. 2008;53(3):547–553
34. American Society for Therapeutic Radiology and Oncology Consensus Panel. Consensus statement: guidelines for PSA following radiation therapy. *In J Radiat*. 1997;37:1035–1041
35. Roach M III, Hanks G, Thames H Jr, et al Defining biochemical failure following radiotherapy with or without hormonal therapy in men with clinically localized prostate cancer: recommendations of the RTOG-ASTRO Phoenix Consensus Conference. *Int J Radiat Oncol Biol Phys*. 2006;65(4):965–974
36. Illing RO, Leslie TA, Kennedy JE, Calleary JG, Ogden CW, Emberton M. Visually directed HIFU for organ confined prostate cancer – a proposed standard for the conduct of therapy. *BJU Int*. 2006;98(6):1187–1192
37. Shipley WU, Thames HD, Sandler HM, et al Radiation therapy for clinically localized prostate cancer: a multiinstitutional pooled analysis. *JAMA*. 1999;281:1598–1604
38. Zelefsky MJ, Kuban DA, Levy LB, et al Multi-institutional analysis of long-term outcome for stages T1-T2 prostate cancer treated with permanent seed implantation. *Int J Radiat Oncol Biol Phys*. 2007;67:327–333
39. Pollack A, Hanlon AL, Horwitz EM, et al Prostate cancer radiotherapy dose response: an update of the fox chase experience. *J Urol*. 2004;171:1132–1136
40. Touma NJ, Izawa JI, Chin JL. Current status of local salvage therapies following radiation failure for prostate cancer. *J Urol*. 2005; 173(2):373–379
41. Nguyen PL, D'Amico AV, Lee AK, Warren Suh W. Patient selection, cancer control, and complications after salvage local therapy for postradiation prostate-specific antigen failure: a systematic review of the literature. *Cancer*. 2007;110:1417–1423
42. Nguyen PL, D'Amico AV, Lee AK, Suh WW. Patient selection, cancer control, and complications after salvage local therapy for postradiation prostate-specific antigen failure: a systematic review of the literature. *Cancer*. 2007;110(7):1417–1428
43. Murat FJ, Poissonnier L, Rabilloud M, et al Mid-term results demonstrate salvage high-intensity focused ultrasound (HIFU) as an effective and acceptably morbid salvage treatment option for locally radiorecurrent prostate cancer. *Eur Urol*. 2009;55:640–647
44. Zacharakis E, Ahmed HU, Ishaq A, et al The feasibility and safety of high-intensity focused ultrasound as salvage therapy for recurrent prostate cancer following external beam radiotherapy. *BJU Int*. 2008;102(7):786–792
45. Ahmed HU, Ishaq A, Zacharakis E, et al Rectal fistulae after salvage high-intensity focused ultrasound for recurrent prostate cancer after combined brachytherapy and external beam radiotherapy. *BJU Int*. 2009;103:321–323
46. Hegarty NJ, Kaouk JH. Radical prostatectomy: a comparison of open, laparoscopic and robot-assisted laparoscopic techniques. *Can J Urol*. 2006;13(suppl 1):56–61
47. Khoo VS. Radiotherapeutic techniques for prostate cancer, dose escalation and brachytherapy. *Clin Oncol (R Coll Radiol)*. 2005;17(7):560–571
48. Ahmed HU, Pendse D, Illing R, Allen C, van der Meulen JH, Emberton M. Will focal therapy become a standard of care for men with localized prostate cancer? *Nat Clin Pract Oncol*. 2007;4(11):632–642
49. Eggener SE, Scardino PT, Carroll PR, et al International Task Force on Prostate Cancer and the Focal Lesion Paradigm. Focal therapy for localized prostate cancer: a critical appraisal of rationale and modalities. *J Urol*. 2007;178(6):2260–2267
50. Nilsson S, Norlen BJ, Widmark A. A systematic overview of radiation therapy effects in prostate cancer. *Acta Oncol*. 2004;43(4): 316–381
51. Meraney AM, Haese A, Palisaar J, et al Surgical management of prostate cancer: advances based on a rational approach to the data. *Eur J Cancer*. 2005;41(6):888–907
52. Barqawi A, Crawford ED. Focal therapy in prostate cancer: future trends. *BJU Int*. 2005;95:273–280
53. Onik G, Narayan P, Vaughan D, Dineen M, Brunelle R. Focal "nerve-sparing" cryosurgery for treatment of primary prostate cancer: a new approach to preserving potency. *Urology*. 2002;60: 109–114
54. Onik G, Vaughan D, Lotenfoe R, Dineen M, Brady J. "Male lumpectomy": focal therapy for prostate cancer using cryoablation. *Urology*. 2007;70(6 suppl):16–21
55. Ahmed HU, Stevens D, Barbouti O, et al Prostate cancer risk stratification and cancer mapping – template transperineal prostate mapping biopsies. In: *European Association of Urology Annual Meeting*; 2008

56. Barqawi A, Lugg J, Wilson S, Kim F, Crawford ED. The role of 3dimensional systematic mapping biopsy of the prostate in men presenting with apparent low risk disease based on extended transrectal biopsy. In: *AUA Annual Meeting, Orlando;* 2008
57. Bahn DK, Silverman P, Lee F Sr, Badalament R, Bahn ED, Rewcastle JC. Focal prostate cryoablation: initial results show cancer control and potency preservation. *J Endourol*. 2006;20(9): 688–692
58. Barqawi AB, Lugg JE, Crawford ED. Target focal therapy in early prostate cancer: initial single institution results. In: *ASCO Annual Meeting*; 2007
59. Donnelly BJ, Saliken JC, Brasher P, Ernst S, Lau H, Trypkov K. A Randomised controlled trial comparing external beam radiation and cryoablation in localized prostate cancer. In: *American Urological Association Annual Meeting*; 2006:Abstract 1141
60. Ellis DS, Manny TB Jr, Rewcastle JC. Focal cryosurgery followed by penile rehabilitation as primary treatment for localized prostate cancer: initial results. *Urology*. 2007;70(6 suppl):9–15
61. Lambert EH, Bolte K, Masson P, Katz AE. Focal cryosurgery: encouraging health outcomes for unifocal prostate cancer. *Urology*. 2007;69(6):1117–1120
62. Muto S, Yoshii T, Saito K, Kamiyama Y, Ide H, Horie S. Focal therapy with high-intensity-focused ultrasound in the treatment of localized prostate cancer. *Jpn J Clin Oncol*. 2008;38(3):192–199
63. Graham J, Baker M, Macbeth F, Titshall V; Guideline Development Group. Diagnosis and treatment of prostate cancer: summary of NICE guidance. *BMJ*. 2008;336(7644):610–612
64. National Institute of Clinical Excellence (UK). NICE Prostate Cancer Management Guidelines, Implementation Advice. http://www.nice.org.uk/nicemedia/pdf/CG58ImplementationAdvice.doc

Tissue Bioengineering

17

Shahin Chandrasoma and Roger De Filippo

Introduction

The growing field of regenerative medicine seeks to counteract injuries in which the body's healing responses fail to respond with new functional tissue. To date, growth factors and cytokines have shown some clinical impact, by stimulating the production of new cells by the body or enhancing function of the existing cells in the body. Newer modalities, however, focus on the formation of new functional tissue substitutes for those lost. Regenerative technology, thus, has wide applications across multiple-organ systems and indeed the entire spectrum of disease processes. The restoration of functional tissue to heart and bone can theoretically provide treatment of congestive heart failure and osteoporosis. The formation of functional skin lessens the reliance on local and free plastic surgical flaps used in reconstruction and skin grafting. Generating neural tissue can treat disease states such as spina bifida. The regeneration of pancreatic tissue can be used to treat diabetes.

Tissue bioengineering represents a radically new field of study, with significant possibilities for implementation that could revolutionize the field of urology, most specifically in the area of reconstructive surgery. Reconstructive surgery is performed by urologists in both pediatric and adult patients for a variety of conditions. Pediatric urologists perform complex plastic surgical reconstructions for cases of ambiguous genitalia, as well as for cloacal and exstrophy malformations. Reconstructive urologists conduct a large variety of posttraumatic procedures for injuries to the genitourinary tract, both cosmetic and functional. Neurourologists and uro-oncologists use bowel segments extensively in bladder augmentation and neobladder formation, respectively. These procedures are technically demanding and can be hindered by a limited availability of local epithelial tissue available for reconstruction. Tissue can be harvested from other sites in the body, but this is also fraught with the potential for new complications in distant body sites.

The goal of tissue engineering is the development and successful implantation of functional biologic substitutes that can supplement or augment the existing function of an organ. It usually involves a matrix of some kind, used as a scaffold on which cells may or be introduced. The cells may be autologous cells or pluripotent precursor cells.

Human embryonic stem cells have been shown to have the capability of differentiating into cells from all three embryonic germ layers, proving them to have true pluripotency. Ectodermal structures, such as skin and neurons[46]; mesodermal structures, such as blood, cardiac cells, and cartilage[29,30] and endodermal structures, such as pancreatic cells[5] have all been formed in vitro. The use of human embryonic stem cells, however, requires fetal demise and is a hotly contested ethical and political dilemma.[4] Because of this, researchers are searching for other more ethically neutral sources of stem cells for use in the study of regenerative medicine.

Fetal cells have been in clinical use for the last decade. Umbilical cord blood has stem-cell potential and has been used both in the treatment of hematological disorders[52] and as a source of mesenchymal stem cells. The fetal kidney, specifically the metanephric mesenchyme, is a potential source of these stem cells as well.[2] Although hematopoietic cells have been used clinically, there are still ethical considerations regarding the actual transplantation of fetal tissue.[1] Progress in these fields is limited by the extensive debate between various political groups. Autologous amniotic fluid stem cells are also under investigation as another source of ethically neutral pluripotent progenitor cells.[43]

Efforts are currently underway to engineer tissue from every cell type of the genitourinary system that a biological substitute for use in reconstructive surgical procedures may be developed. Artificial kidney, ureter, bladder, urethra, and skin, once successfully engineered, could be used in the maintenance, restoration, and improvement of tissue function, all without utilizing tissue from a distant site or separate organ system. Tissue bioengineering may provide a novel source of autologous biocompatible tissues for use in reconstructive urologic procedures. In this chapter, we will investigate current advances in tissue bioengineering on an organ-by-organ basis.

P. Dasgupta et al. (eds.), *New Technologies in Urology,*
DOI: 10.1007/978-1-84882-178-1_17, © Springer-Verlag London Limited 2010

Kidney

Historically, renal failure was invariably fatal. With the advent of hemodialysis and transplantation, mortality has been seen to decrease substantially in these populations. These methods have proved indispensable to the management of patients with end-stage renal disease. Renal transplantation is the gold standard of therapy, with dialysis as a bridge to donor kidney availability. Even so, these are not flawless treatments.

Both dialysis and transplantation carry their own unique morbidities, ranging from effect on lifestyle and problematic vascular access to donor shortage and graft rejection. Both interventions are costly, with dialysis patients costing more than $50,000 per year and posttransplantation patients costing $17,000 per year. Research is continually directed at the restoration of renal function by alternative approaches.

More advanced forms of hemodialysis show promise in decreasing mortality of patients with renal failure, even those on dialysis. A renal assist device is an extracorporeal circuit that seeks to recreate the actual anatomy of the nephron, using human renal proximal tubule cells. Although shown to potentially limit mortality,[51] the renal assist device is still subject to the morbidity of being and externalized dialysis unit with vascular access required. Bioartificial kidneys, which in theory could be implanted and perform continuous dialysis, would be advantageous in limiting the impact on patient lifestyle accorded by hemodialysis. Such a device is largely dependent on technological advancement, and though nanoengineered filtration membranes have been produced,[18] feasible application into a portable transplantable unit is still distant.

Tissue engineering provides a cutting edge alternative to artificial approximation of renal function. The isolation, expansion, and implantation of cells have potential in the development of functional kidney units grown extracorporeally. Renal bioengineering is especially challenging given the multiple functions of the kidney and the intricacy of its structure. Cell transplantation and kidney-cell expansion has been proposed as a method of augmenting or supplementing renal-cell function in impaired kidneys. A possible strategy involves the extraction (via biopsy) of renal cells from an affected kidney, growth of these cells in culture, seeding of the cells onto a scaffold, and subsequent implantation of the scaffold back into the original patient.

In [1995], Atala et al[8] showed in vivo renal-cell growth and nephron organization after extracorporeal attachment to such a biodegradable polymer scaffold. It was later shown that even single cells could redevelop into tubular structures once seeded.[19] Subsequently, functional kidney structures were seen to actually secrete a urine-like fluid, indicating that tissue-engineered units, once implanted, actually have the ability to excrete solutes in a similar fashion to normal kidney tissue.[53] Histologically, vascular structures, glomeruli, and tubules are seen. More recently, three-dimensional culture systems that promote adhesion of expanded cells to one another as opposed to the culture dish have been utilized. This allows for generation of more three-dimensional tissue units.[21] Expanded primary renal cells, when placed in such a system, began to develop into structures that looked like tubules and glomeruli and stained positively for Tamm-Horsfall protein, which is normally expressed in the thick ascending limb of the loop of Henle, as well as the distal convoluted tubules.[27]

Extensive research has gone into the nature of the scaffold. An acellular collagen-based kidney matrix has proven to be a good frame to which renal cells can adhere and develop into tubules.[3] This is a naturally derived lattice that has potential in being the basis for renal augments in the future. Modifications have been made to the scaffold to further enhance survival of engineered tissue, such as incorporation of calcium-peroxide-based oxygen-generating particles.[40] This proved protective to cells when incubated under hypoxic conditions and may have import in the generation of larger implants, which are hindered in their growth by oxygen diffusion limits.

Cell-based approaches have shown promise, both in vitro and in vivo, but the clinical application of this technology is still relatively far away. Current questions address the development of a sizeable enough mass of tissue to functionally augment the kidney, as well as the successful integration of said mass into the patient, establishing circulatory and excretory continuity. Ultimately, perhaps, tissue-engineered kidneys will be transplanted routinely into patients, obviating both the need to await availability of a donor kidney and the need for lifelong immunosuppression, as well as limiting the phenomenon of graft rejection.

Bladder

The bladder can be affected by many disorders that occur across a wide age range. Pediatric patients born with meningomyelocele can be affected with neurogenic bladder of varying degrees of severity. The typical low-volume, low-compliance bladder seen in patients with spina bifida carries with it the risk of transmission of higher storage pressures to the upper tracts. It was for good reason that this population served as the index population in describing the role of bladder augmentation.[37] At the other end of the age spectrum are patients with bladder cancer, whose bladders are removed secondary to a disease process. Whatever the etiology, the end result is the same. Patients with bladder deficiency, with

regard to either function or physical presence, require a substitute reservoir.

The bladder differs from the kidney in that its functions are more limited and defined. It is not nearly as complex, as vital to life, or as intricate in its composition as the kidney. The bladder is primarily a storage organ. If its contractile function is absent or diminished, urine can still be cleared from the body by intermittent catheterization. If catheterization is viewed as an acceptable adjunct to urinary storage from a lifestyle perspective, then defunctionalized bladder needs to be able to accommodate an appropriate volume of urine as well as maintain that urine at a low enough pressure to prevent deleterious transmission of pressure to the upper tracts.

Currently, bladder augmentation and substitution is performed using intestinal segments, most commonly ileum and colon. Many different types of reconstructions have been described. On one end of the operative spectrum are basic bladder augmentations, whereas at the other extreme lie complex continent nonrefluxing orthotopic urinary diversions, such as the T-pouch.[47] Although highly effective and technically impressive, such diversions are accompanied by their own specific constellation of complications, including but not limited to metabolic disturbances,[36] diminished bone health,[32] and stone formation.[50] Because of this, research continues to discover new ways to augment or replace bladder that avoid the manipulation of bowel.

The concept of seeding a scaffold with cells, as mentioned previously, can be found at the center of bladder engineering. The basic idea is that the matrix serves as the lattice on which the cells can grow and differentiate; as this occurs, the scaffold itself degrades until all that remains is engineered bladder tissue. The important criteria for such a matrix are that it is acellular, so that the bladder cells are the only true cells in the graft; that it will degrade to leave only graft behind; and that it is immunologically inert and will not provoke a host response against it.

Cell-seeded bladder matrices were first used in dogs. Autologous cells were grown and applied to matrices, then implanted into dogs. It was seen that tissue-engineered bladder specimens showed a normal capacity to retain urine, normal compliance, and normal histologic organization.[39] This discovery showed for the first time that tissue bioengineering could conceivably reconstitute a transplantable, immune-neutral organ that functioned appropriately and stored urine effectively. This discovery opened the door to clinical trials of tissue-engineered bladder implantation.

In 2006, Atala et al[7] published a report of seven patients with meningomyelocele between the ages of 4 and 19 years who were candidates for augmentation cystoplasty. These patients underwent a bladder biopsy. The specimens were expanded in tissue culture and seeded onto a dome-shaped, collagen-based scaffold. Seven weeks after the biopsy, the scaffolds were implanted onto the existing bladder as an augmentation. Serial urodynamics during follow-up showed decreased bladder pressures and increased compliance, satisfying the requirements of the bladder as a storage organ. Ongoing clinical trials further investigate the utilization of tissue-engineered bladders in human subjects. These studies suggest that tissue-engineered bladders may be a viable option not only for patients of the future but also for patients of the present day.

Ureter

Nonseeded acellular matrix grafts have been implanted in rats, with regeneration of ureteral wall components, but subsequent efforts to use such grafts in tubularized ureteral replacement were unsuccessful. Cell-seeded synthetic scaffolds, however, have shown promise. Cells were expanded in vitro and applied to lattices of tubular polyglycolic acid. After subcutaneous implantation, in vivo layering was noted, with luminal and muscle layers. Continued research seeks to establish successful interposition of tubularized tissue-engineered ureteral structures in continuity with the urinary tract.

Urethra

The urethra can be compromised by congenital abnormalities, but it is most often the acquired maladies that necessitate urethral surgery. Posttraumatic defects, such as urethral disruption or urethral stricture formation, can often not be repaired primarily and may require harvesting of tissue from distant body sites for successful reconstruction. The use of local skin flaps has been described, as have graft harvests of bladder or buccal mucosa[25], but these are still subject to complications. Unwanted intraurethral hair growth can be seen in the use of epidermal grafts, and all areas can potentially contract or scar. Additionally, anastomotic sites are at risk for stone formation, stricture, or conversely, diverticulum development.

Animal studies replacing urethral tissue with segments of acellular collagen-based matrix graft in an onlay fashion have been described,[11] in which the animals were able to void through their newly constructed urethras. No signs of voiding dysfunction were readily apparent, and histologic examination showed wide caliber urethras with normal appearing tissue with a confluent transitional cell layer confirmed by immunohistochemistry. This approach was subsequently applied in human subjects with hypospadias or urethra stricture disease as the impetus for reconstructive

surgery. In addition, anastomosing the acellular matrix in an onlay fashion, good results were seen in 34 of 40 patients, with increased flow rate and good caliber urethras. Six of the 40 patients redeveloped urethral stricture. The advantage of the use of such a matrix is that it does not have to be implanted with host cells and can be packaged and distributed for immediate "off-the-shelf" use, obviating the need for graft harvest and excess morbidity. Acellular matrix grafts are effective for shorter length strictures less than 0.5 cm long.[17]

Acellular matrices are only able to successfully replace urethra if anastomosed in an onlay fashion. Attempts at tubularized repair using acellular matrices proved unsuccessful, with development of recurrent strictures and contracture of the grafts.[33] If tubularized segments of urethra are needed, cell-seeded matrices tend toward more promising results.[14] As shown in animal studies, the tubularized matrices, when seeded with autologous bladder epithelial and smooth muscle cells, develop into strictureless urethras of normal caliber, whereas acellular matrices uniformly result in collapsed urethral sections with stricture development. The implication of this study is that by using autologous cell-seeded tubularized collage scaffolds, the potential for replacement of part or all of the penile urethra exists, without the added morbidity of graft harvest at the time of surgery. Clearly, the potential impact on the urethral or reconstructive urologist is tremendous, as patients requiring urethroplasty represent a population that can become frustrated by continuing urinary difficulties and a relatively high incidence of complications. Human studies are required to assess the practical feasibility of tissue engineering of the male urethra.

Penis

The application of reconstructive surgery in the case of the penis is largely related to erectile dysfunction. The corporal tissue has lost its erectile function, and the main conceptual goals remain the same: either augment existing corporal function or introduce a substitute for it. Currently, these two arms of therapy are approximated by both medical and surgical management. Early medical management with intracavernosal papaverine and intraurethral alprostadil showed reasonably good results, but it was the FDA approval of sildenafil in 1998 that established a new therapy to reestablish function in corporal tissue.[23]

In cases refractive to medical therapy, implantable devices are used as substitutes for languishing corpora. Penile prostheses have been in use for decades since being described[42] and have been composed of various materials. Semirigid devices maintain the penis at a constant level of tumescence, while inflatable implants can be filled to order by siphoning fluid from an implanted reservoir using a pump placed in the scrotum.[20] Although highly effective, complications can arise by virtue of the alien nature of the implant itself, which is continually subject to infection, with early or delayed presentation. Tissue engineering attempts to sidestep these potential complications by utilizing and implant that is either immunologically inert or of autologous origin.

Similar cell-seeding techniques to those described previously have been attempted using culture-expanded corporal smooth muscle cells applied to biodegradable polyglycolic acid polymers. After in vivo implantation, corporal cells could be visible grossly and histologically, indicating the potential for cultivation of tissue-engineered corpora.[41] Acellular nerve grafts have been implanted in rodents with transected cavernous nerves with more rapid return of erectile function.[12] This represents a potential "off-the-shelf" product that could theoretically be used at the time of deep pelvic surgeries with higher risk of disruption of the neural input to the corpora, most notably radical prostatectomy. By approaching the corpora as defunctionalized units in need of augmentation of function, tissue-engineered erectile tissue may provide a means of recovery of function.

If a substitutive effect analogous to a semirigid prosthesis is desired, studies have described the novel formation of cartilaginous rods by seeding chondrocytes on cylindrical scaffolds. The seeded cylinders were implanted in vivo. On retrieval, it was seen that the scaffold had biodegraded to leave behind a milky white rod of cartilaginous tissue. The maintenance of the approximate size and shape of the cylinder was an indication that the development of a possible prosthesis was to some extent customizable, and the rigid elasticity and strength of the rod itself suggested that it may have utility, at least theoretically, as an implantable semirigid prosthesis. Human trials are pending, but given these advancements, it seems that tissue engineering with doubtless play some part in the surgical management of erectile dysfunction.

Testes

The main function of the testis is the production of androgens, in particular testosterone, which in turn have many effects on male development, muscle, bone, and sexual function. Testicular dysfunction can arise in various congenital or acquired conditions ranging from Klinefelter's disease to bilateral mump orchitis. In patients thus rendered functionally anorchic, lifelong androgen requirement therapy may be required to maintain physiological levels of testosterone and avoid adverse impacts on growth and sexuality.

Androgen replacement can be performed in various ways, all with benefits and hindrances. Oral testosterone must be

taken in large amounts to overcome a "first pass" effect whereby a large percent of the dose is rendered metabolically inactive in the liver. Such large doses can actually be hepatotoxic.[24] When administered in a parenteral depot preparation, usually every 3 weeks, testosterone levels are usually initially very high for the first few days only to bottom out by 21 days, a fluctuation that shies away from the typical diurnal pattern of testosterone release. This fluctuation can result in disturbances in mood and libido.[48] Transdermal therapy via testosterone patches can deliver measured doses but are associated with adverse cutaneous side effects at the area of application, such as pruritis, induration, rash, and necrosis of the skin.[26]

One basic approach toward restoration of testicular function in males is the transplantation of Leydig cells (interstitial cells) from a donor into the anorchic male. Leydig cells are the source of 95% of testosterone in men; the rationale is to introduce functional Leydig cells into an affected male to reestablish the integrity of his hypothalamic-pituitary-gonadal axis. Cell transplantation is limited by rejection of the foreign cells by the host's immune system. Currently, studies are focusing on immunoprotection of the transplanted cells via encapsulation in a protective semipermeable membrane that is biologically compatible with the recipient.[10] Encapsulation and subsequent implantation of Leydig cells could conceivably create a transplantable unit that mirrors the hormonal function of the testis and thus mirrors its diurnal secretory pattern in response to signals from the pituitary. In theory, this is a more natural release of testosterone, without dose adjustments or potential for injury to internal organs or skin.

In a study by Machluf et al in 2003, approximately 10% of normal adult rat Leydig cell population was encapsulated in alginate microspheres and injected both subcutaneously and intraperitoneally in castrated rats. They produced serum testosterone levels of up to 40% of normal, with the subcutaneous implants producing testosterone for a longer time period.[35] This study shows the potential that exists in creating an encapsulated Leydig cell implant for in vivo testosterone replacement that approximates normal physiologic release.

Another approach involves the creation of a testicular prosthesis that is capable of eluting testosterone. Testicular-shaped prostheses with a hollow center, made of tissue-engineered chondrocytes, were created in a bioreactor and then filled with 100 μg of testosterone enanthate and both maintained in culture and implanted into athymic mice. Eluted testosterone levels were physiologic for 40 weeks and were calculated as being 60% of the injected volume.[45] Such a prosthesis could have a role in patients who require both prostheses and chronic hormone supplementation; though such a prosthesis would require periodic reinjections of a new testosterone load into the hollow center of the prosthesis, it could provide a more cosmetic option to injectable testosterone that decreased the frequency of injection needed.

Vagina

Vaginal disorders usually stem from congenital malformations and may be grouped into three broad categories, each of which dictates appropriate operative intervention. These three groups comprise the spectrum of vaginal agenesis, ambiguous genitalia, and imperforate anus and urogenital sinus variants. The need for vaginal reconstruction is rare and is a challenging undertaking approached in different manner by different specialties. Plastic surgeon and gynecologists usually embark on dilatation in conjunction with skin grafting, whereas pediatric urologists conduct reconstruction with bowel segments in vaginoplasty.[44]

The discrepancy in preferred tissue source is not so limited; the use of many different tissues from multiple discrete organ systems has been described in animals, including omentum,[22] pericardium,[28] and lyophilized human dura.[31] The use of nonvaginal tissue is to repair the structure, but function remains an issue that is largely not addressed. Additionally, unwanted complications dependent on the type of tissue used can be seen. The primary goal of vaginal reconstruction is the approximation of anatomic normalcy, with functional normalcy a secondary and largely unaddressed goal. In theory, the ability to tissue engineer vaginal tissue would provide a substrate for reconstruction that would not be subject to the compromise in function as associated with other methods.

There are encouraging initial results with regards to the use of tissue engineering of vaginal mucosa. Vaginal epithelium and smooth muscle cells, when expanded in tissue culture and then seeded as mentioned earlier onto synthetic matrices and implanted into athymic mice, can lead to the formation of vaginal tissue, with cells replicating and surviving. By the 6th week following implantation, organization into distinct epithelial and muscular layers was noted.[15]

Recently, using a rabbit model, cells from a vaginal biopsy were expanded in vitro and applied to a scaffold, and subsequently implanted in vivo as an autologous tissue-engineered implant. Six months after vaginal replacement, radiographic studies showed patent vaginas of good caliber with no evidence of stricture. Histologic analysis showed organized epithelial and muscle layers. Physiologic studies showed normal responses of the neovaginas to electrical stimulation and to adrenergic agonism.[13] This exciting new data suggests that a tissue-engineered vagina for vaginal reconstruction is a real possibility in the near future.

It should be noted that this has significant impact in the management of transgendered patients, specifically male-to-female transsexuals. This type of surgery in this patient

population is not routinely performed in the general urologic practice, with such procedures usually limited to specialty centers. This patient population represents not only a shift in the indications for vaginal reconstruction but also an increase in the number of reconstructive procedures that are being performed today. Currently, ileal segments are often used in vaginoplasty, and laparoscopic approaches have been described with good functional results.[34] Bioengineered vaginal tissue could represent a significant advancement in the practice of vaginal reconstruction in this growing population, in that it can result in a neovagina composed of normal epithelium, while obviating the morbidity associate with graft harvest.

Uterus

The application of tissue engineering with regard to the uterus is readily apparent in patients with congenital disorders resulting in a lack of sufficient uterine tissue to reproduce, that is, to maintain a growing fetus and then expel it during labor. Research into the generation of uterine tissue grown in vitro is still in its infancy. Seeded human myometrial cells have been grown on scaffolds that allow them to adhere to each other rather than only to a culture dish, in hopes that thicker tissue samples could be grown.[6] These bridging myocytes were tested for tensile strength and contractile activity. Addition of oxytocin produced irregular contractile activity, which, though not close to the contractions noted with the pattern of human labor, was significant for the demonstration of myocytes grown and bridged in tissue culture contracting in a coordinated manner.

Ovary

Ovarian compromise can be the result of anything that limits the ability of the ovary to produce oocytes capable of differentiation into viable offspring, be it polycystic ovarian syndrome, ovarian failure, or sterility. The role of tissue engineering in these situations is less focused on the generation of de novo oocytes; instead, methods to apply tissue-engineering technology to the preservation of existing immature oocytes have been described. Granulosa cell–oocyte complexes incorporated into an alginate hydrogel culture system showed no degeneration and an intact zona pellucida after 10 days. Approximately 40% of the oocytes retrieved from in vitro growth were capable of progressing to meiosis II. These studies could provide breakthroughs in the preservation of oocytes of women who are at risk for losing ovarian function, be it through progressive cystic disease or impending chemotherapy. Further studies have focused on the incorporation of ligands to the alginate lattice that can affect the behavior and structure of the oocytes themselves.

Injectable Therapies

The urinary system is one governed by flow dynamics. Appropriate one-way flow of urine is essential for proper functioning of the system. Vesicoureteral reflux or backflow of urine from bladder to ureter represents a malfunction in the valve-like nature of the ureter as it tunnels through the bladder wall. Urinary incontinence involves a deficiency in the resistance to outflow of urine from the bladder. Although fundamentally different disorders, both can be treated with injection of bulking agents to limit flow of urine in an undesirable fashion.

Ideal injectable agents are biocompatible and biodegradable. Recently, injection of dextranomer microspheres in a sodium hyaluronan solution (Deflux) has shown good results at treating vesicoureteral reflux.[49] For cases of urinary incontinence, collagen remains a commonly used bulking agent.[38]

Autologous chondrocytes have been expanded in tissue culture, and the resulting solution injected cystoscopically to correct vesicoureteral reflux in children.[16] Similarly, autologous chondrocytes have been used in the treatment of stress incontinence due to intrinsic sphincter deficiency in adults.[9] More recently, attempts to inject the rhabdosphincter itself with myoblasts caused significant strengthening one year later, with attainment of continence.

Tissue engineering of injectable agents for bulking purposes shows promising practical application, largely because such usage is not dependent on scaffolding and structuring the development of a complex organ. Such agents are by definition nonantigenic and thus avoid the potential for allergic or inflammatory reaction in humans. They additionally have the potential to maintain their volumes, avoiding the need for repeat injection as the agent degrades and incontinence returns.

Conclusion

Tissue bioengineering remains on the cutting edge of medical technology. These processes are of significant impact to the urologic surgeon, as every organ in the genitourinary and reproductive system is under investigation. Research is focused on improving methods of cell culture and in vitro expansion of cell lines; improvement of polymers for use as nonantigenic, biodegradable scaffolds for growth and

organization of these cells; and implantation of these seeded scaffolds to assess tissue differentiation in vivo. Tissue bioengineering may provide a means of restoration of lost function without the need for grafts and with much lower morbidity. Despite promising data with regard to virtually all types of urogenital engineering, much remains to be done before tissue engineering is considered a viable corollary to traditional reconstructive urological surgery. Most of the advancements in this field have occurred rapidly and in a relatively short period of time. Continued research is essential to reach the true possibilities in this area of study.

References

1. Abouna GM. Ethical issues in organ and tissue transplantation. *Exp Clin Transplant*. 2003;1(2):125–138
2. Al-Awqati Q, Oliver JA. Stem cells in the kidney. *Kidney Int*. 2002;61(2):387–395
3. Amiel GE, Yoo JJ, Atala A. Renal therapy using tissue-engineered constructs and gene delivery. *World J Urol*. 2000;18(1):71–79
4. Annas GJ, Elias S. The politics of transplantation of human fetal tissue. *N Engl J Med*. 1989;320(16):1079–1082
5. Assady S, Maor G, Amit M, et al Insulin production by human embryonic stem cells. *Diabetes*. 2001;50(8):1691–1697
6. Atala A. Tissue engineering and regenerative medicine: concepts for clinical application. *Rejuvenation Res*. 2004;7(1):15–31
7. Atala A, Bauer SB, Soker S, Yoo JJ, Retik AB. Tissue-engineered autologous bladders for patients needing cystoplasty. *Lancet*. 2006;367(9518):1241–1246
8. Atala A, Retik AB, Schlussel RN. Renal cell growth in vivo after attachment to biodegradable polymer scaffolds. *J Urol*. 1995;153: 209A
9. Bent AE, Tutrone RT, McLennan MT, Lloyd LK, Kennelly MJ, Badlani G. Treatment of intrinsic sphincter deficiency using autologous ear chondrocytes as a bulking agent. *Neurourol Urodyn*. 2001;20(2):157–165
10. Chang TM. Bioencapsulation in biotechnology. *Biomater Artif Cells Immobil Biotechnol*. 1993;21(3):291–297
11. Chen F, Yoo JJ, Atala A. Acellular collagen matrix as a possible "off the shelf" biomaterial for urethral repair. *Urology*. 1999;54(3): 407–410
12. Connolly SS, Yoo JJ, Abouheba M, Soker S, McDougal WS, Atala A. Cavernous nerve regeneration using acellular nerve grafts. *World J Urol*. 2008;26(4):333–339
13. De Filippo RE, Bishop CE, Filho LF, Yoo JJ, Atala A. Tissue engineering a complete vaginal replacement from a small biopsy of autologous tissue. *Transplantation*. 2008;86(2):208–214
14. De Filippo RE, Yoo JJ, Atala A. Urethral replacement using cell seeded tubularized collagen matrices. *J Urol*. 2002;168(4, pt 2): 1789–1792
15. De Filippo RE, Yoo JJ, Atala A. Engineering of vaginal tissue in vivo. *Tissue Eng*. 2003;9(2):301–306
16. Diamond DA, Caldamone AA. Endoscopic correction of vesicoureteral reflux in children using autologous chondrocytes: preliminary results. *J Urol*. 1999;162(3, pt 2):1185–1188
17. Dorin RP, Pohl HG, De Filippo RE, Yoo JJ, Atala A. Tubularized urethral replacement with unseeded matrices: what is the maximum distance for normal tissue regeneration? *World J Urol*. 2008;26(4): 323–326
18. Fissell WH, Humes HD, Roy S, Fleischman A. Initial characterization of a nanoengineered ultrafiltration membrane. *J Am Soc Nephrol*. 2002;13:602A
19. Fung L, Elenius K, Freeman MR, Donovan MJ, Atala A. Reconstitution of EGFr-poor renal epithelial cells into tubular structures on biodegradable polymer scaffold. *Pediatrics*. 1996;98S:631
20. Furlow WL. Surgical management of impotence using the inflatable penile prosthesis. Experience with 36 patients. *Mayo Clin Proc*. 1976;51(6):325–328
21. Giuliani S, Perin L, Sedrakyan S, Kokorowski P, Jin D, De Filippo R. Ex vivo whole embryonic kidney culture: a novel method for research in development, regeneration and transplantation. *J Urol*. 2008;179(1):365–370
22. Goldstein MB, Dearden LC, Gualtieri V. Regeneration of subtotally cystectomized bladder patched with omentum: an experimental study in rabbits. *J Urol*. 1967;97(4):664–668
23. Goldstein I, Lue TF, Padma-Nathan H, Rosen RC, Steers WD, Wicker PA. Oral sildenafil in the treatment of erectile dysfunction. Sildenafil Study Group. *N Engl J Med*. 1998;338(20):1397–1404
24. Gooren LJ. A ten-year safety study of the oral androgen testosterone undecanoate. *J Androl*. 1994;15(3):212–215
25. Hendren WH, Reda EF. Bladder mucosa graft for construction of male urethra. *J Pediatr Surg*. 1986;21(3):189–192
26. Hogan DJ, Maibach HI. Adverse dermatologic reactions to transdermal drug delivery systems. *J Am Acad Dermatol*. 1990;22(5, pt 1):811–814
27. Joraku A, Stern KA, Atala A, Yoo JJ. In vitro generation of three-dimensional renal structures. *Methods*. 2008;47:129–133
28. Kambic H, Kay R, Chen JF, Matsushita M, Harasaki H, Zilber S. Biodegradable pericardial implants for bladder augmentation: a 2.5-year study in dogs. *J Urol*. 1992;148(2, pt 2):539–543
29. Kaufman DS, Hanson ET, Lewis RL, Auerbach R, Thomson JA. Hematopoietic colony-forming cells derived from human embryonic stem cells. *Proc Natl Acad Sci USA*. 2001;98(19):10716–10721
30. Kehat I, Kenyagin-Karsenti D, Snir M, et al Human embryonic stem cells can differentiate into myocytes with structural and functional properties of cardiomyocytes. *J Clin Invest*. 2001;108(3): 407–414
31. Kelâmi A. Lyophilized human dura as a bladder wall substitute: experimental and clinical results. *J Urol*. 1971;105(4):518–522
32. Koch MO, McDougal WS, Hall MC, Hill DE, Braren HV, Donofrio MN. Long-term metabolic effects of urinary diversion: a comparison of myelomeningocele patients managed by clean intermittent catheterization and urinary diversion. *J Urol*. 1992;147(5):1343–1347
33. le Roux PJ. Endoscopic urethroplasty with unseeded small intestinal submucosa collagen matrix grafts: a pilot study. *J Urol*. 2005;173(1):140–143
34. Liguori G, Trombetta C, Bucci S, et al Laparoscopic mobilization of neovagina to assist secondary ileal vaginoplasty in male-to-female transsexuals. *Urology*. 2005;66(2):293–298, discussion 298
35. Machluf M, Orsola A, Boorjian S, Kershen R, Atala A. Microencapsulation of Leydig cells: a system for testosterone supplementation. *Endocrinology*. 2003;144(11):4975–4979
36. McDougal WS. Metabolic complications of urinary intestinal diversion. *J Urol*. 1992;147(5):1199–1208
37. Mitchell ME. The role of bladder augmentation in undiversion. *J Pediatr Surg*. 1981;16(6):790–798
38. Monga AK, Robinson D, Stanton SL. Periurethral collagen injections for genuine stress incontinence: a 2-year follow-up. *Br J Urol*. 1995;76(2):156–160
39. Oberpenning F, Meng J, Yoo JJ, Atala A. De novo reconstitution of a functional mammalian urinary bladder by tissue engineering. *Nat Biotechnol*. 1999;17(2):149–155
40. Oh SH, Ward CL, Atala A, Yoo JJ, Harrison BS. Oxygen generating scaffolds for enhancing engineered tissue survival. Biomaterials. 2008;30:752–762

41. Park HJ, Yoo JJ, Kershen RT, Moreland R, Atala A. Reconstitution of human corporal smooth muscle and endothelial cells in vivo. *J Urol*. 1999;162(3, pt 2):1106–1109
42. Pearman RO. Treatment of organic impotence by implantation of a penile prosthesis. *J Urol*. 1967;97(4):716–719
43. Perin L, Sedrakyan S, Da Sacco S, De Filippo R. Characterization of human amniotic fluid stem cells and their pluripotential capability. *Methods Cell Biol*. 2008;86:85–99
44. Rajimwale A, Furness PD 3rd, Brant WO, Koyle MA. Vaginal construction using sigmoid colon in children and young adults. *BJU Int*. 2004;94(1):115–119
45. Raya-Rivera AM, Baez C, Atala A, Yoo JJ. Tissue engineered testicular prostheses with prolonged testosterone release. *World J Urol*. 2008;26(4):351–358
46. Reubinoff BE, Pera MF, Fong CY, Trounson A, Bongso A. Embryonic stem cell lines from human blastocysts: somatic differentiation in vitro. *Nat Biotechnol*. 2000;18(4):399–404. Erratum in: *Nat Biotechnol*. 2000;18(5):559
47. Stein JP, Lieskovsky G, Ginsberg DA, Bochner BH, Skinner DG. The T pouch: an orthotopic ileal neobladder incorporating a serosal lined ileal antireflux technique. *J Urol*. 1998;159(6):1836–1842
48. Sokol RZ, Palacios A, Campfield LA, Saul C, Swerdloff RS. Comparison of the kinetics of injectable testosterone in eugonadal and hypogonadal men. *Fertil Steril*. 1982;37(3):425–430
49. Stenberg A, Läckgren G. A new bioimplant for the endoscopic treatment of vesicoureteral reflux: experimental and short-term clinical results. *J Urol*. 1995;154(2, pt 2):800–803
50. Takeda M, Katayama Y, Takahashi H, et al Incidence of pouch stones and risk factors for urolithiasis in patients with continent urinary diversion or neobladder using intestine. *Urol Int*. 1994;52(1): 21–25
51. Tumlin J, Wali R, Brennan K, Humes HD. Effect of the renal assist device (RAD)on mortality of dialysis-dependent acute renal failure: a randomized, open-labeled, multicenter, Phase II trial. *J Am Soc Nephrol*. 2005;16:46A (abstracts)
52. Watt SM, Contreras M. Stem cell medicine: umbilical cord blood and its stem cell potential. *Semin Fetal Neonatal Med*. 2005;10(3): 209–220
53. Yoo J, Ashkar S, Atala A. Creation of functional kidney structures with excretion of urine-like fluid in vivo. *Pediatrics*. 1996;98S:605

Renal Radiosurgery

18

David M. Hartke and Lee E. Ponsky

Introduction

The American Cancer Society estimated that there would be more than 54,000 new cases of renal cancer in 2008 in the United States, with the overwhelming majority being renal-cell carcinoma.[1] Surgical excision is widely accepted as the gold standard for the treatment of a localized renal-cell carcinoma. Historically, renal tumors were treated by open-radical nephrectomy. Since the 1990s, however, laparoscopic radical nephrectomy has provided equal efficacy in cancer control with decreased morbidity and a more rapid convalescence.[2–7] Although providing excellent cancer control, radical extirpation also sacrifices many normal nephrons, which may prove problematic over time. Currently, because of the widespread use of abdominal imaging, many renal tumors are small, asymptomatic, and discovered incidentally. Thus, there is a strong motivation to spare as much renal parenchyma as possible while treating these tumors. Surgical excision via partial nephrectomy spares much of the normal tissue, yet it still provides excellent rates of cancer control and long-term survival.[8] Whether done via an open or, more recently, laparoscopic approach, partial nephrectomy is still associated with a hospital stay and several weeks to convalescence. Furthermore, there are risks such as bleeding, infection, and urine leak, which may lead to considerable morbidity. Also, renal hilum clamping and ischemia inherent to the procedure results in nephron injury, although this is usually temporary and recoverable. Finally, surgical difficulties that may be encountered intraoperatively may lead to conversion to radical nephrectomy, though infrequent. This shows that this gold-standard nephron-sparing approach is not exempt from disadvantages.

Just as open surgical approaches have yielded to less-invasive laparoscopic approaches, there is a push toward minimally invasive nephron-sparing treatment modalities as well. The goals of any such modality include definitive destruction of the lesion, preservation of normal surrounding renal parenchyma, and consistent safety with low morbidity. Thermal therapy, using either radio-frequency ablation (RFA) or cryoablation, has been widely available in the past decade. Whether performed laparoscopically or percutaneously, these thermal ablative techniques are certainly associated with little morbidity. However, there have been concerns regarding cancer control. In 2005, Weld and Landman reviewed the available literature on RFA and cryotherapy and compared the results with those from laparoscopic partial nephrectomy.[9] Their efforts confirmed the lower morbidity of these thermal ablative techniques; however, the recurrence rates were 7.9 and 4.6% for RFA and cryotherapy, respectively, compared to only 2.7% for laparoscopic partial nephrectomy. In a single-institution study by Nguyen et al, they demonstrated 25 and 7.4% recurrence rates following RFA and cryotherapy.[10] Furthermore, it has been demonstrated that biopsies of even nonenhancing lesions following thermal ablation can still harbor viable cancer cells, thus challenging our ability to reliably follow patients with imaging after treatment. Lastly, when recurrences do happen, surgical excision is often exceptionally difficult because of extensive perinephric scarring.[10] Certainly, though each modality of therapy has its benefits, there is not a consensus regarding optimal minimally invasive treatment as of yet. Although still in its relative infancy with regard to its application to renal tumors, noninvasive radiosurgical technology is the latest advancement offered for the treatment of localized renal cancer.

Application of Radiation Therapy

Radiation, when delivered at lower doses, changes tissue at the cellular level through the induction of breaks in the DNA and, thus, cellular apoptosis. At high doses, though, radiation can result in complete ablation of tissue. Traditional external beam radiation therapy (XRT) focuses high-energy radiation at a tumor; however, it traditionally subjects the surrounding normal tissue to its effects, and the margins of treatment are indistinct. Because of the unacceptable collateral tissue damage, XRT has been unable to safely deliver ablative doses. Furthermore, XRT must often be delivered in many fractionated doses to protect the skin and surrounding organs in the

P. Dasgupta et al. (eds.), *New Technologies in Urology,*
DOI: 10.1007/978-1-84882-178-1_18, © Springer-Verlag London Limited 2010

path of the radiation beams. In contrast, radiosurgical therapy may deliver a high dose of radiation in very few sessions (fractions) or potentially only a single fraction.

XRT has been studied in the treatment of locally advanced renal tumors, and its role was debated. An early report of a surgeon's experience demonstrated that neoadjuvant XRT may offer improved survival.[11] Other trials, however, have failed to demonstrate any increase in survival associated with XRT in either the neoadjuvant or adjuvant settings.[12–14]

Regardless, complications such as bleeding, radiation nephritis, duodenal stenosis, liver fibrosis, and even death resultant from radiation-induced complications have all but eliminated the use of renal XRT from modern practice.[15–17] Still, in a recent study by Beitler et al, patients who had refused surgical extirpation for localized renal tumors were offered conformal XRT using a stereotactic body frame.[18] They received a dose of 40 Gy delivered in five fractions over 15 days with a 1-cm margin around the tumor. With a median follow-up of 26.7 months, 4 of the 9 patients were still alive; all survivors had a minimum follow-up of 48 months and tumors less than 3.5 cm in diameter. Two patients developed nausea and vomiting during the treatment, and one of these experienced a 30-lb weight loss over 30 days; endoscopic biopsy 6 weeks after radiation revealed glandular atypia in the stomach. The pathologist commented that this was most likely caused by inflammation and radiation injury, even though the stomach received no direct irradiation. The authors concluded that conformal XRT may play a role in the treatment of small, localized renal tumors. However, many potential complications of XRT are due to respiratory excursion (the inherent back-and-forth movement of the kidney associated with the respiratory cycle) that makes precise delivery of traditional XRT to a lesion a near impossibility.

Radiosurgery

Stereotactic radiosurgery was first introduced by Lars Leksell in 1951.[19] The gamma-knife, a radiosurgical delivery system created by Leksell, is now used as the standard of care in the treatment of unresectable or multifocal brain tumors. The gamma knife system employs an immobilization device to keep the patient perfectly still while receiving radiation with pinpoint accuracy. A brain lesion represents a perfect target for radiosurgery because it is unaffected by respiratory motion. If untreated, renal-cell carcinoma metastatic to the brain results in death in only 1–2 months.[20] Radiosurgical therapy has been shown to provide excellent local control of these lesions and may significantly extend survival.[21–24] The study by Brown et al produced a median overall survival of nearly 18 months after stereotactic radiosurgery for metastatic brain tumors due to renal-cell carcinoma.[24] These outcomes support that even the most aggressive and advanced renal-cell carcinomas respond to radiation therapy.

Radiosurgical Technologies

Application of new radiosurgical technologies such as Cyberknife (Accuray Inc; Sunnyvale CA), Novalis System (BrainLab AG; Heimstetten, Germany), and Tomotherapy (Tomotherapy Inc; Madison, WI) allow frameless stereotactic radiosurgery to now be delivered to "moving" organ targets, such as the kidney. The Cyberknife (Fig. 18.1), favored by the authors, contains a lightweight 6-MV linear accelerator mounted to a highly maneuverable robotic manipulator. The manipulator can position and point the accelerator with 0.3 mm precision. Moreover, highly advanced image guidance allows the radiation beam to follow and "correct" for a moving target in real time using Synchrony, a tracking and compensation system. Synchrony uses external markers in conjunction with diagnostic X-ray images to guide the robotic arm so that the beam always remains aligned with the target. With the aid of Synchrony, the tumor motion can be tracked in three-dimensional space, allowing for precise treatment. The Cyberknife is also unique in its ability to deliver ablative-dose radiation with exceptional precision and little effect on surrounding tissue. This is accomplished because the high-dose radiation is divided into hundreds of

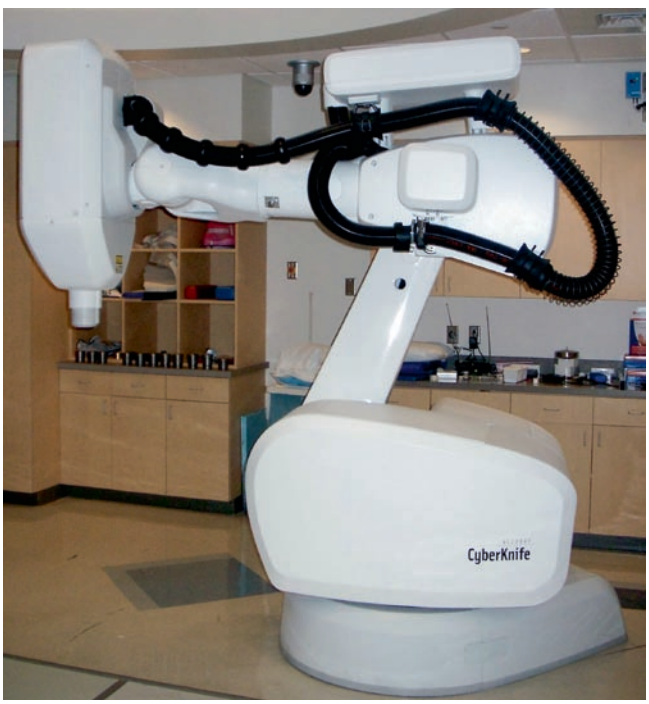

Fig. 18.1 The Cyberknife

beams, with each beam yielding a greatly reduced dose that is essentially benign along its path.[25] However, at the focal point, the dose of the beams are additive and eventually equate to an ablative dose. Finally, because it is mounted on a robotic arm, the Cyberknife directs its beams from numerous positions nearly circumferentially around the focal point with near exact precision.

Before any treatment using the Cyberknife, significant planning must occur. Currently, under an active protocol at our institution, patients undergo a CT scan followed by placement of gold image-guidance markers (fIducials) in or near the tumor using an 18-gauge spinal needle under local anesthesia. Then, the patients are fitted for custom-made plastic immobilization devices that fit snugly over the abdomen and chest and they undergo another CT scan or MRI. During this pretreatment period, the scans are transferred to a computer, and the renal tumor and normal structures (contralateral kidney, spleen, stomach, liver, bowel, and spinal cord) are each carefully outlined (Fig. 18.2). Finally, the team of physicists uses the intricate treatment planning software to calculate the beam arrangement based on the target dose assignment and the anatomy of its relationship to dose-limiting normal structures.

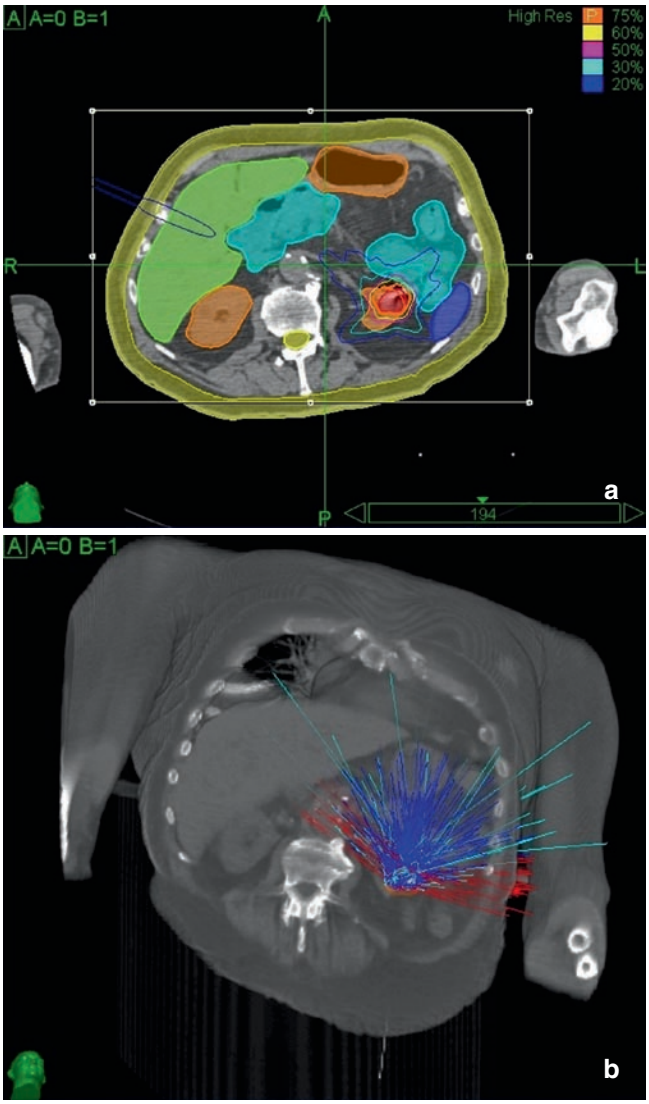

Fig. 18.2 Preprocedural planning CT. (**a**) Using the treatment planning software, the normal organs are outlined so as to direct the beams for dose-limiting purposes; the left renal tumor and treatment zones are mapped. (**b**) The planned beams are directed from multiple angles so as to limit the dose received by the normal organs in their paths

Radiosurgery Outcomes

Radiosurgical technology is still in its relative infancy, and thus, long-term studies are not available. However, short-term analysis has been promising. Our initial evaluation of the Cyberknife was published in 2003.[26] In this study, eight pigs had each of their kidneys treated at predetermined sites – each approximately 2 cm in diameter – throughout the kidneys using a single dose of 24–40 Gy, followed by organ harvest and histological examination 4–8 weeks later (Fig. 18.3). The targeted sites were treated with 40 Gy and evaluated 8 weeks after treatment demonstrated complete tissue ablation surrounded by a small zone of partial fibrosis; the remainder of the kidney was unharmed. Furthermore, on gross inspection at the time of kidney procurement, there was neither any evidence of perinephric scar nor any gross radiation injury to the body wall or surrounding organs. This animal study demonstrated the safety and efficacy of achieving renal ablation using radiosurgical Cyberknife technology.

Initial clinical studies using the Cyberknife to treat renal neoplasms have been promising as well. Following our initial animal study, a clinical protocol was designed to verify the safety of renal radiosurgery. Ponsky et al treated three patients who were good surgical candidates with a mean tumor size of 2.03 cm using a total of 16 Gy divided in four fractions over 2 days.[27] Each patient underwent a CT scan 8 weeks following treatment and then subsequently underwent either open or laparoscopic partial nephrectomy. With follow up ranging from 52 to 62 weeks, no adverse events or acute toxicities were noted. After surgical excision, histological examination in one patient showed a cavity without microscopic evidence of viable tumor. The other two tumors demonstrated pathological evidence of renal-cell carcinoma. This trial confirmed the safety of renal radiosurgery at a low dose. Based on the results of the previous animal study, it was suspected that the low doses used at the initiation of this clinical study would not likely produce complete ablation of the renal tumor. The authors, though, will continue to escalate the dose and monitor patients with regards to safety and tumor ablative

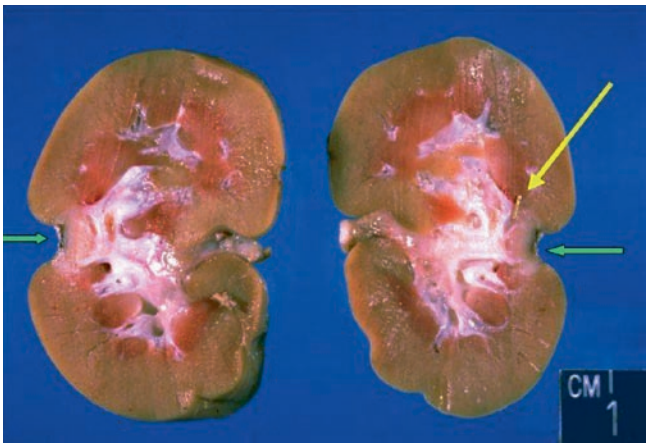

Fig. 18.3 Porcine kidney procured 8 weeks following treatment. The *green arrows* point to the cavity where the ablated tissue resided with a zone of fibrosis beneath. The *yellow arrow* points to the gold fiducial next to the zone of fibrosis

effects. Furthermore, this study will look to correlate the post-treatment CT scan results with the postoperative histology.

Promising work with the Cyberknife is also being done by Hong et al. Their initial evaluation included fourteen patients with a mean tumor diameter of 4.1 cm who were treated with 21 Gy divided in three fractions (7 Gy each).[28] Patients were then imaged with CT scans every 3 months following treatment. Tumor volume decreased by a mean of 9% at 3 months and by 44% at 12 months; and there was not any progression of tumor in the 12-month follow-up period. This study illustrates one of the effects of radiation therapy: as the tumor is replaced by fibrotic scar, it contracts and the lesion appears smaller. At this point, more investigation is necessary not only to determine the optimal dose and fractionation of radiation but also to correlate these CT findings with the probability of complete tumor ablation. Certainly, pathologic correlation would be ideal.

Conclusion

In the past 15 years, the practice of urology has largely shifted from open surgery to laparoscopic approaches to surgery. In recent years, minimally invasive ablative therapies have emerged, and perhaps, they will shift to noninvasive therapies such as radiosurgery. Certainly, renal radiosurgery is an early stage of development, but the early results are exciting. Although renal tumors historically were thought to have been radiation-resistant, radiosurgery offers the potential to treat renal tumors more safely and at a higher dose than traditional XRT. Complete tissue ablation has been achieved in animals, and the safety of lower dose treatments is established in humans. In the coming years, research will focus to determine the optimal dose required for complete tumor ablation, yet still achieve low morbidity. It will also be important to determine whether any tumor characteristics such as size, location, or pathologic subtype will present any limitations or advantages to treatment. Moreover, ideal follow-up protocols will also require development. In the meantime, we will watch with keen interest as tumors in other abdominal and extra-abdominal organs are treated using radiosurgical technology. We will study their successes and failures and apply new technologies in the hope of achieving the best outcomes possible.

References

1. American Cancer Society. *Cancer Facts and Figures 2008*. Atlanta: American Cancer Society; 2008
2. Chan DY, Cadeddu JA, Jarrett TW, et al Laparoscopic radical nephrectomy: cancer control for renal cell carcinoma. *J Urol*. 2001;166(6):2095–2100
3. Ono Y, Kinukawa T, Hattori R, et al The long-term outcome of laparoscopic radical nephrectomy for small renal cell carcinoma. *J Urol*. 2001;165(6):1867–1870
4. Gill IS, Meraney AM, Schweizer DK, et al Laparoscopic radical nephrectomy in 100 patients: a single center experience from the United States. *Cancer*. 2001;92(7):1843–1855
5. Abbou CC, Cicco A, Gasman D, et al Retroperitoneal laparoscopic versus open radical nephrectomy. *J Urol*. 1999;161(6):1776–1780
6. Permpongkosol S, Chan DY, Link RE, et al Long-term survival analysis after laparoscopic radical nephrectomy. *J Urol*. 2005; 174(4):1222–1225
7. Portis AJ, Yan Y, Landman J, et al Long-term follow-up after laparoscopic radical nephrectomy. *J Urol*. 2002;168(3):1257–1262
8. Weight CJ, Fergany AF, Gunn PW, et al The impact of minimally invasive techniques on open partial nephrectomy: a 10-year single institutional experience. *J Urol*. 2008;180(1):84–88
9. Weld KJ, Landman J. Comparison of cryoablation, radio-frequency ablation, and high-intensity focused ultrasound for treating small renal tomours. *BJU Int*. 2005;96:1224–1229
10. Ngyen CT, Lane BS, Kaouk JH, et al Surgical salvage of renal cell carcinoma recurrence after thermal ablative therapy. *J Urol*. 2008; 180:104–109
11. Richie EW. The place of radiotherapy in the management of parenchymal carcinoma. *J Urol*. 1966;95:313–317
12. Juusela H, Malmio K, Alfthan O, et al Preoperative irradiation in the treatment of renal adenocarcinoma. *Scand J Urol Nephrol*. 1977;11(3):277–281
13. Kjaer M, Iversen P, Hvidt V, et al A randomized trial of postoperative radiotherapy versus observation in stage II and III renal adenocarcinoma. A study by the Copenhagen Renal Cancer Study Group. *Scand J Urol Nephrol.* 1987;21(4):285–289
14. Kjaer M, Frederiksen PL, Engelholm SA. Postoperative radiotherapy in stage II and III renal adenocarcinoma. A randomized trial by the Copenhagen Renal Cancer Study Group. *Int J Radiat Oncol Biol Phys*. 1987;13(5):665–672
15. Cox CE, Lacy SS, Montgomery WG, et al Renal adenocarcinoma: a 28 year review with emphasis on rationale and feasibility of preoperative radiotherapy. *J Urol*. 1970;104(1):53–61
16. Kortmann RD, Becker G, Classen J, et al Future strategies in external radiation therapy of renal cell carcinoma. *Anticancer Res*. 1999;19(2C):1601–1603

17. Cassaday JR. Clinical radiation nephropathy. *Int J Radiat Oncol Biol Phys*. 1995;31(5):1249–1256
18. Beitler JJ, Makara D, Silverman P, et al Definitive, high-dose-per-fraction, conformal, sterotactic external radiation for renal cell carcinoma. *Am J Clin Oncol*. 2004;27(6):646–648
19. Leksell L. The stereotaxic method and radiosurgery of the brain. *Acta Chir Scand*. 1951;102(4):316–319
20. Posner JB. Diagnosis and treatment of metastases to the brain. *Clin Bull*. 1974;4(2):47–57
21. Manon R, O'Neill A, Knisely J, et al Phase II trial of radiosurgery for one to three newly diagnosed brain metastases from renal cell carcinoma, melanoma, and sarcoma: an eastern Cooperative Oncology Group Study (E6397). *J Clin Oncol*. 2005;23: 8870–8876
22. Chang EL, Selek US, Hassenbusch III SJ, et al Outcome variation among "radioresistant" brain metastases treated with stereotactic radiosurgery. *Neurosurgery*. 2005;56:936–945
23. Noel G, Valery CA, Boisserie G, et al LINAC radiosurgery for brain metastasis of renal cell carcinoma. *Urol Oncol*. 2004;22(1):25–31
24. Brown PD, Brown CA, Pollock BE, et al Stereotactic radiosurgery for patients with radioresistant brain metastases. *Neurosurgery*. 2002;51:656–667
25. Lunsford LD, Coffey RJ, Cojocaru T, et al Image-guided stereotactic surgery: a 10-year evolutionary experience. *Stereotact Funct Neurosurg*. 1990;54–55:375–387
26. Ponsky LE, Crownover RL, Rosen MJ, et al Initial evaluation of cyberknife technology for extracorporeal renal tissue ablation. *Urology*. 2003;61(3):498–501
27. Ponsky LE, Mahadevan A, Gill IS, Djemil T, Novick AC. Renal radiosurgery: initial clinical experience with histological evaluation. *Surg Innov*. 2007;14(4):265–269
28. Hong YM, Shanmugham L, La Rosa S, et al Cyberknife radiosurgical ablation of primary renal tumors [Personal Correspondence – Presented at World Congress of Endourology]; 2008

Hydro-Jet Technology

19

Sijo J. Parekattil

Introduction

The use of a stream of water or saline to dissect between tissue planes during surgery has been applied for a number of different applications.[1–12] The technology has evolved, and hydro-jet generators and delivery probes that provide more range of pressure control and delivery accuracy have been developed (ERBE Jet 2, ERBE, Inc., Figs. 19.1 and 19.2).

Previous studies have shown that different effects are seen at varying pressure levels of hydrodissection.[1,4,7,9] For fine vascular preservation during dissection in porcine brain tissue, a pressure setting of ten bar [146 psi (pounds per square inch)] is optimal.[7] In the canine parotid gland model, nerve preservation is maintained at a pressure below 40 bar (580 psi).[4] Previous human studies have illustrated that pressure settings in the 225–305 psi (16–21 bar) range can be safely utilized with nerve and microvascular preservation.[5,8,9]

In the field of urology, Shekarriz et al performed pioneering work using the hydrodissection technique for retroperitoneal lymph-node dissection, laparoscopic nephrectomy, and laparoscopic partial nephrectomy (with vascular clamping).[8,9,12] Moinzadeh et al performed leading work using hydrodissection in a calf model for laparoscopic partial nephrectomy without the need for renal hilar clamping.[6]

This chapter presents the clinical human application of the new ERBE™ Jet 2 generator (ERBE, Inc.) with a flexible tip applicator device for use during robotic-assisted laparoscopic procedures. The new flexible applicator tip (Fig. 19.2) allows the surgeon to insert the probe through the abdominal wall (via a 14-gauge angiocatheter sheath), to hold the probe in the fourth robotic arm, that can be molded into angles to allow for more accurate delivery of the water jet in areas with limited access (such as the lower pelvis).

Fig. 19.1 ERBE Jet 2™ – hydro generator

Fig. 19.2 Flexible hydro-jet probe

Hydrodissection Principle

The concept behind hydrodissection is that the hydro-jet may be refined to a pressure setting at which saline dissects around critical structures such as blood vessels and nerves allowing

P. Dasgupta et al. (eds.), *New Technologies in Urology,*
DOI: 10.1007/978-1-84882-178-1_19, © Springer-Verlag London Limited 2010

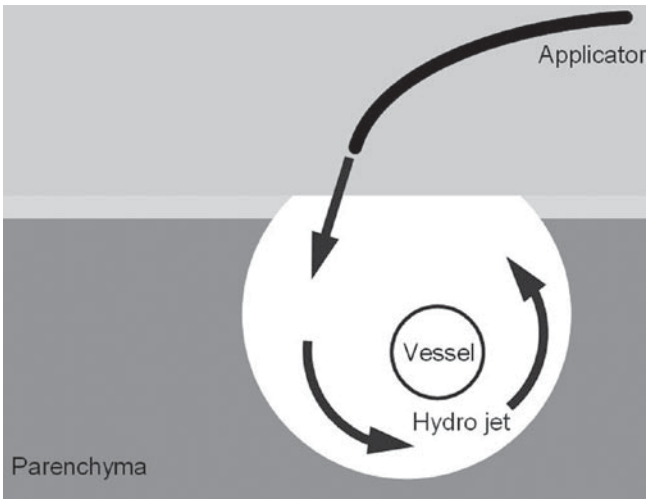

Fig. 19.3 Hydrodissection principle

potential tissue planes between different structures. This would then allow these structures to be separated easily with minimal sharp tissue dissection. Figure 19.3 illustrates this concept. This provides a tool that can be used in a number of operative situations as previously mentioned.

New Clinical Applications in Urology

Robotic-Assisted Laparoscopic Radical Prostatectomy with Hemostatic Hydrodissection of the Neurovascular Bundles

Preservation of continence and potency after robotic-assisted laparoscopic radical prostatectomy (RALP) are two key outcomes that patients consider when comparing treatment options for localized prostate cancer. Ensuring that positive surgical margins are as low as possible provides oncologic control. Various techniques to optimize these outcomes have been employed. The following study presents the early outcomes for hemostatic hydrodissection of the neurovascular bundles (HYNEB) during RALP.

Methods

A review of 100 consecutive RALP HYNEB cases from March 2007 to July 2008 (follow up from 1 to 16 months) was performed. Bilateral HYNEB was performed (in high-risk patients, wide margins were taken) using the ERBE© hydrodissector. Outcomes were measured using validated quality of life measurement tools including the Sexual Health Inventory for Men preoperatively and postoperatively at 3-month intervals.

Surgical Technique

The flexible tip hydrodissector was used to lift the lateral fascia off the prostate, thus separating the neurovascular bundle. A pressure setting of 140 psi (9.7 bar) was used to minimize injury to fine nerves and vessels.[4,7] Direct dissection within the lateral fascia was not performed to prevent potential trauma to the fine nerves in this area. The entire lateral fascia and neurovascular bundle complex was lifted as one entity. Figures 19.4 and 19.5 illustrate the use of the hydrodissector to release the neurovascular bundles.

Results

Overall positive surgical margin rate was 14% (for pathological stage T2 – 11% and stage T3 – 33%). Continence

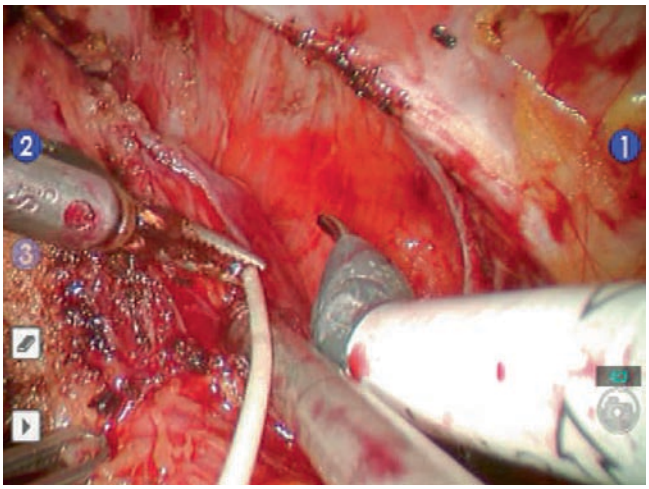

Fig. 19.4 Hydrodissection of the right neurovascular bundle off the prostate

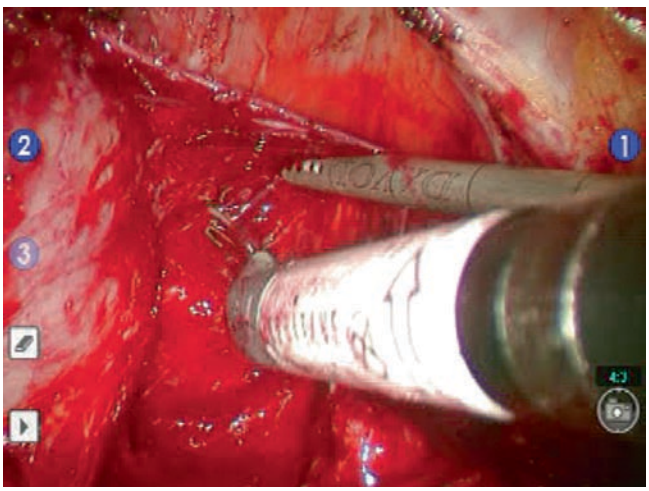

Fig. 19.5 Right neurovascular bundle released from prostate after hydrodissection

(defined as using no pads or one pad for safety daily) was 51% at 1 month, 80% at 3 months, and 95% at 6 months.

For the last 50 patients, the positive surgical margin rate was 8% (for pathological stage T2 – 4.9% and stage T3 – 22%). Continence at 1 month was 65, 83% at 3 months, and 100% at 6 months. In patients with a preoperative SHIM of 25 (19 patients), 74% (14 patients) had return of erections sufficient for intercourse (with or without the use of oral phosphodiesterase inhibitors) by 6 months postoperatively. Two of these patients were able to have intercourse 2 weeks after surgery.

Conclusions

HYNEB may promote the early return of continence and erectile function without significantly compromising positive margin rates.

Robotic-Assisted Laparoscopic Partial Nephrectomy Without Vascular Clamping

Robotic and laparoscopic partial nephrectomy is a treatment option for small renal masses (<4 cm). During these cases, clamping of the renal vessels is usually required to minimize bleeding. This study illustrates the use of hemostatic hydrodissection in combination with bipolar and radiofrequency coagulation during partial nephrectomy to avoid renal vascular clamping and renal ischemia.

Methods

Review of 25 cases from January 2006 to July 2008. Nineteen patients underwent the procedure without vascular clamping using hemostatic hydrodissection (Helix HydroJet™) with bipolar vessel coagulation and radiofrequency coagulation of the margin (RITA Habib probe™). Postoperative follow-up ranged from 1 to 30 months (mean of 14 months).

Surgical Technique

The angled tip hydrodissection probe (Fig. 19.6) or the suction hydrodissector tip were used for this procedure. The pressure was set at 300 psi (21 bar) to allow for renal parenchymal dissection with preservation of vessels.[6,12] Initially, the tumor margins were evaluated using real-time intraoperative ultrasound. These margins were then marked on the renal capsule using monopolar cautery. The RFA ablator was

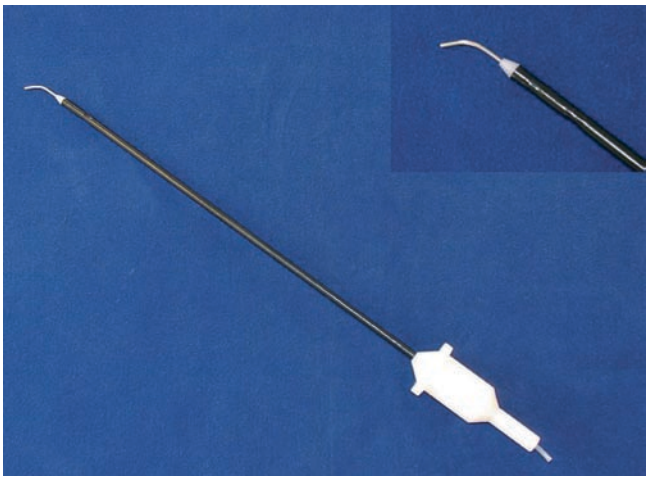

Fig. 19.6 Rigid angled tip hydro-jet probe (ERBE™)

then used to coagulate a rim of renal parenchyma 1 cm beyond the tumor margin. This ablated any large blood vessels traversing this region (Fig. 19.7). The hydrodissector was then used to dissect through the parenchyma at the edge of the coagulated rim (Figs. 19.7 and 19.8). Once any remaining small vessels were encountered, these were cauterized using bipolar cautery and then incised. Using careful dissection with this technique, the entire tumor with a 1-cm margin was safely removed without any vascular clamping of the renal vessels. This allowed the rest of the kidney to be perfused during the entire procedure, and there was no renal warm ischemia. This delicate dissection technique added approximately 15–20 min to the procedure.

Results

None of the 19 cases required vascular clamping. Mean patient age was 58 (range 17–73), mean renal mass size was 2.4 cm (1.1–3.7 cm), mean estimated blood loss was 162 cc

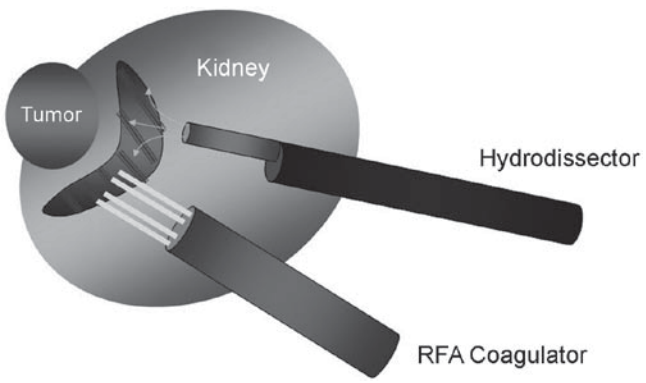

Fig. 19.7 Hydrodissection and RFA ablation technique for robotic and laparoscopic partial nephrectomy

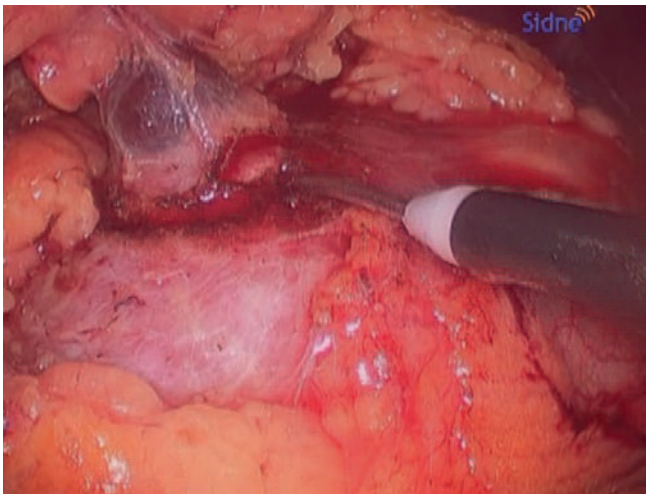

Fig. 19.8 Hydrodissection during robotic-assisted laparoscopic partial nephrectomy

(20–500 cc), and mean operative time was 197 min (105–300 min). All surgical resection margins were negative (tumor and margins sent for frozen pathology exam intraoperatively). One patient had a horseshoe kidney. Ten patients had a transperitoneal approach, and nine patients had a retroperitoneal approach. One patient with a delayed urine leak was treated conservatively. Postoperatively, all patients' serum creatinine remained at baseline. Final surgical pathology was as follows: nine renal-cell carcinomas, three angiomylipomas, one oncocytoma, fige complex hemorrhagic cysts, and one nonfunctioning upper pole. No tumor recurrences or delayed bleeds have occurred thus far. Mean hospital duration of stay was 3 days (range of 1–6 days).

Conclusions

This new technique for robotic and laparoscopic partial nephrectomy appears to be a safe technique that avoids renal vascular clamping and renal ischemia.

Future Goals

The cost of the new hydrodissector device has reduced significantly over the last few years. Comparative effectiveness studies of using the hydrodissector techniques vs. existing standards would be necessary to assess the cost–benefit ratio. Further long-term follow-up and assessment would determine the merit of these techniques.

Conclusion

Hydrodissection technology continues to evolve and new applications will emerge. We should aim to responsibly assess and evaluate these techniques in a structured evidence-based manner.

References

1. Kaduk WM, Stengel B, Pohl A, Nizze H, Gundlach KK. Hydro-jet cutting: a method for selective surgical dissection of nerve tissue. An experimental study on the sciatic nerve of rats. *J Craniomaxillofac Surg*. 1999;27(5):327–330
2. Kaehler GF, Sold MG, Fischer K, Post S, Enderle M. Selective fluid cushion in the submucosal layer by water jet: advantage for endoscopic mucosal resection. *Eur Surg Res*. 2007;39(2):93–97
3. Kockerling F, Yildirim C, Rose J, Scheidbach H, Geers P. Total mesorectal excision with the water-jet-dissection. Technique and results. *Tech Coloproctol*. 2004;8(suppl 1):s217-s225
4. Magritz R, Jurk V, Reusche E, Siegert R. Water-jet dissection in parotid surgery: an experimental study in dogs. *Laryngoscope*. 2001;111(9):1579–1584
5. Meyer L, Uberruck T, Koch A, Gastinger I. Resection of the spleen using the Water Jet dissection technique. *J Laparoendosc Adv Surg Tech A*. 2004;14(5):321–324
6. Moinzadeh A, Hasan W, Spaliviero M, et al Water jet assisted laparoscopic partial nephrectomy without hilar clamping in the calf model. *J Urol*. 2005;174(1):317–321
7. Oertel J, Gaab MR, Knapp A, Essig H, Warzok R, Piek J. Water jet dissection in neurosurgery: experimental results in the porcine cadaveric brain. *Neurosurgery*. 2003;52(1):153–159; discussion 159
8. Shekarriz B. Hydro-Jet technology in urologic surgery. *Expert Rev Med Devices*. 2005;2(3):287–291
9. Shekarriz B, Upadhyay J, Jewett MA. Nerve-sparing retroperitoneal lymphadenectomy using hydro-jet dissection: initial experience. *J Endourol*. 2004;18(3):273–276
10. Shekarriz H, Shekarriz B, Burk CG, Kujath P, Bruch HP. Hydro-jet-assisted pneumonectomy: a new technique in a porcine model. *J Laparoendosc Adv Surg Tech A*. 2002;12(5):371–376
11. Shekarriz H, Shekarriz B, Kujath P, et al Hydro-Jet-assisted laparoscopic cholecystectomy: a prospective randomized clinical study. *Surgery*. 2003;133(6):635–640
12. Shekarriz H, Shekarriz B, Upadhyay J, Burk C, Wood DP Jr, Bruch HP. Hydro-jet assisted laparoscopic partial nephrectomy: initial experience in a porcine model. *J Urol*. 2000;163(3):1005–1008

Chronic Tissue Expansion

20

José R Colombo Jr, Monish Aron Jr., and Inderbir Gill

Tissue substitutes for reconstructive procedures of the urinary tract are required in a variety of acquired and congenital pediatric and adult urological diseases. In the era of rapid growth of tissue engineering and stem cell research and clinical use, the tissue expansion field has fallen behind in the search for viable substitutes in the urologic field. This chapter shows the research and clinical work on tissue expansion in the search of urinary tissue employed in urine conduction and storage.

Among the various self-tissue substitutes such as oral mucosa, pericardium, or allograft tissues that can be used, only vascularized intestinal segments have been successful with regard to the reconstructive surgery of the urinary bladder.[1–5] Nevertheless, the use of bowel segments in the urinary tract reconstruction is associated with significant disadvantages, including metabolic complications, infections, stone and tumor formation, and a variety of surgical risks associated with bowel surgery.[1] These disturbances are exaggerated in patients with compromised renal function and children.

Although it is difficult to assess the total number of surgical cases performed in the United States, where such tissue substitute is needed, a study from a single pediatric hospital reported their experience with almost 500 cases of bladder augmentation in a 25-year timeframe.[6] The potential disadvantages of using intestinal segments in urinary tract reconstruction include metabolic changes, mucus production, high incidence of early and late surgical complications, and stone/tumor formation.[1] In a search for more suitable tissue for bladder reconstruction, a variety of sources have been already explored.[1–5,7] The majority of these sources are still considered experimental, lacking any significant long-term clinical or experimental results.

Chronic tissue expansion is an established concept for creating new tissue in plastic surgery. The growth of native skin has been successfully employed in procedures such as breast reconstruction, craniofacial surgery, and reconstructive surgery in patients with extensive burns.[8] The expanded, new tissue, created by chronic stretch, duplicates the morphologic and functional characteristics of the native tissue. The literature has been accumulated to explore the involved mechanisms in response to tissue chronic stretch, and it demonstrates that the mechanisms behind the principle of stretch-induced cellular growth involve a network of several integrated cascades that include growth factors;[9–14] extracellular, cytoskeletal, and transmembrane structures;[15–19] ion channels;[20–22] protein kinases;[23–25] second messenger systems;[26,27] and transcriptional factors.[28–30] This network is initiated by a mechanical stimulus that sets into play a series of precise reactions through what has been referred to as the stretch-induced signal transduction pathway.[9]

Tissue Expansion Physiology

Chronic stretch-induced tissue is accompanied by increased expression of several growth factors and receptors that may contribute to cell proliferation and tissue remodeling required for expansion. In smooth muscle cells, these proteins include members of the transforming growth factor (TGF), epidermal growth factor (EGF), basic fibroblast growth factor (bFGF), platelet-derived growth factor (PDGF), and nerve growth factor (NGF) families.[9–14] In the bladder smooth muscle cells, mechanical stretch increased the expression of heparin-binding EGF-like growth factor (HB-EGF) and one of its receptors, ErbB1, resulting in inhibition of apoptosis.[10] Tissue expansion also induced production of NGF by urinary tract smooth muscle cells;[11] and lower urinary tract obstruction induced hypertrophy of bladder afferent and efferent neurons that appeared to require increased NGF expression.[12] The latter finding supports the hypothesis that obstruction-induced tissue expansion induces remodeling of the neural networks.

Stretch-induced tissue expansion also involves extracellular matrix production, which is required for stretch-induced cell proliferation.[9] In vascular smooth muscle cells, mechanical strain-induced fibroblast growth and extracellular matrix production were accompanied by increased expression of TGF-β1 and inhibited by a TGF-β1 neutralizing antibody.[13] Rapid tissue expansion may also injure ureteral tissue more seriously than slow expansion, with associated ischemia and

P. Dasgupta et al. (eds.), *New Technologies in Urology,*
DOI: 10.1007/978-1-84882-178-1_20, © Springer-Verlag London Limited 2010

inflammation. TGF-β1 may be the main regulating factor for both the repair process and inflammatory response. We observed 2–3-fold increases in TGF-β2 expression in porcine chronic expanded vs. native ureteral tissues.[31]

Chronic tissue expansion has also been shown to induce angiogenesis, with associated ischemia, which in turn can stimulate the production of vascular endothelial growth factor (VEGF).[14] Ischemia induced by tissue expansion may also determine the degree of any ensuing fibrosis. In our preliminary study, no change in VEGF expression was observed in the expanded ureteral tissue.[31] It should be noted that all of the above-cited literature regarding the mechanisms of stretch-induced tissue remodeling pertains to skin tissue expansion on cultured cells.

Tissue Expansion In Urinary Tract

Tissue expansion techniques have also successfully been used in genitourinary tract tissues in the experimental setting.[31–34] In 1996, Lailas and colleagues initially reported chronic ureteral expansion for subsequent open ureterocystoplasty in a rabbit model.[32] Ten rabbits underwent unilateral ligation at the ureterovesical junction and ipsilateral nephrectomy. A silicone catheter was placed into the proximal ureter and connected to a titanium injection port, which was placed subcutaneously at the level of costal margin. Two weeks later, a saline-antibiotic was injected in the port daily, limited by the pressure in the system. Within 6 weeks, the ureter was opened longitudinally on the anterior aspect, reconfigured into a U-shaped patch, anastomosed to the bladder, and covered with an omental flap. A suprapubic tube was placed for 10 days after the procedure. After 6 months, the animals were euthanized. The cystogram showed a mean increase of 260% in the bladder capacity. Urodynamic studies were compatible with a low pressure, high-capacity bladder.

Ikeguchi and associates[33] performed chronic segmental ureteral expansion in pigs. A latex balloon was located in the distal ureter inserted through the renal parenchyma opened surgically. A nephrostomy tube was also placed. Daily ureteral dilation (150–1,000 mL) was performed with 1–50 cm^3 daily over a period of 2–4 weeks, with no anesthesia required. Subsequently, an open ureterocystoplasty and reconstruction of the ipsilateral ureter were carried out. A transurethral catheter was maintained for 1 week. Cystograms revealed an increased bladder capacity. The animals were sacrificed after 4 weeks, and the histological sections showed preservation of ureteral architecture with epithelial regeneration.

In 2003, Desai and Gill from the Cleveland Clinic reported their initial experience with a completely minimally invasive approach for chronic ureteral balloon expansion followed by laparoscopic augmentation ureterocystoplasty in a survival porcine model.[31]

This study was performed in female farm pigs, and five animals were initially used to develop the prototype design and insertion technique of the ureteral expansion balloon, its inflation schedule, and the technique of laparoscopic ureterocystoplasty. Subsequently, the five animals entered the survival study.

All the five chronic animals underwent unilateral percutaneous insertion of the ureteral expansion balloon (Microvasive, Natick, MA), a dual-channel balloon catheter: one for inflation and the other for proximal nephrostomy drainage (Fig. 20.1). The balloon, flanked by radiopaque markers, was positioned in the juxtavesical ureter and distended with 2.5–3 mL of contrast medium to secure it in position (Fig. 20.2b). The excess proximal length of the catheter exiting the animal's back was tunneled subcutaneously, so that only the inflation and drainage ports were visible outside the skin.

Starting from the day after placement of the ureteral expansion balloon, the ureter was gradually dilated by daily incremental instillation of a dilute (1:4) contrast solution. The inflation was carried out without anesthesia or analgesia. Ureteral expansion was monitored radiologically every 7–10 days (Fig. 20.3).

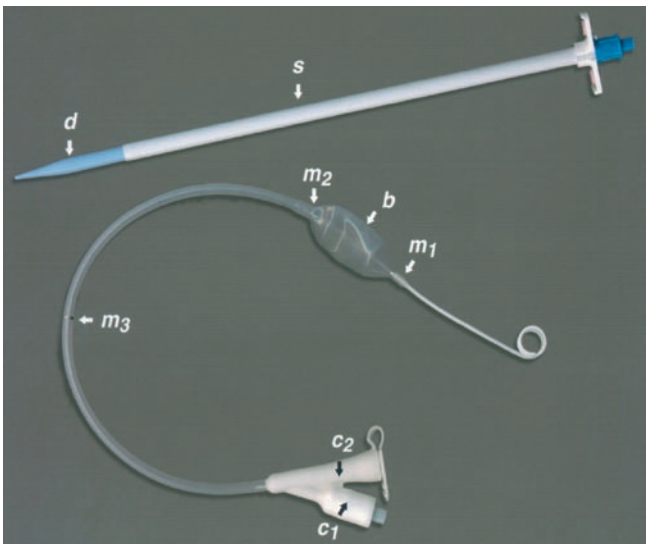

Fig. 20.1 Ureteral expansion was performed using a novel silicone balloon TUEC catheter having two channels: a smaller channel to inflate balloon (*c1*) and a larger fenestrated channel to drain kidney (*c2*). The 14F shaft has multiple holes to facilitate proximal urinary drainage. The balloon (*b*) has one radiopaque marker (*m1* and *m2*) at its either end to facilitate fluoroscopic confirmation during placement. Additional radiopaque marker (*m3*) on shaft immediately proximal to the last drainage hole should lie within the kidney. Terminal end of the catheter is fashioned into a pigtail to facilitate retention in bladder. Single-step dilator (*d*) is used to position 20F peel-away sheath (*s*) within renal collecting system

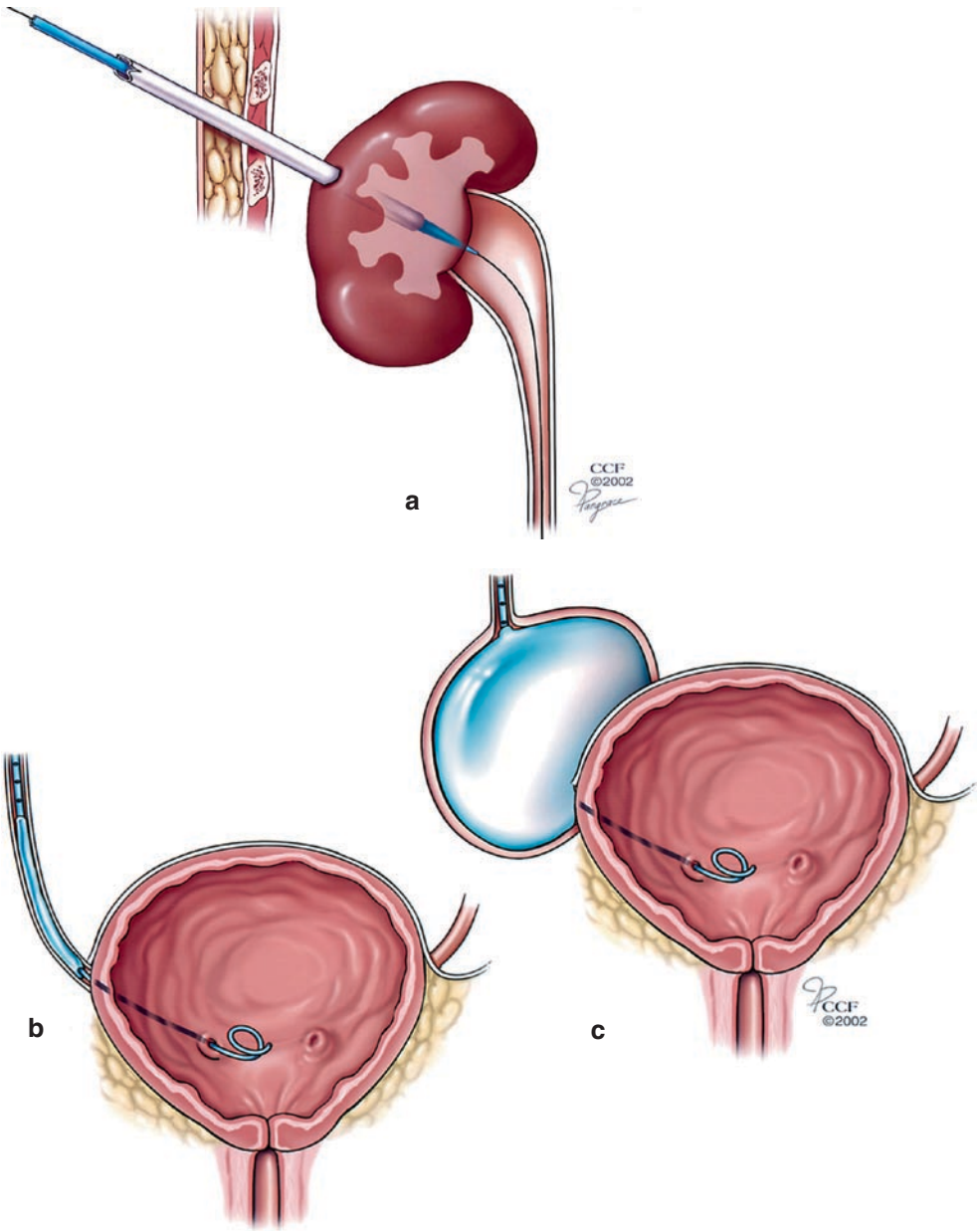

Fig. 20.2 Procedures of percutaneous insertion of TUEC, and inflation of balloon. Balloon position: deflated balloon is positioned in juxtavesical ureter. *Left*: incremental progressive inflation of balloon causes chronic expansion of juxtavesical ureter. (**c**) Expanded juxtavesical ureter. Note: the laterally-based vascular supply to expanded ureteral segment from the internal iliac vessels. Reprinted with the permission from The Cleveland Clinic Center for Medical Art & Photography © 2009. All Rights Reserved

Laparoscopic ureterocystoplasty was performed in all five animals after 3–4 weeks of ureteral expansion. All procedures were performed using a four-port transperitoneal approach with the pig under general anesthesia. Initially, the ureteral balloon was completely deflated, and the amount of fluid aspirated was measured. The balloon was subsequently refilled with the same amount of dilute antibiotic solution to facilitate intraoperative identification, and to prevent intraoperative spillage of potentially infected fluid if inadvertent puncture of the balloon occur intraoperatively. The expanded ureter was identified as a readily visible bulge adjacent to the urinary bladder. The medial peritoneum overlying the expanded ureter was incised to expose the ureteral wall. The fallopian tube and ovary on the ipsilateral side were mobilized away from the ureter. The bladder was mobilized by dividing the medial umbilical ligament and the superior vesical pedicle, and incised laterally in a longitudinal fashion from just above the ureteral orifice up to the dome. The ureteral orifice and intramural ureter were preserved. On the other hand, in the initial two animals, the bladder dome was not excised, and in the latter three, approximately 80% of the bladder was removed. The medial wall of the expanded ureteral segment was then incised using a J-hook monopolar cautery electrode, thus, opening the expanded ureteral segment medially. Care was taken to minimize any mobilization of the ureter, thus, maintaining intact the laterally based

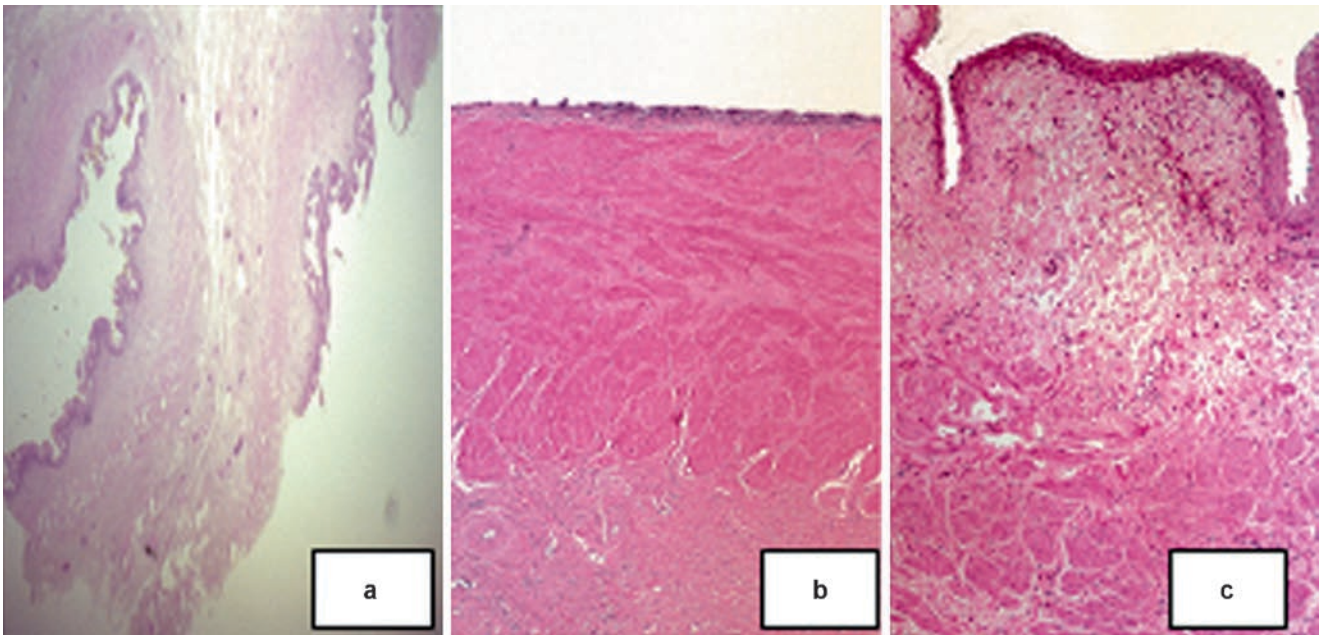

Fig. 20.3 Light microscopic examination of: (**a**) normal ureter, (**b**) tissue-expanded ureter, which reveals muscle hypertrophy and hyperplasia, and variable inflammatory infiltrate, and (**c**) native bladder. Note: the expanded ureter (**b**) more closely resembles the thickness of the bladder wall (**c**) than the normal ureter (**a**)

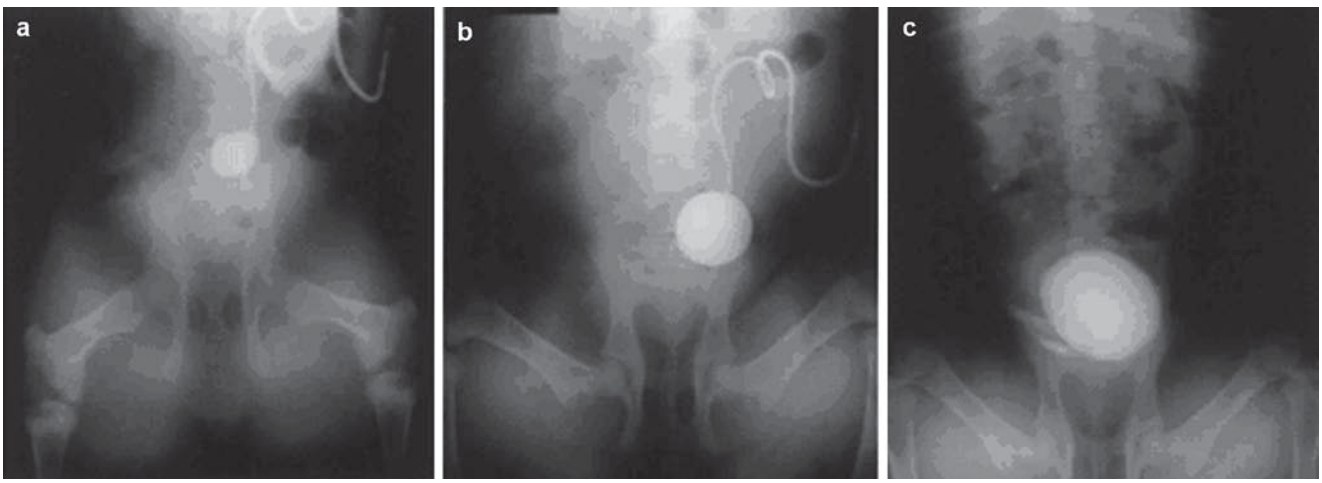

Fig. 20.4 Plain radiographs of the abdomen document progressive ureteral expansion (**a**) At 1 week with 12 mL volume. (**b**) At 2 week, volume in balloon has increased to 46 mL. (**c**) At 25 days just prior to augmentation ureterocystoplasty with 140 mL in the balloon

vascularity of the expanded ureter (Fig. 20.4). The length, site, and orientation of the ureteral incision were tailored to the bladder defect (Fig. 20.5). After the ureteral incision was completed, the balloon was deflated and the catheter removed. The in-line tissue-expanded ureteral patch was then anastomosed to the bladder in a running fashion using 2–0 Vicryl sutures on a CT-1 needle with freehand intracorporeal laparoscopic suturing and knot-tying techniques (Fig. 20.6). After the posterior wall was sutured, an 18F urethral catheter was inserted into the urethra through the bladder neck. The anterior wall was then sutured to complete the augmentation ureterocystoplasty. A 22F suprapubic catheter was left indwelling and brought out through the suture line in the initial two animals only. A drain was positioned in the prevesical space in all five animals and brought out through a port site.

The suprapubic catheter was removed after 7 days, and the urethral catheter was removed after 14 days if not spontaneously expelled earlier. The drain, if not spontaneously expelled, was removed a day after the urethral catheter was removed. All the animals underwent laboratory, radiologic, urodynamic, and histologic investigations (Table 20.1).

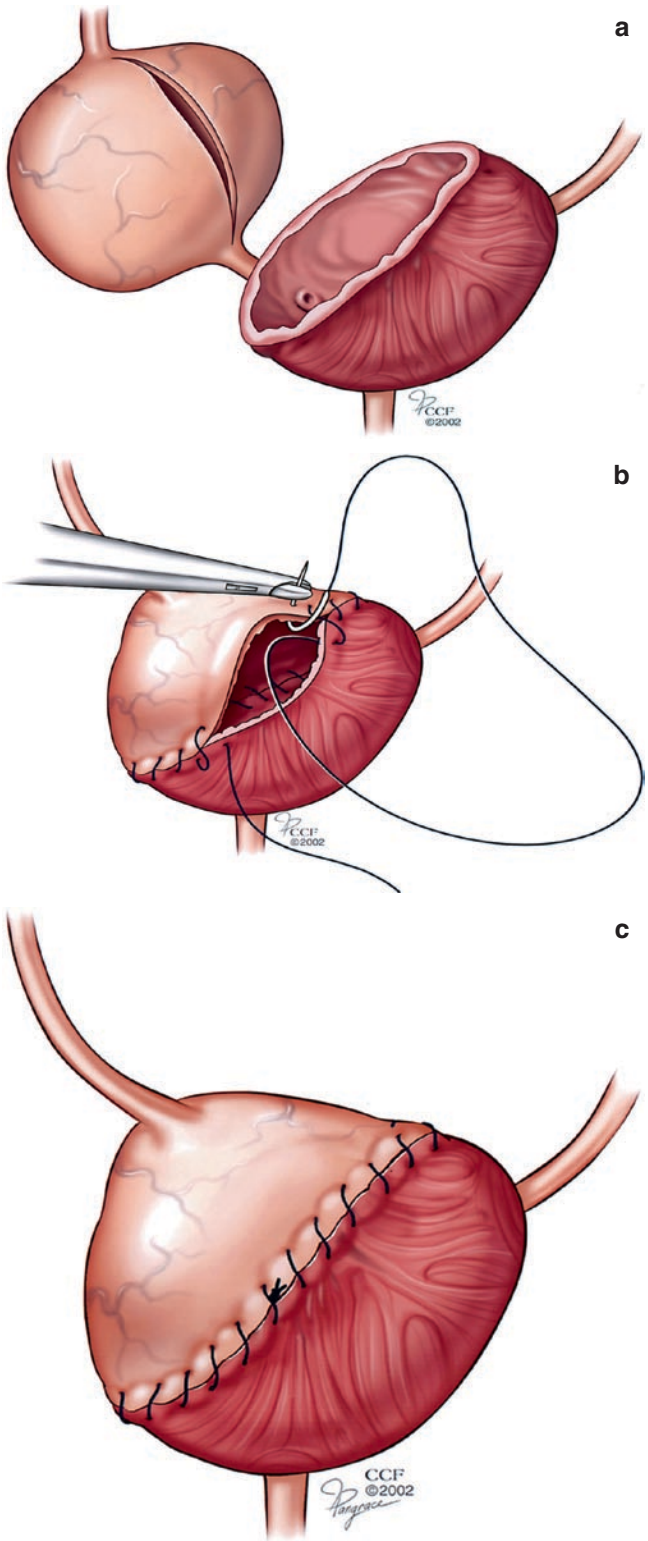

Fig. 20.5 (**a**–**c**) Steps during the laparoscopic ureterocystoplasty. Reprinted with the permission from The Cleveland Clinic Center for Medical Art & Photography © 2009. All Rights Reserved

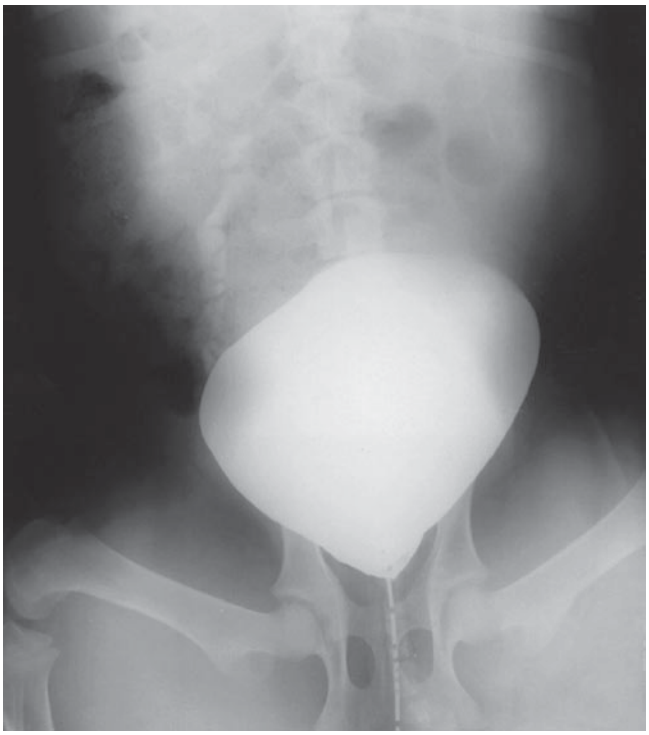

Fig. 20.6 Cystogram performed immediately prior to autopsy at 3 months. Augmented bladder reveals capacity of 600 mL. There is grade II reflux in the right ureter

Table 20.1 Investigation schedule

	Timing
Laboratory: complete blood count, metabolic profile, urinanalysis, and culture	Prior to balloon insertion Prior to augmentation ureterocystoplasty Prior to euthanasia
Radiologic	
Plain film	Weekly during balloon inflation Prior to augmentation ureterocystoplasty
Cystogram	At 1-month follow-up Prior to euthanasia
Intravenous urogram	Prior to euthanasia
Urodynamics	Prior to euthanasia
Cystoscopy	At 1-month follow-up (N 5 2) Prior to euthanasia
Histology	
Light microscopy	During augmentation cystoplasty At euthanasia
Transmission electron microscopy	During augmentation cystoplasty (N 5 2)
Tissue cytokine assay (VEGF and TGF-β2)	During augmentation cystoplasty (N 5)[a]

[a]Seven tissue biopsies were obtained from the five animals at the time of augmentation ureterocystoplasty for cytokine assay

Additionally, electronic microscopy exam of the expanded ureter and measurement of VEGF and TGF-β2 in the expanded ureteral tissue were performed in selected animals. The animals were euthanized at 15 days (N = 1), 1 month (N = 1), 2 months (N = 1), and 3 months (N = 2).

All the five animals underwent successful ureteral expansion over a mean of 25 days. The mean final volume of the ureter was 180 mL. All the animals readily tolerated the daily incremental instillation of dilute contrast solution without apparent pain or discomfort. The ureteral expansion balloon did not malfunction in any case, as judged by leakage of fluid, blockage of the channel, balloon migration, or rupture.

Radiologic volumetric assessment of the ureteral balloon during the phase of ureteral expansion was commensurate with the amount of fluid instilled. We did not note any complications during ureteral expansion. Proximal urinary drainage through the fenestrated channel of the ureteral expansion catheter was adequate in all five animals.

Laparoscopic ureterocystoplasty was feasible in all five animals without the need for open conversion. Periureteral adhesions were encountered close to the expanded ureter, which were lysed laparoscopically. The expanded ureter appeared thick and highly vascular, with areas of urothelial denudation. Intraoperative instillation of saline through the urethral catheter at the end of the ureterocystoplasty revealed a watertight anastomosis in all five cases. Postoperative complications, namely, lower ureteral obstruction and pyelonephritis with sepsis, were seen in two animals (Table 20.2).

Over a follow-up ranging from 15 days to 3 months, the mean bladder capacity was 575 mL (380–940 mL). The P*ves* at maximum capacity was 14 cm H_2O,[6,9–16,31–34] and bladder compliance was 71 mL/cm H_2O (35.3–188 mL/cm H_2O). Uninhibited detrusor contractions were not evident on the urodynamic evaluation in any of the five animals (Table 20.3). Cystography revealed ipsilateral reflux in four renal units: grade II in one animal, grade IV in two animals, and grade V in one animal (Fig. 20.7). At autopsy, one renal unit demonstrated lower-ureteral obstruction and therefore, showed no reflux on cystography. There was no contralateral reflux in any renal unit. In all four refluxing units, the refluxed contrast drained from the kidney immediately after the bladder was emptied, thereby ruling out any ureteral obstruction. Additionally, the cystogram did not reveal contrast extravasation in any case.

Table 20.2 Intraoperative data

Mean time for balloon insertion (min)	52 ± 10 (39–68)
Mean time for bladder augmentation (min)	156 ± 41 (115–210)
Estimated blood loss (mL)	29 ± 16 (10–50)0 00
Subtotal cystectomy performed (N)	3
Ureteral stenting (N)	2
Urethral catheter (N)	5
Intraoperative complications (N)	Serosal bowel tear repaired laparoscopically (1)

Cystoscopy and bladder biopsy was performed in all animals after 1 month and the bladder revealed a fully regenerated mucosa in four animals; one animal euthanized at 15 days still had patchy areas of denuded mucosa. Laboratory examination revealed minimal metabolic alterations in four animals. One animal that developed pyelonephritis and urosepsis had evidence of azotemia, hyponatremia, hyperkalemia, and acidosis. The mean serum creatinine concentration was 1.3 mg/dL at baseline, 0.9 mg/dL at bladder augmentation, and 2 mg/dL at euthanasia.

At autopsy, the ureteral patch appeared well vascularized, and the ureterocystoplasty suture line was healed in all five animals. The ipsilateral renal parenchyma appeared grossly

Table 20.3 Radiologic and urodynamic datas

Animal	Follow-up (weeks)	Subtotal (80%) cystectomy	Cytograma			Urodynamics			
			Ipsilateral reflux (grade)c	Anastomotic leak	Bladder capacity (mL)	Resting	Full capacity (mL/cm)	Compliance H_2O	Involuntary bladder contractions
1	2	No	2	No	600	3.0	20	35.3	Absent
2	4	No	4	No	380	2.0	12	38.0	Absent
3	8	Yes	–	No	940	3.0	8	188	Absent
4	12	Yes	4	No	430	4.0	12	53.8	Absent
5	12	Yes	5	No	520	6.0	18	43.3	Absent
Mean	–	–	–	–	574	3.6	14	71.7	–

[a]Cystographic examination was performed at 1 month (N 5 3) and at autopsy by injecting contrast through a urethral catheter. In all refluxing renal units, obstruction was ruled out by documentation of prompt drainage of contrast from the collecting system

Pves (cm H_2O)

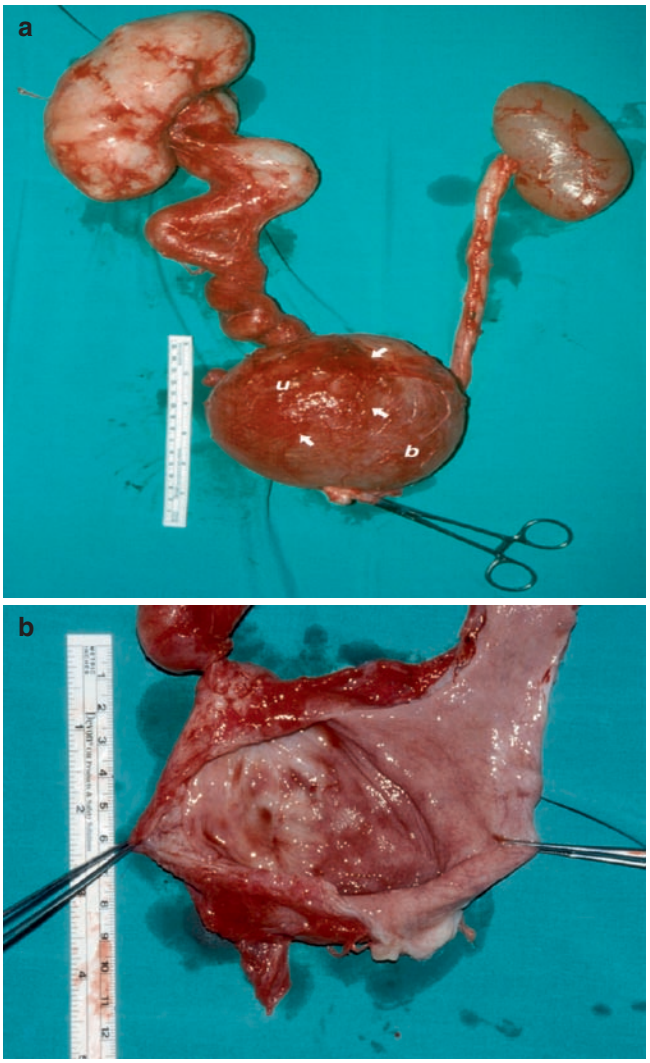

Fig. 20.7 Autopsy photographs. (**a**) Augmented bladder and both renal units. Healed suture line between expanded ureteral patch (*u*) and native bladder (*b*) is seen (*arrows*). (**b**) Interior of the augmented bladder shows demarcation (*arrows*) between expanded ureter (*u*) and native bladder (*b*). Notice the complete epithelialization of the expanded ureteral patch

normal in three cases, with pre-euthanasia intravenous urography (IVU) revealing prompt opacification with mild hydronephrosis. One animal with a lower ureteral obstruction revealed thinning of parenchyma and poor function on IVU. At autopsy, the obstruction was found to be the result of flimsy synechia formation at the junction where the upper, normalcaliber, ureter entered the expanded ureteral segment. The animal with pyelonephritis and urosepsis had a grossly scarred kidney that was nonfunctioning on IVU.

Light microscopic examination of biopsies of the expanded ureter obtained at the time of augmentation cystoplasty revealed muscle hypertrophy and hyperplasia, mucosal atrophy, and variable inflammatory infiltrate. The histological examination of the expanded ureter revealed persistent muscle hypertrophy and hyperplasia, a fully regenerated transitional epithelium, and variable amount of fibrosis.

Transmission electron microscopy performed on the ureteral tissue obtained at the time of laparoscopic augmentation revealed cellular evidence consistent with muscular hypertrophy and hyperplasia.

Preliminary data on growth factor expression in expanded ureteral tissue obtained and snap frozen at the time of augmentation ureterocystoplasty revealed a 2–3-fold increase in TGF-β2 (median 44 pg/mL; range 27–49 pg/mL) over controls (normal ureter 16 pg/mL). There was no increase in VEGF expression in the expanded ureteral tissue when compared with control samples.

Although the potential for ureteral tissue expansion in the context of urinary tract reconstruction has been preliminarily explored, none of the investigators have taken the issue far enough to explore the cellular and molecular mechanism involved in visceral tissue expansion and remodeling. The tissue expansion in the GU system is yet to be advanced to a place where it can have a real practical use by urologists, to the extent that skin expansion has become an accepted part of plastic reconstructive surgery.

Encouraged by the principles mentioned earlier and potential value of expanded ureteral tissue, we pursued development and proof of concept of a methodology that would enable us to obtain excess ureteral tissue with minimally invasive surgical techniques. The expanded ureteral tissue can be used in open or laparoscopic surgical techniques in a variety of reconstruction applications for the lower urinary tract. Further, our preliminary studies have provided motivation for the pursuit of biological markers possibly responsible for visceral tissue remodeling.

Clinical Study

Following the laboratory experiments and upon availability of the opportunity in two outside medical centers, the same authors performed this procedure in three patients (outside the United States), with the approval from the ethical committee at each local institution. Clinical data from these patients have been encouraging, supporting our laboratory data. Specifically, we treated two women and one man, aged 14, 65, and 54 years, respectively. Each patient suffered from a noncompliant bladder with reduced capacity (range 15–150 mL).

After percutaneous placement of the balloon, in-line expansion of the distal ureter was achieved on an out-patient basis over 23–38 days to a volume of upto 218 mL. Notably, all the three patients did not require any analgesia during this entire expansion process.

Operative time for the laparoscopic augmentation ureterocystoplasty ranged from 2 to 3 h, and blood loss was

25–50 mL. Each patient commenced oral intake on the same day and ambulated within 24 h. There were no complications at any stage of this study. Postoperatively bladder capacity increased significantly to 250–280 mL at 2-month follow-up. The first patient has now completed 2-year follow-up with durable success. All the three patients have experienced significant improvement in the voiding symptoms, and the renal function is well preserved.

Clinical Implications

The availability of an urothelium-lined, muscle-backed, vascularized, autogenous, in-line tissue material for the purposes of augmentation, and possibly even replacement of the urinary bladder would indeed be a major advance.

This could eliminate the use of bowel (and its attendant morbidity) in urinary tract reconstruction. Potentially, such a bladder substitute could have mucosal, myogenic, and neurogenic attributes that approximate those of a functionally intact urinary bladder. The study described earlier represents a concerted effort at establishing and developing this novel field of visceral tissue expansion.

The search for the ideal substitute tissue for bladder augmentation is still ongoing. Currently, intestinal segments remain most commonly used for bladder augmentation. Although the results of augmentation cystoplasty using various bowel segments have generally been acceptable, these tissues are associated with absorptive metabolic changes, mucus production, and stone formation, the magnitude of which is dependent on the length and segment of the bowel used.[35] Significant research in the past few decades has focused on alternative tissue substitutes for urinary tract reconstruction. These have included tissue-engineered materials,[36] xenografts such as small-intestinal submucosa (SIS),[37] and techniques such as autoaugmentation and deepithelialized bowel.[38] Some of these techniques, although promising, have either been insufficiently durable or require considerable refinement. The ureter, with its transitional epithelium, is potentially an optimal tissue for bladder augmentation.[39]

Augmentation ureterocystoplasty has been reported, with encouraging long-term urodynamic results, and limited, if any, metabolic changes. However, the amount of ureteral tissue needed to provide an urodynamically acceptable bladder augmentation can be obtained only in a patient with a large megaureter. Therefore, currently, augmentation ureterocystoplasty is limited to the occasional patient with a megaureter and a nonfunctioning kidney, who requires bladder augmentation.

Thus, although the potential for ureteral tissue expansion for urinary tract reconstruction has been demonstrated, further characterization of the biology of ureteral expansion and refinement of the technique are necessary prior to its clinical application. The experimental study published by Desai and Gill was designed specifically to address the following crucial issues: (1) the feasibility of percutaneous insertion of the ureteral expansion device; (2) the efficacy of this novel balloon in expanding the ureter to the desired volume while simultaneously providing adequate drainage of the renal unit; (3) a safe and reliable time-line schedule and regimen for ureteral balloon expansion; (4) the technical feasibility of performing laparoscopic augmentation ureterocystoplasty using the tissue-expanded ureter; and (5) the biologic nature of the expanded ureteral tissue and its efficacy in providing a urodynamically adequate bladder augmentation in a survival porcine model.

Postoperative complications occurred in two animals. One animal developed lower-ureteral stenosis, hydroureteronephrosis, and poor ipsilateral renal function, and the other animal had pyelonephritis with sepsis. At autopsy, the animal with lower-ureteral obstruction revealed flimsy adhesion formation at the junction of the expanded ureter with the proximal normal-caliber ureter. There was no transmural fibrosis on histological examination of the stenotic area. This obstruction probably represents cross-healing of the opposite ureteral walls following mucosal denudation during the expansion process, and can potentially be avoided by stenting at the time of augmentation ureterocystoplasty until reepithelialization is complete.

Moreover, the survival porcine study demonstrated that progressive, incremental ureteral tissue overexpansion can be carried out safely and reliably with a percutaneously placed expansion balloon. This ureteral expansion is well tolerated and can be performed over a 3–4-week period to create a sizeable reservoir for bladder augmentation. The expanded ureter is thick and vascular, and reveals histological and electron microscopic features of durable ureteral smooth-muscle hypertrophy and hyperplasia. This expanded tissue can be used laparoscopically to augment the bladder. Such augmented bladders possess good urodynamic properties over a 3-month follow-up period. This approach has the potential to provide native, urothelium-lined tissue for augmentation or, possibly, replacement of the urinary bladder.

Concerted research on this subject will lead to further development of this novel field of tissue expansion.

References

1. McDougal WS. Metabolic complications of urinary intestinal diversion. *J Urol*. 1992;147:1199–1208
2. Oberpenning F, Meng J, Yoo JJ, Atala A. De novo reconstitution of a functional mammalian urinary bladder by tissue engineering. *Nat Biotechnol*. 1999;17:149–155

3. Elbahnasy AM, Shalhav A, Hoenig DM, Figenshau R, Clayman RV. Bladder wall substitution with synthetic and non-intestinal organic materials. *J Urol*. 1998;159:628–637
4. Snow BW, Cartwright PC. Bladder autoaugmentation. *Urol Clin North Am*. 1996;23:323–331
5. Dewan PA, Close CE, Byard RW, Ashwood PJ, Mitchell ME. Enteric mucosal regrowth after bladder augmentation using demucosalized gut segments. *J Urol*. 1997;158:1141–1146
6. Soergel TM, Cain MP, Misseri R, et al Transitional cell carcinoma of the bladder following augmentation cystoplasty for the neuropathic bladder. *J Urol*. 2004;172:1649–1651
7. Churchill BM, Aliabadi H, Landau EH, et al Ureteral bladder augmentation. *J Urol*. 1993;150:716–720
8. Neumann CG. The expansion of an area of skin by progressive distention of a subcutaneous balloon; use of the method for securing skin for subtotal reconstruction of the ear. *Plast Reconstr Surg*. 1957;19:124–130
9. De Filippo RE, Atala A. Stretch and growth: the molecular and physiologic influences of tissue expansion. *Plast Reconstr Surg*. 2002;109:2450–2462
10. Nguyen H, Park J, Peters C, et al Cell-specific activation of the HB-EGF and ErbB1 genes by stretch in primary human bladder cells. *In Vitro Cell Dev Biol Anim*. 1999;35:371
11. Persson K, Sando JJ, Tuttle JB, Steers WD. Protein kinase C in cyclic stretch-induced nerve growth factor production by urinary tract smooth muscle cells. *Am J Physiol*. 1995;269(4 Pt 1): C1018-C1024
12. Steers WD, Kolbeck S, Creedon D, Tuttle JB. Nerve growth factor in the urinary bladder of the adult regulates neuronal form and function. *J Clin Invest*. 1991;88(5):1709–1715
13. O'Callaghan CO, Williams B. Mechanical strain increases matrix synthesis by human vascular smooth muscle cells: the role of TGF[beta]. J Hypertension. 1998;16(suppl 2):S16
14. Shweiki D, Itin A, Soffer D, Keshet E. Vascular endothelial growth factor induced by hypoxia may mediate hypoxia-initiated angiogenesis. *Nature (Lond.)*. 1992;359:843–845
15. Takei T, Mills I, Arai K, et al Molecular basis for tissue expansion: clinical implications for the surgeon. *Plast Reconstr Surg*. 1998;102:247
16. Schmidt C, Pommerenke H, Durr F, et al Mechanical stressing of integrin receptors induces enchanced tyrosine phosphorylation of cytoskeletally anchored proteins. *J Biol Chem*. 1998;273:5081
17. Wang N, Butler JP, Ingber DE. Mechanotransduction across the cell surface and through the cytoskeleton. *Science* 1993;260:1124
18. Ingber D, Dike L, Hansen L, et al Cellular tensegrity: exploring how mechanical changes in the cytoskeleton regulate cell growth, migration, and tissue pattern during morphogenesis (Review). *Int Rev Cytol*. 1994;150:173–224
19. Vasioukhin V, Bauer C, Yin M, et al Directed actin polymerization is the driving force for epithelial cellcell adhesion. *Cell*. 2000; 100:209
20. Kirber MT, Walsh JV, Jr, Singer JJ. Stretchactivated ion channels in smooth muscle: a mechanism for the initiation of stretch-induced contraction. *Pflugers Arch*. 1988;412:339
21. Sachs F. Mechanical transduction by membrane ion channels: a mini review. *Mol Cell Biochem*. 1991;104:57
22. Nakayama K. Calcium-dependent contractile activation of cerebral artery produced by quick stretch. *Am J Physiol*. 1982;242:H760
23. Ruoslahti E. Stretching is good for a cell. *Science*. 1997;276:1345
24. Nishibe S, Wahl MI, Hernandez-Sotomayor SM, et al Increase of the catalytic activity of phospholipase C-gamma 1 by tyrosine phosphorylation. *Science*. 1990;250:1253
25. Seger R, Krebs EG. The MAPK signaling cascade. *FASEB J*. 1995; 9:726
26. Takei T, Rivas-Gotz C, Delling CA, et al Effect of strain on human keratinocytes in vitro. *J Cell Physiol*. 1997;173:64
27. Tenor H, Hatzelmann A, Wendel A, et al Identification of phosphodiesterase IV activity and its cyclic adenosine monophosphate-dependent up-regulation in a human keratinocyte cell line (HaCaT). *J Invest Dermatol*. 1995;105:70
28. Chien S, Li S, Shyy YJ. Effects of mechanical *Vol. 109, No. 7*/STRETCH AND GROWTH 2461 forces on signal transduction and gene expression in endothelial cells. *Hypertension*. 1998;31(1 pt 2):162
29. Komuro I, Kaida T, Shibazaki Y, et al Stretching cardiac myocytes stimulates protooncogene expression. *J Biol Chem*. 1990;265:3595
30. Bar-Sagi D, Feramisco JR. Induction of membrane ruffling and fluid-phase pinocytosis in quiescent fibroblasts by ras proteins. *Science*. 1986;233:1061
31. Desai MM, Gill IS, Goel M, et al Ureteral tissue balloon expansion for laparoscopic bladder augmentation: survival study. *J Endourol*. 2003;17:283–293
32. Lailas NG, Cilento B, Atala A. Progressive ureteral dilation for subsequent ureterocystoplasty. *J Urol*. 1996;156:1151–1153
33. Ikeguchi EF, Stifelman MD, Hensle TW. Ureteral tissue expansion for bladder augmentation. *J Urol*. 1998;159:1665–1668
34. Liatsikos EN, Dinlenc CZ, Kapoor R, Bernardo NO, Smith AD. Tissue expansion: a promising trend for reconstruction in urology. *Endourol*. 2000;14:93–96
35. McDougal WS. Metabolic complications of urinary intestinal diversion. *J Urol* 1992;147:1199
36. Oberpenning F, Meng J, Yoo JJ, Atala A. De novo reconstitution of a functional mammalian urinary bladder by tissue engineering. *Nat Biotechnol*. 1999;17:149
37. Elbahnasy AM, Shahlav A, Hoenig D, et al Bladder wall substitution with synthetic and nonintestinal organic materials. *J Urol*. 1998;159:628
38. Dewan PA, Close CE, Byard RW, et al Enteric mucosal regrowth after bladder augmentation using demucolized gut segments. *J Urol*. 1997;158:1141
39. Churchill BM, Aliabadi H, Landau EH, et al Ureteral bladder augmentation. *J Urol*. 1993;150:716

Technologies for Imaging the Neurovascular Bundle During Prostatectomy

21

Lawrence L. Yeung and Li-Ming Su

History of the Neurovascular Bundle

In 1904, Hugh Hampton Young was credited for having performed the first radical prostatectomy in the United States by the perineal approach.[1] However, because of the limited visibility afforded by the small incision, identification of critical structures was restricted, making incontinence common and impotence almost universal after surgery. An Irish surgeon by the name of Terence Millin then developed the retropubic approach to prostatectomy in 1947,[2] which allowed for greater visualization of crucial structures; however, morbidity was increased owing to significant blood loss, rectal injury, and urethral strictures, while incontinence remained common, and most men were still impotent.

With the advent of the linear accelerator in the 1960s, external beam radiation became the treatment of choice for most men because of the significant side effects associated with surgery. However, this modality introduced its own set of morbidities in terms of rectal and bladder side effects, in addition to suboptimal treatment of some cancers leading to recurrence of disease. It was not until the early 1970s that urologists began to develop a better understanding of the periprostatic anatomy and vasculature leading to decreased morbidity. In 1977, Walsh performed a prostatectomy on a patient who was fully potent within a year from surgery, leading him to believe that the cavernous nerves did not course through the prostate as most urologists had originally believed.[3] This discovery led Walsh to embark on a journey to further elucidate the anatomy of the pelvic plexus and cavernous nerves.

When Walsh traveled to Leiden, The Netherlands, in 1981 to attend a meeting, he inquired about the work of an acquaintance by the name of Pieter Donker, Chairman of Urology at the University of Leiden, whom he had serendipitously met a few years earlier while attending a meeting of the American Association of Genitourinary Surgeons in Miami.[3] Donker had performed innovative dissections on the nerves innervating the bladder using fetal cadavers, because the tissues proved to be optimal for anatomic dissections and the nerves larger in relation to the surrounding structures.[4] After spending several hours performing dissections, Walsh and Donker had discovered that there were nerves located and traveling outside the prostatic capsule and lateral to the urethra that appeared to innervate the corpora cavernosa[3] (Fig. 21.1). Walsh took this discovery back with him to the operating room where he discovered that the vessels along the capsule of the prostate coincided with the location of the cavernous nerves they had identified in the fetal cadavers. Lepor further confirmed through histologic studies that the cavernous nerves were located on the dorsolateral aspect of the prostate along the pelvic sidewall.[5] Using this information, Walsh determined that the neurovascular bundle (NVB) could be used as a macroscopic landmark for intraoperative identification of the cavernous nerves.[6] This discovery, along with precise understanding of the dorsal venous complex and development of techniques for its ligation and a better understanding of the external striated urethral sphincter anatomy, led to improvements in postoperative potency and urinary continence, and ultimately, the resurgence of radical prostatectomy for the treatment of localized prostate cancer by the mid 1990s.[3]

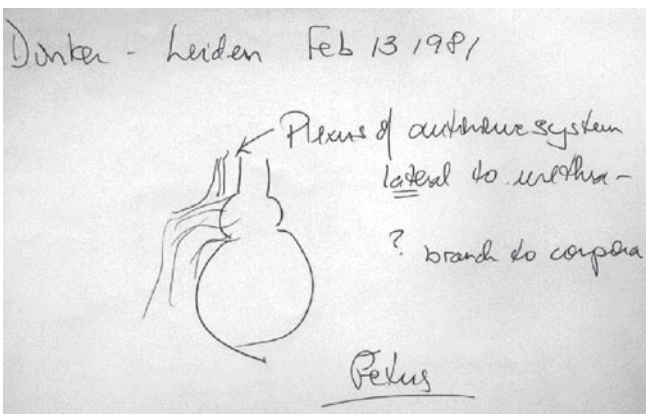

Fig. 21.1 Drawing by Walsh demonstrating autonomic pelvic nerves in a male stillborn infant. (Reprinted from Walsh[3], © 2009, with permission from Elsevier)

P. Dasgupta et al. (eds.), *New Technologies in Urology,*
DOI: 10.1007/978-1-84882-178-1_21, © Springer-Verlag London Limited 2010

Revisiting the Anatomy of the Neurovascular Bundle

Despite having a better understanding of the anatomy of the prostate, reported potency rates have varied widely (i.e., 21–86%) following prostatectomy even with the use of bilateral nerve preservation techniques.[7–9] Sural nerve grafting has been employed in an attempt to enhance cavernosal nerve regeneration in patients who required wide resection of the NVB due to high-risk disease; however, the results have been mixed.[10,11] Several studies have been recently been performed revisiting the periprostatic neuroanatomy to further delineate the anatomic course of the cavernosal nerves.

Costello et al. performed detailed dissections of the NVB and its relationship to the surrounding pelvic structures in male adult cadavers. They discovered that the NVB appears to arise from the most inferior limb of the pelvic plexus and contains divisions that innervate the corpora cavernosa, rectum, prostate, and levator ani musculature (Fig. 21.2). They also demonstrated that the NVB splays laterally between the lateral pelvic fascia and the prostatic fascia, and also posteriorly between the rectum and prostate.[12] They concluded that the cavernosal nerve could not be distinguished from the other divisions of the NVB, thus limiting the success rate of the anastamosis of a single sural nerve graft to distal severed nerve endings.

Takenaka et al. demonstrated that the branches of the hypogastric nerve and pelvic splanchnic nerve splay and interdigitate at multiple levels instead of forming a distinct nerve bundle. They concluded that the cavernous nerves are located beyond the NVB and a surgically reconstructed NVB by graft interposition cannot include the nerve in its entire course.[13] Successful nerve grafting is further complicated by their discovery that there can be significant anatomic variability between patients in the course of the cavernous nerves.

Lunacek et al. performed dissections of the cavernous nerves in fetal and adult cadavers and compared the location of the nerves. They discovered that the cavernous nerves that are initially found running along the lateral lobes of the prostate, as observed in the fetal cadavers (and as Walsh and Donker had discovered), eventually spread anteriorly and form a concave "curtain" when the prostate enlarges as the patient ages (Fig. 21.3). They also demonstrated that the cavernous nerves course lateral and dorsal to the membranous urethra.[14] These findings were also confirmed by Sievert et al., who demonstrated that approximately 25% of the autonomic nerves were located anteriorly at the mid portion of the prostate.[15] Kaul et al. were also able to demonstrate histologically that the prostatic fascia on the anterolateral portion of the prostate contained 25–50% of the total neural tissue (Fig. 21.4).[16] Zvara et al. performed a study in the rat and human model showing that these nerve fibers on the anterolateral aspect of the prostate stained positive for nicotinamide adenine dinucleotide phosphate diaphorase (NADPH-d), which is a cofactor for nitric oxide synthase, the enzyme responsible for the synthesis of nitric oxide (NO).[17] This provided evidence that some of the accessory nerves in the periprostatic fascia produce NO, a principle neurotransmitter responsible for erectile function. All of these anatomic studies, taken together, suggest that accessory neural pathways appear to exist in addition to the main NVB, to provide innervation to the cavernosal bodies. Furthermore, these studies highlight the inherent anatomic

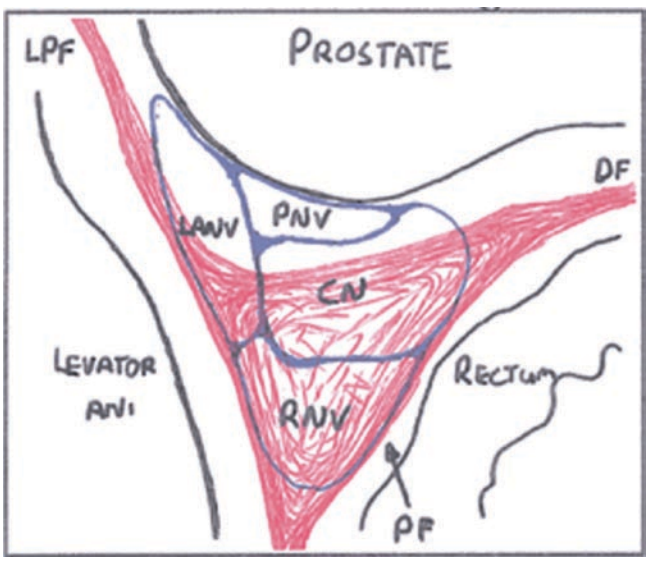

Fig. 21.2 Drawing demonstrating that the *NVB* contains divisions that innervate the corpora cavernosa (*CN*), rectum (*RNV*), prostate (*PNV*), and levator ani musculature (*LANV*). (From Costello et al.[12])

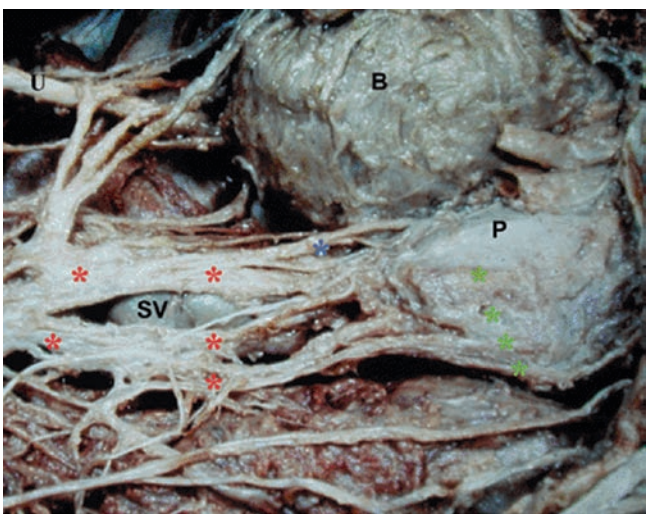

Fig. 21.3 Lateral view of adult cadaver demonstrating splaying of the *CN* (*green asterisks*) along the lateral aspect of the enlarged prostate (*P*) after BPH has developed. The pelvic plexus (*red asterisks*) encase the seminal vesicles (*SV*). *B*, bladder; *U*, right ureter. (From Lunacek et al.[14])

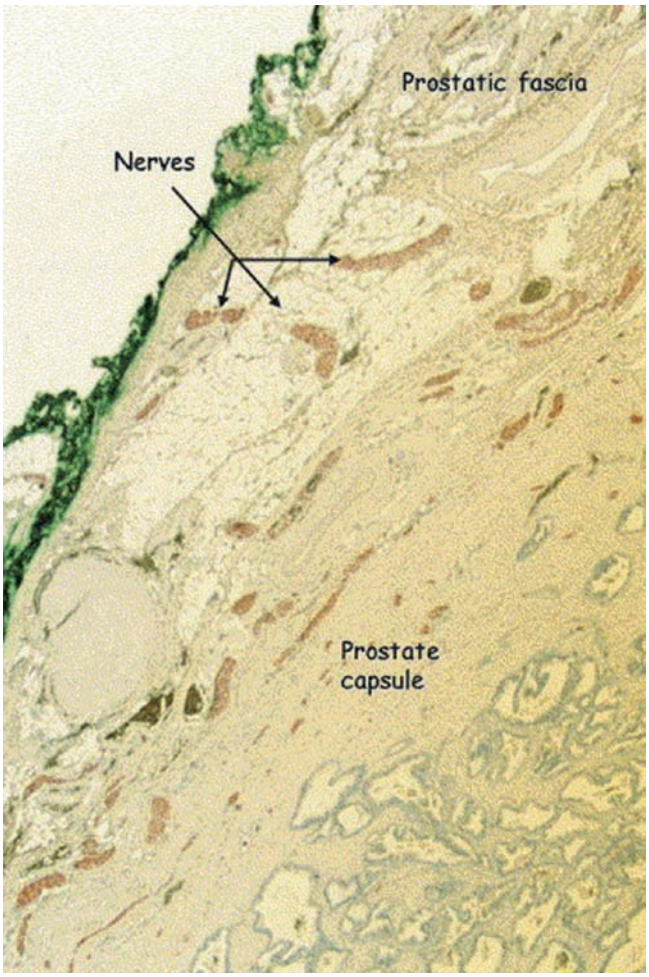

Fig. 21.4 S-100 nerve stain demonstrating accessory nerve fibers within the prostatic fascia. (Reprinted from Kaul et al.[16], © 2005, with permission from Elsevier)

complexity that underlies the cavernous nerves, thus explaining in part the finding that many patients do not recover their full erectile function following bilateral nerve sparing prostatectomy.

Changes in the Technique of Neurovascular Bundle Preservation

The improved knowledge of the anatomic course of the cavernous nerves has allowed for the development of techniques to attempt more precise quantitative and qualitative nerve sparing during radical prostatectomy. With the advent of minimally invasive surgical techniques, including laparoscopic radical prostatectomy (LRP) and robotic assisted laparoscopic radical prostatectomy (RALP), these techniques have allowed for unprecedented intraoperative magnification of the prostate and periprostatic structures including the NVB. These techniques provide a 10× magnification, and in the case of RALP, a high-definition image of the prostatic tissues, thus providing a better opportunity to identify and preserve the putative branches of the cavernous nerves that lie in between layers of the levator, Denonvilliers', and the prostatic fascia.

Because of the anatomic variation in the course of the cavernosal nerves that extend from the posterolateral to the anterolateral surface of the prostate, several surgeons have modified their approach at nerve preservation in patients with low-stage, low Gleason prostate cancer. In 2005, Lunacek et al. reported using a "curtain dissection" technique for nerve preservation during open radical retropubic prostatectomy (RRP) that involved dissection of the NVBs starting anteriorly, while using magnifying lenses to preserve the nerve fibers that are spread in a concave fashion on the anterolateral surface of the prostate.[14]

Menon et al. reported about their RALP nerve-sparing technique termed as the "veil of Aphrodite" that similarly involves incising the prostatic fascia anterioromedially and developing a plane between the prostatic fascia and prostatic capsule in an antegrade fashion using the magnification afforded by the daVinci robotic system, which effectively peels the splayed cavernous nerves off the prostate.[18–20] They believe that the remaining curtains of the periprostatic tissue contain the cavernous nerves and hang from the pubourethral ligament, which creates the image of the so-called "veil".

Nielsen et al. also reported on what Walsh has termed the "high anterior release" nerve preservation technique used during open RRP.[21] His technique is similar to the aforementioned techniques in that the levator fascia is released up high on the anterioromedial aspect of the prostate using the periprostatic fascia as a handle to minimize direct manipulation and traction injury to the true cavernous nerve bundles lying more posterolaterally.

The benefit of intraoperative magnification and the changes in the techniques used to preserve the NVB have resulted in improved potency rates while maintaining acceptable positive margin rates. However, as the cavernous nerves are microscopic and the macroscopic landmarks only serve as a surrogate for the actual cavernous nerves, there is a need for improved mapping of the true cavernous nerve fibers responsible for penile erections. New imaging techniques may assist with localization of the nerves to help target intraoperative nerve dissection and also allow for a successful nerve graft interposition.

Efforts to Achieve Intraoperative Mapping of the Neurovascular Bundle

The goal of intraoperative visual identification of the NVB is mainly twofold: (1) to localize and anatomically map the true nerve fibers responsible for controlling erections and possibly

continence during nerve sparing radical prostatectomy and (2) to locate the cavernous nerve endings during non-nerve sparing radical prostatectomy to facilitate graft anastamosis to the actual ends of the severed nerve. The functional identification of the NVB by electrical stimulation also allows for the evaluation of the continuity of a preserved NVB to aid in determining whether or not a nerve graft should be interposed. A combination of visual and functional identification may allow surgeons to perform a better nerve-sparing prostatectomy and help improve the potency and continence rates, and also improve the success rate of nerve grafting when utilized. Several technologies have been developed to achieve these goals that will be reviewed in the following sections.

CaverMap Surgical Aid

The CaverMap Surgical Aid (Blue Torch Corporation, Norwood, MA) was developed to assist in intraoperative localization of the cavernosal nerves by provoking an erectile response through electrical stimulation of the nerve. It has been shown that electrical stimulation of the cavernous nerve may cause very small changes in tumescence or detumescence of the penis, which may not be visible, but yet physiologically detectable. The CaverMap device was designed to measure changes in penile girth as little as 0.5%. The system is composed of a control unit, a handheld nerve stimulator, and a tumescence sensor placed around the penis to measure changes in the circumference. Mapping of the cavernous nerve is performed by placing the nerve stimulation probe on the tissues suspected to contain the cavernous nerve and using detected changes in penile tumescence during stimulation to, in theory, affirm correct identification of its location (Fig. 21.5). The CaverMap can then be used, after removal of the prostate, to assess the continuity and integrity of the cavernous nerves by proximal stimulation of the nerves and assessing penile tumescence again. It can also be used to localize the distal end of a severed nerve to facilitate nerve graft anastamosis.

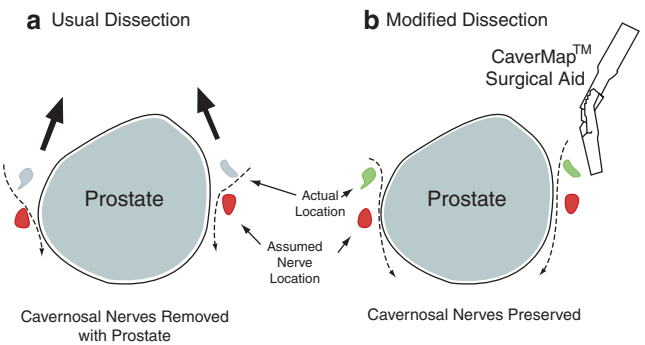

Fig. 21.5 The CaverMap Surgical Aid can be used to map the course of the cavernous nerve along the prostate. (**a**) Dissection resulting the resection of the cavernosal nerve due to incorrect intraoperative identification of the nerves. (**b**) By noting where the probe tip is located when it elicits a tumescence response, the course of the neurovascular bundles becomes apparent and provides an anatomic "map" for the surgeon interested in their preservation. (http://www.bluetorchmed.com/surgeons/index.html)

In concept, the CaverMap Surgical Aid appears to provide a sound solution to precise intraoperative cavernous nerve localization in efforts to achieve optimal cavernous nerve preservation during nerve-sparing radical prostatectomy. Practically, however, results using the CaverMap have been fraught with inconsistency. Klotz et al. reported a 94% potency rate (16 of 17 patients) after the use of CaverMap for intraoperative nerve identification.[22] They also reported a 19% overall positive margin rate (five patients) in that study that included patients with clinical stage T1c and T2a-c disease. However, only three (12%) of the patients had positive margins confined to the apex and/or lateral margin, and it is conceivable that the nerve-sparing approach may have altered the margin status. For the other two patients with positive margins, one had positive margins with seminal vesicle invasion, and the other had extensive positive margins with positive lymph nodes. It is possible that the nerve-sparing approach did not alter the final outcome in those two patients.

Klotz et al. then performed a prospective, randomized, multicenter study using the CaverMap-assisted nerve-sparing prostatectomy technique and compared it with conventional nerve-sparing techniques. They found that, at 1 year, the CaverMap group had a significant improvement in nocturnal tumescence when compared with the conventional nerve-spare group (greater than 60% tumescence for a mean of 15.9 vs. 2.1 min, respectively) as measured by RigiScan, an instrument used to measure penile tumescence and rigidity.[23] However, the improved nocturnal tumescence did not translate into a significant difference in the ability to have an erection sufficient for intercourse (71 vs. 62%, $P = 0.17$). Kim et al. reported that although they had a 77% positive CaverMap response rate, their overall potency rate was only 18% at 1 year.[24] Furthermore, Walsh et al. indicated that the CaverMap device should not be used to determine if a structure should be excised or not, as they found the device to have a low specificity of 54%.[25] This variability and lack of precision was also supported by Holzbeierlein et al. who showed that stimulation of an area on the anterior bladder wall far away from the NVB resulted in tumescence almost half the time.[26] While the CaverMap device had promising early results, efforts to duplicate this have been met with inconsistency and lack of specificity.

Intraoperative Transrectal Ultrasound

Ukimura et al. described a technique to provide real-time intraoperative transrectal ultrasound (TRUS) imaging of the prostate and periprostatic tissues and vessels to assist with

dissection to compensate for the muted tactile feedback present when performing LRP.[27] As opposed to screening TRUS, intraoperative TRUS combines prostate needle biopsy results with real-time imaging, allowing the ultrasonographer to direct the surgeon to a wider plane of dissection in areas of suspicion such as near hypoechoic lesions or regions where the biopsies were positive near the capsule. They reported the potential advantages of real-time TRUS imaging as follows: (1) it identifies the anatomical course of the NVB, (2) it measures the adequacy of NVB preservation, (3) it identifies the apical margin of the prostate, (4) it aids in the dissection of the posterior bladder neck, vas deferens, seminal vesicle, and release of the rectal wall, and (5) it identifies any hypoechoic bulging nodule to help in avoiding positive surgical margins.[28] They found that their positive surgical margin rates decreased from 29 to 9% ($P = 0.0002$) with the use of intraoperative TRUS during LRP, and were able to map the course of the NVB using TRUS by tracing the arterial flow within the NVB.[27] Based on the previous findings by Lepor et al. documenting the lateral location of the cavernous nerve within the NVB with relation to the vascular supply,[5] it was theorized that if the vascular supply in the NVB is preserved after the nerve-sparing dissection, as demonstrated by Doppler waveform analysis using TRUS, then the cavernous nerves should be spared. They were also able to report on the diameter of the NVB and the number of visible vessels within the NVB before and after the dissection to evaluate the quality of the nerve-sparing dissection, and found a decrease in the number of visible vessels from 2.6 to 1.1 and a decrease in the cross-sectional area of the NVB by 11%.[28] However, these findings are yet to be correlated with any improvement in the potency rates after nerve-sparing LRP.

Another serious limitation to the utilization of TRUS during LRP is that it is operator-dependent and requires an experienced and dedicated ultrasonographer. This person is positioned between the patient's legs for a majority of the operation and is constantly involved with the interpretation of the ultrasound and laparoscopic pictures simultaneously. The additional, highly trained, personnel required may also translate into a significant increase in the cost of the operation. In addition, the use of TRUS during RALP poses an additional challenge, as the daVinci robot is situated between the patient's legs where the TRUS operator would normally sit. This may limit the utility and widespread adoption of intraoperative TRUS, as most prostatectomies in the United States are being performed with robot assistance at the time of this writing.

Optical Coherence Tomography

Optical coherence tomography (OCT) is an imaging technique that allows for the real-time, high-resolution, atraumatic, cross-sectional imaging of the tissues, which has been utilized in ophthalmology for retinal and corneal imaging as well as in urology for bladder cancer staging.[29–34] The Niris OCT system (Imalux, Cleveland, OH) has been utilized in urologic applications and is comprised of an 8 F fiberoptic probe and a computer console and screen. The fiberoptic nature of the probe may allow for it to be integrated into the laparoscopic instruments or other flexible devices in the future. OCT is similar to B-mode ultrasonography, but instead of measuring the backscattering of acoustic waves, it measures the backscattering of near-infrared light. However, unlike ultrasound, OCT does not require direct probe contact with the tissue or a transducing medium, decreasing interference with the operative instruments in the surgical field. Image resolution as fine as 1–15 μm can be achieved with a maximal penetration depth of 1.6 mm, which allows for the imaging of the microscopic structures such as the cavernous nerves, lymphatics, blood vessels, and fascial planes.

Rais-Bahrami and Fried et al. demonstrated the use of OCT in imaging of the cavernous nerve and periprostatic tissue in the rat model.[35,36] The rat model proved to be an ideal model for imaging because the cavernous nerve exists as a large, visible structure with minimal intervening vasculature or fat. To confirm the course of the cavernous nerve in the rat, the nerve was identified and stimulated with simultaneous intracorporeal pressure measurements, with penile length and girth measurements recorded. Hematoxylin–eosin stained histologic specimens of the cavernous nerve and periprostatic tissues were then compared with the OCT images obtained from the same location on the prostate and were found to correlate well (Fig. 21.6).[36]

Rais-Bahrami and Aron et al. both reported on the use of OCT to image human *ex vivo* prostatectomy specimens immediately after removal.[36,37] Rais-Bahrami et al. found the OCT images of human cavernous nerve and prostatic tissue to be similar to that of the rat in that there was identical histological correlation with the OCT images. However, identification of the NVB proved to be difficult when compared with the rat prostate owing to the higher density of the prostatic capsule and stroma, as well as the presence of more blood vessels and fat resulting in a degradation of the signal. Aron et al. also found that identification of the NVBs required an experienced operator to distinguish them from adipose tissue, small vessels, and lymphatics.

OCT, like real-time TRUS, also has the limitation of requiring an experienced operator to interpret the images obtained. While OCT has been used to aid in the intraoperative identification and preservation of the NVB,[37] its success has yet to be validated by potency results. Future improvements in the technology resulting in greater depth of penetration and resolution may make OCT more feasible for intraoperative identification of the cavernous nerve during nerve-sparing prostatectomies or for the localization of cavernous nerve endings to allow for a precise nerve-graft anastamosis.

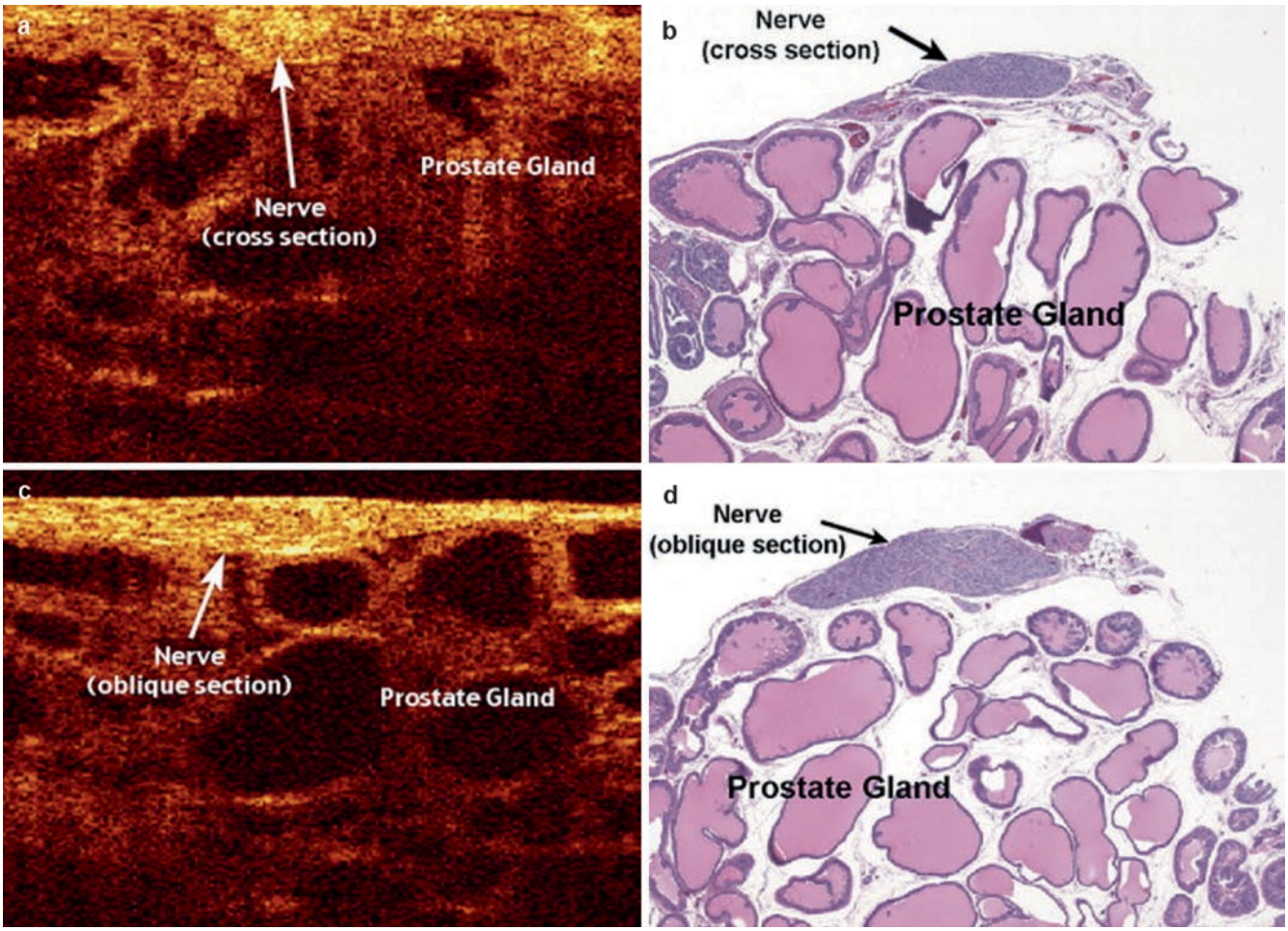

Fig. 21.6 OCT imaging and histologic (hematoxylin–eosin) correlation of rat CN (**a**, **b**) in cross-section and (**c**, **d**) in oblique section overlying prostate glandular tissue. (Reprinted from Rais-Bahrami et al.[36], © 2008, with permission from Elsevier)

Neuropack Nerve Stimulator

Takenaka et al. reported on the first attempt at the intraoperative measurement of intracavernosal and intraurethral pressure using an intracavernosal needle and intraurethral balloon catheter after electrical stimulation of the NVB and the accessory neural pathways in the region of the surgically identified NVB using a Neuropack nerve stimulator device and a bipolar electrode.[38] An increase in intracavernosal pressure signified the presence of cavernous nerve fibers, while an increase in pressure in the intraurethral balloon catheter signified the presence of nerve fibers contributing to urinary continence. By stimulating regions of the nerves away from the identified NVB (i.e., posterolateral rectal wall) and the actual NVB during open radical prostatectomy, the researchers were able to demonstrate that the course of the cavernous nerves did not always correspond to the surgically identified NVB and also showed that the NVB contains nerve fibers contributing to urinary continence. This correlated with their earlier findings that the nerves are actually splayed and located beyond the NVB.[13] These findings support the relative complexity of the cavernous nerve branches and their anatomic course, but also confirm the involvement of some of these fibers with urinary continence.

Animal Studies to Map Neurovascular Bundle

Confocal Fluorescent Microscopy

Confocal fluorescent microscopy (CFM) is a new technology that has been described for use in gastroenterology, dermatology, pulmonology, and urology, and provides such incredibly detailed resolution that it allows for *in vivo* differentiation of cancerous and normal tissue.[39–43] CFM can

also provide adequate resolution to allow distinction between some differentiated and undifferentiated cancers.[44] CFM has also been used to provide real-time *in vivo* images of peripheral nerves and deep-brain structures in rats genetically engineered to express a fluorescent protein in all sensory and motor neurons.[45] CFM allows for sufficient spatial resolution to produce images down to the axonal level. The Cell~Vizio (Mauna Kea Technologies, Paris, France) is a commercially available unit that utilizes CFM technology, and is composed of a laser scanning unit, a small fiberoptic probe, and an image processing unit. Real-time images can be produced up to 12 frames per second, while the probe allows for a lateral resolution of 3.5 μm with a depth of penetration of 15 μm.

Boyette et al. used the CFM technology along with the injection of a fluorescent retrograde nerve tracer to provide *in vivo* real-time images of the cavernous nerve in rats.[46] A recombinant β-subunit of cholera toxin conjugated to a fluorescent compound (AlexaFluor) served as the fluorescent nerve tracer, and was injected into the corpus cavernosum of male rats to allow for retrograde transport along the cavernous nerves. They found that the optimal imaging of the cavernous nerve was obtained after allowing for 9 days of retrograde transport along the nerve. The cavernous nerves were then exposed and imaged using CFM, which produced exceptional images, even allowing for visualization of the branching of the cavernous nerve (Fig. 21.7). Confirmation that the nerves being imaged were actually the cavernous nerve was obtained by electrical stimulation of the fluorescent nerve with simultaneous intracavernosal pressure monitoring.

While CFM technology produces striking images in the rat model, there are limitations to the technology that need to be overcome before successful application in humans. The depth of penetration of the probe is only 15 μm, which works well for the rat model. However, as was encountered in translating OCT technology from the rat to human model, the greater amount of periprostatic fat, vessels, and lymphatics present in the human model may hinder the view of the nerve. Another major limitation to the technology is the need for

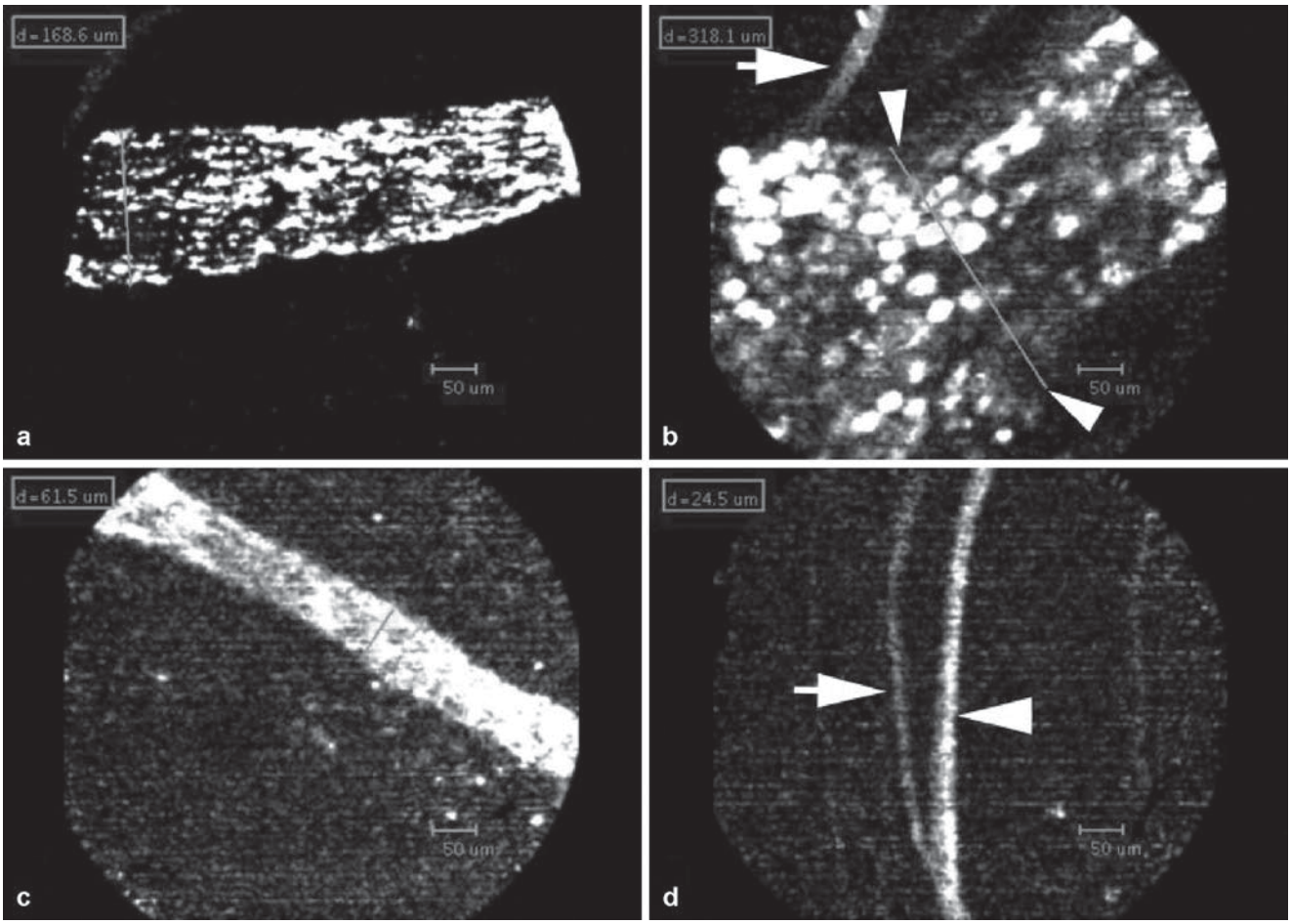

Fig. 21.7 Figures **a, b,** and **c** are CFM images of rat CN obtained 9 days after injection of fluorescent nerve tracer into corpus cavernosum. Figure **d** demonstrates accessory nerve branching into larger and smaller bundles. (Reprinted from Boyette et al.[46], © 2007, with permission from Elsevier)

injection of a fluorescent nerve tracer and waiting for retrograde transport to the cavernous nerve. While transport in the rat model took 9 days, it has been estimated that it may take up to 45 days for optimal imaging to be obtained in the human owing to the four to five times greater distance from the penis to the cavernous nerve the tracer has to travel.[46] Finally, while the short-term safety of the injected tracer composed of the β-subunit of cholera toxin was demonstrated in the rat model, long-term studies need to be performed in humans before the technology can become main stream.

Near-Infrared Fluorescence Imaging

The concept of using an injectable fluorescent nerve tracer to localize the cavernous nerve was also described by Golijanin et al.[47] After the injection of a fluorescent dye called indocyanin green (ICG) into the rat penis and allowing time for retrograde transport to the cavernous nerves, they used a near-infrared fluorescence (NIRF) intraoperative imaging system (SPY, Novadaq Technologies Inc., Mississauga, Ontario, Canada) composed of a laser used to illuminate fluorescent tissue and a camera sensitive to infrared fluorescence to capture images. Nerves were positively identified at 6, 8, 12, 18, 24, and 36 h after ICG injection. The maximal nerve fluorescence was noted at 18 and 24 h postinjection.

The main advantage of NIRF using ICG as a fluorescing agent over CFM with the injection of AlexaFluor is the significantly shorter time required for retrograde transport of the fluorescing agent. Nevertheless, further studies would be required to determine the length of the time needed for adequate transport of ICG from the penis to the cavernous nerves in the human model. However, the downside to using ICG as a fluorescing agent is that the agent contains iodine that would limit its utility to patients without an allergy to iodine.

Future Directions

While technologies such as CaverMap, intraoperative TRUS, OCT, nerve stimulation, and intraoperative fluorescence imaging demonstrate the feasibility of visualizing or approximating the location of the cavernous nerve, precision is hindered in the human model by the lack of resolution and depth of penetration of the imaging modalities. In CFM, a miniaturized confocal microscope can be attached to the end of a conventional endoscope, allowing for point-by-point optical sections to be obtained of the tissue in question and then rendered into a 3D image by a computer, thus providing a real-time virtual histologic image. The downside to this technology is the need for injection of a fluorescing agent such as fluorescein prior to obtaining images. Theoretically, this technology can be applied to RALP for intraoperative identification of the cavernous nerves, while simultaneously scanning for cancerous tissue. Nerve tissue that is seen to be too close to prostate glands with cancerous architecture could then be sacrificed, while nerve tissue well away from the cancerous glands could be spared.

Diffusion tensor imaging (DTI) is an MRI imaging modality that was developed to image white matter tracts in the brain. It has been used to localize brain tumors in relation to white matter tracts for neurosurgical planning, to provide imaging of the cranial nerve pathways, as well as allow for imaging of peripheral nerves such as the sciatic nerve.[48–51] DTI has also been shown to be able provide detailed prostate anatomy as well as allow for delineation of neoplastic lesions and areas of extraprostatic extension.[52,53] Perhaps, in the future, it may be possible that DTI can be used alone or in combination with functional MRI, which has been used for localizing and staging tumor foci in the prostate, to provide a preoperative map of the cavernous nerves and tumor foci, to allow for augmented reality and intraoperative surgical navigation.

Conclusion

Several technologies have been developed and studied in an attempt to provide intraoperative NVB identification during radical prostatectomy; however, unfortunately, none have been reliable or specific enough. In addition, none of the modalities described have been validated with long-term potency outcomes to attest their efficacy at guiding intraoperative cavernous nerve preservation. Future endeavors into new technology will require collaborative work with bioengineers, radiologists, pathologists, and other specialists to find novel techniques for achieving the seemingly difficult goal of optimizing both cavernous nerve preservation and cancer control.

References

1. Anonymous. The early diagnosis and radical cure of carcinoma of the prostate. *CA Cancer J Clin*. 1977;27(5):308–316
2. Miller JA, Staunton MD. The birth of retropubic prostatectomy – Millin. *J R Soc Med*. 1989;82(8):494–495
3. Walsh PC. The discovery of the cavernous nerves and development of nerve sparing radical retropubic prostatectomy. *J Urol*. 2007;177(5):1632–1635
4. Walsh PC. Anatomic radical prostatectomy: evolution of the surgical technique. *J Urol*. 1998;160(6 Pt 2):2418–2424

5. Lepor H, Gregerman M, Crosby R, Mostofi FK, Walsh PC. Precise localization of the autonomic nerves from the pelvic plexus to the corpora cavernosa: a detailed anatomical study of the adult male pelvis. *J Urol*. 1985;133(2):207–212
6. Walsh PC, Lepor H, Eggleston JC. Radical prostatectomy with preservation of sexual function: anatomical and pathological considerations. *Prostate*. 1983;4(5):473–485
7. Walsh PC, Marschke P, Ricker D, Burnett AL. Use of intraoperative video documentation to improve sexual function after radical retropubic prostatectomy. *Urology*. 2000;55(1):62–67
8. Catalona WJ, Carvalhal GF, Mager DE, Smith DS. Potency, continence and complication rates in 1,870 consecutive radical retropubic prostatectomies. *J Urol*. 1999;162(2):433–438
9. Talcott JA, Rieker P, Propert KJ, et al Patient-reported impotence and incontinence after nerve-sparing radical prostatectomy. *J Natl Cancer Inst*. 1997;89(15):1117–1123
10. Zorn KC, Bernstein AJ, Gofrit ON, et al Long-term functional and oncological outcomes of patients undergoing sural nerve interposition grafting during robot-assisted laparoscopic radical prostatectomy. *J Endourol*. 2008;22(5):1005–1012
11. Secin FP, Koppie TM, Scardino PT, et al Bilateral cavernous nerve interposition grafting during radical retropubic prostatectomy: Memorial Sloan-Kettering Cancer Center experience. *J Urol*. 2007; 177(2):664–668
12. Costello AJ, Brooks M, Cole OJ. Anatomical studies of the neurovascular bundle and cavernosal nerves. *BJU Int*. 2004;94(7): 1071–1076
13. Takenaka A, Murakami G, Soga H, Han SH, Arai Y, Fujisawa M. Anatomical analysis of the neurovascular bundle supplying penile cavernous tissue to ensure a reliable nerve graft after radical prostatectomy. *J Urol*. 2004;172(3):1032–1035
14. Lunacek A, Schwentner C, Fritsch H, Bartsch G, Strasser H. Anatomical radical retropubic prostatectomy: 'curtain dissection' of the neurovascular bundle. *BJU Int*. 2005;95(9):1226–1231
15. Sievert KD, Hennenlotter J, Laible I, et al The periprostatic autonomic nerves-bundle or layer? Eur Urol. 2008 Nov;54(5):1109-16
16. Kaul S, Bhandari A, Hemal A, Savera A, Shrivastava A, Menon M. Robotic radical prostatectomy with preservation of the prostatic fascia: a feasibility study. *Urology*. 2005;66(6):1261–1265
17. Zvara P, Spiess PE, Merlin SL, Begin LR, Brock GB. Neurogenic erectile dysfunction: the course of nicotinamide adenine dinucleotide phosphate diaphorase-positive nerve fibers on the surface of the prostate. *Urology*. 1996;47(1):146–151
18. Menon M, Shrivastava A, Kaul S, et al Vattikuti Institute prostatectomy: contemporary technique and analysis of results. *Eur Urol*. 2007;51(3):648–657; discussion 657–648
19. Savera AT, Kaul S, Badani K, Stark AT, Shah NL, Menon M. Robotic radical prostatectomy with the "Veil of Aphrodite" technique: histologic evidence of enhanced nerve sparing. *Eur Urol*. 2006;49(6):1065–1073; discussion 1073–1064
20. Kaul S, Savera A, Badani K, Fumo M, Bhandari A, Menon M. Functional outcomes and oncological efficacy of Vattikuti Institute prostatectomy with Veil of Aphrodite nerve-sparing: an analysis of 154 consecutive patients. *BJU Int*. 2006;97(3):467–472
21. Nielsen M, Marschke P, Walsh PC. High anterior release of the levator fascia improves sexual function following open radical retropubic prostatectomy. In: Abstract presented at *Annual AUA Meeting*, Orlando, FL May 17–22, 2008
22. Klotz L, Herschorn S. Early experience with intraoperative cavernous nerve stimulation with penile tumescence monitoring to improve nerve sparing during radical prostatectomy. *Urology*. 1998;52(4): 537–542
23. Klotz L, Heaton J, Jewett M, et al A randomized phase 3 study of intraoperative cavernous nerve stimulation with penile tumescence monitoring to improve nerve sparing during radical prostatectomy. *J Urol*. 2000;164(5):1573–1578
24. Kim HL, Stoffel DS, Mhoon DA, Brendler CB. A positive caver map response poorly predicts recovery of potency after radical prostatectomy. *Urology*. 2000;56(4):561–564
25. Walsh PC, Marschke P, Catalona WJ, et al Efficacy of first-generation Cavermap to verify location and function of cavernous nerves during radical prostatectomy: a multi-institutional evaluation by experienced surgeons. *Urology*. 2001;57(3):491–494
26. Holzbeierlein J, Peterson M, Smith JJ. Variability of results of cavernous nerve stimulation during radical prostatectomy. *J Urol*. 2001;165(1):108–110
27. Ukimura O, Magi-Galluzzi C, Gill IS. Real-time transrectal ultrasound guidance during laparoscopic radical prostatectomy: impact on surgical margins. *J Urol*. 2006;175(4):1304–1310
28. Ukimura O, Gill IS, Desai MM, et al Real-time transrectal ultrasonography during laparoscopic radical prostatectomy. *J Urol*. 2004;172(1):112–118
29. Browning DJ, McOwen MD, Bowen RM, Jr., O'Marah TL. Comparison of the clinical diagnosis of diabetic macular edema with diagnosis by optical coherence tomography. *Ophthalmology*. 2004;111(4):712–715
30. Feng Y, Simpson TL. Corneal, limbal, and conjunctival epithelial thickness from optical coherence tomography. *Optom Vis Sci*. 2008;85(9):E880–883
31. Manyak MJ, Gladkova ND, Makari JH, et al Evaluation of superficial bladder transitional-cell carcinoma by optical coherence tomography. *J Endourol*. 2005;19(5):570–574
32. Jesser CA, Boppart SA, Pitris C, et al High resolution imaging of transitional cell carcinoma with optical coherence tomography: feasibility for the evaluation of bladder pathology. *Br J Radiol*. 1999; 72(864):1170–1176
33. Lerner SP, Goh AC, Tresser NJ, Shen SS. Optical coherence tomography as an adjunct to white light cystoscopy for intravesical real-time imaging and staging of bladder cancer. *Urology*. 2008;72(1): 133–137
34. Hermes B, Spoler F, Naami A, et al Visualization of the basement membrane zone of the bladder by optical coherence tomography: feasibility of noninvasive evaluation of tumor invasion. *Urology*. 2008;72(3):677–681
35. Fried NM, Rais-Bahrami S, Lagoda GA, Chuang Y, Burnett AL, Su LM. Imaging the cavernous nerves in the rat prostate using optical coherence tomography. *Lasers Surg Med*. 2007;39(1):36–41
36. Rais-Bahrami S, Levinson AW, Fried NM, et al Optical coherence tomography of cavernous nerves: a step toward real-time intraoperative imaging during nerve-sparing radical prostatectomy. *Urology*. 2008;72(1):198–204
37. Aron M, Kaouk JH, Hegarty NJ, et al Second prize: preliminary experience with the Niris optical coherence tomography system during laparoscopic and robotic prostatectomy. *J Endourol*. 2007; 21(8):814–818
38. Takenaka A, Tewari A, Hara R, et al Pelvic autonomic nerve mapping around the prostate by intraoperative electrical stimulation with simultaneous measurement of intracavernous and intraurethral pressure. *J Urol*. 2007;177(1):225–229; discussion 229
39. Hurlstone DP, Baraza W, Brown S, Thomson M, Tiffin N, Cross SS. In vivo real-time confocal laser scanning endomicroscopic colonoscopy for the detection and characterization of colorectal neoplasia. *Br J Surg*. 2008;95(5):636–645
40. Koenig F, Knittel J, Schnieder L, George M, Lein M, Schnorr D. Confocal laser scanning microscopy of urinary bladder after intravesical instillation of a fluorescent dye. *Urology*. 2003;62(1): 158–161
41. Hoffman A, Goetz M, Vieth M, Galle PR, Neurath MF, Kiesslich R. Confocal laser endomicroscopy: technical status and current indications. *Endoscopy*. 2006;38(12):1275–1283
42. Gerger A, Hofmann-Wellenhof R, Langsenlehner U, et al In vivo confocal laser scanning microscopy of melanocytic skin tumours:

diagnostic applicability using unselected tumour images. *Br J Dermatol*. 2008;158(2):329–333
43. Sutedja G. New techniques for early detection of lung cancer. *Eur Respir J Suppl*. 2003;39:57s–66s
44. Kitabatake S, Niwa Y, Miyahara R, et al Confocal endomicroscopy for the diagnosis of gastric cancer in vivo. *Endoscopy*. 2006;38(11): 1110–1114
45. Vincent P, Maskos U, Charvet I, et al Live imaging of neural structure and function by fibred fluorescence microscopy. *EMBO Rep*. 2006;7(11):1154–1161
46. Boyette LB, Reardon MA, Mirelman AJ, et al Fiberoptic imaging of cavernous nerves in vivo. *J Urol*. 2007;178(6):2694–2700
47. Golijanin D, Wood R, Madeb R, et al Intraoperative visualization of cavernous nerves using near infrared fluorescence of indocyanine green in the rat. *http://www.abstracts2view.com/aua_archive/view.php?nu = 200696027 Abstract presented at American Urological Association Meeting*. 2006
48. Lo CY, Chao YP, Chou KH, Guo WY, Su JL, Lin CP. DTI-based virtual reality system for neurosurgery. *Conf Proc IEEE Eng Med Biol Soc*. 2007:1326–1329
49. Kabasawa H, Masutani Y, Aoki S, et al 3T PROPELLER diffusion tensor fiber tractography: a feasibility study for cranial nerve fiber tracking. *Radiat Med*. 2007;25(9):462–466
50. Skorpil M, Engstrom M, Nordell A. Diffusion-direction-dependent imaging: a novel MRI approach for peripheral nerve imaging. *Magn Reson Imaging*. 2007;25(3):406–411
51. Skorpil M, Karlsson M, Nordell A. Peripheral nerve diffusion tensor imaging. *Magn Reson Imaging*. 2004;22(5):743–745
52. Manenti G, Carlani M, Mancino S, et al Diffusion tensor magnetic resonance imaging of prostate cancer. *Invest Radiol*. 2007;42(6): 412–419
53. Kurhanewicz J, Vigneron D, Carroll P, Coakley F. Multiparametric magnetic resonance imaging in prostate cancer: present and future. *Curr Opin Urol*. 2008;18(1):71–77

Part IV

Laparoscopic New Technologies

Inderbir Gill and Prokar Dasgupta

Laparoscopic Partial Nephrectomy

22

Patrick Kenney, Justin Gould, Sheaumei Tsai, and David Canes

Introduction

New technology has been vital for the development of laparoscopic partial nephrectomy (LPN), from the initial description in a porcine model to early descriptions for benign disease in humans, and eventual adoption as an oncologically sound, minimally invasive procedure.[1–5]

Rigorous evaluation and reasoned adoption of new technology is a trademark of the field of urology.[6] This ethos has been central to the ascent of LPN. The evaluation and the adoption of new technologies has impacted all the aspects of the procedure, from preoperative planning, which is crucial to identify appropriate candidates for LPN, to the performance of the procedure itself, and finally postoperative care.

The procedural challenges of LPN are numerous and interrelated. Hilar dissection and identification of renal vasculature can be daunting. Adequate mobilization of the kidney is necessary to achieve a favorable environment for LPN. Resection of the mass with negative margins while minimizing injury to adjacent vasculature, parenchyma, and collecting system is difficult and paramount to the success of the operation. The provision of a bloodless field by clamping, whether en bloc or of the renal artery alone, leads to renal ischemia and consequent deleterious effect on renal function. Renorrhaphy, including hemostasis and collecting system closure if required, can be a challenge to accomplish without damage to the remaining remnant.

From diagnosis in the clinic to treatment in the operating theater, new technologies have great potential to favorably alter the landscape of nephron-sparing approaches to renal masses, in particular LPN.

Beyond Radiographic Diagnosis: Molecular Markers may help Spare Nephrons

The elucidation of the molecular pathways involved in the pathogenesis of renal cell carcinoma (RCC) is revolutionizing the management of metastatic disease. In particular, survival in patients with advanced RCC is improved by novel therapeutics that target the vascular endothelial growth factor-mediated pathways promoting angiogenesis and metastasis.[7] In a similar fashion, translational research has the potential to transform the diagnosis of renal masses.

At present, the evaluation of cystic and solid renal masses focuses primarily on radiographic assessment, with preoperative biopsy rarely performed.[8] With imaging as the principle diagnostic modality, modern nephron-sparing surgery (NSS) series report 15–30% rates of benign final pathology.[9–11] Nonetheless, the role of biopsy has been limited due to an unacceptably high false negative rate due to difficulty differentiating between benign and malignant neoplasms (e.g., chromophobe RCC vs. oncocytoma).[12]

Recent advances in molecular biology are renewing focus on renal biopsy for the diagnosis of renal masses and treatment selection. If biomarkers offer greater sensitivity and specificity than histopathology or cytology, biopsy in the future could potentially obviate the need for surgery in 15–30% of patients.

Despite ample evidence in favor of the safety and oncologic efficacy of NSS, a large percentage of tumors amenable to partial nephrectomy are removed with radical surgery.[13] Moreover, even NSS has an adverse impact on glomerular filtration rate.[14,15] Avoiding unnecessary insults to renal function through improved molecular diagnostics will be a significant technical advance.

Molecular markers of the different subtypes of RCC have been elucidated (Table 22.1).[16,17] Similar to the development of therapeutic alternatives to radical surgery, high-through put techniques to identify DNA, RNA, miRNA, and proteomic signatures associated with benign and malignant renal masses may help spare nephrons.[18–20]

3D CT Scanning

Preoperative planning for LPN is so essential to the ultimate success of surgery that it can be considered as the first surgical step. Based on preoperative imaging, the surgeon should have a clear vision as to the maneuvers that will be required

P. Dasgupta et al. (eds.), *New Technologies in Urology,*
DOI: 10.1007/978-1-84882-178-1_22, © Springer-Verlag London Limited 2010

Table 22.1 Diagnostic and prognostic molecular markers in RCC

Parameter	Marker
RCC histological type:	
Papillary	Loss of 3p, 9p; trisomy 7,17; + p53
Clear cell	Absent VHL gene mutation, gamma-enolase + MN/CAIX
Collecting duct and chromophobe	Vinculin
Progression	Ki67, TS, CD10, erythropoietin, PTEN + STAT protein
Survival	p53, iNOS, CA-125, MN/CA9 + STAT protein
Response to therapy	Neopterin, TPS, Bcl-2, gamma-enolase, TS, MN/CA9 + STAT protein
Urine-based, diagnostic only	NMP-22, extracellular matrix proteins, laminin, collagen IV + fibronectin
Tissue-based markers	Bcl-2, p53, Ki67, CAIX, p21, TPS, PTEN, gamma-enolase, pyruvate kinase, TS, CD10, CD154, erythropoietin, vimentin, vinculin, AgNOR, GP200, P-selectin, mTOR + STAT protein

Reprinted from Hari et al.[78] Copyright 2008, with permission from Elsevier.

intraoperatively to successfully accomplish partial nephrectomy in a minimally invasive environment. Helical computed tomography (CT) scanning with 3D reformatting has become an essential tool in the preoperative evaluation of renal masses.

Obviating the need for more invasive angiographic imaging, 3D reconstructions provide important information about normal renal anatomy, the relationships of a renal mass to main, segmental, and accessory renal vasculature, as well as the proximity to the collecting system. An example is shown in Fig. 22.1. The detail provided by 3D reconstructions can be crucial to surgical planning, not just influencing the global approach (open vs. laparoscopic), but also the technical details (clamped vs. unclamped, wedge resection vs. polar nephrectomy). In an analysis of almost 350 helical CT scans in patients undergoing NSS, Derweesh et al. reported that CT findings were predictive of calyceal entry at the time of surgery. Such detailed preoperative information allows the surgeon to plan and anticipate the need for collecting system closure intraoperatively.[21]

Preoperative virtual reality surgical rehearsal may be feasible in the future, and would represent a significant advance. One might want to determine prior to surgery, for example, if NSS were technically feasible or if radical nephrectomy was the only option. This is yet to materialize for renal surgery, but small steps toward this end have been accomplished. Preliminary proof-of-concept studies have shown that data from 3D CT renderings can be transferred to the virtual reality environment, but this has not yet entered the mainstream clinical practice.[22] Virtual reality surgical simulation will undoubtedly continue to be a focus of future investigation.

Excision Devices for LPN

Despite continued refinement of technique and mounting experience, LPN remains an advanced procedure, with most surgeons facing three common challenges: adequate parenchymal cutting, hemostasis, and reconstruction. This has motivated investigation of new excision devices that address all three technically demanding elements. Lasers are at the forefront of the investigation because of their dual ability to vaporize (i.e., cut) tissue and coagulate.

Lasers are characterized by their wavelength-specific medium, mode of emission (continuous, pulsed, or Q-switched), and power output. The wavelength is proportional to depth of tissue penetration, while emission mode influences the degree of lateral heat conduction. The interplay of these factors with tissue composition, molecular absorption, and perfusion determines the laser end-effect.[23]

The ideal laser for minimally invasive NSS should cut precisely to limit collateral thermal damage, coagulate the tumor bed without destroying tissue architecture to allow margin assessment, and preserve visibility. No laser perfectly satisfies these criteria. For instance, initial clinical studies with the Ho:YAG laser revealed that it cuts and coagulates effectively without the need for hilar clamping, but is handicapped by excessive smoke production and blood splatter.[24] The CO_2 laser has been shown to be ineffective for hemostasis, while the Nd:YAG and diode lasers both cause severe tissue carbonization, obscuring margin analysis.[25]

In an attempt to improve the early experience, two new lasers have been studied for use in LPN: the potassium titanyl phosphate (KTP) laser and the thulium laser. The KTP laser emits a visible green light beam with a wavelength of 532 nm. This wavelength is in the range of hemoglobin absorption, which may explain the KTP laser's superb hemostatic effect, particularly in vascular tissue. In a nonclamping survival calf model, the KTP laser not only demonstrated excellent control of bleeding, but also did so with submillimeter histologic disruption in the adjacent parenchyma.[26] These findings were supported by a subsequent investigation in a porcine model by Hindley et al.[27] The experiments were carried out successfully without hilar clamping. The system delivered very rapid energy pulses, generating nearly continuous power output of 80 W, and hence, minimizing energy scatter. This translated into a superficial 1 mm zone of coagulation necrosis at the

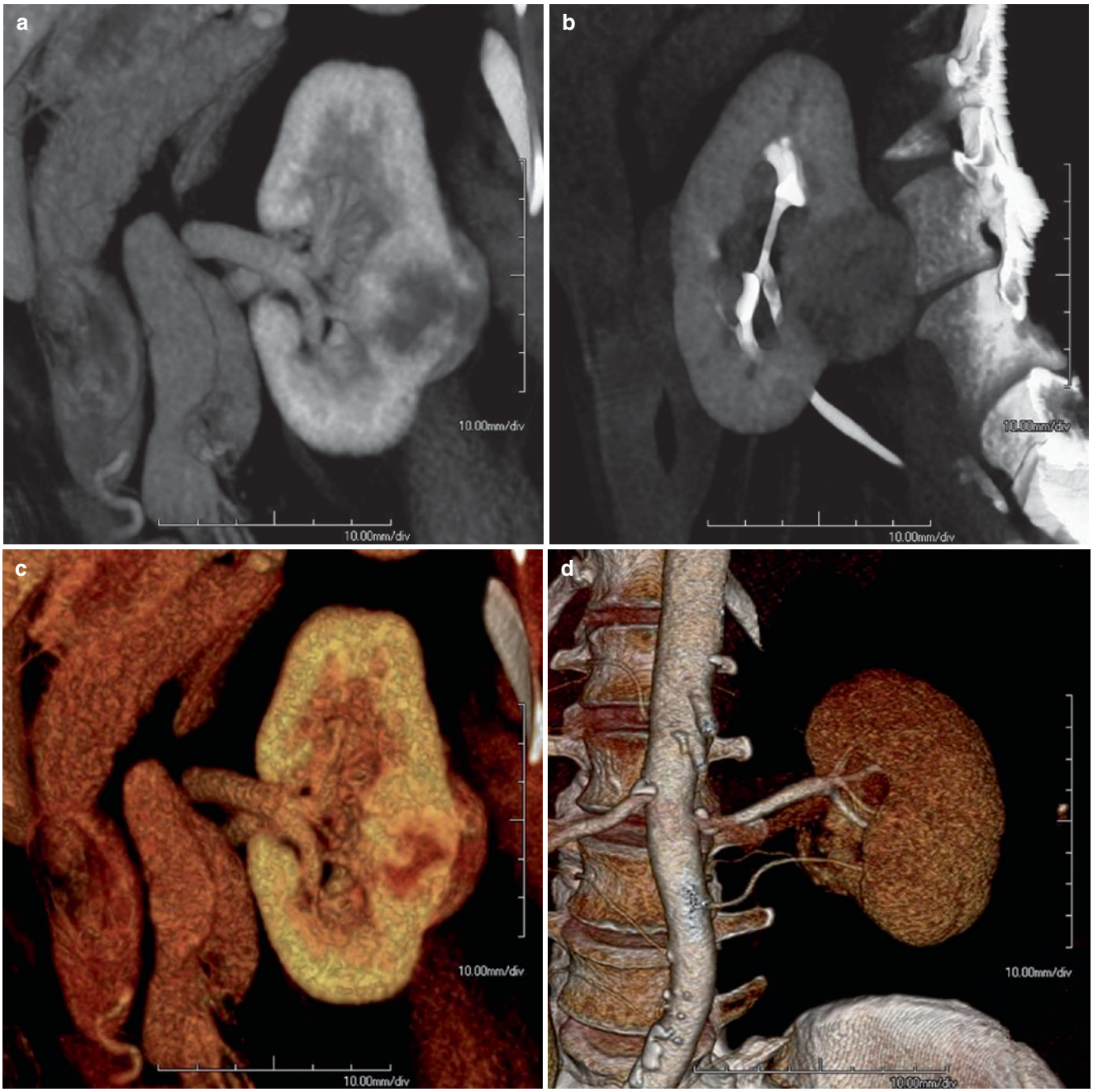

Fig. 22.1 3D CT scan image demonstrating a 4x4.3cm hypervascular interpolar left renal mass. There are two left renal arteries, including a lower polar artery. (Image courtesy of Christoph Wald, Lahey Clinic)

excision margin and a deeper 1 mm zone of tubular lumen collapse, nuclear pyknosis, and erythrocyte loss. Smoke production remained a hindrance with the KTP laser, and modifications are underway to correct this problem before introducing the KTP laser into the clinical arena.

These two studies champion the precision and hemostatic effect of the KTP laser. However, its true efficacy is still uncertain. A recent ex vivo experiment with blood-perfused porcine kidneys deemed the KTP laser inadequate for both tissue coagulation and creation of clean, sharp resection margins.[28] While this study differs significantly in design, it underscores the need for additional research.

The thulium laser is another potential excision device that has been evaluated in a survival animal model. Bui et al. performed successful nonclamping LPN in five pigs using a continuous-wave thulium laser with wavelength of 2 μm and total power of 30 W.[29] The energy was delivered through a 365 μm silica fiber. For improved intracorporeal laser manipulation, the fiber was advanced through the working port of a flexible cystoscope, and the entire unit was then introduced

through a 10 mm laparoscopic port. This system also allowed continuous saline irrigation along the path of laser fiber, thereby reducing smoke production and tissue carbonization. On immediate histological analysis of the cut surface, there was no evidence of charring or necrosis. Furthermore, the continuous emission mode imparted superior cutting precision and eliminated blood splatter. The thulium laser also achieved adequate coagulation of cortical vessels up to 1.6 mm. However, the authors cautioned that the laser incompletely sealed larger vessels near the hilum. Still, these preliminary findings represent a step toward developing an ideal laparoscopic excision device. Additional testing of both the thulium and KTP lasers will probably enable the surgeons to attain that ideal device in the future.

Delineation of Tumor from Normal Parenchyma

Multiple imaging modalities may be employed preoperatively to characterize and localize a renal neoplasm. While preoperative radiographic information provides a guide for tumor excision, intraoperative delineation of tumor from normal parenchyma remains essential for assessing the margin status and achieving complete tumor removal, which is the goal of renal oncologic surgery.[30] Surgeons have long relied on intraoperative frozen section to evaluate tumor margins. However, the technical challenges of LPN along with the time limit on warm ischemia have spurred the development of real-time technologies with the same histologic precision but shorter turn-around time.

Intraoperative laparoscopic ultrasound (ILUS) has been the mainstay of dynamic tumor evaluation in LPN. Studies have demonstrated that ultrasound aids in demarcating tumor-free margins and identifying occult satellite lesions.[31,32] The discriminatory power of ILUS depends on the echotextural differences between neoplastic and normal parenchyma. Thus, if the tumor and the surrounding normal tissue share a similar echo pattern, ILUS will be inadequate. To overcome this limitation, several new technologies have emerged. These include optical reflectance spectroscopy (ORS), optical coherence tomography (OCT), and Smart Needle measurement of bioimpedance.

Optical diagnosis relies on the interaction of light energy with tissue and analysis of the resultant change in the nature of light. In ORS, light energy is applied to tissues, and the light reflected back is detected and recorded as spectral data. Diffuse reflectance, which is characterized in ORS, detects scatter from intracellular components such as nuclei, which are typically altered in neoplastic disease. Thus, ORS can provide real-time structural information about the tissues in question.

Several groups have investigated ORS as a tool for discriminating between normal and neoplastic renal tissue. In a preliminary ex vivo study, Parekh et al. interrogated multiple pathologically confirmed radical nephrectomy specimens using a portable fiber optic-based spectroscopic system.[33] They were able to differentiate cancerous from normal specimens based on fluorescence and diffuse reflectance spectra. Moreover, ORS could distinguish between papillary and clear-cell subtypes. The authors proposed a discriminatory algorithm with high sensitivity and specificity, and concluded that ORS might have a future role in intraoperative margin evaluation.

By applying optical analysis, investigators from UT Southwestern were able to detect a positive margin in their partial nephrectomy specimens.[34] While absorption of light by hemoglobin is cited as a potential limitation of ORS in vivo, one could argue that the promising results from non-perfused ex vivo models are relevant to LPN, which is typically performed under ischemic conditions.

Similarly, OCT analyzes light–tissue interactions, specifically infrared light. OCT is conceptually similar to ultrasound in that it detects a signal reflected back from the tissue, and composes a dynamic, high spatial resolution image of the tissue microstructure to a depth of 11 μm. This yields an "optical biopsy".[35] The technology is suited for minimally invasive surgery, as the fiber-optic device is easily advanced through a laparoscopic port. Although it has found intraoperative applications in bladder and prostate disease, OCT has only recently been employed for renal tumors. Chung et al. conducted a preliminary investigation of OCT in LPN of 11 patients.[36] OCT of parenchyma and capsule, both on and adjacent to the renal mass, detected structural abnormalities in nine RCCs, suggesting possible utility in assessing tumor margins.

Bioimpendance measurement via the percutaneous Smart Needle system is another potential modality for discriminating between normal and neoplastic renal tissue. This technology takes advantage of the distinct electrical properties of malignant versus benign tissue, as previously demonstrated in prostate cancer specimens.[37] With regard to renal disease, the Smart Needle has been used for the confirmation of collecting system entry during percutaneous procedures in a porcine model.[38] Investigators speculate that there may be a role for bioimpedance measurement in renal oncology as well.

Optical technologies such as ORS and OCT, and measurements of bioimpedance hold promise for tumor detection and margin assessment during laparoscopic NSS. These new technologies are investigational but hold promise and merit further study.

Renorrhaphy

Achieving adequate hemostasis along the partial nephrectomy defect is crucial to avoid either immediate or delayed hemorrhage. Sutured renorrhaphy is currently the cornerstone of this effort except for the most superficial resection,

but laparoscopic suturing is perceived to be technically demanding, especially when done under ischemic conditions. The ultimate hemostatic agent obviates suturing, can be easily applied laparoscopically, has a fast onset, and is able to seal large blood vessels and collecting system openings in the deepest portion of the nephrectomy defect. To date, no such agent exists and this goal remains elusive. Several hemostatic agents are predominantly used as hemostatic adjuncts, and these are reviewed as follows.

No single agent or suturing technique has proven superior, and typically depends on surgeon preference.[39] Msezane et al. described four classes of tissue sealants.[40] They include collagen-based adhesives, hydrogel, fibrin sealants, and glutaraldehyde-based adhesives. These agents vary in their mechanism of action, surface type for application, and cost.

Johnson et al. compared seven agents in a hypertensive porcine model.[41] They found that Floseal® and Tisseel® performed well for small resections, but these results were dependent on the systolic blood pressure. They concluded that sutured repair is required for larger resections to adequately control bleeding. Recently, Nogueira et al. performed a prospective study comparing bovine and porcine-derived gelatine matrix-thrombin sealants.[42] Both the agents provided acceptable hemostasis without adverse events, both in the early and late postoperative period. A novel hemostatic agent using a chitosan hemostatic dressing has shown some promise in initial studies.[43] Xie et al. conducted a feasibility study in a porcine model and demonstrated complete hemostasis after deployment of the chitosan dressing in 17 out of a total of 18 procedures.[44]

As mentioned, glues and sealants usually serve as an adjunct to a bolster in the partial nephrectomy defect. The bolster is composed of methylcellulose sheets manufactured by Johnson & Johnson (Surgicel and Surgifoam®) and Pfizer (Gelfoam®). Along with its inherent hemostatic properties, it provides direct mechanical compression on the defect to prevent further bleeding.[41] Porpiglia et al. reported no significant difference between two groups of patients who both received parenchymal sutures, with one group also receiving fibrin glue and collagen fleece.[45] Although suturing has been demonstrated to be the mainstay of hemostasis, facility with intracorporeal suturing requires dedicated training, and minor modifications to the bolster concept have moved away from knot-tying. One innovation using knotless hemostatic parenchymal sutures described by Canales et al. reported a decreased ischemia time using polymer self-locking clips as opposed to traditional free-hand suturing.[46]

A recent technical modification aimed at decreasing ischemia time is an early unclamping technique reported by Nguyen and Gill.[47] A deep running suture is placed under ischemic conditions and then the clamp is released. Bleeding vessels are then sutured in the perfused kidney until all visible bleeding ceases. Adjunctive FloSeal and Tisseel are applied, and a bolster may be omitted in select cases.[48]

Image Overlay and Augmented Reality

Another area where preoperative imaging information is poised to re-shape the intraoperative environment is augmented reality – the superimposition of anatomical data from imaging studies onto the real-time operative images seen through the video endoscope. Particularly for renal masses where the target organ is enveloped within retroperitoneal fat, augmented reality has tremendous appeal. In the field of neurosurgery, where the skull serves as a rigid reference point, augmented reality is already well-integrated into clinical practice.[49]

Marescaux et al. from Strasbourg, France, recently described the use of augmented reality for adrenalectomy, an important advance with implications for all retroperitoneal surgery.[50] In the reported case, superimposed images allowed the surgeon to "see through" the retroperitoneal fat, with cues as to the ultimate location of the right adrenal vein. For renal surgery, similar applications may hasten hilar identification and preclude inadvertent vascular injury.

Surgical navigation and image overlay for the kidney and surrounding structures is more challenging than for the central nervous system. Since the kidney must be mobilized to achieve surgical exposure, anatomical relationships are disturbed. Respiratory motion further complicates image fusion. Nevertheless, Ukimura and Gill described fusing and 3D CT reconstruction of a renal mass with the live intraoperative laparoscopic view.[51] The key to their success was the use of optical sensors on the laparoscopic instruments, as well as the strategically placed fiducials at various fixed points in the surgical field and on the kidney itself. Real-time superimposed color-coded image displayed concentric "zones" around the tumor at increasing distance from the tumor, providing an additional cue as to the dissection plane that would achieve a negative margin (Fig. 22.2).

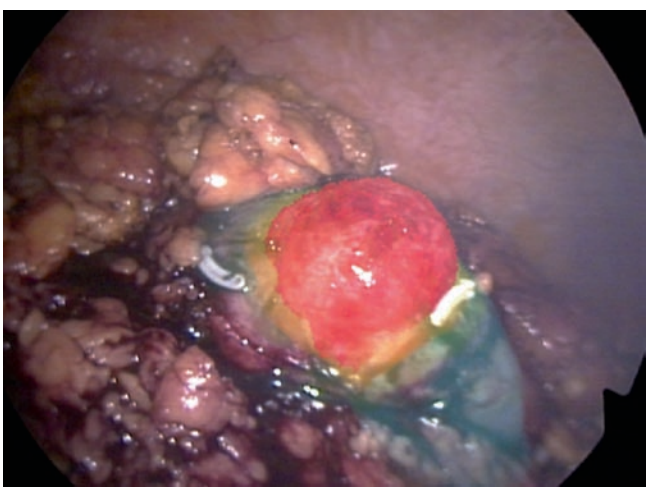

Fig. 22.2 Augmented reality image during laparoscopic partial nephrectomy (Courtesy of Dr. Inderbir Gill, Cleveland Clinic). A *red color* marks the tumor itself, with concentric colored zones at increasing distances from the tumor. The *green stripe* indicates a safe margin for surgical resection

Single-Port Partial Nephrectomy

The drive to decrease incisional morbidity for patients undergoing partial nephrectomy is understandable, considering that the pathologic findings will be benign in up to a third of the patients.[52] The latest advance in minimally invasive surgery attempts to further reduce patient morbidity by consolidating laparoscopic instrumentation through a single port, usually placed in the umbilicus. Numerous abbreviations have been put forth for this approach, including single-port access and laparo-endoscopic single site surgery. Operating through a single port has a rich history in the gynecologic literature, where tubal ligations have been done as outpatient procedures, as far back as in 1969.[53] Recently, surgeons have made strides exploring single-port access for various urologic applications.[54–56]

Aron et al. at Cleveland Clinic reported results of a pilot study of single-port LPN, successfully completed in four patients.[57] These were performed using a single intraumbilical multichannel port that incorporates two 5 mm and one 12 mm gel valve inlet (R-port, Advanced Surgical Concepts, Dublin, Ireland). Tumor sizes ranged from 1 to 5.9 cm, operative time was between 4 and 5.8 h, and warm ischemia was between 11 and 29 min. No intraoperative complications were noted, surgical margins were negative, and one patient experienced postoperative bleeding requiring angioembolization. The authors were able to duplicate steps of the standard laparoscopic procedure. However, with current instrumentation, single-port partial nephrectomy is technically challenging and requires careful case selection. The authors cautioned that single port laparoscopy for partial nephrectomy currently should be limited to small, exophytic lesions at high volume centers where technical expertise exists.

Temporary, Reversible Super-Selective Vascular Occlusion

Regardless of the surgical approach (open, laparoscopic, and robotic), the goals of partial nephrectomy are as follows: (i) remove the entire tumor surrounded by a margin of normal parenchyma, (ii) reliably close the vascular channels and collecting system at the resection bed, and (iii) avoid acute or chronic compromise to normal remaining kidney tissue. These goals are often at odds with each other, contributing to the technical difficulty of the procedure. Hilar clamping permits a bloodless field that allows the surgeon to resect with cold scissors, preserving the natural tissue characteristics so that one can differentiate normal from cancerous tissue. The price of clamping, particularly in patients with compromised baseline renal function, is acute and/or chronic renal impairment.

An attractive solution would be to interrupt blood flow only to the tumor itself, such that partial nephrectomy could proceed while normal parenchyma remains perfused. Nohara et al. described selective clamping of the feeding vessel, and they accomplished partial nephrectomy using this technique.[58] However, this relies on the specific extrarenal anatomy and a dedicated vascular dissection of subsegmental vessels with the attendant risk for vascular injury.

To circumvent these issues, Libertino et al. used biocompatible reverse thermosensitive polymers applied intravascularly through a preoperatively positioned angiographic catheter in a porcine model (Libertino, personal communication). The commercially available thermosensitive polymer, LeGoo™ (Pluromed), is approved in Europe for temporary vascular occlusion and is used in cardiovascular surgery including coronary artery bypass. It has also been used at Lahey Clinic in a porcine autotransplantation model.

LeGoo is part of a family of rapid transition polymers that are liquid at cold temperatures, and become viscous gel as they warm to body temperature. The viscosity and transition temperature can be altered by varying the individual mixture composition. For partial nephrectomy, the concept would proceed as follows: (i) on-table angiography to define tumor feeding vessel, (ii) positioning of catheter tip in segmental vessel feeding the tumor, (iii) kidney and tumor mobilization, (iv) LeGoo injection, which would polymerize at body temperature, (v) completion of partial nephrectomy under segmental occlusion conditions, and (vi) injection of cold saline to dissolve the LeGoo. While still in an experimental phase, temporary superselective vascular occlusion has the potential to allow rapid and safe partial nephrectomy without warm ischemic injury to normal parenchyma (Fig. 22.3).

Assessment of Acute Renal Injury

LPN has equivalent intermediate-term oncologic outcomes to open partial nephrectomy, with both the approaches decreasing the overall risk of end-stage renal disease when compared with radical nephrectomy.[60] Hilar control is often required during these procedures to aid in tumor excision, pelvicalyceal suture repair, and parenchymal hemostasis. Renal hilar clamping causes warm ischemia that can result in permanent renal dysfunction. Although there is no absolute cut-off, 30 min of warm ischemia is usually cited as an acceptable limit. Advancing age and medical renal disease may shorten the acceptable warm ischemia window.[61]

Serum creatinine is an imperfect marker of renal dysfunction in the perioperative period, especially in patients with a normal contralateral kidney. In some cases, elevations in

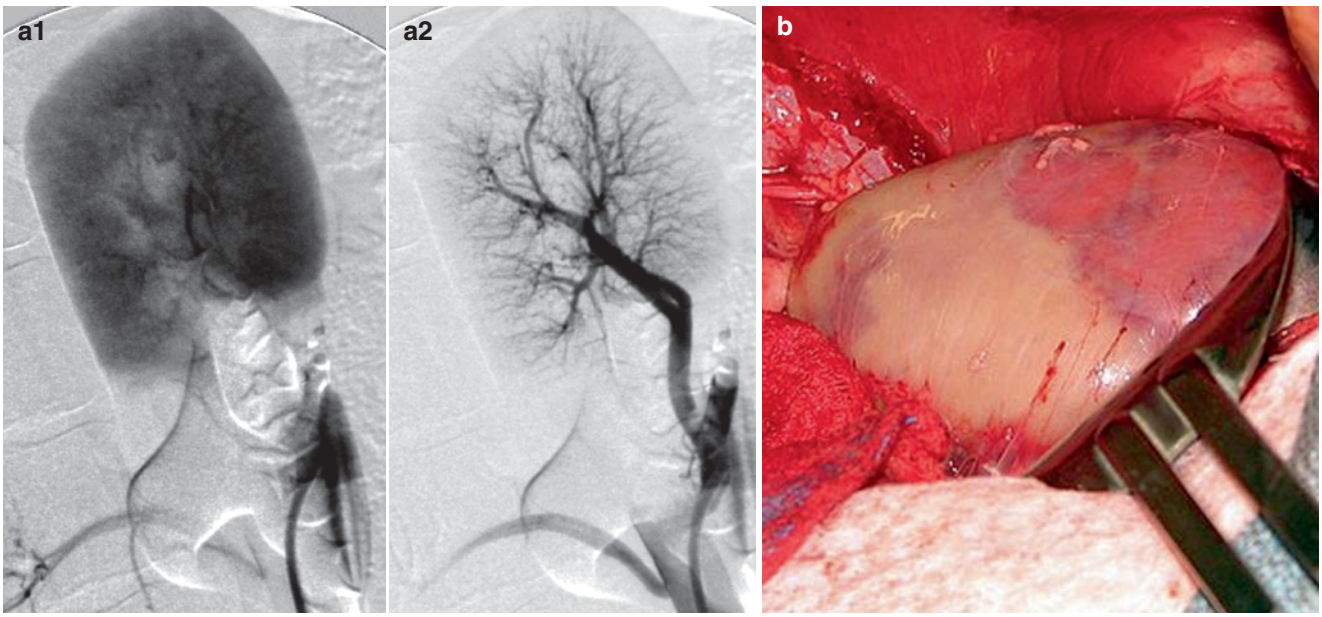

Fig. 22.3 (**a**) Arteriograms demonstrating selective occlusion of the lower segmental branch of the left renal artery. No part of the lower kidney is perfused apart from a small "blush" in the *right-hand image*, which represents flow from a tiny segmental branch not seen in the *left-hand image*. This is the preparation needed to obtain bloodless resection of the renal parenchyma. While the circulation to the lower pole is completely interrupted, flow to the upper portion of the kidney is preserved. (**b**) Gross image of segmental occlusion corresponding to arteriogram above. (Courtesy of John Libertino and Peter Madras, Lahey Clinic Medical Center)

serum creatinine are delayed until 48–72 h after initial insult to the kidney.[62] Furthermore, levels can be influenced by nonrenal factors such as body mass index, muscle metabolism, volume status, and dietary changes. Serum creatinine may not reflect significant damage if there is adequate renal reserve or enhanced tubular secretion of creatinine.[63,64]

A significant need exists for new biomarkers of acute renal injury. Biomarkers may allow earlier detection of acute renal dysfunction, and improve our ability both to assess the degree of renal insult and to predict durable decrements in renal function. Of particular relevance to partial nephrectomy, advanced molecular diagnostics might help to reduce the renal morbidity of partial nephrectomy by signaling the need for intervention.

Trof et al. recently reviewed three main classes of biomarkers.[65] These included tubular enzymes, low-molecular-weight proteins, and markers of glomerular filtration. Tubular enzymes originate from lysosomes, brush-border membranes, and cytoplasm. These include α- and π-glutathione, *S*-transferase, *N*-actyl-glucosaminidase, alkaline phosphatase, γ-glutamyl transpeptidase, and fructose 1,6-biphosphatase. This family of markers detects acute tubular damage at an early stage, typically 12 h to 4 days prior to an increase in creatinine.[66] However, tubular enzymes are released in mild renal injury, limiting its ability to predict irreversible damage.

Urinary low-molecular weight proteins can be used to detect proximal tubule damage, because they are not reabsorbed when these cells are dysfunctional. Some of these markers include α_1 and β_2 microglobulin, retinol-binding protein, adenosine deaminase-binding protein, neutrophil gelatinase-associated lipocalin (NGAL), and kidney injury molecule 1 (KIM-1). These proteins are freely filtered by the glomerulus and reabsorbed, but not secreted by proximal tubular cells. Their predictive value for ultimately requiring renal replacement therapy is superior to tubular enzymuria, but demonstrates wide variability in both sensitivity and specificity.[66]

NGAL is a 25 kDa protein that is usually expressed at very low concentrations in the kidney, but is upregulated in several nephron segments after ischemic injury, predominately in the proximal tubules. [67] Clinically, NGAL is an independent predictor of renal injury in children who underwent cardiopulmonary bypass surgery.[68]

KIM-1 is another promising biomarker that is a type-1 membrane protein that can be determined in urine by Western blot analysis and quantified by ELISA. Patients with a 1-U increase in the urinary KIM-1 levels are subject to a 12-fold increased risk for the presence of acute renal failure (ARF).[69]

Trof et al. also described a class of biomarkers that measure the diminished glomerular filtration.[65] Examples include ProANP and cystatin C. Proatrial natriuretic peptide (1–98) is the prohormone of ANP that does not bind to specific receptors in blood and therefore its clearance depends on renal function.[70] ProANP was a better predictor for the development of ARF in a group of 29 septic patients than standard biochemical markers such as cystatin C.[71]

Coca et al. recently conducted a systematic review of publications that evaluated serum and urinary biomarkers.[72] They reviewed 31 studies involving 21 biomarkers and concluded that serum cystatin C, urine interleukin 18 (IL-18), and urine KIM-1 performed best for the differential diagnosis of established acute kidney injury (AKI). Serum cystatin C, NGAL, IL-18, glutathione-*S*-transferase-π, and γ-glutathione-*S*-transferase performed best for early diagnosis of AKI. Urine *N*-acetyl-β-glucosaminidase, KIM-1, and IL-18 performed best for early mortality risk prediction after AKI.

A new class of biomarkers termed urinary exosomes has recently been discovered. Exosomes are membrane vesicles that are secreted by various cells including the entire nephron. Zhou et al. reported that urinary exosomes such as activating transcription factor 3 (ATF 3) were isolated from patients with AKI, but not from patients with chronic kidney disease or controls.[73] ATF 3 also increases significantly after ischemia-reperfusion injury, peaking between 0 and 2 h after the initial insult. These preliminary results look promising, but more studies are needed to gauge their clinical utility.

Another promising class of markers is the group of netrins, which are laminin-like molecules that were initially described as neuronal guidance cues, but are also abundant in the kidney.[74,75] Netrin-1 is induced in tubular epithelial cells as early as 3 h after ischemia-reperfusion injury and peaks at 24 h.[76] In a recent study of 13 patients with ARF, netrin-1 levels increased dramatically, with no detectable netrin in the urine of six healthy controls.[77]

A wide spectrum of urinary and serum biomarkers are being studied to help identify patients prone to ischemic injury. Owing to the diversity of patient backgrounds, intrinsic renal disease, and etiology of renal insult, it is likely that more than one biomarker will be needed. Individual biomarkers have unique limitations; a broad biomarker panel will therefore be required. In the future, such a panel will allow practitioners to not only avoid ischemic injury in high-risk patients, but to appreciate injury earlier. Furthermore, elucidation of pathways of renal injury may provide molecular targets for targeted intervention.

Conclusion

New technologies have great potential to improve nephron-sparing approaches to renal masses, in particular, LPN. Translational research has the potential to transform the diagnosis of renal masses from a predominantly radiographic diagnosis to one rooted in the DNA, RNA, miRNA, or proteomic profiles associated with the pathologic process itself. Serum, urine, or tissue biomarkers may offer greater sensitivity and specificity than histopathology or cytology, and have the potential of reducing the 15–30% rate of benign operative pathology. Avoiding unnecessary insults to renal function through improved molecular diagnostics will be a significant technical advance.

CT scanning with 3D reformatting has become an essential tool in the preoperative evaluation of renal masses. The detail provided by 3D reconstructions is crucial to surgical planning and has been shown to be predictive of the surgical experience, including calyceal entry. Advances in 3D imaging foretell the possibility of surgical rehearsal in a virtual reality environment, which has been investigated in provocative proof-of-concept studies.

In addition to diagnostic advances, new technology promises to transform the techniques of LPN. New excision devices, such as the thulium and KTP lasers, bring us closer to the ideal of limited collateral thermal damage, excellent hemostasis without destruction of tissue architecture or margins, and preserved visibility. ILUS can be very useful in delineating tumor from normal parenchyma. Similarly, novel optical technologies and bioimpedance tools hold promise for improved tumor detection and margin assessment during LPN.

Moreover, superimposition of anatomical data from imaging studies onto real-time operative images seen through the endoscope may further enhance the intraoperative environment. Fusing of 3D CT imaging with the live laparoscopic view has already been accomplished. Successful use of augmented reality has been described for adrenalectomy, and has the potential to hasten hilar identification and preclude inadvertent vascular injury in LPN.

Single-port partial nephrectomy, the latest advance in minimally invasive surgery, consolidates laparoscopic instrumentation through a single port, usually placed in the umbilicus. This technically challenging approach may decrease incisional morbidity and improve convalescence, but should be limited at present to treatment of small, exophytic lesions at high volume centers.

While LPN is much more favorable than radical surgery from a renal-function perspective, some of the most exciting new technologies aim to further reduce the adverse impact on glomerular filtration. For instance, temporary superselective vascular occlusion has the potential to allow rapid and safe partial nephrectomy without warm ischemic injury to normal parenchyma. Finally, urinary and serum biomarkers are being studied to help identify patients prone to ischemic injury. A biomarker panel may not only allow practitioners to avoid ischemic injury in high-risk patients, but to diagnose durable renal injury sooner and with greater specificity.

LPN is a procedure that was conceived, improved upon, and broadly accepted through the evaluation and adoption of new technologies. This spirit of innovation continues to propel the procedure forward.

References

1. McDougall EM, Clayman RV, Chandhoke PS, et al Laparoscopic partial nephrectomy in the pig model. *J Urol.* 1993;149(6): 1633–1636
2. Winfield HN, Donovan JF, Godet AS, Clayman RV. Laparoscopic partial nephrectomy: initial case report for benign disease. *Endourol.* 1993;7(6):521–526
3. Gill IS, Delworth MG, Munch LC. Laparoscopic retroperitoneal partial nephrectomy. *J Urol.* 1994;152(5 Pt 1):1539–1542
4. Janetschek G Daffner P Peschel R Bartsch G. Laparoscopic nephron sparing surgery for small renal cell carcinoma. *J Urol.* 1998;159(4): 1152–1155
5. Lane BR, Gill IS. 5-Year outcomes of laparoscopic partial nephrectomy. *J Urol*. 2007;177(1):70–74; discussion 74
6. Scardino PT. Urology: a long history of innovation. *Nat Clin Pract Urol*. 2008;5(2):59
7. De Mulder PHM, Patard J, Szczylik C, Otto T, Eisen T. Current status of targeted therapy in metastatic renal cell carcinoma. *Eur Urol Suppl*. 2007;6:665–671
8. Ng CS, Wood CG, Silverman PM, Tannir NM, Tamboli P, Sandler CM. Renal cell carcinoma: diagnosis, staging, and surveillance. *AJR Am J Roentgenol.* 2008;191(4):1220–1232
9. McKiernan J, Yossepowitch O, Kattan MW, et al Partial nephrectomy for renal cortical tumors: pathologic findings and impact on outcome. *Urology.* 2002;60(6):1003–1009
10. Pahernik S, Roos F, Hampel C, Gillitzer R, Melchior SW, Thuroff JW. Nephron sparing surgery for renal cell carcinoma with normal contralateral kidney: 25 years of experience. *J Urol*. 2006;175(6): 2027–2031
11. Gill IS, Matin SF, Desai MM, et al Comparative analysis of laparoscopic versus open partial nephrectomy for renal tumors in 200 patients. *J Urol.* 2003;170(1):64–68
12. Dechet CB, Zincke H, Sebo TJ, et al Prospective analysis of computerized tomography and needle biopsy with permanent sectioning to determine the nature of solid renal masses in adults. *J Urol*. 2003;169(1):71–74
13. Miller DC, Hollingsworth JM, Hafez KS, Daignault S, Hollenbeck BK. Partial nephrectomy for small renal masses: an emerging quality of care concern? *J Urol.* 2006;175(3 Pt 1):853–857; discussion 858
14. Chronic kidney disease after nephrectomy in patients with renal cortical tumours: a retrospective cohort study. *Lancet Oncology*. 2006;7(9):735–740
15. Lucas SM, Stern JM, Adibi M, Zeltser IS, Cadeddu JA, Raj GV. Renal function outcomes in patients treated for renal masses smaller than 4 cm by ablative and extirpative techniques. *J Urol*. 2008; 179(1):75–79; discussion 79–80
16. Lam JS, Leppert JT, Figlin RA, Belldegrun AS. Role of molecular markers in the diagnosis and therapy of renal cell carcinoma. *Urology*. 2005;66(5 Suppl):1–9
17. Tunuguntla HS, Jorda M. Diagnostic and prognostic molecular markers in renal cell carcinoma. *J Urol*. 2008;179(6):2096–2102
18. Junker K, Sanjmyatav J, Mueller J, et al Molecular tumour profiling for detection of biomarkers in renal cell tumours. *Eur Urol Suppl*. 2007;6:611–615
19. Juan D, Gabriela A, Antes T, et al MicroRNA expression profile in clear-cell kidney cancer. *J Urol*. 179:(4):92 (abstract)
20. Thomas JO, Tawfik OW. Recent advances in the diagnosis of renal cell carcinoma. *Diagn Histopathol*. 2008;14:(4):157–163
21. Derweesh IH, Herts BR, Motta-Ramirez GA, et al The predictive value of helical computed tomography for collecting-system entry during nephron-sparing surgery. *BJU Int.* 2006;98(5):963–968
22. Knudsen BE, Campbell G, Kennedy A, et al Design of functional simulation of renal cancer in virtual reality environments. *Urology.* 2005;66(4):732–735
23. Floratos DL, de la Rosette JJ. Lasers in urology. *BJU Int.* 1999;84(2):204–211
24. Rubinstein M, Moinzadeh A, Colombo JR, et al Energy sources for laparoscopic partial nephrectomy – critical appraisal. *Int Braz J Urol*. 2007;33:(1):3–10
25. Janda P, Sroka R, Mundweil B, et al Comparison of thermal tissue effects induced by contact application of fiber guided laser systems. *Lasers Surg Med*. 2003;33:93–101
26. Moinzadeh A, Gill IS, Rubenstein M, et al Potassium-titanyl-phosphate laser laparoscopic partial nephrectomy without hilar clamping in the survival calf model. *J Urol*. 2005;174: 1110–1114
27. Hindley RG, Barber NJ, Walsh A, et al Laparoscopic partial nephrectomy using the potassium titanyl phosphate laser in a porcine model. *Urology*. 2006;67:1079–1083
28. Honeck P, Wendt-Nordahl G, Bolenz C, et al Hemostatic properties of four devices for partial nephrectomy: a comparative ex vivo study. *J Endourol*. 2008;22(5):1071–1076
29. Bui MH, Breda A, Gui D, et al Less smoke and minimal tissue carbonization using a thulium laser for laparoscopic partial nephrectomy without hilar clamping in a porcine model. *J Endourol*. 2007;21(9):1107–1111
30. Timsit M, Bazin J, Thiounn N, et al Prospective study of safety margins in partial nephrectomy: intraoperative assessment and contribution of frozen section analysis. *Urology*. 2006;67:923–926
31. Polascik TJ, Meng MV, Epstein JI, Marshall FF. Intraoperative sonography for the evaluation and management of renal tumors: experience with 100 patients. *J Urol*. 1995;154:1676–1680
32. Fazio LM, Downey D, Nguan CY, et al Intraoperative laparoscopic renal ultrasonography: use in advanced laparoscopic renal surgery. *Urology*. 2006;68:723–727
33. Parekh DJ, Lin W, Herrell SD. Optical spectroscopy characteristics can differentiate benign and malignant renal tissues: a potentially useful modality. *J Urol*. 2005;174:1754–1758
34. Bensalah K, Tuncel A, Peshwani D, et al Optical reflectance spectroscopy to differentiate renal tumor from normal parenchyma. *J Urol*. 2008;179:2010–2013
35. Goel RK, Kaouk JH. Optical coherence tomography: the past, present, and future. *J Robot Surg*. 2007;1:179–184
36. Chung B, Tresser N, Kareta K, et al Niris optical coherence tomography system. Principles of operation and applications in partial nephrectomy. In: *Abstract of the 5th International Kidney Cancer Symposium*. Chicago; 2006
37. Lee BR, Roberts WW, Smith DG, et al Bioimpedance: novel use of a minimally invasive technique for cancer localization in the intact prostate. *Prostate*. 1999;39:213
38. Hernandez DJ, Sinkov VA, Roberts WW, et al Measurement of bioimpedance with a smart needle to confirm percutaneous kidney access. *J Urol*. 2001;166:1520–1523
39. Breda A, Stepanian SV, Lam JS, et al Use of haemostatic agents and glues in during laparascoic partial nephrectomy: a multi-institutional survey from the United States and Europe of 1347 cases. *Eur Urol*. 2007;52(3):798–803
40. Msezane LP, Katz MH, Gofrit ON, et al Hemostatic agents and instruments in laparoscopic renal surgery. *J Endourol.* 2008;22(3): 403–408
41. Johnson WK, Kelel KM, Hollenbeck BK, Daignault S, Wolf JS. Acute integrity of closure for partial nephrectomy: comparison of 7 agents in a hypertensive porcine model. *J Urol*. 2307;2006:175
42. Nogueira L, Katz D, Pinochet R, et al Comparison of gelatine matrix-thrombin sealants used during laparoscopic partial nephrectomy. *BJU Int*. 2008;102(11):1670–1674
43. Pusateri AE, McCarthy S, Gregory KW, et al Effect of a chitosan-based hemostatic dressing on blood loss and survival in a model of severe venous hemorrhage and hepatic injury in swine. *J Trauma.* 2003;54:177–178

44. Xie H, Khajanchee YS, Shaffer BS. Chitosan hemostatic dressing for renal parenchymal wound sealing in a porcine model: implications for laparoscopic partial nephrectomy technique. *JSLS*. 2008; 12:18–24
45. Porpiglia F, Renard J, Billia M, et al Biological glues and collagen fleece for hemostasis during laparoscopic partial nephrectomy: technique and results of prospective study. *J Endourol.* 2007;21(4): 423–428
46. Canales BK, Lynch AC, Fernandes E, et al Novel technique of knotless hemostatic renal parenchymal suture repair during laparoscopic partial nephrectomy. *Urology*. 2007;70:358–359
47. Nguyen MM, Gill IS. Halving ischemia time during laparoscopic partial nephrectomy. *J Urol.* 2008;179(2):627–632
48. Weight CJ, Lane BR, Gill IS. Laparoscopic partial nephrectomy for selected central tumours: omitting the bolster. *BJU Int.* 2007;100(2): 375–378
49. Maciunas RJ. Computer-assisted neurosurgery. *Clin Neurosurg.* 2006;53:267–271
50. Marescaux J, Rubino F, Arenas M, Mutter D, Soler L. Augmented-reality-assisted laparoscopic adrenalectomy. *JAMA*. 2004;292(18): 2214–2215
51. Ukimura O, Gill IS. Imaging-assisted endoscopic surgery: Cleveland Clinic experience. *J Endourol.* 2008;22(4):803–810
52. Frank I, Blute ML, Cheville JC, Lohse CM, Weaver AL, Zincke H. Solid renal tumors: an analysis of pathological features related to tumor size. *J Urol*. 2003;170:2217–2220
53. Wheeless CR. A rapid, inexpensive and effective method of surgical sterilization by laparoscopy. *J Reprod Med*. 1969;5:255
54. Raman JD, Bensalah K, Bagrodia A, Stern JM, Cadeddu JA. Laboratory and clinical development of single keyhole umbilical nephrectomy. *Urology*. 2007;70:1039–1042
55. Desai MM, Rao PP, Aron M, et al Scarless single port transumbilical nephrectomy and pyeloplasty: first clinical report. *BJU Int*. 2008;101:83–88
56. Kaouk JH, Haber GP, Goel RK, et al Single-port laparoscopic surgery in urology: initial experience. *Urology*. 2008;71:3–6
57. Aron M, Canes D, Desai MM, Haber GP, Kaouk JH, Gill IS. Transumbilical single-port laparoscopic partial nephrectomy. *BJU Int*. 2009;103(4):516–521
58. Nohara T, Fujita H, Yamamoto K, Kitagawa Y, Gabata T, Namiki M. Modified anatrophic partial nephrectomy with selective renal segmental artery clamping to preserve renal function: a preliminary report. *Int J Urol*. 2008
60. McKiernan J, Simmons R, Katz J, et al Natural history of chronic renal insufficiency after partial and radical nephrectomy. *Urology*. 2002;59(6):816–820
61. Desai MM, Gill IS, Ramani AP, et al The impact of warm ischemia on renal function after laparoscopic partial nephrectomy. *BJU Int*. 2005;95:377–383
62. Bjornsson TD. Use of serum creatinine concentrations to determine renal function. *Clin Pharmocokinet*. 1979;4:200–20
63. Bosch JP. Renal reserve: a functional view of glomerular filtration rate. *Semin Nephrol*. 1995;15:381–385
64. Herrera J, Rodriguez-Iturbe B. Stimulaton of tubular secretion of creatinine in health and in conditions associated with reduced nephron mass. Evidence for a tubular functional reserve. *Nephrol Dial Transplant*. 1998;13:623–629
65. Trof RJ, Di Maggio F, Leemreis J, Groeneveld J. Biomarkers of acute renal injury and renal failure. *Shock*. 2006;26(3):245–253
66. Westhuyzen J, Endre ZH, Reece G, et al Measurement of tubular enzymuria facilitates early detection of acute renal impairment in the intensive care unit. *Nephrol Dial Transplant*. 2003;18: 543–551
67. Mishra J, Ma Q, Prada A, et al Identification of neutrophil gelatinase-asociated lipocalin as a novel early urinary biomarker for ischemic renal injury. *J Am Soc Nephrol*. 2003;14:2534–2543
68. Mishra J, Dent C, Tarabishi R, Mitsnefes, et al Neutrophil gelatinase-associated lipocalin (NGAL) as a biomarker for acute renal injury after cardiac surgery. *Lancet*. 2005;365:1231–1238
69. Han WK, Bailly V, Abichandani R, Thadhani R, Bonventre JV. Kidney injury molecule-1: a novel biomarker for human proximal tubular injury. *Kidney Int*. 2002;62:237–244
70. Buckley MG, Sagnella GA, Markandu ND, Singer DRJ, MacGregor GA. Concentration of N-terminal ProANP in human plasma: evidence for ProANP(1–98) as the circulating form. *Clin Chim Acta*. 1990;191:1–14
71. Mazul-Sunko B, Zarkovic N, Vrkic N, et al Proatrial natriuretic peptide (1–98) but not cystatin C is predictive for occurrence of acute renal insufficiency in critically ill septic patients. *Nephron Clin Pract*. 2004;97:c103-c107
72. Coca SG, Yalavarthy R, Concato J, Parikh CR. Biomarkers for the diagnosis and risk stratification of acute kidney injury: a systematic review. *Kidney Int*. 2008;73:1008–1016
73. Zhou H, Cheruvanky A, Hu X, et al Urinary exosomal transcription factors, a new class of biomarkers for renal disease. *Kidney Int*. 2008;74(5):613–621
74. Barallobre MJ, Pascual M, Del Rio JA, Soriano E. The Netrin family of guidance factors: emphasis on Netrin-1 signalling. *Brain Res Rev*. 2005;49:22–47
75. Ly NP, Komatsuaki K, Fraser IP, et al Netrin-1 inhibits leukocyte migration in vitro and in vivo. *Proc Natl Acad Sci USA*. 2005;102: 14729–14734
76. Wang W, Reeves WB, Ramesh G. Netrin-1 and kidney injury. Netrin-1 protects against ischemia-reperfusion injury of the kidney. *Am J Physiol Renal Physiol*. 2008;294(4):F739-F347. doi:10.1152/ajprenal.00508
77. Reeves WB, Kwon O, Ramesh G. Netrin-1 and kidney injury. II. Netrin-1 is an early biomarker of acute kidney injury. *Am J Physiol Renal Physiol*. 2008;294:731–738
78. Hari S, Tunuguntla, GR, Jorda M. Diagnostic and prognostic molecular markers in renal cell carcinoma. *J Urol*. 2008;178: 2096–2102

New Advances in Urologic Laparoendoscopic Single Site (LESS) Surgery

23

Brian H. Irwin, Pradeep P. Rao, Mihir J. Stein, and Robert M. Desai

Introduction

The last 30 years has seen an explosion in the development and adoption of laparoscopy as the standard of care for the treatment of many benign and malignant conditions within the majority of areas of surgical practice. Following the initial laparoscopic nephrectomy performed by Clayman, laparoscopic and robotic-assisted surgery has been applied to nearly the entire gamut of the urologic surgical repertoire. While urologic surgeons continue to strive for improvements in morbidity and the cosmetic sequelae of laparoscopic surgery, an effort has been extended toward minimization of size and number of ports required for the performance of these procedures. Laparoendoscopic single site (*LESS*) surgery is a recently coined term that refers to a group of techniques, which allow for laparoscopic interventions to be performed through a single abdominal incision often hidden within the umbilicus. While the term *LESS* has been recently developed, the concept of *LESS* surgery is not singular. Single incision surgery has been performed for decades during percutaneous procedures on the kidney as well as in gynecology[1] and general surgery.[2] The current acceleration in the interest for these techniques has been promoted by the recent introduction of new instrumentation and access devices, incorporation of novel approaches, and new and existing robotic platforms into the repertoire combined with the familiarity of current practitioners with advanced laparoscopic techniques. As such, within the past year, nearly the entire spectrum of extirpative and reconstructive urologic procedures has been performed using *LESS* surgery.

The History of LESS Surgery

The concept of *LESS* surgery has been around for many years and has been used across many surgical specialties. Tens of thousands of tubal ligations have been performed through the years[3] in gynecologic practice, with an offset laparoscope via a single puncture technique.[4] In more contemporary series, the pediatric and general surgical literature has reported on the use of single incision techniques for peritoneal catheter insertions in children[5] and retroperitoneoscopic adrenalectomies using large 4.5-cm trocars without insufflation.[6] Historically, many attempts have been made to minimize the invasiveness of procedures using techniques that would now fall under the heading of *LESS* procedures.[7]

An extension of LESS surgery called natural orifice transluminal endoscopic surgery (NOTES) was first described in 2003. It was developed along the same philosophical basis as *LESS* surgery, with the expressed goal of reducing morbidity and maximizing the cosmetic appeal of the surgical incisional scars associated with interventions.[8] Animal studies, primarily in the porcine model, have been used to explore various NOTES techniques.[9] These procedures have typically been performed with flexible endoscopes passed via the mouth, vagina, or rectum using integral working channels for the introduction and manipulation of surgical graspers, cutting devices, and other instruments within the surgical field. While these techniques have been developed and used relatively extensively in the laboratory setting, they have yet to be applied to any significant number of reported clinical cases. This has been in large part owing to the technical challenge involved in performing these procedures and the unfamiliarity of the clinicians with the flexible instrumentation and optics. As such, most of the reported NOTES animal cases by urologists have been undertaken using a hybrid NOTES technique in which the more familiar laparoscopic approach is used to aid in the surgery with the introduction of an additional 12-mm port in the umbilicus.[10] In contrast to the less familiar NOTES techniques, *LESS* procedures attempt to offer similar reductions in morbidity and improved cosmesis, while using the laparoscopic instrumentation which is more familiar to current surgeons with equivalent results.

A relatively large number and variety of LESS procedures have been reported in the urologic literature shortly following the initial reports of LESS clinical successes. The motivation for this swift expansion in the popularity of *LESS* surgery is likely multi-factorial. Urologists have been comfortable approaching structures through the abdominal wall and via the retroperitoneum for decades. As such, it is logical

P. Dasgupta et al. (eds.), *New Technologies in Urology,*
DOI: 10.1007/978-1-84882-178-1_23, © Springer-Verlag London Limited 2010

that techniques that allow surgeons to approach organs of the urinary tract in a similar manner will be adopted with relative ease when compared with those requiring the surgeon to view and manipulate structures through a hollow viscus.[11] When the surgeon is employed, the opportunity to use more familiar instruments and the learning curve with *LESS* may be shorter, while maintaining the cosmetic benefits seen with a single umbilical incision which can be easily hidden with careful closure.

The approaches for *LESS* surgery generally fall into one of the two categories. In the first, single-site surgery, multiple conventional laparoscopic ports are placed via a single incision to allow for the simultaneous introduction of the required instruments and camera devices. The second general category of LESS procedures involves the introduction of a purpose-designed multi-channel port through the abdominal wall to access the peritoneal cavity. Such single ports surgery can provide a lower profile point of access to the surgical field, minimizing the potential interaction of ports within the small working space afforded by these approaches. Whether carried out by single-incision or single-port technique, the access point may be placed within the umbilicus, an existing cicatrix on the abdomen, or at an extra-umbilical site on the abdomen or flank.

Table 23.1 Acronyms used for LESS procedures

E-Notes	Embryonic natural orifice transumbilical endoscopic surgery
Mini-laparoscopy	
MISPORT	Minimally invasive single port surgery
SILS	Single incision laparoscopic surgery
SLiP	Single laparoscopic port procedure
SPA	Single port access
SPELS	Single port endoscopic and laparoscopic surgery
SPEARS	Single port endoscopic and robotic surgery
SPE	Single port endoscopic surgery
SPIs	Single port intracorporeal surgery
SPLS	Single port laparoscopic surgery
SPL	Single port laparoscopy
SPS	Single-port surgery
TULAs	Translumenal laparoscopic assisted surgery
TUPS	Transumbilical universal port surgery

Adapted with permission from Irwin et al[12]

Nomenclature

Because several techniques have been described for performing single-site surgeries over the course of the past few decades across many specialties, various terminologies and acronyms have been used to describe these laparoscopic procedures (Table 23.1). Owing to the variety of descriptions of these techniques, researchers and potential collaborators have had difficulties in the past identifying studies using similar approaches. *LESS* was proposed as a common nomenclature by a consortium comprised of experts from fields across several surgical specialties to address this problem. Once coined, this term was also endorsed by the Urologic NOTES Working Group in a recent communication.[13]

With the adoption of this common taxonomy, scientific communications, performance of clinical trials, and consistent research practices have been coordinated and standardized. This universal language has allowed for more efficient use of search engines as they are applied to the developing literature to promote the fast dissemination of ideas and results.

Instruments and Technology

Perhaps, the forces that have provided the largest impetus for the quick dissemination of these techniques have been recent improvements in access devices, optics, and instrumentation. In spite of the new developments in instrumentation, the interaction of the necessary elements to perform the case (i.e., instruments, cameras, and access devices) continues to occur at the common point where they are introduced into the abdomen as well as both intra- and extra-corporeally. At times, it is necessary for the surgeon's hands to be crossed to maximize triangulation within the abdomen. This leads to a situation in which the left-handed instrument appears on the right side of the screen and vice versa.

These limitations can largely be overcome with practice, but there remains a very distinct learning curve involved with attempting *LESS* procedures. To facilitate the surgeon along this learning curve, research has focused on developing new technologies to help minimize these limitations, and formal teaching and certifying protocols have been proposed. A brief description of the currently available devices used in LESS surgery is presented in Table 23.2.

Access Devices

LESS surgery can be carried out through a variety of access devices. The initial LESS surgical procedures were carried out using conventional laparoscopic trocars within a single skin incision through separate fascial sites. Ports of varying lengths and with small external components are favored to help reduce the interaction of instruments and ports limiting the movement of instruments intra-abdominally. Reports on the use of shortened ports with reduced intra-abdominal

Table 23.2 Currently available LESS instrumentation

Instrument	Manufacturer	Comments
Access devices		
TriPort	Advanced Surgical Concepts, Co. Wicklow, Ireland	12–25-mm incision Two 5-mm, one 12-mm port and one insufflation port Port introducer available
QuadPort	Advanced Surgical Concepts, Co. Wicklow, Ireland	2.5–6-cm incision Two Configurations available: Four 12-mm ports or Two 12-mm, one 5-mm, and one 15-mm port
Uni-X	Pnavel Systems Inc., Brooklyn, NY	Requires fascial suture to remain in place
Gel port	Applied Medical, Rancho Santa Margarita, CA	Can accept instruments directly or ports Bulges away from patient with use Accommodates multiple instrument configurations Requires at least a 2.5-cm fascial incision
SILS™ access	Covidien/Autosuture, Hamilton HM FX, Bermuda	Three foam insertion sites require low profile ports Insufflation via tubing away from main port body
AirSeal	Surgiquest, Orange, CT	Uses recirculated CO_2 to create seal – no gasket/valve No fulcrum for instruments Requires proprietary insufflator
Articulating instruments		
Roticulator series	Covidien/Autosuture, Hamilton HM FX, Bermuda	Fewer degrees of freedom Dissector, shears, grasper available Lower profile handle
RealHand series	Novare Cupertino, CA	One-handed locking mechanism More degrees of freedom Larger profile handle May be locked in straight position
Autonomy laparo-angle	Cambridge Endo, Framingham, MA	All instruments with locking mechanism More degrees of freedom Larger profile handle
Camera systems		
EndoEYE	Olympus, Center Valley, PA	Low-profile – in-line design Digital chip-on-the-tip technology, available in 0, 30°, and flexible versions
Magnetic anchoring and guidance system MAGS	In development	Inserted completely into abdominal cavity Secured and manipulated through abdominal wall via magnetic handle Current version with poor visibility and wireless not available
EYEMAX	Richard Wolf Medical Instruments Corporation, Vernon Hills, IL	Low-profile – in-line design Digital chip-on-the-tip technology

Adapted with permission from Irwin et al[12]

profiles have also been published, again with the goal of minimizing instrument interaction intracorporeally.[14]

More recently, specific access devices have been developed which allow for the performance of single-port surgery while allowing multiple instruments to be passed into the abdominal cavity at the same time while maintaining pneumoperitoneum. Currently, the most familiar and widely used access system remains the TriPort (Advanced Surgical Concepts, Co. Wicklow, Ire land) (Fig. 23.1).[15] This device has received FDA approval for use in humans. It consists of two components, a retracting ring made up of two semi-rigid rings connected by a double barreled plastic sleeve and a multi-channel valve, which uses a unique elastomeric material similar to that of the more familiar GelPort (Applied Medical, Rancho Santa Margarita, CA) to prevent the loss of pneumoperitoneum alongside the instruments. The currently available TriPorts have one 12-mm and two 5-mm ports to accommodate instruments within the same working space. The size of the incision used with the TriPort can be tailored to the specific application. The device can be placed through

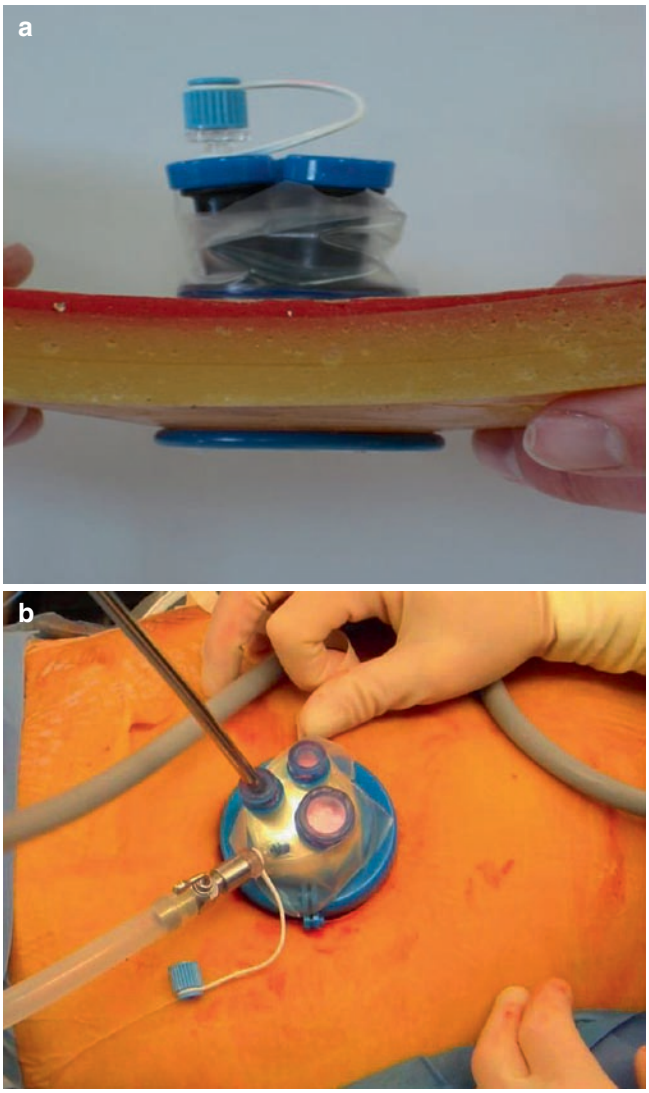

Fig. 23.1 The TriPort (Advanced Surgical Concepts, Co. Wicklow, Ireland) (**a**) applied to a model abdominal wall and (**b**) as viewed from above. Note the presence of three working channels and an insufflation port. Reprinted from Irwin et al[12], Copyright 2009, with permission from Elsevier

a fascial incision measuring between 10 and 30 mm via an open technique but is also supplied with an introducer that allows for the placement of the port into a previously insufflated abdominal cavity. While the larger variation of the device, the QuadPort, does not currently come with such an introducer and must be placed via an open technique, it can be used in even larger incisions of up to 50 mm in length allowing for more working room. Each of the two available configurations for the QuadPort (one 15-mm, one 12-mm, and two 5-mm ports; or four 12-mm ports) can be particularly useful for extirpative procedures in which a larger incision is needed for specimen removal. Both the TriPort and the QuadPort have housings that support the instrument valves, contain a separate insufflation port, and can be removed to facilitate specimen removal through the intact retracting component.

The Uni-X Single Port Access Laparoscopic system (PNavel systems, Cleveland, OH) has been used during the successful completion of a number of LESS procedures. While the device is capable of allowing the introduction of up to three 5-mm instruments simultaneously, it requires placement via an open techniques and suture fixation to the fascia to remain in place.

As a novel use of the familiar GelPort, used more commonly during hand-assisted procedures, radical nephrectomy has been performed using three conventional laparoscopic ports placed through the elastomeric gel.[16] This system has the advantages of allowing for the use of different port configurations within the gel, as well as the placement of different sizes and shapes of ports and instruments directly though the gel without the loss of pneumoperitoneum. The gel can be introduced into an even larger incision during extirpative procedures, allowing the surgeon to take advantage of the entire incisional length from the outset of the procedure. This has been particularly helpful during radical and donor nephrectomy in which the intact specimen must be removed through a sizable incision. One drawback of the GelPort used with LESS procedures is the ballooning effect seen during insufflation. This causes the instruments to be pushed further from the operative field, further limiting the already reduced ability to triangulate within the abdomen, and provides a less stable fulcrum for the instruments than some of the other purpose-designed LESS access devices.

Other single-port devices which remain in various stages of commercialization include the SILS Access (Covidien/Autosuture, Hamilton HM FX, Bermuda) and AirSeal (Surgiquest, Orange, CT). As of the date of this publication, to our knowledge, no published reports using these latter two devices yet exist.

Instruments

The primary hindrances encountered during LESS are (1) the loss of the triangulation familiar to the surgeon from conventional laparoscopy and (2) the "chopsticks" effect leading to the interaction of instruments both intra- and extra-corporeally (Fig. 23.2). The use of special instrumentation has allowed these obstacles to be overcome or minimized in clinical practice. The use of prototype fixed-shaft bent instruments during the performance of single-port LESS procedures was described by Rane et al and Desai et al using the TriPort;[17,18] the use of similar prototype instruments developed by PNavel Systems was reported by Kaouk et al, using the Uni-X device platform.[19]

To further compensate for the loss of triangulation during LESS procedures, various newer articulating instrument

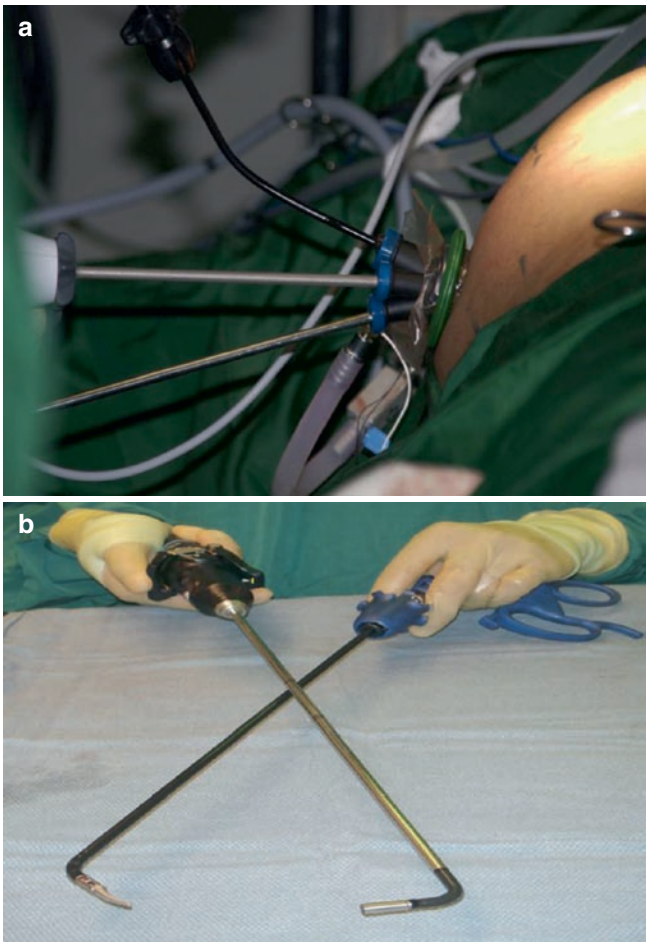

Fig. 23.2 LESS Instrumentation. (**a**) Note that instrument clashing, which is common during LESS surgery, has been somewhat reduced with the use of a fixed-bent instrument. (**b**) The surgeon's left hand holds an articulating dissector while the right holds a flexible camera device. Reprinted from Irwin et al[12], Copyright 2009, with permission from Elsevier

systems have been developed including the RealHand HD series (Novare Surgical Systems, CA), the Roticulator series (Covidien/Autosuture), and those made by Cambridge Endo (Framingham, MA). These companies have attempted to duplicate the full spectrum of available laparoscopic instruments including endo-shears, needle drivers, graspers, and hook electrocauteries in these lines of articulating instruements.[15] The currently available articulating instruments are primarily limited by the technical difficulty involved with training for their use as well as a lack of sufficient strength to provide robust retraction and dissection.

Camera Devices

The clashing of instruments with the camera device as they pass through a common fulcrum continues to be a recurring difficulty seen during LESS surgery. The large profile of the perpendicular light source on most conventional laparoscopes exacerbates this problem. By using a video laparoscope, in which the camera is integrated with a coaxial light cable in line with the shaft of the telescope with a low profile handle, such as the EndoEye (Olympus, Orangeburg, NY), this problem can be minimized.[20] This system is available in 5 and 10 mm sizes in 0 and 30° configurations as well as with a flexible actively deflectable tip of 10 mm size. A 45° telescope with a co-axial light guide attachment has also been developed for use in *LESS* (Karl Storz, Tuttlingen, Germany).

In an elegant way, Park et al have developed a new camera system, which can be introduced completely into the body and manipulated through the abdominal wall with the use of a magnetic anchoring and guidance system, which they have termed "MAGS."[21] This system has already been used successfully in an initial porcine model literature[22] and, more recently, in the first human clinical cases (Cadeddu, personal communication). Currently, this system has been used primarily to control the camera device, but other instruments may be adapted for use in the same manner allowing the surgeon to control them without the use of a port that needs to physically go through the abdominal wall. Another benefit of this type of system is that it allows the surgeon to change the vantage points several times during a given procedure if desired, without the need for the placement of additional ports.

LESS Surgery Clinical Experience

Experience in clinical trials with *LESS* surgery has increased exponentially since the initial reports in the literature of its successful use in human subjects (Table 23.3). Raman et al reported the first human single umbilical incision nephrectomies in three humans (two nonfunctioning kidneys and one renal mass) with the use of three conventional 5-mm laparoscopic ports adjacent to each other as previously described.[11] A 12-mm trocar was placed following dissection for the introduction of a laparoscopic vascular stapling device for the control of the renal hilum. No complications were reported following the surgeries performed with an average operative time of 133 min and patients were discharged on the second postoperative day. A 3-mm subxiphoid port was used in the only right-sided nephrectomy for liver retraction. The authors used an articulating grasper (RealHand HD) for the surgeon's left-hand instrument and a straight instrument in the right hand. Rane et al performed the first LESS procedures – two simple nephrectomies for nonfunctioning renal units resulting from long-standing calculus disease, one orchiopexy, one orchiectomy, and one ureterolithotomy.[18] In this series of five cases carried out with the use of the TriPort, all were completed successfully without complications with a mean operative time of 83 min.

Table 23.3 Summary of current urologic LESS surgery series

References	Number of patients	Procedures	OR time (min)	Hospital stay (days)	Complications	Analgesic use (morphine equivalents)
Raman et al[11]	3	Nephrectomy	133	2	None	–
Kaouk 2007	4	Renal cryotherapy	150	2.8 and 2	1	–
	1	Kidney biopsy				
	1	Radical nephrectomy				
	4	Radical prostatectomy				
Rane et al[18]	1	Simple nephrectomy	–	–	None	–
	1	Right orchidectomy	–	–	None	–
	1	Left ureterolithotomy	–	–	None	–
	1	Left orchidopexy, appendectomy	–	–	None	–
	1	Right simple nephrectomy	–	–	None	–
Kaouk et al[19]	5	Sacrocolpopexy	150	2	None	–
Ponsky et al[16]	1	Radical nephrectomy	96	2	None	34.3
Gill et al[23]	4	Donor nephrectomy	242	–	–	34.8
Goel and Kaouk[24]	6	Renal cryotherapy	170	2.3	1	–
Aron et al[25]	5	Partial nephrectomy	270 (Median)	3 (Median)	1	–
Cadeddu 2008	11	Nephrectomy	122 (Median)	2 (Median)	None	8
Kaouk and Goel[26]	7	Partial nephrectomy (two performed robotically)	163	3.3	One focally positive margin	–
Desai et al[27a]	13	Simple nephrectomy	145	2		64
	4	Radical nephrectomy	208	3.5	Bleeding from gonadal vein – clipped	–
	17	Donor nephrectomy	230	2.9	Corneal abrasion, dyskinesia from anti-emetics	23
	6	Partial nephrectomy	271	7.2	One postoperative bleed required angio-embolization	28
	1	Renal cyst excision	60	1	None	–
	2	Nephroureterectomy	90	5	None	–
	16	Pyeloplasty (2 performed robotically)	236	2	None	28
	2	Ureteroneocystostomy	210	2	None	–
	3	Ileal interposition	330	4	One anastomotic leak required nephrostomy tube	–
	32	Simple prostatectomy (1 performed robotically)	113	3	One mortality in Jehovah's Witness from hemorrhage Two postoperative bleeds required surgical intervention Four postoperative bleeds required transfusion alone 1 bowel injury required exploration 1 UTI	29
	1	Transvesical mesh sling removal	100	1	None	–
	1	Adrenalectomy	150	3	One renal vein injury repaired leading to renal vein thrombosis requiring long term anticoagulation (patent at 3-month follow-up)	–
	1	Hysterectomy	120	2	None	–

[a]Includes patients in series from refs [17,27,28] by Desai published in 2007 and 2008
Adapted with permission from Irwin et al[12]

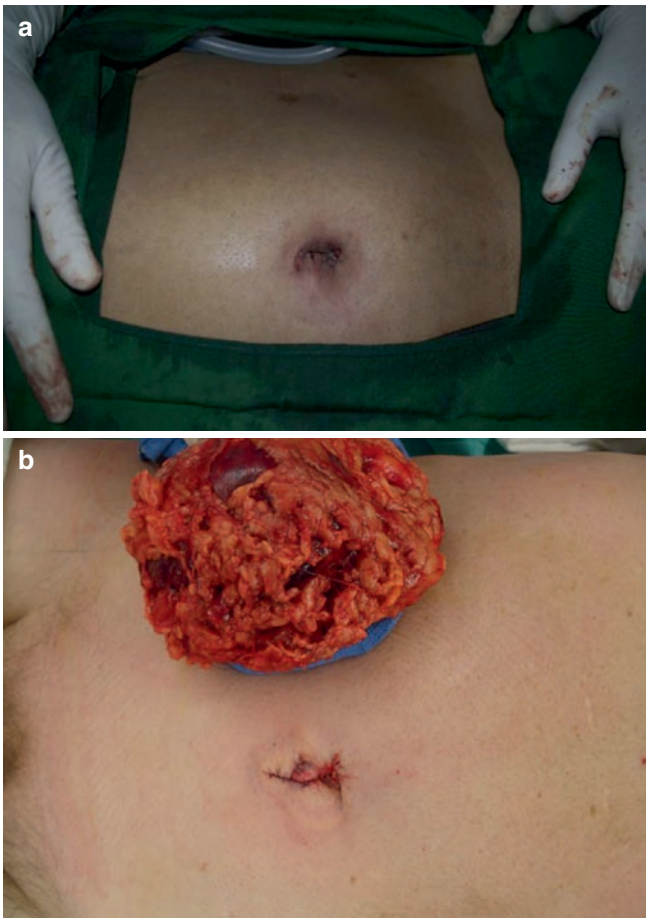

Fig. 23.3 (**a**) Postoperative appearance of surgical incision following LESS simple nephrectomy with morsellation of the specimen. Note that the incision is hidden completely within the umbilicus. (**b**) Postoperative appearance of surgical incision and specimen following LESS radical nephrectomy with intact extraction of the specimen. Notice that the incision extends slightly outside of the borders of the incision. Reprinted from Irwin et al[12], Copyright 2009, with permission from Elsevier

Two early reports followed, which detailed the use of purpose-designed multi-channel single-port surgical platforms. In the first, Desai et al described a simple nephrectomy and a pyeloplasty performed via a transumbilical approach (Fig. 23.3)[17] with mean operative times of 220 and 160 min, respectively. A supplemental 2-mm needlescopic port was placed to aid in reconstruction during pyeloplasty. Patients were discharged on postoperative days 1 and 2, respectively, without complications.

In the second of such reports, Kaouk et al detailed their use of *LESS* techniques in 10 patients undergoing *LESS* nephrectomy ($n = 1$), sacrocolpopexy ($n = 4$), renal cryotherapy ($n = 4$), and renal biopsy ($n = 1$).[19] Using a combination of bent and articulating instruments via the Uni-X port without additional ports, all cases were completed in a mean operating time of 2.5 h. One patient in the cryotherapy group required prolonged oxygen supplementation and transfusion postoperatively.

The indications for *LESS* within the clinical human experience have expanded to include more complex cases since the initial reports of its safe application in benign diseases of the upper and lower urinary tracts. Desai et al described their use of the umbilical LESS approach during six reconstructive procedures in four patients.[27] Two bilateral pyeloplasties, ileal ureteral interposition (Fig. 23.4), and a ureteroneocystostomy were carried out with the aid of a 2-mm needlescopic grasper for dissection and suturing. The ileal ureteral interposition required slight extension of the umbilical incision to perform an extracorporeal bowel reconstruction. All procedures were completed without reported complications.

Donor nephrectomy requires the very judicious use of the newly developed techniques in the process of being established to protect these otherwise healthy altruistic patients. Realizing the potential for significant consequences, Gill and his team attempted this high-profile procedure in four *LESS* donor nephrectomies only after substantial experience with *LESS* techniques.[23] The TriPort was used in all cases again with aid of a 2-mm needlescopic grasper for retraction during hilar dissection and graft extraction within an endoscopic specimen bag. With a mean warm ischemia time of 6.2 min, a median length of 3.3 cm of renal artery, 4 cm of renal vein, and 15 cm of ureter were harvested. Upon transplantation, no delayed graft function or graft loss were seen in this small series; and no intra- or postoperative complications were reported. Donor patients had minimal pain, with all reporting 0/10 visual analog pain scale scores at 2 weeks of follow-up.

The pediatric surgical population has been traditionally treated only with well-established treatments. In their initial report of the application of *LESS* surgery in the pediatric urologic population, Kaouk and Palmer performed unilateral *LESS* varicocelectomy in three adolescents using the Uni-X port and fixed-bent instruments.[29] All procedures were performed as outpatient surgery with operative times of less than 1 h.

Only after the techniques were well established in benign disease and the surgeons felt comfortable with their experience and skill were these techniques applied to the urological oncological arena. The first single-access radical nephrectomy with intact specimen retrieval was reported by Ponsky et al[16] A GelPort was used with three standard laparoscopic ports via a 7-cm paramedian incision using standard laparoscopic instruments. Minimal blood loss was encountered during the 96 min procedure, and the patient was discharged on postoperative day 2 without complication.

Single-port access renal cryoablation (SPARC) was performed in six patients for the treatment of renal masses with a mean tumor size of 2.6 cm by Goel and Kaouk.[24] This group again favored the use of the Uni-X system with bent and articulating instruments. Two transperitoneal procedures were performed transumbilically, and the remaining four

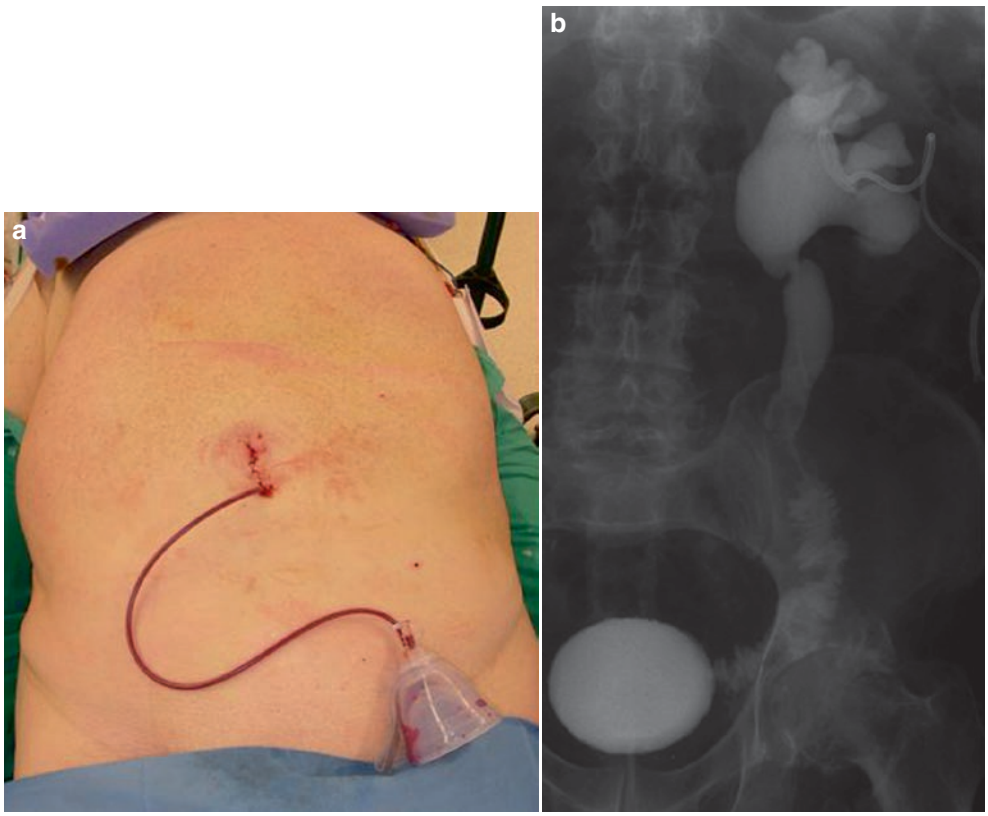

Fig. 23.4 (**a**) Postoperative cosmetic appearance and (**b**) radiographic appearance of cystogram following LESS ileal ureter creation. Note that the umbilical incision has been extended slightly to allow for extracorporeal harvest of the ileal segment and performance of bowel anastomosis. (Reproduced from Irwin et al[12])

were carried out retroperitoneally with the placement of the device at the tip of the 12th rib. Ultrasonic guidance was used for real-time monitoring of the resultant ice ball provided by a laparoscopic ultrasound probe introduced next to the single port through the same incision. A single cryoprobe was introduced through the single port for smaller tumors, while additional probes were placed percutaneously for larger tumors. A mean operative time of 170 min was reported and the resultant hospital stay had a mean of 2.3 days. One patient required a 1-week hospital stay and blood transfusion for the treatment of respiratory difficulty.

By any measure, laparoscopic partial nephrectomy remains a technically demanding procedure. Two series detailing the use of *LESS* surgery in partial nephrectomy have been reported to date. Aron et al described the use of the TriPort in *LESS* partial nephrectomy in four patients for tumors ranging in size from 1 to 5.9 cm (median tumor size 3 cm).[25] A 2-mm grasper was again used to assist in the reconstruction of the renal defect via a needlescopic port. One patient underwent conversion to conventional laparoscopy with the addition of a single 5-mm port. Median warm ischemia time was 20 min (range 11–29) during a total median operating time of 270 min. The median estimated blood loss and hospital stay were 150 mL and 3 days, respectively. Postoperative complications were seen in only one patient who developed postoperative hemorrhage and pulmonary embolism. In a subsequent series, Kaouk et al performed seven *LESS* partial nephrectomies, including two in which robotic assistance was used.[26] Again, one patient required conversion to conventional laparoscopy to control bleeding within the tumor resection bed. A single focally positive margin on final pathology, which was initially read as negative on intra-operative frozen section, was reported.

LESS radical prostatectomy including nerve sparing for the treatment of prostate cancer has been performed successfully in carefully selected patients. These cases are technically challenging as they require the surgeon to be familiar with both precise dissection as well as reconstructive techniques. By selecting patients who were at clinical stage T1c, had had no prior pelvic surgery, and had a BMI ≤35, Kaouk et al carried out *LESS* radical prostatectomy in four patients.[30] They reported a mean total operative time of 285 min consisting primarily of 200 min for prostate excision and an additional 66 min for vesicourethral anastomosis. Within this small series, two (50%) had positive margins and one (25%) developed a recto-urethral fistula 2 months out from surgery. Reporting on their experience in both cadaveric models as well as in the living humans, Barret et al were similarly able to successfully complete *LESS* radical prostatectomies.[31] In the cadaveric model, a combination of both straight rigid and flexible articulating instruments were used. They noted that while the articulating instruments were helpful at times during the case for dissection, the standard instrumentation was

equally necessary. This group also performed a robotic-assisted *LESS* radical prostatectomy in a live patient with an estimated blood loss of 500 mL. Bilateral nerve preservation was achieved with negative surgical margins.

The first comparative study between laparoscopic and *LESS* applications was reported by Raman et al, in which they compared 11 *LESS* nephrectomies to 22 standard laparoscopic nephrectomies.[14] A matching protocol was applied in which patients' age, surgical indication, and tumor size were used to identify the groups in a 2:1 ratio for comparison. Similar outcomes were reported with regard to operative time (122 vs. 125 min), percent decrease from preoperative hemoglobin, analgesic use, length of stay, and complication rate between the two groups. Indeed, to further delineate the benefits of *LESS* procedures, prospective randomized comparative analyses incorporating quality of life investigations are needed.

To date, the largest series compiled in the *LESS* experience was reported by Desai et al, encompassing their experience with 100 *LESS* procedures. The series includes relatively heterogeneous group of procedures, such as nephrectomies ($n = 40$) (simple, partial, radical, and donor), nephroureterectomy ($n = 2$), renal cyst excision ($n = 1$), pyeloplasty ($n = 16$), ureteroneocystostomy ($n = 2$), ileal ureter ($n = 3$), adrenalectomy ($n = 1$) and hysterectomy ($n = 1$), as well as transvesical simple prostatectomy ($n = 32$) and mesh sling removal ($n = 1$). The breadth of possibilities for *LESS* surgery within the urological surgery repertoire is exemplified by this diverse series.

Skepticism regarding the rapidity with which the technique is adopted is expected and can breed a healthy respect for these procedures in the minds of the pioneers, pushing the limits of technology. In a multi-institutional review of three high-volume centers, the authors have found that in our series of over 1,250 upper tract laparoscopic cases, only 11.6% were even attempted using *LESS* techniques despite the surgeons' familiarity with the skill sets and instrumentation needed for both conventional and *LESS* laparoscopy. Of those attempted using *LESS* techniques, only 6.8% were converted to a standard laparoscopic technique requiring the placement of additional ports to safely complete the procedure. This low rate of conversion to standard laparoscopy suggests that the early pioneers in the field have been highly selective in choosing and counseling patients appropriate for *LESS* approaches. In addition, they have been able to identify their own limitations during this early phase of development of the techniques.

Robotics

As the minimally invasive surgical world is being redefined through the use of surgical robotics, a natural extension of this has been the hybridization of the technology with *LESS* surgery. The first group to report on the use of the DaVinci-S (Intuitive Surgical, Sunnyvale, CA) robotic system in conjunction with a TriPort single-port access device was Kaouk et al. They discussed their experience in three patients while performing a radical prostatectomy, a pyeloplasty, as well as a radical nephrectomy, for a 5.6-cm right-sided renal mass.[32] The TriPort was used with a 12-mm 3D camera and 5-mm grasping instrument placed through the device with an additional 8-mm robotic port placed alongside the TriPort in the same incision for the other robotic instrument. All cases were completed successfully using this platform without the need for placement of additional ports. Similar results were reported with regard to operative times (radical prostatectomy = 5 h, pyeloplasty = 4.5 h, radical nephrectomy = 2.5 h), estimated blood loss (radical prostatectomy = 250 mL, pyeloplasty = 80 mL, radical nephrectomy = 200 mL), and hospital length of stay (radical prostatectomy = 1.5 days, pyeloplasty = 2 days, radical nephrectomy = 2 days), as are seen in the conventional robotic-assisted laparoscopic literature. Pain was minimal in all patients (visual analog scale score of 0) at 1 week of follow-up. They described significant "clashing" of the robotic arms, but concluded that this platform might provide an opportunity to shorten the learning curve associated with conventional single-port laparoscopy. While the DaVinci system has a significantly limited range of motion while performing *LESS* surgery, purpose-designed robotic platforms such as flexible robotics and miniature in vivo robotics may, in the future, simplify the performance of *LESS* procedures.

Flexible robotics allows the operator to remotely manipulate a flexible endoscope along with flexible instruments passed through the endoscope's working channel to perform delicate tasks. Such tasks could be carried out via a single skin incision or through a naturally occurring orifice. This could allow the surgeon to overcome some of the limitations encountered while working with rigid systems particularly in *LESS* surgery. Both animal model studies and subsequent patient trials have been reported using this technology while performing ureterorenoscopic procedures for stone disease.[33]

The development of small completely in vivo mini robots, termed "microrobots," has begun to show promise. These microrobots, like the flexible robotic platform or the MAGS system, can be introduced into the abdomen via either a natural orifice or a small single incision. Here, they have been used to perform small tasks such as biopsy[34] and cholecystectomy,[35] and have the potential for use in a large number of applications across many disciplines.

Purpose-built single port robots have yet to be developed. Once available, they may well allow for the dissemination of *LESS* technology beyond a few, highly skilled academic centers. They would allow for the use of articulating instruments in a manner that would prevent inadvertent instrument collision and provide larger ranges of motion in the *LESS* setting than is currently available.

Novel Approaches

LESS surgery has, so far, been primarily applied to standard laparoscopic procedures within a carbon dioxide pneumoperitoneum. With the development of newer access devices has come the proposal for the use of novel approaches. In the conventional and robotic-assisted laparoscopic literature, transvesical procedures including simple and radical prostatectomy[36] as well as ureteral reimplantation[37] have been performed. These cases have typically been prohibitively complex, in large part, owing to the need for several entry points into the bladder. In hopes of simplifying the access to the bladder for these cases, Desai et al described a single-port transvesical enucleation of the prostate procedure using *LESS* techniques. In this procedure, a pneumovesicum is created to take advantage of the potential working space within the bladder while avoiding entry into the peritoneal cavity.[28] Such transluminal surgery has been made possible by the development of new single-incision access devices.

Future Directions

The development of groups such as the Urologic NOTES working groups and the LESSCAR consortium has secured the future of *LESS* surgery as one that will be both well documented and promoted. The LESSCAR consortium has not only helped to develop and disseminate a common nomenclature to assist in the coordination and monitoring of clinical data as they become available, but has also proposed the creation of a *LESS* registry to promote the same ends. With such a registry, a central source would be equipped to design and oversee the development and execution of prospective randomized trials needed to determine the effectiveness and potential benefits of such new techniques.

With the formation of such these organizations, leaders in the field are in a position to formulate teaching platforms and curricula to allow for the safe and efficacious propagation of the techniques within the surgical community. By doing so, they will provide a critical service to the success of *LESS* surgery, which may be mimicked by other newly developing techniques across medical disciplines.

References

1. Wheeless CR Jr. An inexpensive laparoscopy system for female sterilization. *Am J Obstet Gynecol.* 1975;123(7):727–733
2. Buess G, Kipfmuller K, Hack D, Grussner R, Heintz A, Junginger T. Technique of transanal endoscopic microsurgery. *Surg Endosc.* 1988;2(2):71–75
3. Mehta PV. Laparoscopic sterilizations (16,803) without vaginal manipulation. *Int J Gynaecol Obstet.* 1982;20(4):323–325
4. Junker H. [Laparoscopic tubal ligation by the single puncture technique (author's transl)]. *Geburtshilfe Frauenheilkd.* 1974;34(11): 952–955
5. Milliken I, Fitzpatrick M, Subramaniam R. Single-port laparoscopic insertion of peritoneal dialysis catheters in children. *J Pediatr Urol.* 2006;2(4):308–311
6. Hirano D, Minei S, Yamaguchi K, et al Retroperitoneoscopic adrenalectomy for adrenal tumors via a single large port. *J Endourol.* 2005;19(7):788–792
7. Canes D, Desai MM, Aron M, et al Transumbilical single-port surgery: evolution and current status. *Eur Urol.* 2008;54(5):1020–1029
8. Rao GV, Reddy DN, Banerjee R. NOTES: human experience. *Gastrointest Endosc Clin N Am.* 2008;18(2):361–370
9. Gettman MT, Lotan Y, Napper CA, Cadeddu JA. Transvaginal laparoscopic nephrectomy: development and feasibility in the porcine model. *Urology.* 2002;59(3):446–450
10. Clayman RV, Box GN, Abraham JB, et al Rapid communication: transvaginal single-port NOTES nephrectomy: initial laboratory experience. *J Endourol.* 2007;21(6):640–644
11. Raman JD, Bensalah K, Bagrodia A, Stern JM, Cadeddu JA. Laboratory and clinical development of single keyhole umbilical nephrectomy. *Urology.* 2007;70(6):1039–1042
12. Irwin BH, Rao P, Stein RJ, et al Laparoendoscopic single site surgery in urology. *Urol Clin North Am.* 2009;36:223–235
13. Box G, Averch T, Cadeddu J, et al Nomenclature of natural orifice translumenal endoscopic surgery (NOTES) and laparoendoscopic single-site surgery (LESS) procedures in urology. *J Endourol.* 2008; 22(11):2575–2581
14. Raman JD, Bagrodia A, Cadeddu JA. Single-incision, umbilical laparoscopic versus conventional laparoscopic nephrectomy: a comparison of perioperative outcomes and short-term measures of convalescence. *Eur Urol.* 2008;55:1198–1204
15. Tracy CR, Raman JD, Cadeddu JA, Rane A. Laparoendoscopic single-site surgery in urology: where have we been and where are we heading? *Nat Clin Pract Urol.* 2008;5(10):561–568
16. Ponsky LE, Cherullo EE, Sawyer M, Hartke D. Single access site laparoscopic radical nephrectomy: initial clinical experience. *J Endourol.* 2008;22(4):663–666
17. Desai MM, Rao PP, Aron M, et al Scarless single port transumbilical nephrectomy and pyeloplasty: first clinical report. *BJU Int.* 2008;101(1):83–88
18. Rane A, Rao P, Rao P. Single-port-access nephrectomy and other laparoscopic urologic procedures using a novel laparoscopic port (R-port). *Urology.* 2008;72(2):260–263
19. Kaouk JH, Haber GP, Goel RK, et al Single-port laparoscopic surgery in urology: initial experience. *Urology.* 2008;71(1):3–6
20. Raman JD, Cadeddu JA, Rao P, Rane A. Single-incision laparoscopic surgery: initial urological experience and comparison with natural-orifice transluminal endoscopic surgery. *BJU Int.* 2008; 101(12):1493–1496
21. Park S, Bergs RA, Eberhart R, Baker L, Fernandez R, Cadeddu JA. Trocar-less instrumentation for laparoscopy: magnetic positioning of intra-abdominal camera and retractor. *Ann Surg.* 2007;245(3):379–384
22. Zeltser IS, Bergs R, Fernandez R, Baker L, Eberhart R, Cadeddu JA. Single trocar laparoscopic nephrectomy using magnetic anchoring and guidance system in the porcine model. *J Urol.* 2007;178(1): 288–291
23. Gill IS, Canes D, Aron M, et al Single port transumbilical (E-NOTES) donor nephrectomy. *J Urol.* 2008;180(2):637–641
24. Goel RK, Kaouk JH. Single port access renal cryoablation (SPARC): a new approach. *Eur Urol.* 2008;53(6):1204–1209
25. Aron M, Canes D, Desai MM, Haber GP, Kaouk JH, Gill IS. Transumbilical single-port laparoscopic partial nephrectomy. *BJU Int.* 2008;103:516–521

26. Kaouk JH, Goel RK. Single-port laparoscopic and robotic partial nephrectomy. *Eur Urol.* 2009;55(5):1163–9
27. Desai MM, Stein R, Rao P, et al Embryonic natural orifice transumbilical endoscopic surgery (E-NOTES) for advanced reconstruction: initial experience. *Urology.* 2009;73(1):182–187
28. Desai MM, Aron M, Canes D, et al Single-port transvesical simple prostatectomy: initial clinical report. *Urology.* 2008;72(5):960–965
29. Kaouk JH, Palmer JS. Single-port laparoscopic surgery: initial experience in children for varicocelectomy. *BJU Int.* 2008;102(1): 97–99
30. Kaouk JH, Goel RK, Haber GP, Crouzet S, Desai MM, Gill IS. Single-port laparoscopic radical prostatectomy. *Urology.* 2008; 72(6):1190–1193
31. Barret E, Sanchez-Salas R, Kasraeian A, et al A transition to laparoendoscopic single-site surgery (LESS) radical prostatectomy: human cadaver experimental and initial clinical experience. *J Endourol.* 2009;23:135–140
32. Kaouk JH, Goel RK, Haber GP, Crouzet S, Stein RJ. Robotic single-port transumbilical surgery in humans: initial report. *BJU Int.* 2008;103:366–369
33. Desai MM, Aron M, Gill IS, et al Flexible robotic retrograde renoscopy: description of novel robotic device and preliminary laboratory experience. *Urology.* 2008;72(1):42–46
34. Rentschler ME, Dumpert J, Platt SR, Farritor SM, Oleynikov D. Mobile in vivo biopsy and camera robot. *Stud Health Technol Inform.* 2006;119:449–454
35. Lehman AC, Dumpert J, Wood NA, et al Natural orifice cholecystectomy using a miniature robot. *Surg Endosc.* 2009;23(2):260–266
36. Desai MM, Aron M, Berger A, et al Transvesical robotic radical prostatectomy. *BJU Int.* 2008;102(11):1666–1669
37. Gill IS, Ponsky LE, Desai M, Kay R, Ross JH. Laparoscopic cross-trigonal Cohen ureteroneocystostomy: novel technique. *J Urol.* 2001;166(5):1811–1814

Notes

24

D. Nageshwar Reddy, G. V. Rao, and M. J. Mansard

Introduction

Surgery has been rapidly evolving in the past few decades as new technologies are being adopted. Abdominal surgery has traditionally been performed through large incisions into the peritoneal cavity. In the past decade, traditional open surgery has been increasingly replaced by minimally invasive laparoscopic and robotic techniques. As a result, patient outcomes have improved, with faster recovery from smaller incisions. On the other hand, the field of gastrointestinal endoscopy has also been witnessing major advances. Developing from flexible endoscopy to endoscopic retrograde cholangiopancreatography (ERCP) in the 1950s and 1970s to endoscopic ultrasound in the 1980s, endoscopic technology has been transformed from serving purely diagnostic purposes to therapeutic applications.

Some investigators, amalgamating their experiences from the fields of minimal access laparoscopic surgery and of flexible gastrointestinal endoscopy, have proposed the concept of operating in the peritoneal space through natural orifices, such as the mouth, anus, vagina, and bladder. This transluminal approach offers "scarless surgery." There is no abdominal wall incision, and the complications of wound infections, hernias, adhesions, or dehiscence are eliminated. Natural orifice transluminal endoscopic surgery (NOTES) is potentially the next paradigm shift in minimally invasive surgery. It offers the exciting potential to be safer, less invasive, and possibly more cost-effective than the traditional open surgical or laparoscopic approach.

History

Kalloo et al are credited with the fist description of the NOTES procedure in 2000, in which they demonstrated the feasibility and safety of a per-oral transgastric endoscopic approach to the peritoneal cavity with long-term survival in a porcine model. Their published description came out in 2004.[1] Since then, several investigators have pursued NOTES study in animal survival and nonsurvival models, and there has been a surge in the number of different procedures performed with NOTES being reported at national meetings and published in the literature. Initial reports dealt with diagnostic procedures including endoscopic peritoneoscopy, liver biopsy, lymphadenectomy, and abdominal exploration. This was followed by a variety of successful transluminal procedures including oophorectomy, partial hysterectomy, transgastric jejunostomy, and gastrojejunostomy in both survival and nonsurvival porcine models.[2]

To discuss this novel approach, 14 leaders from the American Society of Gastrointestinal Endoscopy (ASGE) and the Society of American Gastrointestinal and Endoscopic Surgeons (SAGES) met in New York City in July 2005.[3] This group published its deliberations as the NOTES Working Group White Paper.[4] The White Paper delineated the anticipated technical barriers to further development of NOTES, emphasized the need for development to be carried out by interdisciplinary teams of surgeons and gastroenterologists and emphasized that any human procedures be performed only with institutional review board (IRB) approval. Subsequently, the first international conference on NOTES was held in Scottsdale, Arizona, in March 2006.

Research in the western part of the world was confined to animal models. The first human experience was gained by Drs. Rao and Reddy from India who presented their series of seven transgastric human appendectomies with good results.[1–5] Today, human NOTES is already being reported from numerous centers, and the results appear promising. The first clinical series of transgastric peritoneoscopy has recently been published;[6] multiple groups are accumulating patients in studies of NOTES cholecystectomy, either via the transgastric or transvaginal route.[7, 8] Cadaveric studies showed the feasibility and safety of performing advanced procedures through NOTES in humans.[9] As expected, there are teething issues, generating vigorous debates from the skeptics and the cautious.

Transgastric NOTES

The peroral transgastric route was chosen to access the peritoneal cavity in initial trials because of a potentially lower risk for surrounding organ injury using the anterior wall of

P. Dasgupta et al. (eds.), *New Technologies in Urology,*
DOI: 10.1007/978-1-84882-178-1_24, © Springer-Verlag London Limited 2010

the stomach.[5] Also, the gastric flora is less contaminating to the peritoneal cavity when compared to the other available natural orifices. It has been shown by a recent study that transgastric instrumentation does contaminate the abdominal cavity, but the pathogens do not mount a clinically significant response in terms of either the species or the bacterial load. Techniques commonly used to reduce the bacterial load are: preoperative overnight fasting, antibiotic lavage of the stomach, perioperative intravenous antibiotic cover, and using sterile overtube through the gastrotomy. The least vascular area, midway between the vascular arcades lying along the greater and lesser curvatures of the stomach, is chosen. The port is placed in the proximal body of the stomach for lower abdominal procedures such as appendectomy. A similar site in the antrum, midway between the arcades, is chosen for upper abdominal procedures such as cholecystectomy. A standard wire-guided needle knife, using blended current, is used to create a stab gastrotomy at the selected site. Adequate pneumoperitoneum is created through this stab, which is further enlarged using a balloon or a sphincterotome for passage of the double-channel endoscope. The most important issue in NOTES that is hotly debated and is an area of active research is the safe closure of the gastric access.[1] Devices ranging from endoscopic clips to stapling devices have been used with considerable success in both animal and human studies.

Transvaginal and Transanal NOTES

The transvaginal route was used to obviate the disadvantages of operating with a retroflexed scope when performing a cholecystectomy.[11] The transvaginal route provides a more direct view of the organs of interest for liver biopsies and cholecystectomies. A triangular area between the uterosacral ligaments, which is avascular without innervations, is chosen for the port placement. The difficulties of port closure are also averted as the port can be hand-sewn under vision. The transvaginal route has also been used to extract laparoscopically divided specimens, in a modification of the hybrid procedure (discussed later).[12] Potential ill-effects of this route from the gynecological point of view are formation of adhesions, spread of preexisting endometriosis, infertility, and dyspareunia.[13]

The transanal route was introduced subsequently to overcome the gender hurdle posed by the transvaginal route. Experience with transanal endoscopic microsurgery instrumentation has been transferred to performance of NOTES procedures.[14] The rectal port of entry allows rigid laparoscopic instruments to be introduced into the peritoneal cavity and enables performance of gastrointestinal procedures the same as in standard laparoscopic surgery. However, extra-long instruments are necessary for dissection from the pelvis. The potential disadvantages of the transanal route are also significant and include issues of sterility, the risk of inadvertent trauma to adjacent organs during transmural puncture, and the risk of colonic wall shearing.[15]

Transesophageal NOTES

Thoracoscopy and mediastinoscopy have been performed in animal models transesophageally.[16] The self-approximating transluminal access technique (STAT) was used to enter the mediastinum. The submucosal tunnel creates a flap-valve that, alone, may be sufficient for preventing esophageal leak. The technique provided excellent visualization of mediastinal and intrathoracic structures. Pleural biopsy could be easily obtained under direct visualization. Structures that are difficult to visualize via traditional cervical mediastinoscopy and thoracoscopy were seen well with this approach. A complete Heller's myotomy of the gastroesophageal junction has also been performed with this approach without complication.[17]

Transumbilical NOTES

In this technique, a single port is introduced through the umbilicus. Operating instruments, flexible or rigid, are passed through the multiple channels available in this port. At the end of the procedure, the scars are hidden inside the umbilicus, thus achieving the "scarless" status. This technique has been termed "single-port NOTES."[18] Since the umbilicus is an embryonical (E) natural orifice, the term E-Notes has also been used.[19] NOTUS (natural orifice transumbilical surgery),[20] SILS (single-incision laparoscopic surgery),[21] and TUES (transumbilical endoscopic surgery)[22] are its other labels. Single-port sleeve gastrectomy,[23] donor nephrectomy, right hemicolectomy, bilateral single-session Anderson-Hynes pyeloplasty, ileal ureter, and ureteroneocystostomy with a psoas hitch[24] have all been shown to be feasible and safe when performed by experienced laparoscopic surgeons.

The Hybrid Technique

Some of the major issues that need to be addressed in NOTES are blindly performed primary incisions, and uncontrolled pneumoperitoneal pressure, no support for the endoscope in the abdominal cavity, inadequate vision, insufficient illumination, limited retraction and exposure, and the complexity of suturing and performing a safe anastomosis. All these

could be overcome by using the hybrid technique.[25] It combines laparoscopy and natural orifice surgery techniques. Transgastric/transvaginal procedures are performed with guidance from another instrument introduced through a laparoscopic port. The hybrid technique offers a superior vision source independent of the working endoscope. The initial puncture and incision can be done safely under laparoscopic observation, thereby avoiding injury to adjacent organs.

While some groups used only a needlescope via the percutaneous route,[26] others have used instruments via the laparoscopic port for retraction,[27] and sometimes even as another working port.[28] Hybrid-NOTES could be an ideal first step before the introduction of "pure" NOTES into clinical practice. Thus far, hybrid procedures have validated the safety of many natural orifice procedures in humans. Human hybrid transvaginal and transgastric peritoneoscopies,[26] cholecystectomies,[27] nephrectomy,[29] and sigmoidectomy[30] have already been reported. Natural orifice (transvaginal or transanal) extraction of laparoscopically dissected specimen is also described as a modification of hybrid notes.

Another variant of the hybrid technique is the "dual lumen" technique.[31] Simultaneous use of transgastric and transvaginal routes provide the same advantages of the hybrid technique while avoiding an external scar. It has also been described as the "rendezvous" technique. Distal pancreatectomy[32] and small bowel resection and anastomosis[31] have been done safely using this variant technique of Hybrid NOTES.

EUS-Guided NOTES

Entering the peritoneal cavity with the echoendoscope has been avoided because this endoscope is rather rigid and difficult to handle and maneuver in a limited space. However, EUS has been used to guide NOTES procedures. Blind NOTES access through the antrum, posterior stomach wall, and rectum could result in catastrophic complications. EUS-guided access through these sites has been shown to substantially reduce this risk.[33] EUS appears promising as an adjunct to NOTES access, particularly as more experience is gained in definitively excluding the presence of at-risk extraluminal structures.[33]

R-NOTES (Robotic Natural Orifice Transluminal Surgery)

Over the past decade, robots have been appearing in the operating room and in the endoscopic suite. It will be no wonder if they will soon have a defined role in NOTES. Using the da Vinci surgical system and accessing the peritoneal cavity through a single-port pyeloplasties, partial nephrectomies and radical nephrectomies have been performed with ease and safety in porcine models.[34] Intracorporeal suturing is significantly enhanced using the robot, especially through the challenging transluminal natural orifice approach. A two-armed dexterous miniature in vivo robot with stereoscopic vision capabilities has successfully demonstrated various capabilities in a nonsurvival natural orifice surgical procedure in a porcine model.[35] The design and kinematic configuration of the robot allows for its complete insertion into the peritoneal cavity and provides intuitive visualization and sufficient force application for tissue manipulation within the dexterous workspace. Further development of robots adaptive to NOTES would boost efforts toward clinical NOTES applications.

Training

The fundamental skill set necessary to perform NOTES includes both minimally invasive surgical skills and endoscopic skills. While the latter is required for appropriate employment of the instrument, the former is required for recognition of anatomy and orientation inside the peritoneal cavity. Hence, the ASGE/SAGES working group had recommended the establishment of multidisciplinary team possessing advanced therapeutic endoscopic and advanced laparoscopic skills to study NOTES.[3] Animal laboratory facilities to perform research and training should be available to the multidisciplinary team for exploration of NOTES techniques and procedures. IRB approval must be obtained before introduction of NOTES procedures in human patients. Some institutions are developing training programs for digestivists incorporating both surgical and gastroenterologic training.[36] A steep learning curve has been reported from one such training program, despite the presence of an investigator with experience in NOTES.

NOTES and Urology

Urologists of the present era possessing both minimally invasive surgical skills and endoscopic skills are ideal candidates to take up the mantle of NOTES specialists. The first experimental application of NOTES in urology was published in 2002 when transvaginal nephrectomy was performed in the porcine model. Confirmatory experimental studies using the gastrointestinal tract for NOTES were first published in 2004.[37] Gettman et al in 2006 described the initial clinical case in which they evaluated the bladder as a portal for NOTES.[38] Subsequently, NOTES has been used to perform

urological procedures in humans starting from transvesical peritoneoscopy to transvaginal donor nephrectomy[39] safely and effectively.

Benefits of NOTES

There are many potential advantages of NOTES over conventional surgery. Much like laparoscopy has demonstrated less physiologic impact than laparotomy, NOTES may cause less physiologic insult than either laparoscopy or laparotomy. Absence of scar has obvious advantages.[3] There is the lack of common complications of conventional surgery such as wound infections and incisional hernia. It may probably reduce the formation of intraabdominal adhesions.[40]

Given the portability of NOTES equipment, NOTES might shift the surgeon from the operating theater to the patient's bedside. Major interventional procedures might be carried out in the future in an intensive care unit (ICU) setting. Moving the equipment to the patient, rather than vice versa, might reduce the resource requirements and potential complications of transporting a patient to the operating room. Moreover, NOTES could be performed under conscious sedation, rather than general anesthesia, again favoring ICU-based procedures.

NOTES offers specific advantages to select population of patients. Patients with no percutaneous access, as in the patient with abdominal wall burns who underwent the first NOTES appendectomy, will derive special benefits from NOTES.[5] Another group is the morbidly obese, who will benefit greatly from NOTES, when done with minimal anesthesia and rapid postoperative convalescence.[41] Studies have already demonstrated the feasibility of obesity surgeries, such as sleeve gastrectomy, by NOTES.[42]

The interest in NOTES has motivated lot of research among the major makers of laparoscopic and endoscopic instruments. Current and future endoscopists and lapraoscopists will reap the benefit of this research, because many techniques and devices that are developed for NOTES will be also put to use in conventional procedures.

Lastly are the cosmetic benefits of NOTES. It has been shown that young people would prefer to undergo a scarless experimental procedure than a well-established conventional procedure even after being educated about the risks involved.[43]

Challenges

NOTES being a new technique requires refinement before it can be employed in daily clinical practice. It has its fair share of skeptics, faces various technical and intellectual challenges, and several key issues need to be addressed.

Infection of the peritoneal cavity by organisms carried in by the scope from the orifices has been an obvious area of concern. Extensive surgical experience with bacteriologic contamination of the peritoneum during bowel surgery shows that if gross spillage is avoided and appropriate antibiotic cover is provided, the contamination is well tolerated. A recent study has shown that transgastric instrumentation does contaminate the abdominal cavity, but the pathogens do not mount a clinically significant response in terms of either the species or the bacterial load.[44] On the other hand, NOTES transgastric ventral hernia repair was found to have a high infection rate, despite adequate antibiotic precautions.[45] Introduction of new organisms that are commensals of the mouth, anus, or the vagina into the peritoneal cavity is another important issue.

Reliable closure of the transgastric defect remains a key component for advancement of NOTES into clinical practice.[46] Peritonitis in even a minor percentage is unacceptable, considering the safety of laparoscopy in this regard. Endoscopic sutures and clips have been used in the earlier reports. T tags have been used for transluminal colonic defects closure with considerable success in the animal model. Today, various stapling devices, including the NDO Plicator,[47] originally designed for endoscopis plication for GERD, the endoscopic tissue plicating devices (TPD),[48] and the automated flexible stapling device (SurgASSIST)[49] among many others, have been evaluated and safety proved in various studies. Fluid- and air-leak tests are simple techniques that can be used to evaluate in vivo the adequacy of the transluminal access site closure after NOTES procedures.[50]

Triangulation, tissue retraction, and apposition are the fundamental principles in any laparoscopic procedure. The current endoscopes, however, have limited ability to manipulate the intraabdominal organs. There is a fixed parallel orientation of the view and instrument axes, reducing the ability for three-dimensional assessment. They have insufficient angulation, tolerate very little push force, and have a very narrow accessory channel. NOTES tools that are being developed are expected to address these issues soon.[51]

Working off the axis of the camera angle (i.e., off axis) as is routine in laparoscopic surgery is a problem surmountable with practice and a little mental exercise when rigid scopes are used.[52] However, when flexible scopes are used in NOTES, the off-axis view results in spatial incongruity, requiring severe mental strain. This will prevent complex procedures from being performed with the speed and facility that in-line visualization would allow. Potential solutions include the use of multiple cameras to achieve the appropriate inline view of the working area[53] and the use of computer interface (live video manipulator)[54] between the video feed and the actual image of the end organ, which automatically adjusts the axis of the camera angle with every deviation.

To date, the advantages of NOTES have been only theoretical. No study has so far shown scientific evidence of the proposed benefits of a scarless surgery. For wider acceptance of this technique in the scientific community, trials comparing NOTES to conventional surgery need to be undertaken.

Pursuit of NOTES in any institute requires animal lab facilities and procurement of advanced tools and devices that incur huge costs. However, when NOTES gains general acceptance, the actual expenditures might be outweighed by decreased consequential costs.[55]

Conclusion

New innovations come to the fore by breaking down older borders in an intelligent fashion. When the flexible endoscope was taken beyond the gastrointestinal lumen into what lies beyond the confines of the gastrointestinal tract, skeptics called it blasphemous. However, continued collaboration between the gastrointestinal endoscopists and minimally invasive surgeons has resulted in the burgeoning growth of NOTES that it now represents a paradigm shift in surgery.

While NOTES may represent a new era in surgery, it is still largely an experimental field. Although clinical NOTES is gaining momentum, the field should remain in check while rigorous laboratory work is performed and cogent clinical trials are undertaken. The zeal for NOTES should not take precedence over the welfare of the patient. Well-managed human studies need to be conducted to determine the safety and efficacy of NOTES in a clinical setting. Although many limitations need to be surmounted before NOTES can reach the human clinical trial stage, the prospect of safe, minimally invasive, and scarless surgery appears very promising. The near future will tell whether current barriers will be broken down and NOTES will acquire a fixed place in the diagnosis and therapy of maladies in humans.

References

1. Giday SA, Kantsevoy SV, Kalloo AN. Principle and history of Natural Orifice Translumenal Endoscopic Surgery (NOTES). *Minim Invasive Ther Allied Technol*. 2006;15(6):373–377
2. de la Fuente SG, Demaria EJ, Reynolds JD, Portenier DD, Pryor AD. New developments in surgery: Natural Orifice Transluminal Endoscopic Surgery (NOTES). *Arch Surg*. 2007;142(3):295–297
3. Rattner D, Kalloo A. ASGE/SAGES Working Group. ASGE/SAGES Working Group on Natural Orifice Translumenal Endoscopic Surgery. October 2005. *Surg Endosc*. 2006;20(2): 329–333
4. Bowman D. ASGE/SAGES Working Group on Natural Orifice Translumenal Endoscopic Surgery White Paper October 2005. *Gastrointest Endosc*. 2006;63(2):199–203
5. Rao GV, Reddy DN, Banerjee R. NOTES: human experience. *Gastrointest Endosc Clin N Am*. 2008;18(2):361–70; x
6. Hazey JW, Narula VK, Renton DB, Melvin WS, et al Natural-orifice transgastric endoscopic peritoneoscopy in humans: initial clinical trial. *Surg Endosc*. 2008;22(1):16–20
7. Marescaux J, Dallemagne B, Perretta S, Wattiez A, Mutter D, Coumaros D. Surgery without scars: report of transluminal cholecystectomy in a human being. *Arch Surg*. 2007;142(9):823–826; discussion 826–827
8. Zorrón R, Filgueiras M, Maggioni LC, Pombo L, Lopes Carvalho G, Lacerda Oliveira A. NOTES.Transvaginal cholecystectomy: report of the first case. *Surg Innov*. 2007;14(4):279–283
9. Can S, Fiolka A, Wilhelm D, et al Set of instruments for innovative, safe and sterile sigmoid access for natural-orifice transluminal endoscopic surgery. *Biomed Tech (Berl)*. 2008;53(4):185–189
10. Forgione A, Maggioni D, Sansonna F, et al Transvaginal endoscopic cholecystectomy in human beings: preliminary results. *J Laparoendosc Adv Surg Tech A*. 2008;18(3):345–351
11. Franklin ME Jr, Kelley H, Kelley M. Brestan L, Portillo G, Torres J. Transvaginal extraction of the specimen after total laparoscopic right hemicolectomy with intracorporeal anastomosis. *Surg Laparosc Endosc Percutan Tech*. 2008;18(3):294–298
12. Thele F, Zygmunt M, Glitsch A, Heidecke CD, Schreiber A. How do gynecologists feel about transvaginal NOTES surgery? *Endoscopy*. 2008;40(7):576–580
13. Sylla P, Willingham FF, Sohn DK, Gee D, Brugge WR, Rattner DW. NOTES rectosigmoid resection using transanal endoscopic microsurgery (TEM) with transgastric endoscopic assistance: a pilot study in swine. *J Gastrointest Surg*. 2008;12(10):1717–1723. Epub 2008 Aug 13
14. Whiteford MH, Spaun GO. A colorectal surgeons viewpoint on natural orifice translumenal endoscopic surgery. *Minerva Chir*. 2008;63(5):385–388
15. Gee DW, Willingham FF, Lauwers GY, Brugge WR, Rattner DW. Natural orifice transesophageal mediastinoscopy and thoracoscopy: a survival series in swine. *Surg Endosc*. 2008;22(10):2117–2122
16. Pauli EM, Mathew A, Haluck RS, et al Technique for transesophageal endoscopic cardiomyotomy (Heller myotomy): video presentation at the Society of American Gastrointestinal and Endoscopic Surgeons (SAGES) 2008, Philadelphia, PA. *Surg Endosc*. 2008;22(10):2279–2280
17. Canes D, Desai MM, Aron M, et al Transumbilical single-port surgery: evolution and current status. *Eur Urol*. 2008;54(5):1020–1029
18. Gill IS, Canes D, Aron M, et al Single port transumbilical (E-NOTES) donor nephrectomy. *J Urol*. 2008;180(2):637–641; discussion 641. Epub 2008 Jun 12
19. Nguyen NT, Reavis KM, Hinojosa MW, Smith BR, Wilson SE. Laparoscopic transumbilical cholecystectomy without visible abdominal scars. *J Gastrointest Surg*. 2009;13(6):1125–1128
20. Raman JD, Cadeddu JA, Rao P, Rane A. Single-incision laparoscopic surgery: initial urological experience and comparison with natural-orifice transluminal endoscopic surgery. *BJU Int*. 2008;101(12):1493–1496
21. Zhu JF, Hu H, Ma YZ, Xu MZ, Li F. Transumbilical endoscopic surgery: a preliminary clinical report. *Surg Endosc*. 2009;23(4):813–817
22. Nguyen NT, Reavis KM, Hinojosa MW, Smith BR, Wilson SE. Laparoscopic transumbilical sleeve gastrectomy without visible abdominal scars. *Surg Obes Relat Dis*. 2009;5(2):275–277
23. Desai MM, Stein R, Rao P, et al Embryonic Natural Orifice Transumbilical Endoscopic Surgery (E-NOTES) for Advanced Reconstruction: Initial Experience. *Urology*. 2009;73(1):182–187
24. Mintz Y, Horgan S, Cullen J, et al NOTES: the hybrid technique. *J Laparoendosc Adv Surg Tech A*. 2007;17(4):402–406
25. Pearl JP, Marks JM, Ponsky JL. Hybrid surgery: combined laparoscopy and natural orifice surgery. *Gastrointest Endosc Clin N Am*. 2008;18(2):325–332; ix

26. Palanivelu C, Rajan PS, Rangarajan M, Parthasarathi R, Senthilnathan P, Praveenraj P. Transumbilical flexible endoscopic cholecystectomy in humans: first feasibility study using a hybrid technique. *Endoscopy*. 2008;40(5):428–431
27. Auyang ED, Vaziri K, Volckmann E, Martin JA, Soper NJ, Hungness ES. NOTES: cadaveric rendezvous hybrid small bowel resection. *Surg Endosc*. 2008;22(10):2277–2278
28. Branco AW, Branco Filho AJ, Kondo W, et al Hybrid transvaginal nephrectomy. *Eur Urol*. 2008;53(6):1290–1294. Epub 2007 Nov 5
29. Leroy J, Cahill RA, Peretta S, Marescaux J. Single port sigmoidectomy in an experimental model with survival. *Surg Innov*. 2008; 15(4):260–265
30. Mintz Y, Horgan S, Cullen J, Falor E, Talamini MA. Dual-lumen natural orifice translumenal endoscopic surgery (NOTES): a new method for performing a safe anastomosis. *Surg Endosc*. 2008;22(2):348–351
31. Ryou M, Fong DG, Pai RD, Tavakkolizadeh A, Rattner DW, Thompson CC. Dual-port distal pancreatectomy using a prototype endoscope and endoscopic stapler: a natural orifice transluminal endoscopic surgery (NOTES) survival study in a porcine model. *Endoscopy*. 2007;39(10):881–887
32. Elmunzer BJ, Schomisch SJ, Trunzo JA, et al EUS in localizing safe alternate access sites for natural orifice transluminal endoscopic surgery: initial experience in a porcine model. *Gastrointest Endosc*. 2009;69:108–114
33. Fritscher-Ravens A. EUS-guided NOTES interventions. *Gastrointest Endosc Clin N Am*. 2008;18(2):297–314; ix.
34. Haber GP, Crouzet S, Kamoi K, et al Robotic NOTES (Natural Orifice Translumenal Endoscopic Surgery) in reconstructive urology: initial laboratory experience. *Urology*. 2008;71(6):996–1000
35. Lehman AC, Dumpert J, Wood NA, Visty AQ, Farritor SM, Oleynikov D. In vivo robotics for natural orifice transgastric peritoneoscopy. *Stud Health Technol Inform*. 2008;132:236–241
36. Kavic MS, Mirza B, Horne W, Moskowitz JB. NOTES: issues and technical details with introduction of NOTES into a small general surgery residency program. *JSLS*. 2008;12(1):37–45
37. Gettman MT, Cadeddu JA. Natural orifice translumenal endoscopic surgery (NOTES) in urology: initial experience. *J Endourol*. 2008;22(4):783–788
38. Gettman MT, Blute ML. Transvesical peritoneoscopy: initial clinical evaluation of the bladder as a portal for natural orifice translumenal endoscopic surgery. *Mayo Clin Proc*. 2007;82(7):843–845
39. Gill IS, Canes D, Aron M, et al Single port transumbilical (E-NOTES) donor nephrectomy. *J Urol*. 2008;180(2):637–641; discussion 641
40. Pham BV, Morgan K, Romagnuolo J, et al Pilot comparison of adhesion formation following colonic perforation and repair in a pig model using a transgastric, laparoscopic, or open surgical technique. *Endoscopy*. 2008;40(8):664–669
41. Fuchs KH, Breithaupt W. Natural orifice transluminal endoscopic surgery in future obesity treatment. *Chirurg*. 2008;79(9):837–842
42. Ramos AC, Zundel N, Neto MG, Maalouf M. Human hybrid NOTES transvaginal sleeve gastrectomy: initial experience. *Surg Obes Relat Dis*. 2008;4(5):660–663
43. Hagen ME, Wagner OJ, Christen D, Morel P. Cosmetic issues of abdominal surgery: results of an enquiry into possible grounds for a natural orifice transluminal endoscopic surgery (NOTES) approach. *Endoscopy*. 2008;40(7):581–583
44. Narula VK, Happel LC, Volt K, et al Transgastric endoscopic peritoneoscopy does not require decontamination of the stomach in humans. *Surg Endosc*. 2009;23(6):1331–1336
45. Buck L, Michalek J, Van Sickle K, Schwesinger W, Bingener J. Can gastric irrigation prevent infection during NOTES mesh placement? *J Gastrointest Surg*. 2008;12(11):2010–2014
46. Voermans RP, Worm AM, van Berge Henegouwen MI, Breedveld P, Bemelman WA, Fockens P. In vitro comparison and evaluation of seven gastric closure modalities for natural orifice transluminal endoscopic surgery (NOTES). *Endoscopy*. 2008;40(7):595–601
47. McGee MF, Marks JM, Onders RP, et al Complete endoscopic closure of gastrotomy after natural orifice translumenal endoscopic surgery using the NDO Plicator. *Surg Endosc*. 2008;22(1): 214–220
48. McGee MF, Marks JM, Jin J, et al Complete endoscopic closure of gastric defects using a full-thickness tissue plicating device. *J Gastrointest Surg*. 2008;12(1):38–45
49. Meireles OR, Kantsevoy SV, Assumpcao LR, et al Reliable gastric closure after natural orifice translumenal endoscopic surgery (NOTES) using a novel automated flexible stapling device. *Surg Endosc*. 2008;22(7):1609–1613
50. Dray X, Gabrielson KL, Buscaglia JM, et al Air and fluid leak tests after NOTES procedures: a pilot study in a live porcine model. *Gastrointest Endosc*. 2008;68(3):513–519
51. Swanstrom LL, Whiteford M, Khajanchee Y. Developing essential tools to enable transgastric surgery. *Surg Endosc*. 2008;22(3):600–604
52. Swanstrom L, Zheng B. Spatial orientation and off-axis challenges for NOTES. *Gastrointest Endosc Clin N Am*. 2008;18(2):315–324; ix
53. Reavis KM, Melvin WS. Advanced endoscopic technologies. *Surg Endosc*. 2008;22(6):1533–1546. Epub 2008 Apr 10
54. Tang SJ, Bergs R, Jazrawi SF, et al Live video manipulator for endoscopy and natural orifice transluminal endoscopic surgery (with videos). *Gastrointest Endosc*. 2008;68(3):559–564
55. Maffei M, Dumonceau JM. The future of "NOTES". *Rev Med Suisse*. 2008;4(169):1879–1881

Augmented Reality for Image-Guided Surgery in Urology

25

Osamu Ukimura, Masahiko Nakamoto, Yoshinobu Sato, Makoto Hashizume, Tsuneharu Miki, Mihir Desai, Monish Aron, and Inderbir S. Gill

Introduction

In conventional open surgery, intraoperative surgical planning was determined by unifying all the human senses, based on a combination of the surgeon's experience and intraoperative information, obtained, for example, from direct vision and tactile feedback. In order to update surgical planning during surgery, the surgeon has needed extensive imagination to combine the intraoperative anatomical information with preoperative 2-D images or with knowledge based on surgical experience. With the significant advantage of minimal invasiveness for the patients, emerging surgical techniques, such as endoscopic surgery, percutaneous intervention, or the extracorporeal approach, have increasingly become alternative therapeutics to the conventional open approach. However, these have distanced the surgeon from the real surgical field, diminishing his understanding through limited access. The emerging 3-D endoscope, the flexible endoscope, and robot arms have successfully compensated for some of the disadvantages during laparoscopic surgery. However, in the modern era of minimally invasive urology, the search for new technology has continued, to compensate for the diminished human understanding, to decrease the learning curve, or even to make the new approach superior to the conventional approach. Emerging computer-aided digital imaging technology provides a powerful new opportunity to obtain real-time 3-D visualization of the surgical fields, even beyond the surgical view, for the surgeon to have an idea of how to optimize the surgical approach and how to decrease surgical morbidity.

Computer-aided imaging technology gives logical information to improve presurgical planning, intraoperative guidance, or predictive surgical navigation, to increase the precision of the expert surgeon as well as to decrease the learning curve of the novice. Intraoperative navigation can lead the surgeon to reduce redundant surgical acts, thus decreasing surgical errors and shortening operating times.

Augmented Reality

Augmented reality (AR) is a novel computer technology for image-guided surgery to display 3-D computer graphics of the surgical space. These are synchronized geometrically and superimposed onto the real endoscopic surgical view, presenting 3-D information of the surgical target beyond the real surgical view. The advantage of this technology is to allow real-time 3-D visualization of the surgical anatomy beyond the endoscopic vision, which it has never been possible to obtain by the human senses alone. It can combine any intraoperatively or preoperatively acquired imaging (including US, CT, MRI, functional MRI, PET, or scintigraphy) and pathological data, and reconstruct them into 3-D computer graphics for surgical navigation.[1–4]

The AR technology system consists of a computer workstation, a tracking system, an imaging modality, an endoscope, and a display system. In this system, since the angle and direction of the endoscope is tracked in real time by a special sensor (such as an optical or magnetic sensor), the 3-D space of the reconstructed 3-D image can be accurately synchronized with the 3-D space of the endoscopic surgical field.

AR and earlier computer-aided techniques have been implemented most prominently in neurosurgery, facilitated by the fact that the brain exists in a relatively fixed space surrounded by a bony reference.[5–7] Because AR images cannot yet be projected in real time, using AR for other surgical specialties is difficult, since most human organs are not rigid, but deform according to the rhythms of heartbeat and respiration, the air pressure of laparoscopic instillation, the progression of the surgery, or when physically probed. Despite these difficulties, AR methods are gaining increasing recognition in multiple fields of surgery, especially in minimally invasive surgery. We believe that the prostate is an attractive target for AR-assisted surgery, because it is a relatively fixed organ on the anterior surface of the rectal wall in the pelvis, which is at the bottom of the abdominal cavity, and dislocations by the rhythms of heartbeat and respiration are minimal compared to other intraabdominal organs. While the kidney may suffer dislocation due to the rhythms of heartbeat and/or respiration, we believe it is also an attractive target for AR-assisted surgery, because it is a relatively fixed organ, in which the 3-D anatomical information of the tumor location and the major vasculature in preoperative CT will provide significant information to help the surgeon.

P. Dasgupta et al. (eds.), *New Technologies in Urology,*
DOI: 10.1007/978-1-84882-178-1_25, © Springer-Verlag London Limited 2010

Recently, a case report of augmented-reality-assisted laparoscopic adrenalectomy was described, using a preoperative CT image.[8] Although the feasibility of using AR was reported, the absolute role and indications for AR in surgery have not yet been established. The outcomes discussed in most published reports to date have included user-friendly features, the accuracy of targeting tissues, and favorable cost as end points. The current limitations of AR systems are related to concerns about feasibility, accuracy, and underappreciation of device sophistication. Existing opinions are that experienced surgeons may benefit from such systems by extending the limits of the safe area to allow for more complete and radical operative therapy, while less experienced surgeons may benefit by more rapidly getting oriented to critical anatomic landmarks.

Initiation of Image-Guided Surgery in Urology

In a contemporary series of studies of localized prostate cancer (clinical T1-T2 disease) treated by radical prostatectomy (RP), pathological extracapsular extension of the cancer (pT3 disease), which has been associated with poor prognosis,[9–10] was reported in 21% to 46% of patients.[11–13] Another occurrence that is likely to increase the risk of cancer positive surgical margins is iatrogenic prostate capsulotomy by the surgeon contending with the cancer in the intricate pelvic anatomy. Since most prostate cancers arise in the peripheral zone close to the capsular margin, generally only minimal normal soft tissue surrounds the cancer nodule. Attempts to achieve wide surgical margins during RP may risk damage to the neurovascular bundle (NVB) or the urethral sphincter. In nerve-sparing RP, the risk of capsulotomy is especially high in the regions of the right and left NVBs, which lie close to the posterolateral surface of the prostate capsule.

Given the difficulties in avoiding capsulotomy during RP while sparing the NVB and urethral sphincter, and the associations of positive surgical margins and the extracapsular extension of prostate cancer with adverse prognosis, it would be of considerable benefit to provide accurate real-time intraoperative information about the location and extent of the cancer in relation to the surrounding tissues. Such information could also help the laparoscopic surgeon overcome the muted tactile feedback during laparoscopic RP (LRP).

Traditionally, during open surgery, surgeons have relied on surgical vision and the palpation of structures in the surgical field, together with surgical planning based on preoperative imaging studies. During surgery, the required abstract assembly of both pre and intraoperative information within the surgeon's brain is suboptimal and can potentially be improved upon. More importantly, the concerned anatomy of the surgical fields continually changes during RP from the preoperative anatomy, because of the progression of the surgical procedures, underscoring the need for a real-time intraoperative imaging modality to assist the surgery.

We recently developed a novel real-time intraoperative TRUS-guided technique of LRP, with energy-free release of the NVBs.[14–16] Intraoperative TRUS is capable of imaging the prostate contour anatomy and a substantial percentage of nonpalpable prostate cancers, as well as periprostatic anatomy such as the course, dimensions, and vascularity of the NVBs. Currently, about 40% of patients undergoing LRP for localized prostate cancer have hypoechoic cancer nodules detectable by TRUS. Intraoperative TRUS monitoring during LRP allows individualized, precise dissection tailored to the specific prostate contour anatomy, thus compensating for the muted tactile feedback of laparoscopy. In our initial experience, real-time TRUS guidance significantly decreased the incidence of positive surgical margins during LRP.

As we described in those recent reports, real-time intraoperative TRUS guidance has been effective in overcoming the disadvantage of muted tactile feedback during minimally invasive LRP. However, the use of that technique with LRP remains limited by the difficulty of mentally synchronizing (registering) the TRUS image on a video screen other than the live video monitor of the laparoscopic surgery. An ideal situation would be to precisely determine the locations in three dimensions of the prostate, prostate cancer, NVBs, and other relevant pelvic tissues, and superimpose 3-D images of those tissues onto the intraoperative laparoscopic view of the surgery, which could then guide appropriate modification of surgical resection. An adaptation of our AR technology has made that possible, and the success of real-time intraoperative TRUS guidance of LRP makes it ideal to provide the images for that next important step of computer-aided image-guided surgery.[17]

Devices and Techniques for the AR System

The AR system includes a workstation (computer and software), a tracking system (sensor and marker), an imaging modality (such as a US probe), an endoscope, and a display system (Fig. 25.1). Essential steps of AR technology include the abilities (1) to calibrate the instruments, (2) to segment the region of interest in imaging and to construct a 3-D virtual model of it, (3) to track laparoscope and surgical instruments in real time, to synchronize the 3-D virtual model fused with the real surgical display, and (4) to register the 3-D space of the model onto the real patient's 3-D surgical space, while minimizing organ movement during progress of the surgery.

The AR System in Operation Room

Figures 25.1 and 25.2 show how our AR system will be arranged in the operating room for use during TRUS-guided LRP. For a generation of AR images during LRP, we have used a Passive Polaris® optical position sensor (Northern Digital Inc., Waterloo, Ontario, Canada) (Fig. 25.1) with the TRUS probe, a laparoscope, and one pair of dissecting scissors each fitted with a triangular planar rigid body (passive tracker probe, Northern Digital Inc.) containing spherical, retroreflective optical markers (Northern Digital Inc.) mounted at each corner. The rigid bodies with markers are attached to parts of the devices that remain outside the patient's body. The dissecting scissors will be used to calibrate superimposition of the initial AR image of the prostate onto the live laparoscopic view. The positions of the TRUS probe, laparoscope, dissecting scissors, and optical position sensor with respect to each other and the patient are shown in the figure. The intraoperative TRUS images, normally viewed only on the US screen, are shown on the workstation screen, where the cancer nodule, prostate, NVB, and other structures are traced on the TRUS images, and the 3-D image is constructed. The 3-D image is then superimposed on the laparoscopic video screen in a geometrically accurate manner.

We are using a US machine (Pro Focus, B-K medical, Herlev, Denmark) with a biplane TRUS probe (type 8808, B-K medical) for US image acquisition (Fig. 25.1). TRUS images are digitized as a 320 × 240 matrix using a Sunvideo Sbus card (Sun Microsystems, Mountain View, CA). Three spherical, retroreflective optical markers for the Polaris system (NDI-1201115, Northern Digital Inc.) have been fixed on the proximal end of the TRUS probe with a triangular planar passive tracker probe (TA-200, Northern Digital, Inc.) and its attachment.

AR image: Intraoperative Real-time imaging vs. Preoperative imaging

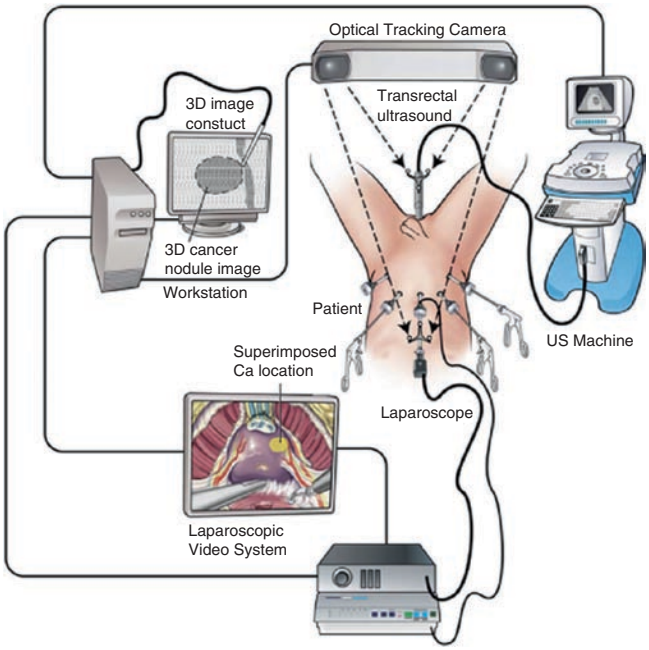

Fig. 25.2 AR system for laparoscopic radical prostatectomy (RP): TRUS and laparoscopic systems in the operating room. The location of the optical position sensor was moved from its actual unobstructed position relative to the TRUS probe and laparoscope for ease of viewing all of the connections in this figure

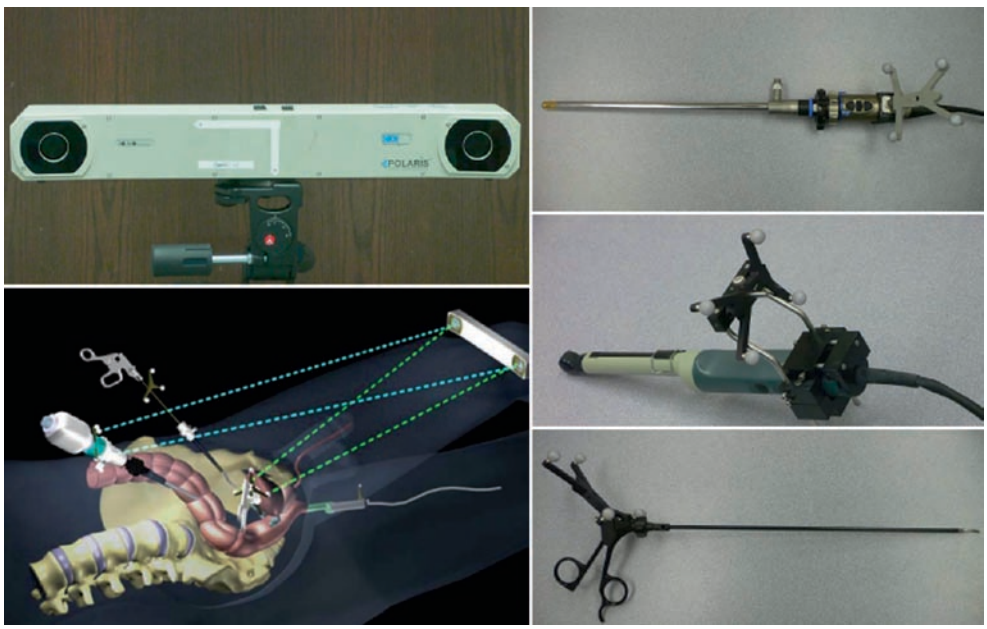

Fig. 25.1 Augmented reality (AR) system: polaris, infrared optical camera (*left upper*) and its role to track the position of the instruments with optical markers attached (*left bottom*), optical marker attached laparoscope (*right upper*), optical marker attached TRUS (*left middle*), and optical marker attached scissors (*right bottom*)

Intraoperatively acquired images such as real-time US or fluoroscopy could be accurately superimposed onto the videoscopic view, if there was no movement in the surgical field between the image acquisition time and the image projection time. However, when preoperatively acquired high-resolution imaging modality scans such as CT or MRI are used for image guidance, the space of the preoperative image needs to be registered to the ongoing real surgical space in the patient during the procedure. In our AR system, we have mainly used reconstructed 3-D surgical models with TRUS and MRI in prostate surgery and CT for kidney surgery.

Preoperative Calibration of the TRUS Probe

A specially shaped acrylic phantom board has been designed for the US calibration (Fig. 25.3). This board was placed under water, and a TRUS probe was positioned over the calibration board in such a way that the US section was completely coincident with the plane of the board. A 2-D US image was then acquired. When a sequence of TRUS images is acquired, the transformation defining the 3-D positions and orientations of the TRUS probe with attached optical trackers is simultaneously acquired along with each image. This acquisition is performed at a rate of about 15 frames/s. One sequence of acquired images usually consists of 240–300 slices of 2-D TRUS images. A 3-D model of the phantom is reconstructed from the US images. The 3-D positions of the tips of the M-shaped part will be used as the control points of the calibration procedure. Digitization of the tips of the calibration board will be performed using the Polaris system.

Preoperative calibration of the laparoscope camera and dissecting scissors

A special projection-point-board was used to obtain the camera calibration images, with each point on the board being used as a control point (Fig. 25.4). The board was positioned so as to be nearly parallel to the image plane at four different depths from the camera. In that way, the control points were arranged as uniformly as possible within the 3-D volume used in the clinical setting. The distance from the camera to the center of this 3-D volume was adjusted so that it lay approximately within the field of view of the camera, which was focused on the volume center. The volume, which should be sufficient to include the entire prostate and bilateral NVB views, ranged typically from $12 \times 12 \times 12$ cm^3 to $15 \times 15 \times 15$ cm^3. The depth of field of the camera should be adequate when the focus is fixed. The distance from the camera to the volume center will be typically around 20 cm.

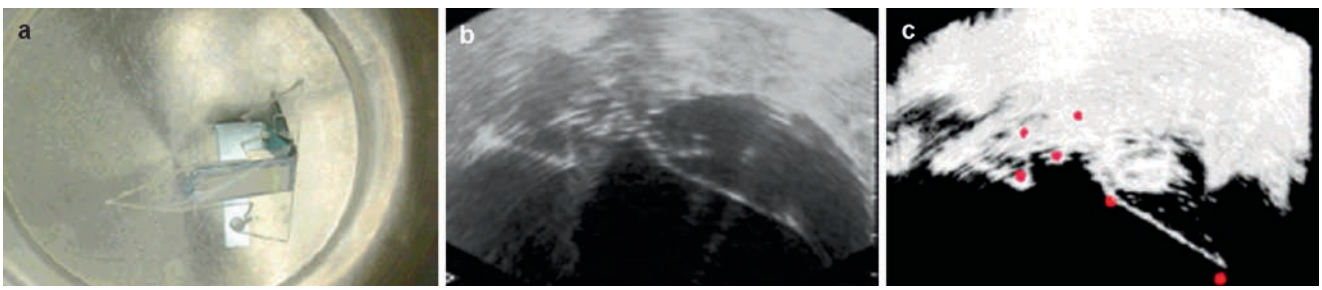

Fig. 25.3 Preoperative TRUS calibration: (**a**) acrylic phantom board; (**b**) 2-D TRUS image of the phantom board; (**c**) 3-D model of the phantom reconstructed from a series of TRUS images. In the process of calibration, the location of the projected *red*-colored points (where the radius is 1.0 mm) as control should be finally corrected to correspond to the center of each point of the M-shaped image of the phantom board

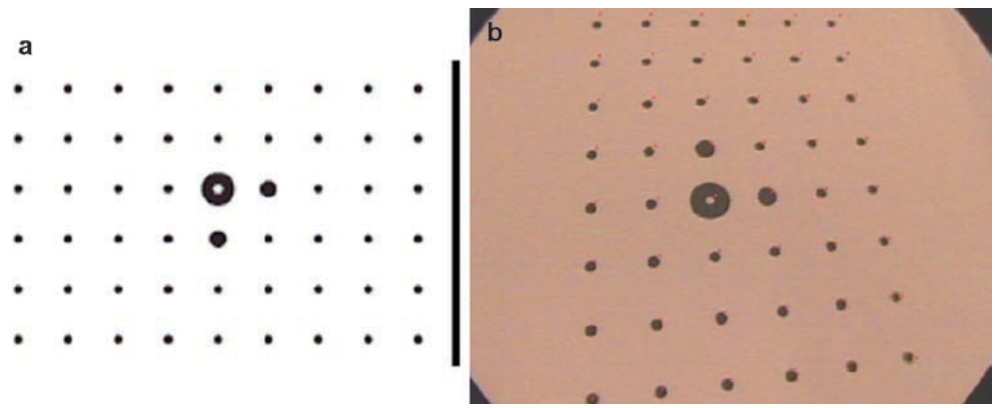

Fig. 25.4 (**a**) Projection-point-board for laparoscopic camera calibration. (**b**) View of calibration process

The 3-D positions of the control points will be measured using a Polaris pen probe. Fitting straight lines to the edge of the board and extracting their intersection points will yield the corresponding 2-D positions in the camera images. In a typical focus setting, the estimated focal length will be about 410 pixels. During the calibration process, the location of the small, red points should be finally corrected to correspond to the center of each of the points on the projection-point-board.

Preoperative Calibration of the Entire System of 3-D Reconstruction and AR

The construction of a 3-D model from TRUS images and the superimposition of the model on the camera images uses the specially shaped acrylic phantom board. The following comparisons will be made for the evaluation and calibration of preoperative errors within 1.0 mm:

- Comparison of the 3-D shape of the phantom reconstructed from US images and the 3-D positions of the vertices of the phantom measured by the Polaris system to evaluate the accuracy of the 3-D US reconstruction.
- Comparison of the projection of the phantom to evaluate the integration accuracy of the 3-D US reconstruction and the superimposition.

For preoperative calibration, a total of six sequences of TRUS images, three each in both transverse and longitudinal views, each at three different depths (5.0 cm, 6.2 cm 7.4 cm, obtained by transverse and longitudinal sweep directions using the biplanar TRUS probe) will be prepared to reconstruct the 3-D models for intraoperative acquisition. In every sequence, the small, red points (red-colored points) (where the radius is 1.0 mm) denote the vertex positions of the phantom accurately measured by the Polaris pen probe. The perceived vertices of the reconstructed model should coincide well with the accurately measured ones in all of the results with different sequences. The preoperative errors will be corrected within 1.0 mm at the five control points of the M-shaped part of the phantom board.

US Image Acquisition and Segmentation for 3-D Model Construction

Construct an intraoperative AR image of the prostate by tracing the outline of the prostate in each 2-D TRUS image using Virtual Place software (Medical Imaging Laboratory, Inc., Tokyo, Japan) and create a 3-D image from those 2-D images by the volume-rendering method. Project the 3-D AR image onto the laparoscopic screen according to the spatial coordinates of the TRUS probe and laparoscope, as registered by the Polaris Position Sensor.

Construct AR images of the cancer nodule, NVBs, lateral pedicles, and the prostate in the region of the lateral pedicles from successive TRUS images and superimpose those images onto the laparoscopic view (Fig. 25.5). The NVBs will be imaged with the US machine in Power Doppler mode, because the blood flow in the NVBs and dorsal vein facilitates Power Doppler resolution of those structures in 3-D. These 3-D images can be used directly by the AR system for superimposition onto the laparoscopic view, requiring only removal of the dorsal vein image, but eliminating the need to make tracings of the 2-D images.

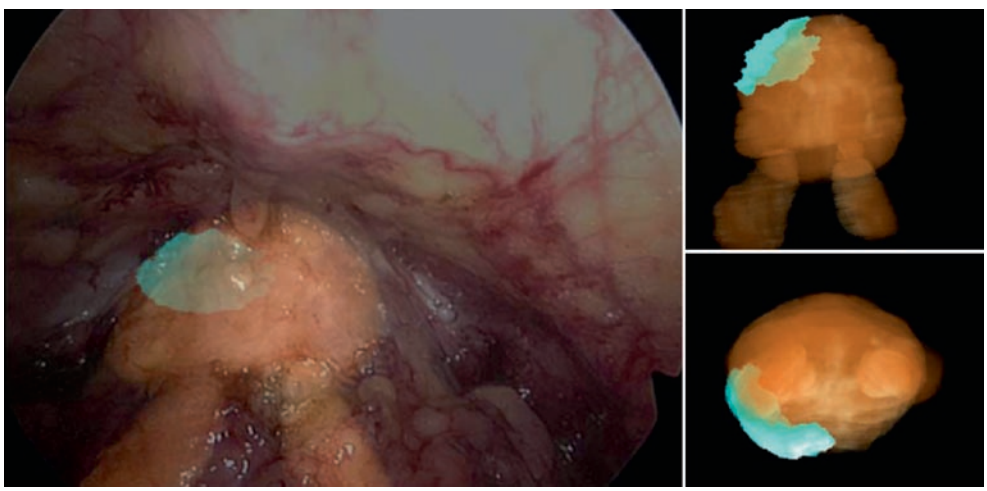

Fig. 25.5 AR visualization (*left*) using the 3-D surgical model with the biopsy confirmed cancer blue area (*right*), which was developed from intraoperatively acquired real-time 2-D TRUS image, to be superimposed onto the real-time laparoscopic view

Registration System of Preoperative Imaging and Tracking

The key to image guidance is to know (1) where the surgical targets are, (2) in which direction the surgical instruments should advance, and (3) how close the tips of the instruments are to the surgical target. The effectiveness of a surgical navigation system is significantly related to the accurate registration of the 3-D surgical model in spatial relationship to the surgical instruments and the surgical anatomy. Using the preoperatively acquired CT or MRI, the preoperative space of the acquired image needs to be registered on the ongoing real surgical space in a patient.

Optical tracking systems are the most prevalent tracking technology with a highly accurate and fast rate of sampling data. There are two primary classes of optical tracker: active and passive. An example of a passive system is the Polaris system (Northern Digital, Inc., Waterloo, Ontario, Canada), which we have used in our system. Three or more reflective optical markers are attached to the instruments in a specific triangulated figure. When an infrared stereo camera unit emits light onto the markers, the reflected light is received as digital data identifying the position and angle data of the instruments with the optical markers attached.

Magnetic tracking systems have the greatest potential in accurate tracking technology. However, their use has been limited because of an inherent feature, the distortion of the magnetic field by the metallic instruments around the surgical space such as the surgical bed, endoscope, scissors, and forceps. The magnetic tracking system consists of three components, including (1) a magnetic field generator, which generates the magnetic fields around the surgical space, (2) a magnetic sensor, which contains specific coils to produce electrical signals within the generated magnetic fields, and (3) a system workstation, which receives the sensor position data and communicates the digital information with the host computer and magnetic field generator.

In the interventional surgical procedure, a stereotactic frame can be used by an interventional surgeon to avoid the use of a highly technological tracking system. Such a frame can be rigidly mounted to the operating room table or patients' body, for example, mounted to the cranium in brain surgery. Mounted needle guidance on it will direct accurate needle placement into the target. These devices were the precursors to magnetic or optical trackers; however, they can still be useful without requiring a continuous tracking system. A robot arm can be also another promising tool for localization of the surgical instruments. The digital coordinates of the tips of scissors or forceps, which can be controlled by the robot arm, can be accurately calibrated and placed in a precise location.

Initial Clinical Experience of the AR System in Urology

In our initial experience, we employed the AR surgical navigation system in 25 laparoscopic surgeries, including 11 renal surgeries and 14 pelvic surgeries. We were able to superimpose the intraoperatively acquired 3-D US and preoperatively acquired 3-D images of CT/MRI, which demonstrated the anatomies of tumor and vital structures (such as the renal artery, the collecting system, and the NVB), onto the real-time laparoscopic view (Figs. 25.5 and 25.6). The accuracy in superimposition was reasonably precise (theoretically, less than 3 mm error in matched points) and sufficient to provide a 3-D perception beyond the surgical view, which has not been achieved by any other imaging guidance system available today.

Among the 11 laparoscopic kidney surgeries, construction of 3-D images of surgical interest (renal tumor, collecting system, and vasculatures) from preoperative CT data was performed one day before the surgery, which required 1–2 h (mean 1.3 h). Once the planned 3-D surgical models of the

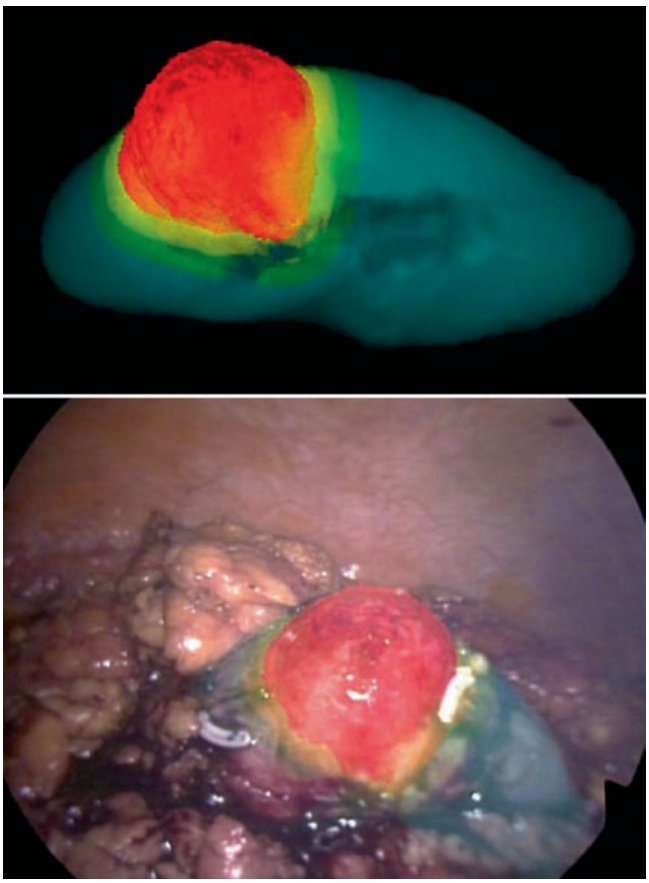

Fig. 25.6 AR visualization (*bottom*) using the 3-D surgical model from original preoperative CT image (*upper*), which is colored by four color-coded-zonal navigation concept, to be superimposed onto the real-time laparoscopic view

preoperative CT were constructed, the registration process required 5–18 min (mean 12 min). Techniques of image registration included the use of the "iterative closest point algorithm" and the "preoperative image to real-time-image algorithm." During laparoscopic partial nephrectomy, the 3-D-constructed tumor image using AR was interpreted directly by the surgeon. The accuracy of the superimposed image was confirmed by the correspondence of the routine electrocauterized surgical marking, which was suggested by 2-D-laparoscopic US in our routine laparoscopic partial nephrectomy procedure.

In laparoscopic partial nephrectomy, we applied our original concept of the four-color coded surgical navigation system. The four sequential, color-coded zones were painted around the surgical target such as a renal tumor: the tumor was colored red, surrounded circumferentially by a 5-mm caution zone in yellow, a 10-mm planned dissection zone in green, and a >10-mm healthy renal tissue zone in blue (Fig. 25.6). This newly developed concept aims to allow the surgeon to achieve a negative surgical margin while maximizing preservation of the renal function, by keeping the surgical dissection line within the green zone (5–10 mm zone from the edge of the tumor). The interval margin can be set at any required length (such as 5 mm), depending on the factors of (1) surgical planning, (2) possible errors of the superimposed image in the surgical navigation system, and (3) possible errors of the surgical procedure itself.

Real-time projection of the color-coded zonal surgical navigation system helped the surgeon to determine intraoperatively where to cut (continuing to cut while staying in the green zone) and what to preserve (preserving renal function in the blue zone), contributing to the achievement of a negative surgical margin in all cases while maximizing preservation of the renal function. In renal surgery, AR facilitated intraoperative identification of the renal artery and vein, which were superimposed onto the renal hilar fat.

Among the 14 pelvic surgeries, including 13 laparoscopic radical prostatectomies and a laparoscopic radical cystectomy, construction of 3-D images of the prostate with a biopsy-proven cancer area from intraoperative gray scale 10 MHz TRUS required 11–24 min (mean 17 min) during surgery, after acquisition of intraoperative TRUS volume data, which required less than 1 min. Another acquisition and construction of 3-D-images of NVB from intraoperative power Doppler TRUS required 3–7 min (mean 5 min) during surgery. Since the 3-D-TRUS image was intraoperatively acquired from the present surgical field, no registration procedure was needed. During LRP, the AR suggested cancer area was interpreted directly by the surgeon, and then intraoperative real-time TRUS guidance confirmed the correspondence of the location in real time in our routine TRUS-guided LRP procedure (Fig. 25.5).

Overall, less than 15 min per case were required for real additional time on our surgical procedures using AR technology. All surgical margins of 9 laparoscopic partial nephrectomies and 14 laparoscopic radical prostatectomies in the series were confirmed by pathology. In two cases, we used preoperative MRI to superimpose the required data. The technique of registration using MRI was the "preoperative image to real-time image algorithm." AR-assisted nerve-sparing LRP contributed to achieve a negative surgical margin for the cancer in all but one case (with a focal positive margin at the site of seminal vesicle involvement in pT3b prostate cancer) with a compatible recovery rate for erectile dysfunction, as shown in our previous report.

Advantages of AR include, first, that it can provide a new opportunity for the surgeon to allow direct interpretation of the 3-D image beyond the surgical view. The newly developed concept of a "color-coded surgical navigation system" provided the surgeon with a 3-D "road map" beyond the surgical view. This demonstrated the precise 3-D locations and extent of the tumor in relation to the surrounding vital anatomies, including vasculature or the collecting system, facilitating the achievement of a negative surgical margin for the cancer while maximizing preservation of the renal function. Second, using a 3-D TRUS model, which was acquired intraoperatively at various time points during nerve-sparing LRP, the position and orientation of the superimposed 3-D models of the prostate cancer and NVB were sufficiently accurate to provide an updated real-time perception of the 3-D anatomy according to each advancing step in the nerve-sparing LRP. This suggests the potential of achieving a negative surgical margin for the cancer while maximizing the preservation of erectile function.

Conclusion

In conclusion, we developed this real-time surgical navigation system using AR technology, for various laparoscopic urologic procedures, using reconstructed 3-D surgical planning models for the specific aims of the surgery, with preoperative CT, MRI, and/or intraoperative US. We developed urological software for our AR navigation system, from software originally developed for the guidance of breast-conservative cancer surgery, and made it compatible with laparoscopic procedures. As far as we know, we reported the initial experience of using AR surgical navigation for a clinical series of various laparoscopic surgeries in urology.

References

1. Sato Y, Nakamoto M, et al Image guidance of breast cancer surgery using 3-D ultrasound images and augmented reality visualization. *IEEE Trans Med Imaging*. 1998;17(5):681–693

2. Nakamoto M, Nakada K, Sato Y, et al Intraoperative magnetic tracker calibration using a magnetooptic hybrid tracker for 3-D ultrasound-based navigation in laparoscopic surgery. *IEEE Trans Med Imaging*. 2008;27:255–270
3. Ukimura O, Gill IS. Imaging-assisted endoscopic surgery: Cleveland clinic experience. *J Endourol*. 2008;22:803–810
4. Ukimura O, Gill IS. Augmented reality for computer-assisted image-guided minimally invasive urology. Ukimura O, Gill S, ed. *Contemporary interventional ultrasonography in urology.* Springer; 2009:179–184
5. Iseki H, Masutani Y, Iwahara M, et al Volumegraph (overlaid three-dimensional image-guided navigation). Clinical application of augmented reality in neurosurgery. *Stereotact Funct Neurosurg*. 1997; 68:(1–4 Pt 1):18–24
6. Kawamata T, Iseki H, Shibasaki T, Hori T. Endoscopic augmented reality navigation system for endonasal transsphenoidal surgery to treat pituitary tumors: technical note. *Neurosurgery*. 2002;50(6): 1393–1397
7. Shuhaiber JH. Augmented reality in surgery. *Arch Surg*. 2004; 139(2):170–174
8. Marescaux J, Rubino F, Arenas M, Mutter D, Soler L. Augmented-reality-assisted laparoscopic adrenalectomy. *JAMA*. 2004;292: 2214–2215
9. McNeal JE, Villers AA, Redwine EA, et al Capsular penetration in prostate cancer. Significance for natural history and treatment. *Am J Surg Pathol*. 1990;14:240
10. Wieder JA, Soloway MS. Incidence, etiology, location, prevention and treatment of positive surgical margins after radical prostatectomy for prostate cancer. *J Urol*. 1998;160:299
11. Guillonneau B, el-Fettouh H, Baumert H, et al Laparoscopic radical prostatectomy: oncological evaluation after 1,000 cases a Montsouris Institute. *J Urol*. 2003;169:1261
12. Rassweiller J, Seemann O, Schulze M, et al Laparoscopic versus open radical prostatectomy: a comparative study at a single institution. *J Urol*. 2003;169:1689
13. Salomon L, Sebe P, De La Taille A, et al Open versus laparoscopic radical prostatectomy: part II. *BJU International*. 2004;94:244
14. Ukimura O, Gill IS, Desai MM, et al Real-time transrectal ultrasonography during laparoscopic radical prostatectomy. *J Urol*. 2004;172:112–118
15. Gill IS, Ukimura O, Rubinstein M, et al Lateral pedicle control during laparoscopic radical prostatectomy; refined technique. *Urology*. 2005;65:23–27
16. Ukimura O, Magi-Galluzzi C, Gill IS. Real-time transrectal ultrasound guidance during nerve-sparing laparoscopic radical prostatectomy: impact on surgical margins. *J Urol*. 2006;175:1304–1310.
17. Ukimura O, Okihara K, Kamoi K, et al Intraoperative ultrasonography in an era of minimally invasive urology. *Int J Urol*. 2008;15: 673–680

Advances in Imaging

26

Gareth Bydawell, Pippa Skippage, and Uday Patel

Kidney

Indeterminate Renal Mass

There has been an extensive investigation in recent times into modalities used in the characterization of indeterminate renal lesions. Unless the benign nature can be confidently diagnosed, suspicious lesions are still subjected to surgery or biopsy.

CT

This readily available modality allows quick and accurate depiction of the renal mass. With different timing of contrast, the lesions can be delineated from normal renal parenchyma and relationships with intrarenal components such as vessels and collecting system and extrarenal structures such as perirenal fascia, IVC, and spleen. Many protocols have been described, but the principle of renal-mass imaging includes the combination of an unenhanced scan with an early[1] and late (nephrographic) scan.[2] Enhancement within the mass or its wall is readily assessed, and this is the single most reliable factor in predicting renal malignancy.[3] Furthermore, accurate tissue characterization allows differentiation between benign and malignant entities. This is particularly relevant in the setting of renal angiomyolipoma where fat content is virtually diagnostic of the condition. A notable, albeit rare, exception is a small percentage of fat-containing RCC. However, in these latter cases, there is often calcification present (which is very rare in AML).[4]

There has been a recent interest in characterizing the histological subtype of the renal tumor using imaging due to the different prognoses and clinical implications. In terms of CT enhancement, clear-cell carcinomas tend to enhance more avidly than the other subtypes. Furthermore, a heterogeneous mass with soft tissue and cystic components also favors a diagnosis of clear-cell carcinoma.[5] Papillary carcinoma has a peripheral or uniform enhancement pattern due to reduced vascularity in comparison to clear-cell subtype.[5] The benign oncocytoma may present as the typical well-defined lesion with a central scar and spoke-wheel configuration of tumoral vessels, but the enhancement pattern overlaps with that of a clear-cell carcinoma.[1] For this reason, some urologists consider oncocytoma as a surgical lesion since imaging, and even biopsy, cannot reliably differentiate this entity from renal-cell carcinoma. Chromophobe renal-cell carcinomas tend to have a variable enhancement pattern.[5] More work is necessary, but it is possible that study of enhancement characterization may aid the risk stratification for renal masses; and that as surrogate for tissue vascularization help assess the response to novel chemoimmunotherapeutic agents.

MRI

High-quality MR imaging is often used to further the investigation of the indeterminate renal mass. Other uses include the assessment of lesions in patients with contraindication to iodinated contrast and in young patients on regular follow up (e.g., AML or hereditary renal tumors). With renal dysfunction, gadolinium-based contrast agents are contraindicated in MR imaging due to the risk of nephrogenic systemic fibrosis,[6] however, unenhanced imaging still provides superior tissue characterization than CT imaging. The assessment of intralesional fat is very sensitive in MR imaging, and other tissue components can be delineated and used to aid diagnosis, e.g., hemosiderin deposition in papillary carcinoma. Chemical-shift imaging is an adaptation of a misregistration artifact in MR imaging where the difference in resonant frequencies between different soft tissue densities (e.g., water and fat) leads to signal drop out, and this has traditionally been used to differentiate the fat-containing adrenal adenoma from metastasis. New adaptations of this technology have been attempted to differentiate subtypes of renal masses.[7]

As with CT, magnetic resonance imaging (MRI) can be used to assess the enhancement patterns of renal lesions, and accurate MR angiograms and venograms can be performed to assist in the planning of nephron-sparing surgery. This topographic information is also invaluable in the imaging of potential donor kidneys. MRI is useful in the interventional

P. Dasgupta et al. (eds.), *New Technologies in Urology,*
DOI: 10.1007/978-1-84882-178-1_26, © Springer-Verlag London Limited 2010

setting, particularly for percutaneous biopsy and ablation techniques. Newer technology even allows for intraprocedural monitoring of both cryoablation and radiofrequency ablation (RFA), and this is predicted to become an important area of research, as MRI is the most suited modality for reproducible monitoring of real-time tissue changes with focal ablative techniques.

Unlike in the assessment of the prostate (see the section on "Prostate") diffusion-weighted MR imaging of the kidney has no clear role in the investigation of renal-mass lesions, although it has been shown to distinguish abnormal tissue from normal parenchyma. It is not clear whether further differentiation is possible, and further research is needed to determine if any clinical applications are possible.

Positron Emission Tomography (PET)

PET imaging using the glucose analog 18-fluoro-deoxy-D-glucose (FDG) has played a limited role in the investigation of the indeterminate renal mass thus far, though it may have limited value in the investigation of the complex renal cyst (to confirm benignity) and to characterize the indeterminate lesion in patients with metastatic renal-cell carcinoma. In terms of sensitivity, PET has similar diagnostic accuracy to CT scanning (ramdave j urol, 2001) and higher documented sensitivity rates of 100% with respect to lymph-node staging,[8,9] but these data have not been confirmed.

Recent work has focused on differentiating clear-cell carcinoma from the other histological subtypes (as with CT, see the section on CT) on the basis that the former is more aggressive and likely to metastasize. Thus, if a nonclear-cell carcinoma is diagnosed, then watchful waiting or minimal access therapy (e.g., RFA) can be considered, especially in elderly patients or those with significant comorbidity. This technique uses a positron-emitting radionuclide, iodine-124, labeled to an antibody (cG250) that recognizes the tumor protein known as carbonic anhydrase IX. This protein is expressed during the active phase of a clear-cell carcinoma. A prospective clinical trial of 26 patients with known renal masses involved PET scanning with I-cG250 antibody prior to their surgery. The results show that the radioisotope is 94% sensitive and 100% specific in diagnosing clear-cell carcinoma,[10] but again this promising data needs to be confirmed with larger studies.

Ultrasound

Conventional B mode ultrasonography is a low cost, easily performed, and safe imaging modality that remains pivotal in the investigation of urinary tract abnormalities. In recent years, however, contrast-enhanced ultrasonography has emerged as a useful adjunct in the study of renal abnormalities. This technique uses microbubbles as a contrast agent and has the ability to study the enhancement pattern of an indeterminate lesion. The gas-filled microbubbles have a lower density than water – this results in acoustic impedance during ultrasound imaging and increases the contrast between the intravascular microbubbles and the surrounding tissues. The technique is especially valuable in patients requiring enhanced imaging, who have contraindications to both CT and MR contrast agents. Other uses include the accurate assessment of the typical centripetal enhancement pattern of lesions such as renal hemangioma.

Urolithiasis

Imaging for urinary stone disease previously included a combination of X-ray, IVU, and ultrasound. However, as the technology has improved, CT scanning has adopted a more frequent role in the assessment of renal colic and the complications of urolithiasis. First, the low-dose unenhanced CT KUB has replaced the IVU in most centers, and second, CT pyelography is being used increasing in preoperative planning for endourological surgery. This technology allows multiplanar reformatted images and 3D volume images and movies to be constructed from the source data (Figs. 26.1 and 26.2). This allows accurate localization of urinary

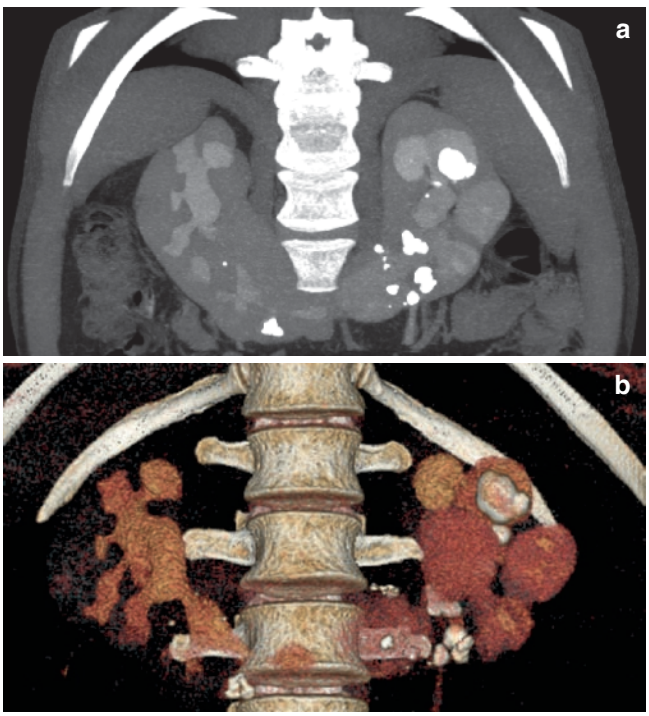

Fig. 26.1 Horseshoe kidney with complex stone burden. Coronal oblique MIP (**a**) and 3D volume rendered images (**b**) enable the endourologist to assess the full distribution of urinary calculi and plan optimal calyceal access for PCNL

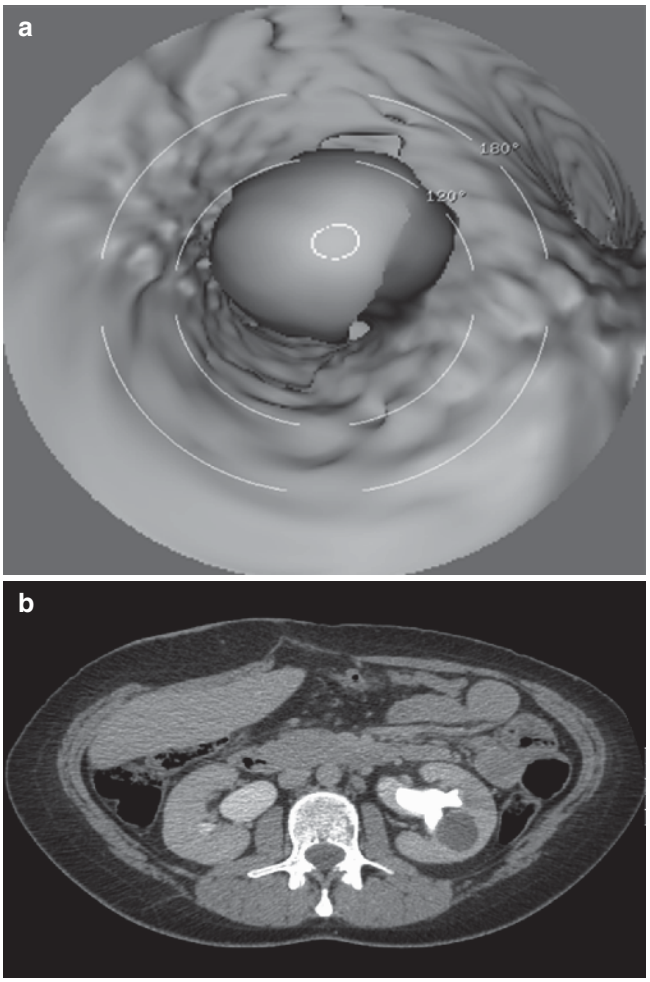

Fig. 26.2 Virtual endoscopic view of a staghorn calculus (**a**). The corresponding axial image of the calculus is seen on the CT urogram (**b**)

calculi and, more importantly, guides the urologist in planning the optimal route of percutaneous access. This technique is particularly useful in planning for percutaneous nephrolithotomy in malpositioned and distorted kidneys and those patients with complex stone burden.[11–14] Another promising area is the ability of CT to characterize the CT density of a given stone, which roughly correlates with the hardness of the stone and hence the likelihood of response to extracorporeal lithotripsy.[15] Most recently, a new CT technique (dual-energy CT) has further expanded the potential of CT for characterization of stone content.[16]

MR urography is not routinely advocated in the work up of patients with urinary calculi, but it is recommended in exceptional circumstances such as renal colic in children or pregnant patients.[17] Similar diagnostic accuracy to CT imaging and IVU has been reported,[17,18] but the foremost limitation of MR urography is that stones are seen as a signal void. No MRI sequence as yet has been able to detect any intrinsic or stone-specific signal.

Urothelial Imaging

CT urography has emerged as a very useful modality in the investigation of urothelial malignancy. To a large extent, it has replaced the IVU in assessment of the ureter and upper tract, but its place in the modern management algorithm is still under review. It is a tempting notion to consider this modality a "one stop shop" for the complete evaluation of the kidneys, ureters, and bladder (including accurate urothelial assessment), but there are important considerations such as radiation dose. A CTU working group of the European Society of Urogenital Radiology recently recommended CTU as a first-line investigation for macroscopic hematuria in high-risk patients (age >50, smokers), and as a problem-solving examination in complex cases.[19] Furthermore, recent studies have shown that CTU imaging of the upper tracts is more sensitive in diagnosing urothelial abnormalities (notably, TCC) than do conventional retrograde pyelography.[20]

Virtual endoscopy of the urinary tract is a promising derivative of CT urography that promises accurate assessment of the urothelium, and several studies have shown increased sensitivity in detecting TCC than CT urography alone.[21,22] This technique utilizes software to generate endoscopic views of the urinary tract from the source axial data from the standard CT urogram procedure (Figs. 26.1 and 26.2). Multidetector scanners are required to acquire thin enough cuts to produce an accurate representation. The limitation of the technique is the added time required to construct the images by the reading radiologist. Further work is required but is possible that faithful 3D anatomical models may be useful for both diagnosis and the teaching of endoscopic navigational skills.

Minimally Invasive Therapy

As the frequency of detection of RCC has increased, there has been an emergence in new therapies aimed at the ablation of small tumors. Examples include RFA, cryotherapy, and microwave ablation.

For RFA, thermal energy is delivered to a targeted lesion (via US or CT) at temperatures designed to cause irreversible cellular damage.

Because of increasing numbers of ablation procedures being performed, there is a concordant increase in the number of posttreatment scans performed to assess treatment response. Current practice usually involves early imaging (within 2 weeks) to assess successful ablation then follow-up scans at an appropriate interval (usually 6 months). Contrast-enhanced CT is the most frequently used modality, and residual enhancement is taken as a surrogate indicator of residual viable tumor tissue. For the immediate postoperative scan,

Table 26.1 CT imaging features of successful tumour ablation

Features of successful ablation
Lack of enhancement
Reduction in size
Replacement with fat/calcification
Postablation halo
Cortical scarring

an unenhanced sequence is recommended to differentiate the high attenuation "reactive hyperemia" in the normal parenchyma from untreated/enhancing tumor. In terms of follow-up imaging, the principle sign of successful therapy is lack of enhancement of a treated lesion. Many other signs have been described, and these have been summarized in Table 26.1.

In terms of untreated or recurrence of the tumor, a crescent of enhancing soft tissue is the cardinal sign detected on contrast-enhanced CT scanning.

Nephron Sparing Surgery

Advances in cross-sectional imaging, CT and MRI, has allowed more accurate assessment of the relationship between renal neoplasm and normal parenchyma. In particular, the proximity to renal vasculature and collecting system and the presence of a pseudocapsule allows the urologist to plan nephron-sparing surgery in appropriate cases. Intraoperative ultrasound is an additional modality that provides real-time ultrasonic localization of renal lesions at the time of operating. This technique has particular advantage in the setting of hereditary renal neoplasia where multiple mass lesions are often encountered in each kidney.

Ureter

Cross-Sectional Imaging

In terms of ureteric calculi, unenhanced CT KUB remains an accurate first-line investigative tool. In pregnant women, magnetic resonance urography (MRU) plays a distinct role in distinguishing between physiologic hydronephrosis and obstructive hydronephrosis secondary to calculi. While ureteric calculi may be difficult to identify on MR imaging (being signal voids, as discussed earlier), the modality is accurate in identifying the secondary signs of ureteric obstruction such as perinephric and periureteral stranding, hydronephrosis, and ureteric dilatation. Heavily T2-weighted sequences are performed in both axial and coronal planes to maximize diagnostic accuracy. Gadolinium-enhanced, or excretory, MRU increases the sensitivity of diagnosing ureteric obstruction. As with CT urography, the contrast and spatial resolution is improved with maximum urine volume within the collecting system – this can be achieved with diuretics, intravenous fluid, and ensuring a full bladder. With the combination of static, excretory MRU, and conventional MRI, a full assessment of the entire urinary tract can be obtained in one procedure. The role of this modality continues to evolve as the quality of MR imaging improves. There are still limitations to overcome such as the insensitivity of detecting calcification, long acquisition time and imaging artifacts, but it possible it may compete with the CT urogram for diagnostic purposes.

Endoscopic Ultrasound

For the most part CT or MR urography provides an accurate assessment of the ureter and any pathology within. There are, however, still occasional clinical scenarios where radiological uncertainty exists, and further investigation is required. Examples include differentiating the underlying cause of pelviureteric junction obstruction, tumor vs. postoperative scarring, and distinguishing primary ureteric malignancy from adjacent lymphadenopathy.[24] Additional abnormalities such as submucosal calculi can also be detected even when this was missed during ureteroscopy. Conventionally, these cases can be closely monitored with interval imaging or more aggressively with diagnostic laparoscopy, but endoscopic ultrasound offers an alternative avenue of investigation. The main advantage is accurate 360° assessment of the ureteric wall and its layers. Technically, the procedure is performed synchronously at the time of cystoscopy and retrograde pyelography and involves collaboration between urologist and radiologist. The ultrasound probe consists of a transducer housed on a 7F catheter and is inserted into the ureter following initial cannulation with wire and catheter. The exact location of the probe can be monitored with fluoroscopy. The disadvantages include the cost of the ultrasound equipment and the necessity for general anesthetic.

Miscellaneous

Functional MR Imaging of the Kidneys

Promising results have been shown in the MR assessment of renal function. The main benefit lies in the combining of anatomic detail with functional information in the assessment of renal disease. This technique has value in the evaluation of living donor kidney, renal artery stenosis, and in patients

prior to nephrectomy. Renal artery perfusion and glomerular filtration rates can be calculated using equations involving the behavior of Gd-DTPA during contrast-enhanced MR imaging.[25]

Image-Augmented Intraoperative Navigation

This technology allows fusion of two imaging modalities or between imaging and real-time sensors that track position of surgical instrumentation. This allows highly accurate localization of abnormalities targeted for biopsy or therapy. Examples include (i) the integration of cross-sectional imaging (CT or MR) with real-time ultrasound imaging to pinpoint RFA and (ii) robotic procedures linking the surgical technology with CT or MR images. The principle of this innovation is the synergy of three-dimensional imaging detail with real-time surgical views, allowing the operator to perform more subtle and delicate procedures in anatomically challenging locations. There is also scope for the development of computer simulation models to assist in the training of future surgeons.

Prostate

Prostate Cancer

Prostate cancer is one of the commonest cancers of the elderly male population. Most prostate malignancies are relatively slow-growing tumors, and gland-confined treatment with curative intent is generally successful. However, once the disease has spread beyond the gland, curative treatment is not feasible. Therefore, it is essential that the initial diagnosis and staging of prostate cancer is as accurate as possible to ensure correct treatment stratification. In the same way, follow-up imaging and the diagnosis of recurrent disease must also be accurate.

Transrectal ultrasound (TRUS), while readily available and cost effective, lacks sensitivity and specificity. MRI is used to stage disease once a diagnosis has been made, but methods lack sensitivity and specificity for cancer detection and localization.[26] More recently, morphologically based prostate imaging is now being complemented by functional and molecular imaging techniques.[27]

Ultrasound

The introduction of TRUS revolutionized the ability to study the prostate gland.[28] Not only did it enable excellent visualization of the gland but also meant that targeted needle biopsies could be performed simultaneously. A systematic biopsy pattern is followed. The number of cores taken varies from 6 to 12. However, multiple studies have shown that systematic biopsy may miss a significant number of clinically relevant cancers.[29] More recently, there has been a trend to increase the number of biopsies taken to ensure a higher positive yield. The saturation biopsy technique samples the whole gland either transrectally by taking 20 or more core biopsies evenly distributed throughout the gland or using a more systematic approach using a transperineal, grid-based method using a brachytherapy template.[30] Transperineal prostate mapping has been shown to improve the accuracy of Gleason grading and, consequently, the disease burden in patients with localized prostate cancer and therefore ensure more accurate disease stratification.[31] As a result, these new techniques have been developed to augment conventional ultrasound and improve the detection of cancer.

Color/Power Doppler Ultrasound

Neovascularity, as a result of tumor angiogenesis, is a well-recognized phenomenon not just limited to prostate cancer. Studies have shown that various different "abnormal" flow patterns are associated with prostate cancer: diffuse increased flow, focal increased flow, and asymmetric flow surrounding the tumor focus. Early studies showed that up to 85% of patients with prostate cancers more than 5 mm have visibly increased flow in the area of tumor involvement. Hypervascularity can also been seen in patients with isoechoic tumors that are more difficult to identify. However, subsequent studies have shown that the use of color and power Doppler will still miss some cancers and therefore does not preclude routine prostate biopsy.[29]

Contrast-Enhanced Ultrasound

Ultrasound-contrast agents are proving to be increasingly useful in the detection and characterization of abnormal prostatic tissue. Contrast agents work by increasing the signal-to-noise ratio and therefore improving the detection of low-volume blood flow. The newer agents developed have many benefits, including being entirely restricted to the vessel lumen resulting in increased detection of small vessels, which are not obscured by surrounding tissue absorption of the agent. They are also many times more reflective than blood, therefore improving flow detection.[29] Used in combination with Doppler imaging, microbubble contrast agents have shown to result in increased signal in areas of increased

vascularity, which (as previously stated) may correlate with areas of malignant change. In a study by Pelzer et al,[32] targeted biopsies, as determined by areas of hypervascularity postintravenous contrast administration, were compared with standard biopsies (ten cores). The results showed that the detection rate of malignancy within the targeted cores was significantly better than that of the standard cores ($p<0.01$).

Elastography

Elastography was first described by Ophir et al in 1991.[33] It is a novel ultrasound technique for assessing tissue elasticity in real time through the application of gentle pressure with a conventional ultrasound probe.[34] Originally, elastography was only possible on organs that could be directly compressed, for example, the thyroid, breast, and testicles. The vast majority of the work on ultrasound elastography has been done on the assessment of breast tissue. However, with the development of intracavitary transducers, it has been possible to apply the technique to deeper organs such as the prostate.[35]

Elastography relies on the principle that abnormal (malignant) tissue is usually stiffer than the surrounding normal parenchyma. This difference in tissue compressibility or elasticity results in an alteration of the ultrasound signal received by the transducer when the tissues are compressed by only a small amount (approximately 2%).[29] The pre- and postcompression-received signals from various regions of interest can then be analyzed and compared for differences. Where tissues are found to be less compressible, a suspicion of malignant change can be raised.

These findings can not only be used to directly assess for possible sites of disease but can also be used to guide biopsy under ultrasound guidance[36] and potentially reduce the number of total biopsies required.[29]

A similar principle is used in sonoelastography. This uses an acoustic vibration in the audible range (30–200 Hz), which is transmitted into the prostate gland. Color Doppler imaging is then used to detect resultant tissue vibrations. Abnormal areas of tissue (i.e., "stiffer" areas) will result in decreased vibrations and therefore be reflected as a signal void in the color Doppler image.[35] Several studies have suggested that sonoelasticity imaging is more sensitive for tumor detection and more accurate for the assessment of tumor localization than conventional ultrasound.[29,37,38]

Although there are undisputed problems with the technique such as failure to detect small tumors and a false-positive detection of hyperplastic nodules and calcium,[38] overall, the recent work on prostate elastography and sonoelastography is promising.

3D

Conventionally, TRUS-guided prostate biopsies are performed using standard two-dimensional (2D) images. Because prostate carcinomas are nonuniformly distributed throughout the gland, it would seem more logical to approach biopsies using three-dimensional (3D) images, therefore, obtaining a more realistic anatomical picture of the prostate gland and increasing the accuracy of the biopsy.[39] New ultrasound machines are capable of delivering 3D images in real-time, referred to as four-dimensional (4D) images.[34] These 4D images have been used in TRUS-guided prostate biopsies and shown to improve diagnostic accuracy.[40]

MRI

MRI is already widely in use for the diagnosis and pretreatment staging of patients with prostate cancer. Standard images are usually obtained using a pelvic phase-array coil. Wide field of view images are useful in determining local nodal spread and the presence of any bony metastases. Multiplanar T2 sequences are routinely obtained, providing good zonal anatomical representation of the prostate gland, with areas of malignant change typically showing as foci of decreased signal. However, low signal in the peripheral zone (where the majority of cancers arise) can also be caused by hemorrhage, prostatitis, hyperplastic nodules, or sequelae from radiation or hormone therapy.[41] This reduces the sensitivity and specificity of conventional MRI. Endorectal coils improve detection of prostate cancer, as well as providing more accurate information on local tumor staging, especially when results are interpreted by experienced readers.[42,43] Endorectal coils work by increasing the signal-to-noise ratio by a factor of 10. This results in higher spatial and spectral resolution.[44]

Faster MR sequences have also much improved imaging of the prostate. The faster scanning times allows more planes to be covered in the same amount of time and also decreases the amount of motion artifact. The scanning parameters can also be adjusted to increase the T2 weighting of the scan, therefore, increasing the detectabilty of lesions.[45]

To further improve the diagnostic capability of prostate MRI, various methods are being developed coupling conventional MR with functional imaging. This shall not only improve the accuracy of diagnosis but may also aid treatment planning.

Dynamic Contrast-Enhanced MRI

The basis for contrast-enhanced MRI is the same as that for contrast-enhanced ultrasound. Within malignant tissue,

angiogenic factors are released, resulting in new vessel formation. Richer vessel density results in a more rapid and sustained period of enhancement postcontrast administration. The development of fast imaging techniques allows the entire volume of the prostate to be covered in a few seconds[41] and therefore allows repeated imaging to be obtained at varying time intervals postinjection of intravenous contrast. From the data collected, various perfusion parameters can be determined, compared with similar data from normal areas of prostate tissue, and analyzed to provide diagnostic information on possible areas of malignant tissue.[26] Studies by Engelbrecht et al[46] and Kim et al[47] have both shown that the relative peak enhancement and contrast washout rates of contrast can be used to confidently identify areas of abnormal prostate tissue. Englebrecht et al[46] concluded that, by analyzing enhancement curves, the relative peak enhancement was the most accurate perfusion parameter for detecting cancer in the peripheral and central zones of the prostate gland. Kim et al[47] demonstrated that the wash-in of the contrast (i.e., how fast an area enhanced) was more accurate for detection of malignancy in the peripheral zone than when using the standard MRI images. The sensitivity and specificity for cancer detection based on the wash-out rate were 96 and 97%, compared with 75 and 53% on the T2 images alone ($p<0.05$). Furthermore, early data suggests that peak enhancement may also be particular to tumors of higher Gleason grade. The promise of dynamic MRI is that it may allow the identification of target or index lesions for focal ablative therapies or directional biopsies for tumor risk stratification.

Magnetic Resonance Spectroscopic Imaging (MRSI)

Conventional MRI detects the nuclear magnetic resonance spectra of water in tissues and provides a combined signal-intensity map of all hydrogen protons within one tissue type. However, the signals from hydrogen protons in different molecules actually have slightly different frequencies, a property known as chemical shift. MRSI detects these different frequencies and produces a map of signal intensity vs. frequency and location.[27,48] As such, MRSI can produce a map of tissue metabolism. Much work had already been done on the metabolic composition of normal prostate tissue, which is known to contain high levels of citrate and low levels of choline. In prostate cancer, there is a decrease in the citrate level and a relative increase in the choline level due to alterations in the tissue metabolism.[26] Therefore, the MR spectra obtained from areas of normal and malignant prostate tissue will differ and may allow localization of tumor.

MR spectroscopy using endorectal coils has also been shown to increase the sensitivity of targeted biopsies in patients with raised PSA levels and previous negative biopsy results.[49]

The disadvantages of MRSI are that it is time consuming, results may vary due to postprocessing factors, and recent biopsies may produce artifacts that degrade the images. While it has been shown to be sensitive for detecting cancer within the peripheral zone, detection of more central cancers has not proved to be as successful, likely reflecting a different metabolic composition of the transition zone tissue.[50]

Diffusion Imaging

Diffusion is the process of thermally induced random molecular displacement or Brownian motion. All tissues have individual diffusion characteristics based on their quantity of free water and the permeability of the tissue itself. In prostate cancer, the normal glandular architecture is disrupted and replaced by aggregated cancer cells and fibrotic stroma.[26] Consequently, there is less free motion of water in the malignant tissue, i.e., restricted diffusion.

Diffusion-weighted images (DWI) can be obtained as part of a routine MRI scan and additional apparent diffusion coefficient (ADC) maps calculated. Areas of restricted diffusion will show as areas of low signal on the ADC map and have been shown to correlate with areas of biopsy proven prostate cancer. The sensitivity of cancer detection is increased when the findings are correlated with the standard T2 images.[51]

DW imaging has the limitation of poor spatial resolution and, as with all MR images, is susceptible to artifact from recent biopsies.

Elastography

Elastography is usually performed with ultrasound as the imaging technique. However, research with MRI elastography is underway.[52]

Conventional MRI vs. 3T MRI

Most work into prostate MRI has been done using standard 1.5 Tesla (1.5 T) scanners routinely found in most departments. The introduction of new localized treatment options such as high-intensity focused ultrasound (HIFU), image-guided brachytherapy, and cryotherapy (see below) has brought about a need for higher quality initial diagnostic and staging imaging. Over the last few years, higher strength 3 T scanners have been developed, and research has been carried

out on the potential benefits for, among others, prostate imaging.

The increase in magnet strength results in a linear increase in signal intensity with a relatively unchanged noise level. This results in a higher signal-to-noise ratio and therefore better spatial, temporal, and spectral resolution. However, the increase in magnet strength does have its disadvantages, namely, alteration in the inherent relaxation properties of tissues, and therefore the acquired signal, as well as an increase in artifact.[53]

Recent studies have been carried out comparing the image quality, tumor delineation and staging accuracy for prostate cancer using 1.5 and 3 T scanners. The results show that images obtained using pelvic phased-array coils at 3 T are comparable with those obtained using an endorectal coil at 1.5 T.[53,54] This is obviously beneficial to the patient as it obviates the need for an invasive procedure. While it is likely that images obtained using an endorectal coil at 3 T will be superior, there is currently only limited data to support this.

At 3 T, imaging has also been shown to improve the sensitivity and specificity of both dynamic contrast-enhanced MR imaging and diffusion imaging.[53,55,56] Work on MRSI at 3 T is currently being undertaken with mixed results.

MRI-Guided Biopsy

A few studies have addressed the feasibility of MRI-guided prostate biopsies. Special biopsy equipment is necessary for targeted MRI biopsy, in particular, the use of nonmagnetic instruments. Data are currently limited but is anticipated that the combination of functional with conventional MR imaging may increase the yield of biopsies in patients with previous negative ultrasound-guided biopsies, but a high clinical suspicion of prostate malignancy.[41] A recent study by Anastasiadis et al showed that MRI-guided biopsy detected cancer in 55.5% of patients who had a previously negative TRUS biopsy but had an elevated PSA, suspicious DRE, and abnormal MRI findings.[57]

CT/PET

PET uses pharmaceuticals containing radionuclides that decay by the release of protons to produce whole-body tomographic images, which can be combined with CT to produce high-resolution images.[27] The most commonly used radionuclide is 2-18F-fluoro-2-deoxy-D-glucose (FDG). However, the use of this in prostate cancer is challenging because of the low-glucose utilization of the prostate gland (and therefore low uptake of the tracer) as well as its urinary excretion meaning that tracer will collect in the bladder and may obscure pathological uptake in the prostate gland and adjacent structures.[58] Consequently, research has been done into alternative PET tracers that are based on metabolic pathways other than glucose. Current avenues of research include the use of ^{11}C- or ^{18}F-choline and ^{11}C-acetate, which are related to membrane lipid metabolism, and ^{11}C-methionine and ^{18}F-fluoro-L-thyosine, which are related to protein turnover.[27] In 2007, Yamaguchi et al compared 11C-choline PET with MRI and MRS in 20 patients with early prostate cancer. The results showed a sensitivity of 100% for the PET images for detection of the primary lesion compared with 60% for MRI and 65% for MRS.[59]

MRI/CT Image Augmented Intraoperative Navigation

Cross-sectional images acquired by CT and MR can be formatted into 3D image sets and linked to sensors that track the position of surgical instruments relative to the image set. These images can be fused with other data sets to form compound images that would aid surgeons in localizing disease sites and to appreciate anatomical boundaries during surgery. These applications can also be used to aid accurate biopsies.[34]

Monitoring Response

With a large number of patients now undergoing localized treatment for prostate cancer rather than radical prostatectomy, it is important that imaging methods are tailored to these patients, to allow regular, routine follow up and to ensure that any recurrence is diagnosed.

Ultrasound

Studies have been done into the use of contrast-enhanced ultrasound and elastography to monitor patients after undergoing HIFU treatment. The initial results have been promising showing a reduction or absence of blood flow in treated areas on both contrast-enhanced and Doppler imaging as well as an alteration in the elastography of the treated tissues.[60–62] However, there has been some discrepancy with reported MRI findings,[60] and further research is required into these methods.

MRI

Specialized MR techniques, such as dynamic contrast-enhanced (DCE) studies, DWI, and MRS, can also be used to

monitor localized treatment to the prostate gland. Essentially, treatment aim is to induce cell death. Therefore, posttreatment monitoring relies on the assessment of this, in terms of lack of vascularity, lack of contrast enhancement, loss of normal tissue signal, and the transformation to signal characteristics consistent with necrosis.

Studies looking at both HIFU and cryotherapy treatment have concluded that while these changes can be identified and in some cases do represent effective treatment, when correlated with histological findings, MRI is not yet sensitive enough to detect all areas of recurrence and therefore biopsy is still required.[63–65]

Testes

Ultrasound

Ultrasound remains the imaging technique of choice in most testicular pathologies. It can be used to differentiate between various tumor types, but, as the vast majority of patients with a suspected tumor will go on to have an orchidectomy, this is not crucial.

More recently, intraoperative ultrasound has been used to guide needle localization for nonpalpable tumors. In patients with bilateral tumors or those with a solitary testicle, testis-sparing surgery has been advocated to avoid the problems associated with castration.[66] Browne et al used intraoperative ultrasound guidance in three such patients and avoided the need for orchidectomy in one of them.[67] Organ-sparing surgery for malignant testicular tumors is a controversial area, as it does not follow the usual radical approaches of cancer surgery. The limited data available is encouraging with respect to disease-free survival, but the potential for local recurrence and residual disease must not be forgotten.[68]

CT/PET

CT is routinely used for staging and follow up of metastatic disease. The disadvantages of this include the radiation dose associated with it and the long-term effect that this may have on the relatively young patient population involved. Possible solutions have been to use low-dose CT or MRI. However, both these techniques need to be validated in suitable surveillance protocols in prospective trials.[69]

FDG PET has been shown to be more sensitive than other modalities for assessment of residual tumors in patients who have previously undergone chemotherapy for seminomatous tumors.[70] Nonseminomatous germ-cell tumors do not take up FDG as readily and therefore use is limited in this patient group. FDG PET has also been shown to be useful in the detection of recurrence when patients have raised tumor markers but no CT evidence of disease.[69]

References

1. Israel GM, Bosniak MA. How I do it: evaluating renal masses. *Radiology*. 2005;236(2):441–450
2. Benjaminov O, et al Enhancing component on CT to predict malignancy in cystic renal masses and interobserver agreement of different CT features. *AJR Am J Roentgenol*. 2006;186(3):665–672
3. Kennelly MJ, Grossman HB, Cho KJ. Outcome analysis of 42 cases of renal angiomyolipoma. *J Urol*. 1994;152(6 Pt 1):1988–1991
4. Zhang J, et al Solid renal cortical tumors: differentiation with CT. *Radiology*. 2007;244(2):494–504
5. Jinzaki M, et al Double-phase helical CT of small renal parenchymal neoplasms: correlation with pathologic findings and tumor angiogenesis. *J Comput Assist Tomogr*. 2000;24(6):835–842
6. Kuo PH, et al Gadolinium-based MR contrast agents and nephrogenic systemic fibrosis. *Radiology*. 2007;242(3):647–649
7. Yoshimitsu K, et al Papillary renal carcinoma: diagnostic approach by chemical shift gradient-echo and echo-planar MR imaging. *J Magn Reson Imaging*. 2006;23(3):339–344
8. Kocher F, Grimmel S, Hautmann R, et al Preoperative lymph node staging in patients with kidney and urinary bladder neoplasm. *J Nucl Med*. 1994;35(suppl):233
9. Levine E. Renal cell carcinoma: clinical aspects, imaging diagnosis, and staging. *Semin Roentgenol*. 1995;30:128–148
10. Larson SM, Schöder H. Advances in positron emission tomography applications for urologic cancers. *Curr Opin Urol*. 2008;18(1):65–70
11. Ghani KR, Pilcher J, Patel U, Rowland D, Nassiri D, Anson K. Three-dimensional ultrasound reconstruction of the pelvicaliceal system: an in-vitro study. *World J Urol*. 2008;26(5):493–498
12. John B, Ghani KR, Patel U, Anson K. Resin polymer and corrosion casting of the porcine pelvi-calyceal system: a useful model for investigating new imaging and endoscopic techniques of the upper urinary tract. *Urol Res*. 2008;36(1):39–42. Epub 2007
13. Ghani KR, Rintoul M, Patel U, Anson K. Three-dimensional planning of percutaneous renal stone surgery in a horseshoe kidney using 16-slice CT and volume-rendered movies. *J Endourol*. 2005; 19(4):461–463
14. Patel U, Ghani K, Walkden RM. Anson 3D CT Pyelography for Planning of Percutaneous Nephrostolithotomy: Accuracy of Stone Measurement, Stone Depiction and Pelvicalyceal Reconstruction *Eur Radiol*. 2009;19(5):1280–1288.
15. Pareek G, Armenakas NA, Fracchia JA. Hounsfield units on computerized tomography predict stone-free rates after extracorporeal shock wave lithotripsy. *J Urol*. 2003;169(5):1679–1681
16. Graser A, Johnson TR, Bader M, et al Dual energy CT characterization of urinary calculi: initial in vitro and clinical experience. *Invest Radiol*. 2008;43(2):112–119
17. Roy C, et al Assessment of painful ureterohydronephrosis during pregnancy by MR urography. *Eur Radiol*. 1996;6(3):334–338
18. Sudah M, et al Patients with acute flank pain: comparison of MR urography with unenhanced helical CT. *Radiology*. 2002;223(1): 98–105
19. Van Der Molen AJ, Cowan NC, Mueller-Lisse UG, et al CT urography: definition, indications and techniques. A guideline for clinical practice, *Eur Radiol*. 2008;18:4–17
20. McCarthy CL, Cowan NC. Multidetector CT urography (MD-CTU) for urothelial imaging. *Radiology*. 2002;225(P):237

21. Battista G, et al Computerized tomography virtual endoscopy in evaluation of upper urinary tract tumors: initial experience. *Abdom Imaging*. 2009;34(1):107–112
22. Takebayashi S. Computerized tomographic ureteroscopy for diagnosing ureteral tumors. *J Urol*. 2000;163(1):42–46
23. Sudah M, et al MR urography in evaluation of acute flank pain: T2-weighted sequences and gadolinium-enhanced three-dimensional FLASH compared with urography. *Am J Roentgenol*. 2001;176:105–112
24. Ingram M, et al Evaluation of the upper urinary tract using transureteric ultrasound- a review of the technique and typical imaging appearances. *Clin Radiol*. 2008;63:1026–1034
25. Nikken JJ, Krestin GP. MRI of the kidney-state of the art. *Eur Radiol*. 2007;17(11):2780–2793
26. Choi YJ, Kim JK, Kim N, Kim KW, Choi EK, Cho K. Functional MR imaging of prostate cancer. *Radiographics*. 2007;27:63–77
27. Oehr P, Bouchelouche K. Imaging of prostate cancer. *Curr Opin Oncol*. 2007;19:256–264
28. Rifkin MD. *Ultrasound of the prostate*. 2nd ed. Philadelphia: Lippincott-Raven; 1997
29. Pallwein L, Mitterberger M, Gradl J, et al Value of contrast-enhanced ultrasound and elastography in imaging of prostate cancer. *Curr Opin Urol*. 2007;17:39–47
30. Raja J, Ramachandran N, Munneke G, et al Current status of transrectal ultrasound-guided prostate biopsy in the diagnosis of prostate cancer. *Clin Radiol*. 2006;61:142–153
31. Ahmed H, Stevens D, Barbouti O, et al The role of transperineal template prostate mapping biopsies in risk-stratifying men with localised prostate cancer. *Eur Urol Suppl*. 2008;7:234
32. Pelzer A, Bektic J, Berger AP, et al Prostate cancer detection in men with prostate specific antigen 4 to 10 ng/ml using a combined approach of contrast enhanced color Doppler targeted and systematic biopsy. *J Urol*. 2005;173:1926–1929
33. Ophir J, Cespedes I, Ponnekanti H, et al Elastography: a quantitative method for imaging the elasticity of biological tissues. *Ultrason Imaging*. 1991;13:111–134
34. Nascimento RG, Coleman J, Solomon SB. Current and future imaging for urologic interventions. *Curr Opin Urol*. 2008;18:116–121
35. Garra BS. Imaging and estimation of tissue elasticity by ultrasound. *Ultrasound Q*. 2007;23:255–268
36. Konig K, Scheipers U, Pesavento A, et al Initial experiences with real-time elastography guided biopsies of the prostate. *J Urol*. 2005;174:115–117
37. Rubens DJ, Hadley MA, Alam SK, et al Sonoelasticity imaging of prostate cancer: in vitro results. *Radiology*. 1995;195:379–383
38. Taylor LS, Rubens DJ, Porter BC, et al Prostate cancer: three-dimensional sonoelastography for in vitro detection. *Radiology*. 2005;237:981–985
39. Shen F, Shinohara K, Kumar D, et al Three-dimensional sonography with needle tracking: role in diagnosis and treatment of prostate cancer. *J Ultrasound Med*. 2008;27:895–905
40. Abul FT, Arun N, Abu-Assi MA, et al Transrectal ultrasound guided biopsy for detecting prostate cancer: can random biopsies be reduced using the 4-dimensional technique? *Int Urol Nephrol*. 2007;39:517–524
41. Aigner F, Pallwein L, Pelzer A, et al Value of magnetic resonance imaging in prostate cancer diagnosis. *World J Urol*. 2007;25:351–359
42. Futterer JJ, Engelbrecht MR, Jager GJ, et al Prostate cancer: comparison of local staging accuracy of pelvic phased-array coil alone versus integrated endorectal-pelvic phased -array coils: local staging accuracy of prostate cancer using endorectal coil MR imaging. *Eur Radiol*. 17(4):1055–1065
43. Futterer JJ, Engelbrecht MR, Jager GJ, et al Staging prostate cancer with dynamic contrast-enhanced endorectal MR imaging prior to radical prostatectomy: experienced versus less experienced readers. *Radiology*. 2005;237:541–549
44. Westphalen AC, McKenna DA, Kurhanewicz J, et al Role of magnetic resonance spectroscopic imaging before and after radiotherapy for prostate cancer. *J Endourol*. 2008;22:789–794
45. Scheibler ML, Schnall MD, Pollack HM. Current role of MR imaging in the s staging of adenocarcinoma of the prostate. *Radiology*. 1993;189:339–352
46. Engelbrecht MR, Huisman HJ, Laheij RJ, et al Discrimination of prostate cancer from normal peripheral and central gland tissue by using dynamic contrast-enhanced MR imaging. *Radiology*. 2003;229:248–254
47. Kim JK, Hong SS, Choi YJ, et al Wash-in rate on the basis of dynamic contrast-enhanced MRI: usefulness for prostate cancer detection and localisation. *J Magn Reson Imaging*. 2005;22: 639–646
48. Rajesh A, Coakley FV, Kurhanewicz J. 3D MR spectroscopic imaging in the evaluation of prostate cancer. *Clin Radiol*. 2007;62:921–929
49. Prando A, Kurhanewicz J, Borges AP, et al Prostatic biopsy directed with endorectal MR spectroscopic imaging findings in patients with elevated prostate specific antigen levels and prior negative biopsy findings: early experience. *Radiology*. 2005;236(3):903–910
50. Zakian KL, Eberhardt S, Hricak H, et al Transitional zone prostate cancer: metabolic characteristics at ^{1}H MR spectroscopic imaging-initial results. *Radiology*. 2003;229:241–247
51. Shimofusa R, Fujimoto H, Akamata H, et al Diffusion-weighted imaging of prostate cancer. *J Comput Assist Tomogr*. 2005;29: 149–153
52. Kemper J, Sinkus R, Lorenzen J, et al MR elastography of the prostate: initial in-vivo applications. *Rofo*. 2004;176(8):1094–1099
53. Kim CK, Park BK. Update of prostate magnetic resonance imaging at 3T. *J Comput Assist Tomogr*. 2008;32:163–172
54. Beyersdorff D, Taymoorian K, Knosel T, et al MRI of prostate cancer at 1.5 and 3.0T: comparison of image quality in tumor detection and staging. *AJR*. 2005;185:1214–1220
55. Ocak I, Bernardo M, Metzger G, et al Dynamic contrast-enhanced MRI of prostate cancer at 3T: a study of pharmacokinetic parameters. *AJR*. 2007;189:W192-W201
56. Kurhanewicz J, Vigneron D, Carroll P, et al Multiparametric magnetic resonance imaging in prostate cancer: present and future. *Curr Opin Urol*. 2008;18:71–77
57. Anastasiadis AG, Lichy MP, Nagele U, et al MRI-guided biopsy of the prostate increases diagnostic performance in men with elevated or rising PSA levels after previous negative TRUS biopsies. *Eur Urol*. 2006;50:738–748
58. Fanti S, Nanni C, Ambrosini V, et al PET in genitourinary cancers. *Q J Nucl Med Mol Imaging*. 2007;51:260–271
59. Yamaguchi T, Lee J, Uemura H, et al Prostate cancer: a comparative study of 11C-choline PET and MR imaging combined with proton MR spectroscopy. *Eur J Nucl Med Mol Imaging*. 2005;32:742–748
60. Curiel L, Souchon R, Rouviere O, et al Elastography for the follow-up o fhigh-intensity focused ultrasound prostate cancer treatment: initial comparison with MRI. *Ultrasound Med Biol*. 2005;31: 1461–1468
61. Sedelaar JP, Aarnink RG, van Leenders GJ, et al The application of three-dimensional contrast-enhanced ultrasound to measure volume of affected tissue after HIFU treatment for localized prostate cancer. *Eur Urol*. 2000;37:559–568
62. Souchon R, Rouviere O, Gelet A, et al Visualisation of HIFU lesions using elastography of the human prostate in vivo: preliminary results. *Ultrasound Med Biol*. 2003;29:1007–1015
63. Kim CK, Park BK, Lee HM, et al MRI techniques for prediction of local tumor progression after high-intensity focused ultrasonic ablation of prostate cancer. *AJR*. 2008;190:1180–1185
64. Kirkham APS, Emberton M, Hoh IM, et al MR imaging of prostate after treatment with high-intensity focused ultrasound. *Radiology*. 2008;246:833–844

65. Donnelly SE, Donnelly BJ, Saliken JC, et al Prostate cancer: gadolinium-enhanced MR imaging at 3 weeks compared with needle biopsy at 6 months after cryoablation. *Radiology*. 2004;232: 830–832
66. Kravets FG, Cohen HL, Sheynkin Y, et al Intraoperative sonographically guided needle localization of nonpalpable testicular tumours. *AJR*. 2006;186:141–143
67. Browne RF, Jeffers M, McDermoot T, et al Intra-operative ultrasound-guided needle localization of impalpable testicular lesions. *Clin Radiol*. 2003;58:566–569
68. Heidenreich A, Weissbach L, Holti W, et al Organ sparing surgery for malignant germ cell tumour of the testis. *J Urol*. 2001;166: 2161–2165
69. Sohaib SA, Koh D, Husband JE. The role of imaging in the diagnosis, staging and management of testicular cancer. *AJR*. 2008;191: 387–395
70. De Santis M, Bechere A, Bokemeyer C, et al 2–18fluoro-deoxy-D-glucose positron emission tomography is a reliable predictor for viable tumour in post chemotherapy seminoma: an update of the prospective multicentric SEMPET trial. *J Clin Oncol*. 2004;22:1034–1039

Advances in Diagnostic and Therapeutic Ultrasonography

27

Charalampos Mamoulakis, Vassilios Tzortzis, Jorge Rioja Zuazu, Maria P. Laguna Pes, Stavros Gravas, Hessel Wijkstra, and Jean J. M. C. H. de la Rosette

Introduction

Ultrasonograpy (US) has been employed to image the human body for over half a century. It represents an established, versatile, and one of the most popular medical imaging modalities. The fact that it is rapid, effective, radiation free, noninvasive, relatively inexpensive, portable, and posing no known risks for human health allows it to be commonly used as a primary diagnostic imaging modality. It is extensively applicable as a reliable guidance tool in a variety of critical interventional procedures and represents an emerging therapeutic tool as well, mainly in the form of high-intensity focused US (HIFU). Modern US is primarily based on the application of a pulse-echo approach with a brightness-mode (B-mode) display, i.e., transmission of small ultrasound pulses, detection of echo signals from structures lying along the pulse path length, and final combination of the signals from many sequential, coplanar pulses into a tomographic "real-time" image.

US possesses a central role in the urologists' armamentarium. Since the first clinical applications in the 1940s, continued advances have expanded its role in the diagnosis, management, and follow-up of urological patients. During the last 15 years, it has undergone tremendous changes, which are about to bring it well beyond its established role as a noninvasive real-time imaging modality. Recent technological developments advanced its position in guiding urological procedures with higher precision and minimalization of morbidity, implementation of innovative treatment options (e.g., laparoscopic surgery or tumor ablation), and monitoring therapy response. This chapter focuses first on the innovations in ultrasound technology and second on their possible application in the field of urology.

Recent Technical Advances in B-Mode Ultrasonography

Latest technical improvements brought on profound alterations in US imaging. Some of these, such as encoded pulses and receive focusing, are nonadjustable and taking effect in the background. Others such as harmonics and compounding are operator-adjustable, representing real-time options. New promising technologies for better characterization of lesions include contrast-enhanced US (CE-US) and elasticity imaging techniques. The recent innovations that improve the performance of modern US equipment applicable in the field of urology are described below and are schematically presented in Table 27.1.[1–4]

Technical Innovations for Improved Resolution

Most new technologies aim at improving spatial resolution. These include digital beam formers, larger channel count, coded pulse excitation, harmonic imaging, spatial compound imaging, electronic focusing using array and matrix transducers, and endoscopic/intraoperative US.[1–4]

Digital Beam Formers and Larger Channel Count

Analog and digital beam formers provide pulse-delay sequences for electronic beam steering, transmit, and receive focusing. Single-element transducers have a sole fixed focal zone and are limited to mechanical steering and focusing. The number and location of focus points on the new systems are operator-assigned for changing the transmit focus. The receive focus is accomplished dynamically and is investigator independent.

Digital beam formers are preferable because they bear a number of advantages, including programmability, acceptance of a wide range of signal frequencies, dynamic aperture, and apodization capabilities. They expedite incorporation of different transducers and novel technologies (programmability function), offer the ability to accept new broad-bandwidth transducers with short-pulse and harmonic technology (wide frequency range), allow for keeping the beam width narrow for best resolution by minimizing the beam-width variation with depth (dynamic aperture), and finally permit

P. Dasgupta et al. (eds.), *New Technologies in Urology,*
DOI: 10.1007/978-1-84882-178-1_27, © Springer-Verlag London Limited 2010

Table 27.1 Recent technical innovations in ultrasonography

A)	**Technical innovations for improved resolution**
	Digital beam formers and larger channel count
	Coded pulse excitation technology
	Harmonic imaging
	Spatial compound imaging
	Electronic focusing by using array and matrix transducers
	Endoscopic and intraoperative ultrasonography
B)	**Technical innovations for improved lesion detection and differentiation**
	Elasticity imaging
	Contrast-enhanced ultrasonography
C)	**Other technical innovations**
	Extended field of view imaging
	Three- and four-dimensional imaging

variation of vibration amplitude during transmission and echo sensitivity during echo reception of adjacent structures (apodization). In conclusion, digital beam formers are desirable because of their improved spatial resolution, upgrade capabilities, use of broad-bandwidth technologies, and reduction of unwanted artifacts.

Channel count, i.e., number of beam formers (crystal elements per data line), determines the aperture size. The larger the channel count, the greater the number of elements that can be simultaneously activated to transmit a pulse/receive echo signals per beam line and the larger the aperture, resulting in improved lateral resolution.

Coded Pulse Excitation Technology

Imaging depth and spatial resolution constitute a fundamental trade-off in US. The effective imaging depth is determined by the pulse amplitude and frequency. The amplitude relates to the power setting on the system and is limited by safety considerations. Higher frequencies improve axial resolution at the cost of penetration depth. This can be overcome by coded pulse-excitation technology, which provides good penetration at the higher frequencies necessary for superior spatial resolution.[5]

This technology employs long high-energy pulses of comparable safety to the short waveform ancestors, specifically shaped for targeted detection by the transducer and submission of the returning echoes to special pulse-compression computer algorithms. The final result is an image with increased signal-to-noise ratio and preserved spatial resolution at larger depths.[5] Coded pulse-excitation is applicable in harmonic, compound, contrast, and Doppler technologies. No inherent disadvantages are encountered apart from increased cost, and therefore it represents a highly desirable feature for diagnostic US imaging.

Harmonic Imaging

Ultrasound imaging is degraded by many factors related to the different body wall layers, which constitute many sound interfaces responsible for reverberations that produce echoes leading to strong ring-down artifacts in the near field. Harmonic US is the detection and display of echoes that are integral multiples of the transmitted pulse frequency (fundamental or 1st harmonic; f_0). For example, the 2nd harmonic has twice the frequency of the fundamental ($2\ f_0$).

Tissue harmonic imaging uses B-mode technology. Harmonic frequencies (2nd, 3rd, etc.) are generated by the tissues, and the amplitude is increasing while the pulse is traveling through the tissue. Therefore, harmonic imaging represents a solution for eliminating the effects of skin surfaces (reverberations and ring-down). The intensity decreases with increasing harmonic order. Furthermore, higher frequency harmonic components are more attenuated. Therefore, harmonic imaging is currently performed mainly with the use of the 2nd harmonic component.

Briefly, the principle is the following[6]: a narrowband f_0 is transmitted, and harmonic frequencies are generated; echoes (f_0 and harmonics) reach the transducer; and the machine system filters out the f_0 and maximizes the harmonic signal. Apart from filtering, additional methods to isolate the harmonic component involve various subtractions and inversion pulse technologies.

In addition to the decreased clutter in the near field caused by ring-down from the body wall, resolution is improved because a higher than the transmitted frequency (2x) is received, lateral resolution is improved since harmonics are generated by the more powerful central portion of the transmitted f_0 beam, volume averaging is avoided since the beam is effectively narrower, and side/grating lobes are too week to generate harmonic signals.[6] As a result, harmonic imaging improves the clinically useful artifacts (shadow and through transmission) and reduces the "nasty" ones (lobe, ring-down and volume averaging), especially in systems with concurrent coded pulse technology.

Spatial Compound Imaging

Electronic steering of parallel beams from an array transducer oriented along different directions is used to image a specific tissue multiple times. Echoes acquired at different angles are averaged together into a single composite real-time image. A greater computational time compared with conventional B-mode imaging is necessary since multiple, rather than one, beams are used. Moreover, spatial compounding is prone to sharpness reduction caused by blurring artifact due to poor registration or misalignment of individual frames as a result of distortions from

refraction and speed-of-sound errors among individual frames.

Similar to tissue harmonic imaging spatial compounding is operator-adjustable and can be optimized. Blurring artifact is related to the number of beams merged into each image. Lower beam compounding rates are more suitable for areas with higher motility, while higher numbers of beams are typically reserved for areas with less motion. Speckle, noise, clutter, and refractive shadows are often reduced, while contrast and marginal definition is improved.[7]

Electronic Focusing by Using Array and Matrix Transducers

Mechanical focusing in the Y axis is achieved by the placement of a lens in front of the piezoelectric element or a shaped element on the surface of the transducer. Array transducers carry a row of crystal elements, allowing for electronic focusing in the X direction. Matrix transducers have multiple rows of elements, which allows for electronic focusing in the X and Y direction. By steering the beam in the X and Y planes, three- and four-dimensional (3D/4D) images can be acquired.

Endoscopic and Intraoperative Ultrasonography

Endoscopic or endoluminal US (EUS) is based on the use of flexible endoscopes carrying high-frequency transducers at their tips, and thereby have a high-axial resolution. Another advantage is that the amount of interactions that affect an ultrasound wave before it interacts with the tissue of interest is decreased. EUS probe can consist of, e.g., 3.5–6.2 F, catheters containing a rotating ultrasound transducer with a frequency in the order of 9–30 MHz. In this case, the catheter-based transducer attached to the ultrasound system rotates continuously resulting in a 360° real-time cross-sectional images.

Intraoperative US can be used in laparoscopic or open surgical procedures, allowing for direct contact of the transducer on the organ of interest. Therefore, higher frequencies can be used since the penetration requirement is reduced, and finally, a better resolution is achieved. Recent advances include the incorporation of new technology such as specially formed probes (endoluminal, laparoscopic, transrectal, and transvaginal) and several functions (Doppler, harmonic, 3D/4D imaging, elastography CE-US, etc.) with the potential to enhance visualization of the surgical anatomy even beyond the surgical view increasing operational precision.[8] It can identify, for example, the location and depth of lesions to guide the proper dissection plane within the kidney; it may be used during partial nephrectomy to identify additional occult tumors and can also be utilized transrectally to guide the plane for neurovascular bundle dissection and reduce the incidence of positive surgical margins during laparoscopic radical prostatectomy.[4]

Technical Innovations for Improved Lesion Detection and Differentiation

Elasticity Imaging

Elastography is a real-time, noninvasive method to image tissue hardness. It represents an extension of the ancient art of palpation and of earlier B-mode US-based methods to view resultant tissue deformation/stiffness by palpation ("sonopalpation"). The basic approach is to measure tissue motion caused by force, to reconstruct the elastic parameters of the tissue. In most cases, US is used to detect the motion or displacement resulting from the applied stress. The excitation stress can be either mechanical (static; slight compression with the transducer or dynamic; mechanical vibrators) or the radiation force of an ultrasound source; either static or dynamic (transient methods, shear-wave methods, and vibroacoustography).[9]

The basic principle is the following[10]: two radiofrequency signal sets are used; a precompression and a postcompression one. The first set of echoes returned to the transducer is analyzed before being converted to the B-mode image and the resultant frame is stored. The second set is produced and stored during applying the excitation force to the tissue. The two radiofrequency waveforms are windowed. The signal in each precompression waveform window is cross-correlated with a similar segment of the postcompression waveform and the amount of shift occurred is found. The shift amount of the signal equals the amount of tissue displacement at that point in the image frame. The same process is followed for each image frame point. The "strain" (rate-of-change) values are displayed to form an "elastogram." Hard tissues move as a unit and are displaced about the same amount when compressed. Therefore, the displacement rate-of-change versus depth tends to zero. Softer tissues present much more displacement closer to the compressing transducer than further away, i.e., a larger displacement rate-of-change versus depth (large strain values). Therefore, harder areas within soft tissues show low strain values and are displayed dark, whereas softer areas show higher strain values and are displayed bright on the elastogram.

Classic parameters to describe tissue stiffness include the *Young elastic modulus* (change in length of a material in relation to the stretching/compressive force applied) and the *shear modulus*, which relates the deformability of a material in response to force applied parallel to one of its surfaces.

The latter is computed directly by US estimation of the shear wave velocity and can be used for the estimation of the former.

Contrast-Enhanced Ultrasonography

The resolution of conventional Doppler US is limited to vessels of approximately 1 mm in size, which is insufficient to image the microvascular bed associated with, e.g., tumor neovascularity (10–50 μm). New functional imaging techniques and the introduction of contrast agents together with special perfusion software (e.g., vascular recognition imaging software, Toshiba) has enabled the detection of even the smallest vessels. Contrast agents consist of intravenously injected microbubbles with a diameter, in the range of 1–10 μm, i.e., small enough to penetrate into the smallest microvssels after passing through the pulmonary circulation.[2, 11, 12]

Microbubbles are nowadays made by a central core of a gas suspension in an aqueous carrier and an outer shell. The gas is innocuous, fluorinated, with low solubility and spreading capability (e.g., sulfur hexafluoride, octafluoropropane, or decafluorobutane). The surrounding capsule is made of albumin or polymer, coated with a lipid or a surfactant for stabilization (prevention of coalescence) and life-span prolongation. The ideal agent should be deprived of significant side effects, allergic potential, or nephrotoxicity and must survive during the journey through the circulation toward the target.

Microbubbles have progressively evolved from the first generation such as Levovist® (Schering, Berlin, Germany) into the "modern" second-generation agents, which use an immunologically inert lipoprotein shell, an inert gas and emit more efficiently the ultrasound signal. Among the most widely used agents today are SonoVue® (Bracco Imaging, Milan, Italy), Optison® (Amersham Health AS, Oslo, Norway), and Definity® (Bristol-Myers Squibb, Billerica, Massachusetts). These agents differ in terms of their physical properties. Modern bubbles are safe to use, and only minor side effects have been reported (alteration of taste, general/facial flush, local pain at the injection site).[13]

Contrast agents contract and expand in response to pressure oscillations of the ultrasound beam generating a scattered field. They are very efficacious ultrasound scatters, producing much stronger backscatter than blood or normal tissue because of the extremely large differences between the acoustic impedances of the gas inside the bubbles and the surrounding liquid. Therefore, contrast agents provide the ideal way for imaging a prostate or kidney tumor, by means of microvessel imaging.

Contrast agents are imaged in general by two basic methods[11]: Color/Power Doppler (CD/PD) US and gray-scale harmonic imaging. Owing to the relative high-energy levels used, conventional Doppler US disrupts most of the microbubbles before their advent to the microvasculature. With PD-CE-US, extra reflections of ultrasound signals in the blood flow after the administration of microbubbles enhance the Doppler signal. When exposed to ultrasound energy, microbubbles display nonlinear behavior because they are able to expand more than they can contract. Signal reflected from tissues is mainly at the transmitted fundamental frequency. However, signal reflected by microbubbles contains harmonics of the fundamental frequency, selectively visualized by ultrasound post-processing techniques providing enhanced visualization. Gray-scale harmonic imaging techniques use lower energies resulting in less bubble destruction.

Continues harmonic imaging has been further improved with the implementation of different techniques such as pulse inversion, intermittent harmonic imaging, flash-replenishment, and cadence contrast-pulse sequence (CPS), allowing for detailed view of the microvasculature. Intermittent harmonic imaging uses low energy to avoid bubble destruction and limited number of frames of high energy to visualize the bubbles.[14] Flash-replenishment techniques involve high-power flash pulses to destroy the microbubbles, followed by low-power pulses to visualize contrast replenishment.[15] CPS processes the reflections of a series of pulses with different amplitudes and phases, which results in an optimized contrast-to-tissue ratio, and a microbubble contrast-only image is constructed.[16–18]

The interpretation of CE-US information is based on a subjective estimation. It is considered highly operator-dependent and a learning curve definitely applies.[13] Various methods have been described for introducing objectivity in the assessment of images and bypass this inherent limitation.[16] Extra time and costs represent further disadvantages. For example, it has been reported that the total investigation time of a prostate CE-US study is increased by 5–10 min.[13]

Other Technical Innovations

Extended Field of View Imaging

Some lesions is impossible to be imaged with a routine ultrasound scan plane, especially superficial lesions, longer than the transducer footprint, or when imaging with array transducers. In these cases, extended field of view technology allows for including the entire lesion in one image. The transducer slowly moves across the large anatomic region of interest, numerous images are acquired from many positions, and the computer algorithm registers the images with respect to each other, accounting for both translation and rotation of the transducer. The relative positions of the images are determined by comparison of data features in the overlapping regions and analyzed appropriately to form the complete

large extended field of view image. This mode is very useful, for example, when the testis is markedly enlarged and cannot fit in one view.[2]

Three- and Four-Dimensional Imaging

The improved resolution achieved to date due to the recent advances in ultrasound technology described earlier, together with the sufficient computing power presently available, has made possible 3D renderings of ultrasound images and their real-time delivery (4D imaging), producing whole volume view of solid structures.[19]

This technology allows for the creation of a 3D image from several 2D images. 4D-US incorporates a temporal dimension to 3D technology, and it is useful for performing volume assessments as a function of time in dynamic systems. It is achieved through rapid refresh rates of consecutive 3D image sets.[20]

Potential advantages of this technology include[2]: (a) elimination of user-dependent scanning variation, (b) increased measuring accuracy of volumes, (c) better appreciation of the anatomic relationships, (d) greater confidence of interpretation, (e) short image-acquisition time, (f) ability of computer enhancement with image registration software that permits postprocessing image manipulation in any plane to derive further information, and (g) easier exam to exam comparison that facilitates follow-up.

Potential limitations are: (a) the need for highly trained personnel to reduce the possibility of artifact introduction during initial scan or data analysis and (b) higher investment costs in a computational infrastructure to meet the hardware, software, transfer/retrieval, and support requirements of this technology. Although the results appear promising, the clinical additional value still has to be determined.

Applications of Novel Ultrasonography Technologies in Urology

Prostate

Elasticity Imaging

The rationale behind the use of elasticity imaging for the detection of prostate cancer (PCa) is that these tumors are firmer than the surrounding normal parenchyma. Prostate was the first organ to be considered for both elastography and sonoelasticity imaging, i.e., the method using CD-US to detect tissue vibrations resulting from acoustic vibrations in the audible range transmitted to the organ.[10]

The results based on a number of recent studies are promising.[21–33] These studies can be schematically divided into two broad, conceptually overlapping categories: (a) Group A (Table 27.2): studies that evaluate the technique as a diagnostic tool for PCa detection based on images (no targeted biopsies obtained),[23–27, 30, 31, 33] (b) Group B: studies that evaluate the method as a tool to support or replace transrectal ultrasound (TRUS)-guided systematic biopsy based on elastography-targeted biopsy results.[21, 22, 28, 29, 32]

Cochlin et al conducted the first clinical trial including 100 patients to investigate whether adding elastography imaging with targeted biopsies of abnormal areas on gray-scale ultrasound-guided systematic biopsy improves PCa detection rate.[21] Although the sensitivity of elastography was not high enough to permit replacement of gray-scale imaging, its addition to the standard biopsy technique was justified because it detected three extra patients at the expense of eight extra cores.

König et al investigated 404 patients with a systematic sextant biopsy protocol under conventional B-mode US in conjunction with elastography imaging.[22] A pathological finding was seen on the elastograms in 84.1% of patients with PCa. Only 64.2% of patients were detected after DRE and/or TRUS. They concluded that PCa can be detected with a high degree of sensitivity using this technique in conjunction with conventional diagnostic methods for guided biopsies.

Elastography-guided prostate biopsy has been compared directly with systematic biopsy in 230 screening volunteers.[28] One investigator performed up to five targeted biopsies in the peripheral zone and subsequently, blindly to previous results, another investigator performed 10 systematic biopsies guided by conventional gray-scale TRUS. PCa was detected in 35% of the population. Targeted biopsy protocol did not detect significantly more patients with PCa compared with systematic biopsy protocol (30% vs. 25%, respectively). However, the difference in detection rates per core was significant (targeted vs. systematic: 12.7% vs. 5.6%). Targeted biopsy in a patient with PCa has been found to be 2.9-fold more likely to detect the tumor. Therefore, targeted biopsy protocol detected more cases of PCa with fewer than half the number of cores. No significant differences have been detected in the distribution of Gleason scores. The detection rate for targeted biopsy has been slightly better in the apical areas.

To compare the detection of PCa and distribution of Gleason scores, targeted biopsies based on conventional TRUS, CD-US, and elastography were obtained along with systematic sextant biopsies in 137 patients.[29] Targeted cores were more likely than systematic cores to detect PCa. Positive results on CD-US and elastography were strongly associated with high-grade and moderate-to-high-grade cancers, respectively. It was concluded that although CD-US and elastography are encouraging adjuncts to improve PCa detection, targeted biopsy alone is not sufficient to replace sextant biopsy technique.

Table 27.2 Studies evaluating the role of elasticity imaging as a diagnostic tool for prostate cancer detection: Review of the literature

Reference	Patients (PCa)	Reference Standard	Diagnostic modalities Compared		Main results
Taylor, 2005[a,23]	19	RPS	3D-SE	3D-US	3D-SE performed considerably better in the depiction of PCa for tumors with volumes ≥1 cm^3
Miyanaga, 2006[24]	29[b]	Biopsy	E	TRUS/DRE	Detection rate was significantly higher for E (93%) compared with TRUS (55%) and DRE (59%) The two patients missed had well-differentiated PCa
	11[c]				Detection rates similar for E (55%), TRUS (55%), and DRE (64%) in previously treated patients
Pallwein, 2007[25]	15	RPS	E	–	E can detect PCa foci with very good accuracy (92%) Best sensitivity at the apex-mid gland
Tsutsumi, 2007[26]	51	RPS	E	TRUS	Detection rate for E (84%) superior to TRUS (31%) Detection rate for combined modalities (100%) Excellent detection for anterior tumors. Lower detection rate for higher-grade tumors
Sumura, 2007[27]	17	RPS	E	TRUS/DRE	Detection rate for E (74.1%) superior to TRUS (48.1%), DRE (33.3%), CD (55.6%), and MRI (47.4%)
				CD/MRI	Detection rates equal at anterior–posterior sides, higher for higher Gleason scores and tumor volumes
Pallwein, 2008[30]	492	Biopsy	E	TRUS	E accurately predicts PCa. Promising results especially in the apex
Salomon, 2008[31]	109	RPS	E	–	E can detect PCa foci with good accuracy (76%) E findings correlate best in the apex The detection rate increases with higher Gleason score (up to 93% for scores >7)
Eggert, 2008[d,33]	351	Biopsy	E	TRUS	Histopathological findings predicted by E in only 44.5% of cases. E does not improve detection rate

PCa = Prostate cancer, RPS = radical prostatectomy specimens, 3D-SE = three-dimensional sonoelastography, US = gray-scale ultrasonography, TRUS = Conventional transrectal ultrasonography, DRE = digital rectal examination, CD = color doppler, MRI = magnetic resonance imaging
E = elastography
[a]Imaging performed in vitro
[b]Previously untreated patients
[c]Patients treated previously with hormone therapy. Elastography detection rate dropped possibly due to lesion softer-rendered consistency by treatment
[d]A randomized clinical trial, in which both arms have been submitted to conventional TRUS-guided 10-core biopsy. One arm has additionally been offered elastography prior to biopsy.

Kamoi et al compared the performance of elastography with conventional TRUS and PD-US in the detection of PCa evaluating a clinical population 107 males.[32] All of them were submitted to transperineal systematic eight-core biopsies. Up to four biopsies were added based on suspicious findings of each modality. Patient analysis showed that the sensitivity of TRUS was significantly lower (50%) than that of PD-US (70%) and elastography (68%), but specificity did not differ significantly. All modalities showed comparable accuracies ranging from 72% (TRUS) to 76% (elastography), and the diagnostic performances did not differ significantly. The diagnostic performances of pair-wise or all-three modalities combinations also did not differ significantly. However, analysis by core showed that the detection rate of the PD-US and elastography combination was significantly higher than that of systematic biopsy. It was concluded that elastography may complement conventional US to minimize the number of missing cancers.

Based on the current data described earlier, elastography combined with TRUS, constitutes a simple, noninvasive, relatively cheap technique, allowing for targeted biopsies and may reduce the number of biopsy cores per patient. Nevertheless, further clinical trials are still necessary and already on the way to better define the advantages and the exact role of this relatively novel technique in the diagnosis of PCa.[34]

Apart from a possible role in the diagnosis of PCa, elasticity imaging techniques may be useful for monitoring HIFU ablation therapy in PCa because HIFU lesions are stiffer than the surrounding normal untreated parenchyma. Promising results have been recently published implying that elastography might be able to replace MRI in these cases, but

further clinical trials are still needed before this application is considered established.[35, 36]

Contrast-Enhanced Ultrasonography

The advent of microbubble-based contrast agents represents a major revolutionary innovation in US. These agents in combination with novel "contrast-specific" imaging modes (e.g., pulse inversion harmonic imaging) pave the way for several new indications for CE-US in urology. In prostate, contrast agents may potentially facilitate the detection of cancer, providing additional information on tumor size (Fig. 27.1) and possibly aggressiveness, as well as the monitoring of antiangiogenic treatment results.[37] This is because prostate cancer shows an increase in both cell density and vascularization. The increased cell density leads to change in elasticity and may be visualized with elasticity imaging techniques as already described earlier; the increased vascularization can be visualized with CE-US.

To determine the value of CE-US in the detection, localization, and treatment follow-up for PCa, a multicenter research coordination project was carried out in four European countries during the period 2002–2006 (CONTRAST, QLRT-2001–2174). Recently, the project results based on 3,746 patients have been reported in comparison to published data outside this research group.[13] The individual studies of this project published, employed various contrast agents imaged by a) CD-US,[38–43] b) 3D-PD-US,[44–47] and c) novel nonlinear imaging techniques (CPS).[16]

The correlation of histological findings in radical prostatectomy specimens with preoperative CE-US images regarding tumor localization seems to be promising, showing that technical improvements have led to an increased sensitivity for the detection of perfusion patterns. Visualization of lesions with increased microvascular density was feasible both with the use of 3D-CE-PD-[46] and CE-CD-US.[48] 3D-CE-PD-US has been found to be a better diagnostic tool than digital rectal examination (DRE), prostate specific antigen (PSA) level, gray-scale, or PD-US, and the most suitable diagnostic predictor for PCa has been found to be the combination of 3D-CE-PD-US and PSA level.[44] Based on wide-band harmonic imaging, it has been shown that CE-US improves the sensitivity for PCa detection but also demonstrates focal enhancement in areas of benign hyperplasia.[49] Nevertheless, accurate detection of localized tumors has been reported in up to 78% of patients with 3D-CE-PD-US.[47, 50] In a larger group of 70 patients evaluated with the same technique, diagnosis by imaging alone has been improved from 61% (standard detection and staging investigations) to an average of 86% of tumors with detection of loci ≥5 mm in 68–79%.[51] In another small series, all T3 tumors could be identified using microvascular imaging (Philips).[13]

The clinical value of these promising results should be tested in a diagnostic setting. The effect of CE-US on the prostate biopsy protocol and detection rate has been

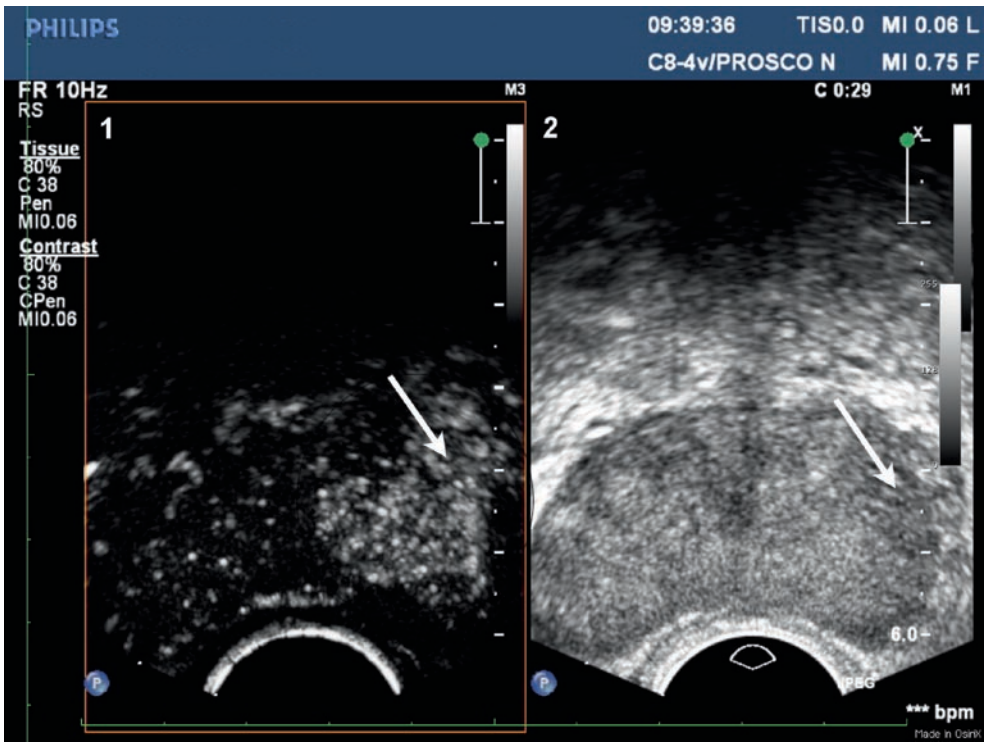

Fig. 27.1 Contrast-enhanced (1) and conventional trans-rectal ultrasonography of the prostate in the same patient with prostate cancer (2) The suspicious lesion is depicted as a hypoechoic area (white arrow) in conventional trans-rectal ultrasonography. A much larger lesion is depicted by contrast enhancement (2: white arrow). Contrast agents may facilitate the detection of cancer providing additional information on tumor size

extensively investigated. The combined research European Community project concluded that a clear association between prostate contrast enhancement and diagnosis of clinically significant PCa exists. The sensitivity for diagnosis is increased by CE-US targeted biopsies, fewer biopsies are needed to achieve the same detection rate, and the tumors detected by targeted biopsies present a higher Gleason score than those detected by random biopsies.[13]

These findings are in accordance with the promising results from studies outside the European research project. By employing various CE-US methods, including novel nonlinear imaging techniques (intermittent harmonic imaging, flash-replenishment, CPS), these studies either directly compared gray-scale ultrasound-guided systematic with CE-targeted biopsy protocols[14, 15, 52, 53] (Table 27.3) or investigated the contribution of CE-US on systematic biopsy protocols[54–57] and its value in predicting the nature of hypoechoic lesions.[17, 18, 58]

Currently, CE-US enables visualization of PCa and targeted biopsies applied upon a random protocol do increase detection rate. However, sensitivity/specificity is still not enough to avoid systematic random biopsies. Therefore, CE-US does not yet have a role in routine clinical practice. Many studies are on the way and a large prospective multicenter study supported by Bracco Imaging, Milan, Italy, has been initiated in an attempt to prove that currently available CE-US techniques can be used in PCa diagnosis and that targeted are superior to systematic biopsies.

The ability of CE-US to image prostate perfusion might enable visualization of minimal invasive or medical treatment effects that influence the perfusion of the organ (HIFU/cryoablation, hormone therapy) in PCa and identify patients with early relapse using the presence or absence of blood signals as an indicator.[59]

In patients submitted to HIFU before radical prostatectomy, it has been shown that the blood flow absence indicated by 3D-PD-US following administration of contrast agent (Levovist®) reflects affected tissue after ablation and volume measurements of these areas can quantify the amount of affected tissue.[45] Unfortunately, in a study investigating the prediction of the HIFU-induced destruction uniformity, it has been shown that pretreatment evaluation cannot identify the nonresponders beforehand.[60] Thirty-five patients with PCa underwent pre- and postcontrast (Levovist®) CD-US of the prostate before HIFU treatment. Tissue destruction seen in posttreatment random biopsies did not correlate with the preoperative US findings.

Another application of CE-US is to monitor hormonal treatment in patients with PCa. It has been reported that the vascular enhancement of the carcinoma detected by CD- and PD-US after the administration of Levovist® declines with hormonal therapy similar to PSA and can be used to monitor therapy.[39]

Apart from the potential "conventional" applications of CE-US discussed earlier, in PCa, other more sophisticated applications in the diagnosis and treatment at a cellular level such as molecular imaging and sonoporation represent an exciting field of urological research and will be the next frontier to be reached.[37]

Molecular imaging (visualization of biological processes at the cellular/molecular level in living systems) aims at viewing and quantifying early molecular changes associated with disease, rather than the resulting morphological changes. The superior sensitivity of contrast-specific imaging modes may render US an ideal tool for noninvasive, real-time observation of in vivo biological events at the molecular level in the vascular compartment. Efforts have been recently put on the design/preparation of specific ligands bound on the phospholipid-stabilized shell. This will result in specific localization of the targeted bubbles on selected vascular receptor sites upregulated in pathologies such as neoangiogenesis. They will then potentially serve as molecular targets for diagnosis and/or as therapeutic agents.

Sonoporation is a physical method that results in increased cell permeability through acoustic cavitation caused by US application in the presence of contrast agents. One of the explanations is that cavitation causes the implosion of microbubbles generating microjets, which open pores through cell membranes, allowing for direct transfer of drugs/genetic material into the cytoplasm. Pore opening is reversible, allowing for preservation of cell viability and transient with duration of a few seconds.[61] Gas and shell properties of the contrast agents have an important influence on cell transfection,[62] and hard-shelled ones (gas microcapsules) are promising candidates for ultrasound-mediated gene delivery.[63]

Recently, it has been shown that PCa cells could be transfected both in vitro and in vivo, via microbubble-enhanced US with short antisense oligodeoxynucleotides that downregulate the androgen receptor, decreasing its expression.[64] In PCa, intratumoral delivery of DNA-Optison followed by therapeutic ultrasound has been proposed as an effective, nontoxic gene delivery method providing a safe clinical alternative to current viral gene-delivery approaches where short-term gene expression is needed.[65] Delivery for example of angiogenic inhibitors in PCa by this method seems to be feasible.[66]

Three- and Four-Dimensional Imaging

Early work on prostate imaging identified several advantages of 3D technology over 2D TRUS imaging with an improved diagnostic capacity,[67] accurate diagnosis of extraprostatic tumor extension, and staging of localized PCa.[68, 69] The 4D technique has been used during TRUS-guided prostate

Table 27.3 Diagnostic performance of contrast-enhanced targeted compared to systematic gray-scale ultrasound guided biopsies of the prostate: Review of the literature

	Reference	Patient analysis					Biopsy core analysis							Contrast-enhanced ultrasound		
		Total	PCa (%)			TB vs SB P value	Total	TB	PCa (%)			TB vs SB		Technique (MHz)	Machine	Contrast Agent
			TB	SB	TB+SB				Total	TB	SB	OR (95% CI)	P value			
European Research Coordination Project	Frauscher, 2002[38]	230	24.4	22.6	30.0	n.s.	3439	1139	7.0	10.4	5.3	2.6 (1.9–3.5)	<0.001	CD (9)	Sequoia 512[a]	Levovist
	Pelzer, 2005[40]	380	27.4	27.6	37.6	n.s.	5700	1900	8.6	32.6[b]	17.9[b]	3.1 (n.a)	<0.01	CD (9)	Sequoia 512[a]	SonoVue
	Mitterberger, 2007[c,41]	690	26.1	24.1	32.0	n.s.	10317	3417	7.6	11.1	5.8	n.a	<0.001	CD (9)	Sequoia 512[a]	SonoVue
	Mitterberger, 2007[d,42]	100	32.0	26.0	29.0	0.04	750	250	9.7	15.6	6.8	–	<0.001	CD (9)	Sequoia 512[a]	SonoVue
	Mitterberger, 2008[e,43]	36	33.3	16.7	33.3	0.04	540	180	12.2	17.0	10.0	2 (n.a)	0.027	CD (9)	Sequoia 512[a]	SonoVue
	Pallwein, 2008[16]	20	40.0	25.0	40.0	n.s.	n.a	n.a	n.a	n.a	n.a	n.a	n.a	CPS (4–5)	n.a	SonoVue
	Frauscher, 2001[52]	84	27.4	20.2	28.6	0.034	1249	409	7.7	13.4	4.9	4.3 (2.6–7.1)	<0.001	CD (9)	Sequoia 512[a]	Levovist
	Halpern, 2005[h,14]	301	27.6	30.9	34.6	n.s.	2939	1133	363	15.4	10.4	2.0 (n.a.)	<0.001	CD/PD/CHI/IHI (6.5)	Sonoline Elegra[f]	AF0150[g]
	Linden, 2007[15]	60	21.7	26.7	30.0	n.s.	825	225	9.6	12.9	8.3	2.0 (n.a.)	0.034	MFI	Aplio	Definity
	Colleselli, 2007[53]	345	77.4	73.0	n.a.	n.s.[i]	5175	1725	–	–	–	–	–	CD (9)	Sequoia 512[a]	SonoVue

PCa = Prostate cancer, TB = targeted biopsy, SB = systematic biopsy, OR = odds ratio, n.s. = not significant, n.a. = not available, CD = color doppler, CPS = cadence contrast-pulse sequence, PD = power doppler, CHI = continues harmonic imaging, IHI = intermittent harmonic imaging, MFI/Aplio= microflow imaging (Toshiba American Medical Systems, Tustin, California; flash replenishment method)

[a]Siemens Medical Mountain View, CA, USA

[b]Detection rate based on number of positive cores per total number of cores in the 143 men with PCa detected by combined approach

[c]Impact on Gleason score was studied: TB detected significantly higher Gleason scores compared to SB and may allow for identification of more aggressive tumors

[d]The only randomized clinical trial to date. Two arms of 50 men undergone either systematic or contrast enhanced targeted biopsies of the prostate

[e]The short-term (14 days) application of dutasteride may be promising to improve cancer detection by contrast-enhanced targeted ultrasound guided biopsies due to blood flow reduction in benign prostatic tissue

[f]Siemens Medical Systems, Issaquah, WA, USA

[g]Imcor, San Diego, CA, USA

[h]IHI provides a statistically significant advantage over gray-scale and Doppler imaging but not over CHI. It improves significantly the characterization of tissue as benign versus malignant and may therefore improve PCa detection but the technique is not sufficient to definitely differentiate benign from malignant tissue without biopsy confirmation

[i]A statistically significant difference in PCa detection rate in favor of contrast-enhanced ultrasound was detected only in small prostate glands (69% vs 88.1% and 70.4% vs 80.8% for prostate volumes of <20 ml and 20–30 ml, respectively)

biopsies improving diagnostic accuracy. Further clinical applications of 3D TRUS include assessing placement for brachytherapy seeds-treatment mapping and guidance for cryoablation of localized PCa in candidates unsuitable for surgery.[67]

Recently, a novel computer-aided US technology, based on tissue characterization algorithms (HistoScanning™; Advanced Medical Diagnostics, Waterloo, Belgium), has been developed. This tissue differentiation, visualization, and quantification tool identifies specific changes in solid-organ morphology by extracting and quantifying statistical features from 3D backscattered ultrasound radio frequency data. The geometric accuracy of the system facilitates identification of minimal, localized tissue structures. The characterization algorithms exploit the physical changes to sound waves that result from the interaction of the ultrasound beam and the cancer tissue (energy loss, erratic spatial energy distribution, and increased entropy). They can be applied in discrete regions of interest in the prostate. Thus, the presence of PCa can be ascertained within minute, discrete tissue volumes. Prostate HistoScanning™ can spatially orientate cancer within the gland, enabling both determination of its location and volume. It has been reported that this technology can accurately detect foci of ≥0.50 mL[70] and has been proposed as a potential triage test for men deemed to be at risk of PCa who wish to avoid biopsy.[71]

Kidney

Contrast-Enhanced Ultrasonography

CE-US can play an important role in differentiating/characterizing solid lesions and complex cystic masses of the kidney. Tamai et al[72] assessed the value of CE-US in the diagnosis of solid renal tumors in comparison to contrast CT. CE-US has been found to be more sensitive in the detection of slight tumor blood flow and a useful tool in the preoperative diagnosis mainly of hypovascular malignant renal tumors.

CE-CD-US has been shown to achieve better results in the detection of tumor vascularity and the discrimination between benign and malignant small renal masses than the conventional CD-US.[73] The detection rate of intra-and/or peritumoral vessels with the use of contrast agents was twice that achieved without their use.

Ascenti et al[74] compared CE-US with triple-phase helical CT in the classification of complex renal cysts using the Bosniak system and found a complete concordance in the differentiation of surgical and nonsurgical complex cysts with a high interobserver agreement. In a similar study comparing CE-US with CT, Park et al[75] found that CE-US has a better diagnostic accuracy, although the difference was not significant. CE-US might better visualize septa number, septa and/ or wall thickness, solid component, and the enhancement of some renal cystic masses, resulting in upgrading of the Bosniak classification and a change in the treatment plan.

The characteristics of renal tumor perfusion detected by CE-US based on CPS technology have been investigated and have been compared with clinical diagnoses and histological findings.[76] It has been reported that CPS may have a future role in determining perfusion patterns in kidney tumors (Fig. 27.2). CE-US based on CPS technology has also been evaluated in the diagnosis of small renal masses (<4 cm).[77] Similar diagnostic accuracy to multidetector CT has been shown for renal masses of 2–4 cm, whereas CE-US has been reported to be superior for lesions smaller than 2 cm.

The increasing use of ablation techniques for the management of small renal masses poses the problem of optimal monitoring of ablated tumors. Since success is defined as absence of contrast enhancement on CT or MRI, CE-US may also play a role in the follow-up of such cases (Fig. 27.3). It has been shown that CE-US has the potential of monitoring radiofrequency ablation (RFA) of renal tumors in animal models.[78] In addition, it has been demonstrated that CE-US based on CPS technology can be used to characterize perfusions defects at different times, during the follow-up, after renal cryoablation[79](Fig. 27.4). Nevertheless, additional clinical studies are necessary to define precisely the potential of this imaging technique for the characterization and follow-up of indeterminate cystic masses, and further larger-scale prospective studies comparing CE-US with CT are still needed.

The new emerging field in CE-US is the generation of targeted microbubbles to specific neoangiogenesis or tumoral antigens to provide a tumor target therapy with antitumor agent-labeled microbubbles in the future.

Other Applications of Novel Ultrasonographic Technologies

Elasticity imaging for visualization of renal masses has only recently been investigated in vivo. Fahey et al[80] evaluated acoustic radiation force impulse imaging for real-time visualization of abdominal malignancies including two renal masses. They provided the first images of renal tumors in the human acquired in vivo using elasticity imaging and concluded that acoustic radiation force impulse imaging improves the visualization of kidney malignancies compared with the sole use of conventional US.

Elasticity imaging has also been recently evaluated as a possible aid in RFA in porcine kidneys by monitoring phase changes in the echo signals caused by speed of sound variations and thermal expansion with temperature.[81] A significant

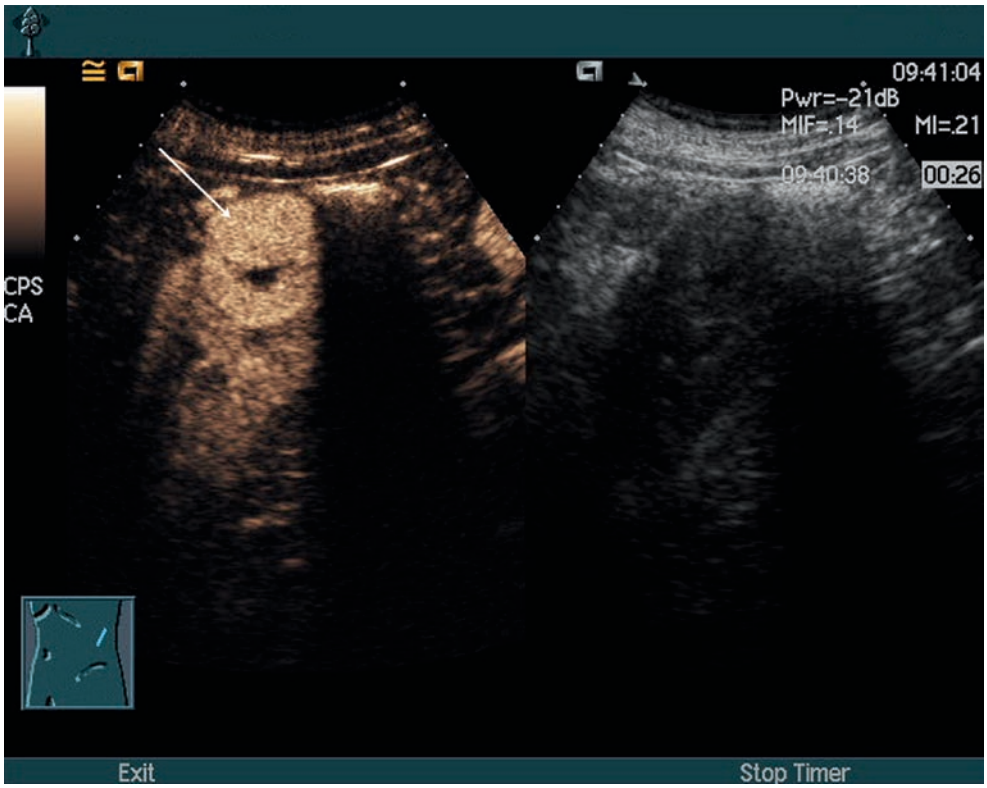

Fig. 27.2 Contrast-enhanced ultrasonography of the kidney. The presence of a renal tumor is imaged by cadence contrast-pulse sequence technology (white arrow). The presence of the tumor is better visualized compared with conventional B-mode imaging

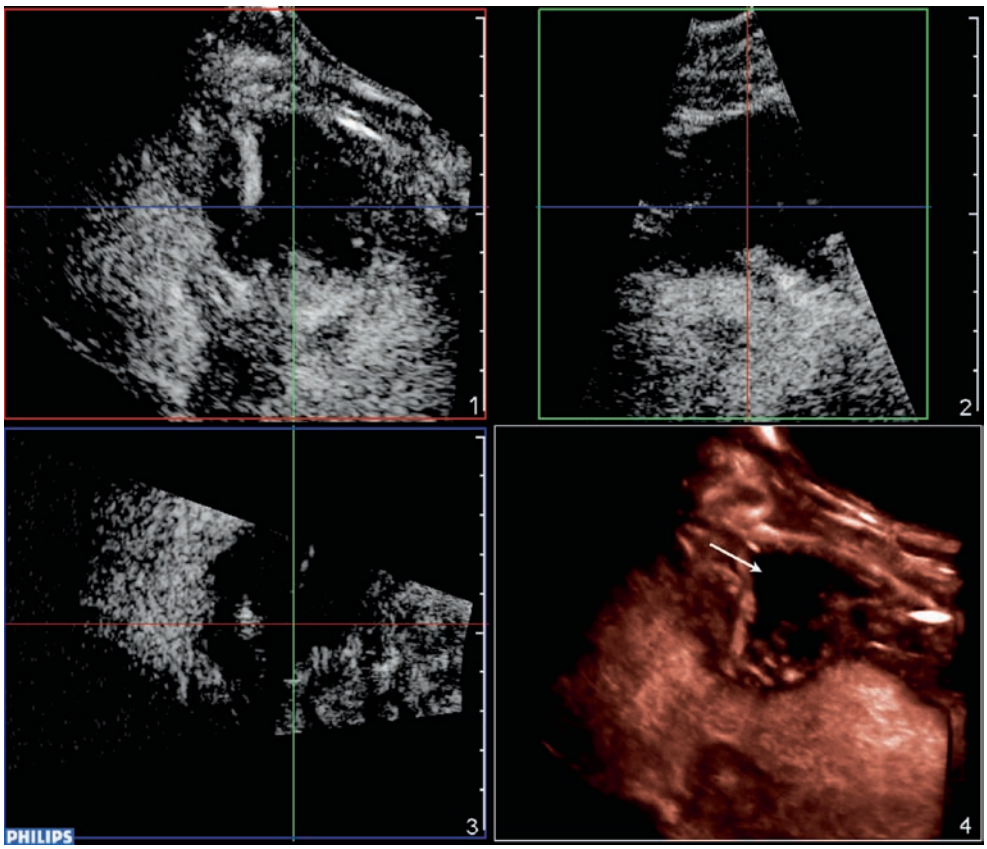

Fig. 27.3 Contrast-enhanced ultrasonography two weeks after cryoablation of a kidney tumor showing the perfusion defect (white arrow). The three respective perpendicular planes are demonstrated (1, 2, 3) as well as the volume rendering of the three-dimensional data set (4)

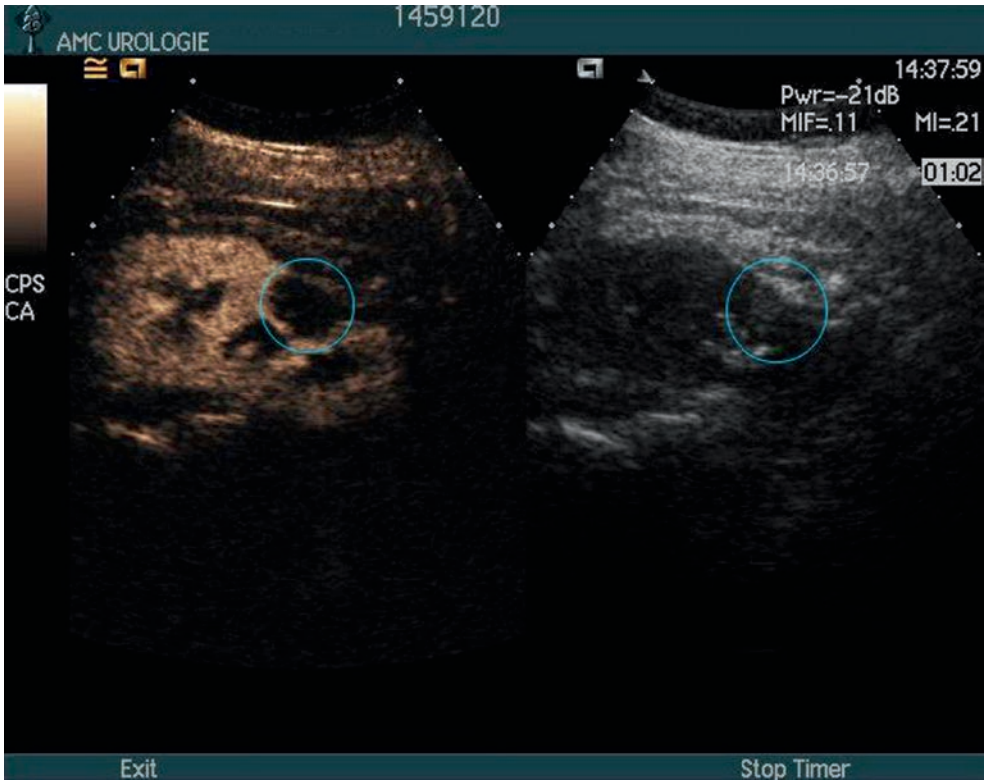

Fig. 27.4 Contrast-enhanced ultrasonography of the kidney based on contrast-pulse sequence technology (left) and the respective conventional B-mode imaging (right). The perfusion defect (within circle) after cryoablation of the renal tumor is more clearly depicted by contrast-enhanced ultrasonography

correlation between elastographic estimations of the area and volume of the thermal lesions and gross pathologic measurements has been found. These results suggest that elastography may prove to be a reliable method for monitoring the RFA zone of renal lesions, overcoming the inaccuracy of the current imaging modalities to provide real-time monitoring, and thus it may result in an improvement of the RFA efficacy.

The percutaneous ablative techniques for renal-cell carcinoma treatment that have been developed require image guiding for the precise placement of the needles. Recently, the use of a novel technology named real-time virtual sonography (RVS, Hitachi Medical Corporation, Japan) has been described. RVS displays simultaneously the images of real-time US with the corresponding CT or MR multiplanar views from a stored volume data set. RVS seems to be a promising alternative imaging tool to CT/MRI, providing excellent anatomical orientation and navigation for percutaneous RFA of solid renal tumors at a lower radiation exposure.[82]

Imaging with 3D/4D-US may have several applications such as, diagnosis and follow-up of hydronephrosis in children, evaluation and follow-up of renal lesions, execution of renal/adrenal biopsies and percutaneous procedures (nephrostomies, ablations).[4] 4D-US has been recently evaluated for guiding percutaneous interventions. 4D-US has been used to refer to both time-resolved and real-time 3D-US. 2D-US has been compared with the time resolved 4D-US for percutaneous access in minimal calyceal dilatation using an in vitro ultrasound phantom.[83] It has been reported that 4D-US is at least as good as 2D-US in terms of quality of punctures. Multiplanar reformatting longitudinal and transverse images were found to be the most useful for needle guidance.

Other Organs of the Urogenital System

Ureter

EUS has been recognized as a complementary technique for obtaining information regarding the ureteral and periureteral anatomy. The ultrasound image is oriented and localized in the upper urinary tract with the aid of real-time fluoroscopy. Its principle indication is to image ureteropelvic junction obstruction. Recently, it has been reported that EUS is more sensitive than helical CT scan for detecting significant crossing vessels, and its use can better prevent bleeding complications.[84] In addition, the use of EUS to direct the choice of treatment during endopyelotomy has been associated with a success rate >90%.[85]

EUS may contribute to the staging of upper urinary tract transitional-cell carcinoma and the detection of submucosal migration of ureteral stones. Moreover, it can be used in the procedure guidance/assessment of other organs of the urogenital system. It can detect bladder cancer muscle invasion,

guide urethral instrumentations, assess sphincter function in cases of urinary incontinence, guide collagen placement to treat sphincter insufficiency, facilitate the diagnosis of closed ostium urethral diverticulum, and contribute even in the locoregional staging of prostate cancer.[4]

Crossing vessel detection in patients with ureteropelvic junction obstruction is also possible with CE-CD-US. The use of this imaging modality in comparison to CT and MRI has been recently evaluated.[86] Results have been correlated with the laparoscopic pyeloplasty findings in 48 patients. Forty-four patients demonstrated crossing vessels at laparoscopy. CE-CD-US and MRI correctly detected all crossing vessels, whereas CT missed four posterior veins. Based on these results, CD-CE-US has been recommended as a first-line imaging modality in these patients.

Results of tissue harmonic imaging combined with plain abdominal radiography have been found to be comparable to those obtained by CT in the diagnosis of ureteral stones in patients with renal colic. It has been suggested that routine use of CT in these patients could be reduced by this strategy.[87]

Bladder

Although the advent of flexible instruments and digital chip technology has significantly increased tolerability during cystoscopy, it still remains an invasive procedure with main drawbacks such as failure to evaluate adjacent structures, a 5–15% risk of urinary tract infection, patient's discomfort and anxiety, and iatrogenic injury of the lower urinary tract.[88] During last years, a lot of effort has been put on the development of new noninvasive techniques for the evaluation of the bladder. The value of 3D- versus 2D-US of the bladder has been evaluated in 42 patients with hematuria.[89] 3D-US has been reported to have a better diagnostic performance, providing an overall correct diagnosis in 86% of the cases. The sensitivity for malignant and benign bladder lesions was 100% and 71%, respectively.

In a similar study, the potential value of the virtual cystoscopy based on 3D sonographic data has been evaluated for the detection of bladder tumors.[90] The sensitivity and specificity of tumor detection has been 96.2% and 70.6%, respectively, with a positive and negative predictive value of 93.9% and 80%, respectively. When combined with gray-scale, multiplanar reconstruction sensitivity, specificity, and positive and negative predictive values have been increased to 96.4%, 88.8%, 97.6%, and 84.2%, respectively.

US estimation of the detrusor wall thickness has been proposed to be a noninvasive predictor of bladder outlet obstruction.[91] Akino et al[92] assessed the efficacy of ultrasound-estimated bladder weight (UEBW) as an indicator for surgery and its outcome in patients with benign prostate hyperplasia. It was found that high UEBW is as important as severe lower urinary tract symptoms in identifying male patients at risk of surgery.

Traditionally, US has been used as diagnostic tool for the evaluation of the urinary tract in children with vesicoureteral reflux (VUR). Contrast-enhanced voiding urosonography (VUS) was used only for the initial diagnosis in females and in the follow-up of children already submitted to voiding cystourethrography (VCUG).[93] Recently, the diagnostic accuracy of VUS compared with that of VCUG in children with VUR has been evaluated.[94] A 96% of diagnostic agreement between the two techniques has been detected, suggesting the use of VUS as a first step in the diagnosis of VUR in children of both genders with a significant reduction in radiation exposure.

Testis

The assessment of the testicular resistive index (RI) by CD-US has been widely used to measure intratesticular blood flow. Pinggera et al[95] investigated the value of the intratesticular arteries RI using high-frequency CD-US in the diagnosis of patients with sperm impairment. The greater RI (>0.6) found in patients with pathological sperm counts seems to be a reliable indicator for routine clinical use to identify subfertile men.

To date, no single reliable test has been able to provide 100% diagnostic accuracy of testicular torsion and the use of CD-US of the testis can be misleading with false-negative results. In a multicenter study, including more than 900 patients, the direct visualization of the twisted cord with high resolution US has been proposed as a diagnostic method for the testicular torsion. The finding of a twisted cord is a highly sensitive and specific sign of testicular torsion, whereas the direct and complete visualization of a linear cord strongly indicates that surgery is unnecessary.[96]

HIFU was first described in 1998 as a minimally invasive technique for the treatment of testicular tumors in a solitary testis.[97] Recently, the long-term results of a phase II trial have been presented.[98] It has been reported that transcutaneous HIFU followed by prophylactic irradiation permits an organ-preserving, curative treatment for tumors in a solitary testis.

Finally, the feasibility of delivering proteins to the testicular extracellular compartment has been recently evaluated.[99] Ultrasound-targeted microbubble destruction is a feasible method for delivering bioactive substances even in organs with moderate to low blood perfusion, as long as they are accessible by ultrasound.

Acknowledgements Dr Charalampos Mamoulakis thanks the Alexander S. Onassis Public Benefit Foundation for a grant offered to attend a clinical fellowship program at the Academic Medical Center University Hospital, Department of Urology, Amsterdam, The Netherlands.

References

1. Hangiandreou NJ. AAPM/RSNA physics tutorial for residents. Topics in US: B-mode US: basic concepts and new technology. *Radiographics*. 2003;23:1019–1033
2. Singer EA, Golijanin DJ, Davis RS, Dogra V. What's new in urologic ultrasound? *Urol Clin North Am*. 2006;33:279–286
3. O'Brien RT, Holmes SP. Recent advances in ultrasound technology. *Clin Tech Small Anim Pract*. 2007;22:93–103
4. Nascimento RG, Coleman J, Solomon SB. Current and future imaging for urologic interventions. *Curr Opin Urol*. 2008;18:116–121
5. Pedersen MH, Misaridis TX, Jensen JA. Clinical evaluation of chirp-coded excitation in medical ultrasound. *Ultrasound Med Biol*. 2003;29:895–905
6. Thomas JD, Rubin DN. Tissue harmonic imaging: why does it work? *J Am Soc Echocardiogr*. 1998;11:803–808
7. Jespersen SK, Wilhjelm JE, Sillesen H. Multi-angle compound imaging. *Ultrason Imaging*. 1998;20:81–102
8. Ukimura O, Okihara K, Kamoi K, Naya Y, Ochiai A, Miki T. Intraoperative ultrasonography in an era of minimally invasive urology. *Int J Urol*. 2008;15:673–680
9. Fatemi M, Greenleaf JF. Probing the dynamics of tissue at low frequencies with the radiation force of ultrasound. *Phys Med Biol*. 2000;45:1449–1464
10. Garra BS. Imaging and estimation of tissue elasticity by ultrasound. *Ultrasound Q*. 2007;23:255–268
11. Linden RA, Halpern EJ. Advances in transrectal ultrasound imaging of the prostate. *Semin Ultrasound CT MR*. 2007;28:249–257
12. Lassau N, Chami L, Benatsou B, Peronneau P, Roche A. Dynamic contrast-enhanced ultrasonography (DCE-US) with quantification of tumor perfusion: a new diagnostic tool to evaluate the early effects of antiangiogenic treatment. *Eur Radiol*. 2007;Suppl 6: F89–98
13. Wink M, Frauscher F, Cosgrove D, et al Contrast-enhanced ultrasound and prostate cancer: a multicentre european research coordination project. *Eur Urol*. 2008;54:982–992
14. Halpern EJ, Ramey JR, Strup SE, Frauscher F, McCue P, Gomella LG. Detection of prostate carcinoma with contrast-enhanced sonography using intermittent harmonic imaging. *Cancer*. 2005;104: 2373–2383
15. Linden RA, Trabulsi EJ, Forsberg F, Gittens PR, Gomella LG, Halpern EJ. Contrast enhanced ultrasound flash replenishment method for directed prostate biopsies. *J Urol*. 2007;178:2354–2358
16. Pallwein L, Mitterberger M, Pelzer A, et al Ultrasound of prostate cancer: recent advances. *Eur Radiol*. 2008;18:707–715
17. Yang JC, Tang J, Li Y, Fei X, Shi H. Contrast-enhanced transrectal ultrasound for assessing vascularization of hypoechoic BPH nodules in the transition and peripheral zones: comparison with pathological examination. *Ultrasound Med Biol*. 2008;34:1758–1764
18. Tang J, Yang JC, Luo Y, Li J, Li Y, Shi H. Enhancement characteristics of benign and malignant focal peripheral nodules in the peripheral zone of the prostate gland studied using contrast enhanced transrectal ultrasound. *Clin Radiol*. 2008;63:1086–1091
19. Lees W. Ultrasound imaging in three and four dimensions. *Semin Ultrasound CT MR*. 2001;22:85–105
20. Claudon M, Tranquart F, Evans DH, Lefèvre F, Correas M. Advances in ultrasound. *Eur Radiol*. 2002;12:7–18
21. Cochlin DL, Ganatra RH, Griffiths DF. Elastography in the detection of prostatic cancer. *Clin Radiol*. 2002;57:1014–1020
22. König K, Scheipers U, Pesavento A, Lorenz A, Ermert H, Senge T. Initial experiences with real-time elastography guided biopsies of the prostate. *J Urol*. 2005;174:115–117
23. Taylor LS, Rubens DJ, Porter BC, et al Prostate cancer: three-dimensional sonoelastography for in vitro detection. *Radiology*. 2005;237:981–985
24. Miyanaga N, Akaza H, Yamakawa M, et al Tissue elasticity imaging for diagnosis of prostate cancer: a preliminary report. *Int J Urol*. 2006;13:1514–1518
25. Pallwein L, Mitterberger M, Struve P, et al Real-time elastography for detecting prostate cancer: preliminary experience. *BJU Int*. 2007;100:42–46
26. Tsutsumi M, Miyagawa T, Matsumura T, et al The impact of real-time tissue elasticity imaging (elastography) on the detection of prostate cancer: clinicopathological analysis. *Int J Clin Oncol*. 2007;12:250–255
27. Sumura M, Shigeno K, Hyuga T, Yoneda T, Shiina H, Igawa M. Initial evaluation of prostate cancer with real-time elastography based on step-section pathologic analysis after radical prostatectomy: a preliminary study. *Int J Urol*. 2007;14:811–816
28. Pallwein L, Mitterberger M, Struve P, et al Comparison of sonoelastography guided biopsy with systematic biopsy: impact on prostate cancer detection. *Eur Radiol*. 2007;17:2278–2285
29. Nelson ED, Slotoroff CB, Gomella LG, Halpern EJ. Targeted biopsy of the prostate: the impact of color Doppler imaging and elastography on prostate cancer detection and Gleason score. *Urology*. 2007;70:1136–1140
30. Pallwein L, Mitterberger M, Pinggera G, et al Sonoelastography of the prostate: comparison with systematic biopsy findings in 492 patients. *Eur J Radiol*. 2008;65:304–310
31. Salomon G, Köllerman J, Thederan I, et al Evaluation of prostate cancer detection with ultrasound real-time elastography: a comparison with step section pathological analysis after radical prostatectomy. *Eur Urol*. 2008;54:1354–1362
32. Kamoi K, Okihara K, Ochiai A, et al The utility of transrectal real-time elastography in the diagnosis of prostate cancer. *Ultrasound Med Biol*. 2008;34:1025–1032
33. Eggert T, Khaled W, Wenske S, Ermert H, Noldus J. Impact of elastography in clinical diagnosis of prostate cancer: a comparison of cancer detection between B-mode sonography and elastography-guided 10-core biopsies. *Urologe A*. 2008;47:1212–1217
34. Pallwein L, Aigner F, Faschingbauer R, et al Prostate cancer diagnosis: value of real-time elastography. *Abdom Imaging*. 2008;33: 729–735
35. Souchon R, Rouvière O, Gelet A, et al Visualisation of HIFU lesions using elastography of the human prostate in vivo: preliminary results. *Ultrasound Med Biol*. 2003;29:1007–1015
36. Curiel L, Souchon R, Rouvière O, Gelet A, Chapelon JY. Elastography for the follow-up of high-intensity focused ultrasound prostate cancer treatment: initial comparison with MRI. *Ultrasound Med Biol*. 2005;31:1461–1468
37. Schneider M. Molecular imaging and ultrasound-assisted drug delivery. J *Endourol*. 2008;22:795–802
38. Frauscher F, Klauser A, Volgger H, et al Comparison of contrast enhanced color Doppler targeted biopsy with conventional systematic biopsy: impact on prostate cancer detection. *J Urol*. 2002;167: 1648–1652
39. Eckersley RJ, Sedelaar JP, Blomley MJ, et al Quantitative microbubble enhanced transrectal ultrasound as a tool for monitoring hormonal treatment of prostate carcinoma. *Prostate*. 2002;51:256–267
40. Pelzer A, Bektic J, Berger AP, et al Prostate cancer detection in men with prostate specific antigen 4 to 10 ng/ml using a combined approach of contrast enhanced color Doppler targeted and systematic biopsy. *J Urol*. 2005;173:1926–1929
41. Mitterberger M, Pinggera GM, Horninger W, et al Comparison of contrast enhanced color Doppler targeted biopsy to conventional systematic biopsy: impact on Gleason score. *J Urol*. 2007;178: 464–468
42. Mitterberger M, Horninger W, Pelzer A, et al A prospective randomized trial comparing contrast-enhanced targeted versus systematic ultrasound guided biopsies: impact on prostate cancer detection. *Prostate*. 2007;67:1537–1542

43. Mitterberger M, Pinggera G, Horninger W, et al Dutasteride prior to contrast-enhanced colour Doppler ultrasound prostate biopsy increases prostate cancer detection. *Eur Urol*. 2008;53:112–117
44. Unal D, Sedelaar JP, Aarnink RG, et al Three-dimensional contrast-enhanced power Doppler ultrasonography and conventional examination methods: the value of diagnostic predictors of prostate cancer. *BJU Int*. 2000;86:58–64
45. Sedelaar JP, Aarnink RG, van Leenders GJ, et al The application of three-dimensional contrast-enhanced ultrasound to measure volume of affected tissue after HIFU treatment for localized prostate cancer. *Eur Urol*. 2000;37:559–568
46. Sedelaar JP, van Leenders GJ, Hulsbergen-van de Kaa CA, et al Microvessel density: correlation between contrast ultrasonography and histology of prostate cancer. *Eur Urol*. 2001;40:285–293
47. Goossen TE, de la Rosette JJ, Hulsbergen-van de Kaa CA, van Leenders GJ, Wijkstra H. The value of dynamic contrast enhanced power Doppler ultrasound imaging in the localization of prostate cancer. *Eur Urol*. 2003;43:124–131
48. Strohmeyer D, Frauscher F, Klauser A, et al Contrast-enhanced transrectal color doppler ultrasonography (TRCDUS) for assessment of angiogenesis in prostate cancer. *Anticancer Res*. 2001;21: 2907–2913
49. Halpern EJ, McCue PA, Aksnes AK, Hagen EK, Frauscher F, Gomella LG. Contrast-enhanced US of the prostate with Sonazoid: comparison with whole-mount prostatectomy specimens in 12 patients. *Radiology.* 2002;222:361–366
50. van Moerkerk H, Heijmink SW, Kaa CA, Barentsz JO, Witjes JA. Computerized three-dimensional localization of prostate cancer using contrast-enhanced power Doppler and clustering analysis. *Eur Urol*. 2006;50:762–768
51. Sedelaar JP, van Leenders GJ, Goossen TE, et al Value of contrast ultrasonography in the detection of significant prostate cancer: correlation with radical prostatectomy specimens. *Prostate.* 2002;53:246–253
52. Frauscher F, Klauser A, Halpern EJ, Horninger W, Bartsch G. Detection of prostate cancer with a microbubble ultrasound contrast agent. *Lancet.* 2001;357:1849–1850
53. Colleselli D, Bektic J, Schaefer G, et al The influence of prostate volume on prostate cancer detection using a combined approach of contrast-enhanced ultrasonography-targeted and systematic grey-scale biopsy. *BJU Int*. 2007;100:1264–1267
54. Halpern EJ, Rosenberg M, Gomella LG. Prostate cancer: contrast-enhanced us for detection. *Radiology.* 2001;219:219–225
55. Halpern EJ, Frauscher F, Rosenberg M, Gomella LG. Directed biopsy during contrast-enhanced sonography of the prostate. *AJR Am J Roentgenol*. 2002;178:915–919
56. Roy C, Buy X, Lang H, Saussine C, Jacqmin D. Contrast enhanced color Doppler endorectal sonography of prostate: efficiency for detecting peripheral zone tumors and role for biopsy procedure. *J Urol.* 2003;170:69–72
57. Taymoorian K, Thomas A, Slowinski T, et al Transrectal broadband-Doppler sonography with intravenous contrast medium administration for prostate imaging and biopsy in men with an elevated PSA value and previous negative biopsies. *Anticancer Res*. 2007;27:4315–4320
58. Tang J, Yang JC, Li Y, Li J, Shi H. Peripheral zone hypoechoic lesions of the prostate: evaluation with contrast-enhanced gray scale transrectal ultrasonography. *J Ultrasound Med.* 2007;26:1671–1679
59. Wondergem N, De La Rosette JJ. HIFU and cryoablation-non or minimal touch techniques for the treatment of prostate cancer. Is there a role for contrast enhanced ultrasound? *Minim Invasive Ther Allied Technol*. 2007;16:22–30
60. Rouvière O, Curiel L, Chapelon JY, et al Can color doppler predict the uniformity of HIFU-induced prostate tissue destruction? *Prostate*. 2004;60:289–297
61. Mehier-Humbert S, Bettinger T, Yan F, Guy RH. Plasma membrane poration induced by ultrasound exposure: implication for drug delivery. *J Control Releas*e. 2005;104:213–222
62. Watanabe A, Otake R, Nozaki T, et al Effects of microbubbles on ultrasound-mediated gene transfer in human prostate cancer PC3 cells: comparison among Levovist, YM454, and MRX-815H. *Cancer Lett*. 2008;265:107–112
63. Mehier-Humbert S, Yan F, Frinking P, Schneider M, Guy RH, Bettinger T. Ultrasound-mediated gene delivery: influence of contrast agent on transfection. *Bioconjug Chem.* 2007;18:652–662
64. Haag P, Frauscher F, Gradl J, Seitz A, Schäfer G, Lindner JR, et al Microbubble-enhanced ultrasound to deliver an antisense oligodeoxynucleotide targeting the human androgen receptor into prostate tumours. *J Steroid Biochem Mol Biol*. 2006;102:103–113
65. Duvshani-Eshet M, Machluf M. Efficient transfection of tumors facilitated by long-term therapeutic ultrasound in combination with contrast agent: from in vitro to in vivo setting. *Cancer Gene Ther*. 2007;14:306–315
66. Duvshani-Eshet M, Benny O, Morgenstern A, Machluf M. Therapeutic ultrasound facilitates antiangiogenic gene delivery and inhibits prostate tumor growth. *Mol Cancer Ther*. 2007;6: 2371–2382
67. Mehta SS, Azzouzi AR, Hamdy FC. Three dimensional ultrasound and prostate cancer. *World J Urol.* 2004;22:339–345
68. Mitterberger M, Pinggera GM, Pallwein L, et al The value of three-dimensional transrectal ultrasonography in staging prostate cancer. *BJU Int*. 2007;100:47–50
69. Zalesky M, Urban M, Smerhovský Z, Zachoval R, Lukes M, Heracek J. Value of power Doppler sonography with 3D reconstruction in preoperative diagnostics of extraprostatic tumor extension in clinically localized prostate cancer. *Int J Urol.* 2008;15:68–75
70. Braeckman J, Autier P, Soviany C, et al The accuracy of transrectal ultrasonography supplemented with computer-aided ultrasonography for detecting small prostate cancers. *BJU Int.* 2008;102: 1560–1565
71. Braeckman J, Autier P, Garbar C, et al Computer-aided ultrasonography (HistoScanning): a novel technology for locating and characterizing prostate cancer. *BJU Int*. 2008;101:293–298
72. Tamai H, Takiguchi Y, Oka M, et al Contrast-enhanced ultrasonography in the diagnosis of solid renal tumors. *J Ultrasound Med*. 2005; 2412:1635–1640
73. Pallwein L, Mitterberger M, Aigner F, et al Small renal masses:the value of contrast-enhanced colour Doppler imaging. *BJU Int*. 2007;1001:47–50
74. Ascenti G, Mazzotti S, Zimbaro G, et al Complex cystic renal masses: characterization with contrast-enhanced US. *Radiology*. 2007;2431:158–165
75. Park BK, Kim B, Kim SH, Ko K, Lee HM, Choi HY. Assessment of cystic renal masses based on Bosniak classification: comparison of CT and contrast-enhanced US. *Eur J Radiol.* 2007;612:310–314
76. Wink MH, de la Rosette JJ, Laguna P, Lagerveld BW, Wijstra H. Ultrasonography of renal masses using contrast pulse sequence imaging: a pilot study. *J Endourol*. 2007;21:466–472
77. Pallwein L, Mitterberger M, Gradl J, et al Diagnostic evaluation of small renal masses: value of contrast-enhanced US in comparison to multidetector CT. *J Urol*. 2008, 179 Suppl:331
78. Slabaugh TK, Machaidze Z, Hennigar R, Ogan K. Monitoring radiofrequency renal lesions in real time using contrast-enhanced ultrasonography: a porcine model. *J Endourol* 2005;19: 579–583
79. Wink MH, Laguna MP, Lagerveld BW, de la Rosette JJ, Wijkstra H. Contrast-enhanced ultrasonography in the follow-up of cryoablation of renal tumors: a feasibility study. *BJU Int.* 2007;99: 1371–1375
80. Fahey BJ, Nelson RC, Bradway DP, Hsu SJ, Dumont DM, Trahey GE. In vivo visualization of abdominal malignancies with acoustic radiation force Elastography. *Phys Med Biol*. 2008;531:279–293
81. Pareek G, Wilkinson ER, Bharat S. Elastography measurements of in-vivo radiofrequency ablation lesions of the kidney. *J Endourol*. 2006;20:959–964

82. Ukimura O, Mitterberger M, Okihara K, et al Real-time virtual ultrasonography radiofrequency ablation of renal cell carcinoma. *BJU Int*. 2008;101:707–711
83. John BS, Rowland D, Ratnam L, et al Percutaneous renal intervention: comparison of 2-D and time-resolved 3-D (4-D) ultrasound for minimal calyceal dilation using an ultrasound phantom and fluoroscopic control. *Ultrasound Med Biol.* 2008;34:1765–1769
84. Hendrikx AJ, Nadorp S, De Beer NA, Van Beekum JB, Gravas S. The use of endoluminal ultrasonography for preventing significant bleeding during endopyelotomy: evaluation of helical computed tomography vs endoluminal ultrasonography for detecting crossing vessels. *BJU Int.* 2006;97:786–789
85. Keeley FX Jr, Tolley DA, Moussa SA. Patient selection before endopyelotomy: can it improve the outcome? *BJU Int*. 2000;86: 773–776
86. Mitterberger M, Pinggera GM, Neururer R, et al Comparison of contrast-enhanced color Doppler imaging (CDI), computed tomography (CT), and magnetic resonance imaging (MRI) for the detection of crossing vessels in patients with ureteropelvic junction obstruction (UPJO). *Eur Urol.* 2008;53:1254–1260
87. Mitterberger M, Pinggera GM, Neururer R, et al Plain abdominal radiography with transabdominal native tissue harmonic imaging ultrasonography vs unenhanced computed tomography in renal colic. *BJU Int*. 2007;100:887–890
88. Newhouse JH, Amis ES Jr, Bigongiari LR, et al Radiologic investigation of patients with hematuria. American College of Radiology. ACR appropriateness criteria. *Radiology.* 2000;215 Suppl:687–691
89. Mitterberger M, Pinggera GM, Neuwirt H, et al Three-dimensional ultrasonography of the urinary bladder: preliminary experience of assessment in patients with haematuria. *BJU Int.* 2007;99:111–116
90. Kocakoc E, Kiris A, Orhan I, Poyraz AK, Artas H, Firdolas F. Detection of bladder tumors with 3-dimensional sonography and virtual sonographic cystoscopy. *J Ultrasound Me*d. 2008;27:45–53
91. Oelke M, Höfner K, Jonas U, de la Rosette JJ, Ubbink DT, Wijkstra H. Diagnostic accuracy of noninvasive tests to evaluate bladder outlet obstruction in men: detrusor wall thickness, uroflowmetry, postvoid residual urine, and prostate volume. *Eur Urol*. 2007;52: 827–834
92. Akino H, Maekawa M, Nakai M, et al Ultrasound-estimated bladder weight predicts risk of surgery for benign prostatic hyperplasia in men using alpha-adrenoceptor blocker for LUTS. *Urology*. 2008 ; 72:817–820
93. Darge K. Voiding urosonography with US contrast agents for the diagnosis of vesicoureteric reflux in children. II. Comparison with radiological examinations. *Pediatr Radiol*. 2008;38:54–63
94. Giordano M, Marzolla R, Puteo F, Scianaro L, Caringella DA, Depalo T. Voiding urosonography as first step in the diagnosis of vesicoureteral reflux in children: a clinical experience. *Pediatr Radiol*. 2007;37:674–677
95. Pinggera GM, Mitterberger M, Bartsch G, et al Assessment of the intratesticular resistive index by colour Doppler ultrasonography measurements as a predictor of spermatogenesis. *BJU Int*. 2008;101:722–726
96. Kalfa N, Veyrac C, Lopez M, et al Multicenter assessment of ultrasound of the spermatic cord in children with acute scrotum. *J Urol.* 2007;177:297–301
97. Madersbacher S, Kratzik C, Susani M, Pedevilla M, Marberger M. Transcutaneous high-intensity focused ultrasound and irradiation: an organ-preserving treatment of cancer in a solitary testis. *Eur Urol.* 1998;33:195–201
98. Kratzik C, Schatzl G, Lackner J, Marberger M. Transcutaneous high-intensity focused ultrasonography can cure testicular cancer in solitary testis. *Urology.* 2006;67:1269–1273
99. Bekeredjian R, Kuecherer HF, Kroll RD, Katus HA, Hardt SE. Ultrasound-targeted microbubble destruction augments protein delivery into testes. *Urology.* 2007;69:386–389

Telementoring

28

Shu Pan, Mohamed A. Atalla, and Louis R. Kavoussi

Introduction

As physicians embrace new technology and incorporate it into practice, traditional approaches will metamorphose into seemingly strange but incredibly useful paradigms. One extraordinary transformation has been the incorporation of telemedicine into daily practice. Defined as the real-time transfer of information between health care providers across various media, telemedicine can take several forms. In its simplest form, telecommunication merely allows information sharing between professionals to help facilitate medical care delivery. In telemedicine's most ambitious application, telesurgery, surgical care in its entirety is delivered over the wire. With surgical fields evolving to incorporate electronic and audio/visual adjuncts, telemedicine has found a new channel for development. This development has been aided by advancements in networking, audio/visual, computer, and robotics technology.

Telementoring, a form of telemedicine, is the practice of using communication technology to assist, guide, and educate other providers over an electronic medium during real-time care delivery. It has been used in space-training missions, naval vessels, and on land.[1] Applications have been most relevant in surgical care, given the urgency and technical demand of surgical care. In the field of urology, telementoring has assumed a central role as communication technology has boomed. As endoscopy and laparoscopy became more widespread in their urologic applications, most urologic procedures have become inherently compatible with this form of remote mentoring.

Minimally invasive urologic surgery benefits patients by conferring improved postoperative cosmesis and expedited convalescence. However, proficiency in laparoscopic surgery is not easily attained. A steep learning curve is associated with the successful acquisition of minimally invasive surgical skills.[2] Additionally, surgeons performing laparoscopic procedures are more than three times more likely to encounter complications if they do not receive additional training after completing their requisites.[3] Although continued training is essential for laparoscopic surgeons, a limited number of expert surgeons have a teaching background. Teaching hospitals thus incur additional expenses and face logistic difficulties in recruiting mentors from outside institutions.

Telementoring eliminates some of these obstacles to attaining laparoscopic surgical proficiency. With the exception of a one-time start-up cost of procuring the necessary equipment, telementoring eliminates variable costs down the road, rendering repeated training sessions economically feasible. Telementoring also makes available the expertise of trained laparoscopic surgeons to patients residing in remote areas. Surgeons working at local hospitals in isolated regions can be assisted directly by expert telementors during complicated procedures. This assistance immediately benefits the patients by bringing specialized care to their home region, reducing the cost of travel, and lowering the risk of delayed medical attention.

This chapter chronicles the history of telementoring and reviews its current state and novel applications. In doing so, it explores the benefits of telementoring and outlines current and future limitations. This review helps the reader to contextualize telementoring and its role in the future of telemedicine.

History

Telementoring is by no means a recent development. Following the invention of the telephone in 1876, an early example of telementoring was recorded in 1906. Einthoven, the renowned father of electrocardiology, transmitted an electrocardiogram via telephone from his lab to a hospital located a mile away.[4] Early forms of telementoring relied primarily on telephone lines or direct video/audio linkups. In the late 1950s, the University of Nebraska established a telemedicine network that aimed to complement clinical training and research in rural areas. Expanding the scope of this trial, two-way audio/video connections were established in 1961 to provide television-based group therapy sessions in the field of psychiatry.[5, 6] Shortly thereafter, Debakey demonstrated the didactic potential of telementoring by performing

P. Dasgupta et al. (eds.), *New Technologies in Urology,*
DOI: 10.1007/978-1-84882-178-1_28, © Springer-Verlag London Limited 2010

transcontinental lectures between the United States and Europe via a direct satellite uplink.[5]

A period of relative stagnancy followed the attempts at telementoring in the 1960s, directly resulting from inadequacies in telecommunication technologies. Cheap, effective transfer of information was not a realizable goal until the implementation of the Internet. Although Vinton Cerf and Robert Kahn coined the term "Internet" in 1974, the physical switch from the older NCP protocol to Transmission Control Protocol/Internet Protocol (TCP/IP) did not occur until 1983. It would be another 5 years before the Internet was open to commercial interests. The commercialization of the Internet served as the catalyst that transformed telemedicine, and more specifically telementoring, to its present form.[7]

Setup

Laparoscopic procedures are inherently compatible with telementoring. Many components of laparoscopic equipment can be easily integrated with a telementoring setup. The most basic arrangement consists of a laparoscopic camera that outputs video footage to a computer equipped with a coder/decoder (CODEC). The audio and visual data are digitized and then transmitted via a local or wide area network. A multitude of connections is available with varying speeds and costs. Earlier trials used mostly modem (operating through telephone lines) or ISDN connections. However, later trials used broadband connections that reduced lag time significantly while improving reliability (Fig. 28.1). Under normal circumstances, a connection speed of 128 Kbps is sufficient to provide high-quality, two-way video transmission. As an additional safeguard, most telementoring institutions use redundant connections in case of connection interruption.

The setup at the mentor side is slightly different. Lacking the operating table and surgical equipment, the mentor's console includes, at a minimum, a computer equipped with a web camera and microphone. More advanced telementoring apparatuses include a telestrator program and interface, which enable the mentor to annotate notable landmarks during surgery (not unlike football commentaries) in an effort to guide the local surgeon. Recent innovations in telerobotics have made it possible for remote surgeons to manipulate robotic assistive devices at the local site. This setup has profound benefits for telementoring, but requires additional connection resources and a specialized software protocol. Overall, the necessary components of a basic telementoring apparatus are not costly or sophisticated, which makes telementoring an ideal form of remote training.

Time Delay

In nearly all instances of telementoring, researchers have strived for greater bandwidth in an effort to reduce time delay. In addition to connection speed, the magnitude of time delay is directly proportional to the distance between two locations. Hardware functions, such as the time required to

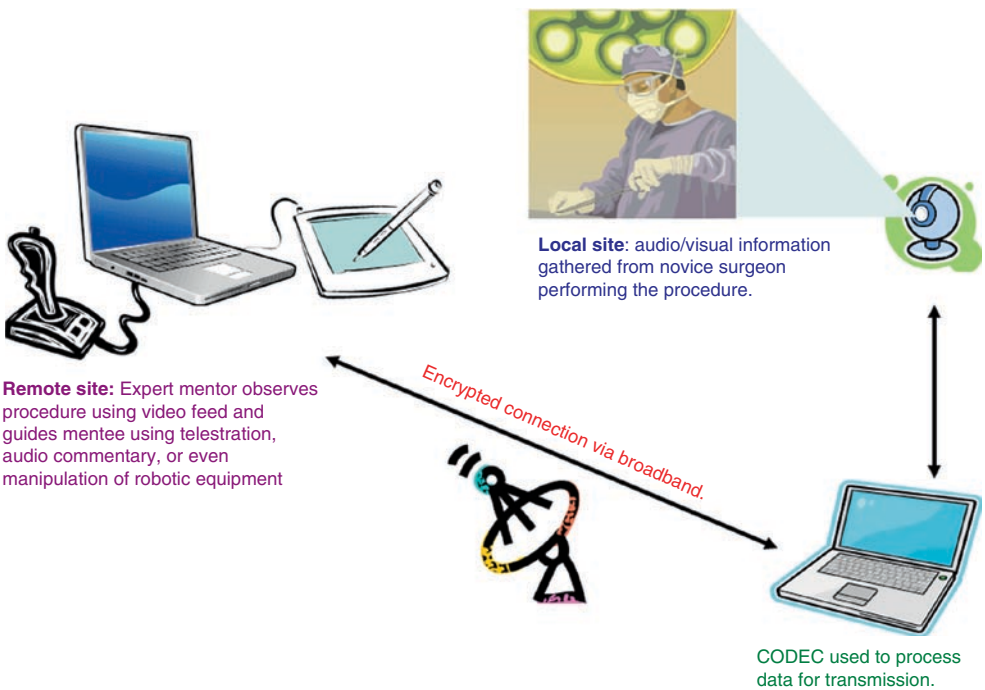

Fig. 28.1 Basic telementoring setup

encode and decode the signal, impose an additional intrinsic lag to the overall signal transmission. Fabrizio et al conducted a unique study to ascertain the effects of time delay on telesurgical manipulations.[8] His group used custom software, Microsoft Plus (Microsoft Corp., Seattle, WA), to artificially impose a controlled time lag on a simulation of operation. It was found that the participating surgeons exhibited a high number of errors, per assigned task, when the time delay was amplified to more than 700 ms. In a second phase of the study, a learning curve was found for surgeons operating with a 500-ms static time lag; the test subjects completed their tasks with fewer errors and fewer movements.

Time delay would most likely pose a lesser detriment to telementoring, in contrast to telesurgery, because the local-site surgeon ultimately is in command of the surgery. Slight pauses in the audio/visual feed from the expert mentor can be tolerated without immediate risks. However, despite tolerable latency from limiting bandwidth, a reliable connection is still essential. Out of the 17 laparoscopic cases recorded by Bove et al, from 1998 to 2000, five could not be telementored because an adequate uplink could not be established.[9]

Robotics

Present telementoring methods transcend basic audio/visual exchange, as illustrated by the incorporation of robotics into the modern repertoire of remote surgical training. The new additions not only benefit the on-site surgeon by providing robotic assistance but also give the expert mentor a greater degree of manipulation. The following robotic devices have been used in telementored laparoscopic trials.

AESOP

The automated endoscopic system for optimal positioning (AESOP) was originally designed for NASA space missions by a team of engineers led by Yulun Wang. It has since been adapted to function as a camera holder in laparoscopic surgeries. A robotic camera holder has the advantage of reducing inadvertent movements and decreasing the overall crowding in the operating room. Later generations of the AESOP are fully compatible with voice-activated commands and can be integrated with the HERMES control center, which acts as the central console to all peripheral devices.[2] With the necessary software and connection, the AESOP can be set up to give the mentoring surgeon direct control. The expert surgeon is then able to manipulate the laparoscope, directing a specific angle of approach for the novice.

Socrates

The Socrates (Computer Motions, Inc., Goleta, CA) is an FDA-approved device for teleeducation, designed for both laparoscopic and open cases. Composed of multiple subunits, the suite has voice-activated controls for the robotic camera arm (AESOP), an insufflator, and external lighting. The Socrates also incorporates the HERMES unit for a centralized console of operation and is fully network compatible, through IP linkup or ISDN connection. Direct connection allows single-party telementoring sessions, whereas a parallel connection enables multiple parties to view the operation. This setup is highly beneficial to physician training. One notable demonstration of its efficacy was a semester-long course held at the Moscow State University, taught from a remote operating room in the United States, some 6,000 mi away.[2]

PAKY

Percutaneous access to the kidney (Urobotics Laboratory, JHMI, Baltimore, MD) is a robotic arm designed to gain renal access for procedures such as nephrostolithotomy (Fig. 28.2). The PAKY can be controlled locally by the on-site surgeon or by the remote mentor, via dedicated ISDN lines. Although this device is undergoing further development, its future implementation could very well minimize radiation exposure for surgeons attempting percutaneous renal access.[9]

Zeus

The Zeus system (Computer Motions, Inc., Goleta, CA) is divided into two constituent units: a surgeon-side console and a patient-side subsystem. The surgeon-side console receives input from the operator, which is then actuated by the robotic arms attached to the operating table (patient side). A myriad of surgical equipment can be interchanged from the two robotic arms, and a third arm controls the endoscopic camera. The primary objective of the Zeus is to minimize tremors from the surgeon, thereby reducing complications. Laparoscopic surgeries completed with the assistance of the Zeus have outcomes comparable to unassisted attempts, but the operative time is generally longer.[10]

The Zeus system was a major contribution to the practice of telementoring; it was the first system to enable the telementor to take over the operation, should complications arise. Its feasibility is evidenced by the first transatlantic telesurgery performed by Marescaux in 2001.[11] Marescaux,

Fig. 28.2 PAKY arm attached to AcuBot console. (Urobotics Laboratory, JHMI, Baltimore, MD)

situated in New York, successfully performed a telerobotic cholecystectomy in a 68-year-old female in Strasbourg, France. Using a dedicated optic fiber network with asynchronous transfer mode (ATM), physical inputs from the surgeon were translated into robotic motion at the patient side. The lag time was determined as approximately 80 ms, which had minimal effect on the overall procedure. This landmark accomplishment demonstrated the feasibility of remote telerobotic surgery, and had profound ramifications on the methodology of telementoring.

Da Vinci

The da Vinci surgical system was developed by Intuitive Surgical, Inc. (Menlo Park, CA). The company merged with Computer Motion, Inc. in 2003, resulting in the discontinued production of the Zeus robot. Like the Zeus, the da Vinci system comprises three subunits: the cart, the console, and the endoscopic stack. A surgeon operator performs surgical tasks with the high-definition, three-dimensional imagery provided by the endoscopic stack. The operator's every movement is translated into corresponding movements in the two robotic arms, which can be fitted with an assortment of surgical instruments. Position sensing effectively eliminates tremors, and cable systems controlling the instrument joints allow emulation of the finest movements.

Supplanting the ZEUS, the da Vinci system has assumed a prominent role in telesurgery and telementoring. Four telementored, laparoscopic right nephrectomies were performed in a porcine model using the da Vinci system. Duplicate consoles were set up so that the experienced surgeon, located in Ohio or Colorado, guided the novice, situated in California. The expert mentor, for three out of the four cases, manipulated two out of the three robotic arms, illustrating the feasibility of rapid switching of console operator. Broadband T1 connections were used, but sporadic packet loss was still detected. If the image got pixelated, the remote surgeon relinquished control and took on a mentoring role. Despite the intermittent time delays, all four cases were completed successfully.[12]

Applications

Long-Distance and International Applications

Telementoring transports the expertise of trained surgeons to rural or remote areas, making complicated surgeries feasible. In one early instance of international telementoring, a surgical training system was established at Johns Hopkins University in 1998.[13] An expert mentor provided remote guidance during three laparoscopic surgeries: varicocelectomy, nephrectomy, and adrenalectomy. The remote sites were in Innsbruck, Austria, and Bangkok, Thailand. Three ISDN lines, narrowband by current standards, formed the dedicated connection. An average delay of less than 1 s was recorded, but the overall outcome of the procedures was unaffected. Even in this early trial of telementoring, the benefits of telestration were discernible: landmarks were annotated in the medium of video or still images.

In 2003, another telementored trial was attempted between the United States and Brazil.[14] The expert surgeon was again located at Johns Hopkins University, but the remote site was in Sao Paulo and Recife, Brazil. Improvements were made to the overall setup, and a new CODEC was adopted. The new Z360 video CODEC featured dual-channel control for robotic arms of the AESOP, the telestrator, and the electrocautery. In this trial, two different connection types were tested. The telementoring session achieved a frame rate of 15 with the dedicated ISDN lines and an enhanced 30 frames per second with the T1 broadband. In addition to using the

AESOP robotic arm for the first case of varicocelectomy, the second case of percutaneous nephrolithotomy was performed with the aid of the PAKY. Urinary access was achieved with the first needle pass. Both cases had good postoperative results; the patients showed minimal blood loss and were discharged 1 and 2 days after surgery, respectively.

In a randomized evaluation study conducted in 2005, it was found that robotic-assisted percutaneous access had an accuracy of 88%, compared with 79% by human operators ($p = 0.046$).[15] The results from this study confirm the benefits of telerobotic assistance in modern urological procedures, and the compatability of Percutaneous Access to the Kidney-Remote Center of Motion (PAKY-RCM) with telementored procedures.

Naval Applications

Medical care is often delayed on the battlefield, due to hostile environments or sheer distance from hospitals. Even if the patient is successfully transferred to field hospitals, it is likely that available physicians may lack the experience to provide specialty care. Telementoring proposes a solution by making available the expertise of specialists. The formation of the Battlegroup Telemedicine System (BGTM) is a prime example of the use of telemedicine in a military setting.

The USS Abraham Lincoln is one of the first military vessels to be fitted with laparoscopic equipment. While deployed in the Pacific Ocean and Persian Gulf, five cases of inguinal hernia were diagnosed among the fleet, facilitating the formation of the BGTM as a solution to treatment.[16] The BGTM comprised three nodes, running on "off the shelf" equipment such as laptops, modems, video cameras, and cellular phones. The battle group is one node, and the two state-side nodes are located at the Johns Hopkins University Applied Physics Laboratory and San Diego Naval Medical Center. Five laparoscopic inguinal hernia repairs were completed successfully under telementoring guidance despite the narrowband connection, which allowed only a choppy video feed of two to four frames per second. The expert mentor nevertheless guided the onboard surgeon through real-time telestration and an exchange of image files, depending on connectivity. Audio exchange was conducted by cellular phone, but the satellite voice communication was frequently haphazard. These accumulated experiences of the BGTM demonstrate the effectiveness of telementoring, despite crude telecommunication equipment.

Applications in Space

In extreme environments, modern telecommunication technologies have eliminated many of the shortcomings encountered in the BGTM experience. The Aquarius habitat is the only underwater laboratory in the world. It is funded by the U.S. National Oceanographic and Atmospheric Administration (NOAA) and operated by the National Undersea Research Center (NURC), based at the University of North Carolina at Wilmington. As a premier training facility, NASA has used the Aquarius to provide specialized training for future astronauts. A series of Neemo undersea missions were carried out at the Aquarius, with the Neemo 7 mission specifically designed to evaluate the effectiveness of telementored surgical procedures in a space mission analog.[17]

In 2004, the crew members participating in the Neemo 7 mission were given minimal training by physicians working at McMaster University's Center for Minimal Access Surgery. The main objective of the training was to familiarize the crew members with equipment operation and relevant medical terminology. None of the participants, which included aquanauts who were physicians, was fully versed in the surgical procedures they would soon perform.

The aquanauts performed diagnostic ultrasonography on fellow crew members and various surgical procedures on simulated patients under telementoring guidance. The procedures included ultrasound-guided abscess drainage, repair of vascular injury, cystoscopy with basket stone extraction, and laparascopic cholecystectomy. Through these simulated exercises, it was concluded that interventional procedures could be performed adequately if telementoring were provided in a similar setting. In the simulated laparoscopic cholecystectomy, all three test subjects successfully completed the surgery. There was no discernible difference between the nonphysician and the physician (nonsurgeon) participants. Mean efficiency scores of 3.3 and 3.1 were given, respectively, and the operative times of 28 and 27.5 min were similar. The laparoscopic cholecystectomies performed with telerobotic assistance (operated by a CMAS mentor) were significantly lengthier than the unassisted cases. This discrepancy in length may suggest a degree of coordination conflict between the mentor and mentee when the mentor operates the robotic endoscope.

Despite this discrepancy, the Neemo 7 mission showcases the capabilities of telementoring during medical emergencies in extreme environments. Under extreme circumstances, even individuals with minimal training can be guided through relatively complex procedures.

Limitations

The numerous opportunities afforded by telemedicine are constrained by several limitations. The first consideration is cost. Establishing a telementoring setup requires an immense start-up cost; an estimate for a relatively advance system runs as high as $20,000.[18] This limitation is especially

detrimental for underdeveloped countries, which may have the most to gain from telementoring. A solution may lie with affiliations with larger, more financially stable hospitals in developed nations. Larger institutions can distribute telementoring systems on lease, and smaller hospitals can use the equipment until training is complete. Once the initial setup cost has been overcome, each successive session of telementoring saves the hosting hospital money. In this scenario, costs associated with travel and lodging for visiting faculty can be averted.

Second, limited resources can be problematic. Physicians who are experts in their fields are highly coveted, and the ones who are trained to use telemedical equipment are even more in demand. Therefore, a relatively small number of viable candidates are available for expert mentor positions.

Third, a basic level of surgical aptitude must be ascertained in the novice surgeon, whether it is through a simulation or by expert assessment. Procedural protocols must be devised before the telementoring session, so that any confusion or dissension can be avoided when the operation begins. In the case of connection interruption or permanent disconnection, the on-site surgeon must know the appropriate course of action. The on-site surgeon also must be capable of converting laparoscopic surgeries to open or continuing without the assistance of the telementor. One safeguard could be the presence of an on-site expert, who can take over the complex procedure, if necessary.

Fourth, telementoring, like telesurgery, is fraught with medicolegal vulnerabilities. Issues corresponding to interstate or international telementored surgeries have to be addressed. Although the on-site surgeon performs the bulk of the surgery, the remote mentor in some instances controls certain aspects of the operation. In fact, there is often the possibility that the remote mentor may take over an operation if extenuating circumstances arise. These circumstances require special consent to be obtained from patients. Moreover, medical qualifications must be reconciled between the two locations. Currently, medical qualifications from the European Union are not recognized in the United States, and the reverse is also true.[18] An international medical authority should be instated to provide oversight and legal protection for the continued development of telemedicine, and its role should facilitate the growth of international medical cooperation.

Establishing Centers for Telemedicine

In recent years, centers dedicated to telemedicine have been established internationally. In Strasbourg, France, the *Institut de Recherche contre les Cancers de l'Appareil Digestif*, in conjunction with the European Institute for Telesurgery (IRCAD/EITS), is the premier organization promoting these novel technologies.[5]

In Canada, the Center for Minimal Access Surgery (CMAS) was established at McMaster University in 1998. Its primary objectives include the provision of clinical training and expert consultations for physicians in rural areas of Canada.[19] The CMAS initiated its telementoring program in 1999 and its telerobotic program in 2003. Between 2003 and 2005, CMAS provided teleassistance for 21 laparoscopic surgeries, including laparoscopic Nissen fundoplications, hemicolectomies, low anterior resections, sigmoid resections, and hernia repairs. Approximately 400 km separate the teaching hospital, St. Joseph's Hospital in Hamilton, Ontario, from North Bay General Hospital in rural Ontario. IP-VPN connections running at 15 Mbps were used, and telemedical transmissions took precedence over other commercial traffic.[19, 20] The surgeons recorded an average time delay of 135–140 ms, which did not hinder overall performance. Zeus control consoles were set up at both sites, enabling the mentor to take over the operation, should the novice surgeon feel unable to proceed.

Canada is also an encouraging environment for cutting-edge medical practices such as telementoring. The Canadian Medical Protective Association (CMPA) covers physicians' liability for all medical practices, and its authority extends across the entire country. The CMPA eliminates many medicolegal and liability concerns that could make telemedicine vulnerable to litigation.

Future

The future bodes auspiciously for telementoring, and we can expect to see its growth coinciding with the development of minimally invasive surgeries. Many of the medicolegal concerns will take center stage as interest increases from the health sector, and those issues will need to be resolved to permit international cooperation.

Developing technological trends also will invariably influence the future of telementoring. Researchers at the Royal Free Hospital in London have used commercial-free software, such as UltraVNC (http://ultravnc.sourceforge.net) and Windows NetMeeting, to establish remote control connections between computer workstations. No IT technicians were involved, and specialized software costs were entirely circumvented.[21] The network-enhanced surgical training (NEST) trials foreshadow the reduced costs of telementoring in the future.

In another innovative attempt of telementoring, urologists at the Johns Hopkins Brady Institute conducted laparoscopic surgeries under the guidance of the RoboConsultant (RemotePresence-7; InTouch Health, Sunnyvale, CA).[22] The telerounding robot not only provided the internal/external camera view complete with telestration capabilities but also

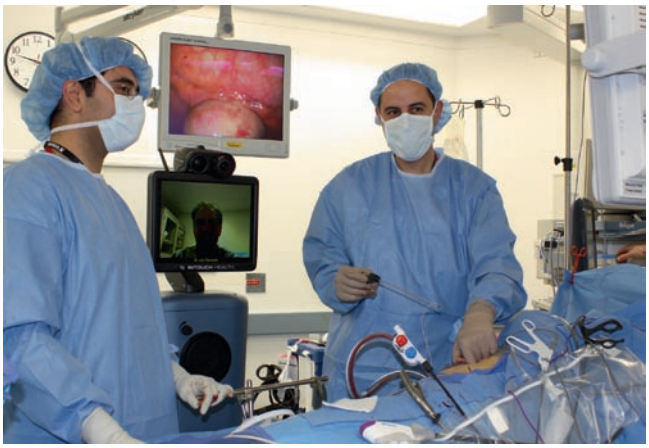

Fig. 28.3 Telementoring in the operating room via RoboConsultant (RemotePresence-7; InTouch Health, Sunnyvale, CA)

had a physical footprint that gave a remote presence to the mentor (Fig. 28.3).

The future of telementoring may lie with remote presence robotics that are fully integrated with surgical robots, so that the mentor could survey external fields and integrate with the endoscopic camera and/or manipulate surgical procedures as necessary. Force feedback, or haptics, should be developed to give the mentor an even greater "feel" of the surgical process, allowing him or her to better direct the novice surgeon.

Plans exist to integrate imaging modalities directly with intelligent robotics. These new designs will incorporate advance sensor systems that use Raman spectroscopy to distinguish and selectively resect tumors automatically.[23] These notions of high-tech medical treatment are no longer fiction but rather attainable goals for the near future. However, until those designs are actualized, telementoring will remain to bridge the gap of disparity in skills among physicians and to facilitate care for the patient.

Telementoring has a bright future; its applications may grow to encompass medicine in remote areas, extreme environments, and even the battlefield. The U.S. Department of Defense has projects underway for rapid battlefield treatment and evacuation. Future space exploration also is likely to enlist more astronauts, particularly with the proliferation of international space stations, and their well-being during such missions is vital for success. Until true robotic surgeries supplant conventional surgeries, telementoring will always have a role in complicated procedures.

References

1. Sibert K, Ricci MA, Caputo M, et al The feasibility of using ultrasound and video laryngoscopy in a mobile telemedicine consult. *Telemed J E Health*. Apr 2008;14(3):266–272
2. Ballantyne GH, Marescaux J, Giulianotti PC. *Primer of Robotic and Telerobotic Surgery*. Philadelphia: Lippincott Williams & Wilkins; 2004
3. See WA, Cooper CS, Fisher RJ. Predictors of laparoscopic complications after formal training in laparoscopic surgery. *JAMA*. Dec 8 1993;270(22):2689–2692
4. Barold SS. Willem Einthoven and the birth of clinical electrocardiography a hundred years ago. *Card Electrophysiol Rev*. Jan 2003;7(1):99–104
5. Anvari M. Telementoring and Remote Telepresence Surgery. In: Faust RA, ed. *Robotics in Surgery*. New York: Nova Science Publisher, Inc.; 2007:35–47
6. Rosser JC, Wood M, Payne JH, et al Telementoring. A practical option in surgical training. *Surg Endosc*. Aug 1997;11(8):852–855
7. Cerf V, Dalal Y, Sunshine C. Specification of Internet Transmission Control Program. December 1974
8. Fabrizio MD, Lee BR, Chan DY, et al Effect of time delay on surgical performance during telesurgical manipulation. *J Endourol*. Mar 2000;14(2):133–138
9. Bove P, Stoianovici D, Micali S, et al Is telesurgery a new reality? Our experience with laparoscopic and percutaneous procedures. *J Endourol*. Apr 2003;17(3):137–142
10. Guillonneau B, Cappele O, Martinez JB, Navarra S, Vallancien G. Robotic assisted, laparoscopic pelvic lymph node dissection in humans. *J Urol*. Apr 2001;165(4):1078–1081
11. Marescaux J, Leroy J, Gagner M, et al Transatlantic robot-assisted telesurgery. *Nature*. Sep 27 2001;413(6854):379–380
12. Sterbis JR, Hanly EJ, Herman BC, et al Transcontinental telesurgical nephrectomy using the da Vinci robot in a porcine model. *Urology*. May 2008;71(5):971–973
13. Lee BR, Bishoff JT, Janetschek G, et al A novel method of surgical instruction: international telementoring. *World J Urol*. 1998;16(6):367–370
14. Rodrigues Netto N, Jr., Mitre AI, Lima SV, et al Telementoring between Brazil and the United States: initial experience. *J Endourol*. May 2003;17(4):217–220
15. Patriciu A, Challacombe B, Dasgupta P, Kavoussi L, Stoianovici D. Robotic telementoring/telesurgical system and randomized evaluation study. *Conf Proc IEEE Eng Med Biol Soc*. 2005;2:2167–2170
16. Cubano M, Poulose BK, Talamini MA, et al Long distance telementoring. A novel tool for laparoscopy aboard the USS Abraham Lincoln. *Surg Endosc*. Jul 1999;13(7):673–678
17. Thirsk R, Williams D, Anvari M. NEEMO 7 undersea mission. *Acta Astronautica*. 2007 ;2007(60):512–517
18. Challacombe B, Kavoussi L, Patriciu A, Stoianovici D, Dasgupta P. Technology insight: telementoring and telesurgery in urology. *Nat Clin Pract Urol*. Nov 2006;3(11):611–617
19. Anvari M. Telesurgery: remote knowledge translation in clinical surgery. *World J Surg*. Aug 2007;31(8):1545–1550
20. Anvari M, McKinley C, Stein H. Establishment of the world's first telerobotic remote surgical service: for provision of advanced laparoscopic surgery in a rural community. *Ann Surg*. Mar 2005;241(3):460–464
21. Gambadauro P, Magos A. NEST (network enhanced surgical training): a PC-based system for telementoring in gynaecological surgery. *Eur J Obstet Gynecol Reprod Biol*. Aug 2008;139(2):222–225
22. Agarwal R, Levinson AW, Allaf M, Markov D, Nason A, Su LM. The RoboConsultant: telementoring and remote presence in the operating room during minimally invasive urologic surgeries using a novel mobile robotic interface. *Urology*. Nov 2007;70(5):970–974
23. Pandya A, Auner G. Robotics technology: a journey into the future. *Urol Clin North Am*. Nov 2004;31(4):793–800

Simulation in Urology

29

James Brewin and Tim Nedas

Introduction

Throughout medicine and surgery, the use of simulation has been increasing as a result of changing professional practice, training, and improved technology. Surgical training has shifted from an apprenticeship model to one of criterion-based training.[1] The traditional Halstead apprenticeship model of surgical training is widely used across Europe and North America, but this concept of training has been challenged over the past few years. The paradigm "see one, do one, teach one" is not applicable to modern surgery, and those in favor of simulation have shifted to the paradigm of "see several, simulate many, do one perfectly." Simulation is becoming an important area of research and is being increasingly integrated into surgical training. Many hope that it may be the answer to reduced working hours as scheduled by the European Working Time Directive.

Urological surgery, particularly endourology, lends itself well to simulation because cameras provide the interface between instrument and user. Minimally invasive procedures tend to allow only one surgeon to operate at a time (as opposed to two or more standing over an open wound); thus, the tyro must be competent before the chief can hand over control.

History of Surgical Simulation

Simulation is defined as: "….an imitation of the conditions of (a situation), e.g., for training."[2] Using an orange to practice suturing skills or practicing surgical knots on a table leg are methods of simulation that have been used by surgeons for many years to practice basic skills. Simulated clinical problems have been used to teach resuscitation skills and management of critically ill patients in the Advanced Life Support™ and Advance Trauma and Life Support™ courses for over 20 years; however, the integration of simulation as a formal training tool to learn surgical skills or entire operations is still in its infancy.

Simulation is established as an important part of training in several other fields such as the military and aviation industries. Indeed, in commercial aviation simulation is a compulsory part of training and assessment. Other industries have set precedents for, and gathered evidence of, the importance of simulation for operator-dependent procedures. Those involved in designing surgical education programs and maintaining surgical standards should look to the airline industry as an example of the power of simulation.

Simulation has the potential to reduce the learning curve in a number of operations and thus may reduce the cost and length of training required to reach competence. It may simulation may also make surgeons safer and more efficient possibly reducing costs and errors in surgery.[3] As a consequence of reduced training time and an increasing number of complex endourological and laparoscopic procedures, medical simulation has developed considerably over the past 10 years.

Role of Simulation in Education

Training time is limited, and therefore, simulators must be shown to be efficient training tools in terms of cost and time if they are to be integrated into surgical training.[4] Rasmussen, a Danish Cognitive Engineer, described three levels of human behavior designed to reduce the potential for accidents in man–machine interface systems,[5] and this model can be applied to the efficacy of surgical training. The three levels of behavior are skill-based behavior (SBB), rule-based behavior (RBB), and knowledge-based behavior (KBB).

SBB takes place without conscious control; tasks using SBB movements are executed as smooth, automated, and highly integrated patterns of behavior. Simple simulators such as knot tying boards are able to teach SBB skills, however, to simulate complicated skills such as those required for endourology and laparoscopy, a more advanced simulator is required. Furthermore, the more realistic the simulator the more likely the SBB learnt in a simulated environment can be translated into the operating room.

RBB reflects the way in which tasks must be completed; in the case of surgery, this reflects the operation protocol. To teach this in a simulated environment, the simulator must be

P. Dasgupta et al. (eds.), *New Technologies in Urology,*
DOI: 10.1007/978-1-84882-178-1_29, © Springer-Verlag London Limited 2010

able to simulate part of a procedure or the whole operation. RBB should be extensively practiced to reduce procedural mistakes; in the commercial world, pilots must practice take off and landing procedures with simulators repeatedly, even when in service, to reduce the risk of error.

KBB relates to unfamiliar situations in which no rules are available and performance must be at higher conceptual level. In the case of pilots, this may be the simulation of a hazardous event requiring emergency action. Simulation of out of the ordinary events increases the ability of an individual to cope with them when they occur, such as the much triumphed landing of an airplane on the Hudson River following a bird strike. For surgery, this relates to unexpected anatomical variation or an inadvertent intraoperative complication.

Simulators may also have a role in assessment; however, a good evidence base must be established to show that a given simulator is an effective assessment tool. Provisional studies support the use of simulators as assessment tools, but before they can be used to select surgical trainees, further research is needed using large cohorts of trainees.[6] If a simulator is able to provide real-time feedback, then it may help trainees to achieve their performance aims and thus be a more efficient training tool.[7] In the short term, it is more likely that performance on a simulator can be used to guide training by identifying areas for development, rather than as a formal selection tool.

Types of Simulators

Simulators may be divided into mechanical simulators, virtual reality simulators, and hybrid simulators. Mechanical simulators utilize real instruments in a simulated environment often using synthetic tissue substitutes to operate on; an example of a mechanical simulator is a box trainer. The instruments used are real, but the simulator needs realistic tissues to work on, it has consumable costs, and it is difficult to monitor errors and other indicators of performance. Metrics are operator parameters that can be measured, and in the case of surgical simulators, some metrics may become reliable performance indicators. Computerized simulators are able to easily produce many metrics for statistical analysis.

The term virtual reality refers to "a computer-generated representation of an environment that allows sensory interaction, thus giving the impression of actually being present."[8] Virtual reality simulators use real instrument handles, but all movements are within an empty structure, the user visualizes their actions on a computer monitor, which displays the virtual world; thus, all tissues and instruments are simulated. The simulator software and processing power must be advanced enough to create a training tool that operates in real time and represents surgery. They are often expensive to purchase but are able to record metric data and do not have the running costs of mechanical simulators.

Hybrid trainers are essentially mechanical simulators that are augmented with computer-based instrument tracking that allows the simulator to monitor performance and errors. One of the principle advantages of hybrid simulation is that it uses real instruments and (depending on the quality of the synthetic tissues used) gives realistic tactile feedback. Hybrid simulators also allow for the tracking of a wide variety of instruments as long as the operating tip has been incorporated into the augmented reality software. The surgeon can inspect their work on the synthetic tissue and also get feedback form the computer-based tracking mechanisms. Although assessment of performance using hybrid simulators has been validated, it is important to note that the metrics generated are often based on visual recognition systems rather than precise tracking and this can lead to the generation of errors.

Simulators can be further divided into low-fidelity and high-fidelity tools. Examples of low-fidelity simulators include mechanical simulators such as box trainers and some virtual reality simulators such as the MIST VR™ (Mentice) during which the trainee has to move, transfer, or diathermy objects. Low-fidelity simulators teach SBB and are generally suited for junior trainees to learn basic skills. There is generally a better evidence for the use of low-fidelity simulators compared with high-fidelity simulators, as they have been available for longer.

High-fidelity simulators more accurately represent real surgery; they require basic skills but also simulate complex tasks or complete operations. Therefore, high-fidelity simulators are able to teach RBB and KBB, in addition to the more basic SBB. Animal models can be considered as high-fidelity simulators of human surgery and are used in surgical training. Several high-fidelity VR simulators, such as the LAP mentor, have been developed for surgery. The operation protocol must be followed; thus, teaching RBB and variations in anatomy and pathology help develop KBB. However, to date, there are no studies that prove that training on high-fidelity simulators can improve operating-room performance.

Mechanical simulators and some virtual reality simulators give the trainee force feedback through the instruments; this is known as haptic feedback. The word haptic is derived from the Greek word "*haphe*," which means pertaining to the sense of touch. Haptics or haptic technology refers to the incorporation of a mechanism, within a mechanical device, inferring the sense of touch to the user by applying forces, vibrations, and motions. In terms of VR, haptics describes the portrayal of sensations from the virtual environment that are equivocal to those felt in the real environment further submerging the user in the virtual world. The science fiction writer Aldous Huxley coined the use of the word haptics with regard to technology in the novel "Brave New World"[9] in which he

described the "feelies," cinemas in which the auditorium seats had hand rests providing haptic stimulation.

Bholat demonstrated that laparoscopic surgery provided haptic feedback (although altered from that felt in open surgery) with a trial in which the tactile properties of objects were compared in three situations during which the subjects were blindfolded; direct palpation, conventional surgical instruments, and laparoscopic instruments.[10] The study demonstrated that direct palpation had the highest accuracy for shape identification, but that fine texture analysis was superior with instrumentation (be it laparoscopic or conventional), and that all three situations were comparable for object consistency.

Haptic devices for VR simulation can use motors, electromagnetic, hydraulics, or gyroscopes to impart tactile sensation to the user. Haptic devices do not usually measure the specific force applied to an object, rather they measure the direction, distance, and speed of movement to calculate force.

Assessment of Simulators

As simulators are introduced into training and incorporated into surgical curricula, an evidence base is gradually developing to support their usefulness as training tools. There is a general consensus in the literature that simulators are important for present-day surgical training, but there is only strong evidence for a small number of surgical simulators. In order for a simulator to be shown to act as a good training tool, it must achieve specific operative and training objectives, and it should be efficient in terms of cost and time.[4] Furthermore, the skills learnt should be transferable to the operating room.

Ideally, a simulator should be able to monitor the performance of a trainee to highlight areas that need to be improved and to develop proficiency-based training programs. VR simulators and hybrid simulators are able to measure numerous metrics of performance, and these must be shown to be valid and reliable indicators of performance before they are used to guide training; there are numerous studies in the literature evaluating various metrics in a number of different simulators.

Validity is a concept borrowed from the social sciences and relates to the property of being true, correct, and realistic.[11] In the case of a simulator, validation looks at how realistically a surgical situation is reproduced and how accurately the metrics relate to proficiency. A valid simulator is realistic and measures true indicators of performance and may thus be used as a training and assessment tool.

There is some variation in the definitions of validity, but generally, it can be divided into face validity, content validity, construct validity, discriminative validity, and most importantly predictive validity. These all look to validate a simulator from different perspectives and build up a picture of the simulator. Face validity and content validity are subjective assessments by experts; Face validity looks at how well the simulator represents real surgery, and content validity analyses the individual components and tasks of the simulator. Construct validity looks at whether a testing instrument measures the attributes it was designed to measure; in the case of surgical simulators, the metrics should reflect the skill of the surgeon. Construct validity is generally evaluated by comparing the performance of experts with novices. Discriminative validity is similar to construct validity, but the simulator must be able to distinguish smaller differences in performance such as when testing surgeons with similar experience.[11, 12]

The ultimate way to validate a simulator is to establish predictive validity by proving that scores achieved on a simulator accurately predict the future proficiency that will be achieved in the operating room. The simulator should also produce similar metrics when used repeatedly in the same situation, and thus demonstrate reliability. Most VR simulators are intrinsically reliable as the computer measures the users movements exactly; however, hybrid simulators rely on they accuracy of the visual-tracking system to produce reliable results.[11]

Some simulators (such as the MIST VR™) have been well validated, and it may be reasonable to use it as a formative assessment tool to guide training. However, to use a simulator as a summative assessment tool for the selection or revalidation of surgeons, there must be a very strong evidence base to prove that the simulator is valid, reliable, and effective. To date, no simulator has shown this.[13]

Simulators for Urology Training

As already discussed, many urological operations are performed either via an endoscope or a laparoscope, and the monitor, along with haptic feedback via the instruments, provides the interface between the surgeon and patient. The images seen by the surgeon are two-dimensional images, while the operation is performed in a three-dimensional environment; this represents a transition from normal practice and must be learnt. Tactile sensation felt through an instrument is of a very different nature to that felt with one's own hand[10] and exposure to the different sensory input is required to allow proficiency in interpretation. Because of the altered force feedback experienced during laparoscopic surgery, altered force application must be learnt.[14]

There is a large discrepancy between the movements possible with a hand compared with those available with an

instrument. Degrees of freedom (DF) are the set of independent displacements that specify the displaced position of the body or the system; the hand gives rise to at least 28 because of its various joints, while the laparoscope and rigid endoscope gives rise to 4; adjustment to this relatively constrained environment must be learned. Furthermore, in laparoscopy, the instruments work via a fulcrum effect in that an upward movement of the hand produces a downward movement of the instrument tip, another feature that extends the length of the learning curve.[15]

Because of these problems, many endourological and laparoscopic operation are difficult to learn, but they are also ideally suited for simulation. Consequently, numerous simulators have been developed for urology and these are discussed below.

Simulators for Laparoscopic Surgery

Early in the introduction of laparoscopic surgical techniques, it became clear that the "learning curve" required to reach a standard of competence compatible with operating independently was steeper than that of open surgery.[16] Moreover, urology, unlike laparoscopic general surgery or gynecology, lacks a relatively simple, high-volume procedure suitable for training.[17] Furthermore, many laparoscopic operations in urology involve complicated reconstruction, and thus, a high degree of skill is required. Simulation in laparoscopy is probably more developed than in the rest of urology as many other specialties operate via a laparoscope, and thus, there is a greater financial incentive to develop simulators for laparoscopy.

Box Trainers

A box trainer is a mechanical simulator in which the student operates using real laparoscopic instruments and real sutures on synthetic tissue substitutes or animal tissue. They are low-fidelity simulators and can vary from the enterprising surgeon's home-made cardboard box equipped with a webcam and instruments to specially designed dry simulators such as the "3-Dmed Laparoscopic trainer™" (Limbs & Things GB) (Fig. 29.1). Any force feedback is limited by the choice of operative material; in the case of dead animal tissue, its properties may differ significantly from that of living tissue. Box trainers have been shown to be effective devices for acquiring basic laparoscopic skills; however, it is debatable how complex the box trainers have to be to be effective. Chung *et al* demonstrated how an inexpensive trainer made of a webcam, cardboard box, desk lamp, and laptop computer was comparable with more expensive commercially available trainers.[18]

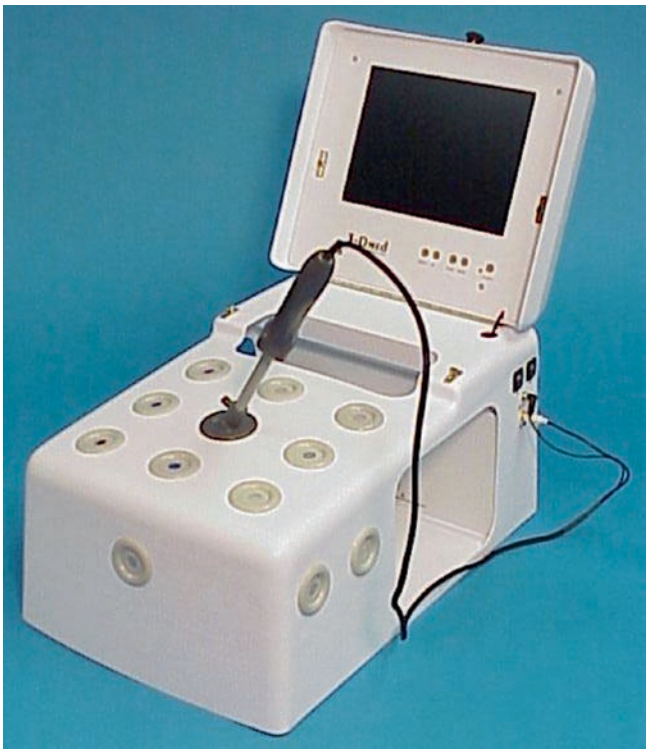

Fig. 29.1 Low-fidelity box trainer

Numerous models have been developed to place inside a box trainer to teach more complicated laparoscopic skills for urology, and these include chicken-skin models to practice the urethral anastamosis following laparoscopic radical prostatectomy[19] and a tumor mimic model for laparoscopic partial nephrectomy.[20]

Hybrid Trainers

Among the best studied hybrid simulators is the ProMIS™ surgical simulator (Haptica Incorporated, USA), but there are other systems on the market such as Surgical SIM LTS™ (METI). Construct validity has been demonstrated by showing that experienced surgeons performed better than novices, but predictive validity has not been established.[21] Several small studies have compared the ProMIS™ with VR trainers; training outcomes were similar in the two groups, but the users generally felt that the ProMIS™ was more realistic than the pure VR trainers.[22] Furthermore, one study has shown that the measurements generated during training on the ProMIS™ compare well to validated observer scoring

systems, and thus, the ProMIS™ also has potential as an assessment tool.[23]

Virtual Reality

Numerous low-fidelity and high-fidelity VR simulators are available for laparoscopic training, and some of the high-fidelity models also include basic low-fidelity training modules (e.g., LapSim™ and LapMentor™).

The best studied low-fidelity simulator is the MIST VR™ (Mentice). Two similar randomized controlled trials have shown that training on the simulator improves real-life performance during laparoscopic cholecystecomies.[24, 25] In both trials, residents performed the operation quicker, with fewer errors and improved economy of movement. Furthermore, in one trial, there were six incidents of "attending takeover" where the attending surgeon felt it necessary to intervene to ensure patient safety; all of these were within the non-VR trained group.[24]

Other low-fidelity models such as the LapSim™ (Surgical Science) and the Lap Mentor™ (Symbionix) have basic laparoscopic modules, in addition to high-fidelity simulation. Studies have established face, content, and construct validity for these two simulators. Interestingly, the LapSIM™ has been compared with box trainers in two trials; both trials showed that the VR and box trainer groups improved more than the control group, but there were only minor differences in performance between the VR and the box trainer groups.[26, 27]

The Procedicus MIST Nephrectomy™ (developed by Guy's Hospital, GSTT Charity and Mentice) is the only high-fidelity simulator available for urology, and recently, face, content, and construct validity have been demonstrated (Figures 29.2–29.6). It has haptic feedback and simulates retroperitoneal and transperitoneal nephrectomy. Other high-fidelity simulators such as the LapSIM™ (surgical sciences) and LapMentor™ (Symbionix) have cholecystectomy modules, but no modules specific to urology. However, some of the skills learnt may be transferable to urology, and a recent study by Lucas *et al* has shown that novices who train on the VR cholecystectomy module (on the Lap Mentor™) perform better than untrained novices when performing porcine nephrectomies.[28] Further studies are needed to see if procedure-specific simulators have any advantage over low-fidelity simulators.

To date, there have been seven trials to assess whether the skills learned on laparoscopic VR simulators are transferable to real surgery (either human or porcine), and all but one have shown a positive transfer of skills.[7] Importantly, three of these used surgical residents rather than medical students and all of these showed a positive transfer of skills.[24, 25, 29]

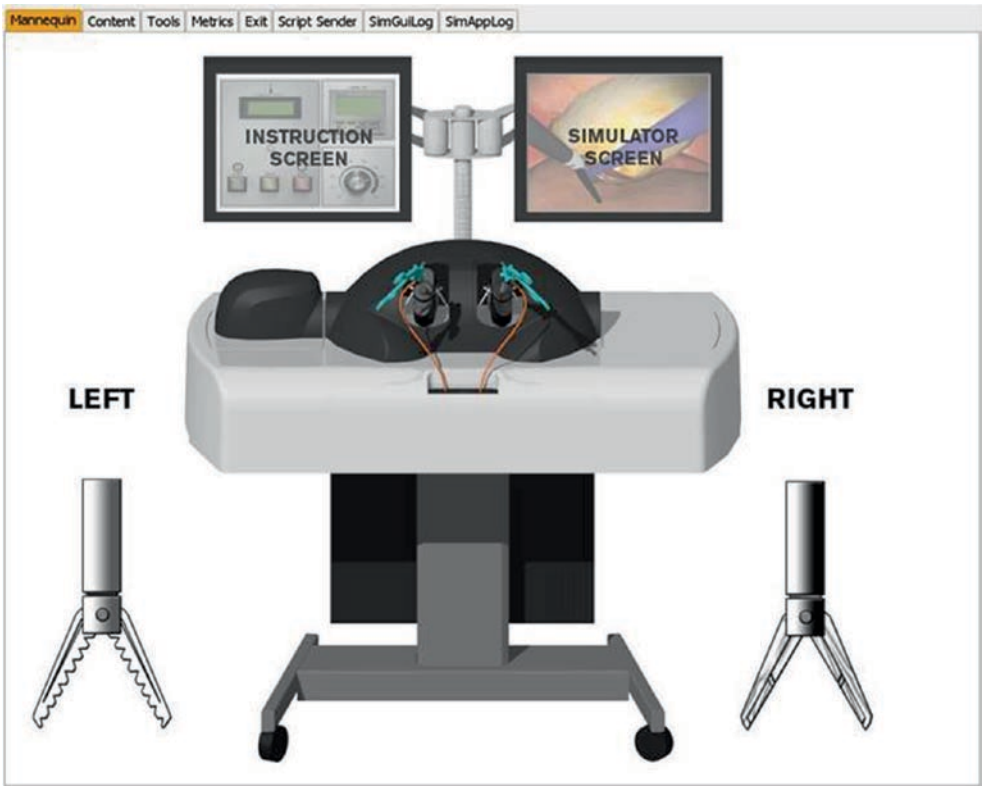

Fig. 29.2 Schematic model of a virtual reality simulator

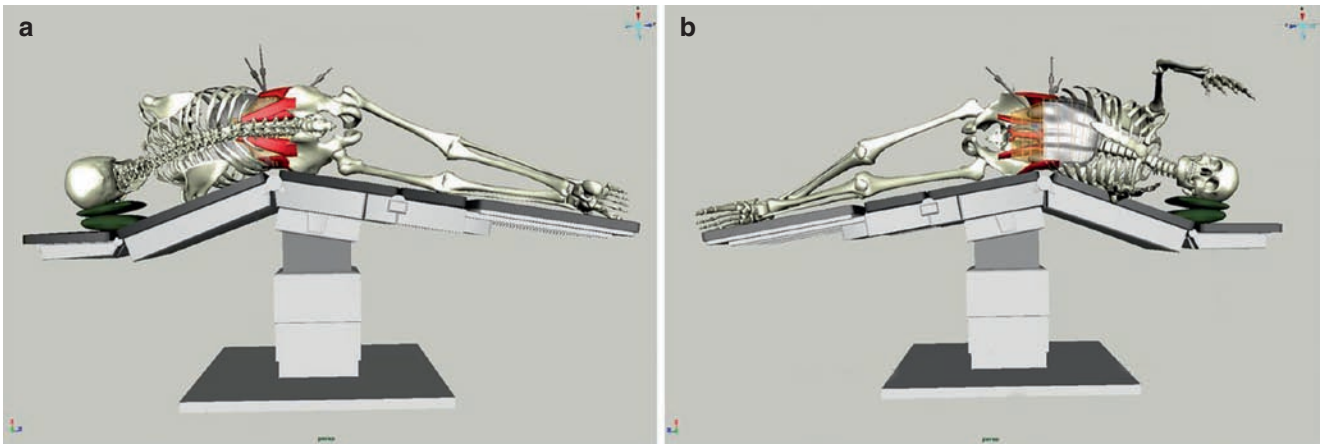

Fig. 29.3 Three-dimensional modeling for virtual reality simulation: (**a**) posterior and (**b**) views of laparoscopic nephrectomy

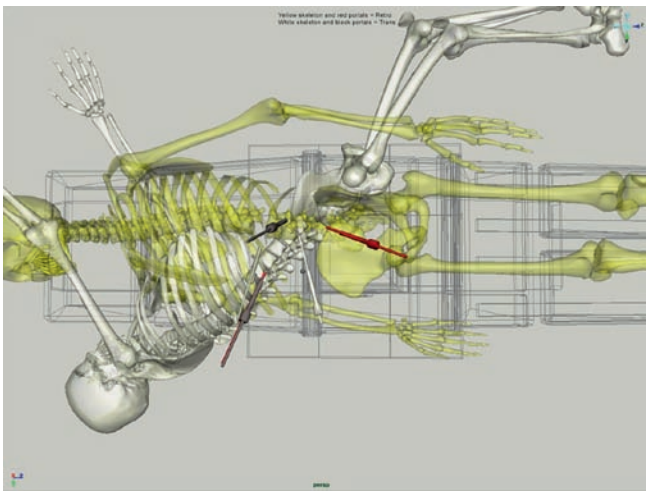

Fig. 29.4 Three-dimensional modeling, comparing the operating positions for different procedures (in this case port positions for retroperitoneal and transperitoneal laparoscopic nephrectomy)

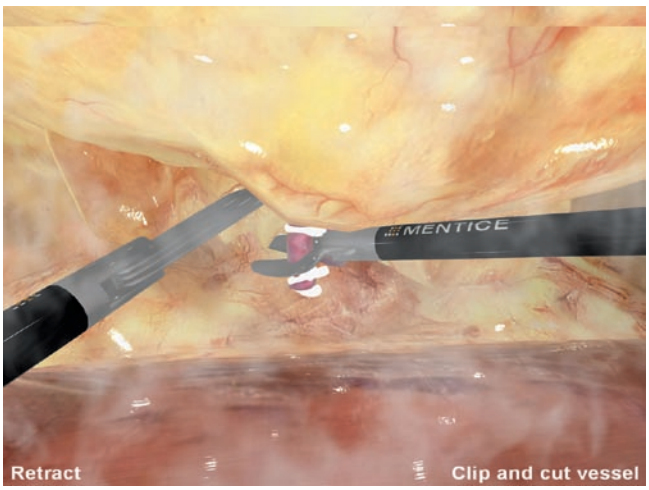

Fig. 29.6 Actual screenshot from a virtual reality laparoscopic nephrectomy simulator

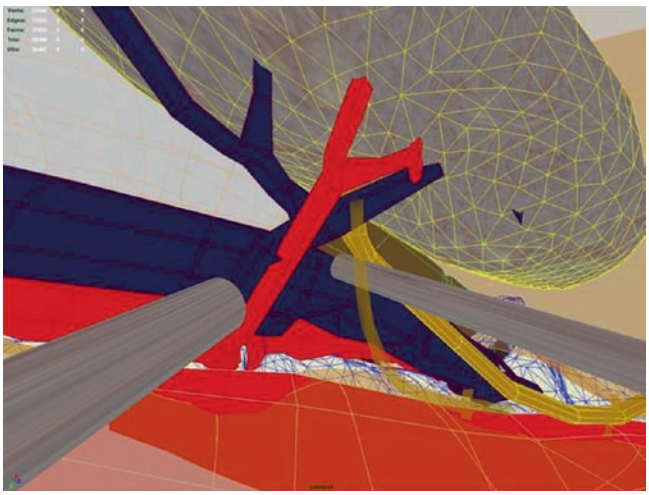

Fig. 29.5 Three-dimensional internal model of laparoscopic nephrectomy constructed from that seen in Fig. 29.3

TURP Simulators

TURP is one of the most commonly performed urological operations and remains the gold standard for the surgical management of BPH. TURP is also one of the most difficult operations to learn as the surgeon has to coordinate the scope, the loop, the diathermy current, and the flow of the irrigation fluid. There are key surgical landmarks that must be avoided, and vision can vary throughout the procedure because of bleeding or debris. Reduced training time and the advent of alternative minimally invasive techniques has resulted in trainees performing fewer TURPs. In 1991, residents in the United States performed on average 120 TURPs before graduating; in 2002, the average was 62.[30] Simulation offers a potential tool to shorten the learning curve and achieve competency, despite the reduced exposure to TURP surgery.

Mechanical simulators for TURP surgery have been developed such as the Bristol TURP Trainer™ (Limbs and Things) that uses a sealed chamber, a real resectoscope, real electrocautery, and real irrigant. The prostate is a synthetic model that does not bleed, but the chips need to be evacuated in the same way as real surgery. As a mechanical simulator, it lacks the ability to measure metrics of performance, but the user is able to look at the synthetic prostate to evaluate their resection.

Several VR TURP simulators have been developed, but the most advanced is the University of Washington VR TURP trainer developed by Sweet and colleagues; it is licensed by Medical Education Technologies Inc. as the SurgicalSIM TURP™.[30] This simulator has haptic feedback and is able to simulate all the components of a TURP, including bleeding and irritant flow; it is also able to measure real-time metrics of performance. Face and content validity have been established by 72 board-certified urologists, and several performance metrics are able to distinguish novices form experts.[31] The investigating group is currently assessing the effect of simulation on operative performance.

Cystoscopy and Ureteroscopy

Cystoscopy and ureteroscopy can be performed with both rigid and flexible instruments, and therefore, simulators must be able to replicate the additional movements possible with flexible instruments. There are several high-fidelity mechanical simulators available for upper and lower tract endourology such as the Uro-Scopic trainer™ (Limbs and Things) and the Scope Trainer™ (Medi Skills). They accurately model the urinary tract, and the user can perform cystoscopy, ureteroscopy, stent insertion, and lithotripsy. The trainee uses the same instruments as in the operating room and, depending on the quality of the model, there is realistic haptic feedback. However, the models do not simulate bleeding and cannot measure performance.

These high-fidelity mechanical models are relatively expensive, and it is not known how realistic a model needs to be to teach the basic skills required for endoscopy. Matsumoto *et al* randomized medical students into three groups: one trained on a low-fidelity model of the renal tract, one trained on a high-fidelity model (Uro-Scopic Trainer™, Limbs, and Things), and one received didactic teaching. The home-made model of the renal tract used a Penrose drain as the urethra, a cup for the bladder, and drinking straws as the ureters and cost $20. There was no significant difference in performance between the low-fidelity and high-fidelity training groups, but the group that received only didactic training performed significantly worse.[32]

VR endourology simulators are also available, and the best studied is the URO Mentor™ (Symbionix), which is able to simulate numerous cystoscopic and ureteroscopic procedures and also has basic skills modules. It has been shown that experienced surgeons perform significantly better than medical students, but that, with training on the simulator, medical students can reach the level of first-year residents.[33] It has also been shown that training on the URO Mentor improves the performance of medical students when performing ureteroscopy on cadavers.[34] The simulator is able to measure performance, and this seems to correlate with the skill of the surgeon.[35] The Uro-Trainer™ (Karl Storz) is a new VR endourology trainer which incorporates haptic feedback; however, only initial validation studies have been performed.[36]

Percutaneous Nephrolithotomy (PCNL)

One of the most difficult parts of performing percutaneous renal surgery is establishing a needle tract into the relevant calyx. The surgeon (or radiologist) must integrate information gained from imaging (fluoroscopy, ultrasound, or a combination), knowledge of renal anatomy, and haptic feedback from the needle. Botoca et al (2006) demonstrated a learning curve of between 40 and 50 PCNL procedures to maximize successful renal puncture and to minimize complications; simulators have the potential to reduce this learning curve.[37]

Several bench models for percutaneous tract simulation have been developed and these can be divided into those that use synthetic models and those that use animal tissues. The Percutaneous Nephrolithotomy Trainer™ (Limbs and Things) consists of synthetic tissues on a translucent slab that can simulate fluoroscopy. It can be used to practice needle puncture, guide-wire insertion, tract dilatation, and stone removal. The Perc Trainer™ (Medi Skills) is a similar synthetic model but can be used with fluoroscopy and ultrasound. Two models using porcine kidneys have also been described; in one model, the kidney is placed in a chicken carcass and in the other it is embedded in silicone. These ex vivo porcine kidney models may provide a more realistic "feel" than the synthetic competitors.[38]

The PERC Mentor™ (Symbionix) is a VR simulator specifically designed to teach percutaneous renal access. A metal needle with a spatial sensor is integrated into a virtual environment in which the trainee has to gain renal access under fluoroscopic guidance. Haptic feedback is provided by a synthetic tissue plate, and there are modules to simulate different clinical situations. User metrics are recorded by the simulator, and construct validity has been established for some of these in a study in which residents performed significantly better than medical students.[38] Studies have also shown that training on the PERC mentor improved performance during porcine percutaneous access, and thus, they

have shown some degree of skill transfer from the simulator to real surgery.[38]

Conclusion

There are numerous simulators available for urology training, and there is a growing body of evidence supporting the use of simulation in surgical training, including several randomized controlled trials.[7] A few simulators have been shown to improve surgical performance in randomized trials, and the evidence for the benefits of simulation is growing.

The use of simulators to improve team working and other areas of "crisis resource management" in addition to clinical skills has been used by anesthetics and other acute medical specialties for a number of years. Urologists may be able to use simulators as part of a simulated operating-room suite and therefore educate the entire surgical team not just the operating surgeon.[39]

Developments in simulation technology, particularly in VR simulation, will result in increasingly realistic and complex simulators. This combined with developments in surgery, such as the use of robotics, will result in new simulators such as the Surgical SIM - RSS™ robotic simulator (METI). Continuing validation studies are needed to assess these new simulators and further work is needed to evaluate how best to incorporate currently available simulators into surgical training. With further research and the continuing improvements in simulation, it should become possible to integrate simulation into urology in an evidence-based and cost-effective way.

The advent of revalidation in the United Kingdom may also provide a role for urological simulation in the assessment of surgical skills. With further developments in technology and a demand for increased patient safety, simulation will have a key role in the training and assessment of tomorrow's urologists.

References

1. Satava RM. The future of surgical simulation and surgical robotics. *Bull Am Coll Surg*. 2007;92(3):13–19
2. The Concise Oxford Dictionary of Current English. 9th ed. New York: Oxford University Press; 1995
3. Nedas T, Challacombe B, Dasgupta P. Virtual reality in urology. *BJU Int*. 2004;94(3):255–257
4. Cuschieri A, Francis N, Crosby J, Hanna GB. What do master surgeons think of surgical competence and revalidation? *Am J Surg*. 2001;182(2):110–116
5. Rasmussen J. Skills, rules and knowledge: signals, signs and symbols and other distinctions in human performance models. *IEEE Transactions on Systems, Man and Cybernetics. SCM*. 1983;13(3):257–266
6. Cadeddu JA, Kondraske GV. Human performance testing and simulators. *J Endourol*. 2007;21(3):300–304
7. Seymour NE. VR to OR: a review of the evidence that virtual reality simulation improves operating room performance. *World J Surg*. 2008;32(2):182–188
8. Coleman J, Nduka CC, Darzi A. Virtual reality and laparoscopic surgery. *Br J Surg*. 1994;81(12):1709–1711
9. Huxley A. *A Brave New World*. London: Chatto and Windus; 1932
10. Bholat OS, Haluck RS, Kutz RH, Gorman PJ, Krummel TM. Defining the role of haptic feedback in minimally invasive surgery. *Stud Health Technol Inform*. 1999;62:62–66
11. Gallagher AG, Ritter EM, Satava RM. Fundamental principles of validation, and reliability: rigorous science for the assessment of surgical education and training. *Surg Endosc*. 2003;17(10):1525–1529
12. Aucar JA, Groch NR, Troxel SA, Eubanks SW. A review of surgical simulation with attention to validation methodology. *Surg Laparosc Endosc Percutan Tech*. 2005;15(2):82–89
13. Carter FJ, Schijven MP, Aggarwal R, Grantcharov T, Francis NK, Hanna GB, et al Consensus guidelines for validation of virtual reality surgical simulators. *Surg Endosc*. 2005;19(12):1523–1532
14. Dankelman J. Surgical simulator design and development. *World J Surg*. 2008;32(2):149–155
15. Gallagher AG, McClure N, McGuigan J, Ritchie K, Sheehy NP. An ergonomic analysis of the fulcrum effect in the acquisition of endoscopic skills. *Endoscopy*. 1998;30(7):617–620
16. Moore MJ, Bennett CL. The learning curve for laparoscopic cholecystectomy. The Southern Surgeons Club. *Am J Surg*. 1995;170(1):55–59
17. Keeley FX, Jr., Eden CG, Tolley DA, Joyce AD. The British association of urological surgeons: guidelines for training in laparoscopy. *BJU Int*. 2007;100(2):379–381
18. Chung SY, Landsittel D, Chon CH, Ng CS, Fuchs GJ. Laparoscopic skills training using a webcam trainer. *J Urol*. 2005;173(1):180–183
19. Nadu A, Olsson LE, Abbou CC. Simple model for training in the laparoscopic vesicourethral running anastomosis. *J Endourol*. 2003;17(7):481–484
20. Taylor GD, Johnson DB, Hogg DC, Cadeddu JA. Development of a renal tumor mimic model for learning minimally invasive nephron sparing surgical techniques. *J Urol*. 2004;172(1):382–385
21. Broe D, Ridgway PF, Johnson S, Tierney S, Conlon KC. Construct validation of a novel hybrid surgical simulator. *Surg Endosc*. 2006;20(6):900–904
22. Botden SM, Buzink SN, Schijven MP, Jakimowicz JJ. Augmented versus virtual reality laparoscopic simulation: what is the difference? A comparison of the ProMIS augmented reality laparoscopic simulator versus LapSim virtual reality laparoscopic simulator. *World J Surg*. 2007;31(4):764–772
23. Kanumuri P, Ganai S, Wohaibi EM, Bush RW, Grow DR, Seymour NE. Virtual reality and computer-enhanced training devices equally improve laparoscopic surgical skill in novices. *JSLS*. 2008;12(3):219–226
24. Seymour NE, Gallagher AG, Roman SA, O'Brien MK, Bansal VK, Andersen DK, et al Virtual reality training improves operating room performance: results of a randomized, double-blinded study. *Ann Surg*. 2002;236(4):458–463; discussion 463–4
25. Grantcharov TP, Kristiansen VB, Bendix J, Bardram L, Rosenberg J, Funch-Jensen P. Randomized clinical trial of virtual reality simulation for laparoscopic skills training. *Br J Surg*. 2004;91(2):146–150
26. Munz Y, Kumar BD, Moorthy K, Bann S, Darzi A. Laparoscopic virtual reality and box trainers: is one superior to the other? *Surg Endosc*. 2004;18(3):485–494
27. Youngblood PL, Srivastava S, Curet M, Heinrichs WL, Dev P, Wren SM. Comparison of training on two laparoscopic simulators and assessment of skills transfer to surgical performance. *J Am Coll Surg*. 2005;200(4):546–551
28. Lucas SM, Zeltser IS, Bensalah K, Tuncel A, Jenkins A, Pearle MS, et al Training on a virtual reality laparoscopic simulator improves

performance of an unfamiliar live laparoscopic procedure. *J Urol*. 2008;180(6):2588–2591; discussion 2591
29. Hamilton EC, Scott DJ, Fleming JB, Rege RV, Laycock R, Bergen PC, et al Comparison of video trainer and virtual reality training systems on acquisition of laparoscopic skills. *Surg Endosc*. 2002; 16(3):406–411
30. Sweet RM. Review of trainers for transurethral resection of the prostate skills. *J Endourol*. 2007;21(3):280–284
31. Sweet R, Kowalewski T, Oppenheimer P, Weghorst S, Satava R. Face, content and construct validity of the University of Washington virtual reality transurethral prostate resection trainer. *J Urol*. 2004; 172(5 Pt 1):1953–1957
32. Matsumoto ED, Hamstra SJ, Radomski SB, Cusimano MD. The effect of bench model fidelity on endourological skills: a randomized controlled study. *J Urol*. 2002;167(3):1243–1247
33. Jacomides L, Ogan K, Cadeddu JA, Pearle MS. Use of a virtual reality simulator for ureteroscopy training. *J Urol*. 2004;171(1):320–323; discussion 323
34. Ogan K, Jacomides L, Shulman MJ, Roehrborn CG, Cadeddu JA, Pearle MS. Virtual ureteroscopy predicts ureteroscopic proficiency of medical students on a cadaver. *J Urol*. 2004;172(2):667–671
35. Wignall GR, Denstedt JD, Preminger GM, Cadeddu JA, Pearle MS, Sweet RM, et al Surgical simulation: a urological perspective. *J Urol*. 2008;179(5):1690–1699
36. Reich O, Noll M, Gratzke C, Bachmann A, Waidelich R, Seitz M, et al High-level virtual reality simulator for endourologic procedures of lower urinary tract. *Urology*. 2006;67(6):1144–1148
37. Botoca MR, Boiborean P, Bucuras V, Herman I, Minciu R, Claici D, et al The learning curve PCNL. Do individual skills prevail over experience? *Eur Urol Suppl*. 2006;5(2):147
38. Stern J, Zeltser IS, Pearle MS. Percutaneous renal access simulators. *J Endourol*. 2007;21(3):270–273
39. Powers KA, Rehrig ST, Irias N, Albano HA, Malinow A, Jones SB, et al Simulated laparoscopic operating room crisis: An approach to enhance the surgical team performance. *Surg Endosc*. 2008;22(4): 885–900

Nanotechnology

30

Declan G. Murphy and Anthony J. Costello

Introduction

The ongoing quest to minimize the invasiveness of surgery is exemplified by robotic-assisted laparoscopic surgery, single-incision laparoscopic surgery, and even natural-orifice transluminal surgery. Surgeons and engineers are pushing the boundaries of technological advancement to allow the performance of complex procedures with minimal trauma to the patient. Miniaturization and robotic-assistance are key components of this progress, and in 2009, we are witnessing increasing enthusiasm for novel systems, which have moved out of the engineering laboratory and into the operating room. While the da Vinci® surgical system (Intuitive Surgical, Mountain View, CA, USA) heralded the first widely implemented generation of surgical "robotics," it is clear that much greater technological advances are on the horizon, which will make systems like the da Vinci® look gargantuan by comparison.

In this chapter, we examine the exciting world of nanotechnology, especially with respect to urological surgery. In the same way, as the development of microtechnology in the 1980s has led to new tools for surgery, emerging nanotechnologies will similarly permit further advances, providing better diagnosis and new devices for medicine. Nanorobots are expected to enable significant new capabilities for diagnosis and treatment of disease for patient monitoring and minimally invasive surgery.[1,2] The ability to manufacture nanorobots may result from current trends and new methodologies in fabrication, computation, transducers, and manipulation. The hardware architecture for a medical nanorobot must include the necessary devices for monitoring the most important aspects of its operational workspace: the human body. Urologists have long been at the forefront of innovation in minimally invasive surgery, and as with endoscopic and laparoscopic surgical systems, we are likely to see urologists adopt the some of the exciting technological developments that nanotechnology offers. Teams of nanorobots may cooperate to perform predefined complex tasks in medical procedures.[3]

Definitions

- Nanotechnology is the study and design of components whose dimensions are measured in nanometers (1 nanometer (nm) = 10^{-9} m). Generally, nanotechnology deals with structures of 100 nm or less and involves the development of materials and devices within those dimensions.
- Nanomedicine: medical and surgical intervention on a nanoscale.

Technical Aspects of Nanotechnology

Miniaturization of Medical Robotics

Medical nanorobotics refers to nanoscale mechanical devices comprising integrated nanocircuits, capable of providing tools for medical instrumentation with dimensions up to few microns. The ongoing developments of molecular-scale electronics, sensors, and motors are expected to make it possible to produce nanorobots with dimensions comparable to bacteria. Such technology could be used in nanosurgery, pharmacokinetics for chemotherapy, or targeted-gene delivery into end organs or cells in remote parts of the body. Such delivery systems should also integrate very well with the development of vaccines and small-molecule agents for renal cancer and laparoscopic surgery.[4] Although developing nanoscale robots presents difficult fabrication and control challenges, the necessary pathway for manufacturing nanorobots should be established based on traditional and new techniques enabled through nanotechnology. A key issue to miniaturizing nanorobots is the further downscaling of integrated circuits and nanobioelectronics.

The research and development of nanorobots with embedded nanobiosensors and actuators offers exciting possibilities for the development of molecular-level medical interventions. A first series of nanotechnology prototypes for

P. Dasgupta et al. (eds.), *New Technologies in Urology,*
DOI: 10.1007/978-1-84882-178-1_30, © Springer-Verlag London Limited 2010

molecular machines are being investigated in different ways around the globe, and some interesting device propulsion and sensing approaches have been presented. In microbiological engineering, the construction of digital circuits in living cells has been demonstrated.[5] Bacteria have been used as physical system components, and radio remote control of biological processes has been demonstrated experimentally.[6] Recent developments in biomolecular computing have demonstrated the feasibility of biocomputers,[7] a promising first step toward future nanoprocessors.

Teleoperation and Actuation

Similar to large-scale robotic arms used in industry or in master–slave robotic surgical systems, miniaturization is enabling nanorobotics systems that can employ enhanced grip actuation for manipulating tissues and objects with extremely small sizes. An actuator with biologically based components has also been proposed. This actuator has a mobile component that moves substantially linearly as a result of a biomolecular interaction between biologically based components within the actuator. Such actuators can be used in nanoscale mechanical devices to pump fluids, open and close valves, or to provide translational movement. These devices will become increasingly complex and versatile as the control and fabrication processes become more adept.

Power Supply

The combination of a remote power supply and a high-frequency, power-receiver antenna coil is already in use for powering implanted medical devices. A similar approach could supply exogenous energy to a molecular machine system possessing embedded nanoelectronics. To help control the nanorobot position, a system for tracking an object in space may comprise a transponder device connectable to the object. The transponder system has a set of antennas through which it is possible to receive and send electromagnetic signals. A series of several transmitters and antennas allow a position calculator associated with the transmitters and receivers to calculate the position of the object as a function of the known delay and the time period between the emission of the radio-frequency (RF) signal and the reception of the RF response from the first, second, and third antennas.

Communication

Monitoring devices coupled to a transceiver and a memory component for remote patient monitoring are currently in use, and provide a central medical system platform for monitoring a large number of physiological parameters. For example, methods of monitoring patients and evaluating the status of a tumor in a patient undergoing treatment includes real-time monitoring in vivo of at least one physiological parameter associated with a tumor, transmitting data from an in situ sensor to a receiver external to the subject, analyzing the transmitted data, repeating the monitoring and transmitting steps at sequential points in time, and then reevaluating the treatment strategy. In situ in vivo biocompatible sensors can also include monitoring systems and telemetry-based operations and related computer program products. An RF telemetry antenna comprises an integrated tank circuit, including an RF head telemetry coil and a tuning capacitor with a predetermined antenna. For the communication, a transmit telemetry pulse is generated for establishing a signal width of the telemetry RF pulse. Thus, equally, a nanorobot can be used to receive data transmitted from an external device and can also transmit data to an external device.

Nanoelectronics Manufacturing

Nanotechnology is moving fast toward nanoelectronics fabrication. Chemically assembled electronic nanotechnology provides an alternative to using complementary metal oxide semiconductor (CMOS) for constructing circuits with feature sizes in the tens of nanometers. Such structures can be operated both as a transistor and as a memory. The thin active silicon channel and the thin front oxide provide dual function of the device, using two voltage ranges. At small voltages, the structure operates as a normal transistor, and at higher voltages, the structure operates as a memory device.

Nanotube/nanofiber electrodes are integrated with electronic devices to form a single-chip nanobiosensor. The single-chip nanobiosensor, which uses nanometer-scale electronic devices, includes sensing transistors in close proximity to nanotube/nanofiber electrodes, and provides an arrangement of the nanotube/nanofiber electrodes into high-density clusters and groups so that sensitive, low noise detection of the activities of small cells, large cells, and a network of cells is possible. The integrated, single-chip approach is such that differential signal extraction is possible. The single-chip nanobiosensor includes small feature size transistors. New fabrication methods allow the manufacture of novel-gated field-emission structures that include aligned nanowire electron emitters localized in central regions within gate apertures, and novel devices using nanoscale emitters for microwave amplifiers, electron-beam lithography, field emission displays, and X-ray sources.

Nanobiosensors

Nanobiosensors are a related area of rapidly progressing research and development. For example, coating nanomagnets with biological molecules produces ultrasmall, highly sensitive, and robust biomagnetic devices that combine molecular and spin electronics (Fig. 30.1). When these nanosensors are integrated into microfluidic channels, highly efficient single-molecule detection chips for rapid diagnosis and analysis of biological agents are constructed. Electromagnetic field sensors can employ the motion of a mechanical oscillator caused by electromagnetic interaction, such as a magnetic polarization with a magnetic field or an electric polarization with an electric field.

Biosensors can incorporate living components including tissues or cells, which are electrically excitable or are capable of differentiating into electrically excitable cells, and which can be used to monitor the presence or level of a molecule in a physiological fluid. Nanotubes and DNA are recent candidates for new forms of nanoelectronics. These may be combined to create new genetically programmed self-assembling materials for facilitating the selective placement of nanotubes on a substrate by functionalizing nanotubes with DNA. Through recombinant DNA technology, targets labeled with distinct detectable biomarkers can be defined, such as fluorescent labels, enzyme labels, and radioactive patterns, and employed in suitable biomolecular transducers. Such biosensors can be used to detect labels selected from among those known, including, but not limited to, radioactive labels, enzymes, specific binding pair components, colloidal dye substances, fluorochromes, reducing substances, latexes, digoxigenin, metals, particulates, dansyl lysine, antibodies, protein A, protein G, electron dense materials, and chromophores.

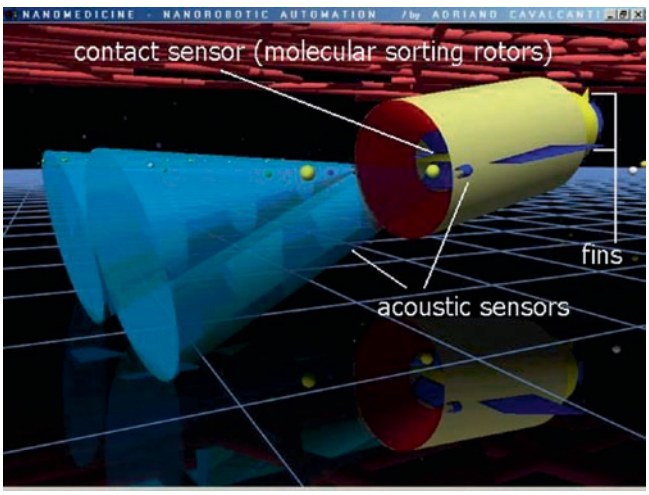

Fig. 30.1 Nanorobot design features: sensors, molecular sorting rotors, fins, and propellers. The depicted blue cones show the sensors "touching" areas. Courtesy of Dr. Adriano Cavalcanti, CAN Centre for Automation in Nanobiotech, Melbourne, Australia

Biocompatibility

Current developments in implant biocompatibility have demonstrated suitable composites that could permit a nanorobot to operate continuously inside the human body. For example, surfactant polymers which are useful for changing the surface properties of biomaterials have been developed. Such surfactant polymers comprise a polymeric backbone of repeating monomeric units having functional groups for coupling to side chains, with separate hydrophobic and hydrophilic side chains linked to polymeric backbone via the functional groups. This "artificial glycocalyx," currently intended for use on biomedical implants, should also provide biocompatibility for nanorobots to operate inside the human body while remaining largely invisible to the immune system.

A Platform for Nanosurgery: Nanorobot Hardware Architecture

Nanorobots for surgical procedures are used as integrated tools and as embedded high-precision transducers for mapping specific areas requiring dissection or indeed any other specific type of biomolecular or tissue intervention. During surgery, they can help to locate surgical targets reporting tumor cell invasion, saving time, and improving productivity. Chemical and thermal patterns can be monitored in real time, providing additional measurements for the surgeon. Teams of nanorobots may cooperate to perform predefined complex tasks in medical procedures.[3] To reach this aim, data processing, energy supply, and data-transmission capabilities can be addressed through embedded integrated circuits, using advances in technologies derived from nanotechnology and very large system integration (VLSI) design. Complementary metal semiconductor (CMOS) VLSI design using deep ultraviolet lithography provides high precision and a commercial way for manufacturing early nanodevices and nanoelectronics systems. The CMOS industry may successfully drive the pathway for the assembly processes needed to manufacture nanorobots, where the joint use of nanophotonic, carbon nanotubes, and nanocrystals may even accelerate further the actual levels of resolution ranging from 248 nm to 157 nm devices. The appropriate interdisciplinary effort will impact on assembly nanodevices and nanoelectronics to build nanorobots.[8] To validate designs to achieve a successful implementation, the use of verification hardware description

language (VHDL) is the most common methodology utilized in the integrated circuit manufacturing industry. Nanorobots can be useful in a large range of biomedical applications for future drug-delivery applications, such as dosage regimens based on predicted pharmacokinetic parameters for chemotherapy in anticancer treatments.[9, 10] A range of different signals are directly correlated to specific medical problems. Chemical signals can serve for medical target identification and actuation.

Factors such as low energy consumption and high sensitivity are among some of the advantages of nanosensors. Nanobioelectronics using nanowires as material for circuit assembly can achieve maximal efficiency for applications regarding chemical changes, enabling new medical applications.[8] Using chemical sensors, nanorobots can be programmed to detect different levels of E-cadherin and beta-catenin as medical targets in primary and metastatic phases. Integrated nanosensors can be utilized for such a task to find different concentrations of E-cadherin signals.[11–13] Beyond sensors, nanorobots may be designed with dedicated space to carry chemotherapy for future cancer drug delivery. This approach allows extremely precise nanotargeting of malignant cells with complete ablation while eliminating adverse effects related to dosing nonmalignant tissues.

Nanorobot Surgical Applications

Cancer

Cancer can be successfully treated with current medical technologies and therapy tools. However, a number of challenges exist for surgeons and cancer specialists. Cancer surgery and chemotherapy often has significant side effects for the patient. This is due to the toxic and destructive nature of the treatment and also due to delivery of this treatment to adjacent structures and organs that do not contain cancer. The key to improving this situation is

- Improved imaging of the malignancy to precisely determine its location and extent
- Improved targeting and delivery systems so that only the tumor receives the treatment

Therefore, how best can one achieve these goals? Currently, cross-sectional imaging using computed tomography (CT) and magnetic resonance imaging (MRI) combined with information from endoscopic and laparoscopic staging is used for preoperative imaging. Preoperative lymph-node staging with CT or MRI scanning has been disappointing since sensitivity and specificity are limited. Considering the possibility of nanorobots navigating as blood-borne devices, they can help on such extremely important process of detection and surgical removal of cancerous tissue (Fig. 30.2).

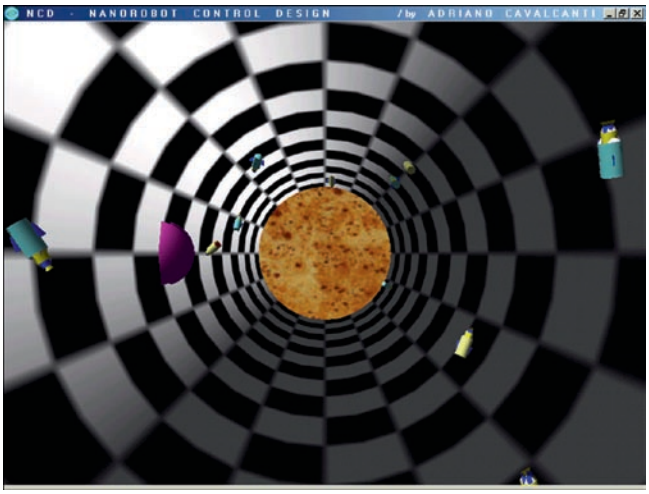

Fig. 30.2 Intravascular view without the red cells. The small solid tumor is the target represented by the pink sphere located on the left wall. All the nanorobots navigate near the wall to detect cancer signals using nanobiosensors. Courtesy of Dr. Adriano Cavalcanti, CAN Centre for Automation in Nanobiotech, Melbourne, Australia

Nanorobots with chemical and electromagnetic sensors can be used for detection of a single tumor cell even in small capillary and intracellular spaces, providing sensing signals at nanoscopic levels. Thus, they can deliver information to the surgeons, helping doctors to deal with the medical procedures through precisely mapping the target areas for dissection. For this purpose, nanorobots can use integrated nanobiosensors to detect changes on gradient intensities of E-cadherin and Bcl-2 signals.[14, 15] Hence, nanorobots can provide a useful addition in biomedical instrumentation to enhance surgical excision of malignant tissues and avoiding tumor recurrence and metastasis following surgery.

Urological Applications of Nanotechnology

Nanobiosensors

The ability of nanoscale sensors to detect clinically significant levels of prostate-specific antigen (PSA) has been reported and correlated with conventional serum PSA testing with good effect, especially at lower levels. Wu et al, using a PSA-labeled antibody, showed that when specific biomolecular binding occurs on one surface of a microcantilever beam, intermolecular nanomechanics bend the cantilever, which can be optically detected using a laser.[16] Shulga et al have developed a new spectrophotometric method using covalently attached capture antibody labeled with alkaline

phosphatase for the detection of free PSA,[17] and Briman et al have described the production and use of a novel electronic device architecture for the quantitative detection and measurement of PSA.[18] The potential of these PSA-based nanotests is the possibility to integrate them into remotely activated nanorobots, allowing for nanosampling and nanodiagnosis of tissue for diagnostic purposes, e.g., lymph nodes and extracapsular prostatic tissue.

Nanotechnology-Enhanced Imaging Techniques

Most diagnostic imaging systems rely on cross-sectional imaging such as computed tomography (CT) or magnetic resonance imaging (MRI) scanning using systemic contrast enhancement with compounds such as gadolinium in the case of MRI scanning. Nanocompounds offer the potential for much more targeted imaging by using nanoparticles to increase the sensitivity and specificity of existing and novel-imaging techniques. The utilization of ultrasmall supermagnetic iron oxides (USPIOs) or monocrystalline iron oxide nanoparticles (MIONs) to improve the detection of lymph-node metastases from prostate cancer has been reported. USPIOs have been shown to extravasate into the interstitial space and are subsequently transported to lymph nodes where they are subsequently taken up by macrophages. Harishinghani et al reported their experience using intravenous injection of USPIOs 24 h before MRI in 80 patients scheduled to undergo radical prostatectomy and pelvic lymph-node dissection. They successfully identified all 33 patients who were proven subsequently to have lymph-node metastases (100% sensitivity). This compares with only 45% who would have been detected using conventional MRI size-based criteria.

Nanocolloids have also been injected to improve the detection rate offered by sentinel node scintigraphy. Warncke et al described their intraprostatic injection technique using technetium-labeled nanocolloid and created a map showing quite varied patterns of lymph-node drainage. Further developments with this technique are expected.

Nanotechnology and Prostate Cancer

One of the challenges facing nanoscale drug-delivery systems has been their degradation in vivo before they achieved their therapeutic goal. However, liposomal delivery systems may overcome in vivo degradation by the reticuloendothelial system, which has a therapeutic potential for the treatment of advanced prostate cancer. The decapetide leuprorelin has been conjugated with polyliposome microspheres as monthly and three-monthly injections in the treatment of advanced prostate cancer.[19]

The use of targeted nanotechnology to deliver cell-destructive therapies is an area of intense interest. Apart from targeted drug-delivery systems, energy-based nanotechnology devices are also under evaluation as potential cancer-killing instruments. Johanssen et al injected superparamagnetic nanoparticles into the prostates of ten men with biopsy-proven locally recurrent prostate cancer following failed primary therapy.[20] Using an alternating current magnetic-field applicator, they excited the superparamagnetic particles leading to hyperthermia (up to 55°C) once weekly for 6 weeks. There was a minimal morbidity, and quality of life was only temporarily impaired. The nanoparticles were detectable within the prostate up to 1 year following treatment. A PSA response was seen in eight of ten patients. This phase-1 study shows some of the potential uses of nanoparticles for the targeted destruction of prostate cancer, and further studies will determine if similar techniques may become available.

The use of therapeutic oligonucleotides to target LNCaP prostate cancer cell lines has also been studied. Santhakumaran et al used polypropylenimine dendrimers to deliver c-myc triplex-forming oligonucleotides to inhibit transcription of the c-myc oncogene.[21] These 130–280 nm nanoparticles exhibited a 65% decrease in c-myc expression demonstrating their potential as candidates for gene transfer in malignancy. Also, Thomas et al have demonstrated that the in vitro targeting of synthesized antibody against prostate-specific membrane antigen with conjugated dendrimer nanoparticles is a potential platform for targeted molecule delivery into appropriate antigen-expressing cells.[22]

Nanotechnology in Urological Surgery

The futuristic vision of autonomous cancer-killing nanorobots coursing throughout the body carrying out precision surgery is a long way distant. However, the progress described earlier in nanorobot control design and manufacture will open the doors to increasing degrees of nanotechnology with clinical applications. The developments are more likely to be evolutionary than revolutionary.

Gommersall et al draw attention to a device that uses nanotechnology to regulate bipolar thermal energy delivery during radical prostatectomy.[19] The Enseal™ device (SurgRx, Palo Alto, CA, USA) has been used to control the dorsal venous complex during laparoscopic radical prostatectomy. It utilizes millions of nanoparticles embedded within the instrument to regulate the thermal spread with theoretical benefits for nerve-sparing and sphincter preservation.

Further nanoscale developments are likely to emerge from the refinement of nanobiosensors for the detection and potential targeting of malignant tissues in situ, and we look forward to such progress.

Conclusion

The huge amounts of funding currently directed toward nanotechnology research will see the rapid development of nanoscale devices and materials in the next decade. Although most of this funding is directed toward nonclinical applications, it is likely that nanoengineering breakthroughs in other sectors will open up opportunities for innovative technologies with clinical applications. Computational nanotechnology should be applied as a useful approach for equipment design, providing insightful information through 3D simulation and clinical data for prototyping, environment test-bed and task analysis, and helping in the development of nanorobots for biomedical applications. Thereby, advanced computational modeling and simulation enables an overview of how surgeons should interface and teleoperate nanorobots for highly precise and minimally invasive surgeries in the future. As before, one can expect the urological community to be among the early adopters of such technologies.

Acknowledgments Many thanks to Dr Adriano Cavalcanti of the CAN Centre for Automation in Nanobiotech, Melbourne, Australia, for his advice in the preparation of this chapter and for his permission to use images reproduced here.

References

1. Cavalcanti A. Assembly automation with evolutionary nanorobots and sensor-based control applied to nanomedicine. *IEEE Trans Nanotechnol*. 2003;2(2):82–87
2. Freitas RA, Jr. Nanomedicine - basic capabilities. www.nanomedicine.com. 1999. Ref Type: Internet Communication
3. Cavalcanti A, Freitas RA, Jr. Nanorobotics control design: a collective behavior approach for medicine. *IEEE Trans Nanobiosci*. June 2005;4(2):133–140
4. Murphy DG, Challacombe B, Khan MS, Dasgupta P. Robotic technology in urology. *Postgrad Med J*. November 1, 2006;82(973): 743–747
5. Yokobayashi Y, Weiss R, Arnold FH. Directed evolution of a genetic circuit. *Proc Natl Acad Sci USA*. December 24, 2002;99(26): 16587–16591
6. Schifferli KH, Schwartz JJ, Santos AT, Zhang S, Jacobson JM. Remote electronic control of DNA hybridization through inductive coupling to an attached metal nanocrystal antenna. *Nature*. 2002; 415(6868):152–156
7. Sand SB, Wiest O. Theoretical studies of mixed-valence transition metal complexes for molecular computing. *J of Physical Chem*. 2003;107(2):285–291
8. Cavalcanti A, Shirinzadeh B, Freitas RA, Jr., Kretly LC. Medical nanorobot architecture based on nanobioelectronics. *Recent Patents on Nanotechnology*. 1 ed. Bentham Science; 2007
9. Kawasaki ES, Player A. Nanotechnology, nanomedicine, and the development of new, effective therapies for cancer. *Nanomed: Nanotechnol Biol Med*. 2005; 1(2):101–109
10. Mutoh K, Tsukahara S, Mitsuhashi J, Katayama K, Sugimoto Y. Estrogen-mediated post transcriptional down-regulation of P-glycoprotein in MDR1-transduced human breast cancer cells. *Cancer Sci*. November 2006;97(11):1198–1204
11. Janda E, Nevolo M, Lehmann K, Downward J, Beug H, Grieco M. Raf plus TGFbeta-dependent EMT is initiated by endocytosis and lysosomal degradation of E-cadherin. *Oncogene*. November 16, 2006;25(54):7117–7130
12. Sonnenberg E, Godecke A, Walter B, Bladt F, Birchmeier C. Transient and locally restricted expression of the ros1 protooncogene during mouse development. *EMBO J*. December 1991;10(12): 3693–3702
13. Trust Sanger Institute. Human chromosome 22 project overview. www.sanger.ac.uk/HGP/Chr22/. 2007. Ref Type: Internet Communication
14. Adams JM, Cory S. The Bcl-2 apoptotic switch in cancer development and therapy. *Oncogene*. February 26, 2007;26(9):1324–1337
15. Ray ME, Mehra R, Sandler HM, Daignault S, Shah RB. E-cadherin protein expression predicts prostate cancer salvage radiotherapy outcomes. *J Urol*. October 2006;176(4 Pt 1):1409–1414
16. Wu G, Datar RH, Hansen KM, Thundat T, Cote RJ, Majumdar A. Bioassay of prostate-specific antigen (PSA) using microcantilevers. *Nat Biotechnol*. September 2001;19(9):856–860
17. Shulga OV, Zhou D, Demchenko AV, Stine KJ. Detection of free prostate specific antigen (fPSA) on a nanoporous gold platform. *Analyst*. March 2008;133(3):319–322
18. Briman M, Artukovic E, Zhang L, Chia D, Goodglick L, Gruner G. Direct electronic detection of prostate-specific antigen in serum. *Small*. May 2007;3(5):758–762
19. Gommersall L, Shergill IS, Ahmed HU et al Nanotechnology and its relevance to the urologist. *Eur Urol*. August 2007;52(2):368–375
20. Johannsen M, Gneveckow U, Taymoorian K et al Morbidity and quality of life during thermotherapy using magnetic nanoparticles in locally recurrent prostate cancer: results of a prospective phase I trial. *Int J Hyperthermia*. May 2007;23(3):315–323
21. Santhakumaran LM, Thomas T, Thomas TJ. Enhanced cellular uptake of a triplex-forming oligonucleotide by nanoparticle formation in the presence of polypropylenimine dendrimers. *Nucleic Acids Res*. 2004;32(7):2102–2112
22. Thomas TP, Patri AK, Myc A et al In vitro targeting of synthesized antibody-conjugated dendrimer nanoparticles. *Biomacromolecules*. November 2004;5(6):2269–2274

Index